Proceedings of the Workshop
on
General Relativity and Gravitation

— TOKYO METROPOLITAN UNIVERSITY, *Hachioji* —

December 4-6, 1991

Editors : K. MAEDA
Y. ERIGUCHI
T. FUTAMASE
H. ISHIHARA
Y. KOJIMA

CONTENTS

PREFACE iii

Wednesday, December 4

Afternoon Session

Chairman: T. FUTAMASE

Perturbation of Black Hole Space-Time and Gravitational Waves
Y. KOJIMA 1

Gravitational Wave Burst Produced by the Merging of Black Holes
T. EBISUZAKI and T. FUKUSHIGE 11

On the Non-Abelian Charged Boson Star
N. JIN and T. FUTAMASE 16

Perturbations of a Boson Star
S. YOSHIDA, Y. KOJIMA and T. FUTAMASE 24

Curvature-Driven Perturbations in Inhomogeneous Cosmological Models
K. TOMITA 34

Quantum to Classical Transition of Density Fluctuation in the Inflationary Model
Y. NAMBU 41

Energy Density Perturbation of Global Textures in the Expanding Universe
M. NAGASAWA and K. SATO 49

Parametric Amplification of Density Fluctuation in the Scalar Field Dominated Universe
Y. NAMBU and S. TAKAYAMA 57

(Coffee Break)

Chairman: K. MAEDA

Checkered (Ichimatsu-Figured) Universe
M. YAMAZAKI 65

Magnitude-Number Count Relation of Galaxies in an Inhomogeneous Universe
– Gravitational Lens Effect –
K. WATANABE 75

Electric and magnetic Parts of the Weyl Curvature in Observational Cosmology
L. GUNNARSEN 88

Topology Changing Solutions of (2+1)-Dimensional Einstein-Yang-Mills Equation
A. HOSOYA 95

Topology Change in Witten Gravity
K. AMANO 104

The Perturbation of the Higher Genus Spatial Surface in (2+1)-Dimensional Gravity
T. OKAMURA and H. ISHIHARA 109

Interaction of Tachyons and Discrete States in c=1, 2-D Quantum Gravity
Y. MATSUMURA and N. SAKAI 114

Spin Precession due to Torsion
K. NOMURA, T. SHIRAFUJI and K. HAYASHI 124

Thursday, December 5

Morning Session

Chairman: M. SASAKI

Numerical Relativity
K. OOHARA 134

Perturbation near the Schwarzschild Black Hole and Test for the Gauge Condition in Numerical Relativity
M. SHIBATA and T. NAKAMURA 151

The Shell Collapse with Scalar Field
Y. OSHIRO, S. KONNO, K. NAKAMURA and A. TOMIMATSU 162

The Oppenheimer-Snyder Space-Time with Λ
K. NAKAO 168

(Coffee Break)

Chairman: K. TOMITA

Experimental Gravity
Y. FUJII 176

Gamma Ray Bursters and Sources of Gravitational Waves
T. NAKAMURA 189

Afternoon Session

Chairman: K. SATO

Black Holes in Astrophysics
F. TAKAHARA 195

Magnetohydrodynamical Accretion onto a Black Hole
M. YOKOSAWA 206

Linear Perturbation Theory of Relativistic Magnetohydrodynamics
T. UCHIDA 213

Time Variation of MHD Accretion onto a Rotating Black Hole
K. HIROTANI, M. TAKAHASHI and A. TOMIMATSU 221

Electromagnetic Radiation from Rotating Objects around a Black Hole
H. HANAMI 231

(Coffee Break)

Chairman: H. ISHIHARA

Cosmic No-Hair Theorem in Exponential and Power-Law Inflation
- Extended Wald's Theorem -
Y. KITADA and K. MAEDA 234

Gravitational Waves in a Planar Universe with Cosmological Constant
H. SHINKAI and K. MAEDA 243

Decaying Cosmological Constant and Inflation
T. NISHIOKA and Y. FUJII 252

Gluing Schwarzschlid-de Sitter Space-Times along the Null Shells
J. SODA 262

Bubble Dynamics and Space-Time Structure in Extended Inflation
N. SAKAI and K. MAEDA 269

Worm Hole Formation in Numerical Cosmology
Y. NAMBU and M. SHIINO 278

Wesson's 5D Space-Time-Mass Theory of Gravity
T. FUKUI 288

Friday, December 6

Morning Session

Chairman: H. KODAMA

Ashtekar Variables and their Applications
H. IKEMORI 296

Vacuum Polarization around Black Holes and Quantum Hair
K. SHIRAISHI 313

Inner-Horizon Thermodynamics and Stability of Kerr Black Holes
O. KABURAKI 319

Rindler Noise and Thermalization Theorem in the Flat Spacetime with a Boundary
K. OHNISHI 321

(Coffee Break)

Chairman: Y. KOJIMA

Equilibrium States of General Relativistic Rotating Stars
Y. ERIGUCHI 331

A General Relativistic Ring around a Black Hole
S. NISHIDA, Y. ERIGUCHI and A. LANZA 353

Afternoon Session

Chairman: A. HOSOYA

Gravitational Soliton Solutions in General Relativity
A. TOMIMATSU 362

Static Gravitational Solitons and the Ring Solution
T. AZUMA 372

Superposed Weyl Solutions – String Connecting Black Holes –
T. KOIKAWA 381

Black Holes from Cosmic Strings
H. MINAKATA 390

Perturbation of Black Hole Space-Time and Gravitational Waves

Yasufumi Kojima

Department of Physics, Tokyo Metropolitan University,
Hachioji, Tokyo 192-03, Japan

Abstract

The perturbations of black hole space-time are reviewed in this paper. Much attention is paid to the gravitational perturbation. To solve this problem, two approaches are possible. One way is to use metric perturbations. The other is to use the Newman-Penrose quantities. Both methods are briefly reviewed. As for this topic, comprehensive reviews[1,2] are available. The mathematical structure is exhaustively studied in Ref.[1], while the application is its main subject of Ref.[2]. These books may be too comprehensive for the most non-experts. The essential points are introduced here.

1. Overview

The perturbation of black hole space-time has a long history. In 1957, Regge and Wheeler[3] first attacked this problem. Their concern was the stability of the black hole space-time. If the space-time is unstable against the modes coupled to the gravitational waves, the black holes never exist. They derived the basic equation governing non-spherical perturbations of "odd" parity-modes, which is a second-order system of differential equations. They showed that the Schwarzschild space-time is stable for such perturbations.

Subsequently, discoveries of pulsars and QSOs in 1960's let lots of astrophysicists draw attention to neutron stars and black holes. Thorne and his collaborators [4] wrote a series of the papers concerning non-radial pulsations of neutron stars. Inside the stars, the non-radial oscillations coupled to density perturbations are

"even" parity-modes. These modes are associated with gravitational waves outside the stars. In their second paper, they derived the basic equation describing the gravitational waves outside the stars. The equation also corresponds to the perturbation equation for the Schwarzschild black hole, because the unperturbed space-time outside the non-rotating star is the Schwarzschild space-time (Birkhoff theorem). They at first derived a third-order system of differential equations for the "even" parity-modes. However, Zerilli [5] showed the basic equation for the "even" parity-modes is also a second-order system, because there is one algebraic identity among the variables and the reduction is possible. Both "even" and "odd" parity-modes can be expressed as a single differential equation of second order, but have different potential terms. See eqs.(18)-(20) in the next section. But this difference is not significant. Chandrasekhar [6] showed both equations are related to each other by a certain transformation. It is also possible to use another function different from Regge-Wheeler or Zerilli functions.

As for the perturbation of the rotating black hole, different technique, that is, Newman-Penrose formalism [7] is necessary. Teukolsky [8] showed gravitational perturbation is described by a single master equation and showed that the separation of variables is possible. Since the background space-time is stationary and axially symmetric, the separation for the variables, t and ϕ is manifestly possible. In addition, the separation for the variable θ is also possible in terms by spheroidal harmonics for the Kerr space-time. Thus, the basic equation governing the gravitational perturbations is a second-order differential equation. He also derived the similar master equations for the perturbations for different fields such as scalar, electron-magnetic and spinor fields. These equations were studied for the superradiance, that is, over-reflection of waves [8]. This is one of the ways to extract energy from the rotating black hole by putting waves. The amplification factor increases with the spin of the fields except the spinor.

The basic equation of gravitational perturbation can be described by a second-order differential equation. There are two independent wave solutions near the horizon and infinity. Two solutions correspond to the ingoing and outgoing waves. We impose purely outgoing waves at infinity and purely ingoing waves at the horizon. Thus, only a certain class of solutions satisfies this boundary condition and the resultant eigen-values are called quasi-normal modes. This concept of the quasi-normal modes was first introduced in Ref. [9]. The quasi-normal frequency is a complex number. The real part corresponds to the oscillation frequency and

the imaginary part to the decay (or growth) rate. The eigen-value thus gives a criterion for the stability of the black hole space-time. Some quasi-normal modes are numerically calculated in several methods [10]. The results show most of black holes are stable, though some instabilities may set in near the extreme Kerr limit [11]. See also e.g., Ref.[12] for the stability.

These quasi-normal frequencies are also the characteristic frequencies of the gravitational waves radiated when the space-time is perturbed. Using the linear perturbation equations, Davis et al. [13] calculated gravitational radiation induced by a small particle falling into a Schwarzschild black hole. In 1977, Smarr [14] first performed fully relativistic non-linear simulation for the collision of two black hole and calculated gravitational waves emitted there. Surprising fact is that the wave form and the efficiency coincide with the estimate from the extrapolation of the linear calculations by Davis et al.. After this remarkable fact was confirmed, a lot of works were done for the estimate of the gravitational radiation [15]. In 1985, Stark and Piran [16] simulated fully relativistic axisymmetric collapse and calculated the gravitational waves. Their results also coincide with the extrapolation of the results based on the linear perturbation.

Recently, cosmological constant revives. Some physicists are interested in the Schwarzschild-deSitter space-time, that is, a black hole solution with non-zero cosmological constant. Several authors [17] examined the perturbation and the quasi-normal modes for the space-time and showed that the space-time is stable.

2. Perturbations of a Schwarzschild black hole

In this section, we shall consider metric perturbations of spherical symmetric space-time as

$$g_{\mu\nu} = g^{(0)}_{\mu\nu} + h_{\mu\nu}, \tag{1}$$

where $g^{(0)}_{\mu\nu}$ is the unperturbed metric. We assume $h_{\mu\nu}$ is a small quantity so that we linearize the Einstein tensor as

$$-2\delta G_{\mu\nu} = h_{\mu\nu;\alpha}{}^{;\alpha} - (h_{\mu\alpha}{}^{;\alpha}{}_{;\nu} + h_{\nu\alpha}{}^{;\alpha}{}_{;\mu}) + 2R^{\alpha}{}_{\mu}{}^{\beta}{}_{\nu}h_{\alpha\beta} + h^{\alpha}{}_{\alpha;\mu;\nu}$$

$$-(R^{\alpha}{}_{\nu}h_{\mu\alpha} + R^{\alpha}{}_{\mu}h_{\nu\alpha}) + g_{\mu\nu}(h_{\alpha\beta}{}^{;\beta;\alpha} - h^{\alpha}{}_{\alpha;\beta}{}^{;\beta}) + Rh_{\mu\nu} - g_{\mu\nu}R^{\alpha\beta}h_{\alpha\beta}, \tag{2}$$

where $R^{\alpha}{}_{\mu}{}^{\beta}{}_{\nu}$, $R^{\alpha\beta}$ and R are Riemann, Ricci and scalar curvatures calculated by the background metric $g^{(0)}_{\mu\nu}$. If we consider Schwarzschild space-time, $R^{\alpha\beta} = R = 0$. It is straightforward but very tedious to write down the basic equations e.g., $\delta G_{\mu\nu} = 0$

for vacuum. Algebraic computer software such as Reduce or Mathematica is helpful. We can furthermore simplify the calculation by the followings.

It is convenient to use tensor harmonics for the angular parts in the calculations. Suppose we solve the Schrödinger equation for the energy levels in the spherical symmetric potential, we expand the function by the spherical harmonics $Y_{lm}(\theta, \phi)$. This technique is useful because the angular part can be separated. The wave function is a scalar under the rotation of 2 dimensional sphere

$$ds^2 = \gamma_{ij} dx^i dx^j = d\theta^2 + \sin^2\theta d\phi^2, \tag{3}$$

so that it is natural to expand the wave function in terms by scalar harmonics. For the metric perturbation, we need another kind of harmonics, because we have to deal with tensors. The spherical harmonic $Y_{lm}(\theta, \phi)$ is a scalar with parity $(-1)^l$. Using this, we can make two kinds of vectors. One is obtained by taking a gradient of the scalar;

$$\nabla_k Y_{lm} = [\partial_\theta Y_{lm}, \partial_\phi Y_{lm}]. \tag{4}$$

The other is obtained by taking a rotation of the scalar;

$$\epsilon_j^k \nabla_k Y_{lm} = [-\partial_\phi Y_{lm}/\sin\theta, \sin\theta \partial_\theta Y_{lm}], \tag{5}$$

where ϵ_j^k is an anti-symmetric tensor. These vectors are valid only for $l \geq 1$ and the vectors (4) and (5) have parity of $(-1)^l$ and $(-1)^{l+1}$. As for the tensor, we have a tensor γ_{ij} with parity of $(-1)^l$;

$$\gamma_{ij} Y_{lm} = \begin{pmatrix} Y_{lm} & 0 \\ 0 & Y_{lm}\sin^2\theta \end{pmatrix}. \tag{6}$$

Taking a gradient of the vector (4), we have $\nabla_i \nabla_j Y_{lm}$. Combining (6), we use traceless form as

$$(2\nabla_i \nabla_j + l(l+1)\gamma_{ij}) Y_{lm} = \begin{pmatrix} W_{lm} & X_{lm} \\ X_{lm} & -W_{lm}\sin^2\theta \end{pmatrix}, \tag{7}$$

where X_{lm} and W_{lm} are functions of θ and ϕ, defined as

$$X_{lm} = 2\partial_\phi(\partial_\theta - \cot\theta) Y_{lm}, \quad W_{lm} = (\partial_\theta^2 - \cot\theta\partial_\theta - \frac{1}{\sin^2\theta}\partial_\phi^2) Y_{lm}. \tag{8}$$

Taking a rotation of the vector (4) and symmetrizing, we have

$$\frac{1}{2}(\epsilon_i^k \nabla_j \nabla_k + \epsilon_j^k \nabla_i \nabla_k) Y_{lm} = \begin{pmatrix} -X_{lm}/\sin\theta & W_{lm}\sin\theta \\ W_{lm}\sin\theta & X_{lm}\sin\theta \end{pmatrix}. \tag{9}$$

Tensors (7) and (9) are valid for $l \geq 2$ and their parity is $(-1)^l$ and $(-1)^{l+1}$.

Since tt, tr rr components are scalars, we can expand these components as

$$h_{tt} = \sum_{l\geq 0,m} H_{0,lm} Y_{lm}, h_{tr} = h_{rt} = \sum_{l\geq 0,m} H_{1,lm} Y_{lm}, h_{rr} = \sum_{l\geq 0,m} H_{2,lm} Y_{lm}, \tag{10}$$

where $H_{n,lm}(n = 0, 1, 2)$ are functions of t and r. Next we consider the vector parts, that is, tj or $rj(j = \theta, \phi)$ components. These components can be written as follows with $C_{n,lm}, h_{n,lm}(n = 0, 1)$, some functions of t and r,

$$h_{tj} = h_{jt} = \sum_{l\geq 1,m} [C_{0,lm} \nabla_j Y_{lm} + h_{0,lm} \epsilon^k_j \nabla_k Y_{lm}],$$

$$h_{rj} = h_{jr} = \sum_{l\geq 1,m} [C_{1,lm} \nabla_j Y_{lm} + h_{1,lm} \epsilon^k_j \nabla_k Y_{lm}]. \tag{11}$$

Finally, $ij(i, j = \theta, \phi)$ components are summation of the three tensors;

$$h_{ij} = h_{ji} = \sum_{l\geq 0,m} K_{lm} Y_{lm} + \sum_{l\geq 2,m} F_{lm}(2\nabla_i \nabla_j + l(l+1)\gamma_{ij}) Y_{lm}$$
$$+ \sum_{l\geq 2,m} d_{lm} [\frac{1}{2}(\epsilon^k_i \nabla_j \nabla_k + \epsilon^k_j \nabla_i \nabla_k) Y_{lm}]. \tag{12}$$

Thus a four-dimensional tensor can be expressed by arbitrary ten functions for a specific l, m. Among the ten functions, $h_{0,lm}, h_{1,lm}$ and d_{lm} have parity of $(-1)^{l+1}$, while remaining seven functions have parity of $(-1)^l$. We call the former set "odd" parity-mode and the latter "even" parity-mode.

There are four degrees of gauze freedom, i.e.,

$$h_{\mu\nu} \longrightarrow h'_{\mu\nu} = h_{\mu\nu} - \xi_{\mu;\nu} - \xi_{\nu;\mu} \quad (x^\mu \longrightarrow x'^\mu = x^\mu + \xi^\mu). \tag{13}$$

It is easily understood that we can generally write down as

$$\xi_t = \sum_{l\geq 0,m} \Lambda_{0,lm} Y_{lm}, \quad \xi_r = \sum_{l\geq 0,m} \Lambda_{1,lm} Y_{lm} \tag{14}$$

and $j(j = \theta, \phi)$ components,

$$\xi_j = \sum_{l\geq 1,m} [U_{lm} \nabla_j Y_{lm} + u_{lm} \epsilon^k_j \nabla_k Y_{lm}]. \tag{15}$$

The functions $\Lambda_{n,lm}(n = 0, 1), U_{lm}$ belong to the "even" parity-mode, while u_{lm} belongs to the "odd" parity-mode. Using these functions, we below show how we can reduce the unknowns.

1) $l = 0$ case.

All quantities for "odd" party-mode vanish. As for "even" parity-mode, there are four functions H_0, H_1, H_2 and K. By a suitable choice of Λ_0 and Λ_1, we can set $H_1 = K = 0$. For the radial oscillation of a star, this coordinate system is usually used. For the black hole perturbation, the solution of this mode corresponds to the change of the black hole mass.

2) $l = 1$ case.

Now we discuss the "odd" parity-mode first. The non-vanishing components are h_0 and h_1. By a suitable choice of u, we can set $h_1 = 0$. The solution for h_0 is related to the change of the angular momentum.

Next, we turn to the "even" parity-mode. We have six functions H_0, H_1, H_2, C_0, C_1 and K and three degrees of freedom Λ_0, Λ_1 and U, so that we can set $C_0 = C_1 = K = 0$. This coordinate system is used for the study of dipole oscillations of a star [18]. For the black hole perturbation, the solution is the gauge mode, that is, we can eliminate it by a certain coordinate transformation. This means the dipole oscillations of the star never disturb the external gravitational field.

3) $l \geq 2$ case.

In this case, there is a degree of freedom for the gravitational waves. The analysis is more complicated. We have one degree of freedom for the "odd" parity-mode and three degrees of freedom for the "even" parity-mode. Using this fact, Regge and Wheeler chose the gauge as

$$C_{0,lm} = C_{1,lm} = F_{lm} = d_{lm} = 0. \tag{16}$$

This gauge condition is normally used. On the other hand, Chandrasekhar chose as

$$H_{1,lm} = C_{0,lm} = C_{1,lm} = d_{lm} = 0. \tag{17}$$

This gauge specification sometimes simplifies the calculation for axisymmetric perturbation, that is, $m = 0$, because $X_{l0} = 0$ and the non-zero components are diagonal for "even" parity-mode. Instead of the gauge specifications, it is possible to use a set of gauge-invariant geometrical objects. See Ref. [19].

Now, we solve ten components of $\delta G_{\mu\nu} = 0$ for vacuum. We can also decompose $\delta G_{\mu\nu}$ by the tensor harmonics. Then we have three equations for "odd" parity-mode and seven equations for "even" parity-mode. The set of "even" parity-mode is more complicated than that of "odd" parity-mode. This is the reason why it took longer time to complete the basic equation for the "even" parity-mode.

We assume the form $e^{-i\omega t}$ for the perturbation and the basic equation can eventually be written as

$$\left[e^{-\lambda}\frac{d}{dr}e^{-\lambda}\frac{d}{dr} + \omega^2 - V^{(\pm)}\right] Z^{(\pm)}_{lm} = 0, \tag{18}$$

where

$$V^{(-)} = e^{-\lambda}\left(\frac{l(l+1)}{r^2} - \frac{6M}{r^3}\right) \tag{19}$$

and

$$V^{(+)} = \frac{e^{-\lambda}[2n^2(n+1)r^3 + 6n^2Mr^2 + 18nM^2r + 18M^3]}{(nr+3M)^2r^3}, \tag{20}$$

where $n = (l-1)(l+2)/2$, $e^{-\lambda} = 1 - 2M/r$ and $(\pm)$ means the "even" and "odd" parity-modes.

If we consider the perturbation of energy-momentum tensor $\delta T^{\mu\nu}$ due to a small particle, it should satisfy the Bianchi identity,

$$\frac{1}{8\pi}\delta G^{\mu\nu}{}_{;\mu} = \delta T^{\mu\nu}{}_{;\mu} = 0. \tag{21}$$

This condition is satisfied for the particle which moves on the geodesics of the background space-time. We can easily include such effect, which results in the source term in the right hand side of eq.(18).

3. Perturbations of a Kerr black hole

In this section, we shall review the perturbation of the Kerr space-time. The essential difference from the previous section is to use the Newman-Penrose formalism. In the formalism, we use four null-vectors $l^\mu, n^\mu, m^\mu, \bar{m}^\mu$, where l^μ and n^μ are real vectors, m^μ is a complex vector and $\bar{m}^\mu$ its complex conjugate. The metric can be expressed as

$$g_{\mu\nu} = -l_\mu n_\nu - n_\mu l_\nu + m_\mu \bar{m}_\nu + \bar{m}_\mu m_\nu. \tag{22}$$

When we derive the basic equation for the gravitational perturbations, we use only following equations among lots of the Newman-Penrose equations; one component of the Riemann tensor (23) and two equations for the Bianchi identities (24),(25);

$$\Delta\lambda - \bar{\delta}\nu = -(\mu + \bar{\mu} + 3\gamma - \bar{\gamma})\lambda + (3\alpha + \bar{\beta} + \pi - \bar{\tau})\nu - \Psi_4, \tag{23}$$

$$\begin{aligned} &-(D + 4\varepsilon - \rho)\Psi_4 + (\bar{\delta} + 4\pi + 2\alpha)\Psi_3 - 3\lambda\Psi_2 \\ &= (\Delta + \bar{\mu} + 2\gamma - 2\bar{\gamma})\Phi_{20} - (\delta + 2\alpha - 2\bar{\tau})\Phi_{21} - 2\nu\Phi_{10} - \bar{\sigma}\Phi_{22} + 2\lambda\Phi_{11}, \end{aligned} \tag{24}$$

$$\begin{aligned} &(\delta - \tau + 4\beta)\Psi_4 - (\Delta + 2\gamma + 4\mu)\Psi_3 + 3\nu\Psi_2 \\ &= (\bar{\delta} - \bar{\tau} + 2\alpha + 2\bar{\beta})\Phi_{22} - (\Delta + 2\bar{\mu} + 2\gamma)\Phi_{21} + 2\nu\Phi_{11} + \bar{\nu}\Phi_{20} - 2\lambda\Phi_{12}, \end{aligned} \tag{25}$$

where D, Δ and δ are directional derivatives along l^μ, n^μ and m^μ, $\alpha, \beta, \gamma, \varepsilon, \lambda, \mu, \nu$, π, ρ, σ are spin coefficients, Ψ_i is a component of Weyle tensor and Φ_{ij} is a component of Ricci tensors. These exact definitions are omitted here. The Ricci tensors can be replaced by the some combinations of the energy momentum tensors through Einstein equation.

The essential point to derive the perturbations of Kerr black hole is its special character of the space-time. The Kerr space-time as well as Schwarzschild space-time belong to the type D space-time in the Petrov classification. Only non-vanishing components is Ψ_2 among five complex Weyle tensors. Due to the Goldberg-Sachs theorem, some spin coefficients can be set to zero. We have for the background space-time,

$$\kappa = \sigma = \nu = \lambda = \Psi_0 = \Psi_1 = \Psi_3 = \Psi_4 = \Phi_{ij} = 0, \tag{26}$$

Now we shall perturb as e.g., $l^\mu = l^{(A)\mu} + l^{(B)\mu}$, $\nu = \nu^{(A)} + \nu^{(B)}$, $\Psi_i = \Psi_i^{(A)} + \Psi_i^{(B)}$ etc., where (A) and (B) mean the unperturbed and perturbed quantities. From eqs.(23)-(25), we can easily observe $\nu^{(B)}, \lambda^{(B)}, \Psi_3^{(B)}, \Psi_4^{(B)}$ and $\Phi_{ij}^{(B)}$ are decomposed from other perturbed quantities. We furthermore assume vacuum case $\Phi_{ij}^{(B)} = 0$ or $\Phi_{ij}^{(B)}$ are given a priori for the test particle case. Eliminating $\nu^{(B)}$, $\lambda^{(B)}$ and $\Psi_3^{(B)}$ from eqs.(23)-(25), we have an equation for $\Psi_4^{(B)}$. The solution for the basic equation can be separated as

$$\Psi_4^{(B)} = (r - ia\cos\theta)^{-4} R_{lm,\omega}(r) S_{lm,\omega}(\theta) e^{-i(\omega t - m\phi)}, \tag{27}$$

where $S_{lm,\omega}(\theta)$ is a spin-weighted spheroidal function. The quantity Ψ_4 corresponds to two polarization modes of outgoing gravitational waves, $h_\times$ and h_+ for large radius. It is therefore sufficient to know the behavior $\Psi_4^{(B)}$, if the information for gravitational perturbations is necessary.

In a similar way, we can derive the basic equation governing $\Psi_0^{(B)}$, which represents ingoing gravitational waves.

The basic equation governing $R_{lm,\omega}$ is not reduced to the Regge-Wheeler or Zerilli equations in Schwarzschild limit. But, we can transform it to different form, which is reduced to Regge-Wheeler equation or others [1,2].

4. Concluding remarks

Two methods, perturbations of the metric and those of the Newman-Penrose equations have been reviewed here. The former has succeeded only for spherical black hole. The extension to the rotating black hole seems to be possible in principle, but practically difficult. Instead, we can extended to include the matter, that is, we can discuss the oscillations of a spherical star in a similar manner. Recently, the non-radial oscillations of a slowly rotating star are studied [20], where the rotation velocity is assumed to be small and the effects are treated perturbatively. Even in such approximation, the basic equation becomes complicated enough. On the other hand, the latter technique is valid for Schwarzschild and Kerr black holes. But, it seems to be difficult to deal with matter. Further studies are indispensable.

Reference

[1] S. Chandrasekhar, " The Mathematical Theory of Black Holes " (Clarendon press, Oxford, 1983)

[2] T. Nakamura, K. Oohara and Y. Kojima, Prog. Theor. Phys. Suppl. 90 (1987), 1.

[3] T. Regge and J.A. Wheeler, Phys. Rev. 108 (1957), 1063.

[4] K.S. Thorne and A. Campolattro, Astrophys. J. 149 (1967), 591.; R. Price and K.S. Thorne, Astrophys. J. 155 (1969), 163.; K.S. Thorne, Astrophys. J. 158 (1969), 1; 997.; J.R. Ipser and K.S. Thorne, Astrophys. J. 181 (1973), 181.

[5] F.J. Zerilli, Phys. Rev. D2 (1970), 2141.

[6] S. Chandrasekhar, Proc. R. Soc. Lond. A343 (1975),289.

[7] E. Newman and R. Penrose, J. Math. Phys. 3 (1962), 566; errata 4 (1963), 998.

[8] S.A. Teukolsky, Astrophys. J. 185 (1973), 635.; W.H. Press and S.A. Teukolsky, Astrophys. J. 185 (1973), 649.; S.A. Teukolsky and W.H. Press, Astrophys. J. 193 (1973), 433.

[9] S. Chandrasekhar and S. Detweiler, Proc. R. Soc. Lond. A344 (1975),441.

[10] S. Detweiler, Astrophys. J. 239 (1980), 292.; B.F. Schutz and C.M. Will, Astrophys. J. 291 (1973), L33.; E.W. Leaver, Proc. R. Soc. Lond. A402 (1985), 285; J. Math. Phys. 27 (1986), 1238.; Phys. Rev. D34 (1986), 384.

[11] S. Detweiler and R. Ove, Phys. Rev. Lett. 51 (1983), 67.

[12] B.F. Whiting, "Proceeding of the 5-th Marcel Grossmann Meeting on General Relativity" (World Scientific, 1989) p.1207.

[13] M. Davis, R. Ruffini, W.H. Press and R.H. Price, Phys. Rev. Lett. 27 (1971), 1466.; M. Davis, R. Ruffini and J. Tiomno, Phys. Rev. D5 (1971), 2932.

[14] L. Smarr, Ann. N.Y. Acad. Sci. 301 (1977), 569.; "Sources of gravitational Radiation" ed, L.L. Smarr (Cambride University Press, 1979).

[15] S.L. Detweiler and E. Szedenits, Astrophys. J. 231 (1979), 211.; S.L. Detweiler, Astrophys. J. 225 (1979), 687.; M.Sasaki and T. Nakamura, Phys. Lett. 89A (1981), 68., Prog. Theor. Phys. 67 (1982), 1788.; T. Nakamura and M. Sasaki, Phys. Lett. 106B (1981), 1627, 89A (1983), 185.; T. Nakamura and M. Haugan, Astrophys. J. 269 (1983), 292.; M. Haugan, S.L. Shapiro and I. Wasserman, Astrophys. J. 257 (1982), 238.; S.L. Shapiro and I. Wasserman, Astrophys. J. 260 (1982), 838.; L. Petrich, S.L. Shapiro and S.A. Teukolsky, Astrophys. J. Suppl. 58 (1985) 297.; K. Oohara and T. Nakamura, Prog. Theor. Phys. 70 (1983), 757., 71 (1984),91.; K. Oohara, Prog. Theor. Phys. 71 (1984), 738.; Y. Kojima and T. Nakamura, Phys. Lett. 96A (1983), 335., 99A (1983), 37, Prog. Theor. Phys. 71 (1984), 79., 72 (1984), 494.;

[16] R.F. Stark and T. Piran, Phys. Rev. Lett. 55 (1985), 891.

[17] R. Balbinot and E. Poisson, Phys. Rev. D41 (1990), 395.; F. Mellor and I. Moss, Phys. Rev. D41 (1990), 403.; J. Guven and D. Nunez, Phys. Rev. D42 (1990), 2577.; H. Otsuki and T. Futamase, Prog. Theor. Phys. 85 (1991), 771.

[18] A. Campolattro and K.S. Thorne, Astrophys. J. 159 (1970), 847.

[19] U.H. Gerlach and U.K. Sengupta, Phys. Rev. D19 (1979), 2268.

[20] S. Chandrasekhar and V. Ferrari, Proc. R. Soc. Lond. A432 (1991), 247, A433 (1991), 423.

Gravitational Wave Burst Produced by the Merging of Black Holes

Toshikazu Ebisuzaki and Toshiyuki Fukushige

Department of Earth Science and Astronomy, College of Arts and Sciences, University of Tokyo, Komaba 3-8-1, Meguro-ku, Tokyo 153

Abstract

When galaxies merge, the central black holes rapidly sink towards the center and make a binary. The orbit of the black holes become highly eccentric and the apocenter distance rapidly decreases. Eventually, gravitational wave emission is significant and the black holes merge. This merging of black holes produce an intense burst of the gravitational wave. We investigated the nature of this gravitational wave bursts and found that the nondimensional amplitude at the earth is as high as 10^{-15} if black holes with the mass of $10^8 M_\odot$ merges at the distance of 2 Gpc. We estimated that the mean time between burst is about 2 yr assuming that the elliptical galaxies are the remnants of the merging of galaxies with central black holes. This assumption is well explained the origin of isothermal core of ellipticals and the positive correlation between core-radius and luminosity.

key word: gravitational wave, black holes, galaxies, quasars

1. Introduction

When galaxies merge, the central black holes rapidly sink toward the common center of the merger remnant due to the dynamical friction of the field star. Eventually, these two black holes make a binary at the center of the parent galaxy. Begelman, Bladford and Rees (1980) and Rees (1990) investigated the orbital decay of this black hole binary at the galactic center. Assuming the orbit of the black holes is circular, they showed that the orbital decay of the black holes slows down because of the depletion of the nearby stars as orbit shrinks. According to them, the life time of the central black hole binary is comparable with Hubble time ($\sim 10^{10} yr$). Roos (1981) performed three-body scattering experiment of the interaction between black holes and field stars and obtained similar results.

However, Ebisuzaki, Makino, Okumura (1991) pointed that the orbit of the black holes become highly eccentric within the core where the mass density of star is nearly uniform. The black holes lose their angular momentum rather than their energy since the dynamical friction is most effective at the apocenter at which black holes have the slowest orbital velocity. In other words, the pericentric distance decreases more rapidly than the apocentric distance. The pericentric distance can become very small because apocentric distance is still large and therefore black hole can interact with a lot of particles at their apocenter.

Fukushige, Ebisuzaki, and Makino (1992) investigated the orbital decay of the black holes in the uniform distribution of the field star. They found that the the orbital angular

momentum exponentially decreases while binding energy does not so much. As angular momentum decreases, the pericentric distance decreases. Eventually, the pericentric distance becomes so small that the energy loss due to the gravitational wave emission is significant. After that two black holes quickly merge due to the energy loss caused by the gravitational wave emission. They concluded that the central black holes merges at most after several dynamical time scale ($\sim 10^7 yr$) of the parent core of the parent galaxy.

This merging of massive black holes produces an intense burst of gravitational wave. In the present paper, we investigate the expected character of this gravitational wave bursts. We found that the mean time between burst is in the range of 2 and 20 yr if we assume elliptical galaxies are the merger remnants of galaxies with the central black holes. This mean time between bursts is consistent with the estimate of Thorne and Braginsky (1976) who used the number of quasars in the universe. The nondimensional amplitude of gravitational wave is as high as 10^{-15} at the earth when black holes with mass of $10^8 M_\odot$ merges at the 2 Gpc distance (Thorne and Braginsky 1976). This level of gravitational wave can be detected by the Doppler tracking of spacecraft (Thorne and Braginsky 1976; Hellings 1979).

In section 2, we figure out the expected character of gravitational wave burst produced by the merging of central black holes. In section 3, we estimate the mean time between bursts assuming that elliptical galaxies are produced by galaxies with central black holes. In section 4, we briefly discuss the detectablity of this bursts.

2. Expected Character of Burst

When two black holes merged, a significant fraction of the rest mass energy is converted into gravitational wave, *i.e.*,

$$E_{gw} = \varepsilon M c^2,$$

where M is the mass of black holes, c is the light velocity, and ε is the efficiency of the energy release. The efficiency ε is estimated as about 0.05 by Nakimura, Oohara and Kojima (1987). The period, P, of the emitted gravitational wave is

$$P = \frac{6\pi\sqrt{3}GM}{c^3} = 2.68 \times 10^3 \left(\frac{M}{10^8 M_\odot}\right)$$

(Press 1971). Thorne and Braginsky (1976) estimated the dimensionless amplitude, $< h >$, of the gravitational wave as

$$< h >= 4.5 \times 10^{-16} \left(\frac{\varepsilon}{0.05}\right)^{\frac{1}{2}} \left(\frac{n}{10}\right)^{-1} \left(\frac{M}{10^8 M_\odot}\right) \left(\frac{R}{2Gpc}\right)^{-1},$$

where R is the distance to the source, n is the number of waves included in one burst. Here we assume that universe is flat. Analytical discussion (Press 1971) and numerical simulations (Ohara and Nakamura 1989) suggests that n is about 10.

3. Mean time between bursts

The mean time between gravitational wave bursts, τ, are calculated as

$$\tau = \frac{1}{4\pi R^2 cnN}$$
$$\sim 2.0 \left(\frac{R}{2Gpc}\right)^{-2} \left(\frac{N}{10}\right)^{-1} \left(\frac{n}{3.7 \times 10^{-3}(Mpc^{-3})}\right)^{-1} \quad (yr),$$

where R and n are, respectively, the distance and the number density of the burst sources, and N is the average number of bursts from each burst source. We estimate these parameters based on the merger hypothesis (Toomre and Toomre 1972; Toomre 1977) that most of elliptical galaxies are formed by the merging of galaxies. This merger hypothesis is strongly supported by recent observations (Schweizer 1982; Bergvall, Rönnbeck, and Johansson 1989; Wright 1990). N-body simulations have shown that merging of two galaxies produces elliptical galaxies (e.g. Barnes 1988; Okumura, Ebisuzaki, and Makino 1991).

The typical distance to the burst sources (merger) is expected to about 2 Gpc. The merging of galaxies is suggested to trigger of quasar activities (Stockton 1990). The distribution of quasars has a peak at around Z=2.7, which corresponds 2 Gpc if we assume the universe is flat and the $H_0 = 100 kms^{-1}Mpc^{-1}$. The number of quasars is consistent with the number density of elliptical galaxies.

We assume that the number density of burst sources is equal to the the number density of the elliptical galaxies. This assumption is justified since merging of two galaxies, which produces an elliptical galaxy, associate with a gravitational wave burst as described as follows.

Elliptical galaxies are strongly suggested to be produced by the merging of galaxies with central black holes. Ebisuzaki, Makino, and Okumura (1991) showed that the core radius expands through merging due to the gravitational energy release of the black hole binary, which is formed after the mergings of parent galaxies. This expansion explains the positive correlation between core radius and absolute luminosity observed in the elliptical galaxies. The core radius dose not increase through merging of galaxies without black holes and is suggested to destroy the positive correlation between core radius and luminosity (Carlberg 1986).

Black hole binary also produces an isothermal core in the merger remnants (Ebisuzaki, Makino, and Okumura 1991). The isothermal core, which is nearly free from the smaller structure, is one of the main characters of the elliptical galaxies. The black hole binary destroys any smaller structure than themselves around the core and make them solved into one isothermal core.

Black holes formed at the center of merger remnant are expected to merge within 10^7 years as described bellow. In the core with nearly uniform density distribution, black holes binary become highly eccentric because the dynamical friction is strongest at the apocenter at which the orbital velocity is slowest (Ebisuzaki, Makino, and Okumura 1991). In other words, the pericentric distance of the black hole binary decreases more rapidly than the apocentric distance. The pericentric distance can become very small because black holes can interacts with a lot of particles at the apocenter which is far from the center. Fukushige, Ebisuzaki, and Makino (1991) performed numerical simulations and the confirmed the results of Ebisuzaki, Makino, and Okumura (1991). According to their

numerical simulation black holes merges at most several dynamical time of the parent galaxies. Therefore, a mergings of galaxies, which produces an elliptical galaxies, associates with a gravitational wave burst. Begelman, Blandford, and Rees (1989) and Rees (1990) estimated the life time of the central black holes binary. However, they overestimated by a large factor it since they assume the orbit of black holes to be circular.

The number density of ellipticals are estimated as $3.7 \times 10^{-3} Mpc^{-3}$ using the data from CfA survey (Huchra, Gellar and de Lapparent 1990). They made acomplete sample of galaxies within $z = 3 \times 10^{-2}$ in a solid angle of $\pi/13$. The number of elliptical galaxies in this sample is about 300.

In the present paper, we assume that burst sources are elliptical galaxies. The elliptical galaxies produces one gravitational wave burst, when it merges with another galaxies. In the case of most brightest ellipticals are expected to experience merging events 100 times since they are typically 100 times massive than the typical ellipticals. Fainter ellipticals probably have probably one or two experiences of merging events. Therefore, we can expected that ellipticals experience 10 times of mergings in average. In other words, $N \sim 10$.

4. Discussion

The merger hypothesis of ellipticals and the theory of active galactic nuclei suggests that one gravitational wave burst with the nondimensional amplitude, h, of 10^{-15} arrives the earth every two years. The detection of this burst is a direct evidence of merger hypothesis of elliptical galaxies.

Since the period and wave length of the gravitational wave are, respectively, as long as 1000 sec and 2 AU, this bursts are detectable by the Doppler tracking of interplanetary space craft (Thorne and Braginsky 1976; Hellings 1979). Using Voyerger I, Hellingth *et al.*(1981) performed one observation of 500 second long and obtain an upper limit of gravitational wave as 3×10^{-14}. It may be easy to reduce the upper limit down to 10^{-16} if we take into account the progress of technology in this decade. Continuous observations are important.

On the other hand, the detection limit of ground-based detectors already is as small as 10^{-18}, which is 1000 times smaller than the expected amplitude of the gravitational wave produce by the black hole mergings. However, these detectors is not sensitive enough to detect gravitational wave with a period of about 1000 s. The improvement of the detection limit of ground based detector at the longer period also quite important.

We thank Junichiro Makino, Daiichiro Sugimoto, Yoshiharu Eriguchi for helpful discussions.

Reference

Barnes, J. E. 1988, *Astrophys. J.*, **331**, 699.
Begelman, M. C., Blandford, R. D., and Rees, M, J. 1980, *Nature*, **287**, 307.
Bergvall, N., Rönnbeck, J., and Johansson, L. 1989, *Astron. Astrophys.*, **222**, 49.
Carlberg, R. L., 1986, *Astrophys. J.*, **310**, 593.

Ebisuzaki, T., Makino, J., and Okumura, S. K., 1991, *Nature*, **352**, 212.
Fukushige, T., Ebisuzaki, T., and Makino, J., 1992, submitted to *Publ. Astron. Soc. Japan.*
Hellings, R. W., 1979, *Phys. Rev. Lett.*, **43**, 470.
Hellings, R. W., Callahan, P. S., Anderson, J. D., and Moffet, A. T., 1980, *Phys. Rev. D*, **23**, 844.
Huchra, J. P., Geller, M. J., and de Lapparent, V., 1990, *Astrophys. J. Suppl.*, **72**, 433.
Nakimura, T., Oohara, K., Kojima, Y., 1987, *Prog. Theor. Phys. Suppl.*, **90**, 135.
Oohara, K., Nakamura, T., 1989, *Prog. Theor. Phys.*, **82**, 535.
Okumura, S. K., Ebisuzaki, T., and Makino, J., 1991, *Publ. Astron. Soc. Japan*, (in press)
Press, W. H. 1971, *Astrophys. J. (Letters)*, **170**, L105.
Rees, M. J., 1990, *Science*, **247**, 817.
Roos, N., 1981, *Astron. Astrophys*, **104**, 218.
Schweizer, F. 1982, *Astrophys. J.*, **252**, 455.
Stockton, A. *Dynamics and Interactions of Galaxies*, (ed. R. Wielen) (Springer-Verlag Berlin: Heidelberg 1990).
Thorne, K. S., and Braginsky, V. B., 1976. *Astrophys. J. (Letters)*, **204**, L1.
Toomre, A. *Evolution of Galaxies and Stellar Populations* (ed. B. M. Tinsely and R. B. Larson)(Yale Observatory: New York 1977).
Toomre, A. and Toomre, J. 1972, *Astrophys. J.*, **178**, 623.
Wright, G. S., James, P. A., Joseph, R. D., and McLean, I. S. 1990, *Nature*, **344**, 417.

On the Non-Abelian Charged Boson Star

N.JIN AND T.FUTAMASE

Department of Physics, Faculty of Science, Hirosaki University
Hirosaki, Aomori-ken 036, Japan

ABSTRACT

Boson star is a gravitationally bound state of complex scalar field. We consider a generalization of the boson star where the scalar field couples to a non-abelian gauge field. We find a way to introduce the time-dependence in the scalar as well as gauge field keeping the staticity of the stress-energy tensor and the space-time metric. This sort of time-dependence seems essential to have a gravitationally bound state. However some difficulties are found to construct the boson star in this case.

§1. Introduction

In cosmology and astrophysics scalar fields play important roles in various situations. For example, a scalar field is used in the inflationary universe scenario which solves the fundamental problems in the standard model. There are also suggestions that the dark matter could be made up of scalar particles. Another interesting suggestion is the possibility of a star-like configuration by scalar field which is now called as the boson star.

The simplest model of boson star is made up of complex scalar field only. The equilibrium configuration is given by a static and spherically equilibrium solution of the Einstein Klein-Gordon equations.[1] [2] [3] It is found that there is a critical mass and particle number. These are $M_{crit} = 0.633(1/G_N m)$ and $N_{crit} = 0.653(1/G_N m^2)$ at $\phi_{crit}(0) = 0.271(1/\sqrt{8\pi G_N})$. [Here $\phi(0)$ is a value at the center and m is the mass of the scalar particle.] The stability for these configurations against the radial perturbations has been studied by Gleiser and Watkins[3] , Lee and Pang[4] and Seidel and Suen.[5] They showed that equilibrium configuration with $\phi(0) < \phi_{crit}(0)$ are stable while the configurations with $\phi(0) > \phi_{crit}(0)$ are unstable.

This model is invariant under a global U(1) phase transformation. Jetzer and Bij[6] extended the analysis to a system of complex scalar field coupled to a U(1) gauge fields. They constructed a series of the static, spherically symmetric solution of the Einstein-Maxwell-Klein-Gordon equations and called them as the charged boson stars. In their treatment the gauge field has only the electric part. The total mass and particle number increases with $\tilde{q} = \sqrt{q^2/8\pi G_N m^2}$ until a critical value of $\tilde{q}$ given by $\tilde{q}_{crit} = \sqrt{1/2}$. Here q is the gauge coupling constant. If $\tilde{q} > \tilde{q}_{crit}$, there is no bounded state because the Coulomb repulsion between two particles becomes larger than the gravitational attraction.

We shall extend their work to a non-abelian case, namely, we study a static spherically symmetric equilibrium configuration of Einstein-Yang-Mills-Higgs system with gauge group SU(2). We found a way to introduce a time-dependence in the gauge and Higgs field without destroying the staticity of the stress-enegy tensor as well as the space-time metric. This kind of time-dependence seems essental to have a bound system. However we find some difficulties integration the basic equilibrium and so far we are not able to constract the desined boson star.

§2. The model and the basic equations

As the most simple example of the non-ablian theory we take the following Einstein-Yang-Mills-Higgs system.

$$S = \int d^4x\sqrt{-g}\left(\frac{R}{16\pi G_N} - \frac{1}{4}tr(F_{\mu\nu}F^{\mu\nu}) - (D^\mu\Phi)^\dagger(D_\mu\Phi) - V(\Phi^\dagger\Phi)\right), \qquad (1)$$

with

$$F_{\mu\nu} = \partial_\mu W_\nu - \partial_\nu W_\mu - \frac{i}{2}g[W_\mu, W_\nu] \qquad (2)$$

$$D_\mu\Phi = (\nabla_\mu - \frac{i}{2}gW_\mu)\Phi \qquad (3)$$

$$V(\Phi^\dagger\Phi) = m^2\Phi^\dagger\Phi \qquad (4)$$

The W_μ and Φ are SU(2) vector potential and Higgs doublet, respectively. Here and after we use $\hbar = c = 1$ unit. This action is invariant under a local SU(2) gauge transformation.

By varying the action with respect to $g^{\mu\nu}$, W_μ and Φ, we obtain Einstein equations

$$G_{\mu\nu} = 8\pi G_N T_{\mu\nu} \tag{5}$$

with

$$\begin{aligned} T_{\mu\nu} = & (D_\mu\Phi)^\dagger(D_\nu\Phi) + (D_\nu\Phi)^\dagger(D_\mu\Phi) - g_{\mu\nu}\{(D^\alpha\Phi)^\dagger(D_\alpha\Phi) + v(\Phi^\dagger\Phi)\} \\ & + tr(F_{\mu\alpha}F_\mu{}^\alpha) - \frac{1}{4}g_{\mu\nu}tr(F_{\alpha\beta}F^{\alpha\beta}) \end{aligned} \tag{6}$$

and the equations of motion for W_μ and Φ,

$$\frac{1}{\sqrt{-g}}\partial_\mu(\sqrt{-g}F^{\mu\nu}) - \frac{i}{2}g[W_\mu, F^{\mu\nu}] - \frac{i}{2}g[\Phi^\dagger\tau^A(D^\mu\Phi) - (D^\mu\Phi)^\dagger\tau^A\Phi]\tau_A = 0 \tag{7}$$

$$D_\mu D^\mu\Phi - m^2\Phi = 0 \tag{8}$$

We would like to find a static spherically symmetric solution of the above set of equations. Thus the space-time metric can be taken as follows.

$$ds^2 = -e^{2\nu(t,r)}dt^2 + e^{2\lambda(t,r)}dr^2 + r^2(d\theta^2 + \sin^2\theta d\varphi^2) \tag{9}$$

The general spherically symmetric ansatz which yields spherically symmetric distribution of the energy takes the following form:[7]

$$W_0 = C(t,r)\,U \tag{10a}$$

$$W_r = G(t,r)\,U \tag{10b}$$

$$W_\theta = [B(t,r)\partial_\theta U + (A(t,r)-1)\frac{\partial_\varphi U}{\sin\theta}] \tag{10c}$$

$$W_\varphi = [B(t,r)\partial_\varphi U - (A(t,r)-1)\sin\theta\partial_\theta U] \tag{10d}$$

$$\Phi = [H(t,r) + iK(t,r)\,U]\begin{bmatrix} 0 \\ 1 \end{bmatrix} \tag{10e}$$

$$U = \frac{x^A\tau_A}{r} = \begin{pmatrix} \cos\theta & \sin\theta e^{-i\varphi} \\ \sin\theta e^{i\varphi} & -\cos\theta \end{pmatrix} \tag{10f}$$

where τ_A is the Pauli matrices.

The above ansatz preserves a U(1) gauge subgroup of the original SU(2) which given by

$$\begin{bmatrix} C \\ G \end{bmatrix} \to \begin{bmatrix} C \\ G \end{bmatrix} + \begin{bmatrix} \dot{f}(t,r) \\ f'(t,r) \end{bmatrix} \tag{11a}$$

$$A + iB \to e^{if(t,r)}(A + iB) \tag{11b}$$

$$H + iK \to e^{\frac{i}{2}f(t,r)}(H + iK) \tag{11c}$$

Here, dot and prime denote ∂_0 and ∂_r, respectively.

It is found that if we take the following time-dependence in the gauge and Higgs field, the metric functions and stress-energy tensor are independent of time.

$$A(t,r) + iB(t,r) = e^{i\omega t}(a(r) + ib(r)) \tag{12a}$$

$$H(t,r) + iK(t,r) = e^{i\frac{\omega}{2}t}(h(r) + ik(r)) \tag{12b}$$

Furthermore we can impose the radial gauge condition: $G = 0$. The basic equations is then given by the two of the Einstein equations

$$\begin{aligned} \frac{2}{r}\lambda' e^{-2\lambda} + \frac{1}{r^2}(1 - e^{-2\lambda}) = 8\pi G_N \Big[& \{\frac{1}{4}e^{-2\nu}(C-\omega)^2 + m^2 \\ & + \frac{1}{2r^2}(a^2 + b^2 - 1)\}(h^2 + k^2) + e^{-2\lambda}(h'^2 + k'^2) + \frac{1}{r^2}a(k^2 - h^2) - \frac{2}{r^2}bhk \\ & + \frac{1}{g^2}\{\frac{1}{2}e^{-2\lambda-2\nu}C'^2 + \frac{1}{r^2}e^{-2\nu}(C-\omega)^2(a^2 + b^2) \\ & + \frac{1}{r^2}e^{-2\lambda}(a'^2 + b'^2) + \frac{1}{2r^4}(a^2 + b^2 - 1)^2\}\Big] \end{aligned} \tag{13a}$$

$$\begin{aligned} \frac{2}{r}\nu' e^{-2\lambda} - \frac{1}{r^2}(1 - e^{-2\lambda}) = 8\pi G_N \Big[& \{\frac{1}{4}e^{-2\nu}(C-\omega)^2 - m^2 \\ & - \frac{1}{2r^2}(a^2 + b^2 - 1)\}(h^2 + k^2) + e^{-2\lambda}(h'^2 + k'^2) - \frac{1}{r^2}a(k^2 - h^2) + \frac{2}{r^2}bhk \\ & + \frac{1}{g^2}\{-\frac{1}{2}e^{-2\lambda-2\nu}C'^2 + \frac{1}{r^2}e^{-2\nu}(C-\omega)^2(a^2 + b^2) \\ & + \frac{1}{r^2}e^{-2\lambda}(a'^2 + b'^2) - \frac{1}{2r^4}(a^2 + b^2 - 1)^2\}\Big] \end{aligned} \tag{13b}$$

and the six of the equations of motion for gauge and Higgs fields.

$$C'' + (\frac{2}{r} - \nu' - \lambda')C' - 2e^{2\lambda}(C-\omega)\{\frac{1}{r^2}(a^2+b^2) + \frac{g^2}{4}(h^2+k^2)\} = 0 \tag{14a}$$

$$a'b - b'a + \frac{g^2}{2}r^2(h'k - k'h) = 0 \tag{14b}$$

$$\begin{aligned} a'' + (\nu' - \lambda')a' - \frac{1}{r}e^{2\lambda}(a^2+b^2-1)a \\ + e^{2\lambda-2\nu}(C-\omega)^2 a - \frac{g^2}{2}e^{2\lambda}\{(h^2+k^2)a + k^2 - h^2\} = 0 \end{aligned} \tag{14c}$$

$$\begin{aligned} b'' + (\nu' - \lambda')b' - \frac{1}{r}e^{2\lambda}(a^2+b^2-1)b \\ + e^{2\lambda-2\nu}(C-\omega)^2 b - \frac{g^2}{2}e^{2\lambda}\{(h^2+k^2)b - 2hk\} = 0 \end{aligned} \tag{14d}$$

$$\begin{aligned} h'' + (\frac{2}{r} + \nu' - \lambda')h' - \frac{1}{2r^2}e^{2\lambda}\{(a-1)^2+b^2\}h + \frac{1}{r^2}e^{2\lambda}bk \\ + e^{2\lambda}\{\frac{1}{4}e^{-2\nu}(C-\omega)^2 - m^2\}h = 0 \end{aligned} \tag{14e}$$

$$\begin{aligned} k'' + (\frac{2}{r} + \nu' - \lambda')k' - \frac{1}{2r^2}e^{2\lambda}\{(a+1)^2+b^2\}k + \frac{1}{r^2}e^{2\lambda}bh \\ + e^{2\lambda}\{\frac{1}{4}e^{-2\nu}(C-\omega)^2 - m^2\}k = 0 \end{aligned} \tag{14f}$$

All the equations are not independent. In fact, Eq. (14b) is the integration of Eqs. (14c)–(14f). The total mass M is defined by

$$M = 4\pi \int_0^\infty \rho r^2 dr \tag{15}$$

where the energy density ρ is the right hand side of Eq. (13a) divided by $8\pi G_N$.

§3. Some difficulties

We wish to solve the above equations numerically. For this we need the boudary conditions at the origin as well as at the infinity. Some of them are obtained by the regularity conditions at the origin. Namely the relevant fuctions may be expanded near the origin in the following way.

$$a = 1 + \alpha r^2 \tag{16a}$$

$$b = -\frac{g^2}{6} h_0 k_1 r^3 \tag{16b}$$

$$h = h_0 + \frac{1}{6} m^2 h_0 r^2 \tag{16c}$$

$$k = k_1 r + k_3 r^3 \tag{16d}$$

$$C = \omega + c_1 r + c_3 r^3 \tag{16e}$$

$$\lambda = \lambda_2 r^2 \tag{16f}$$

$$\nu = \nu_0 + \nu_2 r^2, \tag{16g}$$

with

$$k_3 = \frac{1}{10}\{2(\nu_2 - 3\lambda_2) - 2\alpha - \frac{g^2}{6} h_0^2 - m^2\} k_1 \tag{17a}$$

$$c_3 = \frac{1}{10}\{2(\nu_2 + 3\lambda_2) + 4\alpha + \frac{g^2}{2} h_0^2\} c_1 \tag{17b}$$

$$\nu_2 = 8\pi G_N[-\frac{1}{6} m^2 h_0^2 + \frac{1}{g^2}(\frac{1}{4} e^{-2\nu_0} c_1^2 + \alpha^2)] \tag{17c}$$

$$\lambda_2 = 8\pi G_N[\frac{1}{6} m^2 h_0^2 + \frac{1}{2} k_1^2 + \frac{1}{g^2}(\frac{1}{4} e^{-2\nu_0} c_1^2 + \alpha^2)] \tag{17d}$$

Thus α, c_1, h_0 and k_1 are the free parameter to be specified at the origin. ν_0 is determined by the boundary condition at infinity where the space-time becomes flat. The eigenvalue ω appears in the constant part of C.

Since the space-time is approximately flat near infinity, [i.e. $\nu \sim 0$, $\lambda \sim 0$, $\nu' \sim 0$, $\lambda' \sim 0$ at $r \to \infty$], Eq. (14a) reduces to $(rC)'' \sim 0$. This is obtained by rewriting Eq. (14a) as $C \to rC, h \to rh, k \to rk$ and by ingnoring order of 1/r. Thus C behaves as $C \sim \frac{Q}{r} + \delta$ where Q and δ are the real integration constants. In the same approximation, Eqs. (14c)-(14f) are written as

$$(a + ib)'' + (\delta - \omega)^2 (a + ib) \sim 0$$
$$(rh + irk)'' + \{\frac{1}{4}(\delta - \omega)^2 - m^2\}(rh + irk) \sim 0$$

Therefore Eqs. (14) shows that the fields at the infinity behave as follows.

$$C \sim \frac{Q}{r} + \delta \tag{18a}$$

$$a + ib \sim \beta e^{i(\delta-\omega)r} \tag{18b}$$

$$h + ik \sim \frac{\gamma}{r} e^{-\sqrt{m^2-(\delta-\omega)^2/4}\, r} \tag{18c}$$

Here β and γ are complex numbers. We take a minus sign of exponential factor of Eq. (18c) to consider a bound state of the scalar field for $m^2 > (\delta - \omega)^2/4$. [For $m^2 < (\delta - \omega)^2/4$, the scalar field oscilates, and do not become the bound state. See, however, Seidel and Suen[8]].

In order that the total mass have a finite value, the integland of Eq. (15) must converge to zero at infinity. Thus by substituting Eqs. (18) into the expression for ρ and using the fact that e^{-r} converges to zero faster than r^{-n}, we get

$$\rho r^2 \sim (\delta - \omega)^2 |\beta|^2 = 0, \quad r \to \infty$$

If we take $\delta = \omega$, the effect merely lift the value of C by ω. Then Eqs. (13) and Eqs. (14) becomes purely static system by choosing $C \to C + \omega$. In this case, it seems that these configurations are unstable because there will be no dispersion effect which is needed to support the star-like configuration. Thus we have to take $|\beta| = 0$ at infinity as a physical requirement. For $|\beta| = 0$ at infinity, the θ, φ conponents of gauge field do not vanish at the infinity.

For any value of δ, Eq. (16c) shows that h dose not take a maximum value at the origin because the first and the second term in the Eq. (16c) can not have different sign for any value of $h_0 > 0$. It might be still possible that the scalar field takes a maximum value at some finite distance and gose to zero at a latge distance. If we take $h_0 = 0$, then it may be shown that h vanishes identidcally. Since there might be a configuration where takes a maximum values at some finite distance. Thus in any case, if the non-abelian charged boson star exist, its structure would be rather different from the abelian charged boson star. We hope to study its structures more detail in near future.

ACKNOWLEDGEMENTS

We would like to thank Prof. T. Akiba for useful advice.

REFERENCES

1. R. Ruffini and S. Bonazzola, Phys. Rev. 187 (1969) 1767
2. R. Friedberg, T. D. Lee and Y. Pang, Phys. Rev. D35 (1987) 3640
3. M. Gleiser and R. Watkins, Nucl. Phys. B319 (1989) 733
4. T. D. Lee and Y. Pang, Nucl. Phys. B315 (1989) 477
5. E. Seidel and W. Suen, Phys. Rev. D42 (1990) 384
6. Ph. Jetzer and J. J. Van Der Bij, Phys. Lett. B227 (1989) 341
7. T. Akiba, H. KIkuchi and T. Yanagida, Phys. Rcv. D40 (1989) 588
8. E. Seidel and W. Suen, Phys. Rev. Lett. 66 (1991) 1659

Perturbations of a boson star

SHIJUN YOSHIDA, YASUFUMI KOJIMA * AND TOSHIFUMI FUTAMASE

Department of Physics, Faculty of Science, Hirosaki University
Hirosaki, Aomori-ken 036, Japan

** Department of Physics, Tokyo Metropolitan University*
Hachioji, Tokyo 192, Japan

ABSTRACT

We shall investigate the non-radial pulsation of a boson star and the associated graviational waves. As the first step we here formulate the linearized perturbations around an equilibrium boson star in general relativity using the tensor harmonics and derive the perturbation equations for odd and even parity modes. It is found that the perturbations with odd parity do not couple with gravitational waves and the set of equations for even parity perturbations reduces to sixth-order system of differential equations.

1. Introduction

There is a growing interest for scalar fields in cosmology. For example, many models of the inflationary universe scenario assume the existence of a scalar field called inflaton whose energy density generates the inflationary expansion.[1]

If the scalar fields exist in nature, it is interesting to ask the question if they form gravitationally bound state which is now called as the boson star. This question was answered affirmatively by Ruffini and Bonazzola.[2] They solved the semi-classical Einstein equation and found a gravitationally bound state of the scalar field. Later the boson stars were investigated by many authers.[3] [4] [5] They considered a complex scalar field coupled with gravity and found the equilibrium configuration under the condition that the metric quantities be static, but the complex field ϕ must have a time dependent phase factor as $\phi(r,t) = \phi_0(r)e^{-i\omega t}$. The self-gravity is supported by the dispersion effect due to the wave character of the scalar field.

So far the stability is concerned, the attention is mainly focused to the stability against the radial perturbations around the equilibrium state.[4] However, the detailed study of the non-radial perturbations has not yet done. The detailed information of the emitted gravitational waves is obtained only by such a study. Moreover the gravitational wave observatories are expected to operate in near future and thus it seems very important to predict the detailed features of gravitational waves from various astrophysical sources. In this respect it seems urgent to study the non-radial pulsation of a boson star and the gravitational waves emitted from the pulsation.

As the first step we here present the formulations of the non-radial pulsation of a boson star in the framework of general relativity. The problems of the non-radial pulsations of general relativistic stellar model were studied by Thorne and his coworkers.[6] Here we follow them and the work done by one of us.[7] The perturbations are analyzed in terms of the spherical tensor harmonics and are decomposed into odd and even parity modes.[8] The formulation of the odd parity perturbation for the boson star goes almost the same as that in the perfect fluid star. The difference appears in the treatment of the even parity perturbations.[9]

2. Equilibrium configurations of the boson star

We first review an equilibrium configuration of a boson star. The static and spherical symmetric metric which describes the geometry of an equilibrium boson star can be written as

$$ds^2 = -e^{\nu}dt^2 + e^{\lambda}dr^2 + r^2(d\theta^2 + \sin^2\theta d\varphi^2) \ . \tag{2.1}$$

In this paper, we use the following units.

$$c = \hbar = 1 \ .$$

We take the following self-interacting complex scalar field coupled with Einstein gravity as our model.

$$L = \sqrt{-g}\left(-g^{\mu\nu}\phi^*_{;\mu}\phi_{;\nu} - m^2|\phi|^2 - \frac{\lambda}{4}|\phi|^4\right) \ . \tag{2.2}$$

Then the stress-energy tensor and the scalar field equation are given by

$$T_{\mu\nu} = \phi^*_{,\mu}\phi_{,\nu} + \phi^*_{,\nu}\phi_{,\mu} - g_{\mu\nu}\left[g^{\alpha\beta}\phi^*_{,\alpha}\phi_{,\beta} + m^2|\phi|^2 + \frac{\lambda}{4}|\phi|^4\right] \ , \tag{2.3}$$

and

$$g^{\mu\nu}\phi_{;\mu\nu} - m^2\phi - \frac{\lambda}{2}|\phi|^2\phi = 0 \ . \tag{2.4}$$

As the quilibrium configuration we shall write the scalar field as follows

$$\phi = \phi_0(r)e^{-i\omega t} \ . \tag{2.5}$$

Note that we have anisotropic pressure, $p_r \neq p_t$, where $p_r = T_1{}^1$ and $p_t = T_2{}^2$. This is clear contrast to the perfect fluid source.

Using the above quantities the independent set of equations is chosen as follows

$$\frac{1}{r^2}\left(re^{-\lambda}\right)' - \frac{1}{r^2} = -8\pi G\rho \ , \tag{2.6}$$

$$e^{-\lambda}\left(\frac{\nu'}{r} + \frac{1}{r^2}\right) - \frac{1}{r^2} = 8\pi G p_r \ , \tag{2.7}$$

$$\phi_0'' + \left(\frac{2}{r} + \frac{\nu' - \lambda'}{2}\right)\phi_0' - e^{\lambda}\left(m^2 - e^{-\nu}\omega^2 + \frac{\lambda}{2}\phi_0^2\right)\phi_0 = 0 \ , \tag{2.8}$$

where $\rho = -T_0{}^0$.

It is convenient to introduce the mass function $M(r)$ as follows

$$e^{-\lambda} = 1 - \frac{2GM(r)}{r} , \tag{2.9}$$

where G is the Newton's gravitational constant.

These equations are numerically integrated under the following boundary conditions;

$$\lambda(r=0) = 0,\ \phi(r=0) = \phi(0),\ \phi'(r=0) = 0,\ \phi(\infty) = 0 . \tag{2.10}$$

The equilibrium configuration is obtained only when $\omega^2 e^{-\nu(r=0)}$ takes a particular value. Numerical calculation is straightforward and we shall not show any detail here.

The total mass M is mathematically defined as follows

$$M = 4\pi \int_0^\infty \rho r^2 dr . \tag{2.11}$$

For large r, the metric should coincide with the Schwarzschild metric of the mass defined by $M \equiv M(\infty)$.

$$e^{\nu} = e^{-\lambda} = 1 - \frac{2GM}{r} . \tag{2.12}$$

$\nu(r=0)$ is determined by this relation.

3. Perturbations

The perturbations of static spherical symmetric stars are decomposed by the tensor harmonics for the angular variables θ, φ and the Fourier components for the time variable t. Thus the normal modes are characterized by harmonics index l,m, parity and frequency σ. The metric perturbations in the Regge-Wheeler gauge[10] are given by

$$ds^2 = ds_0^2 + ds_{odd}^2 + ds_{even}^2 , \tag{3.1}$$

$$ds_{odd}^2 = 2h_0 \left(-\frac{1}{\sin\theta} Y_{lm,\varphi} dt d\theta + \sin\theta Y_{lm,\theta} dt d\varphi \right) e^{-i\sigma t}$$

$$+2h_1\left(-\frac{1}{\sin\theta}Y_{lm,\varphi}drd\theta+\sin\theta Y_{lm,\theta}drd\varphi\right)e^{-i\sigma t}\ , \tag{3.2}$$

$$\begin{aligned} ds^2_{even} =& e^{\nu}H_0Y_{lm}e^{-i\sigma t}dt^2-2i\sigma rH_1Y_{lm}e^{-i\sigma t}dtdr+e^{\lambda}H_2Y_{lm}e^{-i\sigma t}dr^2 \\ &+r^2KY_{lm}e^{-i\sigma t}(d\theta^2+\sin^2\theta d\varphi^2)\ , \end{aligned} \tag{3.3}$$

where ds^2_0, ds^2_{odd} and ds^2_{even} correspond to the unperturbed metric, the perturbed metric of "odd parity" and that of "even parity", respectively. The coefficients h_0, h_1, H_0, H_1, H_2 and K are functions of only the radial coordinate r. Here $Y_{lm}(\theta,\varphi)$ is the usual spherical harmonics.

The perturbation of the scalar field has only "even parity" mode which we take the following form;

$$\delta\phi=\phi_0e^{-i\omega t}\{\phi_1(r)+i(-i\sigma\phi_2(r))\}e^{-i\sigma t}Y_{lm}\ , \tag{3.4}$$

$$\delta\phi^*=\phi_0e^{i\omega t}\{\phi_1(r)-i(-i\sigma\phi_2(r))\}e^{-i\sigma t}Y_{lm}\ , \tag{3.5}$$

where ϕ_1 and ϕ_2 are functions of only r.

The above expressions are used to calculate the perturbed Einstein equations;

$$\delta G_{\mu\nu}=8\pi G\delta T_{\mu\nu}\ . \tag{3.6}$$

The perturbation for $T_{\mu\nu}$ is given by

$$\delta T_{\mu\nu}=\delta\phi^*_{,\mu}\phi_{,\nu}+\phi^*_{,\mu}\delta\phi_{,\nu}+\delta\phi^*_{,\nu}\phi_{,\mu}+\phi^*_{,\nu}\delta\phi_{,\mu}+g_{\mu\nu}\delta p_t+h_{\mu\nu}p_t\ , \tag{3.7}$$

where $g_{\mu\nu}$ is the unperturbed metric, $h_{\mu\nu}$ is the perturbed metric and p_t is the unperturbed tangential pressure. By equating each coefficients of the same type of the tensor harmonics in both hand side of (3.6), we obtain the perturbation equations for odd and even parity modes.

1. Perturbation equations for odd parity modes

Since the perturbation of the scalar field may not be expressed by the harmonics with odd parity, we have $\delta\phi = 0$. Following the usual treatment, we introduce a new variable X by

$$h_1 = e^{\frac{1}{2}(\lambda-\nu)}(rX) \ , \tag{3.8}$$

$$h_0 = \frac{i}{\sigma}e^{\frac{1}{2}(\nu-\lambda)}\frac{d}{dr}(rX) \ . \tag{3.9}$$

Then the perturbed equations (3.6) reduces to the following second-order equation for X,

$$\begin{aligned} &e^{\frac{1}{2}(\nu-\lambda)}\frac{d}{dr}\left(e^{\frac{1}{2}(\nu-\lambda)}\frac{d}{dr}X\right) \\ &\quad + \left[\sigma^2 - e^{\nu}\left\{\frac{l(l+1)}{r^2} - \frac{6GM}{r^3} - 4\pi G(p_r - \rho)\right\}\right]X = 0. \end{aligned} \tag{3.10}$$

This equation is our basic equation for odd parity modes. It shows that the perturbations for odd parity modes do not couple to gravitational wave. This is the same as the stellar pulsation of perfect fluid.[6] Thus it expresses the propagation of the gravitational wave through the star. Eq.(3.10) reduces to the Regge-Wheeler equation if the background is the Schwarzschild metric in which $p_r = \rho = 0$, $e^{\nu} = e^{-\lambda} = 1 - 2GM/r$.

2. Perturbation equations for even parity modes

Now we turn to more interesting situation where the perturbations couple to the gravitational degrees of freedom. Namely we consider the even parity perturbations.

It is straightforward to calculate each component of the perturbed Einstein equation (3.6). We follow the procedure taken in the case of perfect fluid star[7] as close as possible and obtain the following set of equations for our basic equations in even parity case.

$$H_0{}' = K' - 2G\frac{e^{\lambda}}{r^2}(4\pi p_r r^3 + M)H_0 - \sigma^2 r e^{-\nu}H_1 + 4F'\phi_1 \ , \tag{3.11}$$

$$H_1{}' = \frac{e^{\lambda}}{r}K + \frac{e^{\lambda}}{r}H_0 + r\left\{4\pi G(\rho - p_r) - \frac{1}{r^2}\right\}e^{\lambda}H_1 - 8\frac{\omega}{r}Fe^{\lambda}\phi_2 \ , \tag{3.12}$$

$$\phi_1{}' = -\frac{\sigma^2 e^{-\nu}}{2F'}(4\omega F e^{\lambda}\phi_2 - e^{\lambda}K + H_1) + G\frac{(4\pi p_r r^3 + M)e^{\lambda}}{2F'r^2}K'$$

$$- \frac{e^{\lambda}}{4F'r^2}\{l(l+1)-2\}K - \frac{e^{\lambda}}{4F'r^3}\{8\pi G(\rho+2p_t-p_r)r^3 - l(l+1)r + 2re^{-\lambda}\}H_0 - \frac{2}{F'r}\left\{F' + 4\pi G e^{\lambda} r(p_r - \frac{\lambda}{4}{\phi_0}^4)\right\}\phi_1 \ , \tag{3.13}$$

$$\begin{aligned}{\phi_2}' =& \frac{1}{4\omega F}K' - \frac{e^{\lambda}}{4\omega r^2 F}(4\pi G p_r r^3 + 3GM - r)K - \frac{1}{4\omega r F}H_0 \\ &+ \frac{1}{8\omega r F}\left\{16\pi G r^2(\rho+p_t) - l(l+1)\right\}H_1 + \frac{F'}{2\omega F}\phi_1 \ ,\end{aligned} \tag{3.14}$$

$$\begin{aligned}K'' =& -\sigma^2 e^{\lambda-\nu}K + \frac{e^{\lambda}}{r^2}\left\{4\pi G(\rho-p_r)r^3 - 2r + 2GM\right\}K' \\ &+ \{l(l+1)-2\}\frac{e^{\lambda}}{r^2}K - \frac{2}{r^2}\{4\pi G(\rho+p_r)r^2 e^{\lambda} - 1\}H_0 \\ &+ \frac{4}{r}\left\{2F' - 4\pi G r e^{\lambda}(\rho - p_r + \frac{\lambda}{2}{\phi_0}^4)\right\}\phi_1 \ ,\end{aligned} \tag{3.15}$$

where $F \equiv 4\pi G{\phi_0}^2$ and we have used the following relation obtained from the 2-3 component of the unperturbed Einstein equations; $H_0 = H_2$.

The above equations are the sixth-order system of differential equations.[9] This is clear contrast to the case of perfect fluid in which basic equations reduce to fourth-order system of equations. The reason for the difference would be that both real and imaginary part of the perturbed scalar field are dynamical degrees of freedom of the material source. It is simple matter to show that the above equations reduce to the Zerilli equation if the background is the Schwarzschild metric in which $p_r = \rho = 0$, $e^{\nu} = e^{-\lambda} = 1 - 2GM/r$.[11]

3. Boundary conditions of even parity modes

These perturbed functions have two independent solutions near the center, due to the regularity condition of the center.

It may be shown that the background configuration ϕ_0 behaves the following way near infinity;

$$\phi_0 \propto e^{-\kappa r} \to 0 \ , \ as \ r \to \infty \ ,$$

where $\kappa = \sqrt{1-\omega^2}$.

The functions will then take the following forms at infinity,

$$(H_0,\ H_1,\ K) \sim A_{\pm} exp(\pm i\sigma r), \tag{3.16}$$

$$(\phi_1,\ \phi_2) \sim \begin{cases} B_{\pm} exp(\pm \kappa_1 r) \\ C_{\pm} exp(\pm \kappa_2 r) \end{cases}, \tag{3.17}$$

where ${\kappa_1}^2 = 1 - (\sigma - \omega)^2$, ${\kappa_2}^2 = 1 - (\sigma + \omega)^2$.

ϕ_1 and ϕ_2 have the following behaviors for three possible ranges of σ at infinity. (Here we have restricted the range of σ to the positive value.)

i) $0 < \sigma < 1 - \omega$

All solutions of perturbed scalar fields behave exponentially. The solutions corresponding to B_+ and C_+ are physically unacceptable, therefore $B_+ = 0$ and $C_+ = 0$.

ii) $1 - \omega < \sigma < 1 + \omega$

Two out of the four independent solutions will behave exponentially and the others will have wave-like behavior. The solution corresponding to B_+ is unacceptable, therefore $B_+ = 0$.

iii) $\sigma > 1 + \omega$

All solutions will have wave-like behavior.

4. Conclusion

As the first step for the study of non-radial pulsation of a boson star and of its associated gravitational waves, we formulated the linearized perturbation around an equilibrium boson star in terms of spherical tensor harmonics. We wrote down the basic perturbation equations for odd and even parity mode.

The perturbations with odd parity mode do not couple to gravitational waves in the Schwarzschild and perfect fluid star backgrounds. This is also the case in our situation since the perturbations of the scalar field may be expressed only by the spherical harmonics of even parity, thus it cannot change the star's density or pressure distributions. In this sense the odd parity mode is trivial.

On the other hand the even parity perturbations do couple with the gravitational waves. We obtained the perturbation equations for even parity which become sixth-order system of differential equations, while they are fourth-order system of differential equations in the perfect fluid star. The difference comes from the fact that the derivatives of both ϕ_1 and ϕ_2 appear in the perturbation of the stress-energy tensor of the scalar field. Thus both fields are the dynamical degrees of freedom for the material source.

In the future we shall use the derived set of equations to calculate numerically the gravitational waves emitted by the boson star and its quasi-normal modes. It should be interesting to see how they are different from that of the perfect fluid star[6][12][13] and black hole.[14][15]

Then in analogy with the quantum mechanical problem we will be able to calculate coefficients of superposition of solutions for all σ at infinity; $A_\pm$, $B_\pm$, $C_\pm$, once the boundary conditions specified. Therefore we will consider the scattering of gravitational radiation by a boson star in similar way done by Vishveshwara for a Schwarzschild black hole.[16] (for $0 < \sigma < 1 - \omega$)

Since the boson star does not have a surface, which is clear difference to the ordinary stars, this system of differential equations have a scalar wave solutions at infinity (for $\sigma > 1 - \omega$). Thus we may also have the following possibility. A scalar wave coming from spatial infinity (the incoming scalar wave) is reflected by the boson star and there is no incoming gravitational wave, thus we will have the outgoing gravitational and the outgoing scalar wave. There will be also the case where an incoming gravitational wave is scattered by the boson star and there is no incoming scalar wave.

We hope to investigate these posibility in detail near future.

REFERENCES

1. K. Sato, Mon. Not. R. Astron. Soc. **195** (1981), 467; Phys. Lett. **99B** (1981), 66; A. H. Guth, Phys. Rev. **D 23** (1981), 347.
2. R. Ruffini and S. Bonazzola, Phys. Rev. **187** (1967), 1767.
3. M. Colpi, S. L. Shapiro and I. Wasserman, Phys. Rev. Lett. **57** (1986), 2485.
4. M. Gleiser, Phys. Rev. **D38** (1988), 2376; M. Gleiser and R. Watkins, Nucl. Phys. **B319** (1989), 733.
5. J. J. van der Bij and M.Gleiser, Phys. Lett. **B194** (1987), 482; Ph. Jetzer and J. J. van der Bij, Phys. Lett. **B227** (1989), 341.
6. K. S. Thorne and A. Campolattaro, Astrophys. J. **149** (1967), 591; R. Price and K. S. Thorne, Astrophys. J. **155** (1969), 163; K. S. Thorne, Astrophys. J. **158** (1969), 1; J. R. Ipser and K. S. Thorne, Astrophys. J. **181** (1973), 181.
7. Y. Kojima, Prog. Theor. Phys. **77** (1987), 297; T. Nakamura, K. Oohara and Y. Kojima, Prog. Theor. Phys. Suppl. 90 (1987).
8. F. J. Zerilli, Phys. Rev. **D2** (1970), 2141.
9. Y. Kojima, S. Yoshida and T. Futamase, Prog. Theor. Phys. **86** (1991), 401.
10. T. Regge and J. A. Wheeler, Phys. Rev. **108** (1957), 1063.
11. F. J. Zerilli, Phys. Rev. Lett. **24** (1970), 737.
12. L. Lindblom and S. Detweiler, Astrophys. J. Suppl. **53** (1983), 73; S. Detweiler and L. Lindblom, Astrophys. J. **292** (1985), 12.
13. S. Chandrasekhar and V. Ferrari, Proc. R. Soc. London **A432** (1991), 247; ibid., **A433** (1991), 423.
14. S. Chandrasekhar and S. Detweiler, Proc. R. Soc. London **A344** (1975), 441; S. Detweiler, Astrophys. J. **239** (1980), 292.
15. E. W. Leaver, Proc. R. Soc. London **A 402** (1985), 285; J. Math. Phys. **27** (1986), 1238.
16. C. V. Vishveshwara, Nature **227** (1970), 936.

Curvature-Driven Perturbations in Inhomogeneous Cosmological Models

KENJI TOMITA

Uji Research Center
Yukawa Institute for Theoretical Physics
Kyoto University, Uji 611, Japan

ABSTRACT

So far the behaviors of inhomogeneities in the Universe have been described using an approximate model consisting of a homogeneous model plus its linear perturbations. Here we treat the nonlinear inhomogeneities driven by the irregular spatial curvature, which are independent of the usual adiabatic linear perturbations. They have the growth factor being a square of that of the adiabatic perturbations, so that they will have interesting influences upon the problem of structure formation, if they are dominant.

1. Introduction

To describe the inhomogeneities in the Universe, we use usually the linear perturbation theory in which the first-order density perturbations are associated with the first-order spatial curvatures. It habeen fully studied and they can be easily treated. However their amplitudes necessary for structure formation are confronted with the difficult problems such as severe upper limit of temperature anisotropy of CBR, while high redshift quasars and galaxies are often found on the other hand.

Here we consider another type of perturbations driven by the irregular spatial curvatures, which may appear owing to general-relativistic nonlinearity in the early stage of the Universe. First we show them in the anti-Newtonian formulation, which will be explained in §2, and find the behaviors of the density perturbations in the gauge-invariant treatment in §3. There we show that they appear also in the exact inhomogeneous cosmological models. The characteristic behavior of this curvature-driven density perturbations is that the growth factor is a square of that of the usual adiabatic perturbations, so that they will have interesting influences upon the problem of structure formation, if they are dominant.

2. Anti-Newtonian Approximation

In the synchronous coordinate condition we can express the line-element as

$$ds^2 = -dt^2 + \gamma_{ij}dx^i dx^j, \tag{2.1}$$

and the Einstein equations for perfect fluid are expressed as

$$\frac{1}{2}\dot{\kappa}^i_i + \frac{1}{4}\kappa^j_i\kappa^i_j = -\frac{1}{2}(\epsilon + 3p) - (\epsilon + p)[(u^0)^2 - 1], \tag{2.2}$$

$$\kappa^j_{j;i} - \kappa^j_{i;j} = 2(\epsilon + p)u^0 u_i, \tag{2.3}$$

$$2P^j_i + \frac{1}{\sqrt{\gamma}}(\sqrt{\gamma}\kappa^j_i)^{\cdot} = 2(\epsilon + p)u_i u^j + \delta^j_i(\epsilon - p), \tag{2.4}$$

where the units $c = 8\pi G = 1$ are used, P^j_i are components of the Ricci tensor in

the three-dimensional space with metric $dl^2 = \gamma_{ij}dx^i dx^j$, κ_i^j is defined by $\gamma^{jl}\dot{\gamma}_{li}$, a dot denotes the derivative with respect to t, γ is the determinant $|\gamma_{ij}|$, and the four velocity $u^\mu(\mu = 0-3)$ satisfies $u_\mu u^\mu = -(u^0)^2[1 - \Sigma_{i=1}^3 (u^i)^2/(u^0)^2] = -1$.

Now approximate inhomogeneous cosmological models are derived using the anti-Newtonian approximation. This approximation consists of the following two steps:

(1) The Einstein equations are solved neglecting the spatial curvature P_i^j (compared with the terms $\approx 1/(ct)^2$) and the squares of the spatial components of the four velocity (compared with unity).

(2) The solutions of first-order with respect to the spatial curvature are derived.

It holds at the early stages of the cosmic evolution, such that main inhomogeneities have curvature radii larger than the horizon size.

In the first step the inhomogeneous models are derived, which start with the generalized Kasner models and evolve to the isotropic Friedmann models. Here it is to be noticed that P_i^j are expressed by the use of the generalized Christoffel symbols corresponding to the above inhomogeneous models and $P_{ij}(= g_{jl}P_i^l)$ change slowly with time, so that they may be nearly constant at the isotropized stage. In the second step the various perturbations caused by the spatial curvature are derived. Their details are shown in Ref. 1[1] (see also the previous papers[2] [3] [4] [5]).

3. Density perturbations in the gauge-invariant treatment

In this section we assume that the Universe has already been isotropized sufficiently and derive the density perturbations in the second step. In order to derive them unambiguously, we shall treat the perturbations in the gauge-invariant form.[6] [7] Then P_i^j play a role of the source terms and are included into the components (T_{ci}^j) of the energy-momentum tensor, like

$$P_i^j = T_{ci}^j - \delta_i^j T_{cl}^l \tag{3.1}$$

or

$$T_{c_i}^{j} = \delta_i^j \Pi_\eta + \Pi_{T_i}^{j}, \tag{3.2}$$

where Π_η and $\Pi_{T_i}^{j}$ are the trace and traceless parts defined by

$$\Pi_\eta \equiv \frac{1}{6} P_l^l, \tag{3.3}$$

$$\Pi_{T_i}^{j} \equiv -P_i^j + \frac{1}{3}\delta_i^j P_l^l, \tag{3.4}$$

where $\Pi_{T_i}^{j}$ are divided into the non-transverse part and the transverse part in the following.

If we put attention only to density perturbations (non-transverse part) in flat space, these are expanded as

$$\Pi_\eta = \int \pi_\eta Q d\mathbf{k}, \tag{3.5}$$

$$\Pi_{T_i}^{j} = \int \pi_{T(0)} Q_i^j d\mathbf{k}, \tag{3.6}$$

where $Q = \exp(i\mathbf{kx})$, $Q_i^j = (k_i k^j/k^2 - \frac{1}{3}\delta_i^j)Q$ and $k^2 = \Sigma_{l=1}^{3}(k^l)^2$. They play similar roles to the isothermal and anisotropic stress appearing in Bardeen's paper.[6] By use of his formulas the equation for the gauge-invariant density perturbations Δ is given by

$$(\epsilon a^3\Delta)'' + (1 + 3(c_s)^2)(a'/a)(\epsilon a^3\Delta)' + [k^2(c_s)^2 - \frac{1}{2}(\epsilon + p)a^2](\epsilon a^3\Delta)$$

$$= k^2 a^3(\frac{2}{3}\pi_{T(0)} - \pi_\eta) + 2(w - {c_s}^2)(\epsilon a^3)(a^2\pi_{T(0)}) - 2a'(a^2\pi_{T(0)})', \tag{3.7}$$

where primes denote derivatives with respect to the conformal time τ defined by $dt = ad\tau$ and it should be noticed that the definition of $\pi_{T(0)}$ and π_η is different from Bardeen's one by the factor of the background pressure. For the gauge-invariant velocity perturbations v_s we have

$$(\epsilon + p)a^3 k v_s = -(\epsilon a^3\Delta)' - 2a^2 a' \pi_{T(0)}. \tag{3.8}$$

After we get Δ solving Eq.(3.7), we can derive v_s from Eq.(3.8).

In the case when $w = {c_s}^2$ is constant and $a \propto \tau^\beta (\beta \equiv 2/(3w+1))$, Eq.(3.7) is simplified and the special solution (Δ_1) representing a component proper to the curvature inhomogeneity is uniquely expressed in terms of the spherical Bessel function j_β and the spherical Neumann function n_β as follows:

$$\Delta_1 = c_s(k\tau)^{2-\beta} \int_0^{k\tau} dy y^\beta \epsilon^{-1} \{(\pi_\eta - \frac{2}{3}\pi_{T(0)})[j_\beta(c_s k\tau) n_\beta(c_s y) - n_\beta(c_s k\tau) j_\beta(c_s y)], \tag{3.9}$$

where we used the relation $(a^2\pi_{T(0)})' = 0$ coming from $\pi_{T(0)} \propto P_i^j \propto a^{-2}$. This Δ_1 gives the perturbation proper to the spatial curvature inhomogeneity. For $c_s k\tau << 1$, we obtain

$$\Delta_1 \simeq (1+2\beta)^{-1}(k\tau)^2 \int_0^{k\tau} dy y^{-1} \epsilon^{-1} [\frac{2}{3}\frac{\beta+1}{2\beta-1}\pi_{T(0)} - \pi_\eta]$$

$$+(2\beta+1)^{-1}(k\tau)^{1-2\beta} \int_0^{k\tau} dy y^{2\beta} \epsilon^{-1} [-2\beta(2\beta+1)y^{-2}\pi_{T(0)} + \pi_\eta].$$

If we neglect the second term (for the decaying mode) from Δ_1 and add the terms with *const* representing homogeneous solutions for comparison, the solution is expressed as

$$\Delta \simeq (1+2\beta)^{-1}(k\tau)^2 \{ \int_0^{k\tau} dy y^{-1} \epsilon^{-1} [\frac{2}{3}\frac{\beta+1}{2\beta-1}\pi_{T(0)} - \pi_\eta] + const\}. \tag{3.10}$$

The first term (for the growing mode) in the right-hand side is of the order of $(k\tau)^2[(\pi_{T(0)} - \pi_\eta)/\epsilon + const]$. For v_s we get from Eq.(3.8)

$$v_s = -\frac{3}{2}\frac{\beta}{\beta+1}(\epsilon a^3)^{-1}\frac{d(\epsilon a^3 \Delta)}{d(k\tau)} - \frac{3\beta^2}{\beta+1}\frac{\pi_{T(0)}}{k\tau\epsilon}. \tag{3.11}$$

In this expression, the first and second terms are of the order of $k\tau[(\pi_{T(0)} - \pi_\eta)/\epsilon + const]$ and $\pi_{T(0)}/(k\tau\epsilon)$, respectively.

Let us express π_η and $\pi_{T(0)}$ as $\pi_\eta = \zeta_\eta (k/a)^2$ and $\pi_{T(0)} = \zeta_T (k/a)^2$, where ζ_η and ζ_T are constant dimensionless normalization factors. Since $\epsilon(a\tau)^2 = 3\beta^2$, we obtain from Eq.(3.10)

$$\Delta \simeq (1+2\beta)^{-1}(k\tau)^2[\frac{1}{6}\beta^{-2}(\frac{2}{3}\frac{\beta+1}{2\beta-1}\zeta_T - \zeta_\eta)(k\tau)^2 + const] \tag{3.12}$$

and the spatial average of Δ^2 is

$$\overline{\Delta^2} \propto (k\tau)^8[\frac{1}{6}\beta^{-2}(\frac{2}{3}\frac{\beta+1}{2\beta-1}\zeta_T - \zeta_\eta) + const/(k\tau)^2]^2. \tag{3.13}$$

From the velocity we obtain from Eq.(3.11)

$$v_s = -3\beta(\beta+1)^{-1}(1+2\beta)^{-1}k\tau[\frac{1}{3}\beta^{-2}(\frac{2}{3}\frac{\beta+1}{2\beta-1}\zeta_T - \zeta_\eta)(k\tau)^2 + const] - \frac{\zeta_T k\tau}{\beta+1}. \tag{3.14}$$

In Ref. 2[8] the density perturbations in inhomogeneous models were analyzed using the exact solutions with plane symmetry and spherical symmetry. In a situation where the spatial curvature radii are larger than the horizon size, it was found that they consist of homogeneous perturbations ($\propto \tau^2$) and curvature driven perturbations ($\propto \tau^4$), and that the latter can be regarded as part of the second-order nonlinear perturbations. This curvature driven perturbations are consistent with the above perturbations caused by the spatial curvature inhomogeneity.

Now let us assume simply that the distribution of irregularities are so random that the occurrence of the irregularities with different k has the same probability at the same interval dk/k. Then we obtain the $n = 5$ spectrum from the term $\propto (k\tau)^8$. Of course this spectrum is not unique and the spectra with other powers can be considered. It is regarded as a representative one, which corresponds to the Harrison-Zeldovich spectrum, because the amplitudes are the same at the horizon crossing time for all k. Here it should be noticed that Δ is proportional to $(k\tau)^4$ rather than $(k\tau)^2$. From the second term in Eq.(3.13) we may have the $n = 1$ and 2 spectra because of the terms $\propto (k\tau)^4$ and $(k\tau)^6$, if *const* in Eq.(3.12) has no dependence on k.

4. Concluding remarks

In this report we showed compactly the derivation of curvature-driven density perturbations, which grow with the growth factor equal to a square of that of usual adiabatic density perturbations. It is expected that the temperature anisotropy of CBR brought by the curvature-driven perturbations are comparatively smaller, when they are normalized in appropriate manner. In a separate work it is being analyzed quantitatively.

In order to treat the clustering of galaxies associated with this type of perturbations, moreover, it is important to clarify the behaviors of this perturbations from the standpoint of post-Newtonian formalism. The general-relativistic nonlinear behaviors of the perturbations will be appear in the post-Newtonian effect in this case. This problem also will be studied in near future.

REFERENCES

1. K. Tomita, Preprint YITP/U-91-28; to be published in *Phys. Rev.* **D**(1992) .
2. K. Tomita, *Prog. Theor. Phys.* **48** (1972) 1503.
3. K. Tomita, *Prog. Theor. Phys.* **50** (1973) 1285.
4. K. Tomita, *Prog. Theor. Phys.* **54** (1975) 730.
5. K. Tomita, *Prog. Theor. Phys.* **67** (1982) 1067.
6. J.M. Bardeen, *Phys. Rev.* **D23** (1980) 1882.
7. H. Kodama and M. Sasaki, *Prog. Theor. Phys. Suppl.* **78** (1984) 1.
8. K. Tomita, Preprint YITP/U-91-49; to be published in *Astrophys. J.* (1992) .

Quantum to Classical Transition of Density Fluctuation in the Inflationary model

Yasusada Nambu
Department of Physics, Tokyo Institute of Technology
Oh-Okayama, Meguroku, Tokyo 152, Japan

January 1992

Abstract

Quantum-classical transition of density fluctuation in an inflationary model is studied. As the environment, short wave length mode of the scalar field is taken. We derived the master equation for the reduced density matrix which describes quantum mechanical time evolution of long wave fluctuation of the scalar field. We show that quantum coherence is lost and classical correlation in phase space appears. Relation to the stochastic treatment of inflation is also discussed.

1 Introduction

The structure of our universe has evolved from small inhomogeneities in the early universe. Inflation is a candidate for explaining the origin of this inhomogeneities. In this model, initial small inhomogeneities are erased out by the de-Sitter expansion in classical level. However, spontaneous quantum fluctuation of inflaton field in the de-Sitter space-time becomes the seed of the structure of our universe. In this scenario, one conceptual problem arises. How does quantum fluctuation change to "classical" fluctuation? The wave length of generated quantum density fluctuation is stretched by de-Sitter expansion and when it exceeds the horizon length, the fluctuation is expected to become "classical" because microscopic interaction is switched off outside of the horizon scale and the coherence of the system is lost.

To formulate such quantum-classical transition, the standard method is to prepare an environment which interacts with the system. Then by tracing out the freedom of the environment, we get the reduced density matrix which describe non-unitary evolution of the system. The system loses its quantum coherence by the interaction with an environment, and macroscopic classical variables appear. To say that the system is "classical", two conditions must be satisfied: the first one is the decoherence of the system. This means that quantum interference becomes negligible and the macroscopic variable appears. In other words, the off-diagonal part of the reduced density matrix becomes zero. The second condition is the establishment of classical correlation on phase space. This means

that strong correlation between canonical variables appear and classical orbit emerges on phase space.

Several authors have already discussed quantum-classical transition of density fluctuation[1]. They introduce an external scalar field which interacts with the inflaton field. Then tracing out the redundant external field, they calculate reduced density matrix. They conclude that the off-diagonal part of the reduced density matrix rapidly becomes zero when the wave length of the scalar field exceeds the Hubble horizon scale. This result implies that microscopic quantum fluctuation becomes macroscopic classical fluctuation when it crosses the Hubble horizon in the de-Sitter space.

In the stochastic approach to inflation[2], the role of the Hubble horizon is vital. The long wave mode of the scalar field is treated as classical variable and the short wave mode is replaced by stochastic noise. This approach suggests that the Hubble horizon scale is a natural boundary between quantum and classical(microscopic and macroscopic) in the inflationary model.

In this paper, we consider the problem of classicalization of quantum fluctuation without introducing the external scalar field. We identify the short wave length mode($k > aH$) of the scalar field with the freedom of an environment as suggested by stochastic approach. We derive the master equation of reduced density matrix for the long wave length mode, and investigate how quantum to classical transition occurs in the inflationary model.

The plan of the paper is as follows. In §2, we derive the master equation which describes the time evolution of the reduced density matrix. In §3, by solving the master equation, we discuss how quantum-classical transition of density fluctuation occurs. Furthermore we discuss the relation to the stochastic approach to inflation. §4 is devoted to discussion.

2 Master Equation

We use the minimally coupled scalar field on de-Sitter space. The equation of motion is

$$\ddot{\varphi} + 3H\dot{\varphi} - \frac{1}{a^2}\nabla^2\varphi + m^2\varphi = 0, \tag{1}$$

where we assume the metric is given by the spatially flat FRW form and the scale factor $a \propto \exp(Ht)$. As mentioned in the introduction, we consider the short wave length mode of the scalar field as an environment. For this purpose we start from the following projection procedure, which separates each k-mode of the scalar field to the long and the short wave length parts by using the step function:

$$\begin{aligned} \phi &= \varphi + \varphi_s, \\ \dot{\phi} &= v + v_s, \end{aligned} \tag{2}$$

where

$$\begin{aligned} \varphi_s &= \int \frac{d^3k}{(2\pi)^{3/2}}\theta(k - \epsilon aH)\phi_k e^{i\vec{k}\cdot\vec{x}}, \\ v_s &= \int \frac{d^3k}{(2\pi)^{3/2}}\theta(k - \epsilon aH)\dot{\phi}_k e^{i\vec{k}\cdot\vec{x}}. \end{aligned} \tag{3}$$

The parameter ϵ defines the scale of an environment and assumed to be smaller than unity. Then the equation of motion for the long wave mode (φ, v) becomes

$$\begin{aligned} \dot{\varphi} &= v + \sigma, \\ \dot{v} &= -3Hv + \frac{1}{a^2}\nabla^2\varphi - m^2\varphi + \tau, \end{aligned} \tag{4}$$

where

$$\begin{aligned} \tau &= \epsilon a H^2 \int \frac{d^3k}{(2\pi)^{3/2}} \delta(k - \epsilon a H)\dot{\phi}_k e^{i\vec{k}\cdot\vec{x}}, \\ \sigma &= \epsilon a H^2 \int \frac{d^3k}{(2\pi)^{3/2}} \delta(k - \epsilon a H)\phi_k e^{i\vec{k}\cdot\vec{x}}. \end{aligned} \tag{5}$$

The above projection is exact in classical level. The Hamiltonian which derives Eq.(4) is

$$H(P,Q) = \int d^3x \left[\frac{1}{2a^3}P^2 + \frac{a^3}{2}m^2Q^2 + (\sigma P - a^3\tau Q) \right]. \tag{6}$$

Here we defined the phase space variables (P,Q) as $P = a^3 v, Q = \varphi$ and the classical equation of motion becomes

$$\begin{aligned} \dot{Q} &= \frac{1}{a^3}P + \sigma, \\ \dot{P} &= -a^3 m^2 Q + a^3\tau, \end{aligned} \tag{7}$$

where we have neglected the spatial derivative term of the long wave variables. Our purpose is to quantize the above dynamical system and obtain a reduced density matrix by tracing out the freedom of short wave length mode(environment):

$$\rho = \mathrm{Tr}_E \rho_{TOT}. \tag{8}$$

We follow the method of Unruh and Zurek and use (Δ, K)-representation of reduced density matrix[5]:

$$\rho(K,\Delta) = \int dQ e^{iKQ} \rho(Q - \Delta/2, Q + \Delta/2), \tag{9}$$

where $\rho(Q - \Delta/2, Q + \Delta/2)$ is "position" representation of density matrix. In this representation, the density matrix of "position" reperesentation is diagonalized if the dispersion of Δ becomes zero, and the density matrix of "momentum" representation is diagonalized if the dispersion of K becomes zero. Then the reduced density matrix at any time can be expressed as

$$\begin{aligned} \rho(\Delta, K) &= \int dq \mathrm{Tr}\delta(Q - q) e^{iP\Delta/2} \rho e^{iP\Delta/2} \\ &= \mathrm{Tr} \exp\left(i \int d^3x (K \cdot Q + \Delta \cdot P) \right) \rho_0, \end{aligned} \tag{10}$$

where $Q(t), P(t)$ are Heisenberg operators that are the solution of Eq.(7), ρ_0 is the initial total density matrix which is product of system and the environment: $\rho_0 = \rho_{0S}\rho_{0E}$. The

symbol Tr means the trace is taken both the system and the environment. To calculate the time derivative of this quantity, we use the formula

$$\frac{d}{dt}e^{A(t)} = \int_0^1 d\lambda e^{\lambda A(t)}\dot{A}(t)e^{(1-\lambda)A(t)}. \tag{11}$$

The time derivative of the density matrix is then given by

$$\dot{\rho} = \mathrm{Tr}\rho_0 \int_0^1 d\lambda e^{i\lambda\int d^3x(K\cdot Q+\Delta\cdot P)}\left[i\int d^3x(K\cdot\dot{Q}+\Delta\cdot\dot{P})\right]e^{i(1-\lambda)\int d^3x(K\cdot Q+\Delta\cdot P)}. \tag{12}$$

Using Eq.(7),

$$K\cdot\dot{Q}+\Delta\cdot\dot{P} = \frac{1}{a^3}KP - a^3m^2\Delta\cdot Q + (K\sigma + a^3\Delta\tau). \tag{13}$$

Therefore we get the following expression by using the formula (11) again:

$$\dot{\rho} = \int d^3x\left[\frac{1}{a^3}K(x)\frac{\delta}{\delta\Delta(x)} - a^3m^2\Delta(x)\frac{\delta}{\delta K(x)}\right]\rho + D(t), \tag{14}$$

where

$$\begin{aligned} D(t) &= i\mathrm{Tr}\rho_0\int_0^1 d\lambda e^{i\lambda\int d^3x(K\cdot Q+\Delta\cdot P)} \\ &\quad\times\left[\int d^3x(K\sigma + a^3\Delta\cdot\tau)\right]e^{i(1-\lambda)\int d^3x(K\cdot Q+\Delta\cdot P)}. \end{aligned} \tag{15}$$

In Eq.(14), the first and the second term correspond to the ordinary Liouville term and the third term $D(t)$ causes the non-unitary evolution of the system. We evaluate this term in detail. To this end we calculate

$$\begin{aligned} K\cdot Q+\Delta\cdot P &= \left(K + a^3\Delta\frac{d}{dt}\right)Q - a^3\Delta\sigma \\ &= S_0(P_0,Q_0) + KF_1 + \Delta\int dua^3\tau \\ &\equiv S_0 + S_1, \end{aligned} \tag{16}$$

where we have written the solution of Eq.(7) as $Q(t) = F_0(Q_0,P_0,t) + F_1(\sigma,\tau)$ and S_0 is the contribution of the term which does not contain "noise" σ,τ and

$$F_1(t,x) = \frac{1}{3H}\int_0^t du(1-e^{-3H(t-u)})(\tau(u,x) + \frac{1}{a^3}(a^3\sigma(u,x))^{\cdot}). \tag{17}$$

Then

$$\begin{aligned} D(t) &= i\mathrm{Tr}(\rho_{0S}e^{iS_0})\mathrm{Tr}\rho_{0E}\int_0^1 d\lambda e^{i\lambda\int d^3xS_1} \\ &\quad\times\int d^3x\left(K\sigma+\Delta a^3\tau\right)e^{i(1-\lambda)\int d^3xS_1} \\ &= \rho(k,\Delta)\frac{\partial}{\partial\alpha}\ln\mathrm{Tr}\rho_{0E}\exp\left[i\int d^3x\left(S_1+\alpha(k\sigma+\Delta a^3\tau)\right)\right]\Big|_{\alpha=0}. \end{aligned} \tag{18}$$

To proceed further we use the formula

$$\mathrm{Tr}\rho_{0E}\exp(iOf) = \exp\left[-\frac{1}{2}\mathrm{Tr}\rho_{0E}(Of)^2\right], \tag{19}$$

which is valid for an arbitrary linear operator O and Gaussian density matrix ρ_{0E}. Then

$$\begin{aligned} D(t) &= \rho(k,\Delta)\frac{\partial}{\partial\alpha}\ln\exp[-\frac{1}{2}\mathrm{Tr}\rho_{0E}\{\int d^3x S_1(\sigma,\tau,t) \\ &\qquad +\alpha\int d^3x(K\sigma+\Delta a^3\tau)\}^2]\Big|_{\alpha=0} \\ &= -\rho\mathrm{Tr}\rho_{0E}\left[\int\int d^3x d^3y S_1(\sigma,\tau,t)(K\sigma+\Delta a^3\tau)\right]. \end{aligned} \tag{20}$$

Inserting the explicit form of S_1 and after some manipulation, we get

$$\begin{aligned} D(t) &= -\rho\mathrm{Tr}\rho_{0E}\Big[\int d^3x d^3y\int_0^t du\left(K\{(e^{-3Hu}-e^{-3Ht})\tau/3H+\sigma\}+\Delta a^3\tau\right) \\ &\qquad \times(K\sigma+\Delta a^3\tau)\Big] \\ &= -\rho\Big[\int_0^t du\int d^3x d^3y\{KK\langle\sigma\cdot\sigma\rangle+K\Delta\langle\sigma\cdot a^3\tau\rangle \\ &\qquad +\Delta K\langle a^3\tau\cdot\sigma\rangle+\Delta\Delta\langle a^3\tau\cdot a^3\tau\rangle\}\Big], \end{aligned} \tag{21}$$

where the symbol $\langle A\rangle$ means tracing over the environment(shot wave length mode), *i.e.*, $\mathrm{Tr}(\rho_E A)$. We can calculate the correlation function of "noise" σ, τ assuming the de-Sitter invariant vacuum state for the short wave length mode:

$$\begin{aligned} \langle\sigma_1\sigma_2\rangle &\approx \epsilon^{(2m^2/3H^2)}\frac{H^3}{4\pi^2}j_0(\epsilon aHr)\delta(t_1-t_2), \\ \langle\tau_1\tau_2\rangle &\approx \epsilon^{(2m^2/3H^2)}\left(\frac{m^2}{3H^2}+\epsilon^2\right)^2\frac{H^5}{4\pi^2}j_0(\epsilon aHr)\delta(t_1-t_2), \\ \frac{1}{2}\langle\sigma_1\tau_2+\tau_2\sigma_1\rangle &\approx -\epsilon^{(2m^2/3H^2)}\left(\frac{m^2}{3H^2}+\epsilon^2\right)\frac{H^4}{4\pi^2}j_0(\epsilon aHr)\delta(t_1-t_2), \end{aligned} \tag{22}$$

where $r=|\vec{x}_1-\vec{x}_2|$. Then the final expression of $D(t)$ to the leading order of ϵ becomes

$$\begin{aligned} D(t) &= -\frac{H^3}{8\pi^2}\epsilon^{(2m^2/3H^2)}\int d^3x d^3y j_0(\epsilon aH|\vec{x}-\vec{y}|)\left[K(x)-Ha^3(\epsilon^2+\frac{m^2}{3H^2})\Delta(x)\right] \\ &\qquad \times\left[K(y)-Ha^3(\epsilon^2+\frac{m^2}{3H^2})\Delta(y)\right]\rho(k,\Delta). \end{aligned} \tag{23}$$

Here we discuss about the value of parameter ϵ. ϵ-dependence disappears in Eq.(23) if we take the value

$$\exp(-3H^2/m^2) \ll \epsilon^2 \ll m^2/H^2. \tag{24}$$

This value nearly corresponds to the Compton wave length of the scalar field $1/m$. Taking the appropriate value of ϵ, we get the final form of the master equation which does not

contain the parameter ϵ:

$$\dot{\rho}(K,\Delta) = \int d^3x \left[\frac{1}{a^3}K(x)\frac{\delta}{\delta\Delta(x)} - a^3m^2\Delta(x)\frac{\delta}{\delta K(x)}\right]\rho$$
$$-\frac{H^3}{8\pi^2}\int d^3xd^3y j_0(\epsilon aHr)\left(K(x) - \frac{a^3m^2}{3H}\Delta(x)\right)\left(K(y) - \frac{a^3m^2}{3H}\Delta(y)\right) \quad (25)$$

3 Classicalization of Quantum Fluctuation

In this section, we discuss the behavior of quantum decoherence by solving master equation (25) for reduced density matrix. For simplicity, we consider the case of $\epsilon \to 0$ limit which means that the long wave length mode is considered to be homogeneous. We can take this limit provided that the condition (24) holds.

$$\dot{\rho}(K,\Delta) = \left(\frac{1}{a^3}K\frac{\partial}{\partial\Delta} - a^3m^2\Delta\frac{\partial}{\partial K}\right)\rho$$
$$-\frac{H^3}{8\pi^2}\left(K - \frac{m^2a^3}{3H}\Delta\right)^2\rho. \quad (26)$$

This equation can be solved by assuming Gaussian form of the density matrix

$$\rho(K,\Delta) = \exp(-\alpha(t)\Delta^2 - \gamma(t)K^2 - 2\beta(t)\Delta K), \quad (27)$$

where α, β, γ satisfies

$$\dot{\alpha} = -2a^3m^2\beta + \frac{H^3}{8\pi^2}\left(\frac{m^2a^3}{3H}\right)^2,$$
$$\dot{\gamma} = \frac{2}{a^3}\beta + \frac{H^3}{8\pi^2}, \quad (28)$$
$$\dot{\beta} = \frac{1}{a^3}\alpha - a^3m^2\gamma - \frac{H^3}{4\pi^2}\left(\frac{m^2a^3}{3H}\right). \quad (29)$$

As mentioned in the introduction, we must check the two conditions: quantum decoherence and classical correlation. To discuss the decoherence, it is convenient to use the "position" representation of density matrix

$$\rho(Q-\Delta, Q+\Delta) = \int dK e^{-iKQ}\rho(K,\Delta)$$
$$\propto \exp\left[-(\alpha - \frac{\beta^2}{\gamma})\Delta^2 + i\frac{\beta}{\gamma}\Delta Q - \frac{1}{4\gamma}Q^2\right]. \quad (30)$$

To measure the degree of decoherence, we use the ratio of the dispersion in Δ and the dispersion in Q[6]:

$$\delta_{QD} = (\alpha\gamma - \beta^2)^{-1/2}. \quad (31)$$

If this ratio becomes small, it means the off-diagonal part of the density matrix becomes small and quantum coherence is lost. Using the asymptotic solution of Eq.(28) for large

t, we can show that $\delta_{QD} \sim e^{-3Ht}$. Therefore quantum coherence of the long wave mode is rapidly lost and we can treat it as classical variable. To discuss quantum-classical transition, classical correlation in phase space is the other indicator to judge whether the system is classical. For this purpose, we use the Wigner representation of the density matrix:

$$\begin{aligned} W(P,Q) &= \int d\Delta e^{iP\Delta}\rho(Q-\Delta, Q+\Delta) \\ &\propto \exp\left[-\frac{1}{4\gamma}\frac{(\gamma P+\beta Q)^2}{\alpha\gamma-\beta^2}-\frac{1}{4\gamma}Q^2\right]. \end{aligned} \tag{32}$$

To measure the degree of classical correlation, we use the ratio of the dispersion in momentum P and the average value of P:

$$\delta_{CC} = \frac{\gamma/\beta}{\sqrt{\alpha\gamma-\beta^2}}. \tag{33}$$

Using the asymptotic solution of Eq.(28), this ratio also becomes small as $\delta_{CC} \sim e^{-3Ht}$. Therefore Q and P have strong correlation in phase space and the peak of the correlation corresponds to classical solution of the system. We can show that the peak appears at $P = -\frac{m^2}{3H}a^3Q$ and this corresponds to the slow rolling version of the classical trajectory.

Now we comment on the relation between master equation (26) and Fokker-Planck equation that appears in the stochastic treatment of inflation. We first transform the master equation (26) to the Winger representation:

$$\begin{aligned} \dot{W}(P,Q) &= \left(-\frac{P}{a^3}\frac{\partial}{\partial Q}+m^2a^3Q\frac{\partial}{\partial P}\right)W \\ &\quad +\frac{H^3}{8\pi^2}\left(\frac{\partial}{\partial Q}+\frac{m^2a^3}{3H}\frac{\partial}{\partial P}\right)^2 W. \end{aligned} \tag{34}$$

Changing the variable to $v = P/a^3$ and defining the new distribution function $P(v,Q) = a^3W(P,Q)$ to preserve normalization, we get the FP equation for $P(v,Q)$[4]:

$$\begin{aligned} \dot{P}(v,Q) &= \left(-\frac{\partial}{\partial Q}v+\frac{\partial}{\partial v}(3Hv+m^2Q)\right)P \\ &\quad +\frac{H^3}{8\pi^2}\left(\frac{\partial}{\partial Q}+\frac{m^2}{3H}\frac{\partial}{\partial v}\right)^2 P. \end{aligned} \tag{35}$$

Under the situation of "slow rolling" $v \approx -m^2Q/(3H)$, we can eliminate the velocity variable v by integrating over v and get the following equation

$$\dot{P}(Q) = \left(\frac{m^2}{3H}\frac{\partial}{\partial Q}Q+\frac{H^3}{8\pi^2}\left(\frac{\partial}{\partial Q}\right)^2\right)P. \tag{36}$$

This is nothing but the basic equation of the stochastic approach. Here realization of the slow rolling condition is equivalent to the appearance of classical correlation in phase space.

4 Discussion

In the inflationary model, the Hubble horizon is a natural scale which defines the environment. On larger distance scales, causal contact is switched off and quantum fluctuation loses its coherence. The stochastic approach is a naive application of this fact, but the relation to the usual field theoretical approach is not clear. We have derived the master equation of the reduced density matrix for the long wave length mode by treating the short wave mode as an environment. We show that the quantum coherence of the long wave mode is lost by solving the master equation. The short wave length mode acts as random noise and the long wave mode loses its coherence through the interaction with the short wave mode. At the same time, classical correlation of the long wave length mode is established. This is because the de-Sitter expansion of the universe "squeezes" the quantum state of the scalar field and the strong correlation which corresponds to classical trajectory appears on the phase space. In this sense, we can say that quantum fluctuation whose wave length is greater than the Hubble horizon becomes classical. After the establishment of classical correlation, the master equation of the long wave mode is essentially equivalent to the basic equation of the stochastic approach.

In this paper we have neglected the freedom of metric perturbations. But to understand the quantum state of the inflation correctly, it is important to include the metric fluctuation because back reaction of the scalar field to the metric becomes significant for the scale greater than Hubble horizon[3]. Furthermore it is interesting to discuss the origin of the master equation for the long wave length mode in the context of quantum cosmology. It is possible to extend our master equation to the arbitrary expansion law of the universe with metric perturbation. So we can analyze the effects of the inhomogeneiety to the classicalization of the universe. This is our future problem to be explored.

References

[1] M. Sakagami, *Prog. Theor. Phys.* **79** (1989) 443; R. Brandenberger, R. Laflamme and M. Mijic, *Mod. Phys. Lett* **5** (1990) 2311.

[2] A. A. Starobinsky, in *Fundamental Interactions*, ed. V. N. Ponomarev (MGPI press, Moscow, 1984) 54; in *Current Topics in Field Theory, Quantum Gravity, and Strings, Lecture Notes in Physics* **246**, ed. H. J. de Vega and N. Sanchez (Springer, Berlin, 1986) 107.

[3] A. S. Goncharov, A. D. Linde and V. F. Mukhanov, *Int. J. Mod. Phys.* **A2** (1987) 561.

[4] M. Sasaki, Y. Nambu and K. Nakao, *Nucl. Phys.* **B308** (1988) 868.

[5] W. G. Unruh and W. H. Zurek, *Phys. Rev.* **D40** (1989) 1071.

[6] M. Morikawa, *Phys. Rev.* **D42** (1990) 2929.

Energy Density Perturbation of Global Textures in the Expanding Universe

Michiyasu Nagasawa and Katsuhiko Sato

Department of Physics, Faculty of Sciences,
The University of Tokyo, Tokyo 113, Japan

Abstract

The properties of the evolution of global textures are studied in the expanding universe. The energy density of textures is investigated by clustering analysis. The spectrum of the energy density perturbation is found to be almost scale invariant. The evolution equation of a texture field is solved numerically and the effect of cosmic expansion is explicitly introduced.

1 Introduction

People have made many attempts to clarify the law of physics for ages. Whereas the instruments for high energy experiments cannot produce sufficiently large energy. The universe, therefore, has come to be a very useful laboratory since a standard big bang model predicts our universe must have experienced a high temperature stage. Actually the recent progress of cosmological observations unveils several remarkable features of the universe.

The idea of spontaneous symmetry breaking is essential to unified theories of elementary interactions. Above the unification energy scale, this symmetry is restored due to the high-temperature correction to the potential of a Higgs field. Standard big bang cosmology enables such a high energy density condition in the early universe. In the course of cosmic evolution, symmetries have been broken and various types of phase transitions should have occurred. Some of these phase transitions may have produced topological defects such as monopoles, cosmic strings or domain walls[1]. These defects have cosmological significance. Particularly cosmic strings can play an important role in constructing various structures in the universe, that is galaxies, clusters of galaxies and so on. Global textures are also generated at the symmetry breaking phase transition $G \longrightarrow H$, when a vacuum manifold $M \equiv G/H$ has a non-shrinkable three-sphere, that is $\pi_3(M) \neq 1$. For example, when global $SU(2)$ is broken this condition is achieved. Textures are the differential energy concentration, which is called a "knot". Unlike other low-dimensional defects, textures are topologically unstable so that they vanish liberating their energy when an event horizon extends enough. This process is called "unwinding" of knots. The spectrum of their distribution is scale-invariant if the unwinding rate of knots is constant in time[2]. Then the

energy density fluctuation caused by knot collapse can be sources of the large-scale structures of the universe. We have calculated numerically the evolution equation of a field for global textures. The result shows that this scenario can be valid.

2 Model and method

We considered the simplest global texture model, $G = O(4)$ and $H = O(3)$. In this case $\pi_3(M) = \mathbf{Z}$ and global textures are possible. We take a real scalar fourplet ϕ with a Lagrangian:

$$\mathcal{L} = \frac{1}{2}(\partial\phi)^2 - V(\phi), \quad V(\phi) = \frac{1}{4}\lambda(|\phi|^2 - v^2)^2. \tag{1}$$

The evolution equation of ϕ in a flat Robertson-Walker universe is written in the form:

$$\frac{\partial^2\phi}{\partial\tau^2} + 2\left[\frac{da}{d\tau}\right]\frac{1}{a}\frac{\partial\phi}{\partial\tau} - \nabla^2\phi = -a^2\frac{\partial V}{\partial\phi}\ , \tag{2}$$

where $a = a(t)$ is a scale factor and τ is conformal time.

When the time evolution of ϕ is followed with Eq.(2), a factor a^2 of the right-hand term prevent us from calculating for an arbitrary long period. The lattice spacing of a simulation box is of constant comoving size. On the other hand, the characteristic length scale of a texture is of constant physical size. Thus with the cosmic expansion, the spatial scale of a texture comes to be smaller than one grid length so as to break the further calculation. To avoid this difficulty, Spergel *et al.* modified the evolution equation[3]. We, however, use an original equation and follow the time evolution for several expansion times, which is enough to know the dynamical feature of global textures in the expanding universe.

A staggered leapfrog algorithm of second-order accuracy[4] was employed with Eq.(2). The equations are expressed by

$$\frac{\phi_{n+1} - \phi_n}{\Delta\tau} = \dot{\phi}_n\ , \tag{3}$$

$$\frac{\dot{\phi}_{n+1} - \dot{\phi}_n}{\Delta\tau} + 2\left[\frac{da}{d\tau}\right]\frac{1}{a}\frac{\dot{\phi}_{n+1} + \dot{\phi}_n}{2} = \nabla^2\phi_n - a^2\frac{\partial V}{\partial\phi_n}\ , \tag{4}$$

where a suffix denotes the number of time steps. Right-hand side terms of Eq.(4) at (x, y, z) are calculated by

$$\nabla^2\phi_{x,y,z} = \frac{\phi_{x+1,y,z} - 2\phi_{x,y,z} + \phi_{x-1,y,z}}{\Delta x^2} + \frac{\phi_{x,y+1,z} - 2\phi_{x,y,z} + \phi_{x,y-1,z}}{\Delta y^2} + \frac{\phi_{x,y,z+1} - 2\phi_{x,y,z} + \phi_{x,y,z-1}}{\Delta z^2}\ , \tag{5}$$

$$\left(\frac{\partial V}{\partial\phi}\right)_{x,y,z} = \lambda\phi_{av}\left(|\phi_{av}|^2 - v^2\right)\ , \tag{6}$$

$$\phi_{av} = \frac{1}{6}\left(\phi_{x+1,y,z} + \phi_{x-1,y,z} + \phi_{x,y+1,z} + \phi_{x,y-1,z} + \phi_{x,y,z+1} + \phi_{x,y,z-1}\right). \tag{7}$$

We set the lattice spacing equal to 1, that is $\Delta x = \Delta y = \Delta z = 1$ in simulations.

3 Dynamical evolution of global textures

We carried simulations on a three-dimensional cubic lattice with 50^3 grids; the values of ϕ are assigned to each lattice point. The length scale of the lattice spacing is equal to the energy scale of the phase transition *i.e.*, v. Initial values of the field are determined under the condition, $|\phi| = v$. Thus the initial time of calculations is the time when the phase transition occurs and ϕ sits on the true vacuum. Phases at each point are random because unit cells correspond to the regions whose sizes are the horizon scale over which there is no causal relation. An expansion law is that in the radiation dominated universe. Hence the scale factor depends on the conformal time such as $a(\tau) \propto \tau$. Boundary condition is periodic. At last we set $\lambda = 1$.

The energy of ϕ at (x, y, z), $E(x, y, z)$ is defined:

$$E(x, y, z) = \frac{1}{2} (\partial\phi)^2_{x,y,z} + V(\phi_{x,y,z}). \tag{8}$$

Figure 1 shows the evolution of an averaged energy over the simulation box, the maximum energy in the box and the median for all the points. As time passes, the median energy remains constant and the maximum one grows larger. This shows the points which have an great amount of energy increase, though the total energy in the simulation box is unchanged. Hence a clustering of energy is implied.

The next figures are those for the relative amplitudes of potential and differential energy to total energy or that of time-differential and space-differential energy. Figure 2 shows

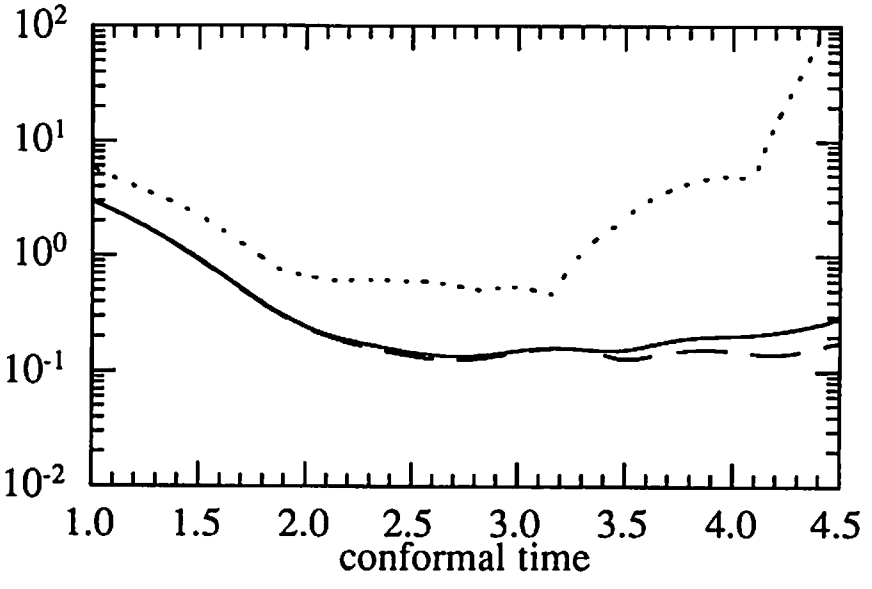

Figure 1 The evolution of energy Eq.(8). A solid line is an energy average. A dotted line is an energy maximum. A broken line is an energy median.

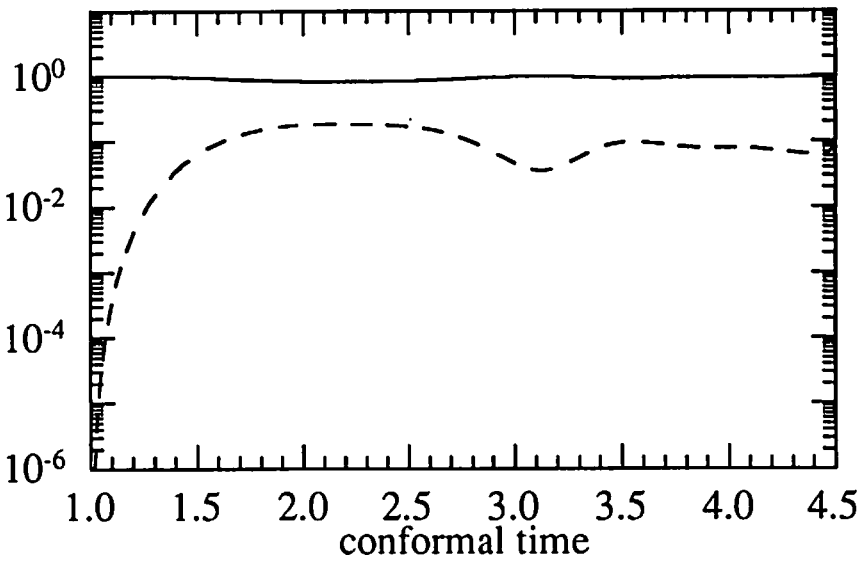

Figure 2 A solid line is the ratio of differential energy to total energy. A broken line is that of potential energy.

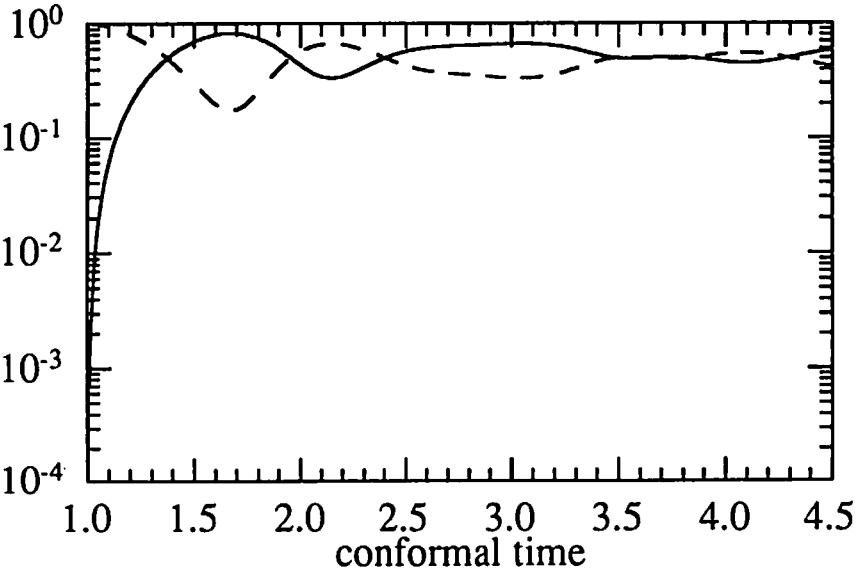

Figure 3 A solid line is the ratio of the time part of differential energy to the total differential energy. A broken line is that of spacial part.

that the differential energy is dominant. This agrees with the fact that textures are clumps of differential energy. Figure 3 indicates the collapses of knots according to the cosmic expansion should take place. The dominance of space-differential energy corresponds to the concentration of energy, *i.e.*, the knot. The increase of time-differential energy is the evidence of radical motion of ϕ, *i.e.*, the unwinding. These are repeated alternately. Thus the growth of causal horizon causes the continuous creation and collapse of knots.

4 The spectrum of energy clustering

To know more detailed properties of energy distribution, we simulated the case that the texture energy scale v is half of that in §3. This change in parameter enables us to follow the time evolution for more than twenty expansion times. For the purpose of the direct determination of a texture's position, the phases of ϕ are evaluated at each point. At all sides of each cell, it is checked if the sign of the ϕ field changes. The cells whick have the side where four components of ϕ changes their signs are counted for topological singularity. The time evolution of the number of these cells is shown in Figure 4. The decrease of texture point, *i.e.*, tha knot corresponds to the energy concentration mentioned in the previous section. After $\tau \cong 5$, the number of knots turns to be almost stable value, $10 \sim 100$. In this region, the rate of knot collapse is frozen.

For the investigation of the energy spectrum of knots, the threshold energy is defined. If the energy of a certain point is larger than the value of the threshold, this point is regarded

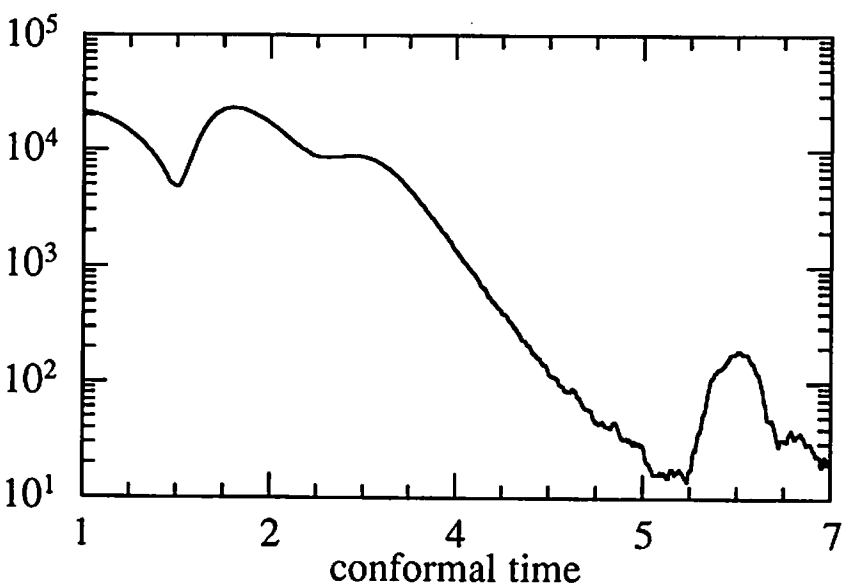

Figure 4 The evolution of the number of knots.

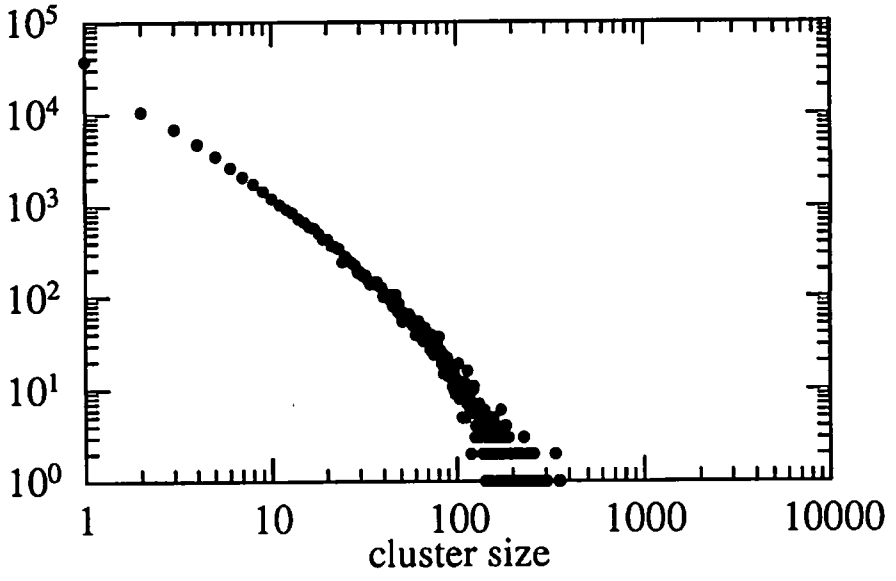

Figure 5 The size distribution of the two-dimensional cluster consisting of the points whose energy is larger than the median value. $\tau = 3.0$. The index of power fitting equals -2.2. The vertical axis is the sum over 10 simulations.

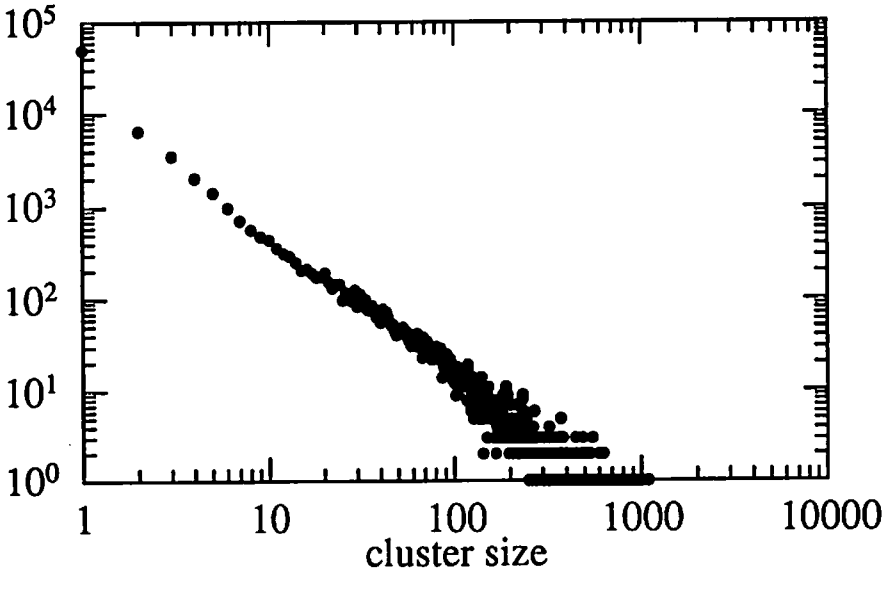

Figure 6 The same figure as Figure 5 at $\tau \cong 6.0$. The power index is -1.6.

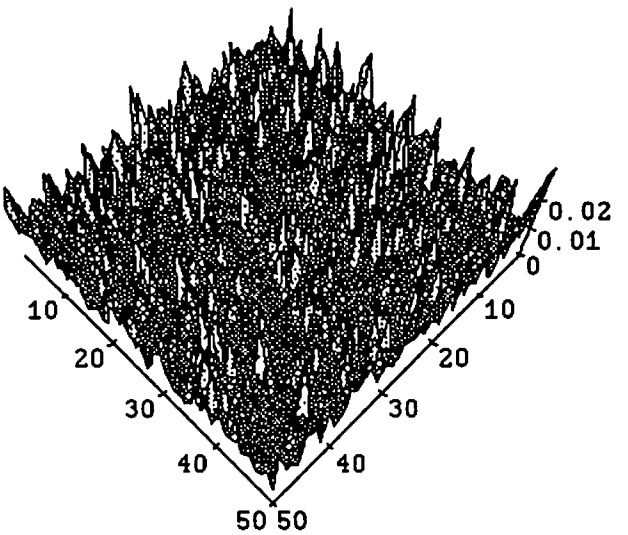

Figure 7 The spatial energy distribution of global textures at the plane $z = 25$. $\tau = 3.0$.

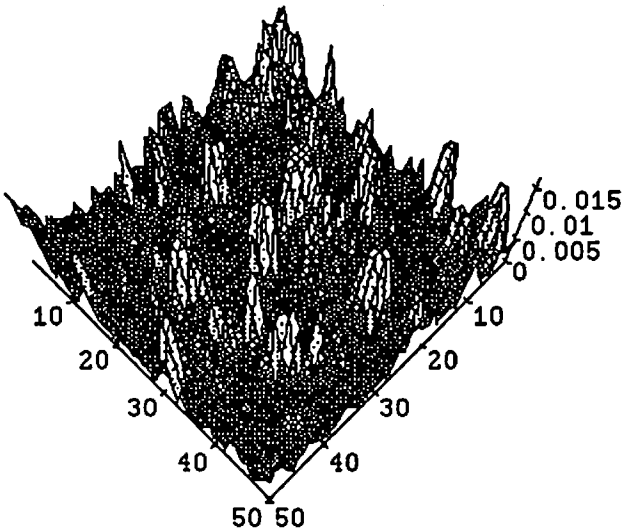

Figure 8 $\tau = 6.0$.

as a high energy point. Then the neighboring high energy points belong to the same energy cluster and the size distribution in two-dimensional plain is examined. Figure 5 and 6 describe the result when the threshold equals the median. We performed the same analysis at various time slices and have found that the power index of fitting line to the cluster

distribution become constant value after $\tau \cong 5$. This has a good agreement with the above prediction about knot collapse. Consequently energy perturbation produced by global textures is found to have a power law profile.

In addition, the decrease of the index number corresponds to the growth of energy cluster. This again implies the energy concentration process. Figure 7 and Figure 8 also confirm this interpretation. These figures show the two-dimensional spatial distribution of texture energy at $\tau = 3.0$ and $\tau = 6.0$. In the former one, the energy of ϕ distributes randomly owing to the initial condition. The figure at later time, however, indicates that clusters of energy develop. This fact agrees well with the implication of Figure 1. Hence the energy concentration is verified in this numerical simulation.

We have made sure that the above results show the true topological properties of ϕ. When the effect of time-differential energy is removed, only the spatial-differential energy of ϕ, *i.e.*, $\frac{1}{2}\nabla^2\phi$ will be left and pure topological structure should be revealed. To this end, we have introduced a dissipating term to the equation of motion. The ϕ configuration at a certain time was evolved using this equation so that the dissipated ϕ at this time was calculated. These simulations reproduced the same figure as Figure 4 about the knot number evolution. The index of power fitting also approaches constant value after $\tau \cong 5$. This is consistent with the result without the artificial dissipation.

5 Conclusion

We have calculated the time evolution of global textures in a radiation dominated universe. The distribution of differential energy depicts the creation and collapse of knots. The change of dominant energy implies the unwinding process. Thus the dynamical process of textures can be characterized by the evolution of knots. About the spectrum of knots, the energy cluster distribution of ϕ is scale invariant; the power index of the distribution comes to be constant when the knot formation process proves to be stable after a few expansion time from the phase transition. Hence global textures generate energy perturbations in various scales. They can be a seed for large-scale structures in our universe. At all events the spontaneous symmetry breaking is inevitable when the universe evolves from an unification state. The texture must be a peculiar defect and is worth further study.

References

[1] T.W.B. Kibble, J. Phys. **A9**(1976)1387.
A. Vilenkin, Phys. Rep. **121**(1985)263.

[2] N. Turok, Phys. Rev. Lett. **63**(1989)2625.

[3] D. N. Spergel, N. Turok, W. H. Press and B. S. Ryden, Phys. Rev. **D43**(1991)1038.

[4] W.H. Press, B.P. Flannery, S.A. Teukolsky and W.T. Vetterling, Numerical Recipes (Cambridge University Press, 1986)p.631

Parametric Amplification of Density Fluctuation in the Scalar Field Dominated Universe

Yasusada Nambu and Shigenobu Takayama
Department of Physics, Tokyo Institute of Technology
Oh-Okayama, Meguroku, Tokyo 152, Japan

January 1992

Abstract

We consider the density fluctuation in a non-minimally coupled scalar field dominated universe. To avoid technical difficulties, we use the conformal transformation from the non-minimal frame into the minimal one. The evolution of the density fluctuation is the same as the minimal scalar case over the Jeans scale, but its amplitude is enhanced within the Jeans scale. It is regarded as a parametric amplification caused by an oscillating Hubble parameter. We find the characteristic scale $\frac{1}{k} \sim |\xi|^{-\frac{1}{6}} \frac{1}{H_0}(\frac{H_0}{m})^{\frac{1}{3}}$ appears.

1 Introduction

The recent galaxy redshift surveys have shown the existence of the large scale structures. The observations over a hundred Mpc reveal the void structure and the deeper pencil beam survey suggests the $128h^{-1}$Mpc periodicity in the galaxy distribution, which is the largest structure as ever known. But it is difficult to explain these structures in the standard scenario of the structure formation which is based on the gravitational instability. One difficulty is that the existence of these non-linear structures causes larger CMB anisotropy than the observed one. Another one is that we do not have the idea to account for the $128h^{-1}$Mpc periodicity.

In order to explain these problems, a model with the oscillating expansion rate has been investigated[1]. This model explains the $128h^{-1}$Mpc periodicity as an apparent structure caused by the oscillation of the Hubble parameter. To realize such an oscillation, the non-minimally coupled scalar field is investigated. Owing to the coupling between the spacetime curvature and the scalar field, the Hubble parameter oscillates and the periodic structure is explained as apparent effect. But in this model the homogeneous scalar field is assumed and the real structure or the density fluctuation is not investigated. It is only suggested that the density fluctuation may be amplified by the oscillating Hubble parameter.

A minimal coupling model has been well investigated in the context of the cold dark matter scenario[2]. The time evolution of the universe and the density

fluctuation is similar to that of the dust dominated model and it can not explain the large scale structures because of the same difficulties as the standard model.

In this paper, we investigate the density fluctuation in the non-minimally coupled scalar field dominated universe. By using the conformal transformation, we avoid the technical difficulties caused by the coupling between the spacetime curvature and the scalar field. Our purpose is to understand the evolution law of the density fluctuation in this model, and discuss the real periodic structure is explained by the oscillating Hubble parameter.

2 Conformal transformation

We consider the scalar field coupled non-minimally to gravity. The action is

$$S = \int d^4x\sqrt{-g}\left[\frac{R}{2\kappa^2} - \frac{\xi}{2}\phi^2 R - \frac{1}{2}g^{ab}\partial_a\phi\partial_b\phi - \frac{1}{2}m^2\phi^2\right], \tag{1}$$

where $\kappa^2 = 8\pi G$ and ξ is the coupling constant. The special case $\xi = 0$ and $\xi = 1/6$ are called minimal and conformal coupling, respectively. We assume that the metric of the Universe can be described by a spatially homogeneous and isotropic background metric plus small fluctuation. As for the fluctuation, for convenience, we choose a Newtonian gauge. Hence the metric takes the form

$$ds^2 = -(1+2\Psi)dt^2 + a^2(t)(1+2\Phi), \tag{2}$$

where Ψ and Φ are the Newtonian potential and the intrinsic spatial curvature perturbation, respectively. The perturbed scalar field is decomposed as follows,

$$\phi(\mathbf{x},t) = \phi_0(t) + \delta\phi(\mathbf{x},t). \tag{3}$$

We would like to know the time evolution of the density fluctuation in this model, but it is difficult to solve it analytically because of the coupling. In the case of the minimal coupling, however, we can solve it analytically within suitable approximations. By using the conformal technique, we can transform the non-minimal model into the minimal one and we can deal with this model easily[3]. The transformation is as follows:

$$\begin{aligned} d\bar{s}^2 &= \Omega^2(\phi)ds^2, \\ d\bar{\phi} &= \left[1 - \xi(1-6\xi)\kappa^2\phi^2\right]^{\frac{1}{2}}\Omega^{-2}d\phi, \end{aligned} \tag{4}$$

where $\Omega^2(\phi) = 1 - \xi\kappa^2\phi^2$. Within the range of the scalar field $1 \gg \xi\kappa^2\phi^2$, we get approximately

$$\begin{aligned} \Omega &\simeq 1 \\ d\bar{\phi} &\simeq d\phi, \end{aligned} \tag{5}$$

and the action(1) reduces to

$$S \simeq \int d^4x\sqrt{-\bar{g}}\left[\frac{\bar{R}}{2\kappa^2} - \frac{1}{2}\bar{g}^{ab}\partial_a\bar{\phi}\partial_b\bar{\phi} - \frac{1}{2}m^2\bar{\phi}^2\right]. \tag{6}$$

The relations between the geometrical quantities in each frame are

$$\Omega_0 dt = d\bar{t}, \qquad \frac{\delta\Omega}{\Omega_0} + \Psi = \bar{\Psi},$$
$$\Omega_0 a = \bar{a}, \qquad \frac{\delta\Omega}{\Omega_0} + \Phi = \bar{\Phi}, \tag{7}$$

where the conformal factor Ω is decomposed as follows

$$\Omega(\phi) = \Omega_0(\phi_0) + \delta\Omega(\phi_0, \delta\phi). \tag{8}$$

3 Minimal coupling frame

In this section we summarize the case of the minimal coupling, but the bar is omitted from each quantity. The Einstein equations and the evolution equation for background quantities become

$$\left[\frac{\dot{a}}{a}\right]^2 \equiv H^2 = \frac{8\pi}{3}G\rho, \qquad \rho = \frac{1}{2}\dot{\phi_0}^2 + \frac{1}{2}m^2{\phi_0}^2,$$
$$\dot{H} = -4\pi G(\rho + p), \qquad p = \frac{1}{2}\dot{\phi_0}^2 - \frac{1}{2}m^2{\phi_0}^2, \tag{9}$$
$$\ddot{\phi_0} + 3H\dot{\phi_0} + m^2{\phi_0}^2 = 0.$$

For late time $mt \gg 1$, eq.(9) have the approximate solution which is consistent with the condition $1 \gg \xi\kappa^2\phi^2$ provided that $\xi \leq 1$:

$$\phi_0 \simeq \frac{1}{\sqrt{3\pi G}}\frac{\sin(mt + \mu)}{mt},$$
$$H \simeq \frac{2}{3t}, \tag{10}$$

where μ is an integral constant, and we put μ equal zero in the following. The time evolution of H is the same as that of the dust dominated universe.

To solve the equations for the fluctuating part, we Fourier-expand Ψ , Φ and $\delta\phi$. Then the Einstein equations for the fluctuating part are

$$3H^2\Psi - 3H\dot{\Phi} - (\frac{k}{a})^2\Phi = -4\pi G\delta\rho,$$
$$H\Psi - \dot{\Phi} = 4\pi G\dot{\phi}\delta\phi,$$
$$\Phi + \Psi = 0,$$
$$\delta\rho = \dot{\phi}\delta\dot{\phi} + m^2\phi\delta\phi - \Psi\dot{\phi}^2. \tag{11}$$

The first equation is the time-time component, the second one is the time-space component and the third one is the traceless part of the space-space component. We do not need the trace part. The evolution equation for $\delta\phi$ is

$$\delta\ddot{\phi} + 3H\delta\dot{\phi} + \left[m^2 + (\frac{k}{a})^2\right]\delta\phi = \dot{\phi}(\Psi - 3\Phi)^{\cdot} - 2m^2\phi\Psi. \tag{12}$$

Up to now we assume only $1/m \ll 1/H$ (i.e. $mt \gg 1$). Now, furthermore, we restrict our attention to the fluctuation whose wavelengths satisfy following inequalities,

$$\frac{a}{k} \gg \frac{1}{m} \quad \text{and} \quad \frac{1}{H} \gg \frac{a}{k}\,. \tag{13}$$

Under these approximations, we can write the solution of $\delta\phi$ as

$$\delta\phi \simeq \frac{1}{\sqrt{3\pi G}}\left[A(t)\sin(mt) + B(t)\cos(mt)\right], \tag{14}$$

where

$$A \simeq \frac{\delta}{2mt}, \quad B \simeq -\frac{3}{2}H(\frac{a}{k})^2\dot{\delta}. \tag{15}$$

And the evolution equation for the density fluctuation of the scalar field is

$$\ddot{\delta} + 2H\dot{\delta} + \left[\left[\frac{1}{2m}(\frac{k}{a})^2\right]^2 - \frac{3}{2}H^2\right]\delta \simeq 0, \tag{16}$$

where $\delta = \delta\rho/\rho$. Eq.(16) is a Bessel equation and the solution is given by

$$\delta \simeq a^{-\frac{1}{4}} J_{\pm\frac{2}{5}}(z), \quad z = \frac{1}{mH}(\frac{k}{a})^2 \sim a^{-\frac{1}{2}}. \tag{17}$$

The time evolution of δ is shown fig.1. From the form of $J_{\pm\frac{2}{5}}(z)$, we find the Jeans scale is given by $z \simeq 1$, that is

$$\frac{a}{k} \sim \frac{1}{\sqrt{mH}}. \tag{18}$$

Using these solutions, we readily obtain

$$\dot{\Omega}_0 \simeq -\xi\kappa^2\phi_0\dot{\phi}_0 = \frac{-4\xi}{3mt^2}\sin(2mt),$$

$$\delta\Omega \simeq -\xi\kappa^2\phi_0\delta\phi = \frac{-2\xi}{3(mt)^2}\left[[1-\cos(2mt)]\,\delta + \sin(2mt)\frac{d\delta}{dz}\right]. \tag{19}$$

4 Time evolution of density fluctuation

In order to find the time evolution of the density fluctuation in the non-minimal frame, we need the relation between each frame's quantities. We obtain the following relation by the conformal transformation:

$$\begin{aligned}\Omega^2\overline{G}^b_c = G^b_c &- 2g^{ba}\left[\partial_a\partial_c ln\Omega - \Gamma^d_{ac}\partial_d ln\Omega\right] \\ &+2\delta^a_c g^{de}\left[\partial_d\partial_e ln\Omega - \Gamma^f_{de}\partial_f ln\Omega\right] \\ &+ 2g^{ba}(\partial_a ln\Omega)\partial_c ln\Omega + \delta^b_c g^{de}(\partial_d ln\Omega)\partial_e ln\Omega,\end{aligned} \tag{20}$$

where G^b_c is the Einstein tensor.

For the background quantities, the time-time component of eq.(20) becomes

$$\overline{H} = \frac{1}{\Omega_0}\left[H + \frac{\dot{\Omega}_0}{\Omega_0}\right]. \tag{21}$$

Therefore the Hubble parameter behaves as follows,

$$H \simeq \frac{2}{3t} + \frac{4\xi}{3mt^2}\sin(2mt), \tag{22}$$

where we put $t = \bar{t}$. This solution coincides with the result of the direct calculations without the conformal technique. Using the Einstein equations, we get the relation of energy density in both frames:

$$\rho \simeq {\Omega_0}^2 \bar{\rho}\left[1 - \frac{2}{\overline{H}\Omega_0}\frac{d\Omega_0}{d\bar{t}}\right]. \tag{23}$$

For the fluctuating part, in a similar manner, we get from eq.(20)

$$\delta\rho \simeq {\Omega_0}^2\delta\bar{\rho} - \frac{{\Omega_0}^2}{\kappa^2}\left[6\overline{H}\frac{d}{d\bar{t}} + 2\frac{k^2}{\bar{a}^2}\right]\delta\Omega. \tag{24}$$

According to these relations, we get

$$\delta \simeq \left[1 + \xi\frac{\overline{H}}{m}\bar{z}[1 - \cos(2m\bar{t})]\right]\bar{\delta} + \left[6\xi\frac{\overline{H}}{m}\cos(2m\bar{t}) + \xi\frac{\overline{H}}{m}\bar{z}\sin(2m\bar{t})\right]\bar{\delta}', \tag{25}$$

where a prime denotes derivative with respect to $\bar{z}$.

We analyze eq.(25) for following two cases distinguished by z, separately. Since $t = \bar{t}$ in our approximations, the bars are omitted from the all quantities except δ in the minimal frame.

a) For $z \gg 1$(i.e. within the Jeans scale), eq.(25) becomes approximately

$$\begin{aligned}\delta &\simeq \left[1 + \xi\frac{H}{m}z[1 - \cos(2mt)]\right]\bar{\delta} + \xi\frac{H}{m}z\sin(2mt)\bar{\delta}' \\ &= \sin z + 2\xi\frac{H}{m}z\sin(mt)\cos(z - mt),\end{aligned} \tag{26}$$

where we set $\bar{\delta} = \sin z$. This solution consists of slowly oscillating part(time scale$\sim \frac{a^2}{k^2}m$) plus rapidly oscillating part($\sim m^{-1}$). If we pay attention to the time scale larger than m^{-1}, we can average the rapidly oscillating part over the time scale $\sim m^{-1}$. By integrating eq.(26) with respect to t from $-\pi/m$ to π/m, we get

$$\delta \simeq \left[1 + \xi\frac{H}{m}z\right]\bar{\delta}. \tag{27}$$

The term $\xi(H/m)z$ goes to zero as time goes on, then we can see that the amplitude of δ at $t = t_0$ is $(1 + \xi\frac{H_i}{m}z_i)^{-1}$ times greater than that of $\bar{\delta}$ if the initial amplitude at $t = t_i$ is the same. This amplification may be caused by the coherent oscillation of the expansion rate. We can regard it as a kind of parametric resonance. For $\xi < 0$, δ is enhanced and for $\xi > 0$, δ is suppressed.

b) For $z \ll 1$, eq.(25) becomes

$$\delta \simeq \bar{\delta} + 6\xi\frac{H}{m}\cos(2mt)\bar{\delta}'. \tag{28}$$

Unlike the case(a), this solution consists of the growing or decaying mode plus oscillation around it. Taking the same average as in the case (a), we get

$$\delta \simeq \bar{\delta}. \tag{29}$$

Therefore in this range of z the amplitude is not affected by the oscillation. Using these solutions, we can discuss about the spectrum of the density fluctuation at $t = t_0$. The initial value of δ at $z = z_i > 1$ is

$$|\delta_i| = \left| \left[1 + \xi \frac{H_i}{m} z_i \right] \bar{\delta}_i \right|. \tag{30}$$

The value of δ at $t = t_0$ is

$$|\delta_0| = |\bar{\delta}_0|. \tag{31}$$

Then the wave number dependence of δ_0 becomes

$$\left| \frac{\delta_0}{\delta_i} \right| = \left| \frac{3 \left[\frac{H_0}{k} \right]^4 \left[\frac{m}{H_0} \right]^2}{1 + \xi \left[\frac{H_0}{k} \right]^6 \left[\frac{m}{H_0} \right]^2 z_i^4} \right|, \tag{32}$$

and we get fig.2. The characteristic scale $1/k_m$ appears:

$$\frac{1}{k_m} \sim |\xi|^{-\frac{1}{6}} \frac{1}{H_0} \left(\frac{H_0}{m} \right)^{\frac{1}{3}}. \tag{33}$$

For this scale, the parametric amplification works effectively. We can also get this scale by the dimensional analysis. By equating the timescale of the sound velocity within the Jeans scale to that of the Hubbel oscillation, we get

$$z_i \approx m t_i. \tag{34}$$

Rewriting eq.(34) yields

$$\frac{1}{k_m} \approx \frac{1}{H_0} \left(\frac{H_0}{m} \right)^{\frac{1}{3}}, \tag{35}$$

where we have assumed ξ is $O(1)$ parameter. The larger scale than this scale is not affected by the oscillation, because the timescale of the sound velocity is shorter than that of the Hubbel oscillation.

5 Conclusion

We have investigated the time evolution of the density fluctuation in the non-minimally coupled scalar field dominated universe, under the condition $1/m \ll a/k \ll 1/H$. Averaging over the time scale m^{-1}, for $z \gg 1$, the amplitude of the fluctuation is enhanced by the factor $(1+\xi \frac{H_i}{m} z_i)^{-1}$ compared to the minimal coupling case, but for $z \ll 1$, the evolution is the same as the minimal case. This is a kind of parametric amplification caused by the oscillation of the expansion rate. With respect to the spectrum, we have found the characteristic scale $\frac{1}{k} \sim |\xi|^{-\frac{1}{6}} \frac{1}{H_0} (\frac{H_0}{m})^{\frac{1}{3}}$ appears. The larger scale than this scale is not affected by the oscillation. If we put m^{-1} equal $128h^{-1}$Mpc, it yields $1/k_m \sim$ 1000Mpc. It is larger than the observed scale. For this scale eq.(27) reduces to $\delta \sim (1 + \xi)\bar{\delta}$.

The amplification factor $(1+\xi \frac{H_i}{m} z_i)^{-1}$ is not large enough to explain the structure formation problems. But it is important that the density fluctuation can grow within the Jeans scale by the parametric amplification. This is completely different from the gravitational instability. In the range of our treatment (i.e. $1/m \ll a/k \ll 1/H$), this factor is not large. But if we give attention to other ranges for which this factor is large (for example in the early universe), this mechanism may play an important role, and we may be able to explain the characteristic scale of the large scale structures. This is our future problem.

References

[1] M. Morikawa, *Ap. J. (Letters)* **362** (1990) L37.

[2] Y. Nambu and M. Sasaki, *Phys. Rev.* **D 42** (1990) 3918.

[3] T. Futamase and K. Maeda, *Phys. Rev.* **D 39** (1989) 399.

[4] H. Kodama and M. Sasaki, *Prog. Theor. Phys. Suppl.* **No.78** (1984) 1.

[5] N. Makino and M. Sasaki, *Prog. Theor. Phys.* **86** (1991) 103.

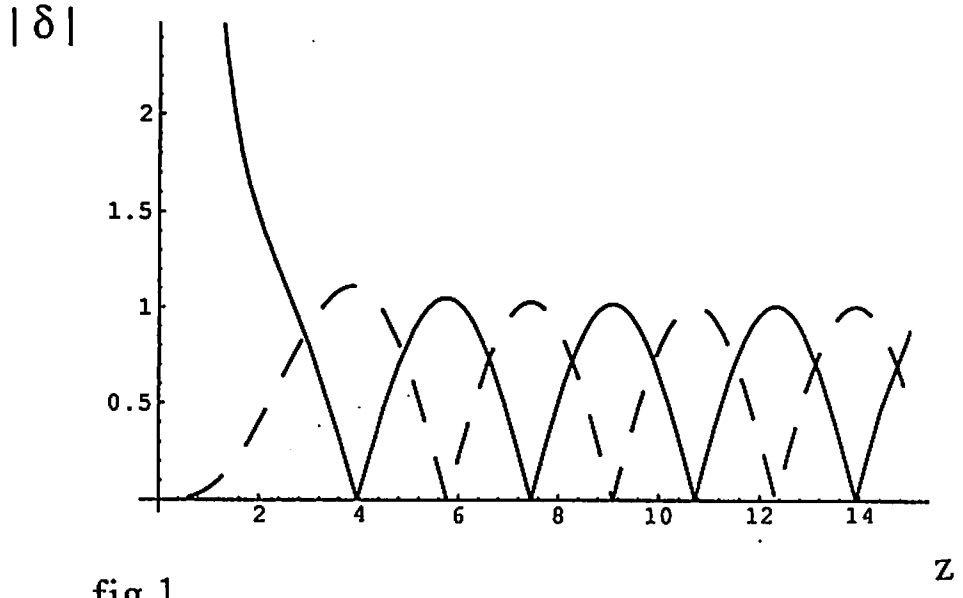

fig.1

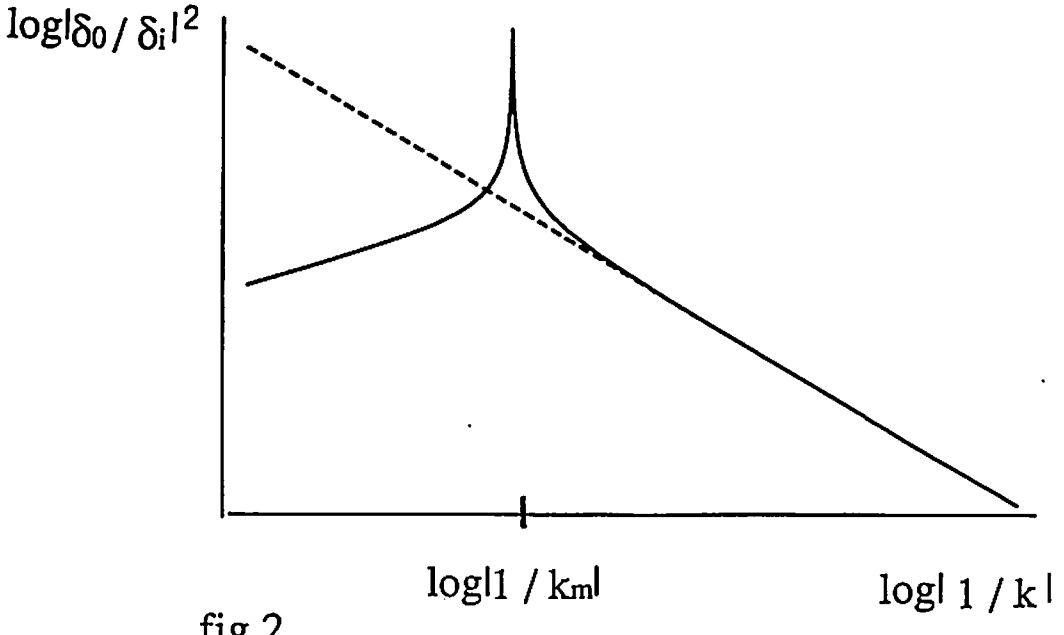

fig.2

Checkered (ichimatsu-figured) universe

Masatoshi Yamazaki

Department of Physics, Kanazawa University, Kanazawa 920

A scenario is suggested that in the early universe, at first, the gluon radiation inevitably has the checkered (ichimatsu-figured) structure with the side 10^{-27}cm just after the end of grand unification and, secondly, the scale factor grows by the factor of 10^{28} and 10^{25} during the subsequent inflation and adiabatic standard phase, respectively. This may yield the observed regularity in the galaxy distribution, the great wall and void, where the size of void is 10^{26}cm = 10^{-27}cm x 10^{28}x 10^{25}.

Geller and Huchra[1] mapped about 10^{-5} of the volume of the visible universe, found that maps of the galaxy distribution in the nearby universe reveal large coherent structure, and detected the great wall where many galaxies lie. Recent surveys by Broadhurst, Ellis, Koo, and Szalay[2] revealed a regularity in the galaxy distribution with a characteristic length scale of 128 Mpc. They compared this regular pattern in the large-scale distribution of galaxies to the picket fence in universe.

Energy densities in great walls and in voids [3)~11)] are 5 and 1/5 times the mean density u_m, respectively[1)]. A typical thickness of the wall is less than 5Mpc[1)]. Volumes of the great wall and of the void are 1/6 and 5/6 times the volume $(128Mpc)^3$, respectively. And energies in the great wall and in the void are 5/6 and 1/6 times the energy $u_m(128Mpc)^3$, respectively. More than 90% of the matter in great walls appears to be dark. This result is called the dark matter problem. The voids are full of dark matter. The anisotropy of 3K microwave background is $\delta T/T<10^{-5}$ [12)].

By means of what scenario grows up this large-scale structure in the universe or the great wall and void, where the size of void is as large as the hundredth of the size of visible universe ? A possible scenario proposed in the present paper, which may yield the large-scale structure, is summarized as follows ((1)~(5)):

(1) The checkered (ichimatsu-figured) structure is a three-dimensional arrayal of black cube, white cube, black cube, white cube, and so on with an identical side length. The gluon configuration distinguishes a black cube from a white cube. The structure constants of SU(3) gluon fields are not uniform

in size in contrast with those of SU(2) fields where $f^{abc}=1$ for abc=123. This fact is the reason why the gluon radiation has the checkered configuration. A higher energy density is provided on the boundary, which will become the great wall, of two adjacent cubes than inside each cube, which will become the void. Of course the black cube and the white cube yield to an identical energy density. Therefore it is inevitable that the gluon radiation has the checkered configuration, because the free energy of which is lower than that of the admixed-at-random configuration.

(2) In the early universe at temperature 10^{14}Gev the checkered (ichimatsu-figured) structure for gluon radiation, with a characteristic Compton length scale of 10^{-27}cm ($=\hbar c/10^{14}$Gev), inevitably begins to appear just after the first step, the quantum tunnelling phase, of the phase transition which results in the end of grand unification. The scale factor grows by the factor of 10^{28} during the subsequent second step of phase transition, the de Sitter phase of exponential expansion and by 10^{25} during the adiabatic standard phase. Thus inevitable is the formation of the large-scale structure observed today or the formation of the great walls and voids with a characteristic

length scale of 0.4 G lt-yr or 10^{26}cm.

(3) At the epoch of the decoupling of matter and radiation the glueball matter, which is a candidate for the dark matter in the present scenario, constitutes the great walls and voids with a characteristic length scale of 10^{23}cm. After the decoupling at temperature 1 ev the baryonic matter begins to fall into the potential wells provided by the glueball matter in the great walls. The falling time is of the order of 10^{8} years ($=10^{23}$cm/3 x 10^{7}cm/sec).

(4) One of two kinds of glueballs gb (1) and gb (2), or $G^{R\to G}{}_{G}{}^{G\to B}{}_{G}{}^{B\to R}$ and $G^{G\to R}{}_{G}{}^{R\to B}{}_{G}{}^{B\to G}$, is a candidate for the dark matter in the present scenario. The gluoniums $G^{R\to G}{}_{G}{}^{G\to R}$, $G^{R\to B}{}_{G}{}^{B\to R}$, and $G^{G\to B}{}_{G}{}^{B\to G}$ have decayed out after the quark-hadron transition. It is hypothesized that the number of glueballs diminished by the factor of $\sim 3 \times 10^{-8}$ after the quark-hadron transition. This is nothing but an analogue of a well-known baryon asymmetry phenomenon. Thus, for every 3 x 10^{7} glueballs gb (2) there were 3 x 10^{7}+1 glueballs gb (1).

(5) Firstly the large-scale structure or the great wall and void, which is composed of the glueball matter, grows continuously from the quark-hadron transition till the matter

domination or till the decoupling of matter and radiation. In other words grows a remarkable contrast of the energy density between the great wall and the void. Secondly the baryonic matter, which is pulled by photons, cannot or can fall into the potential wells provided by the glueball matter dwelling at the great wall in the epoch of radiation domination or of matter domination, respectively.

Some words are complemented to make clear the proposed scheme about the inflation and the glueball dark matter. The following parameters for the inflationary universe are significant : 10^{14} Gev~the critical temperature for the end of grand unification ; 10^{-34} sec~the expansion time scale ; $(2/3)x10^{-32}$sec~the period of exponential expansion ; 10^{-23}cm~ the pre-inflation size of a small causally coherent patch ; and 10^{5}cm~the post-inflation size of the patch which is still causally coherent. During the de Sitter phase of exponential expansion the scale factor grows by the factor of exp $((2/3)x 10^{-32}/10^{-34})=\exp(65)=10^{28}$. During the adiabatic standard phase after the reheating process the scale factor grows by the factor of 10^{25}. The present size of void 10^{26}cm stems from the pre-inflation size 10^{-27}cm and the post-inflation size 10cm, both

of which are of course causally coherent. The number of gluon in a volume $(10^{-27}cm)^3$ is of the order of one at temperature 10^{14}Gev. While the size of checkered structure grows up from a tiny little patch 10^{-27}cm at a much higher temperature of the order of 10^{14}Gev to the size of cell 10^{14}cm at temperature 1 Gev, the coupling constant of gluon field $g^2/\hbar c$ also grows up from $g^2/\hbar c \sim 0.02$ to $g^2/\hbar c \sim 1$. We reasonably assume that initially eight gluon number densities were equal to the photon number density. Just before the quark to hadron transition took place, the energy density and the size of the universe were $10^{17}gm/cm^3$ and 10^{16}cm, respectively. After the transition the gluonium decayed out to red-shifting photons and one of two kinds of glueball became the dark matter, the masses of which were no more red-shifting away. With the present scenario it is reasonably understood that the amount of dark matter is not as much as million times, but of the order of ten times the amount of baryonic matter.

Next we will deduce the scheme of the gluon checkered (ichimatsu-figured) structure. For no net flow of gluon radiation we suppose the following conditions:

1) Everywhere the color neutrality holds.

2) Everywhere the total number density of various gluons is equal, and

3) Everywhere the gluon energy density is equal except some minor region with small measure, namely except the boundary layer between black and white cubes.

R,G, and B mean red, green, and blue, respectively, and the notation is as follows : A red quark emits a gluon $G^{R\to G}$ and becomes a green quark. The energy density u of the gluon radiation is

$$u=2^{-1}(|H^a|^2+|E^a|^2)=A+gL+g^2Q, \text{ and } A=(8\pi^2/15)T^4.$$

Here L and Q are linear and quadratic with respect to the coupling constant g, respectively. We use the approximation $G^a_\mu=n^aG$ for $a=1,2,3,\cdots,8$ and $\mu=1,2,3,4$, where $n^1=n^2=n^{R\to G}=n^{G\to R}$, $n^4=n^5=n^{R\to B}=n^{B\to R}$, and $n^6=n^7=n^{G\to B}=n^{B\to G}$. n^a, $a=1,2,3,\cdots,8$, are the partial number densities of eight gluons. On the analogy of the electromagnetic field the gluon field G^a_μ may have the double summation over the wave vector and the polarization vector. The first summation yields $G^a_\mu \sim n^a G$ and the second $G^a \times G^a \sim G^2$. Under this approximation vanishes the contribution both from all terms in L and from all crossed terms in Q; and remains only the contribution from all squared terms in Q.

The gluon configuration in black and white cubes is represented by three parameters x,y, and z and the consequent energy density is calculated. Three parameters x,y, and z under the conditions $2 \geq x,y,z \geq 0$ and $3 \geq x+z \geq 1$ determine the possible configurations in black and white cubes :

1) The black cube has xN/8 gluons $G^{R \to B}$ and $G^{B \to R}$, zN/8 gluons $G^{G \to B}$ and $G^{B \to G}$, (3-x-z)N/8 gluons $G^{R \to G}$ and $G^{G \to R}$, yN/8 uncolored gluons G^3, and (2-y)N/8 uncolored gluons G^8.

2) The white cube has (2-x)N/8 gluons $G^{R \to B}$ and $G^{B \to R}$, (2-z)N/8 gluons $G^{G \to B}$ and $G^{B \to G}$, (x+z-1)N/8 gluons $G^{R \to G}$ and $G^{G \to R}$, (2-y)N/8 uncolored gluons G^3, and yN/8 uncolored gluons G^8.

Here N is the total number of gluons in one black cube or in one white cube. The boundary layer between a black cube and an adjacent white cube has the configuration with x=y=z=1. The black and the white cubes have an equal energy density when the condition

$$(y-1)[(x-1)^2+(z-1)^2+4(x-1)(z-1)]+9(x+z-2)(x-1)(z-1)=0 \qquad (1)$$

is satisfied. The third term g^2Q in the equation of the energy density u can be written into $g^2Q=g^2qQ'$, where

$$Q'=6+4(y-1)^2[(x-1)^2+(z-1)^2+(x-1)(z-1)+(3/2)]-12(y-1)(x+z-2)$$
$$-[(x-1)^2+(z-1)^2][(x+z-2)^2+8]-(x-1)(z-1)[(x-1)(z-1)+8] \qquad (2)$$

and $q \sim G^4$ is a common constant factor. The minimum value of Eq.(2) in which we are mostly interested is sought under the condition (1). Since it is a hard task to obtain the minimum value of Q' by analytic ways, we study only several cases. The result is that the configurations with 1) x=1, z=2, and y=1, with 2) x=1, z=0, and y=1, with 3) x=0, z=2, and y=1, and with 4) x=2, z=0, and y=1 yield Q'=6-9, while the configuration x=y =z=1 yields Q'=6. More generally, the Helmholtz energy density f=u-Ts must be minimized. The entropy density can be written as $s=s_A(T)+s_B(x,y,z)$, where $s_A=(32\ ^2/45)T^3$ and s_B is the entropy of mixing. In this procedure, more elaborated calculations, namely estimates of the common constant factor q, are necessary so that we can obtain the true minimum of the free energy density f.

References

1) M.J.Geller and J.P.Huchra, Science 246(1989), 897.

2) T.J.Broadhurst, R.S.Ellis, D.C.Koo and A.S.Szalay, Nature 343(1990), 726.

3) M.Joeveer, J.Einasto and E.Tago, Month. Not. Roy. Astron. Soc. 185(1978), 357.

4) R.P.Kirshner, A.Oemler, P.L.Schechter and S.A.Shectman,

Astrophys. J. (Letters) 248(1981), L57.

5) M.P.Haynes and R.Giovanelli, Astrophys. J. (Letters) 306 (1986), L55.

6) R.Giovanelli, M.P.Haynes and G.Chincarini, Astrophys. J. 300(1986), 77.

7) B.A.Peterson, R.S.Ellis, G.Efstathiou, T.Shanks, A.J.Bean, R.Fong and Z.Zen-Long, Month. Not. Roy. Astron. Soc. 221 (1986), 233.

8) H.J.Rood, Ann. Rev. Astron. Astrophys. 26(1988), 245.

9) M.J.Geller, Dark Matter in the Universe, H.Sato and H.Kodama, Eds., (Springer, 1990).

10) S.D.M.White, C.S.Frenk, M.Davis and G.Efstathiou, Astrophys. J.313(1987), 505; C.S.Frenk, S.D.White, G.Efstathiou and M.Davis, Astrophys. J. 351(1990), 10.

11) W.Saunders, C.Frenk, M.Rowan-Robinson, G.Efstathiou, A.Lawrence, N.Kaiser, R.Ellis, J.Crawford, X.Xia and I.Parry, Nature 349(1991), 32.

12) D.J.Fixsen, E.S.Cheng and D.T.Wilkinson, Phys. Rev. Lett. 50(1983), 620; J.Uson and D.Wilkinson, Nature 312(1984), 427; R.D.Davies et al., Nature 326(1987), 462; A.C.S.Readhead et al., Astrophys. J. 346(1989), 566.

Magnitude-Number Count Relation of Galaxies in an Inhomogeneous Universe -Gravitational Lens Effect-

Kazuya Watanabe

Uji Research Center, Yukawa Institute for Theoretical Physics, Gokasho Uji 611 Japan†

1. Introduction

Among the fundamental problems in the astrophysics, the determination of cosmological parameters, *e.g.*, the Hubble parameter, H_0, density parameter, Ω_0, and cosmological constant, λ_0, is the most important subject because they play a crucial role in discussing the origin and evolution of large scale structures of the universe, but their values have not yet been settled.[1] The crucial difficulty has lain in the limitation in our observational strategy. Namely, in order to determine these parameters, accurate observations at high redshift, $z \gtrsim 1$, are required, which have been almost impossible for a long time.

However, owing to the recent rapid progress in relevant technologies, observational cosmology is, now, being more hopeful and interesting. Especially, the development of charge-coupled device (CCD) detectors has made it possible to observe faint objects ($\sim$ 27 mag),[2] which means that the redshift of typical galaxies corresponding to this limiting magnitude is greater than unity. For the determination of the cosmological parameters, the standard homogeneous and isotropic model universe, *i.e.*, the Friedmann model, has been usually assumed, and the light propagation in such a simple model universe has been solved. On the other hand, many authors have pointed out the importance of cosmological inhomogeneities, *e.g.*, galaxies and clusters of galaxies, in interpreting the observational data.[3-10]

On the basis of the previous theoretical works concerning the light propagation, the observational implication of gravitational lens effect has been discussed by many authors.[10] Recently, Omote and Yoshida (1990) investigated the gravitational lens effect on the number count-redshift (N-z) relation of galaxies,[9] and they showed that the gravitational lens effect much affect the N-z relation. We therefore investigate the effects of cosmological inhomogeneities on the m-N relation of galaxies.

2. Amplification probability

Since the amplification probability, $P(\mu)$ (μ is the amplification factor) plays an important role in statistically discussing the realistic m-N relation, in this section we first derive

† On leave of absence from Faculty of Science, Hiroshima University, Japan

the analytic formula for $P(\mu)$ on the basis of the work by Futamase and Sasaki.[7] We then examine the validity of the formula by comparing it with the corresponding numerical results.

The basic equation to derive the probability is the distance-redshift relation in an inhomogeneous universe derived by Sasaki (1987). The most important term, which is also concerned with the gravitational amplification, is given by[11]

$$I \equiv \delta d_L / d_L = -\int_0^{\lambda_s} d\lambda \frac{\sinh^2 \sqrt{-k}\lambda}{\sqrt{-k}} \left(\coth \sqrt{-k}\lambda - \coth \sqrt{-k}\lambda_s \right) \Delta\Psi, \tag{1}$$

where I is the perturbation of the luminosity distance, d_L, $k = 0, \pm 1$ is a curvature signature of space, Ψ is the Newtonian potential generated by inhomogeneities, and λ is the usual conformal affine parameter given by

$$H_0 a_0 \lambda(z) = \int_1^{1+z} \frac{dy}{\sqrt{\Omega_0 y^3 + (1 - \Omega_0 - \lambda_0) y^2 + \lambda_0}} \equiv \tilde{\lambda}(z), \tag{2}$$

in the Friedmann model. The potential, Ψ, is related to inhomogeneities of the density, ρ, by the Poisson equation given by

$$\Delta\Psi = 4\pi G a^2 (\rho - \rho_b), \tag{3}$$

where ρ_b is the background density and Δ is the covariant Laplacian with respect to the spatial metric in the Robertson-Walker spacetime.

Futamase and Sasaki derived the amplification probability on the basis of the equation (1) in the Einstein-de Sitter background universe ($\Omega_0 = 1, \lambda_0 = 0$).[7] Following their work, we extend their formula in the more general cases, where $\Omega_0 + \lambda_0 \leq 1$. Let us represent inhomogeneities by homogeneous spheres whose physical radius and present mean separation are, respectively, R_* and R_0, and let us D and $\tilde{D}$ be, respectively, the angular diameter distance in a Friedmann model and in the corresponding Dyer-Roeder model. The analytic

formula then becomes

$$P(\mu) = P_0(z)\mu^{-2/3}\exp\left[-\frac{\left(I(\mu;z)-I_1(z)\right)^2}{2f(z)}\right] \tag{4}$$

where

$$\begin{aligned}
f(z) &= \begin{cases} (1-\tilde{\alpha})^2\Omega_0^2\left(R_0^3H_0/10R_*^2\right)\tilde{\lambda}^3 & k=0, \\ (1-\tilde{\alpha})^2\Omega_0^2\left(3R_0^3H_0/8R_*^2\right)(1-\Omega_0-\lambda_0)^{-1}h(z) & k=-1, \end{cases} \\
I(\mu;z) &= \sqrt{\frac{\tilde{\mu}(z)}{\mu}}-1, \quad \tilde{\mu}(z) = \left(\tilde{D}/D\right)^2, \\
I_1(z) &= -I_0\left(\exp\left(g(z)\right)-1\right)^{-1}, \quad I_0(z) = \tilde{D}/D-1, \\
h(z) &= \frac{3\left(1-e^{4\tilde{\lambda}}\right)+2\tilde{\lambda}\left(1+4e^{2\tilde{\lambda}}+e^{4\tilde{\lambda}}\right)}{\left(e^{2\tilde{\lambda}}-1\right)^2}, \\
g(z) &= \frac{3R_*^2}{4R_0^3H_0}\int_0^z dz\frac{(1+z)^2}{\chi(z)}, \\
\chi(z) &= \sqrt{\Omega_0(1+z)^3++(1-\Omega_0-\lambda_0)(1+z)^2+\lambda_0},
\end{aligned} \tag{5}$$

and $P_0(z)$ is a normalization factor of the probability function so that

$$\int_1^\infty P(\mu)d\mu = 1. \tag{6}$$

The parameter, $\tilde{\alpha}$, is a smoothness parameter which was introduced by Dyer and Roeder[5] and is defined by

$$\tilde{\alpha} = 1-\rho_L/\rho_b, \tag{7}$$

where ρ_L is the mean density of lens objects. The physical meaning of $\tilde{\mu}$ is the amplification of a Friedmann model relative to the corresponding Dyer-Roeder model. Throughout this

paper, we only discuss the case of $\tilde{\alpha} = 0$, and the angular diameter distance in the Dyer-Roeder model[5] is then given by

$$\tilde{D}(z) = H_0^{-1} \int_0^z \frac{dz'}{(1+z')^2 \chi(z')}. \tag{8}$$

We now examine the validity of our probability function by comparing $P(\mu)$ with the corresponding numerical results. For simplicity, we assume, for a while, the spatially flat dust filled background universe, where inhomogeneities are represented by the Newtonian Potential,

$$\Psi(x,t) = \sum_k \frac{-Gm}{\left(a(t)^2 |x - x_k|^2 + \ell^2\right)^{1/2}}, \tag{9}$$

where m and ℓ are, respectively, mass and size of lens objects, $a(t)$ is the cosmic scale factor, and the index, k, denotes each lens object.

Though our model universe contains two independent parameters, m and ℓ, it is well known that the combination of these parameters are more convenient and fundamental, which are defined as (Futamase 1988)[12]

$$\epsilon^2 = Gm/\ell, \quad \kappa = H_0 \ell. \tag{10}$$

Since $\ell \sim R_*$ and $Gm \sim H_0^2 R_0^3$, the dispersion of $P(\mu)$ is characterized by only one parameter, ϵ^2/κ. We therefore define the strength of gravitational lensing by ϵ^2/κ. Some details about this characterization are found in Watanabe and Sasaki (1990)[13] and Watanabe, Sasaki and Tomita (1991).[6] We then numerically solved optical equations and null geodesics to get the realistic amplification probability.

In figure 1, we compare the analytic formula with corresponding numerical results. We also show the probality function, $P_{ES}(\mu)$, derived by Ehlers and Schneider[14] for comparison. We found that the analytic formula well fits the numerical results for $\epsilon^2/\kappa < 0.5$, and that P_{ES} cannot. On the other hand, for $\epsilon^2/\kappa > 0.5$, our probability function deviates from the numerical results. It is because that the optical depth of lensing becomes smaller so that the asumption made by Futamase and Sasaki is invalid in these cases. In this paper we use $P(\mu)$ (also $P_{ES}(\mu)$ for comparison) when we calculate the realistic m-N relation.

3. Basic formula for the m-N relation

The number of galaxies per unit solid angle whose fluxes are larger than l is given by (Kasai and Sasaki 1987)[15]

$$N(>l) = \int_0^{v(z_F)} \int_{L(l)}^{\infty} n(v, L) d_A^2 \omega dv, \tag{11}$$

where d_A is the angular diameter distance along light rays, $n(v, L)$ is the number density of galaxies with the intrinsic luminosity, L, v is the affine parameter, z_F is the redshift corresponding to the epoch when galaxies are formed, and $\omega = -k^a u_a$ is the frequency of a photon from galaxies measured by the observer whose 4-velocity is u^a. The flux, l, is related to the luminosity, L, in a redshift dependent manner and given by $l = L/(4\pi d_L^2)$, where d_L is the luminosity distance along light rays, and the important relation, $d_L = (1+z)^2 d_A$, holds in any spacetime (Ellis 1971).[16]

Since the distances, d_A and d_L, may be affected by inhomogeneities along light paths, we must solve the equations of null geodesics and optical scalars (Sachs 1961)[17] in order to obtain the realistic m-N relation. However, the equation (11) is too complicated to be easily analyzed in an inhomogeneous universe because the effect of inhomogeneities also appears in the argument, $L = 4\pi l d_L^2$, of the luminosity function due to the gravitational amplification of flux, l. We must therefore approximate the equation (11) under the suitable assumptions about light propagation whose validity is to be carefully investigated.

Our assumptions are

(1) The correlation between inhomogeneities in galaxy distribution and the gravitational amplification of luminosity of galaxies is neglected.

(2) Since the count of galaxies is large, the gravitational amplification of luminosity is taken into account in a statistical manner.

(3) If the surveying area is large, the angular diameter distance in the equation (11) can be replaced by that in a Friedmann model.

(4) Perturbations of the affine parameter and frequency of photons are negligible.

The validity of the first assumption has not yet verified, and actually, there may be some correlations because the galaxies to be counted also play the role of lens objects in causing the gravitational amplification. In this paper we therefore use this assumption as a working

hypothesis. This assumption was also implicitly adopted in Omote and Yoshida. It is noted that the second assumption is the consequence of the first one. Assuming the Schechter function for the luminosity function,[14] we can, in a straightforward manner, extend the formula by Omote and Yoshida to get the realistic m-N relation under the assumptions described above.

The formula becomes

$$N(<m) = \int_0^{z_m} dz \frac{D^2(z)(1+z)^{2+\nu}}{H_0 \chi(z)} \int_1^{\infty} d\mu p(z,\mu) \Gamma[\alpha+1, x(m;z)/\mu], \tag{12}$$

where $\chi(z)$ is defined in the equation (5), and the Schechter function, $\Phi(z, L)$, is parametrized as

$$\Phi(z, L)dL = (1+z)^{3+\nu} \phi^* \exp\left(-\frac{L}{L^*}\right)\left(\frac{L}{L^*}\right)^{\alpha} d\left(\frac{L}{L^*}\right), \tag{13}$$

and $x(m; z)$ is defined by $(1+z)^4 \tilde{D}(z)^2 10^{10+0.4*(M_*-m)}$, and M_* is the absolute magnitude corresponding to L^*. The function, $\Gamma(a, x)$, is the incomplete gamma function defined by

$$\Gamma(a,x) = \int_x^{\infty} dt \exp(-t) t^{a-1}. \tag{14}$$

We now examine the validity of our last two assumptions. In order to do that, we calculate the averaged angular distance as a function of size of a surveying area, $\delta\Omega$. We simulated 400 rays for several values of $\delta\Omega$, and found that the averaged distance, $\left\langle d_A \right\rangle$, coincides with the distance in a Friedmann model for $\delta\Omega$ = 0.1, 1, 5 degree, where inhomogeneities are represented by galaxies with the radius, $\ell = 50h^{-1}$kpc, and the mass, $m = 3.4 \times 10^{12} M_{\odot}$, *i.e.*, $\epsilon^2/\kappa = 0.2$. We also found that the dispersion in the distance, σ_d, is small, which is consistent with the previous works (see Table 1). We also numerically found that the induced error in the m-N relation due to the last assumption is less than 0.1%, which is negligibly small.

z	0.2	0.2	0.2	0.5	0.5	0.5	1.0	1.0	1.0	2.0	2.0	2.0
$\delta\Omega$(deg)	0.1	1	5	0.1	1	5	0.1	1	5	0.1	1	5
$\langle H_0 d_A \rangle$	0.146	0.145	0.145	0.246	0.245	0.244	0.293	0.293	0.292	0.281	0.282	0.281
σ_d	0.001	0.001	0.001	0.06	0.006	0.006	0.016	0.015	0.015	0.025	0.025	0.025
$H_0 D$	0.145	0.145	0.145	0.245	0.245	0.245	0.293	0.293	0.293	0.282	0.282	0.282
$H_0 \tilde{D}$	0.146	0.146	0.146	0.255	0.255	0.255	0.329	0.329	0.329	0.374	0.374	0.374

Table 1 The averaged distances compared with the distances in the Einstein-de Sitter universe (D) and the corresponding Dyer-Roeder model ($\tilde{D}$).

4. Results and discussion

In this section we discuss the m-N relation taking into account the gravitational lens effect. In order to do that, we need to specify the model parameters of luminosity function, lens model, and background cosmological model. For the luminosity function, we adopt the same parameters with those in Fukugita *et al.*[19]

$$\alpha = -1.11, \ M_* = -19.3, \text{ and } \phi_* = 0.0156h^3/\mathrm{Mpc}^3, \tag{15}$$

and the Hubble parameter is $h = 1$. It must be noted that the values of these parameters are irrelevant for us until we compare the theoretical prediction with observational data. We also ignore the K-correction, and assume that $\mu = 0$.

We first summarize the expected changes in the m-N relation due to the gravitational lens effect. Since all galaxies are, in a statistical sense, always amplified relative to the Friedmann model, we will have excess of galaxy counts for all m. However, most of galaxies corresponding to small $m(\lesssim 20)$ are nearby galaxies, and the amplification effect for them is very small. On the other hand, galaxies corresponding to larger $m(\gtrsim 20)$ may be affected much more than nearby galaxies. We therefore expect that we may have much excess of galaxy count for $m \gtrsim 20$, while the count for $\lesssim 20$ remains unchanged. If we are ignorant of the cosmological inhomogeneities, and the gravitational lens effect plays an important role in amplification, we will underestimate Ω_0, or interpret that we have a non-vanishing cosmological term, because the evaluated comoving volume is larger. If this is the true case, the universe with $\Omega_0 \sim 1, \lambda_0 \sim 0$ may be consistent with the present observational data.

To calculate the m-N relation, we must also specify the parameters of a lens model. The probability function, $P(\mu)$, contains only one parameters, ϵ^2/κ, as was described in the previous section. However we must specify another parameter, z_F, which specify the initial time when the first generation of galaxies were formed. We investigated the cases of $z_F = 3$, 5 and 7, changing other parameters, ϵ^2/κ, Ω_0 and λ_0.

In figure 2, we show the m-N relation for $\epsilon^2/\kappa = 0.5$, $z_F = 7$, where the bin of apparent magnitude is 0.5. We also show, for comparison, the gravitational lensed m-N relation in which we adopted the probability function of Ehlers and Schneider in the cases of $\lambda_0 = 0$, where $\tilde{D}$ can be analytically integrated. We found that for both choice of the probability function, *i.e.*, $P(\mu)$ and $P_{ES}(\mu)$, and for any value of (Ω_0, λ_0), the gravitational lens effect on the relation is very weak. It must be noted that our choice of ϵ^2/κ is marginally realistic and therefore provides us with the upper limit of lensing. We can then conclude that the gravitational lens effect does not affect the m-N relation for $m \lesssim 30$. These results are, however, not discouraging but rather encouraging us because they prove that the m-N relation is a comparatively "good" test to determine the cosmological parameters in the sense that the relation is hardly affected by cosmological inhomogeneities.

We also calculate the N-z relation in which we do not integrate over the magnitude, m, but calculate the relation as a function of m, where we examine the cases of $m = 20$, 22 and 28. The bin of m and $\ln(1+z)$ are, respectively, 0.5 and $\ln(1+3)/20 \sim 0.07$, and plot the $z - \ln N$ relation for $\epsilon^2/\kappa = 0.2$, 0.5 in figure 3, where we assume $z_F \gtrsim 2$. We found that for $\Omega_0 = 1$, $\lambda_0 = 0$, the dependence of the relation on ϵ^2/κ appears at the "intermediate magnitude" ($m_c \sim 22$), and the relation seems to be sensitive to inhomogeneities, namely, larger ϵ^2/κ, larger deviation of the relation from that in a smooth universe we have. Furthermore, we empirically found that the results obtained by Omote and Yoshida are almost the same as our results in the cases of $\epsilon^2/\kappa = 0.2$, and confirmed that the N-z relation is comparatively much affected by inhomogeneities, as was pointed out by Omote and Yoshida.[9]

It must be noted that the characteristic magnitude of galaxies, m_c, varies as a function of Ω_0 and λ_0. It is simply because the luminosity distance depends on these parameter, and we have larger m_c in an open universe. We therefore expect that, if the recently reported large scale structures[20] really exist in the universe, the comparison of the sensitive and insensitive observational relations, namely the N-z and m-N relations, may enable us to "detect" the structures in an indirect manner. It also be noted that by determining m_c, we can reassure the values of Ω_0 and λ_0, which are obtained by the m-N relation. The close comparison with observational data is, however, left in future work.

It must be noted that when ϵ^2/κ approaches to unity, the standard Newtonian metric[21]

may be modified by the back-reaction due to inhomogeneities. In that case, the global expansion factor, $a(t)$, given by the Friedmann equation has no meaning in discussing light propagation in an inhomogeneous universe. This means that the picture of amplification given by Futamase and Sasaki may be broken down because the fundamental assumptions to derive it become invalid. However, it must be noted that if this is an actual case in our universe, the notion of "global" cosmological parameters, *i.e.*, H_0, Ω_0, etc., no longer have the well-defined meaning, at least, on the scale compared with the size of the large scale inhomogeneities. These issues are left to be carefully investigated in future work.

Acknowledgment

The author thanks Prof. K. Tomita for his continuous encouragement. The author also thanks Prof. M. Omote for giving a lecture on the gravitational lens effect on observational relations at Uji Research Center, Yukawa Institute for Theoretical Physics, and thanks Prof. Suto for suggesting the possibility of this work. Finally, it was the great pleasure of the author to collaborate on several works concerning with the gravitational lens effect with Prof. Tomita and Prof. Sasaki, because without these collaboration, the author could not complete this work.

REFERENCES

1. M. Fukugita, in *Proceedings of Primordial Nucleosynthesis and Evolution of Early Universe*, Eds. K. Sato and J. Audouze (Kluwer Academic 1991), p.599.
2. J. A. Tyson, *Astron. J.* **96** (1988), 1.
3. R. Kantowski, *Astrophys. J.* **155** (1969), 89.
   C. C. Dyer and L. M. Oattes. *Astrophys. J.* **326** (1988), 50.
4. C. C. Dyer, and R. C. Roeder, *Astrophys. J. Letters* **172** (1972), L115.
5. C. C. Dyer and R. C. Roeder, *Astrophys. J. Letters* **173** (1973), L31.
6. K. Watanabe, M. Sasaki and K. Tomita, sumbitted to *Astrophys. J.*
7. T. Futamase and M. Sasaki, *Phys. Rev.* **D40** (1989), 2502.
8. K. Watanabe and K. Tomita, *Astrophys. J.* **355** (1990), 1.
9. M. Omote and H. Yoshida, *Astrophys. J.* **361**, 27.
10. R. K. Sachs and A. M. Wolfe, *Astrophys. J.* **174** (1967), 73.
    C. R. Canizares, *Nature* **291** (1981), 620.

E. E. Falco, M. V. Gorenstein and I. I. Shapiro, *Astrophys. J. Letters* **289** (1985), L1.
P. Schneider, *Astron. Astrophys.* **179** (1987), 80.
M. Sasaki, *Mon. Not. R. astr. Soc.* **240** (1988), 415.
K. Tomita K. Watanabe, *Prog. Theor. Phys.* **82** (1989), 563.
K. Tomita and K. Watanabe, *Prog. Theor. Phys.* **83** (1990), 467.

11. M. Sasaki, *Mon. Not. R. astr. Soc.* **228** (1987), 653.
12. T. Futamase, *Phys. Rev. Letters* **61** (1988), 2175.
13. K. Watanabe and M. Sasaki, *Publ. Astron. Soc. Jpn.* **42** (1990), 1.
14. J. Ehlers, and P. Schneider, *Astron. Astrophys.* **168** (1986), 57.
15. M. Kasai and M. Sasaki, *Mod. Phys. Letters* **10** (1987), 727.
16. G. F. R. Ellis, in *General Relativity and Cosmology*, Ed. B. K. Sachs (New York Academic 1971), p.104.
17. R. K. Sachs, *Proc. Roy. Soc. London* **A264** (1961), 309.
18. P. Schechter, *Astrophys. J.* **203** (1976), 297.
19. M. Fukugita, T. Takahara, K. Yamashita and Y. Yoshii, *Astrophys. J. Letters* **361**, L1.
20. *eg.*, T. J. Broadhust, R. S. Ellis, D. C. Koo and A. S. Szalay, *Nature* **343** (1990), 726.
21. H. Nariai and Y. Ueno, *Prog. Theor. Phys.*, **23** (1960) 305.
W. M. Irvine, *Annals Phys.* **32** (1965), 322.
K. Tomita, *Prog. Theor. Phys.* **79** (1988), 258.

Figure captions

Fig. 1 The amplification probability, $P(\mu)$, is compared with the numerical results in the background universe with $\Omega_0 = 1$, $\lambda_0 = 0$. The comparison with $P_{ES}(\mu)$ is also made.

Fig. 2 The realistic m-N relation in an inhomogeneous universe is compared with the standard m-N formula, where $z_F = 7$, $\epsilon^2/\kappa = 0.5$, and the model parameters of inhomogeneities and background cosmological models are shown in the figures.

Fig. 3 The realistic N-z relation is calculated as a function of the redshift and magnitude. The model parameters are shown in the figures.

Fig. 1

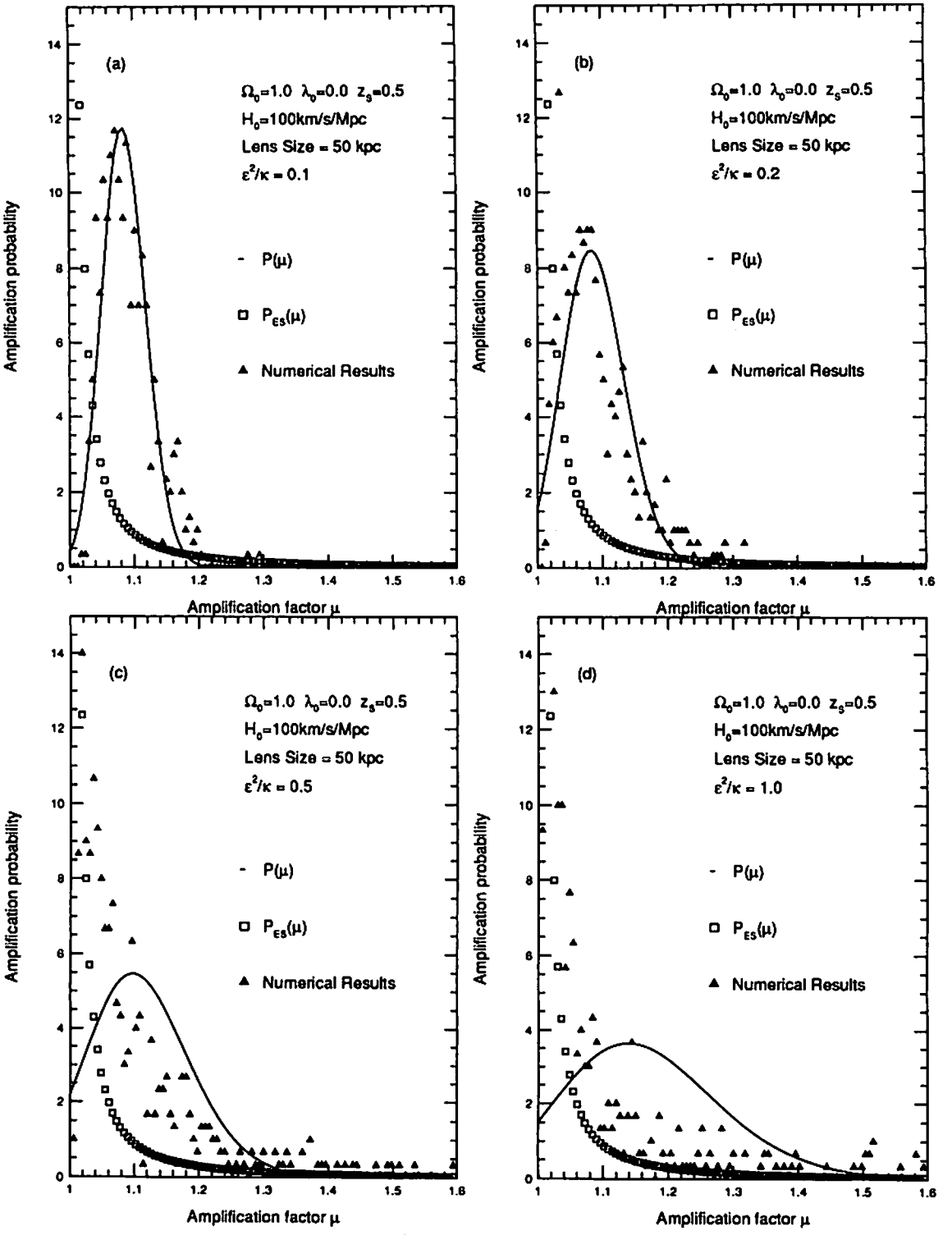
(a)
Ω_0=1.0 λ_0=0.0 z_s=0.5
H_0=100km/s/Mpc
Lens Size = 50 kpc
ε^2/κ = 0.1
- P(μ)
□ $P_{ES}(\mu)$
▲ Numerical Results
Amplification probability
Amplification factor μ
(b)
Ω_0=1.0 λ_0=0.0 z_s=0.5
H_0=100km/s/Mpc
Lens Size = 50 kpc
ε^2/κ = 0.2
- P(μ)
□ $P_{ES}(\mu)$
▲ Numerical Results
Amplification probability
Amplification factor μ
(c)
Ω_0=1.0 λ_0=0.0 z_s=0.5
H_0=100km/s/Mpc
Lens Size = 50 kpc
ε^2/κ = 0.5
- P(μ)
□ $P_{ES}(\mu)$
▲ Numerical Results
Amplification probability
Amplification factor μ
(d)
Ω_0=1.0 λ_0=0.0 z_s=0.5
H_0=100km/s/Mpc
Lens Size = 50 kpc
ε^2/κ = 1.0
- P(μ)
□ $P_{ES}(\mu)$
▲ Numerical Results
Amplification probability
Amplification factor μ

Fig. 2

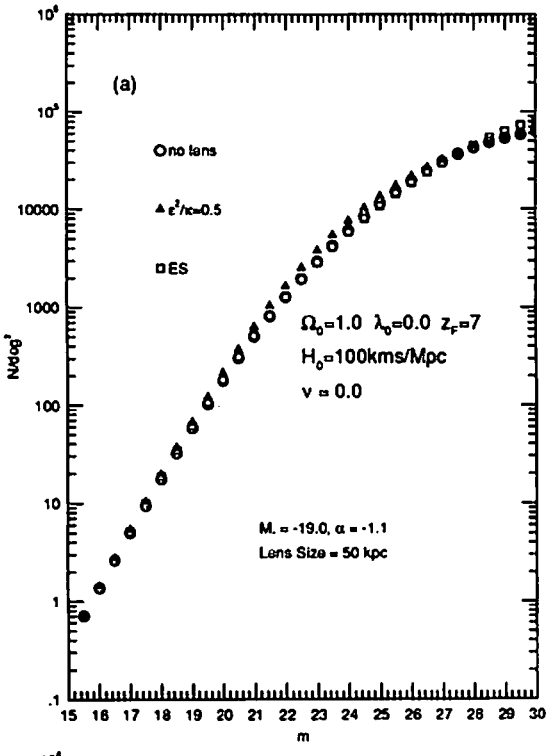
(a)
no lens
ε²/κ=0.5
ES
Ω₀=1.0 λ₀=0.0 z_F=7
H₀=100kms/Mpc
ν = 0.0
M* = -19.0, α = -1.1
Lens Size = 50 kpc
N/deg²
m

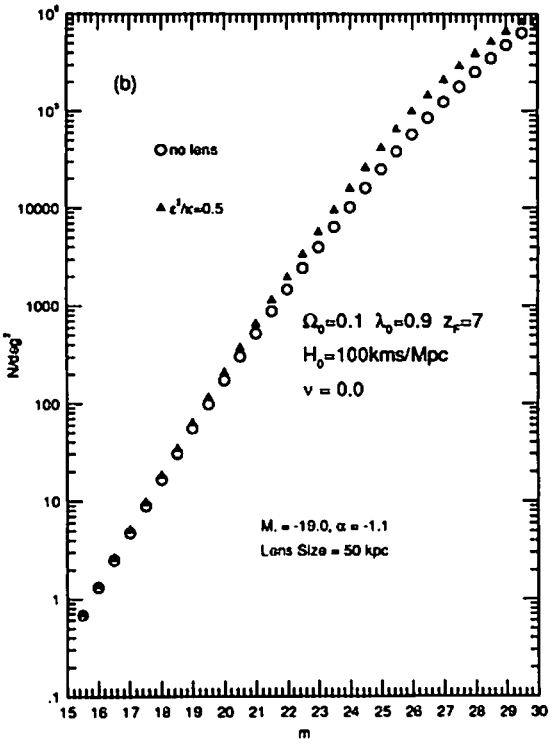
(b)
no lens
ε²/κ=0.5
Ω₀=0.1 λ₀=0.9 z_F=7
H₀=100kms/Mpc
ν = 0.0
M* = -19.0, α = -1.1
Lens Size = 50 kpc
N/deg²
m

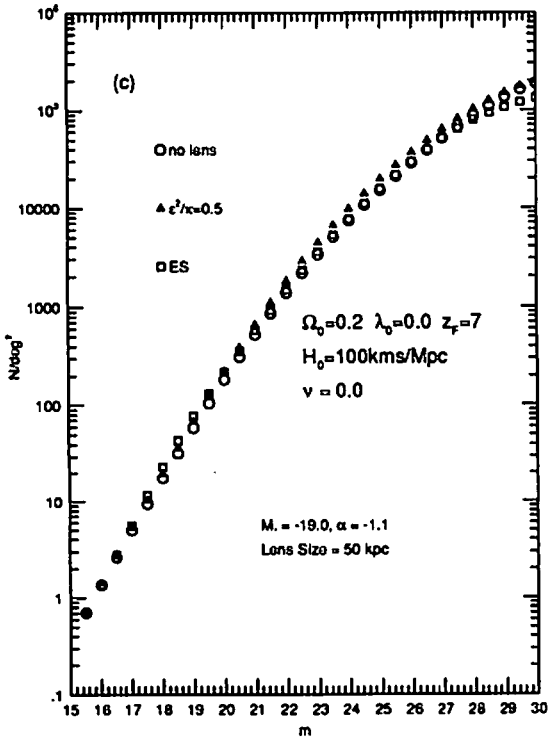
(c)
no lens
ε²/κ=0.5
ES
Ω₀=0.2 λ₀=0.0 z_F=7
H₀=100kms/Mpc
ν = 0.0
M* = -19.0, α = -1.1
Lens Size = 50 kpc
N/deg²
m

Fig. 3

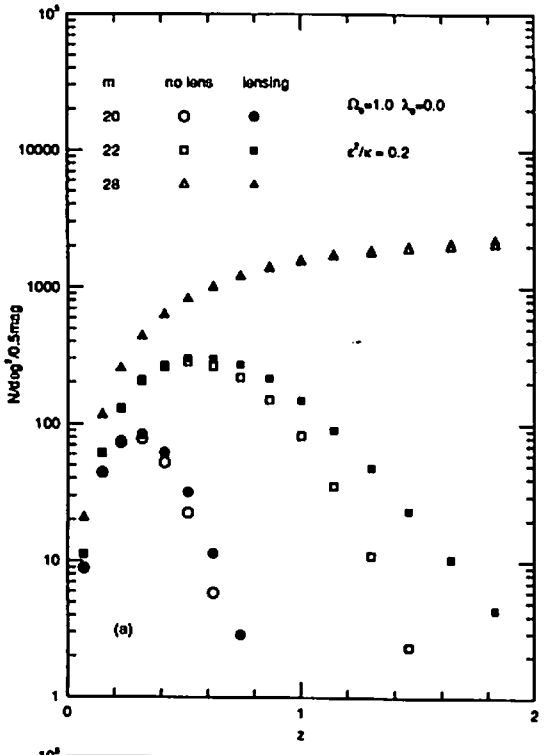
m
no lens
lensing
20
22
28
Ω_0=1.0 λ_0=0.0
ϵ^2/κ = 0.2
(a)
N/deg^2/0.5mag
z

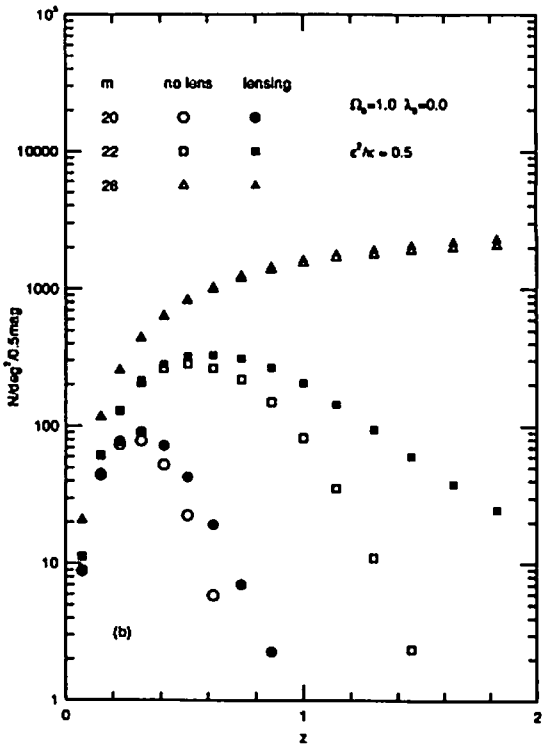
m
no lens
lensing
20
22
28
Ω_0=1.0 λ_0=0.0
ϵ^2/κ = 0.5
(b)
N/deg^2/0.5mag
z

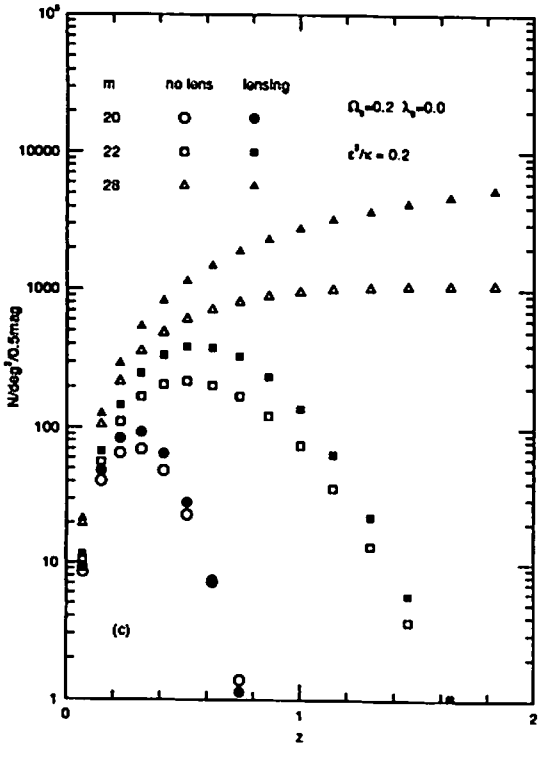
m
no lens
lensing
20
22
28
Ω_0=0.2 λ_0=0.0
ϵ^2/κ = 0.2
(c)
N/deg^2/0.5mag
z

Electric and Magnetic Parts of the Weyl Curvature in Observational Cosmology

LAURENS D. GUNNARSEN*
Department of Physics, Waseda University
Shinjuku-ku, Tokyo 169-50, Japan

January, 1992

Abstract

When Weyl curvature is present in a cosmological model, images of spherical extended light sources have elliptical, rather than circular outlines. This paper shows how the electric and magnetic parts of the Weyl curvature each contribute to this distortion effect. The key result is that only the magnetic part—a field with no Newtonian analog whose inertial frame-dragging effects have yet to be detected in the solar system—contributes any antipodal asymmetry to the distortion effect. It is therefore posible that further observations like those of Tyson, Valdes, and Wenk may reveal cosmological magnetic Weyl curvature in our Universe.

1 Introduction

In 1966, Kristian and Sachs [1] pointed out that Weyl curvature in a cosmological model has a characteristic observational signature: the distortion effect. "In any anisotropic model," they wrote, "all distant objects in a particular direction on the celestial sphere may appear distorted, with a definite preferential direction for their longest dimension." Using a well-defined and physically reasonable approximation scheme, they computed for a general Weyl curvature the induced image distortion as a function of source area distance and position on the celestial sphere.

Now, more than twenty-five years later, observational evidence for Kristian and Sachs's distortion effect is mounting. Particularly strong support comes from the recent observations of Tyson, Valdes, and Wenk [2], which show systematic alignments in the images of faint background galaxies centered on rich foreground galaxy clusters. Since these faint

*e-mail address:shinji@jpnwas00.bitnet

background galaxies seem to be at high redshift ($z \geq 1$), the observed distortion in their images points to the presence of Weyl curvature in our Universe over cosmological scales.

Now, in cosmology, the isotropy of the microwave background radiation determines a preferred frame of reference, and from the point of view of an observer who adopts this frame of reference, there are exactly two kinds of Weyl curvature: electric and magnetic. Electric Weyl curvature has a straightforward Newtonian analog in the tensor field formed by removing the trace from the second derivative of the gravitational potential. Magnetic Weyl curvature, on the other hand, has no Newtonian analog whatever. Its inertial frame-dragging effects, presumably present in the solar system, have yet to be detected.

In Section 2 of this paper, I discuss how the electric and magnetic parts of the Weyl curvature each contribute to the overall distortion effect. My discussion relies on Kristian and Sachs's approximation scheme, which expresses the distortion effect as a power series in a small parameter (essentially the area distance to the source, measured in Hubble units.) Since the coefficients in this power series are all simply tensors in the tangent space to spacetime at the present moment in our history, Kristian and Sachs's approximation scheme effectively reduces the study of cosmological image distortions to a problem in 4-dimensional Lorentzian linear algebra. Adding to this scheme a preferred 4-velocity, t^a, representing the frame of reference in which the microwave background is isotropic simplifies the problem still further, so that it involves only the 3-dimensional Euclidean linear algebra of vectors and tensors orthogonal to t^a. It is in this familiar context, and with this background in mind, that I present my discussion of the role of the electric and magnetic parts in the distortion effect.

The key result of this discussion is that only the magnetic part of the Weyl curvature contributes to the antipodal asymmetry of the distortion effect. I touch briefly on the propects for observing such an asymmetry in Section 3, which also contains my concluding remarks.

2 The Electric and Magnetic Parts of the Weyl Curvature and the Distortion Effect

In this section, a small number of simple mathematical objects play an important role. The first of these, and the most basic, is a real, 4-dimensional vector space, V. Physically, V is just the tangent space to the spacetime we inhabit, at the present moment of our history. As such, it is of course home to a Lorentz-signature inner product, g_{ab}—the second

object on our list. The third object is a timelike unit vector, t^a, which, as I mentioned in the previous section, represents the frame of reference in which the microwave background radiation is isotropic. The fourth and final object may not seem so simple at first glance. It is a tensor $C_{abc}{}^d$ over V that satisfies

$$C_{(ab)c}{}^d = 0, \tag{2.1}$$

$$C_{[abc]}{}^d = 0, \tag{2.2}$$

$$C_{abc}{}^b = 0, \qquad \text{and} \tag{2.3}$$

$$C_{ab(c}{}^e g_{d)e} = 0. \tag{2.4}$$

This tensor of course represents the Weyl curvature of spacetime at our current location. I shall try to show by the end of this section that despite the complicated index permutation symmetry and trace conditions 2.1– 2.4 to which it is subject, the local Weyl curvature is indeed a simple mathematical object—and one with a beautiful physical interpretation.

To achieve this goal, however, I must first define from the members of the quadruple $(V, g_{ab}, t^a, C_{abc}{}^d)$ a variety of related vector spaces and tensors. Let me begin with those that involve only V, g_{ab}, and t^a. First, because t^a is timelike and unit, $T_a{}^b := -t_a t^b$ and $S_a{}^b := \delta_a{}^b - T_a{}^b$ are both projection operators. The range of $S_a{}^b$, a 3-dimensional vector space $S \subset V$, consists precisely of those vectors in V that are orthogonal to t^a. Tensors over S, when viewed as tensors over V, satisfy

$$K^{a\cdots b}_{c\cdots d} = S^a_m \cdots S^b_n S^p_c \cdots S^q_d K^{m\cdots n}_{p\cdots q}; \tag{2.5}$$

I shall call such tensors *spatial*. An example of a spatial tensor is $S_a{}^b$ itself. Two further examples are

$$h_{ab} = g_{ab} + t_a t_b, \qquad \text{and} \tag{2.6}$$

$$\epsilon_{abc} = \epsilon_{abcd} t^d, \tag{2.7}$$

(Here $\epsilon_{abcd} = \epsilon_{[abcd]}$ is the volume element determined by g_{ab}.) The first of these two tensors is the spatial metric; the second is the volume element it determines.

Now let me bring $C_{abc}{}^d$ into the picture. This I do by setting

$$E_{ab} = C_{amb}{}^n T_n{}^m, \qquad \text{and} \tag{2.8}$$

$$B_{ab} = {*C}_{amb}{}^n T_n{}^m, \tag{2.9}$$

where ${*C}_{abc}{}^d = 1/2\epsilon_{ab}{}^{mn} C_{mnc}{}^d$ denotes the dual of the Weyl curvature. As the notation suggests, E_{ab} and B_{ab} are the *electric and magnetic parts* of $C_{abc}{}^d$. It is easy to check that

E_{ab} and B_{ab} are both spatial tensors, and that taken together they completely determine $C_{abc}{}^{d}$: $E_{ab} = B_{ab} = 0$ if and only if $C_{abc}{}^{d} = 0$. This makes it possible to re-express in terms of E_{ab} and B_{ab} the full content of the conditions 2.1- 2.4 on $C_{abc}{}^{d}$:

$$E_{[ab]} = 0, \tag{2.10}$$

$$E_{ab}h^{ab} = 0, \tag{2.11}$$

$$B_{[ab]} = 0, \quad \text{and} \tag{2.12}$$

$$B_{ab}h^{ab} = 0. \tag{2.13}$$

The upshot of all this is that the quadruple $(V, g_{ab}, t^{a}, C_{abc}{}^{d})$ has now outlived its usefulness. Everything there is to be said about Weyl curvature can now be said in terms of the simpler quadruple $(S, h_{ab}, E_{ab}, B_{ab})$, in which S is a real, 3-dimensional vector space, h_{ab} is a positive-definite inner product on S, and E_{ab}, B_{ab} are trace-free, symmetric tensors over S. From now on, therefore, I shall work entirely within this simpler context (e.g., all tensors will now be tensors over S, h_{ab} will be used exclusively to raise and lower indices, etc.)

Physically, the vector space S represents the instantaneous rest space of an observer at our current spacetime location who sees no anisotropy in the cosmic microwave background radiation. A unit vector $r^{a} \in S$ therefore represents a direction in which such an observer might point his telescope to investigate cosmological image distortions. The set of all such unit vectors is simply his *celestial sphere*. The tangent space to this sphere at the point r^{a}, which I shall call P_{r}, is the *plane of the sky in the direction* r^{a}; it consists precisely of those vectors $x^{a} \in S$ that are orthogonal to r^{a}.

Now of course the inner product h_{ab} on S defines an inner product $s_{ab} := h_{ab} - r_{a}r_{b}$ on P_{r}. But even more importantly, it defines a linear mapping $J_{a}{}^{b}$, as follows:

$$J_{a}{}^{b} := r^{c}\epsilon_{ca}{}^{b}. \tag{2.14}$$

It is easy to check that this mapping preserves s_{ab}, and so represents a rotation in the plane of the sky. It is also easy to check that

$$J_{a}{}^{c}J_{c}{}^{b} = -(\delta_{a}{}^{b} - r_{a}r^{b}). \tag{2.15}$$

This equation shws that $J_{a}{}^{b}$ is a *complex structure* on the plane of the sky. $J_{a}{}^{b}$ lets us define *complex* multiples of vectors $x^{a} \in P_{r}$, according to the formula

$$(m + in)x^{a} = mx^{a} + nJ_{b}{}^{a}x^{b}. \tag{2.16}$$

$J_a{}^b$ also plays a crucial role in the formation of the tensor

$$W_{ab} := 2(e_{ab} - J_a{}^c b_{bc}) \tag{2.17}$$

from the trace-free, symmetric 2-tensors e_{ab} and b_{ab} in the plane of the sky. These 2-tensors are simply the trace-free parts of the projections of E_{ab} and B_{ab} into the plane of the sky:

$$e_{ab} := (\delta_a{}^m - r_a r^m)(\delta_b{}^n - r_b r^n)E_{mn} + 1/2 s_{ab}(r^m r^n E_{mn}), \tag{2.18}$$

$$b_{ab} := (\delta_a{}^m - r_a r^m)(\delta_b{}^n - r_b r^n)B_{mn} + 1/2 s_{ab}(r^m r^n B_{mn}). \tag{2.19}$$

It turns out that W_{ab} is also trace-free and symmetric as a 2-tensor in the plane of the sky, and the calculation that establishes this reveals an interesting fact: the tensor J_a^b also defines a complex structure on the vector space of trace-free, symmetric 2-tensors on the plane of the sky. The formula for making complex multiples of these tensors parallels 2.16:

$$(m + in)x_{ab} = mx_{ab} + nJ_a{}^c x_{bc}. \tag{2.20}$$

W_{ab} is therefore an element of a 1-dimensional complex vector space—essentially just a single complex number—and the tensors $2e_{ab}$, $-2b_{ab}$ are just its real and imaginary parts.

Now, the tensor W_{ab} is important for two reasons, one mathematical and one physical. Let me give the mathematical reason first: $W_{ab} = 0$ if and only if the vector r^a points in what is called a *principal null direction* of the Weyl curvature. (For a proof, see [3].) For a non-zero Weyl curvature, there can be at most four such directions, so if $W_{ab} = 0$ for *all* r^a in the celestial sphere, then $E_{ab} = B_{ab} = 0$. This shows that the tensor *field* $r^a \mapsto W_{ab}(r^a)$ determines the Weyl curvature uniquely.

Now let me give the physical reason. Kristian and Sachs have shown that the function

$$e(i^a) := i^a i^b W_{ab} \tag{2.21}$$

achieves its maximum exactly when the unit vector i^a in the plane of the sky points in the direction of maximum Weyl curvature-induced image distortion. This fact, together with the decomposition 2.17 of W_{ab} into its electric and magnetic parts, enables us to see easily how each of these parts contributes to the overall distortion effect.

For my purposes here, one simple fact is crucial: under the replacement $r^a \mapsto -r^a$, the tensor $J_a{}^b$ picks up a minus sign, while both e_{ab} and b_{ab} remain unchanged. From this it follows that the 'magnetic term' in W_{ab} is antipodally asymmetric, while the 'electric term' introduces no antipodal asymmetry whatever. I conclude that if the direction of maximum Weyl curvature-induced image distortion differs at any pair of antipodal points on the celestial sphere, the B_{ab} must be non-zero.

3 Discussion

Let me make just two short remarks, one mathematical and one observational, before I close.

First, the mathematical remark. Although it may not have been obvious, I needed for the analysis of the Weyl curvature $C_{abc}{}^{d}$ that I presented in the previous section only two of the various mathematical structures I ascribed to V. These two essential structures were the 1-dimensional timelike vector space $T \subset V$ to which t^a belongs, and the conformal equivalence class $[g_{ab}]$ to which g_{ab} belongs. This equivalence class makes possible the construction of the tensor field $r^a \mapsto W_{ab}(r^a)$, while the subspace T underlies its decomposition into 'real and imaginary parts.' For further details, see [3].

Second, the observational remark. I have learned in a recent conversation with Professor James E. Gunn of Princeton that the telescopes needed to conduct the image distortion observations of Tyson, Valdes, and Wenk are available in both hemispheres, so that a direct check for antipodal asymmetry in the distortion effect seems possible. Professor Gunn emphasized, however, that the observations of Tyson et al. are very difficult, and that their analysis requires the separation of a very small signal from a very noisy background. The deduction of non-zero magnetic Weyl curvature from such observations might therefore remain controversial for some time.

Acknowledgements

I should like to thank Professor Kei-ichi Maeda of Waseda University for inviting me to speak at this conference, and for agreeing to act as my sponsor under the terms of a fellowship from the Japan Society for the Promotion of Science, whose support I gratefully acknowledge.

References

[1] Kristian, J., and Sachs, R. K., "Observations in Cosmology," Ap. J. **143**(1966), pp.379-99.

[2] Tyson, J. A., Valdes, F., and Wenk, R. A., "Detection of Systematic Gravitational Lens Galaxy Image Alignments: Mapping Dark Matter in Galaxy Clusters," Ap. J. **349**(1990), pp.L1-4.

[3] Gunnarsen, L. D., "Electric and Magnetic Parts of the Weyl Curvature and Principal Null Directions," in preparation.

Topology Changing Solutions of (2+1)-Dimensional Einstein-Yang-Mills Equation

AKIO HOSOYA†

Department of Physics, Tokyo Institute of Technology, Oh-Okayama Meguroku, Tokyo 152, Japan

ABSTRACT

We present an explicit Riemannian solution of classical field equations in the (2+1)-dimensional Einstein-Yang-Mills model with zero or positive cosmological constant. From this solution we can construct various examples of topology changing processes by quantum tunneling in the WKB approximation.

† E-mail address: ahosoya@cc.titech.ac.jp

1. Introduction

In the previous works[1], we have demonstrated explicit examples of topology changing processes by quantum tunneling in the (2+1)-dimensional Einstein gravity with negative cosmological constant in the WKB approximation.

There the tunneling is assumed to be described by a transition between Euclidean and Lorentzian signature regions. Using the hyperbolic geometry we have constructed 3-geometries of Euclidean signature which has totally geodesic boundaries with various topologies. Many Lorentzian signature universes are smoothly glued at the boundaries of the Euclidean signature manifold. The universes are actually Riemann surfaces of genus larger than or equal to two. In the semi-classical picture, this exhibits topology changes and/or branchings of universes.

As shown by Gibbons and Hartle[2], topology change by semi-classical tunneling is impossible if the Euclidean energy-momentum tensor satisfies the positive energy condition. In this sense, our previous model is an extreme case; the energy density is everywhere negative. In this paper we are going to consider gauge fields instead of cosmological constant as an ingredient which drives topology changes, since gauge fields can generally give negative energy density in the Euclidean signature space-time. There the cosmological constant can be either zero or positive.

In contrast with the previous model we have a continuous degrees of freedom for each isospin component of gauge fields, which represents an isotriplet massless mode. In this work we will just put it equal to zero to seek a particular solution.

2. The Model

Our model is the (2+1)-dimensional Einstein-Yang-Mills theory described by the Euclidean action:

$$S_E = -\frac{1}{16\pi G}\int (R - 2\Lambda)\sqrt{g}\; d^3x + \frac{1}{4}\int g^{\mu\nu} g^{\rho\sigma} F^a_{\mu\rho} F^a_{\nu\sigma}\sqrt{g}\; d^3x. \qquad (1)$$

with G and Λ being the Newton constant and the cosmological constant, respectively, in the (2+1)-dimensional space-time. R denotes the scalar curvature and the field strength $F^a_{\mu\nu}$ is given by

$$F^a_{\mu\nu} = \partial_\mu A^a_\nu - \partial_\nu A^a_\mu + e\epsilon^{abc} A^b_\mu A^c_\nu, \qquad (2)$$

in terms of the $SO(3)$ gauge field A^a_μ with e and ϵ^{abc} being the gauge coupling constant and the structure constant of $SO(3)$, respectively. The gauge group can be trivially generalized to any compact Lie groups, which contains $SO(3)$ as a subgroup.

Upon varying the action (1), we obtain the Einstein equation:

$$\begin{aligned} R_{\mu\nu} - \frac{1}{2} g_{\mu\nu} R &= 8\pi G T_{\mu\nu} - \Lambda g_{\mu\nu}, \\ T_{\mu\nu} &= F^a_{\mu\rho} F^{a\rho}_{\nu} - \frac{1}{4} g_{\mu\nu} (F^a_{\rho\sigma})^2 \end{aligned} \qquad (3)$$

and the Yang-Mills equation:

$$D^\mu F^a_{\mu\nu} = 0. \qquad (4)$$

3. Solution

We make an ansatz for the metric and the field strength as

$$g_{\mu\nu} = \Omega^2 \delta_{\mu\nu}, \tag{5}$$

$$F^a_{\mu\nu} = \epsilon_{a\mu\nu} f, \tag{6}$$

where Ω and f are functions of $r^2 = (x^1)^2 + (x^2)^2 + (x^3)^2$ only. Then the energy-momentum tensor becomes

$$T_{\mu\nu} = \frac{1}{2}\Omega^{-2} f^2 \delta_{\mu\nu}. \tag{7}$$

We demand the energy-momentum tensor $T_{\mu\nu}$ be proportional to the metric tensor $g_{\mu\nu}$, since we want a constant curvature space as in the previous work. Namely we set

$$T_{\mu\nu} = \frac{\Lambda\!\!\!^{\prime}}{8\pi G} g_{\mu\nu} = \frac{\Lambda\!\!\!^{\prime}}{8\pi G} \Omega^2 \delta_{\mu\nu} \tag{8}$$

Comparing the above two expressions for the energy-momentum tensor (7) and (8) we obtain

$$f = \sqrt{\frac{\Lambda\!\!\!^{\prime}}{4\pi G}}\,\Omega^2, \tag{9}$$

provided that $\Lambda\!\!\!^{\prime}$ is positive. Later we will confirm that this is indeed the case when the parameter $\Lambda\!\!\!^{\prime}$ is determined by the gauge coupling constant e and the bare cosmological constant Λ.

The Einstein equation now reduces to

$$R_{\mu\nu} - \frac{1}{2} g_{\mu\nu} R = -\bar{\Lambda} g_{\mu\nu} \tag{10}$$

with

$$\bar{\Lambda} = \Lambda - \Lambda\!\!\!^{\prime}$$

. Under the ansatz (5) the solution is given by the Poincaré metric

$$\Omega = \frac{2}{1 + \bar{\Lambda} r^2} \tag{11}$$

provided that $\bar{\Lambda}$ is negative. We will find such a solution in due course.

Let us recall that the Lorentzian energy-momentum tensor is *minus* of the Wick rotation of the Euclidean energy-momentum tensor. So our solution corresponds to the negative energy density as we can recognize this from the signs in front of Λ' and Λ in the expression for the effective cosmological constant.

We are now going to attack the Yang-Mills equation (4). For the vector potential A^a_μ we make an ansatz:

$$A^a_\mu = \epsilon_{a\mu\nu} x^\nu K(r^2). \tag{12}$$

The field strength $F^a_{\mu\nu}$ becomes

$$F^a_{\mu\nu} = -2\epsilon_{a\mu\nu}(K + r^2 K') + \epsilon_{\mu\nu\rho} x^a x^\rho (2K' + eK^2). \tag{13}$$

Comparing (6) (11) and (13), we have $2K' + eK^2 = 0$ and obtain the solution for K and then f as

$$K = \frac{-2}{c - er^2} \tag{14}$$

$$f = \frac{4c}{(c - er^2)^2}, \tag{15}$$

where c is an integration constant. Note that $c > 0$ for the negative effective cosmological constant $\bar{\Lambda}$ as can be seen from FA (11) and (15). The Yang-Mills equation (3) now reduces to

$$\delta^{\rho\sigma} D_\rho F^a_{\sigma\mu} = \epsilon_{a\lambda\mu} x^\lambda (f' + eKf) \tag{16}$$

The right-hand-side of (16) automatically vanishes because of (14) and (15).

Consistency of Eqs.(9) and (15) gives following relations between the parameters $\Lambda\prime$ and c in our solution as

$$-e/c = \bar{\Lambda} = \Lambda - \Lambda\prime \tag{17}$$

$$1/c = \sqrt{\frac{\Lambda\prime}{4\pi G}}. \tag{18}$$

The effective cosmological constant is now given by

$$\bar{\Lambda} = -\alpha - \sqrt{(\Lambda+\alpha)^2 - \Lambda^2} \tag{19}$$

with $\alpha = e^2/8\pi G$. We have chosen the branch of the square root so that the effective cosmological constant $\bar{\Lambda}$ is negative. If we take the other branch, the effective cosmological constant would be positive which we do not want, because such a positive cosmological constant space-time cannot exhibit any topology change as previously remarked. Note also that the bare cosmological constant Λ should be positive in order for the inside of the square root to be positive.

Our solution is summarized as

$$g_{\mu\nu} = \frac{4}{(1+\bar{\Lambda}r^2)^2}\delta_{\mu\nu}, \tag{20}$$

$$A^a_\mu = \epsilon_{a\mu\nu}x^\nu \sqrt{\frac{\Lambda\prime}{4\pi G}}\frac{(-2)}{1+\bar{\Lambda}r^2} \tag{21}$$

$$F^a_{\mu\nu} = \epsilon_{a\mu\nu}\sqrt{\frac{\Lambda\prime}{4\pi G}}\frac{4}{(1+\bar{\Lambda}r^2)^2}, \tag{22}$$

where

$$\Lambda\prime = \Lambda + \alpha + \sqrt{(\Lambda+\alpha)^2 - \Lambda} \tag{23}$$

with $\alpha = e^2/8\pi G$.

4. Construction of 3-manifold

Having found that our Euclidean signature space-time is hyperbolic, we can construct a 3-manifold with totally geodesic boundary in the exactly same way as in the previous works. There we used regular truncated polyhedra as building blocks and glued them together at the faces by a certain gluing rule.

Here we show the simplest example for an illustration which represents the birth of a double torus universe from nothing[4].

We construct this by appropriately gluing two regular truncated tetrahedra together which are embedded in the Kleinian model[3]. In the Kleian model any geodesic is a Euclidean straight line. Next we truncate each vertex of the tetrahedron . It can be verified that there is a unique 2-plane which is perpendicular to all of the three faces with the vertex in common. We cut the four vertices of the tetrahedron along these planes to get a regular truncated tetrahedron embedded completely in the Kleinian model. This embedding induces a metric on the regular truncated tetrahedron.

We prepare two such regular truncated tetrahedra . Then we identify each pair of the faces so as to match the arrows indicated in the Figure and identify all the edges. This gives a topological 3-manifold with a boundary of double torus.

The metric $g_{\mu\nu}$ is perfectly regular everywhere. The field strength contracted with dreibeins $e^{\mu}_{a} = \delta^{\mu}_{a}\Omega^{-1}$

$$F^{a}_{bc} = e^{\mu}_{b} e^{\nu}_{c} F^{a}_{\mu\nu} = \epsilon_{abc}\sqrt{\frac{\Lambda\prime}{4\pi G}} \tag{24}$$

is a constant tensor with an isospin index (a)and two frame indices (b,c). The observable quantity F^{a}_{bc} is invariant under the simultaneous local rotation of the frame and the isospin. Therefore in the gluing procedure the identification of faces of the polyhedra can be achieved by a suitable isometry transformation together with gauge transformation.

This completes the construction.

As is well known, such a Euclidean signature manifold can be interpreted as a quantum tunneling in the WKB approximation in quantum gravity. The tunneling amplitude is calculated as

$$T = N \exp\left(-\frac{1+\frac{|\bar{\Lambda}|}{\alpha}}{4\pi G\sqrt{|\bar{\Lambda}|}}V\right). \tag{25}$$

with V being the hyperbolic volume of the 3-manifold in the unit $|\bar{\Lambda}| = 1$. The minus of the exponent is the Euclidean classical action calculated from our instanton solution. The second term in the exponent represents the effect of the gauge fields, which also modifies the value of the effective cosmological constant as we have already seen.

5. Summary and Discussions

We have obtained a Euclidean classical solution in the (2+1)-dimensional Einstein-Yang-Mills system, which exhibits topology changing processes by quantum tunneling in the WKB approximation.

One will naturally ask; what kind of universes can emerge after tunneling in the Lorentzian signature region? As we previously remarked the boundary surface of the hyperbolic 3-manifold is an initial surface from which the real universe evolves in our picture. the issue is : what is the initial gauge configuration when the universe gets out of the tunnel?

As a final remark, we would like to point out that our present solution is in a sense a three dimensional analogue of the wormhole instanton solution in the Einstein-Yang-Mills system[5].

ACKNOWLEDGMENTS

We are greatly indebted to Y. Fujiwara, S. Higuchi, T. Mishima and S. Siino for useful discussions. The author thanks Professor K. Song at the Dalien University of Technology and Professor L. Liao at the Beijing Normal University for their warm hospitality during the period when this work was initiated. This work is supported in part by the Grant-in-Aid for Scientific Research for the Ministry of Education, Science and Culture No.02640232 (A. H).

REFERENCES

1. Y. Fujiwara, S. Higuchi, A. Hosoya, T. Mishima, M. Siino, *Phys. Rev.* **D44** (1991) 1756,1763 .
2. G. W. Gibbons and J. B. Hartle, *Phys. Rev.* **D42** (1990) 2458.
3. W. P. Thurston, *The Geometry and Topology of 3-manifolds*, to be published by Princeton University Press, 1978/79.
4. J. B. Hartle and S. Hawking, *Phys. Rev.* **D28** (1983) 2960.
5. A. Hosoya and W. Ogura, *Phys. Lett.* **225B** (1989) 117.

Topology change in Witten gravity

Kaoru AMANO

Department of Physics
Tokyo Institute of Technology
Meguro, Tokyo, 152 JAPAN

1. Introduction

2+1 dimensional pure gravity as reformulated by E. Witten [1] provides a computable model for quantum gravity. Witten also shows how his formalism extends to cope with topology changing amplitudes [2]. We show that these amplitudes vanish for certain combinations of 2-space topologies in initial and final states if we require them to be spacelike [3].

Gravity in Witten's formulation, or Witten gravity, is almost identical with (2+1)-dimensional Einstein gravity. Formally the action for Witten gravity is the Einstein-Hilbert action written in terms of dreibein e^a and spin connection $\omega_{ab} = -\epsilon_{abc}\omega^c$:

$$S = \int_M e^a(d\omega_a + \frac{1}{2}\epsilon_{abc}\omega^b\omega^c). \tag{1.1}$$

The main difference from the Einstein theory is that the dreibein e^a is neither restricted to one orientation nor required to be non-degenerate. The action (1.1) with the extended domain of variables has a greater symmetry than the formally identical Einstein-Hilbert action has. These peculiarities will be generally ignored in the following sections for the sake of simplicity.

A basic assumption to be made in order to deal with topology change is that the amplitude is obtained by taking an appropriate compact orientable manifold M with boundary and performing a path integral, or by summing such integrals. Let closed orientable surfaces $\Sigma_1, \ldots \Sigma_N$ be the connected components of the

boundary of M. The amplitude for the transition among the 2-spaces Σ_j via M is given by the path integral

$$\mathcal{I}_M(\omega_1,\ldots,\omega_N) = \int_{\omega=\omega_j \text{ on } \Sigma_j} D\omega \int De \, \exp iS. \tag{1.2}$$

The ω_j are connections on Σ_j, by which we have set boundary conditions for the ω integrated over. This corresponds to taking a representation in which boundary states are given as functionals of the restriction of ω to the boundary. The integral over e can easily be done to give,

$$\mathcal{I}_M(\omega_1,\ldots,\omega_N) = \int_{\omega=\omega_j \text{ on } \Sigma_j} D\omega \; \delta[d\omega + \omega\omega], \tag{1.3}$$

where the delta functional has its support on flat ω. This shows that the amplitude is non-zero for some $(\omega_1,\ldots,\omega_N)$ if and only if there exists a flat ω over M. However, any M admits flat ω. It follows that there are processes with non-vanishing amplitudes for an arbitrary combination of closed orientable 2-spaces. Topology change is quite arbitrary at this level.

The situation alters if we require $\mathcal{I}_M$ to represent an amplitude for transition among space-times with spacelike slices. We shall see that under this condition, the range for (e,ω) can be non-empty only for restricted combinations of 2-space topologies: The Euler characteristics χ_j of the 2-spaces Σ_j must admit some sign assignment $\epsilon_j = \pm$ such that they obey the relation

$$\sum_{j=1}^{N} \epsilon_j \chi_j = 0. \tag{1.4}$$

2. The space condition

First we note that any dreibein-spin connection pair (e,ω) comes with a principal bundle P of the (2+1)-dimensional Lorentz group. That is to say, ω and $\omega+e$ are connections in P. To be precise, in this work we take the structure group to be the maximal connected subgroup G of the Lorentz group; G is the group of the Lorentz transformations that preserve orientation and time orientation.*

So P is the G bundle over M associated with (e,ω). Let Σ be a closed orientable surface (of genus g) embedded in M. Suppose the dreibein e is spacelike. That is, the dreibein e is non-degenerate on Σ and induces a positive definite metric on the surface. Then the Euler class of the portion $P|_\Sigma$ of P over Σ is given by

$$eul(P|_\Sigma) = \pm\chi_\Sigma, \tag{2.1}$$

where $\chi_\Sigma = 2-2g$ is the Euler characteristic of Σ. In fact, by the assumption we can choose local sections of $P|_\Sigma$ so that e^0 is a normal 1-form to Σ. This implies that $P|_\Sigma$ reduces to the bundle of oriented orthonormal tangent frames to Σ, which has Euler class $\pm\chi_\Sigma$ (the sign depending on the orientation of the tangent frames). Hence eq.(2.1).

We call eq.(2.1) the space condition on Σ. Obviously, Σ being spacelike will mean there are other (infinitely many) spacelike slices of the space-time around Σ. Here is a related fact on the space condition. Let N be an arbitrary neighbourhood N of Σ diffeomorphic to $I\times\Sigma$ with $\{t\}\times\Sigma$ at some t of the interval I identified with $\Sigma\subset M$. The portion of P over N is determined by $P|_\Sigma$, and its basic structure is invariably the same over different slices of the cylinder N. If the space condition is satisfied on a slice then the condition is satisfied on any other slice of N.

---

* This is a non-trivial assumption. In particular it implies that e defines a time-oriented metric on the (necessarily orientable) submanifold obtained by excluding the points at which e is degenerate.

3. The selection rule

We propose to impose the space condition on each Σ_j in eq.(1.2). This will be necessarily satisfied for any amplitude of transitions among space-times with spacelike slices. Therefore the range of (e,ω) for such an amplitude has to be restricted at least to those belonging to G bundles obeying the space condition (2.1) for every boundary 2-space Σ_j. We assert that (1.4) holds if the range is non-empty.

Suppose there exists a G bundle P over M that satisfies the space conditions on the boundary and denote $P_j = P|_{\Sigma_j}$. We can reduce P to an $SO(2) \approx U(1)$ bundle Q. Picking an arbitrary $U(1)$ connection ν in Q and using the Gauss-Bonnet formula on the boundary components, we obtain

$$\sum_{j=1}^{N} eul(P_j) = \frac{1}{2\pi i}\int_{\partial M} d\nu = 0. \tag{3.1}$$

We used the orientation of Σ_j induced from M for convenience. Eq.(1.4) follows from eq.(3.1) with the space condition $eul(P_j) = \pm\chi_j$.

4. Comments

We have shown that if there is a topology change involving at initial and final ends only space-times with spacelike slices, then the 2-space topologies at the ends must satisfy the rule (1.4) with some sign assignment $\epsilon_j = \pm$. Surely this selection rule is non-trivial. For example, it forbids two genus one surfaces ($\chi_1 = \chi_2 = 0$) turning into a genus two surface ($\chi_3 = -2$). A generalization of this example is given by Σ_j of genus $g_j \geq 1$, with $g_N = g_1 + g_2 + \cdots + g_{N-1}$, $N \geq 3$. Then $|\chi_N| > \sum_{j=1}^{N-1} |\chi_j|$, so eq.(1.4) cannot be satisfied.

The selection rule does not eliminate the possibility of topology altogether. There are also an infinite number of combinations of surface topologies that satisfy eq.(1.4). Moreover, ref.[3] shows that for any such combinations one can

construct a connected M bounded by the surfaces and a flat G connection ω on M.

In deriving the selection rule we made no essential use of the form of the action or other peculiarities of Witten gravity. The validity of our rule extends to other Lorentzian theories of (2+1)-dimensional gravity. In particular, the relation (1.4) constitutes part of the selection rule of Sorkin [4], which assumes Lorentzian cobordism as the mechanism for topology change.

Finally we note that although we talked about transitions, we did not distinguished between initial 2-spaces and final ones. Perhaps we should integrate over different ranges of (e, ω) depending on what way 2-spaces are divided into initial and final sets. It is not clear if such a distinction can be consistently made in Witten gravity because degenerate dreibeins form an integral part of the formalism.

Acknowledgment

I thank Saburo Higuchi, my co-author of the paper [3] on which this talk is based.

REFERENCES

1. E. Witten, Nucl. Phys. B311 (1988/89) 46
2. E. Witten, Nucl. Phys. B323 (1989) 113
3. K. Amano and S. Higuchi, Tokyo Institute of Technology preprint TIT/HEP-178 (1990)
4. R. D. Sorkin, Phys. Rev. D33 (1986) 978

The Perturbation of the Higher Genus Spatial Surface in (2+1)-Dimensional Gravity

Takashi Okamura

Department of Physics, Kyoto University, Kyoto 606, Japan

Hideki Ishihara

Department of Physics, College of Liberal Arts and Science, Kyoto university, Kyoto 606, Japan

The dynamics of spatial surface with genus $g \geq 2$ in (2+1)-dimensional pure Einstein gravity is studied by the perturbation analysis around the static moduli solution. We find that the action of the perturbed Teichmüller parameters has a harmonic oscillator form with time dependent mass and frequency. It is also shown that the set of the static moduli solutions is an attractor of nearby solutions.

1. Introduction

Many physicists have been interested in a spacetime with a non-trivial topology. For understanding the spacetime as a whole, we must study not only local but also global structure of the spacetime. In usual studies of general relativity, the local structure is analyzed while the global structure is fixed. Here, we would like to shed light on the dynamics of the global structure in this paper.

We study, as a toy model, the vacuum Einstein theory in 3-dimensional spacetime that has no Weyl tensor, *i.e.*, no local dynamical degrees of freedom but finite number (depending on the genus of closed spatial 2-surface) of global degrees of freedom. This fact reduces the technical difficulty. We hope that the global structure in 3-dimensional spacetime mimics the same one in 4 dimensional spacetime essentially. And we will use the conventional ADM approach[1] which is applicable to any dimension and has the clear geometrical meanings. Hosoya and Nakao[2] [3] derived the global deformations of torus-like spatial 2-surface in 3-dimensional pure gravity by the ADM approach. In this case, the Teichmüller parameters move along the geodesics of the Weil-Petersson metric that is naturally defined on the Teichmüller space.

In the higher genus cases, $g \geq 2$, though it is known that there exists the unique solution of constraints,[4] we have not derived the global degrees of freedom yet. The reason is as follows: To derive finite global degrees of freedom from infinite variables, we must solve momentum and Hamiltonian constraints. However, we cannot generally solve Hamiltonian constraint analytically.[2][5] As only exception, we have homogeneous expansion solutions without global deformations, *static moduli solutions.*[3]

In this paper, for the first step to investigate the dynamics of spatial 2-surface with $g \geq 2$, we perform the perturbation analysis around the static moduli solutions. We find that the second order perturbed action for the Teichmüller parameters has a harmonic oscillator form with time dependent mass and frequency. By solving the equation of motion derived from the action, it will be shown that the set of the static moduli solution is an attractor of nearby solutions. This fact is quite different from vacuum torus case.

2. The static moduli solution

The spacetime metric of the static moduli solutions is as follows;

$$ds^2 = -N^2 dt^2 + a(t)^2 dl^2 \ , \tag{2.1}$$

$$dl^2 = \frac{4(dr^2 + r^2 d\theta^2)}{(1-r^2)^2} \equiv \gamma_{ij} dx^i dx^j \ , \tag{2.2}$$

$$a = -\frac{2}{\tau} \quad \text{and} \quad N dt = \frac{2}{\tau^2} d\tau. \tag{2.3}$$

Eq.(2.2)is the line element of Poincaré disk, which is the negative constant curvature space and the covering space of arbitrary genus ($g \geq 2$) closed surface with any moduli.

The spacetime with Eq.(2.1)is nothing but the Milne universe. The closed Riemann surface with an arbitrary genus is obtained by identifying the points in Poincaré disk by Fuchsian group acting on the disk. The comoving coordinate values of the identified points do not change in time. Therefore the spatial 2-surface is stretched by $a(t)$ and the moduli does not change in time. Thus, we call these solutions static moduli solutions. The moduli is determined by the choice of Fuchsian group.

3. The Perturbation Analysis

As seen in the previous section we can construct static moduli solutions easily in the case of the higher genus case ($g \geq 2$) with arbitrary moduli. We perform the perturbation analysis around these solutions.

We divide the variables into background and perturbation parts as

$$\begin{aligned} N &= \hat{N} + n \ , \qquad N_i = \hat{N}_i + n_i \ , \\ h_{ij} &= a^2(t)(\gamma_{ij} + Q_{ij}) \ , \qquad \pi^{ij} = a^{-2}(t)(\hat{\pi}^{ij} + P^{ij}) \ . \end{aligned} \tag{3.1}$$

Hereafter we assign "*hat*" to the background quantities.

Because the background spacetime is spatially homogeneous and isotropic, we can deal with scalar, vector and tensor perturbation separately.[6] So we can derive the part of tensor perturbation, which includes the informations of the global modes, from the total perturbed action;

$$S_2^{red} = \int d^3x (P_{TT}^{ij} \dot{Q}_{ij}^{TT} - H_{(2)}^{red}) \ , \tag{3.2}$$

$$H_{(2)}^{red} = \frac{\hat{N}}{a^2} \left(\frac{P_{TT}^{ij} P_{ij}^{TT}}{\sqrt{\gamma}} + \frac{a^2 \sqrt{\gamma}}{2} Q_{ij}^{TT} Q_{TT}^{ij} - 2a^2 \frac{\hat{H}}{\hat{N}} P_{TT}^{ij} Q_{ij}^{TT} \right) \ , \tag{3.3}$$

$$P_{TT|j}^{ij} = Q_{ij}^{TT|j} = 0 \ , \tag{3.4}$$

$$P_{TTi}^{i} = Q_{TTi}^{i} = 0 \ , \tag{3.5}$$

where indices are raised or lowered by γ_{ij} and the stroke is the covariant derivative with respect to γ_{ij}.

It is worthwhile to note that in the action Eq.(3.2), the perturbation of spatial curvature term in the full Hamiltonian does not contribute because $\hat{N}$ is spatially constant.[7] Therefore the dynamics of the perturbation is fully determined by the kinetic term of the full Hamiltonian, *i.e.*, the structure of the superspace.

It is known that any TT-tensor on the closed orientable 2-surface with genus g(≥ 2) is expanded by finite basis $\{\phi^{(\alpha)ij}; \alpha = 1, 2, ..., 6g-6\}$.

$$P^{ij}_{TT} = \sqrt{\gamma}\sum_{\alpha} P_{(\alpha)}(t)\phi^{(\alpha)ij}(x)/2V \ , \tag{3.6}$$

$$Q^{ij}_{TT} = \sum_{\alpha} \hat{g}_{(\alpha)(\beta)}Q^{(\alpha)}(t)\phi^{(\beta)ij}(x) \ , \tag{3.7}$$

where $V \equiv \int d^2x\sqrt{\gamma}$. And

$$\hat{g}^{(\alpha)(\beta)} = \int d^2x\sqrt{\gamma}\phi^{(\alpha)}_{ij}\phi^{(\beta)}_{kl}\gamma^{ik}\gamma^{jl}/2V$$

is the Weil-Petersson metric of the background Teichmüller parameters about γ_{ij}, which are independent of time. Finally, we obtain the action of the perturbed Teichmüller parameters;

$$S^{red}_2 = \int dt[P_{(\alpha)}\dot{Q}^{(\alpha)} - \frac{\hat{N}}{2Va^2}\{\hat{g}^{(\alpha)(\beta)}P_{(\alpha)}P_{(\beta)} + 2V^2a^2\hat{g}_{(\alpha)(\beta)}Q^{(\alpha)}Q^{(\beta)}$$

$$-4a^2V\frac{\hat{H}}{\hat{N}}P_{(\alpha)}Q^{(\alpha)}\}] \ . \tag{3.8}$$

The equations of motion are

$$\frac{1}{\hat{N}}\frac{d}{dt}(\frac{\dot{Q}^{(\alpha)}}{\hat{N}} + 2\frac{\hat{H}}{\hat{N}}Q^{(\alpha)}) + \frac{2}{a^2}Q^{(\alpha)} = 0 \ , \tag{3.9}$$

and its solution in the proper time gauge ($\hat{N} = 1$) is

$$Q^{(\alpha)} = A^{(\alpha)} + \frac{B^{(\alpha)}}{t} \ , \tag{3.10}$$

where $A^{(\alpha)}$ and $B^{(\alpha)}$ are arbitrary constants. If the scale factor $a(t)$ were constant, the above action (3.8) is just the harmonic oscillator form, but due to the background expansion

$a(t) = t$, the solution approaches to a constant value asymptotically. In other words, every perturbed solution around a static moduli solution evolves towards another static moduli solution. In the framework of the perturbation of the static moduli solutions, it is found that the set of the static moduli solutions is an attractor of nearby solutions because of rapid background expansion. In torus case with a positive cosmological constant, we can find the similar behavior, unlike in vacuum torus case.[8]

ACKNOWLEDGEMENTS

The authors would like to thank Professor M. Sasaki and Dr. K. Nakao for helpful comments and discussions. We are also grateful to Professor H. Sato for continuous encouragement.

REFERENCES

1. R.Arnowitt, S.Deser, and C.W.Misner, in "GRAVITATION" ed. by L.Witten, Wiley, New York-London(1962).
2. A.Hosoya and K.Nakao,Prog.Theor.Phys.84,739(1990).
3. A.Hosoya and K.Nakao,Class.Quant.Grav.7,163(1990).
4. V.Moncrief,Ann.Phys.167,118(1986).
5. J.Soda,Thesis,"Topological aspects of Classical and Quantum (2+1)-dimensional Gravity" Hiroshima University(1990).
6. H.Kodama and M.Sasaki,Prog.Theor.Phys.Suppl.78,1(1984).
7. T.Okamura and H.Ishihara,KUNS-1111 KUCP-0040
8. Y.Fujiwara and J.Soda,Prog.Theor.Phys.83,733(1990).

Interaction of Tachyons and Discrete States in $c = 1$ 2-D Quantum Gravity

YOICHIRO MATSUMURA, NORISUKE SAKAI

Department of Physics, Tokyo Institute of Technology
Oh-okayama, Meguro, Tokyo 152, Japan

and

YOSHIAKI TANII

Physics Department, Saitama University
Urawa, Saitama 338, Japan

Abstract

The two-dimensional (2-D) quantum gravity coupled to the conformal matter with $c = 1$ is studied. We obtain all the three point couplings involving tachyons and/or discrete states via operator product expansion. We find that cocycle factors are necessary and construct them explicitly. We obtain an effective action for these three point couplings. This is a brief summary of our study of couplings of tachyons and discrete states, reported at the workshop in Tokyo Metropolitan University, December 4-6, 1991.

Recently the understanding of two-dimensional (2-D) quantum gravity has advanced significantly. There are two main motivations to study the 2-D quantum gravity coupled to matter. Firstly, it is precisely a string theory when the 2-D space-time is regarded as the world sheet for the string. Secondly, it provides a toy model for the quantum gravity in four dimensions. There are two approaches to study the 2-D quantum gravity: the matrix model as a discretized theory and the Liouville theory as a continuum theory [1, 2]. The former can provide a nonperturbative treatment, but is sometimes less transparent in physical terms since it is not in the usual continuum language. In spite of the nonlinear dynamics of the Liouville theory, a method based on conformal field theory has now been sufficiently developed to understand the results of the matrix model and to offer in some cases a more powerful method in computing various quantities. In particular, we can calculate not only partition functions but also correlation functions by using the procedure of the analytic continuation [3, 4].

So far only conformal field theories with central charge $c \leq 1$ have been successfully coupled to quantum gravity. The $c = 1$ model is the richest and the most interesting, and it is in some sense the most easily soluble. From the viewpoint of the string theory, the $c = 1$ model has at least one (continuous) dimension of target space in which strings are embedded. Hence, we can discuss the space-time interpretation in the usual sense in the $c = 1$ model. Since the Liouville (conformal) mode plays a dynamical role if the dimensions of the target space is different from the usual critical dimensions, the theory is called "noncritical" string theory.

It has been observed that the $c = 1$ quantum gravity can be regarded effectively as a critical string theory in two dimensions, since the Liouville field zero mode provides an additional "time-like" dimension besides the obvious single spatial dimension given by the zero mode of the $c = 1$ matter [5]. We have a physical scalar particle corresponding to the center of mass motion of the string. Though it is massless, it is still referred to as a "tachyon" following the usual terminology borrowed from the critical string theory. Since there are no trans-

verse directions, the continuous (field) degrees of freedom are exhausted by the tachyon field. The partition function for the torus topology was computed in the Liouville theory, and was found to give precisely the same partition function as the tachyon field alone. However, it has been noted that there exist other discrete degrees of freedom in the $c = 1$ matter coupled to the 2-D quantum gravity [6-8]. It has been pointed out that the symmetry group relevant to the dynamics of these discrete states in the $c = 1$ quantum gravity is the area preserving diffeomorphisms whose generators fall into representations of SU(2) [9]. Exploiting the SU(2) symmetry, Klebanov and Polyakov have recently worked out the three point interactions of the discrete states and have proposed an effective action for these discrete states [10].

This paper is a brief report on our study of the interaction of tachyons and discrete states in the $c = 1$ quantum gravity [11]. We have obtained all the possible three point couplings completely including both tachyons and discrete states by using the operator product expansion (OPE) of vertex operators. We have also found that the so-called cocycle factor is needed to obtain the operator product expansion with the proper analytic behaviour.

Let us consider the c=1 conformal matter realized by a single bosonic field X coupled to the 2-D quantum gravity. After fixing the conformal gauge $g_{\alpha\beta} = \mathrm{e}^{\phi}\hat{g}_{\alpha\beta}$ using the Liouville field ϕ, the $c = 1$ quantum gravity can be described by the following action on a surface with a boundary [1, 2, 12]

$$S[\hat{g}, X, \phi] = \frac{1}{4\pi\alpha'}\int d^2z\sqrt{\hat{g}}\Big(\hat{g}^{\alpha\beta}\partial_\alpha X\partial_\beta X + \hat{g}^{\alpha\beta}\partial_\alpha\phi\partial_\beta\phi - 2\sqrt{\alpha'}\hat{R}\phi + 4\alpha'\mu\,\mathrm{e}^{-2\phi/\sqrt{\alpha'}}\Big) + \frac{1}{\pi\sqrt{\alpha'}}\int d\hat{s}\left(-\hat{k}\phi + \sqrt{\alpha'}\lambda\,\mathrm{e}^{-\phi/\sqrt{\alpha'}}\right), \tag{1}$$

where α' is the Regge slope parameter, $\hat{R}$ the scalar curvature, $\hat{k}$ the geodesic curvature along the boundary and $d\hat{s}$ the line element of the boundaries with respect to the reference metric $\hat{g}_{\alpha\beta}$. We have rescaled the Liouville field ϕ. In this paper we will consider only the bulk (or resonant) correlation functions [7],

for which the "energy" and the momentum conjugate to ϕ and X respectively are conserved. For such correlation functions we can use the action without the cosmological terms by putting $\mu = \lambda = 0$.

There are two types of physical operators. The open string vertex operators are given by line integrals of primary fields with boundary conformal weight one along the boundary, while the closed string vertex operators are given by surface integrals of primary fields with conformal weight $(1,1)$. It is convenient to set $\alpha' = 4$ (1) when we discuss the closed (open) string vertex operators. With this convention the integrands of the closed string vertex operators can be constructed by combining the holomorphic operator and the anti-holomorphic operator, both of which have the same form as those of the open string vertex operators. The holomorphic part of the energy-momentum tensor for $\alpha' = 4$ is given by

$$T(z) = -\frac{1}{4}(\partial X)^2 - \frac{1}{4}(\partial\phi)^2 - \partial^2\phi. \tag{2}$$

From the action, we have correlation functions of X and ϕ for closed string

$$\langle X(z,\bar{z})X(w,\bar{w})\rangle = \langle\phi(z,\bar{z})\phi(w,\bar{w})\rangle = -2\ln|z-w|^2. \tag{3}$$

in accord with the convention of Klebanov and Polyakov [10].

Let us first consider the holomorphic part of the vertex operator corresponding to the open string vertex operators. They must be a line integral of a primary field of unit conformal weight. The simplest field for such operators is the tachyon vertex operator

$$\Psi_p^{(\pm)}(z) = e^{ipX(z)}e^{(\pm p-1)\phi(z)} \tag{4}$$

for an arbitrary real momentum p. For higher levels there are non-trivial primary fields only when the momentum is an integer or a half odd integer. They are primary fields for the "discrete states" [6, 7]. They form SU(2) multiplets and

can be constructed as [9, 10]

$$\Psi^{(\pm)}_{J,m}(z) = \sqrt{\frac{(J+m)!}{(2J)!(J-m)!}} \oint \frac{du_{J-m}}{2\pi i} H_-(u_{J-m}) \cdots \oint \frac{du_1}{2\pi i} H_-(u_1) \Psi^{(\pm)}_J(z), \quad (5)$$

where $J = 0, \frac{1}{2}, 1, \cdots$; $m = -J, -J+1, \cdots, J$ and $\Psi^{(\pm)}_J(z)$ is the tachyon operator (4) with the momentum $p = J$. The integrals are along closed contours surrounding a point z with $|u_i| > |u_j|$ for $i > j$. The field $H_-(z)$ corresponds to the lowering operator of the SU(2) quantum numbers and is one of the SU(2) currents

$$H_\pm(z) = e^{\pm iX(z)} = \pm\Psi^{(+)}_{1,\pm 1}(z), \quad H_3(z) = \frac{1}{2} i\partial X(z) = -\frac{1}{\sqrt{2}} \Psi^{(+)}_{1,0}(z). \quad (6)$$

The quantum numbers J and m correspond to the "spin" and the magnetic quantum number in SU(2). Actually, the fields $\Psi^{(\pm)}_{J,m}$ with $m = \pm J$ are not higher level operators but tachyon operators (4) at integer or half odd integer momenta $\pm J$.

In ref. [10] the OPEs of the fields for discrete states (5) were obtained using the SU(2) symmetry. Here we make a remark on the analytic property of the OPEs. The OPE of two vertex operators gives a coefficient different in sign depending on the ordering of the two vertex operators. Even if we use the radial ordering of the two vertex operators as usual in conformal field theory, the OPE is not analytic at $|z| = |w|$. It is desirable to obtain the analytic OPEs since the techniques of conformal field theories make full use of the analyticity. One should multiply the vertex operator (5) by a correction factor as in the vertex operator construction of the affine Kac-Moody algebra [13].

We have succeeded in constructing the necessary correction factor to recover the analyticity. After some lengthy argument using the knowledge of integral cubic lattice, we arrive at the following choice of the cocycle factor [11]

$$\varepsilon(\alpha_1, \alpha_2) = (-1)^{2J_1(J_2 - m_2 - 1)} \qquad \alpha_i = \sqrt{2}(m_i, J_i - 1), \quad i = 1, 2. \quad (7)$$

The sign of J in the cocycle factor should be changed according to the sign of J

in the two-vector α corresponding to the $(-)$ type. It is easy to see that eq. (7) indeed satisfies the cocycle conditions. With this cocycle the correction factor is constructed as [13]

$$c_\alpha = \sum_{\beta \in \Lambda} \varepsilon(\alpha, \beta) \, |\beta\rangle \, \langle\beta| \,, \tag{8}$$

where $|\beta\rangle$ is an eigenstate of the energy and the momentum with an eigenvalue β. Then the corrected operators

$$\Psi'^{(s)}_{J,m}(z) = \Psi^{(s)}_{J,m}(z) c_\alpha, \quad \alpha = \begin{cases} \sqrt{2}(m, J-1) & \text{for } s = + \\ \sqrt{2}(m, -J-1) & \text{for } s = - \end{cases} \tag{9}$$

satisfy the OPEs which are analytic in the complex z plane.

We find that after an appropriate rescaling the corrected operators (9) satisfy the same OPEs as those given in ref. [10]. The non-trivial OPEs are given by

$$\begin{aligned} \tilde{\Psi}'^{(+)}_{J_1,m_1}(z) \, \tilde{\Psi}'^{(+)}_{J_2,m_2}(w) &\sim \frac{1}{z-w} (J_2 m_1 - J_1 m_2) \, \tilde{\Psi}'^{(+)}_{J_1+J_2, m_1+m_2}(w), \\ \tilde{\Psi}'^{(+)}_{J_1,m_1}(z) \, \tilde{\Psi}'^{(-)}_{J_1+J_3-1, -m_1+m_3}(w) &\sim \frac{1}{z-w} (-J_1 m_3 - J_3 m_1) \, \tilde{\Psi}'^{(-)}_{J_3,m_3}(w). \end{aligned} \tag{10}$$

Other OPEs have no singular term. We have used rescaled fields

$$\begin{aligned} \tilde{\Psi}'^{(+)}_{J,m}(z) &= \tilde{N}(J,m) \, \Psi'^{(+)}_{J,m}(z), \\ \tilde{\Psi}'^{(-)}_{J,m}(z) &= (-1)^{J(2J-1)+J-m} \left[\tilde{N}(J,m)\right]^{-1} \Psi'^{(-)}_{J,m}(z), \end{aligned} \tag{11}$$

$$\tilde{N}(J,m) = (2J-1)! \sqrt{\frac{J}{2}} N(J,m), \quad N(J,m) = \left[\frac{(J+m)!(J-m)!}{(2J-1)!}\right]^{\frac{1}{2}}. \tag{12}$$

We shall now generalize these results of the OPEs to include tachyon operator (4). We have succeeded to generalize the cocycle operator to the tachyon case, but we merely refer our paper [11] for the full account of the construction and write down only the OPE without the cocycle factors because of lack of space.

From the conservation of the energy and the momentum we find that only four non-trivial OPEs are possible:

$$\begin{aligned}
\Psi^{(+)}_{p_1}(z)\,\Psi^{(+)}_{p_2}(w) &\sim \frac{1}{z-w}\,F^{(+)}_{p_1p_2}\,\tilde{\Psi}^{(-)}_{J_3,1-J_3}(w) \quad (J_3=-p_1-p_2+1),\\
\Psi^{(-)}_{p_1}(z)\,\Psi^{(-)}_{p_2}(w) &\sim \frac{1}{z-w}\,F^{(-)}_{p_1p_2}\,\tilde{\Psi}^{(-)}_{J_3,J_3-1}(w) \quad (J_3=p_1+p_2+1),\\
\tilde{\Psi}^{(+)}_{J_1,J_1-1}(z)\,\Psi^{(+)}_{p_2}(w) &\sim \frac{1}{z-w}\,G^{(+)}_{J_1p_2}\,\Psi^{(+)}_{p_3}(w) \quad (p_3=J_1-1+p_2),\\
\tilde{\Psi}^{(+)}_{J_1,1-J_1}(z)\,\Psi^{(-)}_{p_2}(w) &\sim \frac{1}{z-w}\,G^{(-)}_{J_1p_2}\,\Psi^{(-)}_{p_3}(w) \quad (p_3=1-J_1+p_2).
\end{aligned} \tag{13}$$

The coefficient in the third and fourth OPE in eq. (13) can be obtained by using the representation (5) for $\Psi^{(+)}_{J_1,J_1-1}$ or the similar expression for $m=1-J$ and directly evaluating the OPE

$$\begin{aligned}
G^{(+)}_{J_1p_2} &= \frac{\Gamma(1-2p_2)}{2\Gamma(-2p_3)} = (-1)^{2J_1-1}\,\frac{\tilde{N}(p_3,p_3)}{\tilde{N}(p_2,p_2)}\,p_2,\\
G^{(-)}_{J_1p_2} &= (-1)^{J_1(2J_1-1)}\frac{\Gamma(1+2p_2)}{2\Gamma(2p_3)} = (-1)^{J_1(2J_1-1)}\,\frac{\tilde{N}(p_2,p_2)}{\tilde{N}(p_3,p_3)}\,p_3,
\end{aligned} \tag{14}$$

where $\tilde{N}(p,p)=\frac{1}{2}\Gamma(1+2p)$. To obtain the coefficient of the first OPE in eq. (13), we apply the operator $\oint\frac{du}{2\pi i}H_-(u)$ to both hand sides of the equation, where the integration contour surrounds both of z and w. The coefficient of the second OPE in eq. (13) can be obtained similarly by applying $\oint\frac{du}{2\pi i}H_+(u)$. We find

$$\begin{aligned}
F^{(+)}_{p_1p_2} &= \frac{\Gamma(1-2p_1)}{2\Gamma(2p_2)} = \left[\tilde{N}(p_1,p_1)\tilde{N}(p_2,p_2)\right]^{-1}\,\frac{\pi p_1p_2}{2\sin(2\pi p_1)},\\
(-1)^{J_3(2J_3-1)}F^{(-)}_{p_1p_2} &= -\frac{\Gamma(1+2p_2)}{2\Gamma(-2p_1)} = \frac{2}{\pi}\,\tilde{N}(p_1,p_1)\tilde{N}(p_2,p_2)\sin(2\pi p_1).
\end{aligned} \tag{15}$$

The coefficients of the OPE determine the three-point correlation functions of the physical operators, which can be summarized by the effective action. Introducing a variable $g^{(s)}_{J,m}$ $(s=\pm)$ for each discrete state, the cubic terms of the

effective action for discrete states determined by the OPEs (10) are [10]

$$S_3 = \frac{1}{2} \sum_{J_1,m_1,J_2,m_2} (J_2 m_1 - J_1 m_2) f^{ABC} g^{(-)A}_{J_1+J_2-1,-m_1-m_2} g^{(+)B}_{J_1,m_1} g^{(+)C}_{J_2,m_2} \int d\phi, \quad (16)$$

where we have introduced the Chan-Paton index A in the adjoint representation of some Lie algebra and have factored out the Liouville volume $\int d\phi$.

In ref. [10] it was shown that the terms in the cubic interaction (16) which depend only on the integer modes $g^{(s)A}_{J,m}$ $(J,\, m \in \mathbf{Z})$ can be written in a compact form by introducing a scalar field on $\mathbf{R} \times \mathrm{S}^2$

$$\Phi_0(\phi,\theta,\varphi) = \sum_{s,A,J,m} T^A g^{(s)A}_{J,m} M^s(J,m) D^J_{m0}(\varphi,\theta,0)\, \mathrm{e}^{(sJ-1)\phi}. \quad (17)$$

Here, T^A are the representation matrices of the the Lie algebra, D^J_{m0} are components of the SU(2) rotation matrix [14] and $M^s(J,m)$ are the normalization factor

$$D^J_{mm'}(\varphi,\theta,\psi) = \left\langle Jm \right| \mathrm{e}^{-i\varphi J_z}\, \mathrm{e}^{-i\theta J_y}\, \mathrm{e}^{-i\psi J_z} \left| Jm' \right\rangle. \quad (18)$$

$$M^+(J,m) = \frac{N(J,m)N(J,0)}{J}, \quad M^-(J,m) = \frac{(-1)^m}{4\pi} \frac{J(2J+1)}{N(J,m)N(J,0)}. \quad (19)$$

The effective action can be written in terms of the field Φ_0 using $x^i = (\theta,\varphi)$

$$S^{(1)}_3 = \int d\phi\, \mathrm{e}^{2\phi} \int_{S^2} d\theta d\varphi\, \epsilon^{ij}\, \mathrm{Tr} \left(\Phi_0 \frac{\partial \Phi_0}{\partial x^i} \frac{\partial \Phi_0}{\partial x^j} \right). \quad (20)$$

We have succeeded to generalize this construction to the terms containing half odd integer modes as well as integer modes. We introduce two spinor fields

$\Phi_{\frac{1}{2}}$ and $\Phi_{-\frac{1}{2}}$ on $\mathbf{R}\times\mathrm{S}^2$ for half odd integer modes $g^{(s)A}_{J,m}$ $(J,\, m\in\mathbf{Z}+\frac{1}{2})$

$$\Phi_\mu(\phi,\theta,\varphi)=\sum_{s,A,J,m} T^A g^{(s)A}_{J,m} M^s_\mu(J,m) D^J_{m\mu}(\varphi,\theta,0)\,\mathrm{e}^{(sJ-1)\phi} \quad \left(\mu=\pm\frac{1}{2}\right), \tag{21}$$

where

$$M^+_\mu(J,m)=\frac{N(J,m)N(J,\frac{1}{2})}{J+\frac{1}{2}}, \quad M^-_\mu(J,m)=\frac{(-1)^{m+\mu}}{4\pi}\frac{2J(J+1)}{N(J,m)N(J,\frac{1}{2})}. \tag{22}$$

Note that $\Phi_{\frac{1}{2}}$ and $\Phi_{-\frac{1}{2}}$ have the same coefficients $g^{(s)A}_{J,m}$ and are not independent. In order to write down the effective action in terms of these fields we need covariant derivatives on S^2 acting on spinor fields Φ_μ. They are given by

$$\nabla_\pm=\mp\partial_\theta-\frac{1}{\sin\theta}(i\partial_\varphi-\mu\cos\theta) \tag{23}$$

when acting on Φ_μ. The effective action can be written as

$$S^{(2)}_3=\int d\phi\,\mathrm{e}^{2\phi}\int_{S^2} d\theta d\varphi\sin\theta\,\mathrm{Tr}\left(\Phi_0\left[\nabla_+\Phi_{-\frac{1}{2}},\nabla_-\Phi_{\frac{1}{2}}\right]\right). \tag{24}$$

The sum of eqs. (20) and (24) gives the complete cubic terms for the discrete states (16).

Apart from the special case of the compact boson X with the self-dual radius, we have tachyons with momenta other than integer or half odd integer which should be included in the effective action. The OPE results (13) can be summarized as two types of terms in the effective action involving tachyons: two tachyons with the same chirality (+) or (−) couple to the single discrete state of the (+) type. We have succeeded to write down the local effective action involving tachyons, for which we refer our paper [11].

References

[1] J. Distler and H. Kawai, *Nucl. Phys.* **B321** (1989) 509; J. Distler, Z. Hlousek and H. Kawai, *Int. J. of Mod. Phys.* **A5** (1990) 391; 1093; F. David, *Mod. Phys. Lett.* **A3** (1989) 1651.

[2] N. Seiberg, *Prog. Theor. Phys. Suppl.* **102** (1990), 319.

[3] M. Goulian and M. Li, *Phys. Rev. Lett.* **66** (1991), 2051.

[4] P. Di Francesco and D. Kutasov, *Phys. Lett.* **261B** (1991), 385; Y. Kitazawa, *Phys. Lett.* **265B** (1991), 262; N. Sakai and Y. Tanii, *Prog. Theor. Phys.* **86** (1991), 547; V.S. Dotsenko, Paris preprint PAR-LPTHE 91-18 (1991).

[5] J. Polchinski, *Nucl. Phys.* **B324** (1989) 123; *Nucl. Phys.* **B346** (1990) 253.

[6] D.J. Gross, I.R. Klebanov and M.J. Newman, *Nucl. Phys.* **B350** (1991) 621.

[7] A.M. Polyakov, *Mod. Phys. Lett.* **A6** (1991) 635.

[8] N. Sakai and Y. Tanii, Tokyo Inst. of Tech. and Saitama preprint TIT/HEP-173, STUPP-91-120 (1991); TIT/HEP-179, STUPP-91-122 (1991).

[9] E. Witten, Princeton preprint IASSNS-HEP-91/51 (1991).

[10] I.R. Klebanov and A.M. Polyakov, *Mod. Phys. Lett.* **A6** (1991) 3273.

[11] Y. Matsumura, N. Sakai and Y. Tanii, Tokyo Inst. of Tech. and Saitama preprint TIT/HEP-186, STUPP-92-124 (1992).

[12] M. Bershadsky and D. Kutasov, Princeton and Harvard preprint PUPT-1283, HUTP-91/A047 (1991); Y. Tanii and S. Yamaguchi, Saitama preprint STUPP-91-121 (1991), to appear in *Int. J. of Mod. Phys.* **A**.

[13] P. Goddard and D. Olive, in *Vertex Operators in Mathematics and Physics*, eds. J. Lepowsky et al., (Springer, Heidelberg, 1985) p. 51; *Int. J. of Mod. Phys.* **A1** (1986) 303.

[14] M.E. Rose, *Elementary Theory of Angular Momentum* (John Wiley & Sons, New York, 1957).

Spin Precession Due To Torsion

Koichi Nomura, Takeshi Shirafuji and Kenji Hayashi*
Physics Department, Saitama University, Urawa, Saitama 338
*Institute of Physics, Kitasato University, Sagamihara, Kanagawa 228

Abstract

The Fock-Papapetrou (FP) method is applied to the motion of spinning test particles moving in the Riemann-Cartan (RC) spacetime. With the aid of the WKB method, we can then derive the equations of world line and spin precession due to torsion for particles with arbitrary spin. The world line is the geodesics of the metric, while the intrinsic spin is not Fermi-Walker transported along the world line relative either to the nonsymmetric connection or to the symmetric connection.

§1 Introduction

In general relativity, the problem of motion of extended bodies was first been studied by Fock[1] and developed by Papapetrou,[2] who derived the equations of world line and spin for spinning test particles moving in a background gravitational field.[3] According to their result, test particles behave in the single-pole approximation like spinless mass points, while the world line deviates in the pole-dipole approximation from the geodesics of the metric due to the spin-curvature coupling.

In this paper we apply the FP method to the motion of test bodies moving in a background RC spacetime.[4] The torsion of spacetime, if it exists, is coupled to intrinsic spin of matter fields like the fundamental fields with spin 1/2, thus giving rise to nontrivial and observable effects on the motion of particles with intrinsic spin. It has been suggested by Adamovicz and Trautman[5] using a spin-fluid model[6] that intrinsic spin is Fermi-Walker transported along the world

line relative to the nonsymmetric connection. The result obtained by the WKB method does not agree with theirs, however.[7] It seems highly desirable to apply the FP method to spinning test particles moving in the RC spacetime.

The resultant equations of spin and world line for spinning test particles are found to involve a quantity $N^{\mu\nu\lambda}$ which we call the spin-current. For wave packets of fields with arbitrary spin, the spin current can be calculated with the aid of the WKB method. Using the resut for $N^{\mu\nu\lambda}$ in the equations derived by the FP method, we can then get the equations of world line and spin for particles with arbitrary spin.

Throughout this paper we use the same notation and convention as Refs.4), 7) and 8).

§2 The FP method applied to test particles in RC spacetime

The starting point of the FP method is the response equations of the energy-momentum tensor density $\mathbf{T}^{\mu\nu}$ and the spin tensor density $\mathbf{S}^{mn\nu}$ of matter fields in the background RC spacetime.[4] Using Noether's theorem, we can get

$$\nabla_\nu \mathbf{T}^{\mu\nu} - K_{\rho\sigma}{}^{\mu}\mathbf{T}^{\rho\sigma} + \frac{1}{2}F^{mn\mu\nu}\mathbf{S}_{mn\nu} = 0\,, \tag{2.1}$$

$$\partial_\nu \mathbf{S}^{mn\nu} + A^{m}{}_{k\nu}\mathbf{S}^{kn\nu} + A^{n}{}_{k\nu}\mathbf{S}^{mk\nu} - (\mathbf{T}^{mn} - \mathbf{T}^{nm}) = 0\,, \tag{2.2}$$

where $\mathbf{T}^{\mu\nu}$ and $\mathbf{S}^{mn\nu}$ are defined by

$$\mathbf{T}^{\mu\nu} = \frac{\delta \mathbf{L}_M}{\delta e_{k\nu}} e_k{}^{\mu}\,, \qquad \mathbf{S}^{mn\nu} = -2\frac{\delta \mathbf{L}_M}{\delta A_{mn\nu}} \tag{2.3}$$

with $\mathbf{L}_M$ being the Lagrangian density of matter fields under consideration. Accordingly, we shall adopt (2.1) and (2.2) as the basic response equations.

An extended body sweeps a world tube in spacetime. Inside the tube we take an arbitrarily chosen, timelike world line L which will 'represent' the motion of the body as a whole. The coordinates of the points on L will be denoted

by $X^\mu(\tau)$ with τ being the proper time on L. Putting $\delta x^\mu = x^\mu - X^\mu(\tau)$ with $\delta x^0 = x^0 - X^0(\tau) = 0$, we define the total spin of the body by

$$J^{\mu\nu} = \int \left(\delta x^\mu \mathbf{T}^{\nu 0} - \delta x^\nu \mathbf{T}^{\mu 0} + \mathbf{S}^{\mu\nu 0}\right) d^3x\,, \tag{2.4}$$

and the spin-current by

$$N^{\mu\nu\lambda} = -U^0 \int \mathbf{S}^{\mu\nu\lambda}\, d^3x\,, \tag{2.5}$$

where U^μ denotes the four-velocity, $U^\mu = dX^\mu(\tau)/d\tau$, and the integration is carried out over the three-dimensional space with x^0 =constant. The intrinsic spin tensor $S^{\mu\nu}$ is given by $S^{\mu\nu} = N^{\mu\nu\lambda}U_\lambda$.

If the dimensions of the extended body are very small, all integrals with one or more factors of δx^ρ should be also very small. Then the single-pole approximation is characterized by ,

$$\int \mathbf{T}^{\mu\nu}\, d^3x \neq 0 \qquad \text{but} \qquad \int \delta x^\lambda \mathbf{T}^{\mu\nu}\, d^3x = 0, \cdots. \tag{2.6}$$

and the pole-dipole approximation by

$$\int \delta x^\lambda \mathbf{T}^{\mu\nu}\, d^3x \neq 0 \qquad \text{but} \qquad \int \delta x^\rho \delta x^\lambda \mathbf{T}^{\mu\nu}\, d^3x = 0, \cdots. \tag{2.7}$$

The main results can be summarized as follows.[4)]

Single-pole approximation

In the single-pole approximation for $\mathbf{T}^{\mu\nu}$ and $\mathbf{S}^{mn\nu}$, intrinsic spin is Fermi-Walker transported along the world line relative to the nonsymmetric connection, and the world-line equation has a spin-curvature coupling similar to that in general relativity.

However, the validity of the single-pole approximation seems doubtful because of the following reasons. Firstly, the spin equation does not agree with that for elementary particles with spin 1/2 and 1 derived by the WKB method. Secondly and more seriously, it turns out that the Dirac particle behaves like a spinless point particle because $S^{\mu\nu}$ vanishes in this approximation. Thus, higher-order approximation is indispensable in order to treat the intrinsic spin of fundamental particles.

Pole-dipole approximation

Assuming the pole-dipole approximation for $\mathbf{T}^{\mu\nu}$ and the single-pole approximation for $\mathbf{S}^{\mu\nu\lambda}$, we can obtain the covariant equation of spin;

$$\frac{\nabla J^{\mu}}{\nabla \tau} = \left(U^{\mu} \frac{\nabla U^{\nu}}{\nabla \tau} - U^{\nu} \frac{\nabla U^{\mu}}{\nabla \tau} \right) J_{\nu} - \frac{1}{2} \epsilon^{\mu\nu\rho\sigma} U_{\nu} \left(2 K_{\rho\lambda\tau} N_{\sigma}{}^{\lambda\tau} + K_{\lambda\tau\rho} N^{\lambda\tau}{}_{\sigma} \right) \quad (2.8)$$

with $J^{\mu} = \frac{1}{2} \epsilon^{\mu\nu\rho\sigma} U_{\nu} J_{\rho\sigma}$. In the present approximation the total spin $J^{\mu\nu}$ and the spin-current $N^{\mu\nu\lambda}$ are tensors under general coordinate transformations, which implies that $S^{\mu\nu}$ is also a tensor. We have also used the fact that the constraint $J^{\mu\nu} U_{\nu} = 0$ can be imposed by appropriately choosing the world line L. It is physically reasonable to assume another constraint $S^{\mu\nu} U_{\nu} = 0$, which ensures that the intrinsic spin has only three independent components.

The covariant equation of world line is, on the other hand,

$$\frac{\nabla \tilde{P}^{\mu}}{\nabla \tau} + \frac{1}{2} R^{\rho\sigma\mu\nu} J_{\rho\sigma} U_{\nu} - \frac{1}{2} \left(\nabla^{\mu} K^{\rho\sigma\nu} \right) N_{\rho\sigma\nu} = 0 \,, \quad (2.9)$$

where the four-vector $\tilde{P}^{\mu}$ stands for

$$\begin{aligned} \tilde{P}^{\mu} = \tilde{m} U^{\mu} - U_{\nu} \Big(& \frac{\nabla J^{\mu\nu}}{\nabla \tau} + K^{\mu}{}_{\rho\sigma} N^{\nu\rho\sigma} - K^{\nu}{}_{\rho\sigma} N^{\mu\rho\sigma} \\ & + \frac{1}{2} K_{\rho\sigma}{}^{\mu} N^{\rho\sigma\nu} - \frac{1}{2} K_{\rho\sigma}{}^{\nu} N^{\rho\sigma\mu} \Big) , \end{aligned} \quad (2.10)$$

and the scalar $\tilde{m}$ is

$$\begin{aligned}\tilde{m} &= -P^\nu U_\nu + U_\nu \{^\nu_{\rho\sigma}\} \frac{J^{0\rho} U^\sigma}{U^0} + U_\nu \{^\nu_{\rho\sigma}\} \frac{N^{0\rho\sigma}}{U^0} - \frac{1}{2} K_{\rho\sigma\nu} U^\nu \frac{N^{\rho\sigma 0}}{U^0} \\ &= -\tilde{P}^\nu U_\nu \end{aligned} \tag{2.11}$$

with P^μ being given by $P^\mu = \int \mathrm{T}^{\mu 0} d^3x$. Here $R^{\rho\sigma\mu\nu}$ denotes the Riemann-Christoffel curvature tensor formed of the metric.

It should be noticed that (2.8) and (2.9) involve the spin-current $N^{\mu\nu\lambda}$ coupled to the torsion of spacetime.

§3 The semiclassical particles with arbitrary spin in the RC spacetime

Let us now apply the result obtained above to the motion of wave packets with arbitrary intrinsic spin.[8] Theory of higher-spin fields was initiated by Dirac, Fierz, and Fierz and Pauli. The Lagrangian formulation for massive fields with spin higher than 2 was later constructed by Singh and Hagen,[9] and its massless limit was investigated by Fronsdal and Fang.[10] A first-order formalism for boson fields with arbitrary spin was also formulated,[9] which allows us to introduce the electromagnetic interaction and other gauge couplings unambiguously: Thus, the Poincaré gauge invariant Lagrangian for higher-spin fields can be derived in an unambiguous manner both for the boson and fermion cases.

Fields with half-interger spin

Consider first a spin-s fermion field described by the Dirac-Rarita-Schwinger symmetric tensor-spinor $\psi^{(n)}_{l_1 \cdots l_n}$ of rank $n = s - 1/2$ $(n = 0, 1, 2, \cdots)$ satisfying the spinor-trace condition,*) $\gamma^{l_1} \psi^{(n)}_{l_1 \cdots l_n} = 0$. The Lagrangian given by Singh and Hagen[9] takes a complicated form involving many auxiliary fields $\psi^{(n-1)}, \cdots, \psi^{(0)}$ and $\chi^{(n-2)}, \cdots, \chi^{(0)}$, which are also Dirac-Rarita-Schwinger tensor-spinors. The

*) This condition implies the tracelessness with respect to Lorentz indices.

Lagrangian density in the RC spacetime can be obtained by the minimal prescription as follows:

$$\mathbf{L}_M = e\Bigg[\frac{1}{2}\overline{\psi}^{(n)}{}_{l_1\cdots l_n}\left(i\hbar\gamma^k D_k - m\right)\psi^{(n)l_1\cdots l_n} + \text{c.c.} \\ + (\text{terms involving the auxiliary fields})\Bigg], \tag{3.1}$$

where the terms of the auxiliary fields are chosen so that all the auxiliary fields automatically vanishes for the free field case, and the covariant derivative D_k operates on both spinor and tensor indices. The field equation derived from (3.1) is very complicated.

Now let us look for a WKB solution of the form

$$\psi^{(p)}{}_{l_1\cdots l_p}(x) = A^{(p)}{}_{l_1\cdots l_p}(x)\exp(iS(x)/\hbar). \tag{3.2}$$

In the lowest onder of $\hbar$, it can be shown that all the $A^{(p)}(x)$ corresponding to the auxiliary fields are vanishing, and that the $A^{(n)}$ satisfies

$$(\gamma^k\partial_k S + m)A^{(n)}{}_{l_1\cdots l_n}(x) = 0, \qquad (\partial^{l_1}S)A^{(n)}{}_{l_1\cdots l_n}(x) = 0\,. \tag{3.3}$$

The first equation implies that the function S obeys the Hamilton-Jacobi equation, $g^{\mu\nu}(x)\partial_\mu S\,\partial_\nu S + m^2 = 0$: As is well known, the complete solution of the equation has three independent parameters $\alpha_i\,(i = 1,2,3)$ besides an additive constant. We shall denote the solution as $S(x,\alpha)$. In conformity with this, we shall write the corresponding solutions as $A^{(n)}{}_{l_1\cdots l_n}(x,\alpha)$ and $\psi^{(n)}{}_{l_1\cdots l_n}(x,\alpha)$. We form a wave-packet solution by superposing $\psi(x,\alpha)$ over a small region in the α-space:

$$\begin{aligned}\psi^{(n)}{}_{l_1\cdots l_n}(x) &= \int d^3\alpha\, W(\alpha-\overline{\alpha})\,\psi^{(n)}{}_{l_1\cdots l_n}(x,\alpha) \\ &\approx A^{(n)}{}_{l_1\cdots l_n}(x,\overline{\alpha})\int d^3\alpha\, W(\alpha-\overline{\alpha})\exp(iS(x,\alpha)/\hbar) \\ &\equiv A^{(n)}{}_{l_1\cdots l_n}(x,\overline{\alpha})\,\Omega(x,\overline{\alpha})\,,\end{aligned} \tag{3.4}$$

where $W(\alpha-\overline{\alpha})$ is a weight function peaked at $\alpha_i = \overline{\alpha}_i\,(i = 1,2,3)$ so sharply

that $A^{(n)}{}_{l_1\cdots l_n}(x,\alpha)$ can be approximated by $A^{(n)}{}_{l_1\cdots l_n}(x,\overline{\alpha})$, and the last equation defines $\Omega(x,\overline{\alpha})$. Because $|S| \gg \hbar$, the integrand oscillates rapidly in the integrals of (3.4), and therefore compensation takes place almost everywhere in the spacetime: The only exception is a thin tube around the world line satisfying $\partial S(x,\overline{\alpha})/\partial\alpha_i = 0$. Thus $\psi^{(n)}{}_{l_1\cdots l_n}(x)$ of (3.4) indeed represents a wave packet. The world line $X^\mu(\tau)$ defined above satisfies

$$U^\mu(\tau) \equiv \frac{dX^\mu(\tau)}{d\tau} = \frac{1}{m} g^{\mu\nu}(X(\tau))\partial_\nu S(X(\tau),\overline{\alpha}), \tag{3.5}$$

and hence obeys the geodesic equation, $\nabla U^\mu/\nabla\tau = 0$.

Since $e_k{}^\nu$ and $A^{(n)}{}_{l_1\cdots l_n}$ are assumed to be slowly varying over the size of the wave packet, they can be approximated by $e_k{}^\nu(X(\tau))$ and $A^{(n)}{}_{l_1\cdots l_n}(X(\tau),\overline{\alpha})$, respectively.

If we use $U_k = e_k{}^\nu(X(\tau))U_\nu(\tau)$, (3.3) can be rewritten as

$$(\gamma^k U_k + 1)A^{(n)}{}_{l_1\cdots l_n}(X(\tau),\overline{\alpha}) = 0, \qquad U^{l_1}A^{(n)}{}_{l_1\cdots l_n}(X(\tau),\overline{\alpha}) = 0. \tag{3.6}$$

Now we are ready to calculate the spin-current $N^{\mu\nu\lambda}$ for the wave packet: The final result is

$$N^{\mu\nu\lambda} = -S^{\mu\nu}U^\lambda - \frac{1}{s}U^{[\mu}S^{\nu]\lambda} \tag{3.7}$$

with

$$\begin{aligned} S^{\mu\nu} &= N^{\mu\nu\lambda}U_\lambda \\ &= 2is\hbar\overline{A}^{(n)l_1\cdots[\mu}A^{(n)}{}_{l_1\cdots}{}^{\nu]}\left(-U^0\int|\Omega|^2\,e\,d^3x\right), \end{aligned} \tag{3.8}$$

where $s = n + \frac{1}{2}$ stands for the spin of the particle under consideration. It should be noticed that $S^{\mu\nu}U_\nu = 0$ holds owing to (3.6). We can also show that the rotational spin $L^{\mu\nu} = J^{\mu\nu} - S^{\mu\nu}$ is negligibly small for the wave packet solution.

Now let us turn to the boson case. The Lagrangian density can be obtained by applying the minimal prescription to that in the Minkowski spacetime. Since we start from the first-order formalism of Singh and Hagen, no ambiguity arises in replacing ordinary derivative ∂_k by the covariant one D_k. Then the spin-current can be calculated for wave packets in the same manner as in the fermion case: The result is precisely the same as (3.7) with $S^{\mu\nu}$ now being given by an appropriate expression in terms of the boson field:[8] The $S^{\mu\nu}$ is shown to satisfy $S^{\mu\nu}U_\nu = 0$.

Using the above results for the spin-current in (2.8), we arrive at the equation of spin precession due to torsion:

$$\begin{aligned}\frac{\nabla S^\mu}{\nabla\tau} = &\left(U^\mu\frac{\nabla U^\nu}{\nabla\tau} - U^\nu\frac{\nabla U^\mu}{\nabla\tau}\right)S_\nu \\ &+ f_1\epsilon^{\mu\nu\rho\sigma}U_\rho a_\sigma S_\nu + f_2\left(U_\rho t^{\rho[\mu\nu]} - 3U^{[\mu}t^{\nu]\rho\sigma}U_\rho U_\sigma\right)S_\nu ,\end{aligned} \tag{3.9}$$

where f_1 and f_2 are dimensionless, spin-dependent parameters defined by

$$f_1 = -\frac{1}{2}\left(1+\frac{1}{s}\right), \qquad f_2 = \frac{4}{3}\left(1-\frac{1}{2s}\right), \tag{3.10}$$

and a_σ and $t^{\rho\mu\nu}$ are the axial-vector part and the tensor part of the torsion tensor, respectively. The equation (3.9) agrees with our previous result for spin 1/2 and 1 derived by the WKB method alone. Furthermore, since it is impossible to have both $f_1 = 0$ and $f_2 = 0$ at the same time, the intrinsic spin vector is not Fermi-Walker transported along the world line with respect to the ordinary, symmetric connection. Thus, the intrinsic spin necessarily precesses due to torsion irrespective of the spin value. We also note that $S^\mu S_\mu$ is a constant of motion.

We can rewrite (3.9) into an alternative form in terms of the covariant derivative $D/D\tau$ with respect to the nonsymmetric connection:

$$\begin{aligned}\frac{DS^\mu}{D\tau} = &\left(U^\mu\frac{DU^\nu}{D\tau} - U^\nu\frac{DU^\mu}{D\tau}\right)S_\nu \\ &- \frac{1}{2s}\epsilon^{\mu\nu\rho\sigma}U_\rho a_\sigma S_\nu - \frac{2}{3s}\left(U_\rho t^{\rho[\mu\nu]} - 3U^{[\mu}t^{\nu]\rho\sigma}U_\rho U_\sigma\right)S_\nu .\end{aligned} \tag{3.11)}$$

This equation shows that the intrinsic spin vector is not Fermi-Walker transported along the world line relative to the nonsymmetric connection: We notice, however, that the Fermi-Walker transport is realized in the limiting case $s \to \infty$. It should also be emphasized that the equation of spin precession due to torsion depends on the spin s.

Finally, we briefly comment on the world line equation derived by the FP method. The intrinsic spin $S^{\mu\nu}$ is of the first-order in $\hbar$, and hence its magnitude is negligible in the semiclassical limit $\hbar \to 0$: According to (3.7), this means that the spin-current $N^{\mu\nu\lambda}$ is also negligibly small. Thus, the world line equation (2.9) is reduced to the geodesic one with respect to the Christoffel symbol. This result is consistent with the Hamilton-Jacobi equation, since the latter equation is derived by the WKB method in the lowest order in $\hbar$.

§4 Summary

We have applied the FP method developed in general relativity to the motion of extended bodies in the RC spacetime. The resultant equations of motion are found to involve the spin-current $N^{\mu\nu\lambda}$ coupled to torsion. We have then calculated the spin current for semiclassical particles with arbitrary spin represented by wave packet with the aid of the WKB method. Combining the above results, we have obtained the equations of world lined and spin precession for semiclassical particles with arbitrary spin. The world line is the geodesics of the metric, while the equation of spin precession has two spin-dependent parameters.

References

1) V.A. Fock, *J. Phys. U.S.S.R.* **1** (1939), 81.

2) A. Papapetrou, *Proc. Roy. Soc.* **A209** (1951), 248.

   E. Corinaldesi and A. Papapetrou, *Proc. Roy. Soc.* **A209** (1951), 259.

3) For other approaches to the problem of the equation of motion in general relativlty see, for example, the review article

   W.G. Dixon, Proceedings of the international school of physics ⟨*Enrico Fermi*⟩; course **67**, ed. J. Ehlers, *Isolated Gravitating Systems in General Relativity* (North-Holland, 1979), p.156.

4) K. Nomura, T. Shirafuji and K. Hayashi, *Prog. Theor. Phys.* **86** (1991), 1239.

5) W. Adamowicz and A. Trautman, *Bull. Acad. Polon. Sci., Sér.Sci. Math., Astr. Phys.* **20** (1975), 339.

6) J. Weyssenhoff and A. Raabe, *Acta Phys. Polon.* **9** (1947), 7.

7) K. Hayashi, K. Nomura and T. Shirafuji, *Prog. Theor. Phys.* **84** (1990), 1085.

8) K. Nomura, T. Shirafuji and K. Hayashi, STUPP-92-123, Kitasato-92-1.

9) L.P.S. Singh and C.R. Hagen, *Phys. Rev.* **D9** (1974), 898, 910.

10) C. Fronsdal, *Phys. Rev.* **D18** (1978), 3624.

    J. Fang and C. Fronsdal, *Phys. Rev.* **D18** (1978), 3630.

Numerical Relativity

KEN-ICHI OOHARA
National Laboratory for High Energy Physics
Oho, Tsukuba, Ibaraki 305, Japan

1. Introduction

Any theory of physics should be proven by experimental and observational facts. In order to compare a theory with experiment or observation, we should solve equations, which are in general complicated and non-linear partial differential equations. Such equations cannot be solved by analytical means without any approximation. For example, we assume some symmetry, spatial and/or temporal, or introduce some small quantity and expand the equation into its power series. Many of important problems, however, does not have such symmetry or a small quantity. Many of problems in classical relativity force to solve Einstein equations for strong gravitational field and/or dynamical and asymmetric space-time. If you consider the formation of a black hole or the gravitational radiation from the coalescence of a binary system, we should solve equations for highly dynamical and general relativistic space-time. Furthermore an asymmetric process is very important since the gravitational instability causes fragmentation of matter and a lot of gravitational waves are emitted from an asymmetric system. For these problems, we should solve Einstein equations (and hydrodynamic equations) by numerical means; that is numerical relativity.

Numerical relativity involves the application of advanced computer technology and modern computational algorithms. The condition is severer for general relativity than for Newtonian gravity. For self-gravitating system in both cases, we should solve Poisson equations, or more generally elliptic partial differential equations, which are usually the most time-consuming in view of numerical calculation. In Newtonian gravity, we have only to solve a Poisson equation for the gravitational potential ψ. But in general relativity, we need calculate the metric tensor $g_{\mu\nu}$, for which we should often solve more than one elliptic equation in connection with the singularity avoidance. Numerical relativity usually requires more memory of a computer not only because there are more variables, the potential ψ vs. the metric tensor $g_{\mu\nu}$ for example, but also because the gravitational radiation should be calculated at the region sufficiently far from the source.

In this article, I will review approaches of numerical relativity. For more detailed, see reviews of Smarr[1], Piran[2] and Nakamura, Oohara and Kojima.[3] For the frontiers of numerical relativity after the mid-seventies, see an informal series for numerical relativity published by Cambridge University Press.[4, 5, 6]

2. Progress in Numerical Relativity

Before explaining the method of numerical relativity, I show a brief history of numerical relativity. For more details, see the review of Hobill and Smarr.[7]

May and White[8] succeeded in numerical calculation for collapse of a spherically symmetric star in the mid-sixties for the first time. In the same era, Hann and Lindquist[9] tried to study collision of two black holes. However both groups obliged to face the singularity formation. A singularity appeared soon after calculations started unless a black hole was never formed, and then they could not continue numerical calculation. Subsequently the modern technique for numerical relativity, including application of ADM-formalism, was developed and numerical relativity gained momentum only in the mid-seventies when Smarr, Cadez, DeWitt and Eppley solved head-on collision of two black holes.[10] The computer they used was CDC 6600 and CDC 7600, whose performance (the theoretical peak speed) was 7MFLOPS and 30MFLOPS, respectively, and the available memory was 256Kbytes and 512Kbytes. Note that such performance can be achieved on a workstation now and the memory for them is less than that for a present personal computer. In 1980, Nakamura, Maeda, Miyama and Sasaki published their success in numerical simulation of the axially symmetric collapse of a rotating star.[11] A modern supercomputer CRAY-1 was shipped in 1976. By the mid-eighties, supercomputers, CRAY-1, CRAY-XMP, FACOM VP-series, HITAC S810 and NEC SX-series became available for researchers in physics including numerical relativity. The peak performance and the maximum memory of these supercomputers is several hundred MFLOPS and a few hundred Mbytes. In this time, Bardeen and Piran developed an axisymmetric general relativistic code[12] and Stark and Piran calculated axisymmetric collapse and the resulting gravitational wave emission[13] on a CRAY supercomputer. Subsequently, the rapid progress was made in supercomputers; the peak speed and the maximum memory increased to more than 1GFLOPS and 1Gbytes. As the first step to three-dimensional numerical relativity, Oohara and Nakamura solved the coalescence of binary neutron star systems using a three-dimensional post-Newtonian code[14] on HITAC S820/80, whose performance is 3GFLOPS and 512Mbytes. To complete the study of the coalescence of binary black hole or neutron star systems and the resulting gravitational radiation, we need a three-dimensional general relativistic code. In order to perform fully general relativistic simulation of collapse of a star or coalescence of binary neutron star systems with good accuracy, we may need more powerful supercomputers such as machines on the order of 100's of GFLOPS and 10's of GFLOPS. They might be available in the mid- or late-nineties.

3. General Formalism

Numerical relativity is a method of numerical solutions to Einstein equations as Cauchy problems. It yields an approximate solution to Einstein equations. Like in perturbation calculation, it requires an expansion parameter. The crucial difference

between numerical calculation and other approximation methods is the nature of the expansion parameter. The numerical expansion parameter is not a physical parameter of the problem. For the finite difference method, it is the grid spacing divided by the typical length scale of the system and for the (smoothed) particle method the mass of each particle divided the total mass of the system. Since the expansion parameter is not physical, numerical methods can be applied for strong field, non-linear problems even when all natural expansion parameter are large.

Einstein equations in the form

$$G_{\mu\nu} = 8\pi T_{\mu\nu}. \tag{1}$$

is not suitable for numerical solution, since there are six equations of second order in time as well as four first order equations. To construct a successful numerical scheme, they have to be written as a set of quasi-linear partial differential equations of first order in time;

$$\frac{\partial Q}{\partial t} = L(Q, x). \tag{2}$$

In order to do it, I use the 3+1 ADM formalism[15] in this article. Other approaches, such as 2+2 formalism[16] or Regge calculus,[17] will not be discussed, because almost all the successful results were presented in 3+1 formalism and I think it is the most promising for the future.

In 3+1 formalism, initial values are defined on an initial spacelike hypersurface and then evolved through their future development. The evolution is performed from one hypersurface to a nearby surface. The space-time is foliated into a set of three-dimensional spacelike hypersurfaces. (Other types of foliation can be considered. In a characteristic 2+2 formalism, it is foliation to two-dimensional null hypersurfaces.)

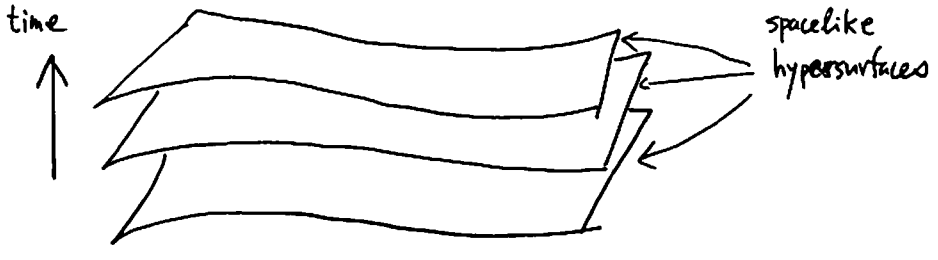

Fig. 1. Slicing of space-time.

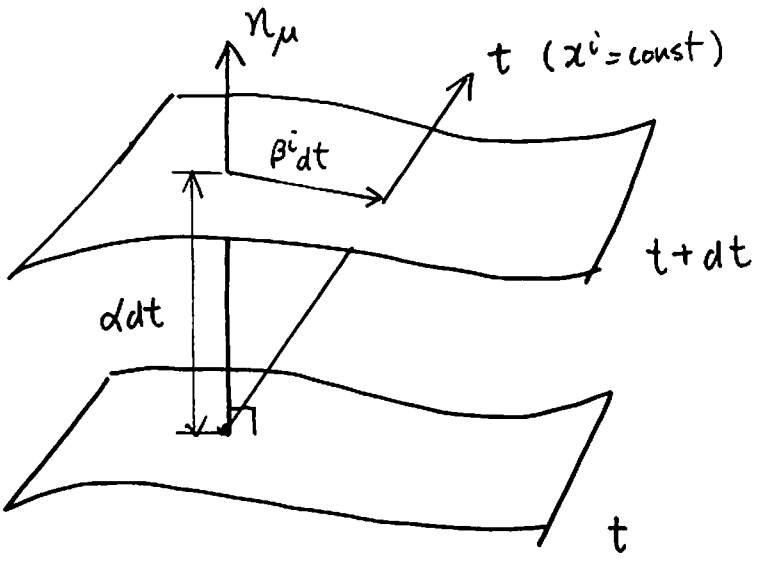

Fig. 2. The lapse function and the shift vector.

The four-dimensional line element is written in the form

$$ds^2 = -(\alpha^2 - \beta_i\beta^i)dt^2 + 2\beta_i dx^i dt + \gamma_{ij}dx^i dx^j. \tag{3}$$

The time coordinate labels spacelike hypersurfaces with intrinsic geometry specified by the spatial metric tensor γ_{ij}. The unit timelike four-vector normal to the hypersurface is given by

$$n_\mu = (-\alpha, 0, 0, 0), \qquad n^\mu = \left(\frac{1}{\alpha}, -\frac{\beta^i}{\alpha}\right). \tag{4}$$

The proper time interval along n^μ between two neighboring hypersurfaces is α times the coordinate time interval Δt. The three-vector $\beta^i\Delta t$ on the next hypersurface is the vector from the intersection point of the normal line to that of the coordinate line. So α and β^i are called the lapse function and the shift vector, respectively. The unit tensor of projection into the hypersurface is defined by

$$h^\mu{}_\nu = \delta^\mu{}_\nu + n^\mu n_\nu. \tag{5}$$

For any vector, say V^ν, the projected vector $h^\mu{}_\nu V^\nu$ is the vector in the hypersurface or $n_\nu h^\mu{}_\nu V^\nu = 0$. The extrinsic curvature defined by

$$K_{ij} = -h_i{}^\mu h_j{}^\nu n_{\mu;\nu} = -\frac{1}{2\alpha}\left(\gamma_{ij,0} - \beta_{i|j} + \beta_{j|i}\right) \tag{6}$$

describes how the hypersurface is locally embedded in the four-dimensional spacetime. Here " ; " denotes a four-dimensional covariant derivative with respect to $g_{\mu\nu}$,

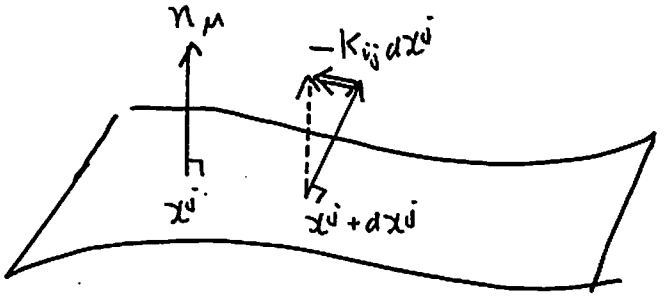

Fig. 3. Extrinsic curvature.

" | " a three-dimensional covariant derivative with respect to γ_{ij} and " , " an ordinary partial derivative.

The (3+1)-decomposition of Einstein equations is performed by multiplying them by $n^\mu n^\nu$, $n^\mu h_i{}^\nu$ to get

(1) the Hamiltonian constraint

$$2G_{\mu\nu}n^\mu n^\nu = R + K^2 - K_{ij}K^{ij} = 16E, \tag{7}$$

where $R = R_{ii} = \gamma^{ij}R_{ij}$, and

(2) the momentum constraints

$$-G_{\mu\nu}n^\mu h_i{}^\nu = K_i{}^j{}_{|j} - K_{|i} = 8\pi J_i, \tag{8}$$

where $K = K^i{}_i$, and multiplying Einstein equations in the form

$$^{(4)}R_{\mu\nu} = 8\pi(T_{\mu\nu} - g_{\mu\nu}T/2) \tag{9}$$

by $h_i{}^\mu h_j{}^\nu$ to get

(3) the evolution equations

$$\begin{aligned}\partial_t K_{ij} \;=\; & \alpha(R_{ij} + KK_{ij}) - 2\alpha K_{ik}K^k_j - 8\pi\alpha\,(S_{ij} + \gamma_{ij}(E-S)/2) \\ & -\alpha_{|ij} + \beta^k{}_{|j}K_{ki} + \beta^k{}_{|i}K_{kj} + \beta^k K_{ij|k}.\end{aligned} \tag{10}$$

For the evolution of γ_{ij}, we use Eqs.(6) or

$$\partial_t \gamma_{ij} = -2\alpha K_{ij} + \beta_{i|j} + \beta_{j|i} \tag{11}$$

Here ${}^{(4)}R_{\mu\nu}$ is the four-dimensional Ricci tensor with respect to $g_{\mu\nu}$ and R_{ij} is the three-dimensional Ricci tensor with respect to γ_{ij}. The energy density E, the momentum density J_i and the stress tensor S_{ij} of the matter measured by the normal line observer are, respectively, defined by

$$E = n^\mu n^\nu T_{\mu\nu}, \tag{12}$$

$$J_i = -h_i{}^\mu n^\nu T_{\mu\nu}, \tag{13}$$

$$S_{ij} = h_i{}^\mu h_j{}^\nu T_{\mu\nu}, \tag{14}$$

and $S = S^i{}_i$.

Evolution equations of matter are given by the energy-momentum conservation equations, or the contracted Bianchi identities

$$T_\mu{}^\nu{}_{;\nu} = G_\mu{}^\nu{}_{;\nu} = 0. \tag{15}$$

For a perfect fluid, $T_{\mu\nu}$ is given by

$$T_{\mu\nu} = (\rho + \rho\varepsilon + P)u_\mu u_\nu + P g_{\mu\nu}, \tag{16}$$

where ρ is the proper mass density (or baryon mass density), ε is the internal energy per unit mass, P is the pressure and u_μ is the four velocity of the matter. The pressure P and the internal energy ε are related to the mass density ρ by an equation of state. The conservation of mass (or baryon number) implies $(\rho u^\alpha)_{;\alpha} = 0$, by definition. It can be written as

$$D_t(\alpha u^0 \rho) = 0, \tag{17}$$

where

$$D_t Q \equiv \partial_t(\gamma^{1/2} Q) + \partial_k(\gamma^{1/2} V^k Q) \tag{18}$$

with γ being the determinant of γ_{ij} and $V^i = u^i/u^0$. The "(3+1) variables" E, J_i and S_{ij} defined by Eqs.(12)-(14) are related to ρ, ϵ, P and u^μ by

$$E = (\rho + \rho\varepsilon)(\alpha u^0)^2 P\left[(\alpha u^0)^2 - 1\right], \tag{19}$$

$$J_i = (\rho + \rho\varepsilon + P)\alpha u^0 u_i, \tag{20}$$

$$S_{ij} = (\rho + \rho\varepsilon + P)u_i u_j + P h_{ij}. \tag{21}$$

In order to obtain the evolution equations of E and J_i, write the energy-momentum tensor in the form

$$\begin{aligned} T_{\mu\nu} &= (h_{\mu\alpha} - n_\mu n_\alpha)(h_{\nu\beta} - n_\nu n_\beta)T^{\alpha\beta} \\ &= E n_\mu n_\nu + J_\mu n_\nu + J_\nu n_\mu + S_{\alpha\beta} h_\mu{}^\alpha h_\nu{}^\beta \end{aligned} \tag{22}$$

and project Eq.(15) along u^μ and $(\delta_i{}^\mu - u_i u^\mu)$. Then we have

$$D_t E = -\partial_k \left(\gamma^{1/2} P(V^k + \beta^k)\right) + \alpha\gamma^{1/2} P K - \gamma^{1/2} J^k \partial_k \alpha + \frac{\alpha\gamma^{1/2} J^k J^m K_{km}}{P+E} \tag{23}$$

and

$$D_t J_i = -\alpha\gamma^{1/2}\partial_i P - \gamma^{1/2}(P+E)\partial_i \alpha + \frac{\alpha\gamma^{1/2} J^k J^m}{2(P+E)}\partial_i \gamma_{km} + \gamma^{1/2} J_k \partial_i \beta^k. \tag{24}$$

Now we have 4 constraint equations, Eqs.(7) and (8), 12 evolution equations, Eqs.(10) and (11), of the metric and 4 evolution equations, Eqs.(23) and (24), of the matter. However, these equations are not independent because of the Bianchi identities. To illustrate it, define the deviations from the constraints:

$$H = \gamma^{1/2}(K_{ij}K^{ij} - K^2 - R - 8\pi E) \tag{25}$$

$$H_i = -2\gamma^{1/2}(K_i{}^j{}_{|j} - K_{|i} - 8\pi J_i). \tag{26}$$

If we assume H and H_i do not vanish and α and β^i are not functionals of γ_{ij} and K_{ij}, the deviations H and H_i evolve as

$$\partial_t H = 2H^i \partial_i \alpha + \alpha \partial_i H^i - \partial_i (H\beta^i) \tag{27}$$

$$\partial_t H_i = H\partial_i \alpha - \partial_j(\beta^j H_i) - H_j \partial_i \beta^j. \tag{28}$$

These equations assure that H and H_i vanish if $H = H_i = 0$ at $t = 0$. Therefore, if we solve the constraint equations in the initial Cauchy slice, we need not solve them afterward, when we have only to solve evolution equations. This is called the free evolution method. In this method, the deviations of the constraint defined by Eqs.(27) and (28) can be used to check the accuracy of numerical solution. Alternative methods can be chosen to evolve the metric. In constrained evolution, all the constraint equations are solved. In partially constrained evolution, some of the constraint equations are solved. Chopped evolution is free or partially constrained evolution which is fully constrained every fixed time interval. In any case, we solve 12 (or less if the system has some symmetry) evolution equations for the metric in each time step. This corresponds only 6 degrees of freedom and their time derivatives, while there are 10 degrees of freedom in the four-dimensional metric tensor $g_{\mu\nu}$. The rest of degrees of freedom is determined by coordinate (or gauge) conditions, which we will discuss later.

In a numerical point of view, it is more time consuming to solve a constraint equation than an evolution equation since a constraint equation is generally an elliptic partial differential equation. This difficulty disappears in some gauges, where a constraint equation become parabolic. It has been shown that fully constraint schemes are likely to be numerically stable in some cases.[18]

4. Initial Data

In any scheme described the previous section, the Hamiltonian and the momentum constraint equations, Eqs.(7) and (8), are solved in the initial hypersurface to obtain the initial data. York and his collaborators gave a general scheme for solution of constraint equations.[19, 20] In York's procedure, only the conformal factor of three-dimensional metric and the longitudinal part of the extrinsic curvature tensor are governed by the constraint equations while the conformed metric and the transverse-traceless and the trace parts of the extrinsic curvature tensor are freely specified. In principle it is possible to specify other parts of the metric tensor and the extrinsic curvature tensor using the constraint equations. However, York's procedure is up to now the only one that leads to an elliptic set of equations for which proofs of existence of a unique solution exists.[21] In this procedure, the three-dimensional metric tensor γ_{ij} is decomposed into a conformal factor ψ^4 and a conformed metric $\tilde{\gamma}_{ij}$:

$$\gamma_{ij} = \psi^4 \tilde{\gamma}_{ij} \tag{29}$$

We consider that $\tilde{\gamma}_{ij}$ is given. Then the three-dimensional Ricci scalar R is given by

$$R = \psi^{-4}\tilde{R} - 8\psi^{-5}\tilde{\Delta}\psi. \tag{30}$$

Here the tilde " ~ " denotes quantities or operators with respect to the conformed metric $\tilde{\gamma}_{ij}$; $\tilde{\Delta} = \tilde{\gamma}^{ij}\tilde{\nabla}_i\tilde{\nabla}_j$ is the Laplacian with respect to $\tilde{\gamma}_{ij}$. If $\tilde{K}^{ij}$ is defined by

$$K^{ij} = \psi^{-10}\tilde{K}^{ij}, \tag{31}$$

then its divergence and trace part are given by

$$\nabla_j K^{ij} = \psi^{-10}\tilde{\nabla}_j\tilde{K}^{ij} \qquad \text{and} \qquad K = \psi^{-6}\tilde{K}. \tag{32}$$

Any symmetric tensor $\tilde{K}_{ij}$ can be decomposed as

$$\tilde{K}_{ij} = \tilde{K}^{TT}_{ij} + (\tilde{L}W)_{ij} + \frac{1}{3}\tilde{\gamma}_{ij}\tilde{K}, \tag{33}$$

where $\tilde{K}^{TT}_{ij}$ and $\tilde{K}$ are the transverse-traceless part and the trace of $\tilde{K}_{ij}$. The longitudinal part $(\tilde{L}W)_{ij}$ is given, using a "vector potential" W_i, by

$$(\tilde{L}W)_{ij} = \tilde{\nabla}_i W_j + \tilde{\nabla}_j W_i - \frac{2}{3}\tilde{\gamma}_{ij}\tilde{\nabla}_k W^k. \tag{34}$$

Since $\tilde{K}^{TT}_{ij}$ is transverse, its divergence vanishes, $\tilde{\nabla}^j\tilde{K}^{TT}_{ij} = 0$, by definition; $(\tilde{L}W)_{ij}$ is longitudinal since

$$\int_\Sigma K^{TT}_{ij}(\tilde{L}W)^{ij}\tilde{\gamma}^{1/2}\, d^3x = 0. \tag{35}$$

Using transformed quantities, the Hamiltonian and the momentum constraint equations are written as

$$8\tilde{\Delta}\psi - \tilde{R}\psi + \left(\tilde{K}_{ij}\tilde{K}^{ij}\right)\psi^{-7} - \frac{2}{3}\tilde{K}^2\psi^5 = -16\pi\rho_B\psi^{-1} \tag{36}$$

and

$$\tilde{\Delta}W_i + \frac{1}{3}\tilde{\nabla}_i\tilde{\nabla}^j W_j - \frac{2}{3}\tilde{\nabla}_i\tilde{K} = 8\pi\tilde{J}_i, \tag{37}$$

where $\rho_B = \psi^6 E$ and $\tilde{J}_i = \psi^6 J_i$. The conformal factor ψ^4 and the vecotr potential W_i are determined by these equations, while $\tilde{\gamma}_{ij}$, $\tilde{K}_{ij}^{TT}$, $\tilde{K}$, ρ_B and $\tilde{J}_i$ are freely specified. In many cases, $\tilde{\gamma}_{ij}$ is chosen as the metric of the flat space and $\tilde{K}_{ij}^{TT} = \tilde{K} = 0$. In this choice, $\tilde{R} = 0$ and it simplifies the constraints equations.

Asymptotic flatness requires the boundary condition as $\psi \to 1$ and $W_i \to 0$ for $r \to \infty$. However, in numerical calculation the numerical boundary is not infinity but finite though it is far from the source. Therefore we need the boundary condition at the numerical boundary. For ψ, it is

$$\psi = 1 + \frac{M}{2r} + O(r^{-2}), \tag{38}$$

where M is the total energy. Usually it is used in the form

$$\frac{\partial u}{\partial r} + \frac{u}{r} = O(r^{-3}), \tag{39}$$

where $u = \psi - 1$.

As for W_i, at the region where $\tilde{J}_i = 0$, for Eq.(37) with $W_i \to 0$ for $r \to \infty$, there are three solutions which, combined, yield[22, 20]

$$W_i = -\frac{1}{4r}(n_i n_k + 7\tilde{\gamma}_{ik})P^k + O(r^{-2}), \tag{40}$$

where P^i is a constant vector and $n_i = x^i/r$ is the unit normal of a sphere. With this vector potential, $\tilde{K}_{ij}$ is given by

$$\tilde{K}^{ij} = \frac{3}{2r^2}\left[P^i n^j + P^j n^i - (\tilde{\gamma}^{ij} - n^i n^j)P^k n_k\right] + O(r^{-3}). \tag{41}$$

Thus P^i is the total linear momentum of the system;

$$P^i = \frac{1}{8\pi}\int_\infty (\tilde{K}^{ij} - \tilde{\gamma}^{ij}K)\, d^2S_j = \int \tilde{J}^i\, dV \tag{42}$$

Since $\tilde{J}^i$ can be freely specified and it determined P^i, the boundary condition can be written as

$$\frac{\partial V^i}{\partial r} + \frac{2V^i}{r} = O(r^{-3}), \tag{43}$$

where

$$V_i = W_i + (n_i n_k + 7\tilde{\gamma}_{ik})P^k/(4r). \tag{44}$$

5. Coordinate Conditions

The coordinate conditions specify the lapse function α and the shift vector β^i, which, in principle, can be freely specified since they are not determined by Einstein equations. The coordinate conditions are related also to the choice of the coordinate system; Cartesian (x, y, z), spherical (r, θ, ϕ), cylindrical (R, ϕ, z), etc. How to foliate the four-dimensional space-time into a set of three-dimensional hypersurfaces is determined by α and the coordinate system in each hypersurface is by β^i. What coordinate conditions are imposed plays a crucial role in success in a numerical solution. Here I will present a brief review of various coordinate conditions.

We have the following demands on the coordinate conditions.

1. Singularity avoidance:

   If a singularity appears in the numerical region, we can not continue the numerical calculation. So we should use the coordinates that do not develop singularities. For example, the coordinate conditions are imposed so that the time advances slowly near physical singularities but the whole space-time region that is physically important can be covered. Moreover the coordinates must not develop coordinate singularities, apart from simple singularities that can be factored out.

2. Simplification:

   We should use a coordinate system that simplifies the metric and Einstein equations. A complicated form of the equations, in general, causes difficulty in accurate solution and in stability of numerical calculation.

3. Calculation of gravitational radiation:

   Gravitational waves can propagate in the region away from sources. It is possible if the coordinates turn to a natural radiation gauge asymptotically. In order to calculate the energy and the waveform of gravitational waves, the gravitational degree of freedom should be isolated as much as possible.

4. Unique form of known exact solutions:

   In order to identify the final destiny of the space-time evolution, it is advantageous if known exact solutions have a unique form in the chosen coordinate system.

5.1. Lapse function and slicing condition

Slicing conditions, or the conditions on α, are particularly related to singularity avoidance. Thus it is very important for success in numerical solution.

Gaussian coordinates

The choice of

$$\alpha = 0 \qquad \text{(usually with } \beta^i = 0\text{)} \tag{45}$$

is called Gaussian coordinates. This is the simplest and used in early works.[9] However it does not leads to any simplification of Einstein equations except for elimination of α (and β^i). This coordinates has a tendency to form caustics and singularities that are pure coordinate singularity. Physical singularities can not be avoided.

Lagrangian slicing

In slicing

$$\alpha u^0 = 1, \tag{46}$$

where u^0 is the t-component of the matter four-velocity, the spatial components of the velocity u^i vanish and the spacelike hypersurfaces are orthogonal to the flow lines. If $\beta^i = 0$, the spatial coordinates follow the matter flow lines. So this slicing is called Lagrangian slicing. It simplifies the hydrodynamics equations. However, the matter flow lines converge towards a singularity if it forms. The Lagrangian hypersurfaces touch the black hole's singularity as soon as it forms long before all the matter falls into the black hole.

Maximal slicing

Maximal slicing condition is that

$$K = 0, \tag{47}$$

where K is the trace of the extrinsic curvature tensor. The variation δV of three-volume of each spacelike hypersurface V defined by

$$V = \int_S \gamma^{1/2}\, d^3x \tag{48}$$

vanishes on this condition; $\delta V = 0$. It means that this condition maximizes the three-volume. With $K = 0$ in the initial hypersurface, $\partial K/\partial t = 0$ yields the maximal slicing condition. Thus the lapse function α is determined by

$$\frac{\partial K}{\partial t} = -\triangle \alpha + \left[K_{ij}K^{ij} + 4\pi(E+S)\right]\alpha = 0. \tag{49}$$

Asymptotic flatness requires the boundary condition

$$\alpha \to 1 + \frac{\text{const}}{r} \qquad \text{for } r \to \infty. \tag{50}$$

Maximal slicing has excellent singularity avoidance features. The lapse function α decreases exponentially near the singularity where $E+S$ is large, allowing the maximal slices to span the rest of the future development of the initial data.[23, 24, 25] Gravitational radiation can propagate nicely on maximal slices.[26] In the equation for α Eq.(49), the shift vector β^i does not appear. Thus α can be determined independently of β^i. Therefor maximal slices are very popular in recent numerical works, although one needs to solve an elliptic equation at each time step.

Constant mean curvature hypersurface

Maximal slicing is generalized as

$$K = k(t), \tag{51}$$

where $k(t)$ is constant in each hypersurface, while it may depend on time t. It has singularity avoidance feature like maximal slicing.[23] Constant mean curvature hypersurfaces become asymptotically null and reach null infinity (either $^+$ or $^-$ depending on the sign of $k(t)$), while maximal hypersurfaces reach spacelike infinity I^0. This may be advantageous for studying propagation of gravitational radiation. For cosmological problems, this slicing leads to the natural generalization of the constant time slices of the Robertson-Walker metric.[27]

Polar hypersurfaces

Polar hypersurfaces,

$$K - K^r{}_r = 0, \tag{52}$$

are compatible with spherical polar coordinates (r, θ, ϕ).[12] This slicing condition yields the equation for α given by

$$\frac{\partial K}{\partial t} - \frac{\partial K^r{}_r}{\partial t} = 0, \tag{53}$$

which is a parabolic equation since the second order derivative of α with respect to r disappears. Solution of the parabolic equation is less time consuming than solution of the elliptic equation Eq.(49). With the radial gauge discussed later, the polar slicing seems to have singularity avoidance feature that is even stronger than that of maximal slicing. Unlike in prior slicing conditions, the shift vector β^i appears in the equation for α. If equations for α and β^i are solved simultaneously, the equations become an elliptic system. Moreover the behavior of polar hypersurfaces becomes irregular at the origin. To avoid the irregularity, an inner portion of the polar hypersurface must be replaced by another. For example, the condition that hypersurfaces are maximal near the origin and polar outside the intermediate region, and they are fitted smoothly as

$$K = C(r/r_c)K^r{}_r, \tag{54}$$

where C is a smooth function with $C(0) = 0$ and $C(x) = 1$ for $x \geq 1$.

5.2. Shift vector

The condition on the shift vector β^i is not so crucial as that on the lapse function α. However it is related to simplification of Einstein equations and isolation of the gravitational degrees of freedom.

Normal coordinates

The normal coordinate condition:

$$\beta^i = 0, \tag{55}$$

is the simplest. The trajectories fo these coordinates are orthogonal to the spacelike hypersurfaces. Thus this condition never leads to a coordinate singularity. Disappearance of β^i makes evolution equations simple but this simplification is very minor in the numerical point of view. It might be very difficult to identify the formation of a specific geometry. In spite of such drawbacks, the normal coordinate condition was used in many works.

Lagrangian coordinates

Lagrangian coordinates,

$$\beta_i = -u_i/u_0, \tag{56}$$

leads to u^i and follow the matter, while u_i does not generally vanish. (Note that Lagrangian slicing Eq.(46) with $\beta^i = 0$ leads to $u^i = u_i = 0$.) These coordinate will not develop coordinate singularity unless a physical hydrodynamic singularity appears. However, if shock waves appear, they causes difficulties. Moreover it may be very hard to propagate the gravitational radiation through the coordinate shear produced by the matter motion.

Minimal distortion

The minimal distortion condition specify β^i as the solution of

$$\sigma_{ij}{}^{|j} = 0, \tag{57}$$

where σ_{ij} is the distortion tensor defined by

$$\sigma_{ij} = \partial_t \gamma_{ij} - \frac{1}{3}\gamma_{ij}\gamma^{\ell m}\partial_t \gamma_{\ell m} \tag{58}$$

$$= -2\alpha\left(K_{ij} - \frac{1}{3}\gamma_{ij}K\right) + \beta_{i|j} + \beta_{j|i} - \frac{2}{3}\gamma_{ij}\beta^{\ell}{}_{\ell}. \tag{59}$$

It leads to

$$\triangle\beta_i + \frac{1}{3}\beta^k{}_{|k|i} + R_{ij}\beta^j = \left[2\alpha(K_{ij} - \frac{1}{3}\gamma_{ij}K)\right]^{|j}. \tag{60}$$

It has not been shown yet that this condition will not develop coordinate singularities. However it seems to be an excellent radiation gauge.[28] The greatest disadvantage of the minimal distortion condition is that very complex vector elliptic equations Eq.(60) should be solved in each time step.

Simplifying gauge

In order to simplify Einstein equations and to isolate the gravitational degrees of freedom, it is advantageous that one determines the form of the metric γ_{ij} in advance. For example, particular components of γ_{ij} is assumed to vanish. Or more generally, assume that γ_{ij} satisfies a general algebraic relation,

$$F(\gamma_{ij}, x^i) = Q(x^i), \tag{61}$$

and the condition

$$\partial_t F = \frac{\partial F}{\partial \gamma_{ij}}\frac{\partial \gamma_{ij}}{\partial t} \tag{62}$$

$$= \frac{\partial F}{\partial \gamma_{ij}}(\beta_{i|j} + \beta_{j|i} - 2\alpha K_{ij}) = 0 \tag{63}$$

determines β^i. With three components of β^i, we can impose up to three coordinate conditions of the form of Eq.(61).

In diagonal gauge, where the three-metric is given by

$$ds^2 = \gamma_{xx}dx^2 + \gamma_{yy}dy^2 + \gamma_{zz}dz^2, \tag{64}$$

the shift vector equations are

$$\begin{aligned} \gamma_{xx}\partial_y\beta^x + \gamma_{yy}\partial_x\beta^y &= 2\alpha K_{xy}, \\ \gamma_{yy}\partial_z\beta^y + \gamma_{zz}\partial_y\beta^z &= 2\alpha K_{yz}, \\ \gamma_{zz}\partial_x\beta^z + \gamma_{xx}\partial_z\beta^x &= 2\alpha K_{zx}. \end{aligned} \tag{65}$$

Usually this set of equations does not have a solution or it is not unique even if it exists.

With spherical coordinates (r, θ, ϕ), the radial gauge is particularly useful.[12] The three-metric has the form

$$ds^2 = A^2dr^2 + r^2B^{-2}d\theta^2 + r^2B^2(\sin\theta d\phi + \xi d\theta)^2. \tag{66}$$

The simplifying conditions are

$$\gamma_{r\theta} = \gamma_{r\phi} = 0 \tag{67}$$

and

$$\gamma_{\theta\theta}\gamma_{\phi\phi} - \gamma_{\theta\phi}^2 = r^4 \sin^2\theta. \tag{68}$$

Note that from Eq.(68) the coordinate r obtains a direct geometrical meaning, that is, the area of a constant-r sphere is $4\pi r^2$. The radial gauge is a natural generalization of Schwarzschild coordinates. The shift vector equations are

$$\begin{aligned}(2\beta^r/r)_{,r} - \frac{1}{\sin\theta}(A^2\beta^{r,\theta}\sin\theta)_{,r} - (A^2\beta^{r,\phi})_{,\phi} \\ = \left[2\alpha(K_\theta^\theta + K_\phi^\phi)\right]_{,r} - \frac{1}{\sin\theta}(2\alpha K_r^\theta \sin^2\theta)_{,\theta} - (2\alpha K_r^\phi)_{,\phi}\end{aligned} \tag{69}$$

$$\beta^{\theta,r} = 2\alpha K^{r\theta} - \beta^{r,\theta} \tag{70}$$

$$\beta^{\phi,r} = 2\alpha K^{r\phi} - \beta^{r,\phi} \tag{71}$$

The isothermal gauge,

$$ds^2 = \phi^4\left[B^{-2}(dr^2 + r^2 d\theta^2) + r^2 B^2(\sin\theta d\phi + \xi d\theta)^2\right], \tag{72}$$

gives another simplifying condition. In this gauge

$$\gamma_{r\theta} = \gamma_{r\phi} = 0, \qquad \gamma^{rr} = \gamma^{\theta\theta}, \tag{73}$$

and the shift vector equations are

$$\alpha(K^{\theta\theta} - r^{-2}K^{rr}) = -r^{-1}\left(r^{-1}\beta^r\right)^{,r} + \beta^{\theta,\theta} \tag{74}$$

together with Eqs.(70) and (71).

6. Conclusions

Numerical solution of the evolution equations requires boundary conditions at the outer boundary and the inner boundary. The inner boundary condition is related to the regularity condition at the origin or the polar axis when the polar coordinates are used. This condition, together with isolation of the gravitational degrees of freedom, leads choice of the numerical variable. For three dimension problems, it is particularly difficult to impose completely the regularity conditions. Thus it seems to be better to use Cartesian coordinates (x, y, z), where there is no inner boundary. In addition, choice of numerical schemes for integration of elliptic equations and evolution equations is very important to stable and accurate numerical calculation. However we do not discuss these problems here.

According to development of computer technology and computational algorithms, the best choice of the coordinate conditions and the scheme of evolving the space-time is altered. For three-dimensional problems, it is natural to use Cartesian coordinates. It does not lead so serious difficulties in numerical algorithms as to use polar coordinates. However it is more memory consuming. If a supercomputer with a lot of memory, 100Gbytes or more, this drawback is not so serious. Development of computer technology affects computational algorithms as well as coding technique. Since vector supercomputers are presented, algorithms suitable for vector processors have been developed. During the next five years, a wide vaiety of parallel supercomputers with a large number of processors (more than a thousand processors) will become available and their use will be essential to achieve the speed-ups. This will require a new generation of codes that take advantage of parallelism; we will have to consider distribution of programs and data to processors and communication between them. Moreover handling output data will become increasingly important as numerical computation becomes larger in scale.

References

1. L. Smarr, Ann. N.Y. Acad. Sci. **302** (1977), 569.
2. T. Piran, in *Proceedings of the Second Marcel Grossmann Meeting on General Relativity*, ed. R. Ruffini (North-Holland, Amsterdam, 1982);
   in *Gravitational Radiation*, eds. M. Deruelle and T. Piran, (North-Holland, Amsterdam, 1983).
3. T. Nakamura, K. Oohara and Y. Kojima, Prog. Theor. Phys. Suppl. No. 90 (1987).
4. *Sources of Gravitational Radiation*, ed. L. Smarr (Cambridge University Press, Cambridge, 1979).
5. *Numerical Relativity and Dynamical Spacetimes*, J. M. Centrella (Cambridge University Press, Cambridge, 1986).
6. *Frontiers in Numerical Relativity*, eds. C. R. Evans, L. S. Finn and D. W. Hobill (Cambridge University Press, Cambridge, 1989).
7. D. W. Hobill and L. Smarr, ibid., p. 1.
8. M. May and R. White, Phys. Rev. **141** (1966), 1232.
9. S. G. Harn and R. W. Lindquist, Ann. Phys. **29** (1964), 304.
10. L. Smarr, in *Sources of Gravitational Radiation*, ed. L. Smarr (Cambridge University Press, Cambridge, 1979).
    L. Smarr, A. Cadez, B. DeWitt and K. Eppley, Phys. Rev. **D14** (1976), 2443.
11. T. Nakamura, K. Maeda, S. Miyama and M. Sasaki, Prog. Theor. Phys. **63** (1980), 1229.
12. J. M. Bardeen and T. Piran, Phys. Rep. **96** (1983), 205.
13. R.F. Stark and T. Piran, in *Proceedings of the Fourth Marcel Grossmann Meeting on General Relativity*, ed. R. Ruffini (Elsevier, Amsterdam, 1986), p. 327.

14. K. Oohara and T. Nakamura, in *Proceedings of the Sixth Marcel Grossmann Meeting on General Relativity,* ed. H. Sato and T. Nakamura (World Scientific, Singapore, 1992), in press.
15. R. Arnowitt, S. Deser and C. W. Misner, in *Gravitation—An Introduction to Current Research*, ed L. Witten (Wiley, New York, 1962).
16. R. Gómez and J. Winicour, in *Frontiers in Numerical Relativity* (1989) p. 385.
17. M. R. Dubal, in *Gravitational Collapse and Relativity,* (World Scientific, Singapore, 1986) p. 339.
18. T. Piran, J. Comp. Phys. **35** (1980), 254.
19. N. ÓMurchadha and J. W. York, Jr., Phys. Rev. **D10** (1974), 428.
20. in *Gravitational Radiation* eds. M. Deruelle and T. Piran, (North-Holland, Amsterdam, 1983).
21. M. Cantor, J. Math. Phys. **20** (1979), 1741;
D. Christodonlon and N. ÓMurchadha, Comm. Math. Phys. **80** (1981), 271.
22. K. Oohara and T. Nakamura, Prog. Theor. Phys. **81** (1989), 360.
23. D. M. Eardley and L. Smarr, Phys. Rev. **D19** (1980), 2239.
24. K. Maeda, Prog. Theor. Phys. **63** (1980), 425.
25. K. Maeda, S. Miyama, M. Sasaki and T. Nakamura, Prog. Theor. Phys. **63** (1980), 1048.
26. L. Smarr and J. W. York, Jr., Phys. Rev. **D17** (1978), 1945.
27. J. W. York, Jr., Phys. Rev. Lett. **28** (1972), 1082.
28. J. M. Bardeen, in *Gravitational Radiation*, eds. M. Deruelle and T. Piran, (North-Holland, Amsterdam, 1983).

Perturbation near the Schwarzschild Black Hole and Test for the Gauge Condition in Numerical Relativity

Masaru Shibata

Department of Physics, Kyoto University, Kyoto 606, Japan

and

Takashi Nakamura

Research Institute for Fundamental Physics
Kyoto University, Kyoto 606, Japan

1. Introduction

One of the most important purposes in numerical relativity is to calculate the wave form and the radiation efficiency of gravitational waves emitted in the stellar core collapse and the collision of two compact stars. However there have been only a few analyses of gravitational waves in the general relativistic way. The most crucial reason is that we do not know an appropriate gauge condition for each problem in numerical relativity well. Therefore we must find them, but even if we just think of a good idea of gauge condition, it is very hard to confirm the suitability of it by carrying out a numerical relativistic calculation. Accordingly we need some testbed calculations of it.

One effective method is a perturbative calculation on fixed spacetime of a black hole. This is because it is much easier than a fully relativistic calculation, and still we can investigate features of the situations with the fast motion and the strong gravitational field. Furthermore previous authors showed that the results in the perturbative calculations are fairly coincident with the results in numerical relativistic calculations in respect to the wave form and the radiation efficiency of gravitational waves. For these reasons perturbative calculations have been extensively performed by many authors[1] . But all of them calculated gravitational waves only at infinity and did not utilize these analyses to investigate the behavior of the metric perturbations in the strong field near the black hole. In numerical relativity we need to know the behavior of the metric in the strong

gravitational field and have to estimate gravitational waves and its energy flux at a finite radius. Therefore it is important to know the behavior of the metric perturbations, especially the gravitational waves, near the black hole.

So we calculate the metric perturbations near the Schwarzschild black hole under a few gauge conditions used in numerical relativity and evaluate the minimum radius at which one can estimate the wave form and the energy flux accurately.

2. Formulations

The metric perturbations on the Schwarzschild geometry when a test particle of mass μ falling straightly into a Schwarzschild black hole of mass $M \gg \mu$ were studied by Regge and Wheeler[2] and Zerilli[3] . According to them, all of the metric perturbations can be expressed by $R_{l\omega}(r)$. In this case the system is axisymmetric and nonrotational, so $R_{l\omega}$ obeys,

$$\frac{d^2 R_{l\omega}}{dr^{*2}} + [\omega^2 - V_l(r)]R_{l\omega} = S_{l\omega}(r), \tag{2.1}$$

where r^* is the tortoise coordinate defined by

$$r^* = r + 2M \ln(\frac{r}{2M} - 1). \tag{2.2}$$

V_l is the potential defined by

$$V_l = \frac{(r-2M)}{r^4(\lambda r + 3M)^2}[2\lambda_l^2(\lambda_l + 1)r^3 + 6\lambda_l^2 M r^2 + 18\lambda_l M^2 r + 18M^3], \tag{2.3}$$

where $\lambda_l = (l-1)(l+2)/2$. $S_{l\omega}$ are the sources for $R_{l\omega}$, which is

$$S_{l\omega} = \frac{4}{\lambda r + 3M}\sqrt{l + \frac{1}{2}}(1 - \frac{2M}{r})[\sqrt{\frac{r}{2M}} - \frac{2i\lambda}{\omega(\lambda r + 3M)}]e^{i\omega T(r)}, \tag{2.4}$$

where

$$T(r) = 2M[-\frac{2}{3}(\frac{r}{2M})^{3/2} - 2(\frac{r}{2M})^{1/2} + \ln\frac{(r/2M)^{1/2}+1}{(r/2M)^{1/2}-1}], \tag{2.5}$$

describes the time when the particle passes the radius r.

Eq.(2.1) should be solved under the boundary conditions of purely outgoing waves at infinity ($r^* \to \infty$) and purely ingoing waves at Schwarzschild radius ($r^* \to -\infty$).

Now we carry out the gauge transformation from the Regge-Wheeler gauge to some other gauge conditions. We write the metric perturbation as h_{ab}. Under the gauge transformation $(x^a)^{new} = x^a - \xi^a$, the metric h_{ab} is transformed to

$$h_{ab}^{new} = h_{ab}^{RW} + \nabla_a \xi_b + \nabla_b \xi_a, \tag{2.6}$$

where 'new' and 'RW' denote a new gauge which we may use in numerical relativity and Regge-Wheeler gauge, respectively. ∇_a is the covariant derivative operator assosiated with the Schwarzschild metric.

2.1 Radial gauge

Radial gauge was suggested by Bardeen and Piran[4] and its gauge conditions are written as

$$\gamma_{r\theta} = \gamma_{r\varphi} = 0,$$

and

$$\gamma_{\theta\theta}\gamma_{\varphi\varphi} - \gamma_{\theta\varphi}^2 = r^4 \sin^2\theta. \tag{2.7}$$

The linear approximation of the last gauge condition becomes

$$h_{\theta\theta} + \frac{h_{\varphi\varphi}}{\sin^2\theta} = 0. \tag{2.8}$$

When we perform the gauge transformation from the Regge-Wheeler gauge to the radial gauge using the above gauge condition, we get the following equations for the gauge variables.

$$\partial_r \xi_\theta + \partial_\theta \xi_r - \frac{2\xi_\theta}{r} = -h_{r\theta}^{RW} = 0,$$

and

$$\frac{1}{\sin\theta}\partial_\theta(\sin\theta\xi_\theta)+2(r-2M)\xi_r=-(h^{RW}_{\theta\theta}+\frac{h^{RW}_{\varphi\varphi}}{\sin^2\theta})/2. \tag{2.9}$$

Now we expand ξ_i by the vector harmonics

$$\xi_i=(\xi_1 Y_{l0},\quad \xi_2 Y_{l0,\theta},\quad 0), \tag{2.10}$$

where ξ_1 and ξ_2 are functions of r, which depend on l. We also expand h^{RW}_{ab} by the tensor harmonics, then the equations of the Fourier coefficient of ξ_i become (we omit the subscript ω, l and m)

$$\xi_{2,r}-2\xi_2/r+\xi_1=0,$$

and

$$2(r-2M)\xi_1-l(l+1)\xi_2=-K(r)r^2, \tag{2.11}$$

where $K(r)$ is the Fourier transform of one of the metric perturbations in the Regge-Wheeler gauge[3] . Accordingly the gauge variable ξ_i can be found by solving the first order ordinary differential equations.

Now we are interested in the gravitational wave perturbations η[4] , so we calculate them from the gauge variables. Then

$$\eta=-\frac{1}{r^2}\sum_{l\geq 2}\int\frac{d\omega}{\sqrt{2\pi}}e^{-i\omega t}\xi_2 W_{l0}, \tag{2.12}$$

In the above treatment we only consider the spatial gauge variables, but the time component of gauge variable can be added. However in the case of radial gauge it does not affect η, so it is sufficient to consider only the spatial displacement.

2.2 Isothermal gauge(Quasi isotropic gauge)

Isothermal gauge or quasi isotropic gauge was proposed by several authors[4] [5] [6] and its gauge conditions are written as

$$\gamma_{r\theta} = \gamma_{r\varphi} = 0,$$

and

$$\gamma_{rr}\gamma_{\varphi\varphi}r^2 = \gamma_{\theta\theta}\gamma_{\varphi\varphi} - \gamma_{\theta\varphi}^2. \tag{2.13}$$

The linear approximation of the last equation becomes

$$\gamma_{rr} = \gamma_{\theta\theta}/r^2. \tag{2.14}$$

In the case of the isothermal gauge, the radial coordinate r corresponds to the isotropic one, which is related to the Schwarzschild radial coordinate r_{Sch} by

$$r = \frac{1}{2}[r_{Sch} - M + \sqrt{r_{Sch}^2 - 2r_{Sch}M}]. \tag{2.15}$$

In the following since we consider the metric perturbations in the isotropic coordinate, we must rewrite the Regge-Wheeler gauge to isotropic form.

Using the gauge conditions, we get the equations of the Fourier coefficients of the gauge variables as follows.

$$\partial_r\xi_\theta + \partial_\theta\xi_r - 2(2\frac{\phi_{,r}}{\phi} + \frac{1}{r})\xi_\theta = 0,$$

and

$$\partial_\theta\frac{\xi_\theta}{r^2} + (4\frac{\phi_{,r}}{\phi} + \frac{1}{r})\xi_r - \partial_r\xi_r = \phi^4\sum_l \frac{1}{2}(H_2 - K)Y_{l0}, \tag{2.16}$$

where $\phi = 1 + M/2/r$, and the functions H_2 and K are the Fourier transforms of the metric perturbations in the Regge-Wheeler gauge, but their argument is r, not r_{Sch}.

The + mode of gravitational waves η[4] can be written as

$$\eta = -\frac{1}{\phi^4 r^2}\partial_\theta \xi_\theta. \tag{2.17}$$

In this gauge condition the time component of the gauge variable does not affect the above gravitational wave variables just as in the radial gauge.

3. Numerical Results

3.1 Wave Forms of Gravitational Waves

We show the wave forms of gravitational waves at some finite radii in the case of a test particle or a spheroidal dust shell falling straightly into a Schwarzschild black hole. Detailed nemurical methods are shown in our paper[7] , so we omit them here.

Gravitational waves variable η in the radial gauge and the isothermal gauge can be written as

$$\begin{aligned} \eta &= -\sum_l \eta_l W_{l0}, && \text{for radial gauge} \\ &= -\sum_l \eta_l[(1-x^2)T_{l,x} - xT_l]. && \text{for isothermal gauge.} \end{aligned}$$

In Figure 1 we show η_2 in both the radial gauge and the isothermal gauge at $r = 20,\ 30,\ 50M$ in Schwarzschild coordinate. In both gauge condition the amplitude of η does not go to zero for $t \geq 200M$. It shows that η includes not only the wave part, but also the mutipole moment part(nonwave part). As for the wave part it is made of two modes, a quasi-normal mode and a long wavelength mode, and we can see the wave form of the quasi-normal mode clearly at $r = 30M$.

In Figure 2 we show the wave forms in both the radial gauge and the isothermal gauge in the case of the spheroidal dust shell falling from infinity. It shows that the amplitude of η goes to zero for large t, in contrast to one particle case. This is because there are no multipole moments in η for large t. As to the wave

part, the results are almost the same as those of one particle case. In the case of the radial gauge this results are consistent with the simulations of Stark and Piran ,[8] who explained in the radial gauge the wave form is almost unchanged at $r \geq 25M$.

3.2 The Energy Flux

In this section we discuss the method to estimate the energy flux of gravitational waves at a finite radius. Usually we calculate the energy flux of gravitational waves by the formalism defined by the Landau-Lifshitz pseudotensor or the fourth Newman-Penrose quantity. Surely they are good methods to estimate the energy flux of gravitational waves at null infinity because they only include the gravitational waves among the metric components. However if we try to estimate the energy flux at a finite radius, we should be very careful to apply these formalisms becauce they also include the information of the other metric components[7] .

In numerical relativity, since we have to estimate the energy flux at a finite radius, we must find an appropriate formalism to estimate the energy flux of gravitational waves. So we try to find it taking the case of radial gauge. Stark and Piran used the following formula to calculate the energy flux in their simulation[8]

,

$$\Delta E = \frac{r^2}{4} \int dt \int dx [K_+^2 + \frac{1}{4} A^{-2} B^{-4} \eta_{,r}^2]^2, \tag{3.1}$$

where A^2 is γ_{rr}, $B^2 = 1 + \eta$ and K_+ is the extrinsic curvature which is conjugate to η. In the case that the dust shell falls from infinity, Eq.(3.1) is fairly good to estimate the total energy flux at $r \geq 40M$, but in the case of a particle it is not good. This is due to the same reason why the estimation of the energy flux by the Newman-Penrose quantity fails: Nonwave mode is included in η, and $\eta_{,r}$ does not go to zero for $t \to \infty$, so ΔE diverges[7] . Therefore in order to calculate the energy flux of gravitational waves, we must eliminate the time independent part of η. So we suggest the following quantity as the definition of the energy flux of

gravitational waves.

$$\Delta E = \frac{r^2}{4}\int dt \int dx [K_+^2 + \frac{1}{4}A^{-2}B^{-4}\eta_{,t}^2]^2. \tag{3.2}$$

At infinity Eq.(3.2) is equal to Eq.(3.1) because $\eta_{,r} = \eta_{,t}$ at infinity. So Eq.(3.2) gives the energy flux of gravitational waves accurately at infinity. In our perturbative calculations, Eq.(3.2) is written as

$$\Delta E = \frac{1}{16}(r-2M)r\sum_l (l-1)l(l+1)(l+2)\int d\omega\omega^2|\eta_{l\omega}|^2. \tag{3.3}$$

In Figure 3 and 4 we show

$$\Delta E(l=2)_r/\Delta E(l=2)_\infty$$

at each radius when a particle and a spheroidal dust shell, respectively, fall from infinity. $\Delta E(l=2)_\infty$ is the total energy flux of gravitational waves for $l=2$ mode, so the above quantity indicates the accuracy of the estimation of the energy flux at each radius.

In the case of the spheroidal dust shell falling from infinity, if we try to estimate the total enrgy flux with the accuracy within 20 percent, we need the radius at most $r \sim 40M$. Therefore when we estimate the energy flux of gravitational waves by the dust collapse in numerical relativity, we will make fairly acculate estimation of the energy flux of gravitational waves by Eq.(3.2).

By contrast, in the case of one particle falling from infinity it is found that we overestimate the energy flux twice larger at $r = 50M$ and one and half times larger at $r = 100M$. If we try to estimate the total energy flux within 20 percent accuracy, we need the radius $r > 150M$ and it is difficult to take so many grids as to perform the sufficiently accurate calculations in numerical relativity.

4. Conclusions and Discussion

In this paper we investigate both the wave forms and the method to estimate the radiation efficiency of gravitational waves near Schwarzschild black hole for

a few gauge conditions used in numerical relativity. We find that in the case of the radial gauge and the isothermal gauge the wave forms of gravitational waves become clear at $r = 30M$. We also find that the definition of the energy flux by either the Newman-Penrose quantity or the Landau-Lifshitz pseudotensor may be inadequate to estimate the flux at a finite radius. So we must find a good method to calculate the energy flux of gravitational waves for each gauge condition and for each problem in numerical relativity. It is found in the radial gauge Eq.(3.2) is fairly a good formula to estimate the energy flux compared with Eq.(3.1). The essence of our method is to extract the wave part and to eliminate the nonwave part. We must also find the formula for the isothermal and other gauge conditions, and it is a problem to be solved.

In the above calculations the global slice is the polar slice and it is not trivial whether the results change or not if we choose other slices instead of the polar slice. However if we use the maximal slice condition in the above, it can be shown the results are almost unchanged as to the wave forms of gravitational waves for $r \geq 20M$[7] .

REFERENCES

1. T. Nakamura, K. Oohara and Y. Kojima, Prog. Theor. Phys. supple. **90** 110 (1987) and reference therein
2. T. Regge and J. A. Wheeler, Phys. Rev. **108**, 1063(1957)
3. F. Zerilli, Phys. Rev. **D2** 2141(1970)
4. J. M. Bardeen and T. Piran, Phys. Rep. **96**, 203(1983)
5. J. Wilson, in Sources of Gravitational Radiation, ed. L. Smarr (Cambridge Univ. Press, Cambridge, England, 1979)
6. C. Evans, in Dynamical Spacetimes and Numerical Relativity, ed. J. Centrella(Cambridge Univ. Press, Cambridge, 1986)
7. M. Shibata and T. Nakamura, KUNS 1116
8. R. F. Stark and T. Piran, Phys. Rev. Lett. **55** 891(1985)

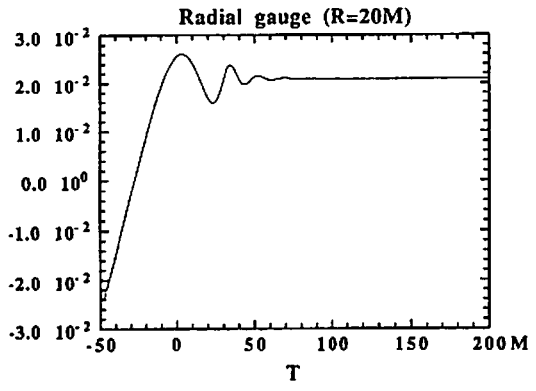
Radial gauge (R=20M)
3.0 10-2
2.0 10-2
1.0 10-2
0.0 100
-1.0 10-2
-2.0 10-2
-3.0 10-2
-50 0 50 100 150 200 M
T

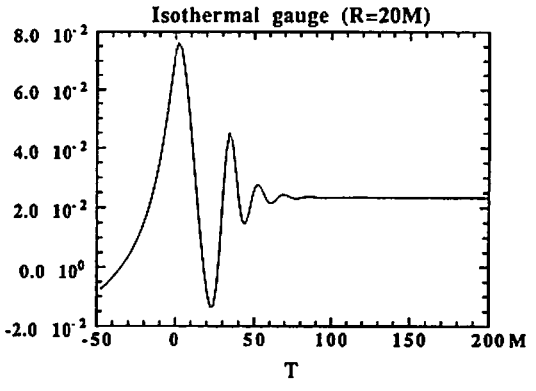
Isothermal gauge (R=20M)
8.0 10-2
6.0 10-2
4.0 10-2
2.0 10-2
0.0 100
-2.0 10-2
-50 0 50 100 150 200 M
T

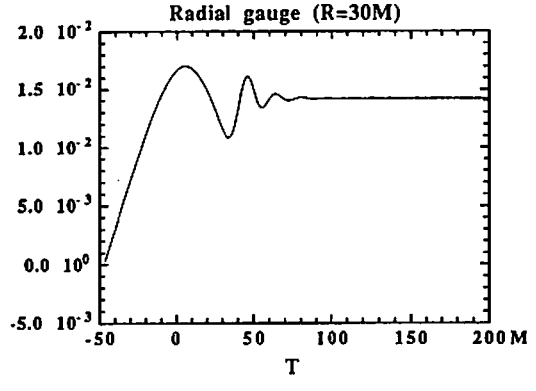
Radial gauge (R=30M)
2.0 10-2
1.5 10-2
1.0 10-2
5.0 10-3
0.0 100
-5.0 10-3
-50 0 50 100 150 200 M
T

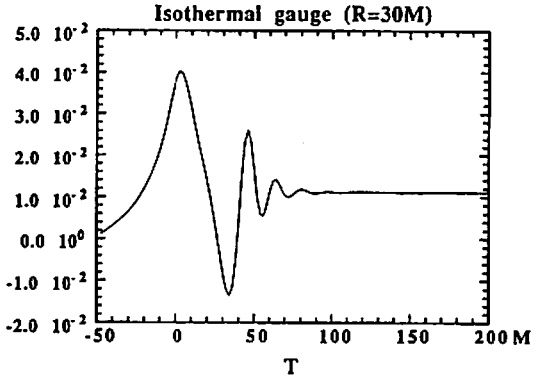
Isothermal gauge (R=30M)
5.0 10-2
4.0 10-2
3.0 10-2
2.0 10-2
1.0 10-2
0.0 100
-1.0 10-2
-2.0 10-2
-50 0 50 100 150 200 M
T

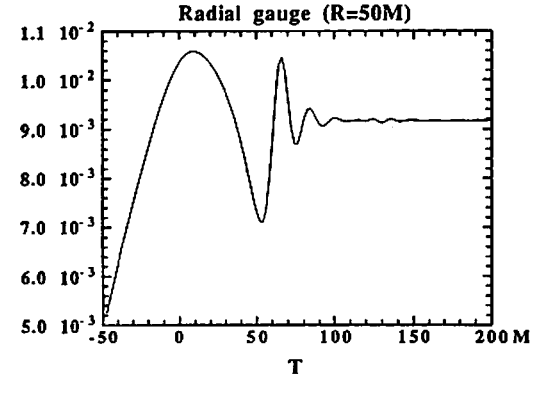
Radial gauge (R=50M)
1.1 10-2
1.0 10-2
9.0 10-3
8.0 10-3
7.0 10-3
6.0 10-3
5.0 10-3
-50 0 50 100 150 200 M
T

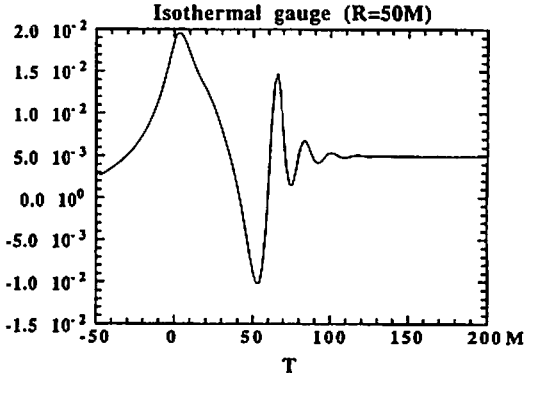
Isothermal gauge (R=50M)
2.0 10-2
1.5 10-2
1.0 10-2
5.0 10-3
0.0 100
-5.0 10-3
-1.0 10-2
-1.5 10-2
-50 0 50 100 150 200 M
T

Figure 1.

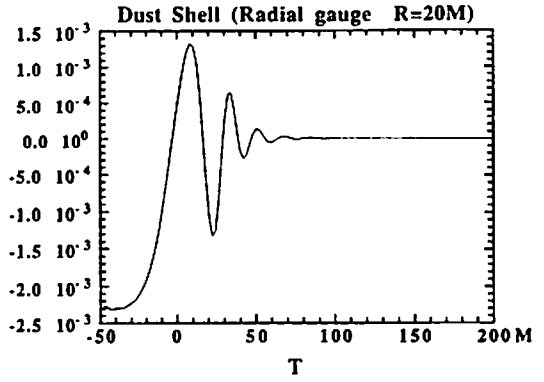

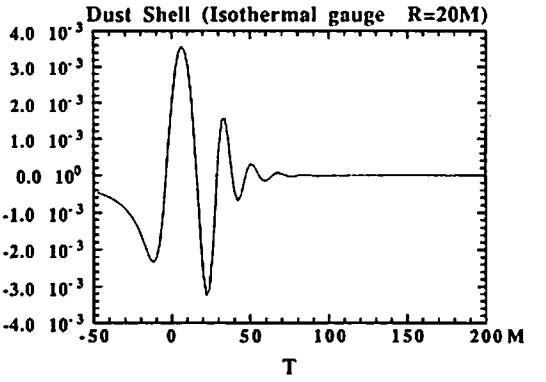

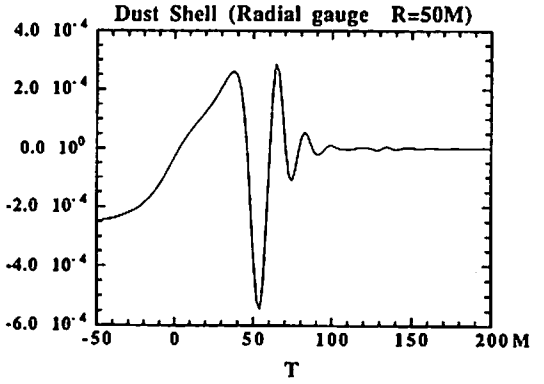

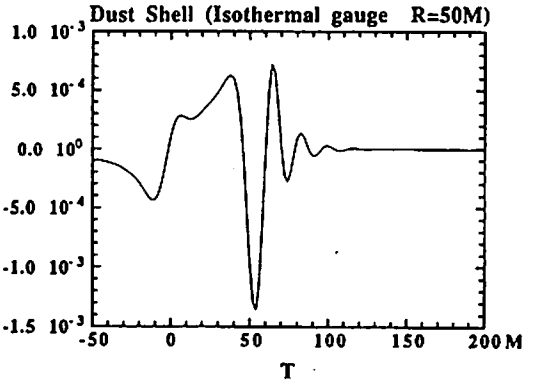

Figure 2.

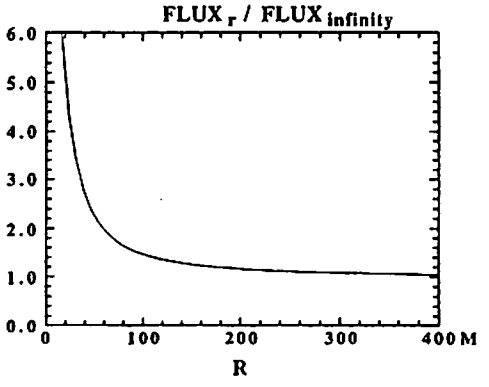

Figure 3.

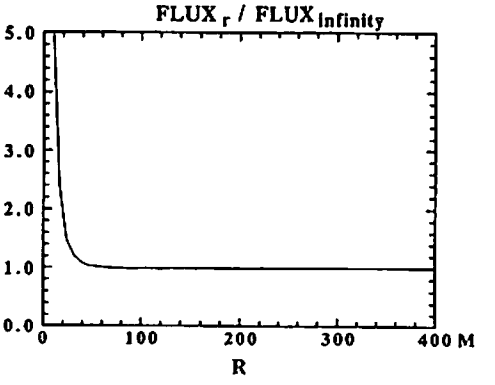

Figure 4.

THE SHELL COLLAPSE WITH SCALAR FIELD

Yosimi Oshiro, Sigeru Konno, Kouji Nakamura,
and Akira Tomimatu

Department of Physics, Nagoya University
Chikusa-ku, Nagoya 464-01, Japan

ABSTRACT

We studied the shell evolution near the apparent horizon using the junction condition. The spherically symmetric dust shell model coupled with a scalar field is considered. In the classical theory we show that the shell can evaporate when the backreaction of the scalar field becomes effective. The time derivative of the mass of shell is proportional to $-M^{-1}$ (M is a mass of the shell).

I. INTRODUCTION

The discovery by Hawking that a black hole emits particle like a blackbody with temperature proportional to its surface gravity [1] has acted as a great stimulus to research on the quantum gravity and the quantum field theory on curved-space time. It must be emphasized that Hawking evaporation is inferred from a semiclassical approximation where the gravitational field is classical and not consider backreaction of matter fields. It is necessary to surpass the linearized theory on fixed background in order to really understand these effects.

The primary approach to the backreaction problem has been through the semiclassical theory of gravity, wherein one has a classical gravitational field coupled to the expectation value of the stress-energy tensor of quantized matter fields via the semiclassical Einstein equations $G_{\mu\nu} = 8\pi\langle T_{\mu\nu}\rangle$. Although solutions to these equations representing evaporating black-hole spacetimes have not yet been found, substantial progress has been made in studying the semiclassical theory.

To consider the importance of backreaction we study a shell which coupled to massless scalar filed. It is known that a collapsing shell with constant mass will became a black-hole. However, it is not even clear that mass emitting shell will became a black-hole. In classically we show that shell can evaporates when backreaction is effectively on the Einstein equation, and shell become black hole when backreaction is not dominant on the Einstein equation. Thus, this result indicate that one must be consider backreaction when discuss about black hole evaporation.

In this paper we use a junction condition which was developed primarily by Israel [2], and which has been used by several previous authors [3]. The basic approach is to examine the embedding properties of the timelike three-hypersurfaces formed by the histories of the shell. Israel first elaborated this sort of attack, in a general discussion of shock waves, boundary surfaces, and thin shells. Usually shell model and junction condition are use to inflationary universe model. We applied it to the problem of a collapsing dust shell.

In the next section we will review the Gauss-Codazzi formalism, in which four-dimensional spacetime is parametrized by a one-parameter family of three-dimensional hypersurface; four-dimensional geometric quantities are then expressed in terms of three-dimensional geometric quantities related to these hypersurface. The Einstein equation in this (3 + 1) dimensional language yield junction conditions which determine the dynamics of the shell. In Sec. III we analyze the shell evolution near the apparent horizon. Our conclusions are presented in Sec. IV.

II. JUNCTION CONDITION

To describe the behavior of the shell, it is simplest to introduce a Gaussian normal coordinate system in the neighborhood of the shell. Denoting the (2 + 1) dimensional spacetime hypersurface swept out by the shell as Σ,we introduce a coordinate system on Σ. For definiteness, two of the coordinates can be taken to be the angular variables θ and ϕ which are always well defined, up to overall rotation, for a spherically symmetric configuration. For the third coordinate, one can use the proper-time variable τ that would be measured by an observer moving along with the shell. The fourth coordinate η is taken as the proper distance from Σ. Thus, the full set of coordinates is given by $x^\mu = (x^i, \eta)$, where $x^i = (\tau, \theta, \phi)$, and i runs from 1 to 3.

In these coordinates the metric can be written as

$$ds^2 = -\alpha^2 d\tau^2 + d\eta^2 + R^2 d\Omega^2, \tag{1}$$

$$d\Omega^2 = d\theta^2 + \sin\theta d\phi^2,$$

where α, R is function of τ, η. (τ, η)coordinate is the co-moving along with shell, than α can taken to 1 on the shell.

In this coordinates,the components of the normal vector n_μ is given by

$$n_\mu = (0, 1, 0, 0).$$

The extrinsic curvature corresponding to each η =const hypersurface is a three-dimensional tensor whose components are defined by

$$K_{ij} = -n_{i;j} = -\frac{1}{2} g_{ij,\eta}. \tag{2}$$

Here the semicolon represents the four dimensional covariant derivative. The nonzero components of the affine connection are given by

$$\Gamma^k_{ij} = {}^3\Gamma^k_{ij},\ \Gamma^\eta_{ij} = K_{ij},\ \Gamma^i_{\eta j} = K^i{}_j,$$

where the superscript (3) denotes three-dimensional geometric quantities.

The energy-momentum tensor $T^{\mu\nu}$ is expected to have a δ-function singularity at the shell,so one can define the surface stress-energy $S^{\mu\nu}$ by writing

$$T_{\mu\nu} = S_{\mu\nu}\delta(\eta) + (\text{regular terms}). \tag{3}$$

We assume the shell constructed from dust them surface stress-energy $S^{\mu\nu}$ can be written as

$$S^{\mu\nu} = \sigma U^{\mu} U^{\nu}, \tag{4}$$

where

$$U^{\mu} = (1/\alpha, 0, 0, 0), \tag{5}$$

is the four-velocity of the shell.

Thus, the energy-momentum tensor $T^{\mu\nu}$ is given by

$$T_{\mu\nu} = S_{\mu\nu}\delta(\eta) + \frac{1}{4\pi}(\partial_{\mu}\psi\partial_{\nu}\psi - \frac{1}{2}g_{\mu\nu}\partial^{\beta}\psi\partial_{\beta}\psi). \tag{6}$$

It can be shown that the Einstein equations become

$$G^{\eta}{}_{\eta} = \frac{1}{2}(K^2 - K^i{}_j K^j{}_i) - \frac{1}{2}{}^3R = 8\pi T^{\eta}{}_{\eta}, \tag{7}$$

$$G^{\eta}{}_{i} = K_{|i} - K^j{}_{i|j} = 8\pi T^{\eta}{}_{i}, \tag{8}$$

$$\begin{aligned} G^i{}_j &= (K^i{}_j - \delta^i{}_j K)_{,\eta} - K K^i{}_j + \frac{1}{2}\delta^i{}_j(K^2 + K^k{}_l K^l{}_k) \\ &= 8\pi T^i{}_j, \end{aligned} \tag{9}$$

where a comma denotes an ordinary derivative and subscript vertical bar denotes the three dimensional covariant derivative.

To discover the effect of the surface stress-energy tensor, perform a η integration of the Einstein field equation provided that g_{ij} is continuous at $\eta = 0$. Thus, equation (8) then leads to the junction condition

$$\gamma^i{}_j - \delta^i{}_j Tr\,\gamma = 8\pi S^i{}_j, \tag{10}$$

where $\gamma^i{}_j$ is the "jump" in the components of the extrinsic curvature

$$\begin{aligned} \gamma^i{}_j &\equiv [K^i{}_j] \\ &= \lim_{\varepsilon\to 0}\{(K^i{}_j(\eta = +\varepsilon) - K^i{}_j(\eta = -\varepsilon)\}. \end{aligned} \tag{11}$$

By taking the trace of the Eq. (10) we obtain $Tr\,\gamma = 4\pi G\,Tr\,S$, which can be substituted back into Eq. (10) to give

$$\gamma^i{}_j = 8\pi\,(S^i{}_j - \frac{1}{2}\delta^i{}_j\,Tr\,S). \tag{12}$$

In analyzing the shell, one uses not only the junction condition (12), but also the four-dimensional Einstein field equation applied on each side of the surface Σ separately, and also an equation of motion for the surface stress-energy. The equation of motion is derived by

energy-momentum conservation law. Using Eq. (6) one can write down the equation for energy-momentum conservation

$$T^{\alpha\beta}{}_{;\beta} = A^{\alpha}\,\delta'(\eta) + B^{\alpha}\,\delta(\eta) + C^{\alpha} = 0, \tag{13}$$

by setting the coefficient of $\delta(\eta)$ in Eq.(13) to zero, one deduce that

$$S^{ij}{}_{|j} + [T^{i\eta}_{scalar}] = 0, \tag{14}$$

$$\widehat{K}_{ij}S^{ij} + [T^{\eta\eta}_{scalar}] = 0, \tag{15}$$

where

$$\widehat{K}_{ij} = \lim_{\varepsilon\to 0}\frac{1}{2}\{K_{ij}(\eta = +\varepsilon) + K_{ij}(\eta = -\varepsilon)\}. \tag{16}$$

The vanishing of the term in $\delta'(\eta)$ then implies that

$$S^{\eta}{}_{\eta} = 0. \tag{17}$$

$$S^{\eta}{}_{i} = 0. \tag{18}$$

One see that (17) and (18) are satisfied automatically by Eq. (4).

The Einstein equation on one side of the shell can be derive from the Einstein field equation on another side of the shell and junction condition. Thus, there are six independent equations that need for analyzing the shell. By combining (5) with the expression (4) for the surface stress-energy $S^{\mu\nu}$, one finds

$$[R'] = -4\pi\sigma R, \tag{19}$$

$$[\alpha'] = 4\pi\sigma, \tag{20}$$

$$[\alpha'^2 + \dot{\psi}'^2] = 0, \tag{21}$$

$$4\pi(\dot{\sigma} + 2\sigma\frac{\dot{R}}{R}) = \dot{\psi}[\psi'], \tag{22}$$

where a dot denotes a partial derivative of τ, and a prime denotes a partial derivative of η. The $\tau\eta$ and $\eta\eta$ component of the Einstein equations on one side of the shell

$$\dot{R}\alpha' - \dot{R}' = R\dot{\psi}\psi', \tag{23}$$

$$\ddot{R} - R'\alpha' + \frac{1}{2R} + \frac{1}{2R}\dot{R}^2 - \frac{1}{2R}R'^2 = -\frac{1}{2}R(\dot{\psi}^2 + \psi'^2). \tag{24}$$

III. SHELL EVAPORATION

It is useful to eliminate the mass M of shell by following combination [5]

$$M = \frac{R_+}{2}(1 - g^{\mu\nu}\partial_\mu R_+\partial_\nu R_+). \tag{25}$$

The quantity M has simple interpretation thus, gravitational mass. With the help of Eq. (19) $\sim$ Eq. (24) one calculates $\dot{M}$ to be

$$\dot{M} = R_+^2 \{ R'_+ \dot{\psi}_+ \psi'_+ - \frac{1}{2} \dot{R}_+ (\dot{\psi}_+^2 + \psi_+'^2) \}. \tag{26}$$

We assume scalar field on outside satisfy outgoing condition

$$\dot{\psi}_+ + \psi'_+ = 0. \tag{27}$$

Because, this condition is most efficacious for emission of the mass.

To solve Eq. (19) $\sim$ Eq. (24) let expand all quantity by η.

$$R(\tau, \eta) = R(\tau) + R_1(\tau)\eta + \ldots,$$

$$\alpha(\tau, \eta) = 1 + \alpha_1(\tau)\eta + \ldots,$$

$$\psi(\tau, \eta) = \psi(\tau) + \psi_1(\tau)\eta + \ldots,$$

$$etc.,$$

We interested in neighborhood horizon. One usually defines the apparent horizon to be such a point, at which one has [4]

$$\partial_v R = 0 \, , \, \partial_u \partial_v R \leq 0, \tag{28}$$

where v is the advanced time and u is the retarded time.

To see the behavior of the shell near the horizon we expand all quantity by τ, Thus

$$A(\tau) = \varepsilon^{\omega}(A_0 + A_1\varepsilon + \ldots),$$

$$R(\tau) = \varepsilon^{\delta}(R_0 + R_1\varepsilon + \ldots),$$

$$\psi(\tau) = \varepsilon^{\gamma}(\psi_0 + \psi_1\varepsilon + \ldots),$$

$$etc.,$$

where

$$A(\tau) = \partial_v R_+ = \dot{R}_+ + R'_+,$$

$$\varepsilon \equiv \tau_0 - \tau.$$

This expansion insert in Eq. (19) $\sim$ Eq. (24) and determine δ, ω, *etc.*, to consist with basic equation Eq. (19) $\sim$ Eq. (24). When $\delta = 0$, the shell falls in the horizon. When $\delta > 0$, shell collapse to origin without enter into the horizon.

There are two consistent solutions, that is, $\delta = 0$ and $\delta = 1/2$. In the case of $\delta = 1/2$, the mass M of shell became zero in the same order with R. Thus, the shell can evaporate.

When shell evaporation scalar field become the same order of τ to gravitational field in Einstein equation, Eq. (23) and Eq. (24). However, shell collapse to a black-hole in this time scalar part much smaller than gravitational part. This result suggest that backreaction is important when the shell evaporate.

In the evaporating case, time derivative of M is in inverse proportion to M itself,

$$\dot{M} \propto -M^{-1}. \tag{29}$$

It is an interesting result because the relation is $\dot{M} \propto -M^{-2}$ in the case of the Hawking radiation. It is worth remarking that there is a difference between quantum and classical results.

IV. CONCLUSION

We have analyzed the behavior of a spherically symmetric dust shell interacting with scalar field in the neighborhood of the horizon. The shell can emit its mass and may collapse to the origin, though it never enter inside of the horizon. The mass of shell tends to vanish as fast as the shell radius R. Thus, this model reduce interesting result that a shell can evaporate in classical level when the backreaction of scalar field becomes effective. This result suggests that the backreaction has a key role in the dynamics.

Additionally, the time derivative of the mass of shell is proportional to $-M^{-1}$. Although this result reminds us of the Hawking evaporation, the time derivative of the black-hole mass is proportional to $-M^{-2}$ in the Hawking radiation.

At this point it is interesting to note that in a shell evaporation one can derive the result such that $\dot{M} \propto M^{-1}$. And backreaction has a key role in the dynamics.

REFERENCE

[1] S.W.Hawking,Commum.math.Phys.43,199,(1974).

[2] W.Israel,Nuovo Cimento44 B,463 (1966).

[3] S.K.Blau, E.I.Guendelman and A.H.Guth, Phys.Rev. **D 35**, 1747, (1987).

[4] W.Hawking ans G.F.Ellis, The Large Scale Stracture of space-time (Cambridge University Press, Cambridge, 1973).

[5] W.Fischer, D.Morgan and J.Polchinski, Phys.Rev.D 42,4042,(1990).

The Oppenheimer-Snyder Space-Time with Λ

Ken-ichi Nakao
Department of Physics, Kyoto University, Sakyo-ku, Kyoto 606, Japan

1. Introduction

Since our universe observed today is homogeneous and isotropic, its geometry is well described by the Friedmann-Robertson-Walker space-time. That feature of our universe is one of the mystery (so-called the homogeneity problem) within the framework of the standard Big Bang universe model. The inflationary universe scenario is a favorable model to answer the above problem.[1] In this scenario, there is a period in which our universe undergoes the de Sitter-like exponential expansion due to the vacuum energy of the inflaton scalar field which plays a role of the effective cosmological constant during the phase transition. After the phase transition, the vacuum energy is transformed into radiation and the standard Big Bang scenario is recovered. In the framework of this scenario, the present homogeneity of our universe is attributed to that rapid cosmic expansion, based on the cosmic no hair conjecture which states that if a positive cosmological constant exists, all space-times approach the de Sitter space-time asymptotically.[2] However, even though there is a positive cosmological constant, it is not likely that highly inhomogeneous initial conditions would lead to the de Sitter-like expansion. In reality, there are several counter examples. For example, the Kerr-Newman-de Sitter space-time is one of those.[3] Of course, such a strong statement as the original cosmic no hair conjecture is not necessary for the practical inflationary scenario since we do not observe the whole universe and therefore there may exist regions which do not undergo inflation if those regions are not observable. But it is important to obtain the knowledge about

the behavior of general inhomogeneities in the space-time with a cosmological constant, in order to understand the early stage of our universe.

For the practical inflationary scenario, inhomogeneities of the cosmological constant itself is crucial and have been investigated by analytic and numerical approaches.[4 - 7] On the other hand, we should also understand inhomogeneities with a homogeneous cosmological constant Λ. In this paper, we investigate the Oppenheimer-Snyder space-time with a positive cosmological constant Λ, which describes spherically symmetric motion of a homogeneous dust sphere.

In the Oppenheimer-Snyder space-time, the interior of the dust sphere is described by the Friedmann-Robertson-Walker (FRW) solution with dust and Λ while the exterior of the dust sphere is the Schwarzschild-de Sitter space-time. The evolution of the FRW space-time is essentially determined by the ratio between the total energy of the dust and Λ. On the other hand, the global structure of the Schwarzschild-de Sitter space-time depends on the relation between the gravitational mass M_0 and Λ. Therefore there are various cases for the motion of the dust sphere in the Oppenheimer-Snyder space-time. Garfinkle and Vuille studied the Oppenheimer-Snyder space-time for the case of $M_0^2\Lambda < 1/9$ and they concluded that in this case "the weak cosmic no hair conjecture " holds, which which states that only a portion of the universe undergoes inflation and is sufficient for the practical inflationary scenario.[8] However the other cases are also important to understand the behavior of general inhomogeneities in the early stage of our universe. Thus we investigate all possible cases for the motions of the dust sphere in the Oppenheimer-Snyder space-time. As will be shown in Sec.4, these results show that the inhomogeneity with the large gravitational mass M_0 does not necessarily obstruct inflation because the large gravitational mass M_0 gives the same effect as the large cosmological constant Λ, which leads to the strong cosmic expansion.

2. The Interior and Exterior Solutions

The interior solution is described by the closed FRW space-time in which the metric with the cosmic time τ is expressed as,

$$ds^2 = -d\tau^2 + a^2(\tau)(d\chi^2 + \sin^2\chi d\Omega^2), \tag{1}$$

with

$$d\Omega^2 \equiv d\theta^2 + \sin^2\theta d\varphi^2. \tag{2}$$

The Friedmann equation is given by

$$\left(\frac{da}{d\tau}\right)^2 = \frac{2m}{a} + H_0^2 a^2 - 1 \equiv -V_i(a), \tag{3}$$

where

$$m \equiv \frac{4\pi}{3}\rho a^3 = \text{constant},$$
$$H_0 \equiv \sqrt{\frac{\Lambda}{3}},$$

with the energy density of the dust ρ.

We can understand the behavior of the solutions, regarding Eq.(3) as an energy equation for a particle with the potential $V_i(a)$.

When $m^2 H_0^2 < 1/27$, there are two positive roots of the equation $V_i(a) = 0$ as follows,

$$\begin{aligned} a_1 &= \frac{2}{H_0\sqrt{3}}\cos\left(\frac{1}{3}(\pi + \tan^{-1}\sqrt{\omega_i})\right), \\ a_2 &= \frac{2}{H_0\sqrt{3}}\cos\left(\frac{1}{3}(\pi - \tan^{-1}\sqrt{\omega_i})\right), \end{aligned} \tag{4}$$

where

$$\omega_i \equiv \frac{1}{27m^2H_0^2} - 1. \tag{5}$$

Since a_1 and a_2 correspond to the turning points, there are two kinds of the solutions, i.e., the recollapsing and bouncing solutions.

For the case of $m^2H_0^2 = 1/27$, there is only one positive root,

$$a_0 = \frac{1}{\sqrt{3}H_0}. \tag{6}$$

This is the unstable equilibrium point of the potential $V_i(a)$ and thus if the scale factor a is equal to a_0 initially, the solution is static, i.e., the Einstein's static universe.

In the last case of $m^2H_0^2 > 1/27$, there are two kinds of solutions. In one solution, the scale factor a merely increases and becomes infinite asymptotically and the other goes to the singularity $a = 0$ within a finite cosmic time.

The exterior solution is the Schwarzschild-de Sitter space-time in which, by the use of the Schwarzschild coordinates, the metric is expressed as,

$$ds^2 = -Cdt^2 + C^{-1}dR^2 + R^2d\Omega^2, \tag{7}$$

with

$$C = 1 - \frac{2M_0}{R} - H_0^2R^2,$$

where M_0 is the gravitational mass.

In contrast with the Schwarzschild space-time, there are three cases in accordance with the value of M_0H_0 as follows. When $M_0^2H_0^2 < 1/27$, there are two kinds of the event horizons. One is the black hole (or white hole) horizon at $R = R_H$ and the other is the cosmological horizon at $R = R_C$. These radii are given by

$$\begin{aligned} R_H &= \frac{2}{H_0\sqrt{3}}\cos\Big(\frac{1}{3}(\pi + \tan^{-1}\sqrt{\omega_e})\Big), \\ R_C &= \frac{2}{H_0\sqrt{3}}\cos\Big(\frac{1}{3}(\pi - \tan^{-1}\sqrt{\omega_e})\Big), \end{aligned} \tag{8}$$

where

$$\omega_e \equiv \frac{1}{27M_0^2H_0^2} - 1. \tag{9}$$

In the case of $M_0^2H_0^2 = 1/27$, there is only one kind of the event horizon at

$R = 3M_0$ while in the case of $M_0^2 H_0^2 > 1/27$ there is no event horizon.

3. Junction of the Metric and Motion of the Dust Sphere

Now we consider the junction between the interior and exterior solutions. Since the areal radius $\tilde{r}$ is a C^1 function on the surface of the dust sphere, $\tilde{r} = a \sin\chi = R$ and $g^{\mu\nu}(\nabla_\mu \tilde{r})(\nabla_\nu \tilde{r})$ is continuous on it.[8] From this condition, we obtain the following relation,

$$M_0 = m \sin^3 \chi_s, \tag{10}$$

where χ_s is the interior radial coordinate of the surface. Since the interior coordinate of the surface is constant, the motion of it is along a timelike geodesic in the interior space-time and also in the exterior space-time by the continuity of the metric. Therefore we investigate the timelike radial geodesics in the Schwarzschild-de Sitter space-time which obey the following equation,

$$\left(\frac{d\bar{R}}{d\bar{t}}\right)^2 = \frac{1}{E^2}(E^2 - C) \equiv -V_g(R). \tag{11}$$

Here the proper time $\bar{t}$ and radius $\bar{R}$ are given by

$$d\bar{t} = C^{\frac{1}{2}} dt,$$
$$d\bar{R} = C^{-\frac{1}{2}} dR,$$

and E is an integration constant corresponding to the energy of the particle with unit mass because the four velocity is given by

$$u_\mu = (E, \pm\sqrt{E^2 - C}/C, 0, 0). \tag{12}$$

If we realize the above geodesic as the motion of the surface of the dust sphere, from the continuity of the derivative along the normal to the surface of the dust

sphere $n^\mu \nabla_\mu \tilde{r}$, we obtain

$$E = \cos \chi_s, \tag{13}$$

where n^μ is the spacelike unit normal of the surface of the dust sphere:

$$n^\mu = \begin{cases} (0, a^{-1}, 0, 0) & \text{for the interior,} \\ (\pm\sqrt{E^2 - C}/C, E, 0, 0) & \text{for the exterior.} \end{cases} \tag{14}$$

Therefore the interior coordinate of the surface of the dust sphere should be $\chi_s < \pi/2$ in order that $0 < E$. We can, then, easily see the following relation

$$V_i(a) = V_g(R = a \sin \chi_s) \tan^2 \chi_s. \tag{15}$$

Fig.1 depicts the region, in which the potential V_g is positive and the motion of the dust sphere surface is forbidden, by the shaded one in $(M_0 H_0, H_0 R)$ plane, fixing E.

4. Conclusion and Remarks

The boundary of the shaded region in Fig.1 corresponds to the turning point of the motion of the dust sphere surface. It should be noted that when $M_0 > \sqrt{(1-E)^3/27}/H_0$, there is no turning point and therefore, if the dust sphere expands initially, it does continuously expand and the space-time approaches to the de Sitter space-time asymmptotically. Furthermore, for the case of $M_0 > \sqrt{1/27}/H_0$, by imposing the asymptotic de Sitter boundary condition, there dose not exist collapsing solution.[10] Therefore the dust sphere with a large gravitational mass M_0, i.e., a large inhomogeneity does not necessarily obstruct inflation. The reason of the above fact is because the large gravitational mass M_0 gives the same effect as the large cosmological constant Λ, which leads to the strong cosmic expansion.[10]

On the other hand, in the case of $M_0^2 H_0^2 < 1/27$, there are collapsing solutions which goes to the singularity within a finite cosmic time but this singularity is enclosed by the black hole event horizon. There are, furthermore, static solutions which do not collapse and do not expand, either. However these are all in accordance with the weak cosmic no hair conjecture as discussed by Garfinkle and Vuille.[8]

REFERENCES

1. A.H.Guth, Phys. Rev. **D23**, 347 (1981);
   K. Sato, Mon. Not. Roy. Astron. Soc. **195**, 467 (1981);
   A. Albrecht and P. J. Steinhardt, Phys. Rev. Lett. **48**, 1220 (1982);
   A. D. Linde, Phys. Lett. **108B**, 389 (1982).

2. G. W. Gibbons and S. W. Hawking, Phys. Rev. **D15** 2738 (1977);
   S. W. Hawking and I. G. Moss, Phys. Lett. **110B**, 35 (1982);
   e.g. K. Maeda, "*Inflation and Cosmic No Hair Conjecture*", in the Proceedings of 5th Marcel Grossmann Meeting, ed. by D. G. Blair and M. J. Buckingham (World Scientific, 1989) p.145.

3. B. Carter, Commun. Math. Phys. **17**, 1067 (1970).
   in *Black Holes* ed. C. DeWitt and B. S. DeWitt (Gordon and Breach, New York, 1973).

4. K. Sato, M. Sasaki, H. Kodama, and K. Maeda, Prog. Theor. Phys. **65** 1443 (1981);
   K. Maeda, K. Sato, M. Sasaki and H. Kodama, Phys. Lett. **108B**, 98 (1982);
   K. Sato, in the Proceedings of I. A. U. Symposium No.130 " *The Large Scale Structure of the Universe*" (1987).

5. H. Kurki-Suonio, J. Centrella, R. A. Matzner and J. R. Wilson, Phys. Rev. **D35**, 435 (1987).

6. K. A. Holcomb, S. J. Park and E. T. Vishniac, Phys. Rev. **D39**, 1058 (1989).

7. D. S. Goldwirth and T. Piran, Phys. Rev. **D40**, 3269 (1989);
   D. S. Goldwirth and Piran, Phys. Rev. Lett. **64**, 2852 (1990).

8. David Garfinkle and Chris Vuille, Gen. Rel. Grav. **23**, 471 (1991).

9. L. Smarr and J. W. York, Phys. Rev. **D17**, 2529 (1978);
   D. M. Eardley and L. Smarr, Phys. Rev. **D19**, 2239 (1979).

10. K. Nakao, Kyoto University preprint, KUNS-1112 (1991).

FIGURE CAPTIONS

1. This figure depicts the region, in which the potential V_g is positive and the motion of the dust sphere surface is forbidden, by the shaded one in (M_0H_0, H_0R) plane, fixing and E.

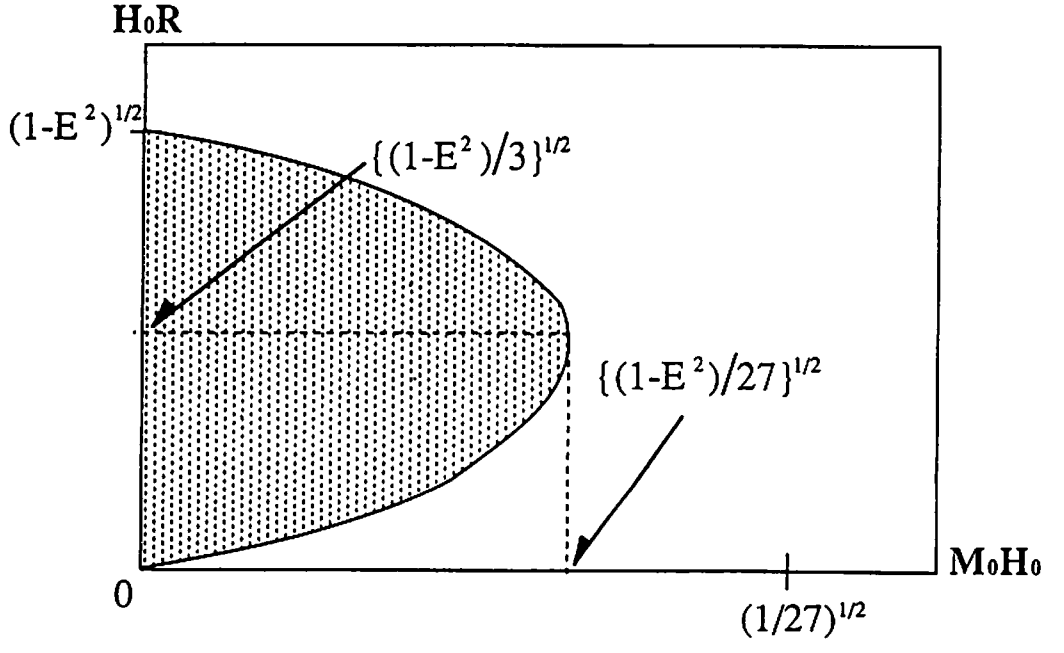

Fig.1

Experimental Gravity

Yasunori Fujii

Institute of Physics, University of Tokyo-Komaba
Meguro-ku, Tokyo, 153 Japan

Experimental gravity, or sometimes called experimental relativity, is now an established branch of physics, which owes its birth largely to Dicke and Schiff in the early 1960's. Efforts have been made to verify Einstein's general relativity (GR) by using various types of precision experiments. This has been done often through the attempts to rule out experimentally many "alternative theories" having arbitrary parameters, choosing particular values of which selects GR. Remarkably enough, results of extensive studies have pointed steadily toward narrowing down the ranges in which GR is allowed. A brief survey of this unique field is attempted for non-experts. For more general and extensive reviews, readers are referred particularly to Will's papers [1].

The subjects to be discussed will include:

I. Equivalence principle,
II. Solar system experiments,
III. Binary pulsars,
IV. Fifth force.

Serious attempts at detecting gravitational waves are not included because many other reviews are available. The appendix discusses a theoretical aspect of the choice of conformal frame, an important but poorly understood subject in connection with the implication of $\dot{G}/G$.

I Equivalence principle

The equivalence principle (EP) is the physical basis of GR, as is well-known, and has been the subject of experimental scrutiny. In the literature, however, EP appears under three or four different names: Weak equivalence principle (WEP), Einstein equivalence principle (EEP), and Strong equivalence principle (SEP). Sometimes WEP is further divided into two: WEP(I) and WEP(II).

WEP means that any object falls in the gravitational field with the same acceleration irrespective of its mass and composition. This is the most naive expression of EP recognized first by Galiley. In the sense of mechanics, this implies the equivalence between the inertial and gravitational masses. Another familiar expression is composition-independence of the gravitational force. WEP(II) asserts that the acceleration should be independent also of the spin states.

As modern tests of WEP, refinement of the Eötvös experiment, Dicke et al [2] and Braginski et al [3] verified the null result to the accuracy of 10^{-11} and 10^{-12}, respectively. These experiments were carried out by using the Sun as the source of the gravitational force. Recently, however, the suggestion of the fifth force, Non-Newtonian force of finite force-range, stimulated the renewed interest of the experiment but with the Earth or nearby objects as the source. The same type of experiment using torsion-balance [4] reached almost the same level of the accuracy of 10^{-11}, demonstrating the remarkable improvement in the measuring techniques during the past two decades.

In 1962 Schiff showed [5] that the experiment due to Pound and Rebka [6], who were the first to bring GR in the arena of modern experimental physics, can be understood only in terms of special relativity and EP. Since then the red-shift experiment which had been proposed originally to test GR has been categorized as the test of EP. The improved version of the Pound-Rebka experiment was carried out by Vessot et al [7] by using a rocket climbing up to the altitude of 10,000 km, narrowing the possible discrepancy to 2×10^{-4}, an improvement of 2 orders of magnitude compared with Pound-Rebka's result. Incidentally, in this experiment, code named Gravity Probe (GP) A in NASA, the launching tower was 23 meters high, nearly the same as the tower in the classic Princeton experiment in 1964.

Schiff went ahead further to offer a conjecture that WEP does imply EEP which asserts that gravity is a metric phenomena. The concept of the metric theory is more general than Einstein's GR. It incorporates Brans-Dicke theory (BD), among others, in which the effect of the scalar field shows up only through the metric; objects remain to fall along geodesics. Alternative metric theories are distinguished from GR only through the different manners in which the gravitational potential (of the Sun, for example,) enters in each component of the metric tensor.

The conjecture was verified to be true, at least within some fairly realistic models. According to the "$TH\epsilon\mu$ formalism" developed by Lightman and Lee, and by Haugan [8], the Lagrangian of a massive particle and the electromagnetic field in a static and spherically symmetric gravitational filed is formulated in term of the arbitrary functions T, H, ϵ and μ of the gravitational potential; in any metric theories these function must obey the relation

$$\epsilon = \mu = \sqrt{H/T}. \tag{1}$$

Interesting enough one finds that a violation of (1) results in the difference between the

maximum speed of massive particles $c_m = \sqrt{T/H}$ and the speed of light $c_\gamma = 1/\sqrt{\epsilon\mu}$, implying violation of local Lorentz invariance.

The authors of ref. [8] applied this $TH\epsilon\mu$ formalism to the system of charged particles bound by the Coulomb interaction. They computed the acceleration of a bound system in the gravitational field, finding certain contributions depending on the details of the composition. Requiring WEP amounts to requiring these contribution to vanish. This in turn results in the condition (1), hence leading to EEP.

As mentioned before, the violation of WEP and hence EEP would result in the violation of the local Lorentz invariance, suggesting an interesting type of experiment. In the above calculation the composition-dependent terms come in as a form of the mass-tensor involving a velocity of the object. This velocity should be interpreted as the one relative to certain frame of reference, presumably fixed to the solar system, our Galaxy or the 3K cosmic background radiation which is falling toward the center of Virgo cluster. The preferred direction introduced in our space might be detected through an uneven spacing in Zeeman splittings of an atom in a magnetic field. This was an attempt first carried out by Hughes and by Drever in 1960 [9].

A better measurement of the Hughes-Drever experiment was carried out by Prestage et al [10] who tried to see if one of the hyper-fine splittings of $^9Be^+$ (having nuclear spin 3/2) shows any variation of 24-hour-period when compared with the hydrogen maser which should remain unaffected because both its nuclear and electron spins are 1/2. Using such techniques as Penning trap and optical pumping, they saw no evidence of the variation to the accuracy of 70 μHz against the splitting of 508.856 MHz. This implies the equality between c_m and c_γ to the accuracy of 10^{-8} if the relevant velocity of the preferred frame is $10^{-3}c$. Even better constraint has been obtained by Lamoreaux et al [11] who used ^{201}Hg and ^{199}Hg nuclei. Their upper bound on the frequency variation is 0.48 μHz corresponding to the energy determination to the accuracy of 2×10^{-21}eV.

We now turn to WEP(II), the significance of which was pointed out first by Ni [12], who showed that the $TH\epsilon\mu$ formalism can be further generalized in the portion of the electromagnetic field, represented by a scalar field. Only with the vanishing of this field added to the condition (1) can one recover EEP. On the other hand, the presence or the absence of this field can be tested only by checking if an object falls with the acceleration independent of its spin state. The experiments using torsion balances with substances with nuclear spins polarized but magnetically shielded carefully by using superconducting coating are still under way [13].

SEP asserts that any object falls along the geodesic even if the effect of the gravitational self-interaction is included. In other word, the inertial and gravitational masses are the same even with the gravitational binding energy is included. The effect can be significant only with objects as large as astronomical bodies. It might sound somewhat curious to find that

GR which started with accepting EP does not always observe the equality between the two kinds of mass in the higher order terms with respect to the gravitational coupling constant. As early as 1938 Eddington showed that the equality holds only if the second time derivative of the moment of inertia of an object vanishes [14]. Late Professor Ryoyu Utiyama told the author that Einstein used EP in a heuristic approach, ending up with a mathematical theory from which strict EP follows only in the lowest-order effects.

More recently Nordtvedt analyzed the problem in a general framework [15] in terms of the post-Newtonian parameters β and γ, which are given also for the later use:

$$\begin{cases} -g_{00} &= 1 - \frac{GM}{r} + 2\beta\left(\frac{GM}{r}\right)^2, \\ g_{0i} &= 0, \\ g_{ij} &= \delta_{ij}\left(1 + 2\gamma\frac{GM}{r}\right), \end{cases} \tag{2}$$

where we chose $c = 1$ and the isotropic coordinates employed in the static, spherically symmetric and non-rotating field due to a mass M. GR predicts the standard values $\beta = \gamma = 1$, while BD gives $\gamma = (1 + \omega^{-1})/(1 + 2\omega^{-1})$, for example. Nordtvedt studied a 2-body system in a circular orbit, showing that the violation of EP is proportional to $\eta \equiv 4\beta - \gamma - 3$, also multiplied by $\Delta \sim GM/\bar{r}$ which measures the relative contribution of the gravitational binding energy, where $\bar{r}$ is the size of the body. The above factor η is 0 for GR, whereas it is $(2 + \omega)^{-1}$ for BD.

Nordtvedt proposed to apply the analysis to the Earth-Moon system orbiting around the Sun. Due to the difference in Δ for the Earth and the Moon ($\sim 5 \times 10^{-10}$ and 2×10^{-11}, respectively), they would fall toward the Sun with different accelerations if $\eta \neq 0$. As a result the lunar orbit would be "polarized" always in the direction of the Sun (the Nordtvedt effect). Two groups [16] tried to detect the possible variation of the Earth-Moon distance with the synodic period of 29.53 days by the way of laser-ranging using the reflector placed on the lunar surface by Apollo 11. This "Lunar Laser Ranging" technique is capable of measuring the distance to the accuracy of 30 cm.

The expected effect is so small that they relied on the extensive least-squares fit of many parameters representing various perturbations. After 4-6 years of measurements since 1970, they confirmed SEP, namely $\eta = 0$ to the accuracy of 3%. This places a constraint $\omega \gtrsim 30$ for the BD parameter.

It might be worth keeping in mind that SEP can be violated even with GR if the motion in a body is not circular, but the effect vanishes if averaged over periods of rotation.

II Solar system experiments

In this section we discuss

(i) Deflection of light around the Sun,
(ii) Time delay in radar ranging,
(iii) Perihelion shift of Mercury,
(iv) Time variability of the gravitational constant.

The deflection angle θ of light passing at the distance d in units of the solar radius is given by

$$\Delta\theta = \frac{1}{2}(1+\gamma)\frac{1}{d} \times 1.75''. \tag{3}$$

The original proposal to taking advantage of solar eclipses has never reached the accuracy better than 10%. Since the end of the 1960's, however, using long-baseline radio interferometry and very-long-baseline interferometry measuring the signal of groups of strong quasi-stellar radio sources made it possible to confirm (3) to the accuracy of 1%.

A much better experiment on essentially the same quantity is obtained by measuring the time-delay of the radar-echo from the Earth to an object at the occasion of superior conjunction:

$$\Delta t \approx \frac{1}{2}(1+\gamma)(1 - 0.16 \ln d) \times 250\mu\text{s}. \tag{4}$$

The best result was obtained from the data collected from the Viking Landers and Orbiters during the period from 1976 through 1982. The latest of the results shows $\gamma = 1 \pm 0.001$.

The perihelion shift of the Mercury was the first triumph of GR due to Einstein himself, but was shadowed in 1966 by Dicke who measured solar oblateness finding it sufficiently large ($J_2 \sim 2 \times 10^{-5}$ as compared with the value $\sim 10^{-7}$ expected from centrifugal flattening) to be comparable with the effect of GR. The calculation including this effect shows

$$\dot{\omega} = 42.98''\text{yr}^{-1}\left[\frac{1}{3}(2 + 2\gamma - \beta) + 0.0003\left(J_2/10^{-7}\right)\right]. \tag{5}$$

Dicke viewed this discrepancy caused by a large J_2 as favored to his scalar-tensor theory. Many of the experiments performed subsequently, however, supported smaller values like $J_2 \sim 1.7 \times 10^{-7}$ [17], though others reported larger values around $\sim 10^{-6}$ [18], suggesting time-dependent oblateness due to complicated solar dynamics. If J_2 is in fact "small," then the recent ranging data yields $\gamma = 1.000 \pm 0.002$ and $\beta = 0.99 \pm 0.02$.

It is emphasized that the results of all these modern experiments have been derived on the basis of the "parametrized post-Newtonian ephemerides," programs of extensive least-squares fit of a large number of parameters including not only β and γ but also such diverse parameters as the masses and the initial data of 9 planets and masses of asteroids.

The current value of $\dot{G}/G$ was also obtained as one of such parameters: $\dot{G}/G = (0.2 \pm 0.4) \times 10^{-11}\text{yr}^{-1}$ [19]. This already rules out what is expected from Dirac's Large-numbers Hypothesis; $\sim 10^{-10}\text{yr}^{-1}$. The main source of uncertainty in the above result comes from the uncertainty in the mean densities of 200 of the largest asteroids.

Future proposed experiments include Galileo flying by Mercury, Venus, Jupiter and Mercury Orbiter. An order or two magnitudes improvement of the result is expected, possibly with J_2 determined separately from other parameters.

Another kind of experiment has been in preparation; gyroscope, called GP-B in NASA, conceived originally by Schiff. This intends to measure the precession angle of a spinning object (gyroscope on board a space shuttle on the polar orbit) predicted by $\frac{1}{2}(1+\gamma) \times 0.''042\mathrm{yr}^{-1}$ [20]. The launching is currently scheduled in 1996. This experiment if successful will be the first detection of the gravitomagnetism, also known as dragging of inertial frame or the Lense-Thirring effect.

There is another proposal [21] of detecting gravitomagnetism by observing the nodal advance (predicted to be $\sim 0.''031\mathrm{yr}^{-1}$) of LAGEOS II, to be paired with the existing LAGEOS (Laser-Ranged Geodynamics Satellite) which has been in the sky since 1976. A similar experiment is also proposed [22] to use a superconducting 3-axis gradiometer on board yet another project of LAGEOS III.

It should be noticed that all the experiments are done using atomic clocks. According to this we must choose a conformal frame in which masses of elementary particles remain time-independent provided e, c and h are assumed truly constant. The theoretical implication is discussed in Appendix, particularly in connection with $\dot{G}/G$.

III Binary pulsar

Seventeen years of continued extensive measurement of the binary pulsar PSR 1913+16 have passed. The successful arrival time analysis made it possible to determine the pulse period of about 60 ms with precisions of 14 digits. The rate of decrease of the orbital period P_b ($\sim$8 hours, also 12 digits) was also measured very accurately: $\dot{P}_b = (-2.425 \pm 0.01) \times 10^{-12}\mathrm{ss}^{-1}$. This agreed surprisingly well with the rate of the gravitational energy radiated calculated according to the quadrupole formula, thus providing the first "evidence" of the gravitational waves.

Both of the pulsar and its companion are interpreted as compact neutron stars. The orbital semi-major axis is about 2 lightseconds, with the eccentricity 0.6171312(8), and the periastron shift is $4.226605(30)\mathrm{deg}\cdot\mathrm{yr}^{-1}$. With all of these and other orbital data, PSR1913+16 is now an ideal testing ground of GR. It is emphasized that in contrast to the solar-system experiments in which gravitation is relatively weak (notice $GM_\odot/R_\odot \approx 2 \times 10^{-6}$), the binary system is unique in much stronger gravity ($GM/R \sim 0.2$).

One can finally determine the masses of the pulsar and the companion by fully including the PN parameters affecting the time dilation in the binary system as well as in the solar system. This is in fact an over-determination of the masses, serving as consistency checks. All

the data are mutually consistent, also agreeing with GR to an impressive accuracy. Readers are advised to refer to the latest report [23], for example. The most recent determination of the masses are 1.439 ± 0.001 and 1.389 ± 0.001 for the pulsar and the companion, respectively, in units of the solar mass.

The agreement with the data and GR is so good that Damour, Gibbons and Taylor went further to see how the experimental uncertainties constrain the value of $\dot{G}/G$ [24]. For this purpose they applied a detailed analysis of the orbital motion including the terms up to the order $(v/c)^5$. Their conclusion is $\dot{G}/G = (1.2 \pm 1.3) \times 10^{-11}\mathrm{yr}^{-1}$, still somewhat less stringent than the result of [19]. This seems nevertheless to be a promising approach because the result on several other binary pulsars are now available. Particularly important is PSR 1534+12 detected first in February of 1990, providing the data with the precision approaching the same level as PSR1913+16.

IV Fifth force

A fifth force is "defined" phenomenologically by the static potential between two point masses:

$$V(r) = G_\infty \frac{m_i m_j}{r}\left(1 + \alpha_{ij} e^{-r/\lambda}\right), \tag{6}$$

where the coefficient α_{ij} is expected to be of the same order of magnitude or somewhat smaller than 1, implying that the force would be nearly as weak as or somewhat weaker than gravity. Its dependence on the substance i and j is anticipated because the force is likely to be composition-dependent, in contrast to the "authentic" gravity. The force-range λ will be of the order of a macroscopic distance, presumably somewhere between cm and km. The possible occurrence of this type of force was first suggested based on the theoretical conjecture on the mass hierarchy in the attempts to unify particle physics and gravity [25].

Two types of experiments have been carried out to probe (6). The "composition-independent experiments" tried to discover any departure from the inverse-square law of the Newtonian gravity, both in the laboratory scale and the geophysical scale (upward and downward). The "composition-dependent experiments," on the other hand, searched for the apparent violation of WEP, as revealed dramatically by Fischbach et al who reanalyzed the old Eötvös experiment [26].

In spite of a number of "discoveries" reported, it is fair to say that no firm evidence is present at this time. In some occasions, the sources of the error were pinned down, but not in other cases yet. See the review articles [27] for more details. This does not imply that the experiments were conducted with insufficient care. The real situation was exactly the opposite, simply showing that the effect was so small that unexpected new kinds of "noise"

were often unavoidable. By serious efforts to reduce these noises our understanding of the gravitational force has increased considerably for the past years. Any new development in the technique of precision experiments should be applied to this subject beyond the now available level of accuracy.

It should be emphasized that most theoretical predictions based on a variety of motivations are only crude estimates allowing a latitude of few orders of magnitude. This is true both on the magnitude α and the force-range λ. Also the two types of experiments mentioned above can be correlated only on specific models on the coupling of the force (e.g. the baryon number coupling). See ref. [28] for more detailed explanation. For these reasons further efforts to search for the force are strongly encouraged.

As one of new experiments which might be feasible, the author proposed [29] the use of the ultra-sensitive laser interferometer similar to the device now under development for gravity-wave detection. Further improvement will be reported elsewhere, replacing the Fabry-Perot cavities by active lasers used as very narrow resonators.

Appendix Choice of conformal frame

Possible time variability of G is usually formulated in terms of a scalar field ϕ that has a nonminimal gravitational coupling, chosen as the BD-type for simplicity:

$$\mathcal{L} = \sqrt{-g}\left(\frac{1}{2}\xi\phi^2 R - \frac{1}{2}g^{\mu\nu}\partial_\mu\phi\partial_\nu\phi + L_{\text{matter}}\right), \tag{A.1}$$

where ξ is related to BD's ω by $\xi = (4\omega)^{-1}$. The first term inside the parenthesis of (A.1) is compared with the standard term $(16\pi G)^{-1}R$, hence the effective gravitational constant G_{eff} is given by

$$G_{\text{eff}} = \frac{1}{8\pi}\xi^{-1}\phi^{-2}, \tag{A.2}$$

where we use the unit system of $c = \hbar = 1$. In cosmology we may reasonably assume that ϕ depends only on the cosmic time t as a first approximation. Eq.(A.2) thus gives a time-dependent G_{eff}.

This, however, does not immediately imply nonzero $\dot{G}/G$ to be measured in the experiments using atomic clocks. Consider a fairy-tale situation, for example, in which time is recorded by a pendulum, with its length, the mass and the size of the Earth assumed to remain unchanged. Then, by definition, G is time-independent. To meet this physical situation we apply a Weyl rescaling (conformal transformation) $ds^2 \to ds_*^2$ as defined by

$$g_{\mu\nu} = \Omega^2 g_{*\mu\nu}, \qquad \text{with} \qquad \Omega^{-1} = \sqrt{8\pi G}\xi^{1/2}\phi, \tag{A.3}$$

where G is certain constant, at the moment. The Lagrangian (A.1) is now expressed in terms of the quantities in the new (starred) conformal frame (CF):

$$\mathcal{L} = \sqrt{-g_*}\left(\frac{1}{2}\frac{1}{8\pi G}R_* - \frac{1}{2}g_*^{\mu\nu}\partial_\mu\sigma\partial_\nu\sigma + L_{*\text{matter}}\right), \tag{A.4}$$

where the new scalar field σ is given by $\sigma \sim \ln\phi$. In this CF, R_* is multiplied by a pure constant, indicating the constancy of the gravitational constant. This illustrates that one can always go a CF in which the gravitational constant is a true constant.

In the more realistic situation, masses of elementary particles must be true constants because the time scale of atomic clocks is provided by the Rydberg constant and we may reasonably assume that the fundamental constants c, $\hbar$ and the fine-structure constant are pure constants. To be able to discuss particle masses we must specify the matter part L_{matter}. In the BD model the mass term is given as usual. Corresponding to this we choose the usual Dirac Lagrangian of a massive particle as an illustration:

$$L_{\text{D}} = -\bar{\psi}(\not{D} + m)\psi, \tag{A.5}$$

where m is the mass and $\not{D}$ contains the spin connection as usual.

The kinetic energy part can be made conformally invariant if ψ is transformed into ψ_* according to $\psi = \Omega^{-3/2}\psi_*$. This implies, however, that the mass term is not invariant. We find in fact

$$\sqrt{-g}\,\bar{\psi}\psi = \Omega\sqrt{-g_*}\,\bar{\psi}_*\psi_*. \tag{A.6}$$

It follows that the effective mass $m_* = m\Omega \sim \phi^{-1}m$ is no longer a constant in CF in which G is constant. The CF in which m is constant is the original CF in which (A.1) is given. This implies time-dependent G if measured by atomic clocks.

Let us simplify the discussion by assuming that the present experiment rules out the time variability of G. If this is indeed the case, we must design L_{matter} in such a way that we find a CF in which both of G_{eff} and m_{eff} are time-independent. An example is provided by replacing the mass term in (A.5) by an interaction term

$$L_{\text{int}} = -f\bar{\psi}\psi\phi, \tag{A.7}$$

where f is a dimensionless coupling constant. This will give a mass approximately if ϕ varies sufficiently slowly as a function of t. An inspection of (A.6) shows that the effective mass m_* in the starred CF is given by $m_* = f\phi\Omega = f\xi^{-1/2}$, which is constant; the starred CF is a CF corresponding to the physical situation in which time is recorded by atomic clocks.

It is one of the premises of the BD model to rule out any matter interaction of ϕ because the term would violate the property that a particle falls along the geodesic. The requirement can be loosened if the coupling constant f is sufficiently weak. Moreover it is likely that ϕ is massive, making the force due to the scalar field finite-range, thus leaving the effect

relatively unimportant in solar system experiments, for example. A simple estimate shows that $f \sim 10^{-19}$ or less.

The above argument shows clearly that one must take microscopic physics into account in order to fully appreciate the result on $\dot{G}/G$. In other word, $\dot{G}/G$ provides a precious information about how gravity enters in microscopic physics. It seems, however, there is a wide-spread confusion on the nature of conformal transformation. Some says that physics looks the same in any CF, making it unnecessary to choose a particular CF. In this connection we hasten to point out that any of realistic theories of gravitation are noninvariant under conformal transformation. (The title and some of the statements in Dicke's classic paper "Mach's Principle and *Invariance* under Transformation of Units" [30] might be partly blamed.) Others also say that physics will look different only if quantum effects come in. In the following simple but explicit example we first demonstrate that physical effects show up differently in different CF even in the classical level.

Again as an exercise consider a perfectly standard theory of GR, and apply a Weyl rescaling of an arbitrary function Ω of time t. Also assume that $\Omega(t)$ varies so slowly that one can approximate it by

$$\Omega(t) \approx 1 + t\dot{\Omega}, \tag{A.8}$$

where $\dot{\Omega}$ is a derivative at the present time $t = 0$; we assume $|t\dot{\Omega}| \ll 1$ with the normalization $\Omega(0) = 1$.

The geodesic equation is transformed into

$$\frac{D^2x^\mu}{D\tau_*^2} = \Omega^2 \frac{D^2x^\mu}{D\tau^2} - f_\nu \left(g_*^{\mu\nu} + \frac{dx^\mu}{d\tau_*}\frac{dx^\nu}{d\tau_*} \right), \tag{A.9}$$

where $f_\nu \equiv \partial_\nu \ln \Omega$. This shows that a particle that falls along a geodesic in the original CF does not do so in the starred CF; depending on the choice of CF, GR may look as if it were not a metric theory! In the nonrelativistic limit, (A.9) gives an equation corresponding to the Newtonian equation of motion:

$$\frac{D^2x^i}{D\tau_*^2} \approx -\dot{\Omega}\frac{dx^i}{d\tau_*}. \tag{A.10}$$

It appears as if a dissipative force were present.

In the application to solar system experiments we notice that x^i and t are not the correct PN coordinates since the $g_{*\mu\nu}$ are not asymptotically flat due to the presence of Ω^2 in (A.3) if $g_{\mu\nu}$ are. This can be remedied by applying a general coordinate transformation to $\tilde{x}^i$ and $\tilde{t}$ [31]:

$$\begin{cases} t = \left(1 + \frac{1}{2}\tilde{t}\dot{\Omega}\right)\tilde{t} + \frac{1}{2}\tilde{r}^2\dot{\Omega}, \\ x^i = \left(1 + \tilde{t}\dot{\Omega}\right)\tilde{x}^i. \end{cases} \tag{A.11}$$

Suppose the Newtnonian equation in the original CF is given by

$$\frac{d^2x^i}{dt^2} = -GM\frac{x^i}{r^3} + \text{PN terms.} \tag{A.12}$$

Using (A.10) and (A.11) we obtain

$$\frac{d^2\tilde{x}^i}{d\tilde{t}^2} = -\left(1 - 2\tilde{t}\dot{\Omega}\right)GM\frac{\tilde{x}^i}{\tilde{r}^3} - \dot{\Omega}\frac{d\tilde{x}^i}{d\tilde{t}} + \text{PN terms.} \tag{A.13}$$

Let the solution of (A.12) be denoted by $\tilde{x}^i(t)$. We then show that the solution of (A.13) is given by [31]

$$\tilde{x}^i(\tilde{t}) = \tilde{x}^i(\tilde{t}) - \frac{1}{2}\dot{\Omega}\tilde{t}^2\dot{\tilde{x}}^i(\tilde{t}), \tag{A.14}$$

which shows explicitly that the particle moves in a different way from the way in the original CF. The different behavior should come as no surprise because of conformal noninvariance of the theory. It is something like different motions in different noninertial frames of coordinate in the Newtonian mechanics.

Obviously choosing a correct CF is an indispensable part of any theoretical analysis. Also obvious is that there is no apriori criterion to select a particular one. In the analysis of the solar system experiments in the above sense, a CF in which the particle masses are constant seems to be a right CF. This is, however, not sufficient if we go back to the past to discuss the early universe in which atomic clocks had not been available yet.

The same universe looks expanding differently in different CFs. Suppose the scale factor behaves like $a(t) = t^\alpha$ in the original CF, and the scalar field dynamics gives $\Omega \sim t^{-\zeta}$. The time variable t_* and the scale factor $a_*(t_*)$ are defined by the relations $dt = \Omega dt_*$ and $a = \Omega a_*$. We then find $a_* = t_*^{\alpha_*}$ and $t_* = t^{\zeta+1}$, where $\alpha_* = (\alpha+\zeta)/(1+\zeta)$. An example of the theoretical models [32] gives $\alpha_* = 1/2$ and $\zeta = 1$ with $m_* = \text{const}$, and hence $t = t_*^{1/2}$, $m \sim t$ and $\alpha = 0$. The radiation-dominated universe in the starred CF shows no expansion in the original CF, because rods now expands in the same proportion as the universe.

The difference in quantum effects will be even more drastic, because in many occasions quantum theories are defined as small perturbations around classical solutions. Choosing CF and quantization procedure may not be commutable. It is something like the effects in phase transitions. See ref. [32] for an example.

References

1. C. Will, *Theory and Experiment in Gravitational Physics*, Cambridge University Press, (1981): Phys. Rep. **113** (1984), 345: Science **250** (1990), 770.

2. P.G. Roll, R. Krotokov and R.H. Dicke, Ann. Phys. (N. Y.) **26** (1964), 442.

3. V.B. Braginski and V.I. Panov, Sov. Phys. JETP **36** (1971), 464.

4. E.G. Adelberger, C.W. Stubbs, B.R. Heckel, Y. Su, H.E. Swanson, G. Smith, J.H. Gundlach and W.F. Rogers, Phys. Rev. **D 42** (1990), 3267: R.D. Newman, D. Graham and P. Nelson, Proc XXIVth Rencontre de Moriond, (Editions Frontieres, 1989), p. 459.

5. L.I. Schiff, Am. J. Phys. **28** (1960), 340.

6. R.V. Pound and G.A. Rebka, Phys. Rev. Lett. **4** (1960), 337.

7. R.F.C. Vessot, M.W. Levine, E.M. Mattison, E.L. Blomberg, T.E. Hoffman, G.U. Nystrom, B.F. Farrel, R. Decher, P.B. Eby, C.R. Baugher, J.W. Watts, D.L. Teuber and F.D. Wills, Phys. Rev. Lett. **45** (1980), 2081.

8. A.P. Lightman and D.L. Lee, Phys. Rev. **8** (1973), 364: M.P. Haugan, Ann. Phys. (N. Y.) **118** (1979), 156.

9. V.W. Hughes, H.G. Robinson and Beltran-Lopez, Phys. Rev. Lett. **4** (1960), 342: R.W.P. Drever, Phil. Mag. **6** (1961), 683.

10. J.D. Prestage, J.J. Bollinger, W.M. Itano and D.J. Wineland, Phys. Rev. Lett. **54** (1985), 2387.

11. S.K. Lamoreaux, J.P. Jacobs, B.R. Heckel, F.J. Raab and E.N. Fortson, Phys. Rev. Lett. **57** (1986), 3125.

12. W.T. Ni, Phys. Rev. Lett. **38** (1977), 301.

13. C.-H. Hsieh, P.-Y. Jen, K.-L. Ko,K.-Y. Li, W.-T. Ni, S.-S. Pan, Y.-H. Shih and R.-J. Tyan, Mod. Phys. Lett. **A4** (1989), 1597: Y. Chou, W.T. Ni and S.L. Wang, preprint: W.-T. Ni, Y. Chou, S.-S. Pan, C.-H. Lin, T.-Y. Hwong, K.-L. Ko and K.-Y. Li, Proc. 3rd ROC-ROK Metrology Symposium, May, 1990, p. 107.

14. A. Eddington and G.L. Clark, Proc. Roy. Soc. **166A** (1938), 465.

15. K. Nordtvedt, Jr., Phys. Rev. **169** (1968), 1014; 1017: **170** (1968), 1186.

16. J.G. Williams, R.H. Dicke, P.L. Bender, C.O. Alley, W.E. Carter, D.G. Currie, D.H. Eckhardt, J.E. Faller, W.M. Kaula, J.D. Mulholland, H.H. Plotkin, S.K. Poultney, P.J. Shelus, E.C. Silverberg, W.S. Sinclair, M.A. Slade and D.T. Wilkinson, Phys. Rev. Lett. **36** (1976), 551: I.I. Shapiro and C.C. Caounselman, III, Phys. Rev. Lett. **36** (1976), 555.

17. T.M. Brown, J.Christensen-Dalsgaard, W.A. Dziembowski, P. Goode, D.O. Gough and C.A. Morrrow, Astrophys. J. **343** (1989), 526.

18. H.A. Hill, P.D. Clayton, D.L. Patz, A.W. Healy, R.T. Stebbins, J.R. Olesin and C.A. Zanoni, Phys. Rev. Lett. **33** (1974). 1497.

19. R.W. Hellings, P.J. Adams, J.D. Anderson, M.S. Keesey, E.L. Lau, E.M. Standish, V.M. Canuto and I. Goldman, Phys. Rev. Lett. **51** (1983), 1609.

20. R.A. Van Pattern and C.W.F. Everitt, Phys. Rev. Lett. **36** (1976), 629.

21. I. Ciufolini, Phys. Rev. Lett. **56** (1986), 278.

22. B. Mashhoon, H.J. Paik and C. Will, Phys. Rev. **39** (1989), 2825.

23. J.H. Taylor, A. Wolosczan, T. Damour and J.M. Weisberg, Nature **535** (1992), 132.

24. T. Damour, G.W. Gibbons and J.H. Taylor, Phys. Rev. Lett. **61** (1988), 1151.

25. Y. Fujii, Nature Physical Science **234** (1971), 5.

26. E. Fischbach, D. Sudarsky, A. Szafer, C. Talmadge and S.H. Aronson, Phys. Rev. Lett. **56** (1986), 3.

27. E. Fischbach and C. Talmadge, Nature to be published.

28. Y. Fujii, Int. J. Mod. Phys. **A6** (1991), 3505.

29. Y. Fujii, Phys. Lett. **255B** (1991), 439.

30. R.H. Dicke, Phys. Rev. **125** (1962), 2163.

31. P.J. Adams, V.M. Canuto, I. Goldman and R.W. Hellings, Phys. Rev. **D28** (1983), 1822.

32. Y. Fujii and T. Nishioka, Phys. Rev. **D42** (1990), 361.

Gamma Ray Bursters and Sources of Gravitational Waves

Takashi Nakamura

Yukawa Institute for Theoretical Physics,
Kyoto University, Kyoto, 606, Japan

Almost twenty years have passed since gamma ray bursters were discovered. The main observational results as well as theoretical arguments up to 1990 are reviewed by Higdon and Lingenfelter.[1] We do not discuss topics treated in this review paper. Here we only discuss recent astonishing observational results by BATSE science team in GRO(Gamma Ray Observatory)[2],[3] whose gamma ray detector has 2000cm^{2}x8 area with energy range from 20 to 2000keV and can determine the position of the source within the accuracy of 5 to 10 degrees. BATSE reported that the distribution of 153 located events is isotropic within the statistical limit. A measure of the dipole moment with respect to the galactic center is $< \cos\theta >= 0.002 \pm 0.006$ (vs. 0 ± 0.046 for an isotropic distribution) and that of the quadrupole moment with respect to the galactic plane is $< \sin^2 b >= 0.310 \pm 0.006$ (vs. 0.333 ± 0.023 for an isotropic distribution). The quoted errors for the measured values are the instrumental errors due to inaccuracy of the burst locations only, while those for the isotropic model distribution are the standard statistical ones for the sample of 153 events. The value of the dipole moment suggests that the source distribution is a symmetric function of $\cos\theta$. There are equal number of sources toward the galactic center and anti-center directions. The quadrupole moment, however, does not necessarily suggest the isotropy as stated by Meegan et al.[3] . To show this we consider a model distribution of gamma ray bursters such that the source luminosity and the number density are both constants within the spheroid given by

$$\frac{x^2+y^2}{a_1^2}+\frac{z^2}{a_3^2}=1. \tag{01}$$

If we identify xy plane with the galactic plane , $< \sin^2 b >$ is given by

$$< \sin^2 b >= \frac{(1-e^2)(\frac{1}{2}\log\frac{1+e}{1-e}-e)}{e^3}, \tag{02}$$

where

$$e = \sqrt{1 - \frac{a_3^2}{a_1^2}}.$$

From the observation, $< \sin^2 b >$ can be 0.25 for 3σ lower bound. In the above model this corresponds to e=0.7 or $a_1 : a_3$=1:0.7. Even for $< \sin^2 b >$=0.295 (i.e.1σ lower bound) , e=0.5 (or $a_1 : a_3$=1:0.86). This shows that more located events are needed to distinguish whether the source distribution is isotropic or not.

The integral brightness distribution has a slope of -0.8 (vs. -1.5 for homogeneous and isotropic distribution). The average value of V/V_{max} is 0.348±0.024(vs. 0.5 for a homogeneous and isotropic distribution), while *Ginga* found V/V_{max}=0.35±0.035[4] , where V/V_{max} for each burst is the ratio of spherical volume defined by the distance of the burst and the maximum volume from which the burst could have been detected. In the homogeneous spheroid model distribution of Eq. (01) V/V_{max} is given by

$$< V/V_{max} >= (2(1-e^2)^{1.5} + 3(1-e^2)^{0.5} + 3\frac{1}{e}\tan^{-1}\frac{e}{\sqrt{1-e^2}})/16, \qquad (03)$$

where $V_{max}=4\pi a_1^3/3$ is assumed. Then the value of $< V/V_{max} >$ are 0.387 and 0.43 for e=0.7 and 0.5, respectively. Thus the spheroid model can be compatible with V/V_{max} tests of GRO and GINGA satellites if e$\sim$ 0.7 and $V_{max} \sim 4\pi a_1^3/3$. Note that the spheroid model yields 0.5 for $< V/V_{max} >$ if $V_{max} \leq 4\pi a_3^3/3$. The larger value of $< V/V_{max} >$ in the range of 0.4-0.5, which are reported by the other satellite experiments[1] , might be interpreted in terms of the V_{max} smaller than $\sim 4\pi a_1^3/3$. This suggests that a homogeneous spheroid model which is anisotropic might be consistent with the dipole and quadrupole moments of the angular distribution as well as the V/V_{max} tests of GRO and other satellites. On the other hand, if we assume the isotropy of the distribution, the index of integral brightness distribution -0.8 and $< V/V_{max} >$=0.348 is compatible with the inhomogeneity of the number of sources decreasing as $r^{-1.5}$ as a function of distance r from the earth.

From the rise time of the bursts[1] , the size of the sources should be smaller than 300km. This suggests that gamma ray bursts are the phenomena near compact objects such as neutron stars or black holes. In reality cyclotron features measured in three out of 23 events by Gamma-ray Burst Detector on board the *Ginga* satellite corresponds to a magnetic field of $\sim 10^{12}$ gauss, which strongly suggests neutron stars[5] . *Ginga*

also detected X-ray emission in the 2-10kev energy range ~10s before the onset of the gamma ray bursts as well as a tail of X-ray emission for ~30s afterwards. The spectra of the precursor is well fitted by the black body with a temperature 1.5keV, which also suggests emission from a neutron star at near Eddington limit. In view of these facts, we do not consider sources other than neutron stars and black holes in this paper although gamma ray bursters might be completely new compact objects about which we know nothing.

If future observations confirm the isotropy of the distribution, we may abandon galactic disk models as well as halo models. One inclines to consider a cosmological model. If typical gamma ray bursters are at the distance of $\sim$ 4Gpc($\sim 10^{28}$cm), the total energy amounts to $\sim 10^{50}$ergs . If this is the gravitational energy liberated by the matter falling onto the neutron star, the total mass is $\sim 0.1 M_{\odot}$. Even in the dense core of globular cluster the collision time between a neutron star and a low mass star is too long ($\sim 10^{18}$y). Although there are many pulsars which have a low mass companion($\sim$ 20) , the decay time of the orbit due to the gravitational radiation is much longer than the age of universe. The most probable candidate seems to be coalescing binary neutron stars. There are at least three systems, PSR1913+16, PSR2127+11C and PSR1534+12 in the galactic disk. Two neutron stars in these systems will coalesce after 3×10^8y, 2×10^8y and 3×10^9y, respectively, due to the emission of the gravitational waves. Then an ultra-conservative lower limit to the rate of coalescing binary neutron star gives $\sim$ 200events/y within 4Gpc[6] . Phinney's best estimate gives $\sim 10^4$events/y.

Coalescing binary neutron stars at cosmological distance as gamma ray bursters are consistent with the isotropy of sources. As for V/V_{max} test, two aspects exist. Since binary neutron stars coalesce $\sim 3 \times 10^8$ to 10^{10}y after formation, the number of sources should decrease as a function of distance, i.e. the backward time, from us. This favors the small value of V/V_{max} qualitatively. Even if the number density of sources is constant in co-moving coordinate, V/V_{max} becomes smaller due to cosmological redshift. As for the energy, potentially a part of binding energy of neutron stars $\sim 10^{53}$ ergs might be liberated as gamma rays[7] . What is difficult in this model is the time scale problem. Nakamura and Oohara performed post Newtonian 3D numerical simulations of coalescing binary neutron stars including radiation reactions of gravitational waves[8] . They performed several simulations with different mass ratio. The final product is a rotating black hole with a Kerr parameter a/m$\sim$ 0.35. The time from the contact of

two neutron stars to the formation of the black hole is at most 10ms or so. Even if we include the accretion phase before the contact or tidal disruption of the smaller mass neutron star, the time scale is at most 1sec while there exist gamma ray bursters with duration $\sim$ 100 sec[1] . Even the existence of event with duration 1000s was reported[9] . Regardless of energetics and radiation mechanism, it seems highly difficult to make an phenomena with duration of 1000sec in coalescing binary neutron stars.

In numerical simulations by Nakamura and Oohara[8] when the initial mass of each coalescing binary neutron stars is different, the smaller mass neutron star is tidally disrupted. The tail of the tidally disrupted star makes spiral like structure due to the differential rotation. After several rotation, these spiral structure disappear by winding and a disk is formed around a rotating Kerr black hole. Here there are two energy sources, one is the rotational energy of Kerr black hole which amounts to

$$E_{rot} = 6 \times 10^{52} ergs (\frac{a/m}{0.35})^2,$$

and the gravitational energy of the disk estimated as

$$E_{acc} = 10^{51} ergs (\frac{M_{disk}}{0.01 M_\odot}).$$

If neutron stars have magnetic fields of $\sim 10^{12}$ gauss before coalescence, it is not so unreasonable to assume that a magnetic field may be amplified up to 10^{15}gauss due to the winding and the differential rotation of the disk. Then E_{rot} as well as E_{acc} may be liberated by Blandford-Znajeck effect with the luminosity[10] given by

$$L \sim 10^{50} ergs/s (\frac{a/m}{0.35})^2 (\frac{M}{3M_\odot})^2 (\frac{B}{10^{15} gauss})^2.$$

$\tau = (E_{rot} + E_{acc})/L$ will give a time scale of the event which depends on the strength of magnetic fields. In order to produce gamma ray we may use positron and electron pair creation in the spark-gap and subsequent curvature radiation as in radio pulsar[11] . The energy of electron pairs are estimated as[11]

$$E_e \sim 10^{12} eV (\frac{B}{10^{15} gauss})^{-1/7} (\frac{a/m}{0.35})^{1/7}.$$

Then the energy of the curvature radiation becomes

$$E_\gamma \sim 1 MeV (\frac{10^7 cm}{\rho}),$$

where ρ is the curvature of the magnetic fields. In this case we can see gamma ray

bursts only from a certain direction. Then the beam factor of ~ 0.1 will give us ~ 1000 events/y which is the correct rate.

If gamma ray bursters are coalescing binary neutron stars, they should be the sources of gravitational waves certainly. Numerical simulations of coalescing binary neutron stars by Nakamura and Oohara[8] suggest that the maximum amplitude of the gravitational waves amounts $h \sim 10^{-21}$ if the source is at the distance of 50Mpc. This shows that the maximum amplitude will be $h \sim 10^{-23}$ if the source is at the distance of 4Gpc. At present the goal of the gravitational wave detectors is to achieve the sensitivity of $h \sim 10^{-21}$ at the frequency of $\sim$kHz. However, in the advanced phase of detectors such as LIGO[12] , the goal is $h \sim 10^{-23}$. Then we may observe almost all the gamma ray bursts by the gravitational waves also. Such observations will give us important information on physics in strong gravity such as black hole physics. At the same time the gamma ray bursters will give us unambiguous standard candles which have been sought for in cosmology. From the measurement of amplitude, the frequency and the time scale of the increase of the frequency $\sim$1sec before the coalescence of binary neutron stars, we can determine the distance to the source directly[13] , i.e. without using any empirical relations often used in cosmology. The simultaneous observation of events by several gravitational wave detectors as well as gamma ray detectors can determine the position of the source. From the value of the redshift of the host galaxy and the directly determined distance, we may determine various important cosmological parameters such as Hubble constant, energy density, deceleration parameter and the cosmological constant unambiguously.

This paper is based on the paper *Possible Origins of Gamma Ray Bursts* by T. Nakamura, N. Shibazaki, T. Murakami and A. Yoshida.(YITP/K-960) This work was partly supported by a Grnat-in-Aid for Scientific Research on Priority Area of Ministry of Education, Science and Culture(03250103)

REFERENCES

1. J.C.Higdon and R.E.Lingenfelter, Ann.Rev.Astron.Astrophys. **28**(1990),401.
2. C.A.Meegan, G.J.Fishman, R.B.Wilson, W.S.Paciesas, M.N.Brock, J,M,Horack, G.N.Pendelton and C.Kouveliton, IAU Circular No5358, 1991 October 4
3. C.A.Meegan, G.J.Fishman, R.B.Wilson, W.S.Paciesas, M.N.Brock, J,M,Horack, G.N.Pendelton and C.Kouveliton, Nature in press.
4. Y. Ogasaka, T. Murakami, J. Nishimura, A. Yoshida and E. E. Fenimore, Apj. L., **383**(1991), L 61.
5. A.Yoshida. T.Murakami, J.Nishimura, I.Kondo, and E.Fenimore , P.A.S.J, **43** (1992) no 6.
   T.Murakami, M,Fujii, K.Hayashida, M.Itho, J.Nishimura, T.Yamagami, J.Conner, W.D.Evans, E. E. Fenimore, R.W. Klebesadel, A. Yoshida, I.Kondo and N. Kawai, Nature **335**(1988), 234.
6. E.S.Phinney, Caltech preprint GRP-270
7. D. Eichler, M. Livio, T. Piran and D. Schramm, Nature, **340**(1989),126.
   P.Haensel, B.P. Pacynski and P.A. Amsterdamski, Astrophys. J. **375**(1991) 209.
   A. Shemi and T. Piran, ApJ. L.**365**(1990), L55.
8. T. Nakamura and K. Oohara, Prog. Theor. Phys, **82**(1989),535. Prog. Theor. Phys, **82**(1989),1066. Prog. Theor. Phys, **83**(1990),906. Prog. Theor. Phys, **86**(1991),73.
9. R. Klebesadel et al., Bull. Am. Astron. Soc. **16**(1984), 1016.
10. R.D. Blandford and R. L. Znajek, Mon. Not. R. astr. Soc. **179**(1976),433.
    K. S. Thorne , R. H. Price and D. A. Macdonald, *Black Hole; the Membrane Paradime*Yale University Press 1986.
11. M. A. Ruderman and P.G. Sutherland, Astrophys. J. **196**(1975),51.
12. R. E. Vogt, in proceeding of the 6th Marcell Grossman Meeting on General Relativity (1991, June Kyoto,Japan)
13. B. Schutz, Nature, **323**(1986),310.

Black Holes in Astrophysics

Fumio Takahara

Department of Physics, Tokyo Metropolitan University
Minamiohsawa 1-1, Hachioji, Tokyo 192-03

Abstract

Astrophysical aspects of black holes are reviewed. Firstly, observable signatures of black holes are examined in the context of dense stellar systems and X-ray sources. Then, basic ideas of accreting black holes in explaining X-ray stars and active galactic nuclei are presented. Finally, cosmological evolution of black holes in galactic nuclei is discussed.

1. Introduction

For modern physicsists who investigate the real world around us, the black hole is not just a mathematical solution of the Einstein equation but an object which can be studied observationally. The existence of the black hole is a natural outcome of stellar evolution as was first noted by Oppenheimer and Snyder in 1939[1]. As the stellar energy source was understood in terms of the thermo-nuclear fusion, the fate of stars after the consumption of the nuclear fuel has gathered much attention. Theoretical study of stellar evolution predicts that a star of the initial mass more than about $30M_{\odot}$ leaves behind a black hole. The problem is how to recognize the existence of the black hole, because, by definition, the black hole does not emit any radiation from inside the event horizon and it is unobservable. The breakthrough occurred in 1960s that was the era when many important astrophyical objects were discovered such as pulsars, X-ray stars, quasars and cosmic microwave background. It is rather surprising that they remain to be major topics in astrophysics in 1990s, even 30 years later after their discovery. It was soon recognized that most X-ray stars

in our Galaxy are in binary systems and emit X-rays through the gravitational energy release by gas accretion from the companion star. Among them, one particular star called Cyg X-1 proved to have a mass of about $10M_\odot$ which is well above the theoretical upper limit for the mass of the neutron star which is about $2M_\odot$. Thus, such a massive compact star should be necessarily regarded as a black hole.

It should be noted that the idea of accreting black holes was proposed as early as 1964 by Salpeter[2] and Zeldovich[3] to explain an enormous luminosity of quasars. This idea had not received much attention for an initial decade but eventually revived in mid 70s. In the initial decade most theoretitians had developed models in terms of supermassive stars and very dense stellar systems. Those studies had finally lead to tha recognition that the formation of a black hole in the center is inevitable and it plays a major role in explaining quasars and active galactic nuclei[4),5]. Today we believe that various activities seen in quasars and active galactic nuclei are caused by accretion onto supermassive black holes of about $10^8M_\odot$, although detailed understanding of physical processes has not been fully appreciated. Such physical processes are one of the most important topics in astophysics in 1990s.

In this review I treat basic concepts of black holes in the astrophysical point of view. First, I present a basic idea of how to recognize the existence of a massive black hole in dense stellar systems. Then, I describe observable signatures of black holes in X-ray sources. The present status of theoretical understanding of accreting black holes is also presented. Finally, cosmological considerations of the formation and evolution of black holes in galactic nuclei are discussed.

2. Black holes in stellar systems

Stellar systems such as globular clusters and galactic nuclei are only moderately dense. We may recognize the existence of a massive black hole by its dynamical effect on the surrounding stellar system. A pioneering investigation of such an effect was made by Peebles in 1972[6]. Following his paper much work has been done in 1970s[7),8),9]. For a detailed discussion and a list of references, readers may consult a recent review paper by Dokuchaev[10] in which many physical processes of stellar systems are discussed.

Dense stellar systems may be described by an isothermal sphere model which is characterized by the one-dimensional velocity dispersion σ, the central density ρ_c,

and the core radius r_c. They are mutually related by the equation

$$\rho_c = \frac{9\sigma^2}{4\pi G r_c^2}. \tag{1}$$

The density distribution is approximately constant for $r < r_c$ and decreases as r^{-2} for $r > r_c$. While real stellar systems show a somewhat steeper density distribution in the envelope region, this is not essential for the present discussion. The core mass of the system is roughly given by

$$M_c = \frac{4\pi}{3}\rho_c r_c^3 = \frac{3\sigma^2 r_c}{G}. \tag{2}$$

For reference, representative values are tabulated for globular clusters, galactic nuclei, and hypothetical dense stellar systems which once had been considered a model of quasars.

	σ(km/s)	r_c(pc)	$\rho_c(M_\odot/pc^3)$	$M_c(M_\odot)$
Globular Clusters	10	1	10^4	10^4
Galactic Nuclei	100	10	10^4	10^7
Hypothetical system	1000	1	10^8	10^8

The gravitational field of the central black hole dominates that of the stellar system if the mass of the black hole M_H is more massive than the stellar mass within the radius r. This leads to the condition

$$r < r_c(\frac{M_H}{M_c})^{1/3}, \tag{3}$$

for $M_H < M_c$. In this case, however, actual gravitational effects appear only for $r < r_H = GM_H/\sigma^2$ which is smaller than the above radius. Alternatively, if $M_H > M_c$ the condition is

$$r < 3r_c(\frac{M_H}{M_c}) = r_H. \tag{4}$$

Thus the gravitational effect of the black hole appears for $r < r_H$ for both cases. In this region, velocity dispersion of stars increases as $r^{-1/2}$. If the stellar system is

rotationally supported, the rotation velocity increases in the same power. Observationally this is seen as a prominent jump in the rotation velocity at the both sides of the black hole.

The number density distribution of stars around a black hole is more complicated to treat. Sufficiently near the black hole, stars are tidally disrupted and eventually swallowed into the hole. If the number density of stars is large enough, mutual stellar collisions disrupt the stars. In any case a net flow of stars occurs in the direction to the hole. The relaxation between stars owing to stellar distant encounters will make up for swallowed stars. The relaxation time T_R is proportinal to $\sigma^3 n^{-1}$, where n is the number density of stars. The steady state condition may be written as $nr^3/t_s \sim$ const., where t_s is the time scale of the flow of stars. Accompanying the flow of stars, a net energy flow should occur outwards since the hole swallows stars with a negative energy. The condition of the steady energy flow is written as $nr^3 E/t_E \sim$ const., where E is the total energy of a star and may well be proportional to r^{-1} and t_E is the time scale of the energy flow. At the minimum radius $r_{\rm min}$ where stars are disrupted we can take $T_E = T_s = T_R$. Then, we obtain from the two steady state conditions $t_E = (r_{\rm min}/r)t_s$. Since the relaxation time should be identified with the minimum of t_s and T_E, we should take $T_E = T_R$. Thus, we finally have the distibution proportional to $r^{-7/4}$, which is called a cusp around the black hole.

As was shown above, observational search for massive black holes in stellar systems relies on the velocity and density distribution in the central region. The corresponding angular scale becomes

$$\theta = \frac{r_H}{d} = 21 \frac{r_H}{1\mathrm{pc}} \frac{10\mathrm{kpc}}{d} \mathrm{arcsec} \tag{5}$$

where d is the distance. Nearby galaxies are within the reach of such study. Observations have suggested the existence of a massive black hole in several galactic nuclei such as M31, M32, NGC4549, M87, NGC3311 and NGC3377[11),12),13)]. The mass derived ranges from $3\times10^6 M_\odot$ to $3\times10^9 M_\odot$. For our galaxy, a stellar system cannot be observed due to heavy absorption, but it is also suggested that there exists a black hole of $3 \times 10^6 M_\odot$ using infrared lines emitted by a gaseous component[14)]. Hubble Space Telescope is expected to greatly improve the reliability of such observations as well as extend the number of target galaxies.

A cusp in the density distribution can be also formed by the gravothermal catas-

trophe without the central black hole as is frequently discussed for globular clusters. It is to be noted that the velocity structure is very different from a cusp around massive black hole and observationally discriminated.

3. Black holes in X-ray binaries and active galactic nuclei

As was stated in the Introduction, the first detection of the black hole was made for Cyg X-1 which belongs to X-ray stars in the Galaxy. From the analysis of binary motion we can infer the mass of the X-ray star and if the mass exceeds the theoretical upper limit for the neutron star of about $2M_{\odot}$, we may identify it with a black hole. At present we have four such X-ray stars, Cyg X-1, LMC X-3, A0600-00 and LMC X-1. The characterictics of X-ray emission from such black hole candidates is in fact distinct from those from X-ray stars containing the neutron star[15]. The latter population belongs to a majority of X-ray sources and is classified into two categories. One category is the X-ray pulsars which show a modulated emission pattern with its rotation period and a spectral feature of a steep cutoff above about 20keV due to the cyclotron resonance. The second category is called low mass X-ray binaries for which the spectrum is fitted by a superposition of two component quasi-black body radiation and occasionally phenomena called X-ray bursts occur. The two components are interpreted as the emission from the stellar surface and from the accretion disk. It should be reminded that the emission from stellar surface is definitely observed for both categories of X-ray stars.

In contrast, for black hole candidates, no stellar emission, no regular pulsation and no X-ray bursts have been observed. They are characterized by rapid time variabilities with no characteristic time scale and their emission is composed of two components, too. One is a hard component with a power law spectrum extending up to 100keV and the other is an ultrasoft component that is peaked at 1keV or less. Usually the latter is ascribed to the emission from an optically thick accretion disk, while the former origin is still in debate, while the Compotonization in a hot plasma with the temperature of about 100keV is most likely[16]. Similar emission properties are observed for quasars and active galactic nuclei[17]. A hard X-ray emission with a power law spectrum is a ubiquitous feature of active galactic nuclei and a strong UV emission which seems to have a quasi-black body spectrum is also observed for many active galactic nuclei. The latter seems to correspond to an ultrasoft X-ray

emission from galactic black hole candidates.

Thus for black holes, the power law component seems to replace the emission from the stellar surface in the case of neutron stars. However, theoretical models of such a hard X-ray emission with a power law spectrum in the vicinity of the black hole remain to be further developed. Recent detection of X-ray lines from iron atoms has given another diagnostics of black holes in X-ray sources since in principle they carry the information of the properties of the black hole through the effect of space-time structure[18),19)]. However, to make it possible we need a reliable astrophysical model as well as very detailed observational data.

4. Accreting balck holes

As was briefly stated in the introduction, gravitational energy release due to accretion is considered to provide the energy source of X-ray stars and active galactic nuclei. Since accreting gas posseses some amount of angular momentum in general, it forms a disk around the central gravitating object, which is called the accretion disk. A theory of accretion disks was developed by Shakura and Sunyaev[20)] and independently by Novikov and Thorne[21)], and it is now called the standard accretion disk model. They assumed that the disk is geometrically thin and rotating obeying the Kepler law. Through the action of the viscosity, angular momentum is transferred outwards and the rotating gas slowly moves into the central black hole and at the same time frictionally generated heat is radiated away from the disk. For the viscosity, they assumed that the off-diagonal component of the stress energy tensor is proportional to the pressure. Although at first sight this may seem to drastically affect the resultant disk structure, steady state structure of accretion disks seems to be fairly robust, while stabilities of the disk much depend on the assumed shape of the viscosity.

The solution of the standard accretion disk is not unique and two solutions are known near the black hole where a major portion of energy release occurs. One solution is an optically thick solution in which the radiation pressure dominates the gas pressure and the disk emits the black body radiation at the local temperature. The temperature is determined independent of the details since the luminosity is an order of the Eddington luminosity and the surface area is given by the square of the Schwarzschild radius. The typical temperature turns out to be 10^7K for a stellar

mass hole and 10^5K for $10^8 M_\odot$ hole in active galactic nuclei. Those temperatures correspond to the ultrasoft component from galactic black hole candidates and the UV bump from active galactic nuclei, respectively. While this incidence implies some success of the theory, there is no room for explaining hard X-ray emission from these sources. An alternative solution is an optically thin solution where the ion temperature is much higher than the electron temperature[22),23)]. In this model the dissipated energy is first used to heat ions, then electrons are heated by Coulomb collisions, and electrons cools by repeated Compton scattering to produce a power law X-ray emission. While this model is successful in explaining the X-ray emission, emission at other wavelengths is not explained.

Thus we need a more complicated modelling of accretion disks even in the context of explaining the electromagnetic emission properties. Moreover, jet production in radio galaxies and quasars has been completely neglected in the model, which is one of the most challenging problems in the contemporary astrophysics. Certainly we need to incorporate many aspects of physics such as radiation hydrodynamics, hydromagnetics and particle acceleration to fully understand the physics of accretion onto massive black holes.

From the view point of general relativity, it is an important issue to obtain the efficiency of energy conversion. The inner boundary of the standard accretion disk is identified with the radius of the inner most stable circular orbit. For Schwarzshild hole, this radius is 3 times the Schwarzschild radius with the specific angular momentum of $\sqrt{3}$ and the conversion efficiency becomes 5.7%. For comparison for Kerr hole, this radius becomes smaller as the rotation of the hole increases when the orbit is co-rotating with the hole. In contrast when the orbit is counter-rotating, this radius becomes larger. For the extreme Kerr hole, the innermost stable orbit coincides with the event horizon with $0.5r_g$ with the specific angular momentum of $1/\sqrt{3}$ and the conversion efficiency becomes as large as 42%. It is fairly surprising that most astrophysical applications have been made only for the Schwarzschild case. It should be noted that accreting matter should have angular momentum and spin up the hole in a relatively short time scale. We should use Kerr holes in astrophysical applications; a factor of 8 difference of the conversion efficiency may change the emergent spectra and affect interpretation of observations.

Above argument relies on the thin disk approximation and a fairly complicated treatment is required to take the effect of the finite temperature of accreting plasma

into account. Some authors have argued that thick disks are formed in the vicinity of the hole when the efficiency of angular momentum transfer is low[24),25)]. A comment on this model is that it leads to a very low efficiency of the enrgy conversion. As an accreting plasma piles up with a large angular momentum, the plasma swallowed into the hole has a large angular momentum as well as a large internal energy. Thus, the conversion efficiency should be very low and larger accretion rate is required to produce observed luminosities than for the thin disk.

Final comment on accreting black hole is made on the Penrose processes[26)]. While a particle orbit has always positive energy for a positive angular momentum, a negative energy orbit becomes possible in the ergosphere of the Kerr hole. Since such a negative energy orbit is bounded by a barrier in the effective potential within the ergosphere, a negative energy particle can be produced only in situ by breaking a particle of positive energy which comes from the infinity. If negative energy particles are preferentially swallowed into the hole and the positive energy particles that are a counterpart of the break up leave for infinity, the eventual outcome is that an energy can be extracted from the rotation energy of the hole. This is called the Penrose process. Maximum energy extractable from the extreme Kerr hole is 29% in theory. The astrophysical plausibilities of this process have been extensively examined such as the disruption of a star, Compton scattering of a photon, and electron-positron pair production. However, the efficiency has proved to be extremely low since positive energy particles are also swallowed into the hole at the same time[27)]. The effect of magnetic field is now a current topic but it seems to be very difficult to realize afavorable situation because a surrounding plasma which is rotating slower than the hole is necessarily free falling.

5. Cosmological evolution of black holes in galactic nuclei

The existence of supermassive black holes in active galactic nuclei and galactic nuclei in nearby galaxies suggests that it is a ubiquitous feature. It is an unsolved problem when and how such black holes are formed and evolved. As was stated in the last section, a black hole accrete ambient gas and becomes a very bright and active object. A black hole in nearby galaxies is considered to be accreting only a tiny amount of gas for some reason. The accretion rate which is given by an ambient gas is called Bondi's rate and written by

$$\dot{M} = 4\pi(\frac{GM}{c_{s\infty}^2})^2 \rho_\infty c_{s\infty}. \tag{6}$$

This rate critically depends on the sound velocity $c_{s\infty}$ and density ρ_∞ of the ambient gas. If we choose appropriate values, the rate proves to be sufficient large to provide observed high luminositites. However, the Bondi's rate does not take account of the effect of the back reaction of the radiation that is produced by the accretion. In actual case, owing to radiation force, accretion rate is limited by the Eddington's rate which is given by

$$\dot{M} = \frac{4\pi GMm_p}{\eta\sigma_T c}, \tag{7}$$

where η, m_p and σ_T are the conversion efficiency, the proton mass, and Thomson cross section respectively. Since this rate is proportional to the mass, the black hole mass evolves exponentially with time as

$$M = M_0 \exp(t/t_E), \tag{8}$$

where the Eddington time t_E is written by

$$t_E = \frac{\eta\sigma_T c}{4\pi G m_p} = 4.6 \times 10^8 \eta \text{ years}. \tag{9}$$

For a typical efficiency of η=0.1, the evolution time is 5×10^7years. This finite age has a fairly strong cosmological significance as discussed below based on the argument by Turner[28].

Recent search for distant quasars has revealed many quasars of the redshift greater than four. Take an example of PG1158+4635 with redshift of 4.73. Bolometric luminosity is estimated as 2×10^{46}erg/s for H_0=100km/s and Ω_0=1. Then, the minimum mass is $1.6 \times 10^8 M_\odot$ assuming that the quasar is accreting at the Eddington rate. Then, the time required to grow from the intitial mass of $10M_\odot$ is 7.6×10^8years and 3.4×10^8years from $10^5 M_\odot$. These time scales are compared to the age of the universe at z=4.73 which is 4.6×10^8years. It is found that the initial mass should be far greater than the stellar mass scale, unless the formation process of a hole is inefficient in producing radiation. Thus the growing process of black holes in galactic nuclei seems to be prolonged in the high redshift range. This is reinforced by the fact that metal emission lines are seen in the spectra of quasars,

which implies that nucleosynthsis of metals had proceeded before z=5 in the host galaxy.

Dynamical argument also suggests that quasars and their host galaxies were formed in a rather early epoch. Equating the growth time t_E with the free fall time scale of the region which eventually becomes a black hole $1/\sqrt{4\pi G\rho_H}$, we obtain the characteristic density as

$$\rho_H = \frac{4\pi G m_p^2}{\eta^2 \sigma_T^2 c^2} = 6 \times 10^{-25} (\frac{0.1}{\eta})^2 \ \mathrm{gcm}^{-3}. \tag{10}$$

Comparing this with the average density in the universe we obtain the density contrast in the cosmological context as

$$\frac{\rho_H}{\rho} = 3 \times 10^4 (\frac{0.1}{\eta})^2 (\frac{H_0}{100\mathrm{km/s}})^{-2} \Omega^{-2} (1+z)^{-3}. \tag{11}$$

This suggests that quasar host galaxies have attained a fairly large density contrast and have been formed at al least around the redshift of z=10-30. The age constraint may be alleviated for open universe but in this case the adopted luminosity and the resultant mass become larger and similar constraint is obtained. Furthermore, the density constrast argument becomes more severe.

Epilogue

As was briefly described in this article, astrophysics of black holes has opened many new aspects in various fields in astrophysics ranging from dense stellar systems, X-ray stars and quasars to cosmology. It provides us many challenging problems which are still developing and awaiting further studies by an increasing number of physicists.

References

1) J.R.Oppenheimer and H.Snyder, Phys.Rev., 56 (1939) 455.
2) E.E.Salpeter, Astrophys.J., 140 (1964) 796.
3) Ya.B.Zeldovich and I.D.Novikov, Dokl.Acad.Nauk.USSR, 158 (1964) 811.
4) M.J.Rees, Ann.Rev.Astron.Astrophys., 22 (1984) 471
5) J.G.Hills, Nature, 254 (1975) 295.
6) P.J.E.Peebles, Gen.Rel.Grav., 3 (1972) 63.

7) A.P.Lightman and S.L.Shapiro, Astrophys.J., 211 (1977) 244.
8) J.N.Bahcall and R.A.Wolf, Astrophys.J., 209 (1976) 214.
9) J.Frank and M.J.Rees, Mon.Not.R.Astron.Soc., 176 (1976) 633.
10) V.I.Dokuchaev, Sov.Phys.Uspekhi, 34 (1991) 447.
11) J.Kormendy, Astrophys.J., 335 (1988) 40.
12) A.Dressler and D.O.Richstone, Astrophys.J., 324 (1988) 701.
13) J. Kormendy, to appear in 'TESTING AGN Paradigm' (eds. S.S. Holt, S.Neff and C.M.Urry, New York, AIP) (1992).
14) R.Gensel and C.H.Townes, Ann.Rev.Astron.Astrophys. 25 (1987) 377.
15) H.Inoue, to appear in 'TEXAS/ESO-CERN SYMPO.', (1991).
16) F.Takahara, S.Tsuruta and S.Ichimaru, Astrophys.J., 251 (1981) 26.
17) J.N.Bregman, Astron.Astrophys.Rev., 2 (1990) 125.
18) Y.Kojima, Mon.Not.R.Astron.Soc., 250 (1991) 629.
19) L.Stella, Nature, 344 (1990) 747.
20) N.I.Shakura and R.A.Sunyaev, Astron.Astrophys., 24 (1973) 337.
21) I.D.Novikov and K.S.Thorne, in 'Black Holes' (eds. C.de Witt and B.S.de Witt, Gordon and Breach) (1973) 343.
22) S.Ichimaru, Astrophys.J., 214 (1977) 840.
23) S.L.Shapiro, A.P.Lightman and D.M.Eardley, Astrophys.J., 204 (1976) 187.
24) M.Abramowicz, M.Jaroszynski and M.Sikora, Astron.Astrophys., 63 (1978) 221.
25) B.Paczynski and P.J.Witta, Astron.Astrophys., 88 23.
26) S.M.Wash and N.Dadhich, Phys.Rep., 183 (1989) 137.
27) E.S.Phinney, PhD Thesis at University of Cambridge (1983).
28) E.L.Turner, Astron.J., 101 (1991) 5.

MAGNETOHYDRODYNAMICAL ACCRETION ONTO A BLACK HOLE

M. YOKOSAWA
Dept. of Physics, Ibaraki University, Mito 310, Japan

ABSTRACT. Extraction processes of black hole's spin energy by electromagnetic effects are briefly reviewed. The computational method of general relativistic magnetohydrodynamics(MHD), MHD structure around a black hole and the energy transfer by magnetic field are given. The evolution of magnetosphere of a black hole and the instability in the sphere are discussed.

1. Introduction

X-ray emission has been observed in many active galactic nuclei (AGN). Observations have showed the X-ray spectra of a substantial sample of Seyferts to be remarkably uniform, being well described by a simple power-law model (Pounds 1977; Elvis et al. 1978; Turner and Pounds 1989). If the bulk of the X-ray luminosity is synchrotron or inverse Compton radiation, it would require an AGN structure in which nonthermal emission is far superior to the thermal type. The magnetic field could play a principal role in the required AGN model since, for instance, the magnetic fields interacting with a black hole bring about electromagnetic power (Blandford and Znajek 1977; Macdonald and Thorne 1982), or a magnetic field interacting with infalling "cold clouds" (Guilbert and Rees 1988) would supply a large bulk of energetic particles in the same way as in solar flares (Osawa and Sakai 1987). Thus, in this paper we discuss the structures of the magnetic fields formed near a black hole and the energy extraction from a black hole by magnetohydrodynamical process.

The two types of processes were proposed regarding the extraction of rotational energy from a Kerr black hole by means of magnetic fields. One is an electromagnetical extraction (Blandford and Znajek 1977) and the other is a hydromagnetical-type extraction (Ruffini and Wilson 1975). The former type magnetic field is a force-free field generated by the surrounding matter outside the event horizon. The interaction of a magnetic field with the hole's rotation produces a "battery-like" behavior of the hole's horizon (Thorne et al. 1986). The latter extraction process is caused by the fact that two shells of different radii formed outside the event horizon are dragged due to the rotation of the black hole with a characteristic angular velocity. If connections between the two shells are made (ropes, springs or in the case of the magnetosphere magnetic lines of forces), rotational energy can be pumped out from the innermost shell to an external one, and the rotational energy can be extracted from a black hole (Ruffini 1977). Whereas electromagnetic extraction processes have been studied by many authors, the latter case has not. When the magnetic energy builds up to equipartition with the kinetic energy of infalling gas, the extraction energy could be comparable with the observed radiation energy from AGN. Therefore, we investigate the hydromagnetical extraction process.

The magnetic field lines near a rotating black hole are twisted by a frame-dragging effect and, thus, the rotational energy of the black hole is stored in the magnetosphere around the black hole(Ruffini 1977). The twisted magnetic field exerts a torque on an ambient plasma. The particles acted on by magnetic stress either increase or decrease their angular momentum. The increased kinetic energy of particles is changed in some cases to thermal energy, wave energy or radiation energy. The actual extraction process should be determined by many parameters, e.g. the strength of the magnetic field, angular momentum and density of infalling particles. We first consider the possible structures of the magnetic field formed around a black hole in a simple case in which initially a homogeneous field is changed by infalling gas with no angular momentum at infinity. We evaluate the extracted energy from the Kerr black hole.

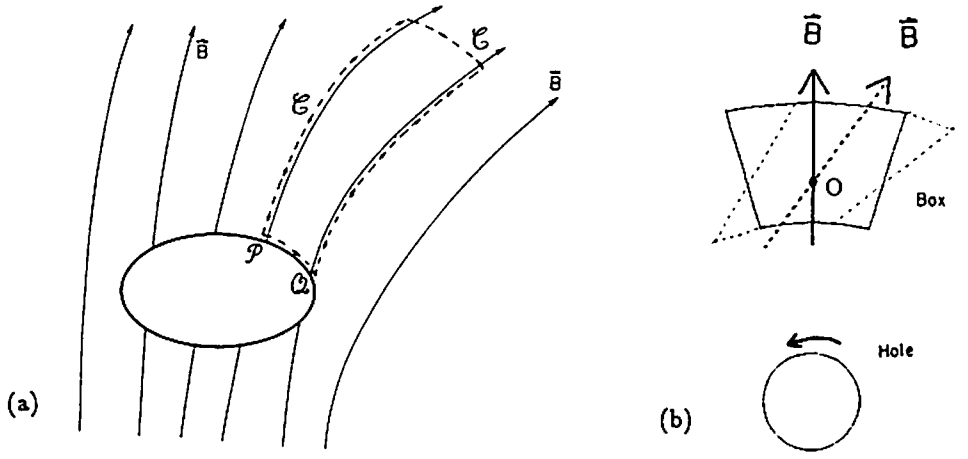

Figure 1 (a) A rotating black hole immersed in a magnetic field that is time-independent, $(\partial\vec{B}/\partial t)_x = 0$. The coupling of the hole's GM potential $\vec{\beta}$ to the magnetic field $\vec{B}$ produces an EMF around the closed curve L. This EMF can be regarded as due to a magnetic-gravitomagnetic "surface battery" in the stretched horizon (Thorne et al. 1986). (b) The deformation in time, as viewed in rigid coordinates attached to the LNRF at O, of a box whose walls are at rest in absolute space. The rotation of the box about the hole is not shown. The differential motion (shear) of absolute space deforms the box from its initial shape (solid line) into an elogated shape (dashed line). The hole's dragging of inertial frames rotates a magnetic force line at O from its initial position (solid arrow) to a new position (dashed arrow).

2. Extraction Processes of Rotating Energy from a Black Hole by Electromagnetic Effects

The physics of electromagnetics is clearly understood by the 3+1 formalism. The 3+1 formulation chooses a preferred family of 3-dimensional, spacelike hypersurfaces in spacetime (surfaces of "constant time") and treats them as though they were a single 3-dementional space that evolves as time passes ("decomposition of 4-dimensional spacetime into 3-dimensional space plus 1-dimensional time")(Thorne et al. 1986). The general relativistic physics of black holes, plasmas, and accretion disks takes place in this 3-dimentional space; and the relativistic laws of physics that govern them, written in 3-dimensional language, resemble the nonrelativistic laws. Several recent works on black hole electrodynamics (Thorne and MacDonald 1982 ; MacDonald and Thorne 1982 ; MacDonald 1984 ; MacDonald and Suen 1985) relativistic MHD (Phinney 1983 ; Sloan and Smarr 1985 ; Camenzind 1986a, 1986b, 1987 ; Evans and Hawley 1988 ; Petrich et al. 1989 ; Zhang 1989 ; Punsly and Coroniti 1989, 1990a, 1990b ; Punsly 1991 ; Takahashi et al. 1991 ; Yokosawa et al. 1991) were presented.

The 3 + 1 form of the Maxwell's equations becomes

$$\vec{\nabla}\cdot\vec{E} = 4\pi\rho_e, \tag{1}$$

$$\left(\frac{\partial}{\partial t} - L_{\vec{\beta}}\right)\vec{E} = -\vec{\nabla}\times(\alpha\vec{B}) - 4\pi\alpha\vec{j}, \tag{2}$$

$$\vec{\nabla}\cdot\vec{B} = 0, \tag{3}$$

$$\left(\frac{\partial}{\partial t} - L_{\vec{\beta}}\right)\vec{B} = -\vec{\nabla}\times(\alpha\vec{E}). \tag{4}$$

Here $L_{\vec{\beta}}$ denotes the "Lie derivative" along $\vec{\beta}$:

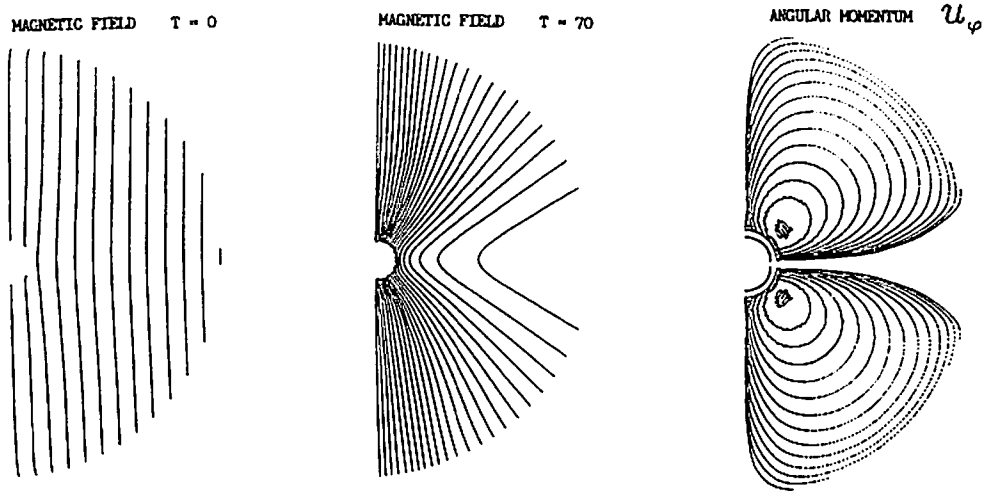

Figure 2 Time evolution of an initially homogeneous magnetic field in Kerr spacetime with $a = 0.999M$. The initial geometry of the magnetic field lines, which are uniform at infinity and modified by the presence of the Kerr black hole, is shown in the upper left-hand diagram in $r - \theta$ coordinates with $\varphi = constant$. The evolutionary time is displayed in units of M. The infalling matter forms a paraboloidal configuration with a growing scale. In the central region the "radial" flow rapidly increases the radial component of the field, so that the configuration turns out to be "radial". In the vicinity of the event horizon, however, the tangential component is yet to be predominent.

$$L_{\vec{\beta}}\vec{E} = (\vec{\beta}\cdot\vec{\nabla})\vec{E} - (\vec{E}\cdot\vec{\nabla})\vec{\beta}. \tag{5}$$

The "lapse function" and "shift vector" are represented by α and $\vec{\beta}$.

As our first model problem we consider a Kerr black hole immersed in a time-independent magnetic field [i.e., a field with $(\partial\vec{B}/\partial t)_{\chi^j}$, where χ^j are star-fixed coordinates]; see figure 1. We can gain insight into the interaction of the B field with the hole's rotation by applying Faraday's law of induction to a carefully chosen closed curve L(figure 1). The curve begins at some arbitrary point Q on the stretched horizon, extends out of the stretched horizon and up a magnetic field line to a point far from the hole, then crosses over to some other field line and descends down it to the stretched horizon at point P, then extends along the stretched horizon back to the starting point Q. Faraday's law is represented as follows :

$$\oint \alpha(\vec{E} + \vec{v}\times\vec{B})\cdot d\vec{l} = -\frac{d}{dt}\int \vec{B}\cdot d\vec{A} = 0, \tag{6}$$

where $\vec{v}$ is the velocity of the closed-curve boundary measured by the observer in the locally non-rotating frame (LNRF)(Bardeen 1972). Faraday's law says that

$$EMF = \oint \alpha\vec{E}\cdot d\vec{l} = \oint -\alpha\vec{v}\times\vec{B}\cdot d\vec{l} = \int_P^Q -\vec{\beta}\times\vec{B}\cdot d\vec{l}. \tag{7}$$

This EMF can be regarded as due to a magnetic-gravitomagnetic "surface battery" in the stretched horizon (Thorne et al. 1986). The EMF around a massive black hole is given :

$$EMF = \int_{equatorialplane}^{ploe} \vec{\beta}\times\vec{B}\cdot d\vec{l} \sim \frac{1}{2}\Big(\frac{a}{M}\Big)MB_n \sim 10^{19} volts\Big(\frac{M}{10^8 M_\odot}\Big)^2\Big(\frac{B_n}{10^4 G}\Big). \tag{8}$$

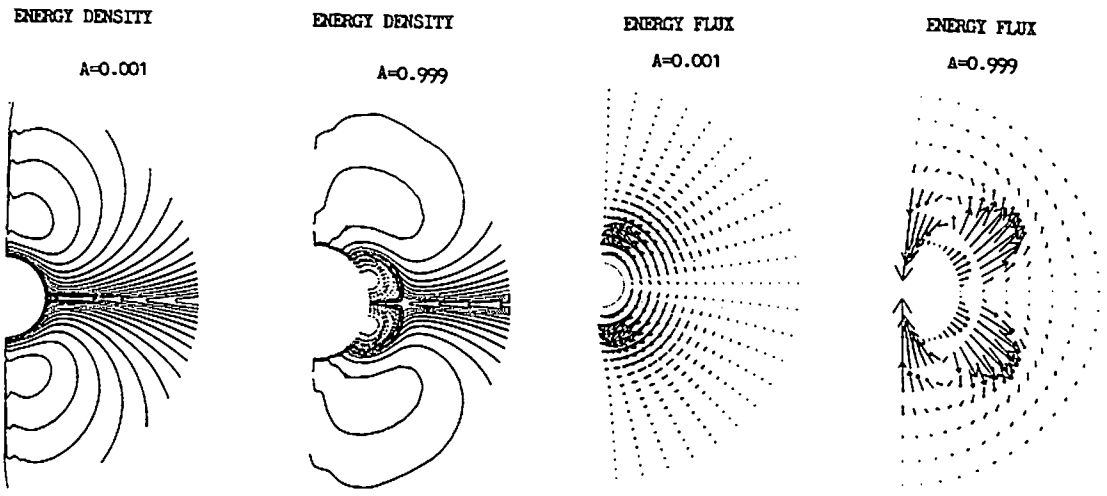

Figure 3 (a) Energy flux of electromagnetic field. (b) Energy density of electromagnetic field.The lower part shows the energy density at infinity $\epsilon_\infty(x)$. The positive region of the energy density is shown by solid lines and the negative region is by broken lines.

As our second model problem we consider a Kerr black hole immersed in a freezing nmagnetic field in surrounding gas. The freezind condition gives

$$\vec{E} = -\vec{v} \times \vec{B}, \tag{9}$$

where $\vec{v}$ is the flow velocity of the gas measured in LNRF. Faraday's law then becomes

$$\frac{\partial \vec{B}}{\partial t} = \vec{\nabla} \times [\alpha(\vec{v} - \vec{\beta}) \times \vec{B}]. \tag{10}$$

Even if there is no gas motion, $\vec{v} = 0$, the magnetic field is induced due to the differential rotation of the space-time, $\vec{\beta}(\chi^r)$, (see figure 2).

The extraction rate of the hole's spin energy in the above cases is obtained by summing the energy flux of the electromagnetic field over the horizon :

$$\begin{aligned} Power = \oint_H \alpha \vec{S}_\infty \cdot d\vec{S} &= \oint_H \left[\frac{1}{4\pi}(\vec{E} \times \vec{B}) - \frac{\Omega}{4\pi} r_L B_\varphi B_r \vec{n}\right] \cdot d\vec{S} \\ &\sim 10^{45} erg/sec \left(\frac{a}{M}\right)^2 \left(\frac{M}{10^8 M_\odot}\right)^2 \left(\frac{B_n}{10^4 G}\right). \end{aligned} \tag{11}$$

3. Numerical Calculation Methods of General Relativistic MHD

The magnetohydrodynamic calculations are performed in a fixed gravitational field; for accretion problems this field is represented by the Kerr metric in Boyyer-Lindquist coordinates. The line element is:

$$ds^2 = g_{tt}dt^2 + 2g_{t\phi}dtd\phi + g_{\phi\phi}d\phi^2 + g_{rr}dr^2 + g_{\theta\theta}d\theta^2. \tag{12}$$

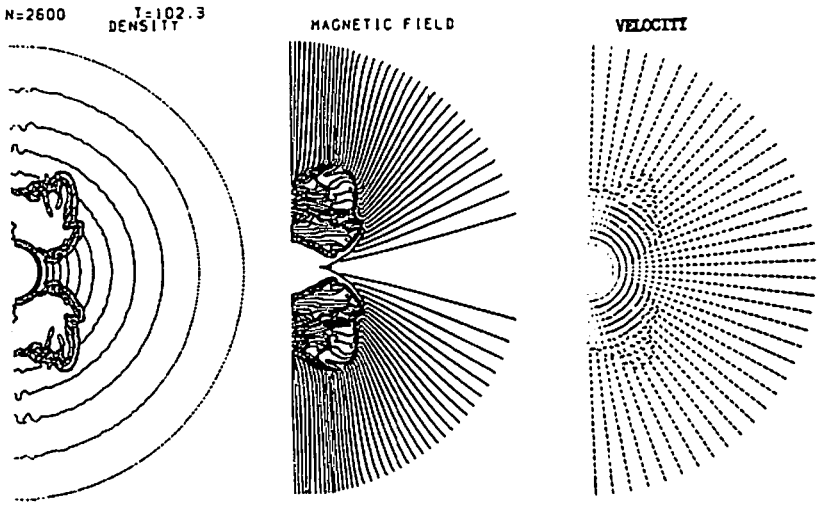

Figure 4 Dynamical evolution of accretion flows bounced by the magnetic stress. The first bounce occurs at the poles in the vicinity of the horizon . The meridian motion is remarkable in the bounced region , which is a characteristic common to all strong magnetic stress either in the case of rapidly rotating black hole or in slow rotating black hole. When the gas pressure is comparable with the magnetic stress at the bounced region, no remarkable meridian motion appears .

The motion of the fluid is governed by the equation of motion

$$T^{\alpha\beta}{}_{;\beta} = 0. \tag{13}$$

Here, the energy-momentum tensor is given by

$$T^{\alpha\beta} = (\rho + P + \frac{B^2}{4\pi})u^\alpha u^\beta + (P + \frac{B^2}{8\pi})g^{\alpha\beta} - \frac{B^\alpha B^\beta}{4\pi}, \tag{14}$$

where B^α is a magnetic field component represented in terms of the comoving magnetic field

$$B_\alpha = \frac{1}{2}\eta_{\alpha\beta\delta\psi}u^\beta F^{\delta\psi} \tag{15}$$

with $\eta_{\alpha\beta\delta\psi} = (-g)^{1/2}\epsilon_{\alpha\beta\delta\psi}$.

We calculate the magnetic field in LNRF and then transform its components into the Boyyer-Lindquist coordinate for a fluid calculation. The 3 + 1 decomposition of the line element is

$$ds^2 = -\alpha^2 dt^2 + \gamma_{ij}(dx^i + \beta^i dt)(dx^j + \beta^j dt), \tag{16}$$

in terms of the lapse function α, shift vector β^i and spatial three- metric γ_{ij}. The magnetic induction equation is represented by

$$\partial_t \tilde{B}^i = \partial_j[(\alpha v^i - \beta^i)\tilde{B}^j - (\alpha v^j - \beta^j)\tilde{B}^i], \tag{17}$$

where, $\tilde{B}^i = \gamma^{1/2}B^{\hat{i}}$, and $B^{\hat{i}}$ is the magnetic field component observed in LNRF.

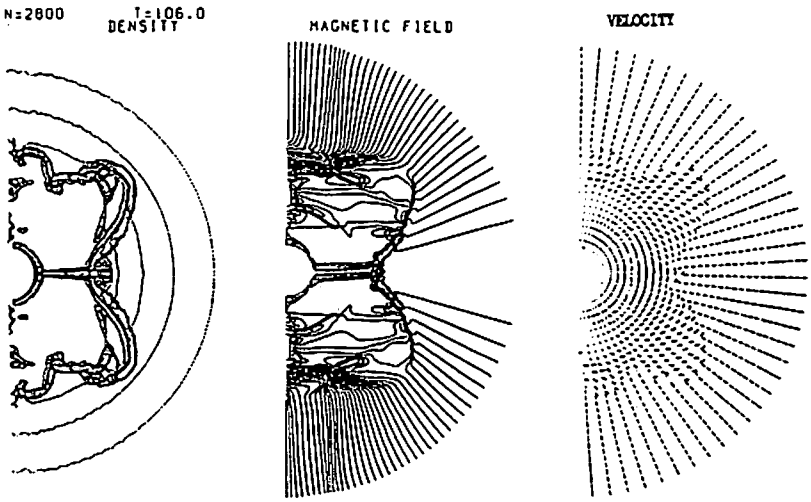

Figure 4(to be continued)

4. Magnetohydrodynamical Accretion

Wr set the initial conditions such that the magnetic field and the gas are homogeneous, and the gas observed in LNRF is rest. Two types of boundary condetions are adopted at the outer boundary. One is the free fall condition in which the gas density and the magnetic field strength are given by the analytic solutions of the free fall (Yokosawa, Ishizuka and Yabuki 1991). Other is the quasi-stationary condition in which the gas density is constant and the magnetic field strength slowly increases. The latter case is calculated in order to evaluate the energy and angular momentum transport rate of a black hole to the ambient matter in a stationary state. The initial gas temperature is selected either to be cool or to be hot. In the hot case, the gas pressure behind the shock front is comparable with the magnetic pressure. The calculating space is $r = 1.07r_h \sim 10r_h$ and $\theta = 0 \sim \pi/2$, where r_h is the horizon radius. The mesh size is 125 in the r-direction and 100 in the θ-direction. Computations were performed on the workstation, MIPS RS3230.

5. Dynamical Evolution of Magnetosphere around a Black Hole

(a) We discuss the dynamical evolution of the energy density distribution of the field and also discuss the energy transfer through the surface of a stretched horizon. The radially infalling gas enhancese both the radial componet of the magnetic field $\tilde{B}_r$ and the meridian one $\tilde{B}_\theta$. The hole's rotation strengthens the toroidal component $\tilde{B}_\phi$. Therefore the gravitational binding energy and the hole's rotation energy are stored in the magnetosphere formed around the black hole. The stored energy in a region should be evaluated by " the energy-at-infinity" E_∞. Initially the energy density $\epsilon_\infty(x)$ is negative over the most of the area around the horizon. After the delayed time , $t > t_d$, the positive peak in $\epsilon_\infty(x)$ is formed at the stretched horizon and then the electromagnetic energy density at any position in the magnetosphere increases with time (figure 3). The large amount of the electromagnetic energy caused by the hole's rotation is stored in the region whose distance from the center of the black hole is several times as long as the horizon radius. We investigate the transfer of the electomagnetic energy through the surface of the stretched horizon. When $(\tilde{B}_\phi \tilde{B}_r)_{at\ r_{st}} < 0$,

this part acts as the extraction of the energy from the black hole, that is , the rotational energy of the hole is tranferred to the outer space by means of the magnetic field.
(b) Next we discuss the Dynamics of accretion flows bounced by the magnetic stress. The first bounce occurs at the poles in the vicinity of the horizon (figure 4). The meridian motion is remarkable in the bounced region , which is a characteristic common to all strong magnetic stress either in the case of rapidly rotating black hole or in slow rotating black hole. When the gas pressure is comparable with the magnetic stress at the bounced region, no remarkable meridian motion appears .

(c) The maximum energy density of the magnetic field obtained in quaisi-stationary accretion flows is $B^2_{MAX} \approx 10^{-3}\rho c^2$. The more strong magnetic field produces the shock structure in the flow. The rotational velosity of the fluid reaches to $v_{\phi,MAX} \approx 0.1c$. The stored energy in the magnetospher around a black hole is about 0.1 percent of the rest mass energy of the accreting matter.

References

Bardeen, J. M., Press, W. H., and Teukolsky, S. A. 1972, *Astrophys. J.*, **178**, 347.
Blandford, R. D., and Znajek, R. L. 1977, *Monthly Notices Roy. Soc.*, **179**, 433.
Camenzind, M. 1986a, *Astron. Astrophys.*, **156**, 137.
Camenzind, M. 1986b, *Astron. Astrophys.*, **162**, 32.
Camenzind, M. 1987, *Astron. Astrophys.*, **184**, 341.
Elvis, M., Maccacaro, T., Wilson, A. S., Ward, M. J., Penston, M. V., Fosbury, R. A. E., and Perola, G. C. 1978, *Monthly Notices Roy. Astron. Soc.*, **183**, 129.
Evans, C. R. and Hawley, J. F. 1988, *Astrophys. J.*, **332**, 659.
Guilbert, P. W., and Rees, M. J. 1988, *Monthly Notices Roy. Soc.*, **233**, 475.
Macdonald, D. A. 1984, *Monthly Notices Roy. Soc.*, **211**, 313.
Macdonald, D. A., and Suen W. -M. 1985, *Phys. Rev. D* , **32**, 848.
Macdonald, D., and Thorne, K. S. 1982, *Monthly Notices Roy. Soc.*, **198**, 345.
Ohsawa, Y., and Sakai, J. 1987, *Astrophys. J.*, **313**, 440.
Punsly, B., and Coroniti, F. V. 1989, *Physical Rev. D*, 40, 3834.
Punsly, B., and Coroniti, F. V. 1990a, *Astrophysical J.*, **350**, 518.
Punsly, B., and Coroniti, F. V. 1990b, *Astrophysical J.*, **354**, 583.
Punsly, B. 1991, *Astrophysical J.*, **372**, 424.
Petrich, L. I., Shapiro, S. L., Stark, R. F., and Teukolsky, S. A. 1989, *Astrophys. J.*, **336**, 313. Pounds, K. A. 1977, *Ann. New York Acad. Sci.*, **302**,361.
Phinney, E. S. 1983, Ph.D. diss., Univ. of Cambridge.
Ruffini, R. 1977, in *Proceedings of the First Marcel Grossmann Meeting on General Relativity*, ed. R. Ruffini (North-Holland Publishing Company, Amsterdam), p349.
Ruffini, R., and Wilson, J. R. 1975, *Phys. Rev. D*, **12**, 2959.
Sloan, J., and Smarr, L. L. 1985, in *Numerical Astrophysics*, ed. J. Centrella, J. LeBlance, and R. Bowers (Boston : Jones and Bartlett).
Takahashi, M., Nitta, S., Tatematsu, Y., and Tomimatsu, A. 1990 *Astrophysical J.*, **363**, 206.
Thorne, K. S., Price, R. H., Macdonald, D. A.,Suen, W. M., and Zhang, X. H. 1986, in *Black Holes: The Membrane Paradigm*, ed. Thorne, K. S., and Price, R. H., Macdonald, D. A (Yale University Press, New Haven and London), p.67.
Turner, T. J., and Pounds, K. A. 1989, *Monthly Notices Roy. Soc.*, **240**, 833.
Yokosawa, M, Ishizuka, T., and Yabuki, Y. 1991, *Publ. Astron. Soc. Japan*, **43**, 427.
Wilson, J. R. 1977, in *Proceedings of the First Marcel Grossmann Meeting on General Relativity*, ed. R. Ruffini (North-Holland Publishing Company, Amsterdam) , p393 .
Zhang, Xiao-He 1989, *Physical Rev. D*, **39**, 2933.

Linear Perturbation Theory of Relativistic Magnetohydrodynamics

Toshio Uchida

Astronomical Institute, Faculty of Science, Tohoku University, Sendai 980, Japan

Abstract

We formulate a Lagrangian linear perturbation theory of relativistic magnetohydrodynamics. The Lagrangian displacement is introduced as a basic variable and small changes in all the physical quantities are expressed up to second order by this vector field. The basic equation becomes three components second-order partial differential equation whose independent variables are components of the Lagrangian displacement normal to u^μ. The action principle and the geometric optical approximation are also formulated.

1. Introduction

Recently, relativistic magnetospheres around black holes or accretion disks draw much attention as energy sources of the active galactic nuclei or quasars. Most of previous works were concerning with the stationary and axisymmetric configuration, and now more general consideration will be necessary for deeper understanding. For this purpose, we study a linear perturbation theory which enables to treat arbitrary small perturbation around any solution of relativistic ideal magnetohydrodynamics. Since changes in gravitation are small, we completely neglect changes in the metric in the following.

2. Unperturbed configuration

It is assumed that the unperturbed configuration is obeying the following set of equations:

$$\nabla_\mu(nu^\mu) = 0, \tag{1}$$

$$u^\mu\nabla_\mu s = 0, \tag{2}$$

$$\nabla_\lambda F_{\mu\nu} + \nabla_\mu F_{\nu\lambda} + \nabla_\nu F_{\lambda\mu} = 0, \tag{3}$$

$$\nabla_\nu F^{\mu\nu} = 4\pi J^\mu, \tag{4}$$

$$F_{\mu\nu} u^\nu = 0, \tag{5}$$

$$\nabla_\nu T^{\mu\nu} = 0, \tag{6}$$

$$\rho = \rho(n, s), \tag{7}$$

where n is the particle number density, s is the specific entropy, $F_{\mu\nu}$ is the electromagnetic field, and ρ is the energy density. The energy momentum tensor $T^{\mu\nu}$ is given by

$$T^{\mu\nu} = (\rho + p)u^\mu u^\nu + pg^{\mu\nu} + \frac{1}{4\pi}(F^{\mu\lambda}F^\nu_\lambda - g^{\mu\nu}F^{\lambda\tau}F_{\lambda\tau}), \tag{8}$$

where p is the pressure of the fluid. By introducing the projection tensor on the hypersurface normal to u^μ by

$$\gamma^{\mu\nu} = u^\mu u^\nu + g^{\mu\nu},$$

equation (6) is reduced to

$$u^\mu \nabla_\mu \rho + (\rho + p)\nabla_\mu u^\mu = 0, \tag{9}$$

$$(\rho + p)u^\nu \nabla_\nu u^\mu + \gamma^{\mu\nu}\nabla_\nu p = F^{\mu\nu}J_\nu, \tag{10}$$

where equation (9) is the energy conservation law and equation (10) is Euler equation, of course. Then our aim in this paper is to develop a linear perturbation theory which is applicable to the small perturbation around any solution of these equations.

3. Lagrangian displacement

When treating small perturbations, two schemes are known, i.e. Eulerian perturbation theory and Lagrangian perturbation theory. Here, we adopt the latter approach. Thus we must first introduce the Lagrangian displacement as a auxiliary variables. To do this, we assume that the perturbed configuration relates to the unperturbed configuration by a

one-parameter family of maps $\psi^\mu(\lambda, x)$, having following properties;

$$\psi^\mu(x, 0) = x^\mu, \tag{11}$$

and if

$$\overline{x}^\mu = \psi^\mu(x, \lambda_1),$$

then

$$\psi^\mu(\overline{x}, \lambda_2) = \psi^\mu(x, \lambda_1 + \lambda_2). \tag{12}$$

Here different value of λ corresponds to a different perturbed configuration. The Lagrangian displacement ζ^μ is defined by

$$\frac{\mathrm{d}\psi^\mu(x, \lambda)}{\mathrm{d}\lambda} = \zeta^\mu(\overline{x}). \tag{13}$$

By integrating this equation iteratively, ψ^μ is written explicitly as

$$\psi^\mu(x, \lambda) = x^\mu + \lambda\zeta^\mu(x) + \frac{1}{2}\lambda^2(\zeta^\nu\partial_\nu\zeta^\mu)(x) + O(\lambda^3). \tag{14}$$

(Hereafter we omit λ and make order-counting by ζ^μ itself.)

Perturbations can be represented by two ways. The Eulerian changes in quantity f is defined by

$$\delta f = \overline{f}(x) - f(x), \tag{15}$$

where $\overline{f}$ is a quantity in the perturbed configuration. The Lagrangian change is defined by

$$\Delta f = \psi^*\overline{f}(\overline{x}) - f(x), \tag{16}$$

where ψ^* is a pull back of ψ. Then the Eulerian and Lagrangian change relate as

$$\begin{aligned}\Delta^{(1)}f &= \delta^{(1)}f + \pounds_\zeta f,\\ \Delta^{(2)}f &= \delta^{(2)}f + \pounds_\zeta\delta^{(1)}f + \frac{1}{2}\pounds_\zeta\pounds_\zeta f,\end{aligned} \tag{17}$$

where $\pounds_\zeta$ is the Lie derivative with respect to ζ^μ.

4. Expressions of perturbed quantities

Next we are going to express changes in physical quantities by ζ^μ. First, let us consider the velocity field. Let $x^\mu = z^\mu(\tau)$ be the trajectory of the fluid element parametrized by the proper time τ. Then perturbed trajectory is given by $\overline{x}^\mu = \overline{z}^\mu(\tau) = \psi^\mu(z, \lambda)$, and its tangent vector is given by

$$\frac{\mathrm{d}\overline{z}}{\mathrm{d}\tau}(x) = u^\mu - \pounds_\zeta u^\mu + \frac{1}{2}\pounds_\zeta \pounds_\zeta u^\mu.$$

However τ is no longer the proper time along the perturbed trajectory, because length along curves is not preserved by map ψ. Then above expression implies that the proper time τ' along the perturbed trajectory is relating to τ as

$$\frac{\mathrm{d}\tau'}{\mathrm{d}\tau} = 1 + 2u_\mu \pounds_\zeta u^\mu - (g_{\mu\nu}\pounds_\zeta u^\mu \pounds_\zeta u^\nu + u_\mu \pounds_\zeta \pounds_\zeta u^\mu).$$

Since

$$\overline{u}^\mu = \frac{\mathrm{d}\overline{z}^\mu}{\mathrm{d}\tau}\frac{\mathrm{d}\tau}{\mathrm{d}\tau'},$$

we have

$$\begin{aligned}
\delta^{(1)}u^\mu &= \frac{1}{2}u^\mu u^\lambda u^\tau \pounds_\zeta g_{\lambda\tau} - \pounds_\zeta u^\mu, \\
\delta^{(2)}u^\mu &= \frac{1}{2}(\gamma^{\mu\nu}\delta^{(1)}u^\lambda \nabla_\lambda \zeta_\nu - \zeta^\lambda \nabla_\lambda \delta^{(1)}u^\mu) \\
&\quad + \frac{1}{2}(\delta^{(1)}u^\mu u^\nu + u^\mu \delta^{(1)}u^\nu)u^\lambda \nabla_\lambda \zeta_\nu
\end{aligned} \tag{18}$$

To construct changes in the particle number density, the entropy, and the electromagnetic field, we put following requirements:

$$\begin{aligned}
&\Delta s = 0, \\
&\Delta(n\varepsilon_{\mu\nu\lambda\tau}u^\tau) = 0, \\
&\Delta F_{\mu\nu} = 0,
\end{aligned} \tag{19}$$

where $\varepsilon_{\mu\nu\lambda\tau}$ is Levi-Civita tensor. These condition implies that we consider only perturbations which can be attained by changes which conserve the specific entropy and the particle number

density and preserve the flux-freezing condition from the unperturbed configuration. Then these conditions yield

$$\delta^{(1)}s = -\zeta^\lambda \nabla_\lambda s, \tag{20}$$

$$\delta^{(2)}s = \frac{1}{2}\zeta^\lambda \nabla_\lambda (\zeta^\tau \nabla_\tau s), \tag{21}$$

$$\delta^{(1)}n = -\nabla_\mu (n\zeta^\mu) - nu^\lambda u^\tau \nabla_\lambda \zeta_\tau, \tag{22}$$

$$\delta^{(2)}n = -\frac{1}{2}\nabla_\mu (\delta^{(1)} n\zeta^\mu) - \frac{1}{2}\delta^{(1)} nu^\lambda u^\tau \nabla_\lambda \zeta_\tau - \frac{1}{2}(\delta^{(1)}u^\mu u^\nu + u^\mu \delta^{(1)}u^\nu)\nabla_\lambda \zeta_\tau, \tag{23}$$

$$\delta^{(1)}F_{\mu\nu} = \nabla_\mu (F_{\nu\lambda}\zeta^\lambda) - \nabla_\nu (F_{\mu\lambda}\zeta^\lambda), \tag{24}$$

$$\delta^{(2)}F_{\mu\nu} = \frac{1}{2}\{\nabla_\mu (\delta^{(1)}F_{\nu\lambda}\zeta^\lambda) - \nabla_\nu (\delta^{(1)}F_{\mu\lambda}\zeta^\lambda)\}. \tag{25}$$

The change in the energy density is determined by the first law of the thermodynamics, $\mathrm{d}\rho = T\mathrm{d}S - p\mathrm{d}(1/n)$. The results are

$$\delta^{(1)}\rho = -\nabla_\mu (\rho\zeta^\mu) - (\rho u^\mu u^\nu + p\gamma^{\mu\nu})\nabla_\mu \zeta_\nu, \tag{26}$$

$$\delta^{(2)}\rho = \mu\delta^{(1)}n + \frac{1}{2}\frac{c_s^2 \mu}{n}\delta^{(1)}n\,\delta^{(1)}n, \tag{27}$$

where μ is the specific enthalpy, i.e. $\mu = (\rho + p)/n$, and c_s is the speed of sounds.

The essential point here is that these expressions already satisfy the perturbed version of the energy conservation (9), the entropy conservation (2), the particle number conservation (1), the degenerate condition (5), and the one of Maxwell's equation up to second-order in ζ^μ. Thus only the perturbed Euler equation is equation we must solve. That is,

$$\begin{aligned}(\rho + p)u^\lambda \nabla_\lambda \delta^{(1)}u^\mu &+ (\nabla_\nu p)(u^\nu \delta^{(1)}u^\mu + u^\mu \delta^{(1)}u^\nu) \\ &+ (\rho + p)(\nabla_\lambda u^\mu)\delta^{(1)}u^\lambda + \gamma^{\mu\nu}\nabla_\nu \delta^{(1)}p + (\delta^{(1)}\rho + \delta^{(1)}p)u^\nu \nabla_\nu u^\mu \\ &= F^{\mu\nu}\delta^{(1)}J_\nu + \delta^{(1)}F^{\mu\nu}J_\nu,\end{aligned} \tag{28}$$

where we regard that all the first-order quantities are already expressed by the Lagrangian displacement ζ^μ.

5. Action principle

The equation of motion for unperturbed configuration can be derived by extremizing the action I_0,

$$I_0 = \int \rho\sqrt{-g}\mathrm{d}^4x - \frac{1}{16\pi}\int F^{\mu\nu}F_{\mu\nu}\sqrt{-g}\mathrm{d}^4x, \tag{29}$$

under the constrained variation of the form in equations (24) and (26).

Thus the action which yield our equation of motion (28) will be derived by expanding (29) using equations (20) $\sim$ (27). After tedious calculation and disregarding the total four-divergence term, we have

$$I_2 = \int L_2\mathrm{d}^4x, \tag{30}$$

where

$$\begin{aligned}\frac{1}{\sqrt{-g}}L_2 &= \frac{1}{2}n\mu\gamma^{\lambda\tau}(u^\mu\nabla_\mu\zeta_\lambda - \zeta^\mu\nabla_\lambda u_\mu)(u^\nu\nabla_\nu\zeta^\tau - \zeta^\nu\nabla_\nu u^\tau)\\ &+\frac{1}{2}\mu\{\nabla_\lambda(n\zeta^\lambda) - n(u^\tau\nabla_\tau u_\lambda)\zeta^\lambda\}\{-c_s^2\nabla_\mu\zeta^\mu + (1+c_s^2)\zeta^\nu u^\lambda\nabla_\lambda u_\nu\}\\ &-\frac{1}{16\pi}\{\nabla_\mu(F_{\nu\lambda}\zeta^\lambda) - \nabla_\nu(F_{\mu\lambda}\zeta^\lambda)\}\{\nabla^\mu(F^\nu_{\ \lambda}\zeta^\lambda) - \nabla^\mu(F^\nu_{\ \lambda}\zeta^\lambda)\}\\ &-\frac{1}{8\pi}(\nabla_\tau F^{\mu\tau})\zeta^\lambda\{\nabla_\mu(F_{\nu\lambda}\zeta^\lambda) - \nabla_\nu(F_{\mu\lambda}\zeta^\lambda)\}.\end{aligned} \tag{31}$$

It should be noted that this Lagrangian permits a sort of gauge transformation.

5. Geometric optical approximation

Unfortunately, the basic equation (28) is complex and explicit knowledge of the unperturbed configuration is necessary to investigate in detail. However, it is possible to develop a systematic approximation when the wave length of perturbations are much less than the typical length in which physical quantities in unperturbed configuration change, i.e., in the geometric optical regime.

The formulation of the geometric optical approximation is achieved as follows:
First, we expand the lagrangian displacement as

$$\zeta^\mu = (a^\mu + \epsilon b^\mu + \cdots)\exp(i\theta/\epsilon), \tag{32}$$

where ϵ is a dimensionless small quantity. By substituting this into equation (28), the leading order $O(\epsilon^{-2})$ term is

$$(\rho+p)\{u^\mu u^\nu \nabla_\mu\theta\nabla_\nu\theta\gamma_{\lambda\tau} - c_s^2\gamma_\lambda^\mu\nabla_\mu\theta\gamma_\tau^\nu\nabla_\nu\theta\}a^\tau$$
$$+\frac{1}{4\pi}\{F_\lambda{}^\mu F_\tau{}^\nu\nabla_\mu\theta\,\nabla_\lambda\theta - F_{\mu\lambda}F^\mu_\tau g^{\nu\rho}\nabla_\nu\theta\nabla_\rho\theta\}a^\tau = 0. \tag{33}$$

The next order term is complex, but its inner product with a^μ reads

$$\nabla_\mu\{[(\rho+p)(u^\mu u^\nu\gamma^\rho_\tau\gamma_{\rho\nu} - c_s^2\gamma^\lambda_\tau\gamma^\mu_\nu)$$
$$+\frac{1}{4\pi}(F^\mu_\tau F^\nu_\lambda - F^\rho_\tau F_{\rho\nu}g^{\mu\lambda})]\nabla_\lambda\theta a^\nu a^\tau\} = 0. \tag{34}$$

These two are the basic equation in the geometric optical approximation.

After some manipulations, the first equation yields the dispersion relation,

$$(\rho+p)(1-c_s^2)(u^\mu k_\mu)^4 - (\rho+p)(c_s^2+v_A^2)k^2(u^\mu k_\mu)^2$$
$$+\frac{1}{4\pi}c_s^2k^2(B^\mu k_\mu)^2 = 0, \tag{35}$$
$$\{\rho+p+\frac{B^2}{4\pi}\}(u^\mu k_\mu)^2 - \frac{1}{4\pi}(B^\mu k_\mu)^2 = 0, \tag{36}$$

where $k_\mu = \nabla_\mu\theta$, v_A is Alfven velocity and B^μ is the magnetic field defined by $B^\mu = *F^{\mu\nu}u_\nu$. Equation (35) is the dispersion relation of the fast and slow mode, and equation (36) is the dispersion relation of the Alfven mode. In general, the former equation cannot be divided into the product of the quadratic form of k_μ, but in the cold limit, i.e. $p\to 0, c_s^2\to 0, \rho\to nm$, the slow mode vanishes and the dispersion relation of the fast mode becomes

$$\{(nm+\frac{B^2}{4\pi})u^\mu u^\nu - \frac{B^2}{4\pi}\gamma^{\mu\nu}\}k_\mu k_\nu = 0. \tag{37}$$

Substituting this relation into equation (35) again, we see that a^μ must be written as

$$a^\mu = \frac{\mathcal{A}}{(\overline{H}^{\mu\nu}k_\mu k\nu)^{1/2}}\overline{H}^{\mu\nu}k_\nu, \tag{38}$$

where $\mathcal{A}$ is the amplitude of the perturbation, $(\overline{H}^{\mu\nu}k_\mu k_\nu)^{1/2}$ is the normalization factor, and $\overline{H}^{\mu\nu}$ is defined by

$$\overline{H}^{\mu\nu} = \gamma^{\mu\nu} - B^\mu B^\nu/B^2.$$

Substituting equation (38) into equation (34), we have equation for $\mathcal{A}$

$$\nabla_\mu\{\mathcal{A}^2[(nm+p)u^\mu u^\nu - \frac{B^2}{4\pi}g^{\mu\nu}]k_\nu\} = 0. \tag{39}$$

Equations (37) and (39), together with $\nabla_\mu k_\nu = \nabla_\nu k_\mu$, determine behaviour of the fast mode completely.

By the same way, equation (36) yields equations for the Alfven mode as

$$a^\mu = \frac{\mathcal{A}}{(\overline{H}^{\mu\nu}k_\mu k_\nu)^{1/2}}\varepsilon^{\mu\nu}k_\nu, \tag{40}$$

$$\nabla_\mu\{\mathcal{A}^2[(\rho+p+\frac{B^2}{4\pi})u^\mu u^\nu - \frac{B^\mu B^\nu}{4\pi}]k_\nu\} = 0. \tag{41}$$

Then equations (40) and (41) determine θ and $\mathcal{A}$ for the Alfven mode. It should be noted that $(\rho + B^2/4\pi)u^\mu u^\nu - B^\mu B^\nu/B^2$ is rank two as a matrix, and well-known characteristic behaviour of the Alfven wave results from this fact.

6. Conclusion

The formulation which enables us to treat small disturbances of the relativistic ideal magnetohydrodynamics is presented. More complete exposition of this theory and applications to the black hole magnetospheres will appeare elsewhere.

TIME VARIATION OF MHD ACCRETION ONTO A ROTATING BLACK HOLE

Kouichi HIROTANI, Masaaki TAKAHASHI, AND Akira TOMIMATSU

Department of Physics, Nagoya University
Chikusa-ku, Nagoya 464-01, Japan

ABSTRACT

We examine non-stationary and non-axisymmetric perturbations on a Kerr black hole magnetosphere which will exist in an active galactic nucleus (AGN). In the high wave number limit, relations between perturbed quantities are derived and especially the influence of a small perturbation in the magnetic field on fluid quantities are analyzed in detail. The most important aspect of this study is to make a convincing argument that the time-dependent nature of the magnetohydrodynamic (MHD) accretion flows onto a black hole appears prominently near the fast-magnetosonic point in the magnetically dominated limit. Some implications of the present results are briefly discussed with respect to observed short-term variations in luminosity of AGNs.

subject headings: accretion – black hole physics – galaxies: active

1 INTRODUCTION

Short-term variations in luminosity have been reported in various classes of AGNs, which are thought to contain accretion disks and magnetospheres around central black holes (e.g., Rees 1984). Such variations may be caused by some kind of instabilities in accretion disks or by the time-dependent nature of accretion in the magnetosphere. The former problems have been explored by many authors (e.g., Papaloizou & Pringle 1984, Abramowicz & Kato 1989). Nevertheless, the latter problems have hardly been studied in spite of the fact that the energy output from the magnetosphere can become comparable with that from the accretion disk.

In this paper we study the possibility that the observed short-term variations in luminosity can be attributed (at least to some degree) to the time variation of the accretion in the black hole magnetosphere which comprises ingoing and outgoing flows. Both flows start from a region where plasma particles are injected with very low poloidal velocity;

this injection region may be the disk surface. We expect that plenty of plasma can be supplied from the disk into the magnetophere, and as a consequence we may treat the flows by MHD approximation. Then the causality requires that the inflows must pass through the fast magnetosonic point where the poloidal flow velocity is equal to the wave velocity of fast-magnetosonic mode (Phinney 1983).

Basic equations for general relativistic MHD flows are presented in the next section. In Section 3 we display critical conditions for stationary and axisymmetric flows and describe the equilibrium configurations. Then we consider the non-stationary and non-axisymmetric perturbations superposed on the equilibrium state in Section 4. In Section 5 we will show that the time-dependent nature of the MHD accretion onto a rotating black hole appears prominently at the fast-magnetosonic point in the magnetically dominated limit that the rest mass density of particles is negligible compared with the magnetic energy density. The final section is devoted to discussion.

2 BASIC EQUATIONS

The self-gravity of electromagnetic field and plasma around the black hole is very weak, hence the background geometry of the magnetosphere is described by the Kerr metric

$$ds^2 = \frac{\Delta - a^2 \sin^2\theta}{\Sigma} dt^2 + \frac{4Mar\sin^2\theta}{\Sigma} dt d\phi - \frac{A\sin^2\theta}{\Sigma} d\phi^2 - \frac{\Sigma}{\Delta} dr^2 - \Sigma d\theta^2, \qquad (1)$$

where $\Delta \equiv r^2 - 2Mr + a^2$, $\Sigma \equiv r^2 + a^2\cos^2\theta$, $A \equiv (r^2+a^2)^2 - \Delta a^2 \sin^2\theta$ and $a \equiv J/M$. Throughout this paper we use geometrized units such that $c = G = 1$.

Under ideal MHD conditions the electric field vanishes in the fluid rest frame, thus we have $F_{\mu\nu}u^\mu = 0$, where $F_{\mu\nu}$ is the electromagnetic field tensor satisfying the Maxwell equations and u^μ is the fluid four velocity. The motion of the fluid is governed by the equations of motion

$$T^{\mu\nu}{}_{;\nu} = 0, \qquad (2)$$

where the energy-momentum tensor $T^{\mu\nu}$ decomposes into a material part

$$T^{\mu\nu}_{(M)} = m_p n u^\mu u^\nu \qquad (3)$$

in the cold limit and an electromagnetic part

$$T^{\mu\nu}_{(em)} = \frac{1}{4\pi}\left(F^{\mu\rho}F_\rho{}^\nu + \frac{1}{4} g^{\mu\nu} F_{\alpha\beta}F^{\alpha\beta}\right). \qquad (4)$$

Here, the semicolon denotes a covariant derivative and m_p the rest-mass of a proton. The proper number density n obeys the continuity equation $(nu^\mu)_{;\mu} = 0$.

3 CRITICAL CONDITIONS FOR STATIONARY FLOWS

As an unperturbed state, we consider stationary and axisymmetric accretion flows in a Kerr black hole magnetosphere. From the analysis of stationary and axisymmetric ideal MHD equations above, it is known that there exist four integration constants conserved along each flow line (e.g. Bekenstein & Oron 1977; Camenzind 1986a,b). These conserved quantities are the angular velocity of a magnetic field line (Ω_F), particle flux per unit magnetic flux tube (η), total energy (E) and total angular momentum (L). They are defined as follows:

$$\Omega_F = \frac{F_{tr}}{F_{r\phi}} = \frac{F_{t\theta}}{F_{\theta\phi}}, \tag{5}$$

$$\eta = -\frac{\sqrt{-g}nu^r}{F_{\theta\phi}} = -\frac{\sqrt{-g}nu^\theta}{F_{\phi r}} = -\frac{\sqrt{-g}nu^t(\Omega - \Omega_F)}{F_{r\theta}}, \tag{6}$$

$$E = m_p u_t - \frac{\Omega_F}{4\pi\eta} B_\phi, \tag{7}$$

$$L = -m_p u_\phi - \frac{1}{4\pi\eta} B_\phi, \tag{8}$$

where $\Omega \equiv u^\phi/u^t$ is the angular velocity of the fluid, and the magnetic field B^μ is covariantly defined by

$$B^\mu = \frac{1}{2\sqrt{-g}} \epsilon^{\mu\nu\rho\sigma} F_{\rho\sigma} \xi_\nu, \tag{9}$$

where $\xi^\mu = (1,0,0,0)$ is the time-like Killing vector. The poloidal flow lines are identical with the poloidal field lines and are given by $\Psi(r,\theta) =$ constant, where Ψ is the ϕ-component of the electromagnetic vector potential. The conserved quantities are functions of Ψ only. We assume that Ψ is arbitrarily given in unperturbed state.

Since we are interested in an active state of the black hole, we impose the condition $E < 0$ which means that the energy extraction due to the Blandford-Znajek process can work (Blandford & Znajek 1977).

Fluids must pass through the so-called critical points before they fall into the horizon. In order to derive this critical condition, we first write down the poloidal wind equation (Camenzind 1986b),

$$u_p^2 + 1 = \left(\frac{E}{\mu}\right)^2 \frac{k_0 k_2 - 2k_2 \mathcal{M}_A{}^2 - k_4 \mathcal{M}_A{}^4}{(k_0 - \mathcal{M}_A{}^2)^2}, \tag{10}$$

where the poloidal velocity u_p and the Alfvénic Mach number $\mathcal{M}_A{}^2$ are defined as

$$u_p^2 \equiv -\left[g_{rr}(u^r)^2 + g_{\theta\theta}(u^\theta)^2\right], \tag{11}$$

$$\mathcal{M}_A{}^2 \equiv \frac{4\pi\mu\eta^2}{n}, \tag{12}$$

and k_0, k_2, k_4 are abbreviations of the following quantities,

$$k_0 \equiv g_{\phi\phi}\Omega_F^2 + 2g_{t\phi}\Omega_F + g_{tt}, \tag{13}$$

$$k_2 \equiv (1 - \Omega_F \tilde{L})^2, \tag{14}$$

$$k_4 \equiv \frac{g_{\phi\phi} + 2g_{t\phi}\tilde{L} + g_{tt}\tilde{L}^2}{\rho_w^2}, \tag{15}$$

where $\rho_w^2 \equiv g_{t\phi}^2 - g_{tt}g_{\phi\phi} = \Delta \sin^2\theta$ and $\tilde{L} \equiv L/E$. Equation (10) determines the evolution of $\mathcal{M}_A{}^2$ along a flow line

Differentiating equation (10) along a poloidal flow line, we obtain (Takahashi *et al.* 1990)

$$(\ln\ u_p)' = \frac{1}{2}\left(\frac{E}{m_p}\right)^2 \frac{N}{D}, \tag{16}$$

where

$$N = k_4'\mathcal{M}_A{}^6 + \left\{ k_0 k_4 \left[\ln \frac{(k_0 \tilde{B}_p)^2}{k_4}\right]' + 2k_2(\ln \tilde{B}_p)' \right\} \mathcal{M}_A{}^4 + 3k_2 k_0' \mathcal{M}_A{}^2 - k_0 k_2 k_0', \tag{17}$$

$$D = (k_0 - \mathcal{M}_A{}^2)^3 \left[u_p{}^2 - \left(\frac{E}{\mu}\right)^2 \mathcal{M}_A{}^4 \mid \frac{k_2 + k_0 k_4}{(k_0 - \mathcal{M}_A{}^2)^3} \mid \right], \tag{18}$$

and the prime denotes the derivative $\partial_r - (\Psi_r/\Psi_\theta)\partial_\theta$. The Alfvén or the fast magnetosonic critical point appears when D vanishes. In order that the flows may smoothly pass through these critical points, N also must vanish there (Waber & Davis 1967). Thus the critical condition is given by

$$N = 0 \quad \text{and} \quad D = 0. \tag{19}$$

With the help of (10), $D = 0$ is satisfied when

$$u_p{}^2 = U_{\rm FM}{}^2 \equiv \frac{(e/m_p)^2 - k_0}{\mathcal{M}_A{}^2}, \tag{20}$$

where $e \equiv E - \Omega_F L$. We define $U_{\rm FM}$ as the fast-magnetosonic velocity.

In the black hole magnetosphere, there are two light surfaces which are defined by $k_0 = 0$ (see e.g., Znajek 1977). One is called the outer light surface which is formed by the centrifugal force in the same manner as in pulsar models. The other is called the inner light surface which is formed by the gravity of the black hole. In a region between the horizon and the inner light surface plasma must stream inwards, while in a region beyond the outer light surface it must stream outwards. The plasma source where both inflows and outflows start with low poloidal velocity ($\mathcal{M}_A{}^2 \approx 0$) can be located between these two light surfaces (Nitta et al. 1991). It can be understood from equations (16)–(18) that inward acceleration $u_p u'_p < 0$ (outward acceleration $u_p u'_p > 0$) occurs in the region where $k'_0 > 0$ ($k'_0 < 0$) and $\mathcal{M}_A{}^2 \approx 0$ hold. The injection region of plasma inflows is separated with that of plasma outflows. We call the boundary surface defined by $k'_0 = 0$ the separation surface. If we consider plasma injection from a thin disk ($\theta = \pi/2$), the separation point corresponds to the corotation point where Ω_F is equal to the angular velocity of circular orbits in Kerr geometry. The accretion starts from the disk surface between the inner edge and the corotation point. Along magnetic field lines plasma inflows pass through the Alfvén point ($r = r_A$), the light cylinder ($r = r_L$) and the fast magnetosonic point ($r = r_F$) successively, and at last reach the event horizon ($r = r_H$).

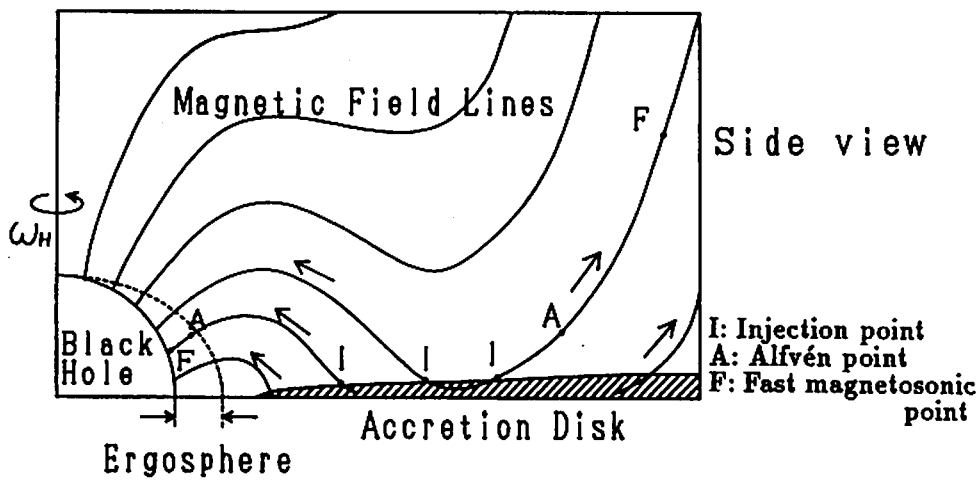

Figure 1. Schematic picture of the black hole magnetosphere. Both inflows and outflows start from the surrounding disk.

4 NON-AXISYMMETRIC PERTURBATIONS ON MHD FLOWS

We next consider a small-amplitude non-axisymmetric perturbations superposed on the unperturbed state discussed in the last section. In the perturbed state all perturbed quantities are solved self-consistently including trans-field equation, in contrast to the unperturbed state in which the poloidal magnetic field is arbitrarily assumed.

Since the terms containing the derivatives of quantities in the equilibrium state are very complicated, we adopt the approximation in which all such terms can be neglected comparing with those containing derivatives of quantities in the perturbed state. In this approximation, neither the acceleration due to gravity nor the curvature of the magnetic field will be taken into account, because all covariant derivatives can be replaced by normal derivatives and all the derivatives of magnetic field in the equilibrium state will not contribute. From now on, we will call this approximation high wave number limit. As perturbed quantities, we use $\tilde{u}^\mu$, $\tilde{n}$, and $\tilde{F}^{\mu\nu}$ for perturbations of u^μ, n, and $F^{\mu\nu}$, respectively. And we sometimes use a symbol (0) such as $u^\mu{}_{(0)}$ to indicate that the quantity is in the equilibrium state. We will investigate the mode distinguished by $k_\mu = (-\omega, k_r, k_\theta, m)$; perturbed quantities are expressed as

$$\partial_\mu \tilde{u}^\alpha = i k_\mu \tilde{u}^\alpha .$$

We treat all the quantities in the equilibrium state to be already known and thus we have 11 independent perturbation equations for 11 quantities $\tilde{u}^\mu$, $\tilde{n}$, and $\tilde{F}^{\mu\nu}$.

In this paper, we wish to examine the behavior of fluid quantities in response to the variation in the electromagnetic field, we shall henceforth focus our attention on the relations between perturbed quantities. By ignoring terms of the second and higher orders in perturbations, we obtain the following results after a tedious analysis (Hirotani et al. 1992b):

$$\tilde{\epsilon} = \Omega_F \tilde{l} = -\frac{{u_p}^2 \Omega_F}{u^\phi - \Omega_F u^t} \frac{\tilde{u}_p}{u_p}, \tag{21}$$

and

$$\frac{\tilde{u}_p}{u_p} = -\frac{2(u^\phi - \Omega_F u^t) u^r u^\theta \sqrt{g_{rr} g_{\theta\theta}}\, u^\mu k_\mu}{{u_p}^2 [u^\mu k_\mu + (\omega - m\Omega_F) u^t]} \frac{k_\perp}{F} \tilde{b}, \tag{22}$$

for the Alfvén mode,

$$\frac{\tilde{u}_p}{u_p} = \frac{2(u^\phi - \Omega_F u^t) u^r u^\theta \sqrt{g_{rr} g_{\theta\theta}}\, {\rho_w}^2 u^\mu k_\mu}{(e^2 - k_0) {u_p}^2 [u^\mu k_\mu + (\omega - m\Omega_F) u^t]} \frac{F}{k_\perp} \tilde{b}, \tag{23}$$

for the fast-magnetosonic mode, where

$$F \equiv u_p (k^\phi - \Omega_F k^t) + k_{||} (u^\phi - \Omega_F u^t), \tag{24}$$

$$k_{\parallel} \equiv \frac{1}{u_p}(u^r k_r + u^\theta k_\theta)\ , \quad k_\perp \equiv \frac{\sqrt{g_{rr} g_{\theta\theta}}}{u_p}(u^r k^\theta - u^\theta k^r), \tag{25}$$

$$\tilde{b} \equiv \frac{1}{2}\left(\frac{\tilde{B}^r}{B^r} - \frac{\tilde{B}^\theta}{B^\theta}\right). \tag{26}$$

Here, $\tilde{\epsilon}$ and $\tilde{l}$ denote the energy and angular momentum of the fluid in the perturbed state, respectively. If the poloidal part of k_μ is longitudinal to the unperturbed poloidal magnetic field, then $k_\perp$ becomes 0. $\tilde{b}$ expresses the variation of the poloidal magnetic field in the direction perpendicular to the unperturbed field. The Alfvén and the fast-magnetosonic modes are given by the following equations (Lichnerowicz 1967);

$$\text{Alfven mode :} \quad (k_0 - {\mathcal{M}_A}^2)(u^\mu k_\mu)^2 + (\omega - m\Omega_F)[\omega - m\Omega_F + 2eu^\mu k_\mu] = 0, \tag{27}$$

$$\text{fast mode :} \quad (u^\mu k_\mu)^2 + {U_{\rm FM}}^2 k^\mu k_\mu = 0. \tag{28}$$

In the next section, we study the behavior of $\tilde{u}_p/u_p$ in response to $\tilde{b}$ for both the Alfvén and the fast-magnetosonic modes.

5 ANALYSIS OF ALFVÉN AND FAST-MAGNETOSONIC MODES

Let us now examine qualitatively the behavior of fluid quantities represented by $\tilde{u}_p/u_p$ at several typical points along the flow line for both the Alfvén and the fast-magnetosonic modes. We shall first consider the Alfvén mode. The dispersion relation (27) gives

$$\omega - m\Omega_F = \frac{e - (k_0 - {\mathcal{M}_A}^2)u^t \pm \sqrt{e^2 - k_0 + {\mathcal{M}_A}^2}}{1 - 2eu^t + (k_0 - {\mathcal{M}_A}^2)(u^t)^2} u_p \left(k_{\parallel} + \frac{u^\phi - \Omega_F u^t}{u_p} m\right), \tag{29}$$

which shows there exist two modes.

We analyze equation (22) for each mode at three typical points $r_A < r < r_I$, $r = r_A$ and $r = r_H$. (i) In the sub-Alfvénic region ($r_A < r < r_I$), one mode is out-going and the other mode is in-going. In this case, no quantities in equation (22) diverge, and as a consequence, we obtain

$$|\ \tilde{u}_p/u_p\ | \lesssim |\ \tilde{b}\ | \tag{30}$$

in order of magnitude, except when the special mode which cancels the leading order in $u^\mu k_\mu + (\omega - m\Omega_F)u^t$ or F occurs. (ii) At the Alfvén point ($r = r_A$), the one mode stagnates and the another mode is in-going and no quantities in equation (22) diverge.

Thus the same relation as (30) holds. (iii) At the horizon ($r = r_H$), the dispersion relation (27) is satisfied only when

$$\omega - m\omega_H = -k_{r*} + O(\Delta) \tag{31}$$

holds, where $k_{r*} \equiv [(r^2 + M^2)/\Delta]k_r$. This means that the both modes become in-going with the same velocity. In this case,

$$F = O(\Delta^{-1/2}) \ , \quad u^\phi - \Omega_F u^t = O(\Delta^{-1}) \ , \quad {u_p}^2 = O(\Delta^{-1})$$

$$u^\mu k_\mu = O(1) \ , \quad u^\mu k_\mu + (\omega - m\Omega_F)u^t \approx (\omega - m\Omega_F)u^t = O(\Delta^{-1})$$

hold, and as a consequence, we have

$$| \tilde{u}_p/u_p | \lesssim (\Delta/M^2) | \tilde{b} | \tag{32}$$

in order of magnitude, except when the special mode which cancels the leading order in F occurs. From (i)-(iii), we can conclude that the perturbations in fluid quantities such as $| \tilde{u}_p/u_p |$ will not become large comparing with those in poloidal magnetic field $| \tilde{b} |$.

Let us next consider the fast-magnetosonic mode by introducing the magnetically dominated limit ($| E/m_p | \gg 1$). In this limit, the fast magnetosonic point is located very close to the horizon (Phinney 1983). We analyze equation (23) at the following three regions: $r_F < r < r_I$, $r = r_F$ and $r = r_H$. (iv) In the sub-fast-mangetosonic region ($r_F < r < r_I$) no quantities in equation (23) diverge, because we can put $\Delta/M^2 \sim 1$ in order on magnitude in this region. We thus have the same relation (30) as in the Alfvén mode. (v) At the fast-magnetosonic point ($r = r_F$), we have the following two modes:

$$\omega - m\omega_H = O\Big(-\frac{m_p}{E}\Big) \qquad (\text{ mode I }), \tag{33}$$

$$\omega - m\omega_H = -k_{r*} + O\Big(-\frac{m_p}{E}\Big) \qquad (\text{ mode II }), \tag{34}$$

where $\omega_H \equiv (a/2mr_H)$ is the angular velocity of the black hole. On the other hand, we have

$$\frac{\tilde{u}_p}{u_p} = C\frac{(\omega - m\omega_H + k_{r*})^2}{[(\omega_H - \Omega_F)m - k_{r*}][k_\theta + 2P(Mk_{r*})]}\Big(-\frac{E}{m_p}\Big)\tilde{b}, \tag{35}$$

where C is in order of unity and does not depend on k_μ, and $P \equiv -(r\partial_r\Psi/\partial_\theta\Psi)_H$ represents the shape of the field line near the horizon. Substituting equation (33) and (34) into (35), we obtain

$$| \tilde{u}_p/u_p | \sim (-E/m_p) | \tilde{b} | \qquad (\text{ for mode I }), \tag{36}$$

$$| \tilde{u}_p/u_p | \sim (-m_p/E) | \tilde{b} | \qquad \text{(for mode II)} \tag{37}$$

in order of magnitude. (vi) At the horizon ($r = r_H$), we have

$$\omega - m\omega_H = -k_{r_*} + O(\Delta) \tag{38}$$

from equation (28). Substituting equation (38) into (23), we obtain

$$| \tilde{u}_p/u_p | \lesssim (\Delta/M^2) | \tilde{b} | \tag{39}$$

in order of magnitude. Note that $-E/m_p \gg 1$ is finite. From (iv)-(vi), we can conclude that in the magnetically dominated limit $| \tilde{u}_p/u_p |$ becomes much larger than $| \tilde{b} |$ for mode I at $r = r_F$ even if $| \tilde{u}_p/u_p | \lesssim | \tilde{b} |$ holds at other points. This is because the physics changes disruptly between $r_H < r < r_F$ for the mode I: the wave stagnates at $r = r_F$ but must fall inside at $r = r_H$. A small perturbation in the electromagnetic field of which energy density is dominant compared with the fluid's can exert a significant influence on fluid quantities near the horizon.

In summary, we have calculated the relation between quantities perturbed by non-stationary and non-axisymmetric perturbations in the high wave number limit. The magnetically dominated limit is crucially essential to the results that $| \tilde{u}_p/u_p | \gg | \tilde{b} |$ holds for the fast-magnetosonic mode at the fast magnetosonic point, because this point is located very close to the horizon in this limit. In addition to this result, we also showed that $| \tilde{u}_p/u_p | \lesssim | \tilde{b} |$ holds for the fast-magnetosonic mode at the remote place from the fast-magnetosonic point and that $| \tilde{u}_p/u_p | \lesssim | \tilde{b} |$ holds for the Alfvén mode at an arbitrary point along the flow line. Therefore we can conclude that the time-dependent nature of the MHD accretion flows onto a black hole appears prominently near the horizon in the magnetically dominated limit.

6 DISCUSSION

The results derived in the previous section lead to a conjecture that the motion of fluid will become time-dependent as it approaches to the fast-magnetosonic point in the magnetically dominated limit. Thus when the magnetic field is not very dominant, say when $(-E/m_p) \approx 10$, the flow may perturbed by several tens of percent in amplitude in somewhat extended regions around the black hole. Radiation will be emitted from such regions provided that several part of the kinetic energy of the fluids changes into thermal energy. If the perturbation period is longer than the dynamical time scale (i.e., $M\omega \lesssim 1$), the luminosity of these regions will vary with frequency ω. Note that the high wave number limit is still valid even if $M\omega \lesssim 1$, because $m, Mk_{r_*} \gg 1$ holds. The short-time variations in luminosity observed in AGNs may be caused by such mechanisms.

Let us next consider the MHD energy flux $T^A{}_t = T^A_{(M)t} + T^A_{(em)t}$, where A is r or θ. By ignoring terms of the second and higher orders in the perturbations, we have

$$\frac{\tilde{T}^A{}_t}{T^A{}_t} = \frac{\tilde{T}_{(em)}{}^A{}_t}{T_{(em)}{}^A{}_t} + \frac{T_{(M)}{}^A{}_t}{T_{(em)}{}^A{}_t}\left[\frac{\tilde{T}_{(em)}{}^A{}_t}{T_{(em)}{}^A{}_t} + \left(\frac{T_{(M)}{}^A{}_t}{T_{(em)}{}^A{}_t} - 1\right)\frac{\tilde{T}_{(M)}{}^A{}_t}{T_{(M)}{}^A{}_t}\right]. \tag{40}$$

At the fast-magnetosonic point, this equation reduces to

$$\frac{\tilde{T}^A{}_t}{T^A{}_t} = \frac{\tilde{T}_{(em)}{}^A{}_t}{T_{(em)}{}^A{}_t} + \frac{m_p}{E}u_t{}^{(0)}\frac{\tilde{T}_{(M)}{}^A{}_t}{T_{(M)}{}^A{}_t} \tag{41}$$

in the magnetically dominated limit which gives $(T_{(M)}{}^A{}_t/T_{(em)}{}^A{}_t)_{(0)} = (m_p/E)u_t{}^{(0)}$. Note that this equation is valid only for the small perturbations such that $|(E/m_p)\tilde{b}| \ll 1$. In the right hand side of equation (41), both the first and the second terms are in order of $\tilde{b}$. This implies that the fluid part has almost the same contribution as the electromagnetic part. This could be understood that the inertia of fluid becomes essential near the horizon. Such feature would never been seen in the force-free approximation in which we neglect the fluid part in $T^A{}_t$. The same discussion can be applied to the angular momentum flux $T^A{}_\phi$. Thus we can suggest that the force-free approximation should be abandoned near the horizon in the perturbed state and that we should take the inertia of fluid into account.

We have seen that the flows tends to become time-dependent as they approach to the horizon in the magnetically dominated limit. This is due to the effects of a critical point, the horizon and the inertia of fluid. Nevertheless, we have neglected the effect of gravitational acceleration by adopting the high wave number limit in this work. Such nature of MHD flows would be clearly seen if we would analyze the fully time-dependent flows near the horizon without using the high wave number limit.

REFERENCES

Abramowicz, M. A. & Kato, S. 1989, ApJ, 336, 304
Bekenstein, J. D., & Oron, E. 1977, Phys. Rev. D, 18, 1809
Camenzind, M. 1986a, A & A, 156, 137
———. 1986b, A & A, 162, 32
Hirotani, K. Takahashi, M., Nitta, S., & Tomimatsu, A. 1992a, ApJ, 386, in printing
Hirotani, K. Takahashi, M., & Tomimatsu, A. 1992b, in preparation
Lichnerowicz, A. 1967, in *Relativistic Hydrodynamics and Magnetohydrodynamics*, (New York: W. A. Benjamin, Inc.), p. 107
Nitta, S., Takahashi, M., & Tomimatsu, A. 1991, Phys. Rev. D, 44, 2295
Papaloizou, J. C. B. & Pringle, J. E. 1984, MNRAS, 208, 721
Phinney, E. S. 1983, Ph. D. thesis, Univ. Cambridge
Rees, M. J. 1984, Ann. Rev. Astron. Astrophys., 22, 471
Takahashi, M., Nitta, S., Tatematsu, Y., & Tomimatsu, A. 1990, ApJ, 363, 206
Waber, J., & Davis, L. Jr. 1967, ApJ, 148, 217
Znajek, R. L. 1977, MNRAS, 179, 457

Electromagnetic Radiation from Rotating Objects around a Black Hole

Hitoshi HANAMI

Laboratory of Physics, College of Humanities and Social Sciences,
Iwate University, Morioka, 020 Japan

Abstract

This paper examines the nature of the eletromagnetical radiation emitted from a test particle with magnetic field as it rotates around a Schwarzshild black hole.

Electromagnetic Fields around Schwarzshild Black Hole

We will formulate the dynamical approach of general relativistic plasma based on the "3+1" formalisum. This approach has been extensively applied to numerical relativity. Thorne and Macdonald (1982) have formulated Maxwell equations with the familiar langauge for astrophysicists. Around a Schwarzschild black hole (B.H), by using the "3 + 1" formalism, we can write the Maxwell's equations for the electromagnetic field,

$$\frac{\partial \mathbf{E}}{\partial t} = \nabla \times (\alpha \mathbf{B}) - 4\pi\alpha \mathbf{j}\,, \qquad \nabla \mathbf{E} = 4\pi\rho\,,$$
$$\frac{\partial \mathbf{B}}{\partial t} = -\nabla \times (\alpha \mathbf{E})\,, \qquad \nabla \mathbf{B} = 0\,, \tag{1}$$

where the lapse function $\alpha = (1 - 2M/r)^{1/2}$.

The electric and magnetic fields can be derived from a scalar potential ϕ and a vector potential $\mathbf{A}$, $\mathbf{B} = \nabla \times \mathbf{A}$, $\mathbf{E} = -\frac{1}{\alpha}\nabla\alpha\phi - \frac{1}{\alpha}\frac{\partial \mathbf{A}}{\partial t}$. The solenoidal gauge derives the final equation for the vector potential,

$$-\frac{1}{\alpha^2}\frac{\partial^2 \mathbf{A}}{\partial t^2} = \frac{1}{\alpha}\nabla \times (\alpha \nabla \times \mathbf{A}) - 4\pi \mathbf{j}\,. \tag{2}$$

Representation with Vector Spherical Harmonics

Any vector field can be expressed by the spherical vector harmonics. Then, with introducing the "tortoise coordinate " r^* as Regge and Wheeler (1957) defined $dr^* = \frac{dr}{1-\frac{2M}{r}}$, $r^* = r + 2Mln\left[\frac{r}{2M} - 1\right]$. We obtain the equation for the solution with the radial dependent as

$$\left[\frac{\partial^2}{\partial r^{*2}} - \frac{\partial^2}{\partial t^2} - V(r)\right] \hat{g}_{lm}(r,t) = -4\pi\alpha^2 \hat{j}_{lm} = S(r,\omega), \tag{3}$$

$$V(r) = \left(1 - \frac{2M}{r}\right)\left[\frac{l(l+1)}{r^2}\right]\,, \tag{4}$$

where $\hat{g}_{lm} = r\alpha_{lm}$ or $r\beta_{lm}$ and $\hat{j}_{lm} = j_{\alpha,lm}\frac{r^2}{\alpha}$ or $j_{\beta,lm}r$. The electric transverse mode β is important.

Formal Solutions

Let g_{in} and g_{out} be the homogeneous solutions to Eq.(3) without the source term in the right hand. Then the solution for the Fourier compornents of Eq.(3) can be expressed as

$$g(r^*,\omega) = \frac{1}{W(\omega)}\times$$
$$\left[g_{out}(r^*,\omega)\int_{-\infty}^{r^*} g_{in}(r^{*'},\omega)S(r^{*'},\omega)dr^{*'} + g_{in}(r^*,\omega)\int_{r^*}^{\infty} g_{out}(r^{*'},\omega)S(r^{*'},\omega)dr^{*'}\right] . \quad (5)$$

where the Wronskian is represented as $W(\omega) = g_{in}\frac{dg_{out}}{dr^*} - g_{out}\frac{dg_{in}}{dr^*} = 2i\omega\left(\frac{1}{T(\omega)}\right)$.

Since our interest is in the emitting radiation to infinity, we only need the form of g for the outgoing compornet at $r^* \to \infty$. Then,

$$g(r^* \to \infty,\omega) = G(\omega)T(\omega)e^{-i\omega r^*} , G(\omega) = -\frac{i}{2\omega}\int_{-\infty}^{\infty} g_{in}(r^{*'},\omega)S(r^{*'},\omega)dr^{*'} . \quad (6)$$

Properties of Sources

We will write the source terms of the current by the bases introduced for the representation of the vector potential. Our interest is the radiation from a moving moment. Then, we can obtain effective polarization induced by the moving magnetization from Lorentz transformation. From the similarity between the transformation of $(\mathbf{E},\mathbf{B})$ and that of $(\mathbf{P},-\mathbf{M})$ we can obtain the effective current sources for the moving magnetized objects

$$\begin{aligned} \mathbf{j}_{eff} &= \frac{\partial}{\partial t}(\mathbf{v}\times\mathbf{M}') + \nabla\times(\alpha\mathbf{M}) \\ &= \mathbf{j}_{pol} + \mathbf{j}_{mag} , \end{aligned} \quad (7)$$

where we have defined $\mathbf{j}_{pol} = \frac{\partial}{\partial t}(\mathbf{v}\times\mathbf{M}')$ and $\mathbf{j}_{mag} = \nabla\times(\alpha\mathbf{M})$.

For the point dipole source with its moment $\mathbf{m}$ at $\mathbf{r}'$, the magnetization can be represented as,

$$\mathbf{M} = \delta(\mathbf{r}-\mathbf{r}'(t))\mathbf{m}(\mathbf{r}'(t)) , \quad (8)$$

In this paper, we will assume that the velocity is perpendicular to the magnetization. It means that $\mathbf{M}' = \mathbf{M}$. Furthermore, we will consider that the direction of the moment at the point $\mathbf{r}'$ is parallel to its radial position vector $\mathbf{r}'$. Then, the magnetic moment can be represented as

$$\mathbf{m} = m_d\frac{\mathbf{r}'}{r'} . \quad (9)$$

We obtain the source term,

$$\begin{aligned} S_{s,\beta,lm}(r,\omega) &= 4\pi\alpha^2 j_{s,\beta,lm}(r,\omega)r \\ &= Q_{s,lm}\frac{1}{\sqrt{l(l+1)}}\sqrt{\frac{(l-m)!(2l+1)}{4\pi(l+m)!}}P_{lm}(0)\delta(r-r')\delta(\omega-m\Omega) , \end{aligned} \quad (10)$$

where $s = mag$ or pol,

$$\left.\begin{array}{c} Q_{mag,lm} \\ Q_{pol,lm} \end{array}\right\} = \left\{\begin{array}{c} \frac{4\pi}{3} m_d \alpha^2 \frac{l(l+1)}{r^2} \\ i\frac{4\pi}{3} m_d \alpha^2 m^2 \Omega^2 \end{array}\right\} \delta(r - r')\delta(\omega - m\Omega) \,. \tag{11}$$

Radiation around Schwarzshild Black Hole

We can see the source term is only non zero at the radius of the particle. For a pure multipole of order (l,m), the power-radiated per unit solid angle per unit frequency interval is the angular distribution reduces to a single term,

$$\begin{aligned} \frac{d^2 P_{lm}}{d\omega d\Omega} &= \frac{\omega^2}{4\pi} \mid G_{lm}(\omega) T_{lm}(\omega) \mid^2 \mid \mathbf{S}_{\beta,lm} \mid^2 \\ &= \frac{1}{4\pi} \mid g_{in,lm}(r'^*, \omega) \mid^2 \left\{ \mid S_{mag,lm}(r'^*, \omega) \mid^2 + \mid S_{pol,lm}(r'^*, \omega) \mid^2 \right\} \mid T_{lm}(\omega) \mid^2 , \end{aligned} \tag{12}$$

where we had used the property that $Q_{mag,lm}$ and $Q_{pol,lm}$ is pure real respectively. The solution g_{in} and g_{out} can be well approximated using hypergeometric functions as shown by Ferrari and Mashhoon (1984). From the approximation, we can represent the refrection and transmission coefficients with gamma function. From the relation between the frequency and the orbit radius

$$\mid \omega \mid = \mid m\Omega \mid = \mid m \mid \left(\frac{M^{1/2}}{r'^{3/2}}\right) , \tag{13}$$

The asymptotic solutions are well approximation as long as $r' < 2.5M$ or $r' > 10M$, which are represented as,

$$\frac{dP_{lm}}{d\omega} \simeq \left\{\begin{array}{ll} \frac{1}{4\pi} \mid e^{i\omega r'^*} \mid^2 \mid T(\omega) \mid^2 \mid S(r'^*, \omega) \mid^2 & : r'^* \to -\infty \\ \frac{1}{4\pi} \mid e^{i\omega r'^*} + R(\omega) e^{-i\omega r'^*} \mid^2 \mid S(r'^*, \omega) \mid^2 & : r'^* \to \infty \end{array}\right.$$

When $r' > 3M$, we can see $\mid \omega \mid < \frac{1}{3\sqrt{3M}} l$. Then, we can treat the reflection and transmission coefficients as $\mid R(\omega) \mid \sim 1$, and $\mid T(\omega) \mid \sim e^{\pi\left\{\left|\frac{m}{\omega}\right| - (l(l+1) - 1/4)^{1/2}\right\}}$ in usual cases for the orbiting objects.

References

Ferrari, V. and Mashhonn, B. 1984, Phys. Rev. D **30**, 295.
Macdonald, D. A., and Thorne, K. S. 1982, Mon. Not. Roy. Astron. Soc. **198**, 345.
Regge, T., and Wheeler, J. A. 1957, Phys. Rev. **108**, 1063.
Thorne, K. S., and Macdonald, D. A. 1982, Mon. Not. Roy. Astron. Soc. **198**, 339.

Cosmic No-Hair Theorem in Exponential and Power-Law Inflation

— Extended Wald's Theorem —

YUICHI KITADA

Department of Physics, Faculty of Science, University of Tokyo, Bunkyo-ku, Tokyo 113, Japan

and

KEI-ICHI MAEDA

Department of Physics, Waseda University, Shinjuku-ku, Tokyo 169, Japan

Abstract

Generalizing an inflaton potential as $\exp(-\lambda\kappa\phi)$ $(0 \leq \lambda < \sqrt{2})$, we prove an extended version of Wald's cosmic no-hair theorem. For $\lambda \neq 0$, we find that an isotropic power-law solution is the unique attractor and that anisotropies always enhance inflation for any initially expanding Bianchi-type models except type-IX, with an inflaton and matter fluid which satisfies the dominant and strong energy conditions. For Bianchi IX, this conclusion is also valid except for the effect of anisotropies, if the following two conditions are initially satisfied; the ratio of the vacuum energy $\Lambda_{\rm eff}$ to the maximum three-curvature ${}^{(3)}R_{\rm max}$ is larger than $1/[3(1-\lambda^2/2)]$ and time derivative of this ratio is initially positive. Setting $\lambda = 0$, we can show that it guarantees inflation for a wider class of Bianchi type-IX spacetimes than Wald's one.

1 Basic Equations

Assuming Bianchi-type homogeneous anisotropic spacetimes with an exponential potential $\exp(-\lambda\kappa\phi)$, we investigate whether or not a power-law inflationary solution [1] is the unique attractor and such anisotropic spacetimes are really isotropized in finite time [2]. Such a potential appears at least approximately in some inflation models, *e.g.*, in (hyper-)extended inflation [3,4] and in soft inflation [5].

In the present paper, we show two types of cosmic no-hair theorems for Bianchi models as extensions of Wald's theorem [6,7], based on our recent works; Ref.[8] (limited case of $0 \leq \lambda < \sqrt{2/3}$) and Ref.[9] (general case of $0 \leq \lambda < \sqrt{2}$). In addition, we give a recollapse theorem for Bianchi-IX models and discuss the relation to the so-called closed-universe-recollapse theorem [10].

Our model Lagrangian is

$$S = \int d^4x\sqrt{-g}\left[\frac{1}{2\kappa^2}R - \frac{1}{2}(\nabla\phi)^2 - V(\phi) + L_{\rm matter}\right], \tag{1}$$

where $\kappa^2 = 8\pi G$, ϕ is an inflaton field and $L_{\rm matter}$ is the matter Lagrangian aside from ϕ. The potential of the inflaton is assumed to be an exponential type $V(\phi) = V_0\exp(-\lambda\kappa\phi)$, where $V_0 (> 0)$ and $\lambda (\geq 0)$ are constants. In order for power-law inflation to occur, λ must be smaller than $\sqrt{2}$ in our notation [11,12], and our discussion is for λ in this range $(0 \leq \lambda < \sqrt{2})$. This corresponds to $\omega > 1/2$ for JBD theory [5], which is consistent with observations ($\omega > 500$).

The Einstein equations are written as $G_{ab} = \kappa^2(T^{(\phi)}_{ab} + T_{ab})$, where $T^{(\phi)}_{ab}$ and T_{ab} are the energy-momentum tensors of the inflaton and of the ordinary matter fluid. Hereafter we assume the matter fluid satisfies the dominant and strong energy conditions [13]. The dominant energy condition implies the weak energy condition.

For our purpose, it is convenient to use a new time coordinate τ, which is defined by

$$d\tau = \exp(-\lambda\kappa\phi/2)dt\ , \tag{2}$$

with t the cosmic time. In an isotropic homogeneous spacetime, the attractor (an inflationary solution) becomes a time-independent fixed point with this time coordinate [11,12]. Hereafter an overdot denotes differentiation with respect to τ.

In the following, we may use "power-law" and "exponential potential", which are correct just for the case of $\lambda \neq 0$. However every discussion below is also valid for the case of $\lambda = 0$, which corresponds to the original-type of inflation, if we replace those with "exponential" and "cosmological constant".

We analyze three basic equations given below. Following Wald [6], we consider two components of the Einstein equations. One is the Hamiltonian constraint

$$\widetilde{K}^2 = 3\kappa^2\left(\frac{1}{2}\dot{\phi}^2 + V_0\right) + \frac{3}{2}\tilde{\sigma}_{ab}\tilde{\sigma}^{ab} - \frac{3}{2}{}^{(3)}\tilde{R} + 3\kappa^2\tilde{T}_{\rm W}(n)\ , \tag{3}$$

and the other is the Raychaudhuri equation

$$\dot{\widetilde{K}} = \kappa^2(-\dot{\phi}^2 + V_0) + \frac{\lambda\kappa}{2}\widetilde{K}\dot{\phi} - \frac{1}{3}\widetilde{K}^2 - \tilde{\sigma}_{ab}\tilde{\sigma}^{ab} - \kappa^2\tilde{T}_{\rm S}(n)\ , \tag{4}$$

where $\tilde{T}_{\rm W}(n) \equiv T_{ab}n^an^b \geq 0$ and $\tilde{T}_{\rm S}(n) \equiv \left(T_{ab} - \frac{1}{2}Tg_{ab}\right)n^an^b \geq 0$ result from the weak and the strong energy conditions for a unit timelike vector n^a, respectively.

And the last is the scalar-field equation, which is written as

$$\ddot{\phi} = \frac{\lambda\kappa}{2}\dot{\phi}^2 - \widetilde{K}\dot{\phi} + \lambda\kappa V_0\ , \tag{5}$$

where we introduced a new variable $\widetilde{K}$ defined by $\widetilde{K} = K\exp(\lambda\kappa\phi/2)$, and K is the trace of the extrinsic curvature with respect to time t. The other variables with tilde relations are defined similarly, *e.g.*, shear $\tilde{\sigma}_{ab}\tilde{\sigma}^{ab} = \sigma_{ab}\sigma^{ab}e^{\lambda\kappa\phi}$ and three-curvature ${}^{(3)}\tilde{R} = {}^{(3)}Re^{\lambda\kappa\phi}$. Our argument is always reduced to the case of original inflation (a constant vacuum energy) by setting $\lambda = 0$ and $\phi = 0$, that means exponential inflation. The terms with $\widetilde{K}\dot{\phi}$ in (4) and with $\dot{\phi}^2$ in (5) appear due to the new time coordinate and new variables.

2 Cosmic No-Hair Theorem

We can show that Wald's cosmic no-hair theorem is simply extendable to power-law inflationary models for a limited case ($0 \leq \lambda < \sqrt{2/3}$) [8], by the replacement of the "positive cosmological constant Λ" with a positive exponential potential of an inflaton ϕ as the effective cosmological constant: $\Lambda_{\rm eff} \equiv \kappa^2 V(\phi) \equiv \kappa^2 V_0 \exp(-\lambda\kappa\phi)$.

The theorem is as follows.

Theorem 1. Cosmic No-Hair Theorem for Bianchi Models (Wald's Type) *Assume there exists a scalar field ϕ which has an exponential potential $V(\phi) = V_0\exp(-\lambda\kappa\phi)$, where $V_0 (> 0)$ and λ ($0 \leq \lambda < \sqrt{2/3}$) are constants, and that the ordinary matter fluid satisfies the dominant and strong energy conditions. Then any initially expanding Bianchi-type spacetime except type-IX approaches asymptotically to the power-law ($0 < \lambda < \sqrt{2/3}$) or exponential ($\lambda = 0$) inflationary solution. Anisotropy, three-curvature, and all components of the energy-momentum tensor of the matter fluid, vanish faster than the inflaton potential. For initially expanding type-IX models, these results are also valid under the following additional initial condition*

$$\frac{\Lambda_{\rm eff}}{{}^{(3)}R_{\rm max}} > \frac{1}{2}\,, \tag{6}$$

where $\Lambda_{\rm eff} \equiv \kappa^2 V(\phi)$ is the effective cosmological constant, and ${}^{(3)}R_{\rm max}$ is the maximum three-curvature for a fixed proper volume.

For the general case $0 \leq \lambda < \sqrt{2}$, the simple way used in Ref.[8] does not apply to Bianchi models except type-IX for a mathematical reason, although the no-hair conjecture is still valid for non type-IX. As for type-IX, even if the above condition (6) is satisfied initially, some spacetimes do not inflate but recollapse to the singularity in the case of $\sqrt{2/3} < \lambda < \sqrt{2}$ (see Fig.2.3 and the discussion in §3). Hence we have to generalize the Wald's theorem or Theorem 1. Fortunately, for the general case of $0 \leq \lambda < \sqrt{2}$, we can prove a new version of cosmic no-hair theorem by a detailed phase-space analysis [9]. In particular,

this new theorem is an extension of Theorem 1. and guarantees inflation for a wider class of Bianchi-IX spacetimes than the Wald's-type theorem (Theorem 1) even for $0 \leq \lambda < \sqrt{2/3}$.

Theorem 2. Extended Cosmic No-Hair Theorem for Bianchi Models
Assume there exists a scalar field ϕ which has an exponential potential $V(\phi) = V_0 \exp(-\lambda\kappa\phi)$, where $V_0 (> 0)$ and λ $(0 \leq \lambda < \sqrt{2})$ are constants, and that the ordinary matter fluid satisfies the dominant and strong energy conditions. Then any initially expanding Bianchi-type spacetime except type-IX approaches asymptotically to the power-law $(0 < \lambda < \sqrt{2})$ or exponential $(\lambda = 0)$ inflationary solution. Anisotropy, three-curvature, and all components of the energy-momentum tensor of the matter fluid, vanish faster than the inflaton potential. For type-IX models, these results are valid under the following two additional initial conditions:

$$\text{(a)} \quad \frac{\Lambda_{\rm eff}}{{}^{(3)}R_{\rm max}} > \frac{1}{3(1-\lambda^2/2)} \tag{7}$$

and

$$\text{(b)} \quad \frac{d}{dt}\left(\frac{\Lambda_{\rm eff}}{{}^{(3)}R_{\rm max}}\right) > 0\,, \tag{8}$$

in place of the requirement of initial expansion.

If we apply Theorem 2 to Bianchi-IX spacetimes in the cosmological-constant case: $\lambda = 0$ with $\phi = 0$ (exponential inflation), the required initial conditions (a) and (b) reduce to $\Lambda/{}^{(3)}R_{\rm max} > 1/3$ rather than $1/2$ and initial expansion, respectively. Hence we would say that Theorem 2 is more general than the original Wald's theorem, even in the case of original inflationary model, under the same energy conditions for the matter fluid.

3 Recollapse Theorem for Bianchi Type-IX

Halliwell systematically studied the evolution of FRW spacetimes with only an exponential potential [11,12] for all $\lambda \geq 0$, and obtained the phase diagrams shown in Ref.[11]. However, his classification is not complete for the power-law inflationary case $(0 < \lambda < \sqrt{2})$ (Note that $\lambda_{\rm Halliwell}$ in his notation is related ours as $\lambda_{\rm Halliwell} = \sqrt{6}\lambda$). We have to refine the classification for the power-law inflationary case into three cases: (i) $0 < \lambda < \sqrt{2/3}$ (Fig.2.1), (ii) $\lambda = \sqrt{2/3}$ (Fig.2.2), (iii) $\sqrt{2/3} < \lambda < \sqrt{2}$ (Fig.2.3). The case with a constant vacuum energy $(\lambda = 0)$ is also shown in Fig.1. Note that the Fig.2 in Ref.[11] is valid only for the case (i).

In the $(\dot{\phi}, \widetilde{K})$-plane, we can define a "recollapse region", as a sufficient condition such that any spacetime that enters once into the region recollapses inevitablly.

In the anisotropic (homogeneous) case, the boundary of recollapse region coincides with the curve of the isotropic case in general, except for some modification near the repeller only in the case $0 < \lambda < \sqrt{2/3}$ (see Fig.2.1).

We stated above that, in the case (iii), some spacetimes which initially satisfy the condition (6) do not inflate but recollapse. That is due to the following reason. The condition (6) requires (but not equivalent to)

$$\widetilde{K}^2 - \frac{3}{2}\kappa^2\dot{\phi}^2 > 0 \tag{9}$$

(see Fig.2.3), and in case (iii), some spacetimes in the region of the inequality (9) that have relatively small anisotropy (and small matter energy-density) can satisfy both the condition (6) and the recollapse condition, to result in the fate of recollapse.

4 Evolution of Bianchi Models and Effects of Anisotropies

For Bianchi models except IX, because of the nonpositive spatial curvature ${}^{(3)}R \leq 0$, we can easily see from the constraint equation (3) that anisotropies (as well as energy density of matter) always enhance inflation. So, here, we shall focus our discussion on effects of anisotropy in the case of type IX.

The above extended theorem (Theorem 2) is also interpreted as a restriction condition to initial anisotropy which leads to inflation. We define two quantities: one is a measure of anisotropy (including energy density of ordinary matter)

$$\tilde{S}_{\rm aniso} \equiv \frac{3}{2}\tilde{\sigma}_{ab}\tilde{\sigma}^{ab} + \frac{3}{2}\left({}^{(3)}\tilde{R}_{\rm max} - {}^{(3)}\tilde{R}\right) + 3\kappa^2\tilde{T}_{\rm W}(n) \quad (\geq 0)\,, \tag{10}$$

and the other is

$$\tilde{S} \equiv \tilde{S}(\dot{\phi}, \widetilde{K}) \equiv \widetilde{K}^2 - 3\kappa^2\left(\frac{1}{2}\dot{\phi}^2 + V_0\right) = \frac{3}{2}\tilde{\sigma}_{ab}\tilde{\sigma}^{ab} - \frac{3}{2}{}^{(3)}\tilde{R} + 3\kappa^2\tilde{T}_{\rm W}(n)\,, \tag{11}$$

where the last equality comes from Eq.(3), which is nothing but the Hamiltonian constraint equation.

From Eqs.(10) and (11), the condition (a) (Eq.(7)) implies

$$\text{Condition (a)} \iff \text{Condition (c)} : \quad (0 \leq)\ \tilde{S}_{\rm aniso} < \tilde{S}(\dot{\phi}, \widetilde{K}) - \tilde{S}_{\rm S} \tag{12}$$

$$\implies \quad \tilde{S}(\dot{\phi}, \widetilde{K}) > \tilde{S}_{\rm S}\,, \tag{13}$$

where $\tilde{S}_{\rm S} \equiv -\frac{9}{4}(2-\lambda^2)\kappa^2 V_0$ (=constant). Note that contour curves of $\tilde{S}$ are hyperbolas in the $(\dot{\phi}, \widetilde{K})$-plane, and $\tilde{S} = \tilde{S}_{\rm S}$ is the special hyperbola that passes through two of saddle

points and represents a part of the boundary of the inflation region (see all figures). While, the condition (b) is equivalent to $2\widetilde{K} - 3\lambda\kappa\dot{\phi} > 0$.

In order for a spacetime to inflate, a sufficient condition is that the spacetime is initially in the inflationary region ($\tilde{S} > \tilde{S}_S$ with $2\widetilde{K} - 3\lambda\kappa\dot{\phi} > 0$) with an additional requirement, *i.e.*, "small-anisotropy condition" (Condition (c)) (see all figures). These conditions are equivalent to the conditions (a) and (b). This provides the constraint on initial anisotropy. Since both the shear term due to anisotropy and the energy density term affect in the same way in Eq.(3), moderate anisotropy ($\tilde{S}_{\rm aniso} \lesssim \tilde{S}(\dot{\phi}, \widetilde{K}) - \tilde{S}_S$) enhances inflation. However, too large anisotropy which is estimated by the initial condition of $(\dot{\phi}(\tau_0), \widetilde{K}(\tau_0))$, tends to lead the spacetime to the recollapse region, for the shear term in Eq.(4) acts so that the spacetime evolves downward in the phase diagram. It is, in particular, much more effective if the point is or comes near the recollapse region. This result is consistent with and explains the qualitative result by the numerical simulation [2]. The above tendency is intuitively understood by setting $\lambda = \sigma_{ab}\sigma^{ab} = 0$, ${}^{(3)}R = {}^{(3)}R_{\rm max}$, and $\kappa^2 T_{\rm W}(n) \gg \Lambda$, when the spacetime reduces to a matter-dominated closed FRW universe with a positive cosmological constant, that recollapses and is a well-known counter-example against the naive cosmic no-hair conjecture.

Finally, we shall mention to the so-called closed-universe-recollapse theorem recently proven by Lin and Wald [10] for Bianchi-IX spacetimes, assuming matter-fluid satisfies the dominant energy condition and a trace of the spatial projection of the stress-energy tensor is non-negative. The latter condition is not always satisfied if we have an inflaton field ϕ. Since we have shown the recollapse theorem in the case with an inflaton, it applies to a wider class of spacetimes than their theorem. In fact, if we show their condition in our phase diagram, it is a subset of our recollapse region [9].

Acknowledgements

We would like to thank Prof. K. Sato, Dr. A.L. Berkin and Dr. J. Yokoyama for useful discussions. This work was supported in part by the Grant-in-Aid for Scientific Research Fund of the Ministry of Education, Science and Culture No. 02640238 and No. 03250213.

References

[1] L.F. Abbott and M.B. Wise, Nucl. Phys. **B244**, 541 (1984);
F. Lucchin and S. Matarrese, Phys. Rev. **D32**, 1316 (1985).

[2] A.B. Henriques, J.M. Mourão and P.M. Sá, Phys. Lett. **B256**, 359 (1991);
H. Ishihara and M. Den, in proceedings of the 20th Yamada conference on *Big Bang, Active Galactic Nuclei and Supernovae*, ed. by S. Hayakawa and K. Sato (Universal Academy, Tokyo, 1988), p.79.

[3] D. La and P.J. Steinhardt, Phys. Rev. Lett. **62**, 376 (1989); Phys. Lett. **B220**, 375 (1989);
R. Holman, E.W. Kolb, and Y. Wang, Phys. Rev. Lett. **65**, 17 (1990).

[4] P.J. Steinhardt and F.S. Accetta, Phys. Rev. Lett. **64**, 2740 (1990).

[5] A.L. Berkin, K. Maeda, and J. Yokoyama, Phys. Rev. Lett. **65**, 141 (1990);
A.L. Berkin and K. Maeda, Phys. Rev. **D44**, 1691 (1991).

[6] R.M. Wald, Phys. Rev. **D28**, 2118 (1983).

[7] I. Moss and V. Sahni, Phys. Lett. **B178**, 159 (1986).

[8] Y. Kitada and K. Maeda, Phys. Rev. **D45**, (to be published, 1992).

[9] Y. Kitada and K. Maeda, preprint UTAP-138/92, WU-AP/19/92.

[10] X.-F. Lin and R.M. Wald, Phys. Rev. **D40**, 3280 (1989); Phys. Rev. **D41**, 2444 (1990).

[11] J.J. Halliwell, Phys. Lett. **B185**, 341 (1987).

[12] J. Yokoyama and K. Maeda, Phys. Lett. **B207**, 31 (1988);
A.B. Burd and J.D. Barrow, Nucl. Phys. **B308**, 929 (1988).

[13] S.W. Hawking and G.F.R. Ellis, *The large scale structure of space-time*, (Cambridge Univ. Press, Cambridge, 1973);
R.M. Wald, *General Relativity*, (Univ. of Chicago Press, Chicago, 1984).

Figure Captions

Fig.1: Phase diagram on $(\dot{\phi} - \widetilde{K})$ plane for inflation and recollapse in Bianchi IX spacetime with a constant vacuum energy ($\lambda = 0$). There are four critical points for isotropic Friedomann-Robertson-Walker spacetimes with the scalar field : A is the attractor (inflationary solution), R is the repeller, and two of S are saddle points. The attractor and the repeller are on either of two branches of a hyperbola $\tilde{S} = 0$. If a spacetime-point initially exists in the cross-hatched region under the small anisotropy condition (c) (see text), inflation always occurs and the spacetime is isotropized with time. While, if a spacetime is in the shaded region at some time, it eventually recollapses. Both conditions are sufficient conditions. We set $\kappa^2 = 8\pi$ and $V_0 = 1$.

Fig.2: The same phase diagrams for the case of a power-law inflation with an inflaton potential $V = V_0 \exp(-\lambda\kappa\phi)$. We classify the model into three cases; (i) $0 < \lambda < \sqrt{2/3}$ (**Fig.2.1**), (ii) $\lambda = \sqrt{2/3}$ (**Fig.2.2**), (iii) $\sqrt{2/3} < \lambda < \sqrt{2}$ (**Fig.2.3**).

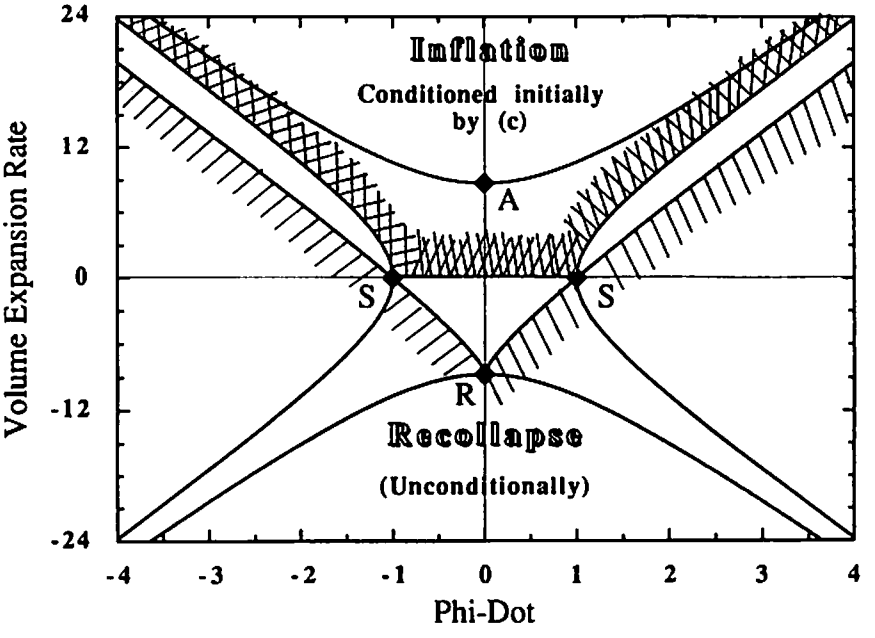

Fig.1 Exponential Inflation (λ=0)

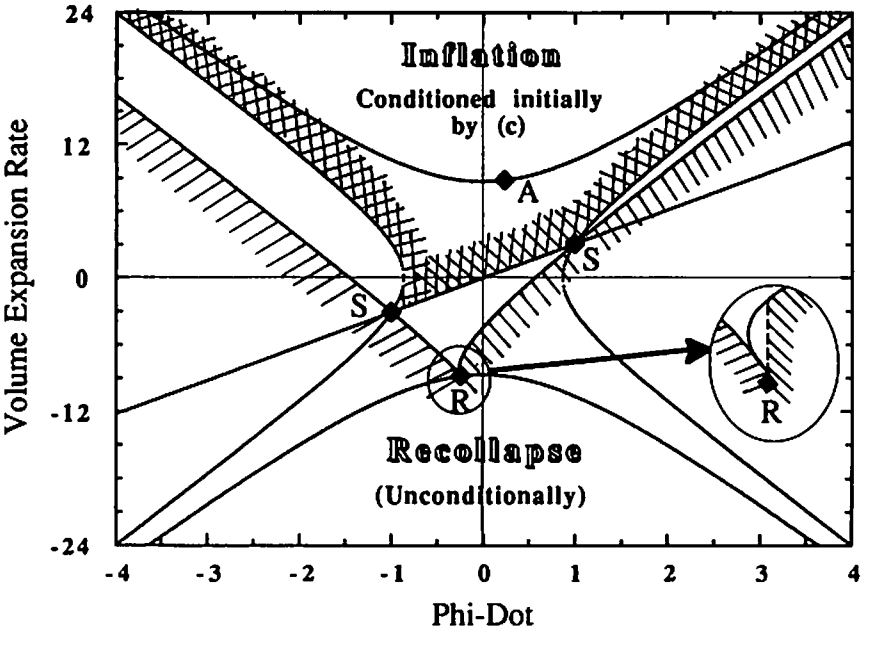

Fig.2.1 Case (i) $0<\lambda<\sqrt{2/3}$

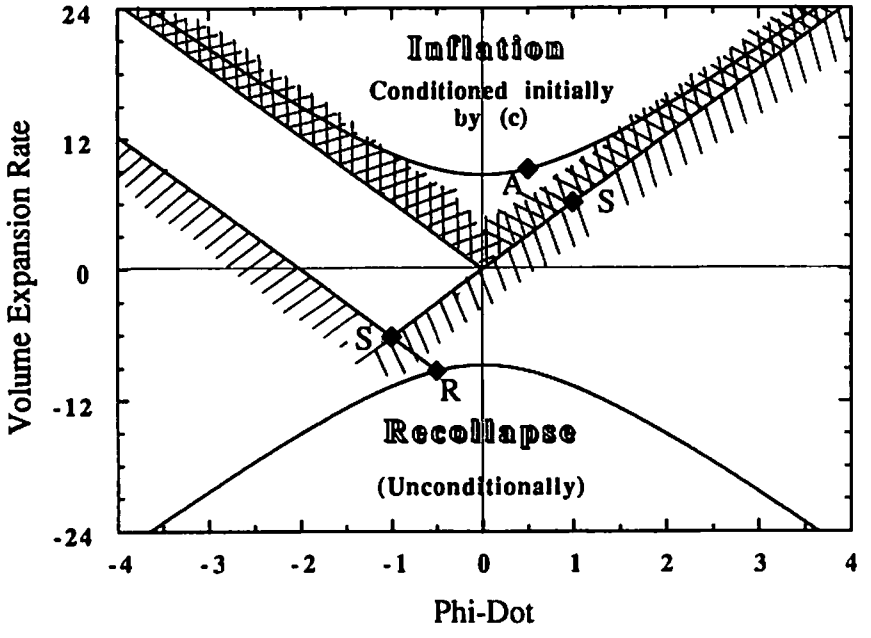

Fig.2.2 Case (ii) $\lambda=\sqrt{2/3}$

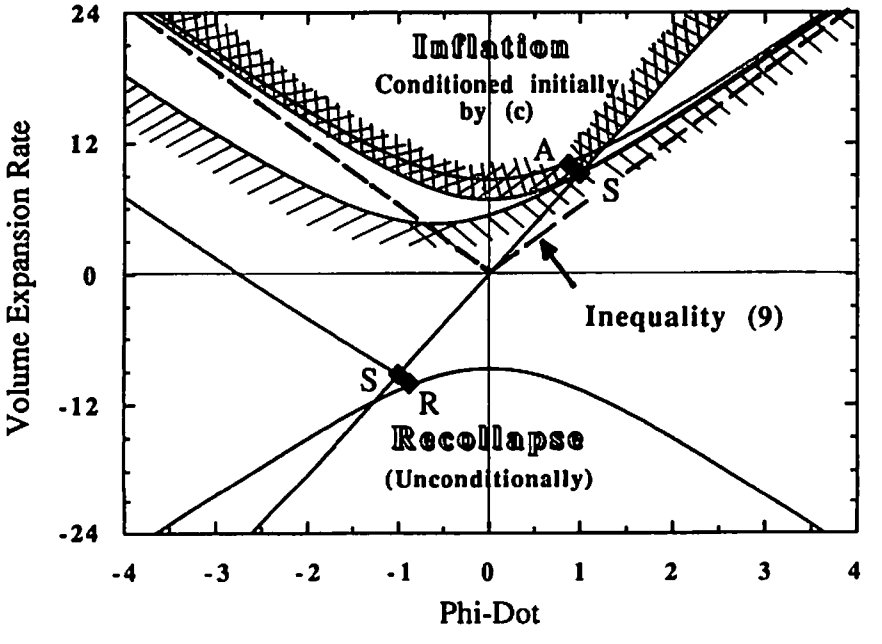

Fig.2.3 Case (iii) $\sqrt{2/3}<\lambda<\sqrt{2}$

Gravitational Waves in a Planar Universe with Cosmological Constant

Hisa-aki Shinkai and Kei-ichi Maeda*
Department of Physics, Waseda University
Shinjuku-ku, Tokyo 169, Japan

January, 1992

Abstract

To investigate the so-called cosmic no hair conjecture, we numerically analyze the behavior of 1-dimensional inhomogeneous space-times. The spacetimes we analyze are to be a plane symmetric and vacuum with a positive cosmological constant. This is a complementary work to the Goldwirth-Piran spherically symmetric case, because their inhomogeneity is due to a matter fluid while ours is due to gravitational waves. We find that the scale of an initial inhomogeneity and its curvature invariant characterize the later evolution of the spacetime. In our simulations, all initial inhomogeneities damp out within one Hubble expansion time, although the curvature invariant increases once in the early stage for which inhomogeneous scale is small compared to the horizon scale.

1 Introduction

The widely accepted inflationary cosmology model [1] is an attempt to solve many long-standing cosmological difficulties—such as the flatness, horizon, monopole and galaxy formation problems—in the standard big-bang model. Although no successful and natural particle physics model has yet been found to support it, we believe that inflation occurred in the early stages of the Universe's history. However, even if we accept the inflationary scenario, we still face one more important and unsolved problem: the explanation of present isotropy and homogeneity of the Universe. In order to see whether inflation, which is usually studied in an isotropic and homogeneous spacetime, is natural, we have to study an inflationary model in anisotropic and inhomogeneous spacetimes as well. If inflation occurs in such spacetimes and homogenizes and isotropizes the universes, then inflation is a universal and natural phenomenon in the history of the Universe.

*BITNET address: maeda@jpnwas00

On the other hand, we know the so-called cosmic no hair conjecture [2]. The conjecture is: "All initially expanding universes with positive cosmological constant Λ approach the de Sitter spacetime asymptotically". There exist, however, simple counter examples. For example, a closed Friedmann-Robertson-Walker spacetime with positive Λ collapses if the initial energy density is large enough. Hence, to prove this conjecture, we have to look for additional criteria.

For homogeneous but anisotropic spacetime, many works have done. Wald [3] showed that initially expanding spacetimes (except Bianchi IX) with positive Λ approach the de Sitter spacetime within one Hubble expansion time $\tau_H = \sqrt{\Lambda/3}$. And for Bianchi IX, with one additional initial condition that Λ be larger than a half of the maximum value of 3-dimensional Ricci scalar, this result is still valid.

For inhomogeneous spacetimes, on the other hand, one practical method we have at present is to solve the Einstein equation numerically. Some groups have already started to investigate this subject. Assuming a spherically symmetric spacetime, Goldwirth and Piran [4] studied the behaviour of inhomogeneous distributions of scalar field and matter. They proposed a criterion for inflation to occur such that

$$\frac{\text{a physical scale of inhomogeneous distribution}}{\text{horizon scale}} > \text{a few times } \frac{\delta\phi}{m_{pl}} \qquad (1)$$

where $\delta\phi$ is a relative spatial deviation of the scalar field to the mean value and m_{pl} is Planck mass. They showed this criterion is true for most chaotic inflationary models but not for any new inflationary model. In the latter case, they found any inhomogeneity prevents the onset of inflation immediately.

In the Einstein theory, however, there are gravitational waves, which are another source for inhomogeneity and have not been, so far, discussed. This type of inhomogeneity due to gravitational waves may play a different role in a homogenization process in an inflationary scenario. In this report, therefore, we analyzed numerically this type of inhomogeneity driven by gravitational waves, especially in the case with 1-dimensional inhomogeneity. Our simulation may be thought of as complementary to the spherically symmetric case discussed by Goldwirth and Piran.

2 Setting the Problem and Numerical Code

To analyze the behaviour of 1-dimensional inhomogeneities due to gravitational waves, we consider the following case:

- Spacetime is vacuum.

- Positive cosmological constant Λ exists.
- Spacetime is plane symmetric so that we can deal with gravitational waves.

Here we mean by plane symmetric that spacetime has two commuting spacelike Killing vectors $(\partial/\partial y, \partial/\partial z)$. Since such a metric allows different behaviour in y- and in z-directions, our definition of "plane symmetry" is not exactly equivalent with the usual mathematical definition (for example, see Kramer *et al.*[5] §13). Under these assumptions, we examine whether such a spacetime leads to an inflationary era, and whether such initial inhomogeneities and anisotropies be smoothed out during inflation periods.

We use the ADM formalism [6,7] to solve the Einstein equation

$$R_{\mu\nu} - \frac{1}{2} g_{\mu\nu} R + \Lambda g_{\mu\nu} = 0, \tag{2}$$

with the metric

$$ds^2 = -(\alpha^2 - e^{-F}\beta^2)dt^2 + 2\beta dt dx + e^F dx^2 + e^H dy^2 + 2L dy dz + e^U dz^2, \tag{3}$$

where the lapse function α, the shift vector $(\beta, 0, 0)$, and the "3-metric" F, H, U and L all depend on only time t and position x. We set the speed of light $c = 1$.

So far, the Texas group [8] has constructed a numerical code for planar cosmology. Their metric is different from (3). They adopt a diagonized spatial metric, which fixes the shift vector.

As for a procedure of simulation, we follow Nakamura *et al.*[9]: (i) Determine initial values by solving the two constraint equations. We use the York-O'Murchadha's formalism [10] to set initial values. (ii) Evolve time slices by using the dynamical equations. (iii) The accuracy of the simulation is checked by the constraint equations. In our all simulations, the accuracy is under 10^{-4} on the initial slice, and decreases monotonically with time steps.

As a measure of inhomogeneity, we use Riemann invariant $I = {}^{(3)}R_{ijkl}\,{}^{(3)}R^{ijkl}$, where ${}^{(3)}R_{ijkl}$ is the Riemann tensor of the 3-metric on the hypersurface Σ [11]. We calculate the ratio of the Riemann invariant I to the cosmological constant Λ,

$$C(t,x) \equiv \frac{\sqrt{{}^{(3)}R_{ijkl}\,{}^{(3)}R^{ijkl}}}{\Lambda} \quad \text{on } \Sigma(t) \tag{4}$$

which we call the "curvature" hereafter. We estimate the strength of inhomogeneities by the maximum value of this "curvature", $C_{\max}(t)$, on each slice. We also define the width l of the distorted range by the proper distance between two points where the 3-volume (trace γ of 3-metric γ_{ij}) drops to a half of its maximum value, γ_{max}, at the center.

The range of the x direction in our computations is several times larger than the width of the distortions initially assumed. We solve the Hamiltonian constraint equation on the initial slice by a fourth order Runge-Kutta method. We use a finite difference method to calculate dynamical evolutions with 400 meshes in the x direction.

3 Evolutions of Pulse-like Inhomogeneities

We may consider two initial complementary situations: (1) The 3-metric is conformally flat and all distortions are produced by the transverse-traceless(TT) part K_{ij}^{TT} of the extrinsic curvature. (2) All distortions are given by the 3-metric γ_{ij} and $K_{ij}^{TT} = 0$. Plane symmetry is, however, not consistent with the case (1). Hence we examine only the case (2) with a pulse-like distortion expressed by the metric in York's conformal frame, defined by $\hat{\gamma}_{ij} = \phi^{-4}\gamma_{ij}$,

$$\hat{\gamma}_{ij} = \begin{pmatrix} 1 - c\, e^{-(x/x_0)^2} & 0 & 0 \\ 0 & 1 - a\, e^{-(x/x_0)^2} & 0 \\ 0 & 0 & 1 \end{pmatrix} \tag{5}$$

where a and x_0 are free parameters but c is fixed so that the conformal scale ϕ is not singular on the boundary. An image of this type of distortion is shown in Fig.1.

We set the trace K of the extrinsic curvature on the initial slice as

$$K = \sqrt{3\Lambda} = \text{const.} \qquad \text{on } \Sigma(t = 0) \tag{6}$$

to make the Hamiltonian constraint simple. The coordinate conditions are imposed as a geodesic slicing $\alpha = 1$ for the time coordinate and $\beta = 0$ for the spatial coordinates.

Giving a and x_0 in (5), an initial form of gravitational waves is determined and the width l and $\mathcal{C}_{\max}(0)$ are calculated. Since a pulse-like wave has two characteristic parameters, a width and an amplitude, we describe those two by the above l and $\mathcal{C}_{\max}(0)$. Since we have one dimensional parameter Λ, we have typical and natural units. So we use the Hubble expansion time $\tau_H = \sqrt{\Lambda/3}$ as our time unit, which is a characteristic expansion time of the expanding Universe. And our unit of length is also normalized to the horizon length of the de Sitter universe $l_H = (\Lambda/3)^{-1/2}$. Ranges of l and $\mathcal{C}_{\max}(0)$ calculated here are $0.040 l_H \leq l \leq 1.8 l_H$. $0.220 \leq \mathcal{C}_{\max}(0) \leq 13.1$.

In Fig.2 we show a typical time evolution of the "curvature" $\mathcal{C}(t, x)$ corresponding to $l = 0.14 l_H$ and $\mathcal{C}_{\max}(0) = 0.88$. The dotted line shows $\mathcal{C}(0, x)$, and the dashed and solid line shows $\mathcal{C}(t, x)$ at $t = 0.137\tau$ and 0.271τ, respectively. We see that the initial inhomogeneity is decaying and is almost smoothed out within 0.3τ, and this final stage is commonly seen in all simulations we tried.

Changing the width of the initial pulse, we display evolutions of $\mathcal{C}_{\max}(t)$ for $\mathcal{C}_{\max}(0) =$ 1.0 (Fig.3(a)) and $\mathcal{C}_{\max}(0) = 2.0$ (Fig.3(b)). In both cases, as the initial width becomes greater, the slower homogenization proceeds monotonically. While as the width gets narrower, we see $\mathcal{C}_{\max}(t)$ goes to a growing phase for a while after it starts decaying. In particular for the case of $\mathcal{C}_{\max}(0) = 2.0$ in Fig.3(b), we find "curvature" is enhanced beyond its initial given value. This growth of inhomogeneities may be an effect of the nonlinearity of gravity, which is suppressed later by the expansion of the Universe due to the cosmological constant.

Fig.3 indicates that such a nonlinear effect of gravity, which may produce a singularity, appears for a narrow-width pulse. To test for such a possibility, we search a wide range of the parameters, l and $\mathcal{C}_{\max}(0)$. All the results we get are summarized on the "curvature"-width plane in Fig.4. From this figure, we can classify the evolutions of the "curvature" into four types: (1) $\mathcal{C}_{\max}(t)$ decays monotonically (dotted with o), (2) $\mathcal{C}_{\max}(t)$ stays constant for a while or grows up little like the dotted line in Fig.3(a) (dotted with • in Fig.4), (3) $\mathcal{C}_{\max}(t)$ is once enhanced larger than its initial $\mathcal{C}_{\max}(0)$ like the dotted line in Fig.3(b) (dotted with $\triangle$), and (4) "curvature" starts growing up from the beginning (dotted with $\times$). The results depend strongly on the width l, but very weakly on $\mathcal{C}_{\max}(0)$. From this fact, we conclude that it is the width of an initial distortion that characterizes its time evolution. Although the chosen values of the parameters in Fig.4 are restricted, we believe that we are able to deal with the nonlinear effects of gravity enough to check the reliability of the cosmic no hair conjecture.

The same phenomena were found in the case of another form of gravitational waves, *i.e.*, $(1 + a\cos^2(x/x_0))$-type in the (xx) and (yy) components in (5).

4 Discussion

We examined the evolution of inhomogeneities driven by gravitational waves in plane symmetric vacuum spacetimes with a cosmological constant. We assumed a one-dimensional pulse-like distortion of space and integrated the Einstein equations, calculating the "curvature" (the ratio of Riemann invariant to the cosmological constant) as a measure of the strength of the inhomogeneity. For a wide range of widths and "curvatures" present initially, all inhomogeneities decay below 5 % of their initial "curvatures" within 0.3 Hubble expansion times.

A temporal growth of the "curvature" in earlier stages for some sharp pulses was found, which may be a reflection of the nonlinear effects of gravity. However the expansion of the Universe later overcomes this nonlinearity.

The result that all initial inhomogeneities we assumed decay and disappear does not give any additional condition to the cosmic no hair conjecture, but it gives a strong and positive support to the conjecture. This result, however, does not agree with that by Goldwirth and Piran [4] who simulated effects of inhomogeneities due to a matter field. We have not yet determined whether our results are characteristic behaviors of inhomogeneities driven by gravitational waves, or due to our ansatz of plane symmetry. In order to answer these questions, further simulations including matter or a scalar field, or in some other or more general spacetimes—for example, cylindrical or axially symmetric or fully 3-dimensional—are required. It is one direction of our future works.

Acknowledgement

H.S. would like to thank Dr. Laurens D.Gunnarsen for useful discussions and his careful reading of our report. This work was supported partially by the Grant-in-Aid for Scientific Research Fund of the Ministry of Education, Science and Culture Nos. 02640238 and 03250213.

References

[1] The original idea is in
A.H. Guth, Phys. Rev. **D23**, 347 (1981);
K. Sato, Mon. Not. Roy. Astron. Soc. **195**, 467 (1981).
Reviews are, *e.g.*,
S.K.Blau, A.H.Guth, in *300 Years of Gravitation*, ed. by S.Hawking and W.Israel, (Cambridge, 1987);
K. Olive, Phys. Rep. **190**, 309 (1990).

[2] The original idea is in
G.W.Gibbons, S.W.Hawking, Phys. Rev. **D15**, 2738 (1977);
S.W.Hawking, I.G.Moss, Phys. Lett. **110B**, 35 (1982); Nucl. Phys. **B224** 180 (1983);
W.Boucher, G.W.Gibbons, in *The Very Early Universe*, ed. by G.W.Gibbons, S.W.Hawking and S.T.Siklos, p.273 (Cambridge, 1983);
W.Boucher, G.W.Gibbons, G.T.Horowitz, Phys. Rev. **D30**, 2447 (1984).
Reviews are, *e.g.*,
K.Maeda, in the Proceedings of the Yamada Conference XX on *Big Bang, Active Galactic Nuclei and Supernovae*, ed. by S.Hayakawa and K.Sato, p.51 (Universal Academy Press, 1988); in the Proceedings of 5th Marcel Grossman Meetings, ed. by R.Ruffini, p.145 (World Scientific, 1989);
K.Sato, in the Proceedings of I.A.U. Symposium No.130, *The Large Scale Structure of the Universe*, ed.by J.Audouze *et al.*, p.67 (IAU, 1988)

[3] R.M.Wald, Phys. Rev. **D28**, 2118 (1983)

[4] D.S.Goldwirth and T.Piran, Phys. Rev. **D40**, 3263 (1989); Phys. Rev. Lett. **64**, 2852 (1990); Gen. Rel. Grav. **23**, 7 (1991)
D.S. Goldwirth, Phys. Lett. **B243**, 41 (1990); Phys. Rev. **D43**, 3204 (1991)

[5] D.Kramer, H.Stephani, M.MacCallum and E.Herlt, *Exact solutions of Einstein's field equations*, (Cambridge, 1980)

[6] R.Arnowitt, S.Deser and C.W.Misner, in *Gravitation: An Introduction to Current Research*, ed. by L.Witten, (Wiley, New York,1962)

[7] J.W.York,Jr., in *Sources of Gravitational Radiation*, ed. by L.Smarr, (Cambridge, 1979) ;
L.Smarr and J.W.York,Jr., Phys. Rev. **D17**, 2529 (1978)

[8] P.Anninos, J.M.Centrella, R.A.Matzner, Phys. Rev. **D39**, 2155 (1989);
in *Frontiers in Numerical Relativity*, ed. by C.R.Evans, L.S.Finn and D.W.Hobil, (Cambridge, 1989); Phys. Rev. **D43**, 1808 (1991); Phys. Rev. **D43**, 1825 (1991)

[9] T.Nakamura, K.Maeda, S.Miyama and M.Sasaki, Prog. Theo. Phys. **63**, 1229 (1980)

[10] N.O'Murchadha and J.W.York,Jr., Phys. Rev. **D10**, 428 (1974)

[11] K.Nakao, T.Nakamura, K.Oohara and K.Maeda, Phys. Rev. **D43**, 1788 (1991)

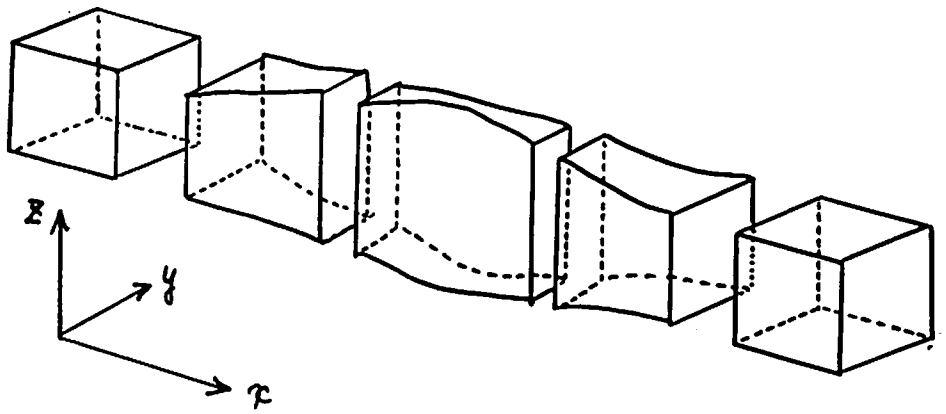

Figure 1: An image of assumed distortion at the initial time. Physical scale of space that expressed by the present metric is drawn on a virtual flat coordinate.

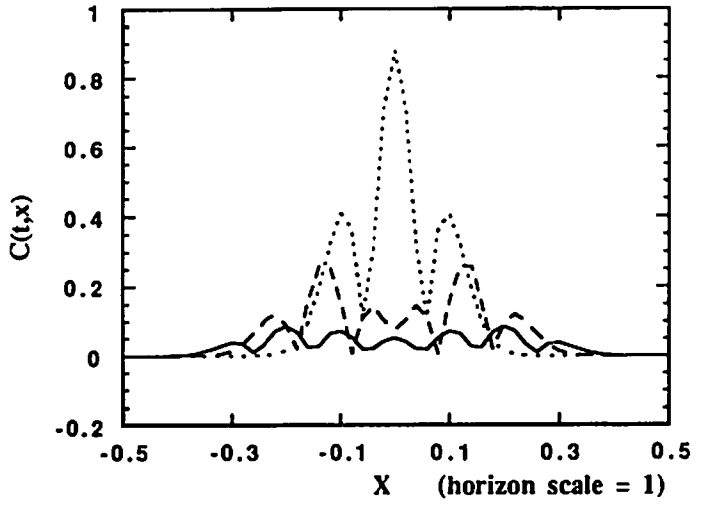

Figure 2: Spatial profiles of "curvature" $C(t,x)$ for the case of initial width $l = 0.07 l_H$, and an amplitude $a = 0.1$. The dotted line shows initial state ($t = 0$), the dashed line and the solid line correspond to $t = 0.137\tau_H$ and $t = 0.271\tau_H$, respectively.

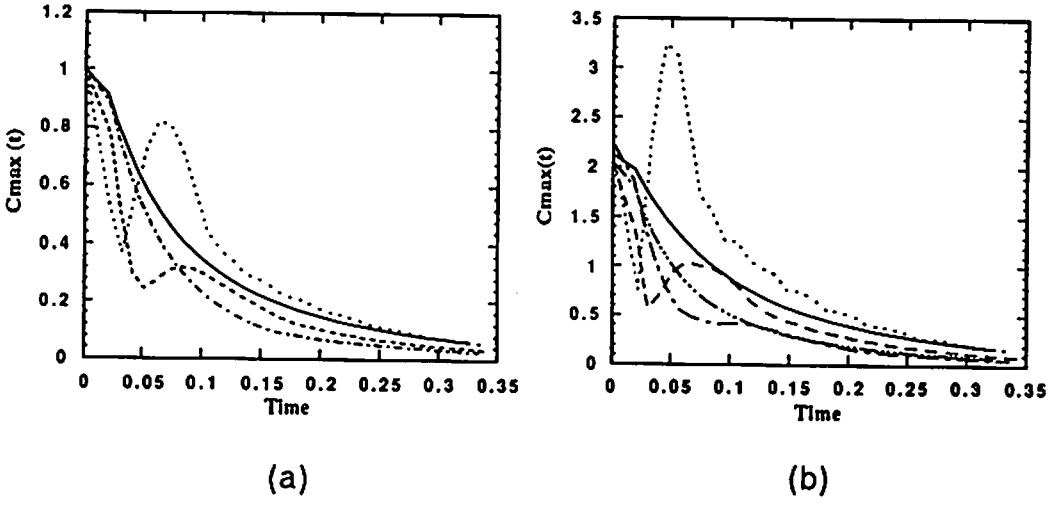

Figure 3: Evolutions of $C_{max}(t)$ for the initial data with the same "curvature" $C_{max}(0)$ but different width l. (a) $C_{max}(0) = 1.00$, l=0.14 (dotted line), 0.23 (dashed line), 0.48 (dot-dashed line), 0.97 (solid line). (b) $C_{max}(0) = 2.00$, l=0.088 (dotted line), 0.16 (dashed line), 0.31 (dot-dashed line), 0.68 (three-dot and solid line), 1.80 (solid line).

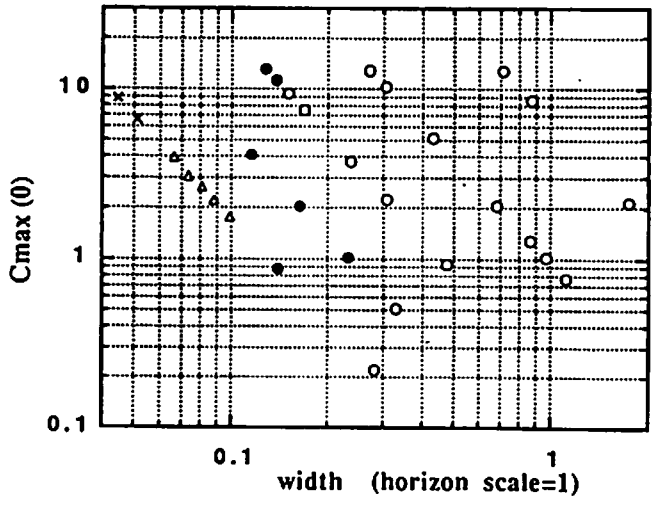

Figure 4: All results are summarized on (width-"curvature") plane. They are classified into four types: (1) monotonous decaying are found at o, (2) small nonlinear effects are discovered at •, (3) "curvature" grows up larger than the initial $C_{max}(0)$ at Δ data and (4) at $\times$ we see "curvature" starts growing up from the beginning.

Decaying Cosmological Constant and Inflation

Tsuyoshi Nishioka and Yasunori Fujii
Institute of Physics, University of Tokyo-Komaba, Tokyo, Japan

The cosmological constant is a problem because it requires an extreme fine-tuning or cancellation to the unimaginable order of 120 or so. One of the natural ways out is the scenario of a decaying cosmological constant;[1,2,3,4] $\Lambda \sim t^{-2}$. We use the unit system $c = \hbar = 8\pi G = 1$. The present age of the universe is $t \cong 14\mathrm{Gyr} = 1.68 \times 10^{60}$, hence giving $\Lambda \sim 10^{-120} = 10^{-57}\mathrm{cm}^{-2}$. According to this idea, the present-day cosmological constant is small only because our universe is old.

This idea is implemented by a scalar field ϕ which has a nonminimal gravitational coupling. The field is much like the JBD field, and will be called a "gravitational scalar field." It appears that the gravitational constant also decays with time. This is not only in conflict with the observed constancy of G, but also invites a cynical comment; how is Λ a worry in the world without gravity? The question is, however, ill-addressed. One can always go to a conformal frame (CF) in which G is a true constant. The real question is if Λ in this CF still decays with time.

We start with a generalized scalar-tensor theory with the cosmological constant Λ;[2,4]

$$\mathcal{L} = \sqrt{-g}\left[\frac{1}{2}F_G(\phi)R - \frac{1}{2}F_K(\phi)g^{\mu\nu}\partial_\mu\phi\partial_\nu\phi - \Lambda\right] + \mathcal{L}_{\mathrm{matter}} + \mathcal{L}_{\mathrm{coupling}}, \tag{1}$$

where we choose

$$F_G = 1 + \xi\phi^2, \tag{2}$$

and

$$F_K = (1 + \chi\xi\phi^2)/F_G, \tag{3}$$

for simplicity (ξ and χ are constants). The essential behavior of F_K is

$$F_K(\phi) = \begin{cases} 1 & \xi\phi^2 \ll 1 \\ \chi & \xi\phi^2 \gg 1. \end{cases} \tag{4}$$

The constant χ may not be positive because ϕ is not a canonical field. Even if χ is negative, ϕ is not necessarily a ghost. Later we choose a negative χ, to obtain successful cosmology, in the choice of which ϕ is not a ghost because another contribution to the kinetic term of ϕ is induced from the nonminimal coupling.

The effective gravitational constant is given by $G_{\rm eff} = (8\pi F_G)^{-1}$ and changes with time. The observed upper bound on $\dot{G}/G$, however, seems to exclude such time variability of G.[5] Moreover, it is hard to understand the real nature of ϕ because ϕ is not a canonical field. To avoid these difficulties we apply a conformal transformation

$$g_{\mu\nu} \to g_{*\mu\nu}; \qquad g_{\mu\nu} = F_G^{-1} g_{*\mu\nu}, \tag{5}$$

such that the curvature scalar is multiplied by a pure constant;

$$\mathcal{L} = \sqrt{-g_*}\left[\frac{1}{2}R_* - \frac{1}{2}g_*^{\mu\nu}\partial_\mu\sigma\partial_\nu\sigma - \Lambda F_G^{-2}\right] + \mathcal{L}_{*\rm matter} + \mathcal{L}_{*\rm coupling}, \tag{6}$$

where σ is the new canonical field defined by

$$\frac{d\sigma}{d\phi} = F_G^{-1}\sqrt{D}; \qquad D = 1 + (\chi + 6\xi)\xi\phi^2. \tag{7}$$

If this D is negative, then σ is a ghost. We avoid this by imposing a condition $\chi \geq -6\xi$ to ensure that σ is a canonical field. Our choice of χ satisfies this condition. From (2),(7), the relation between σ and ϕ is given by

$$\phi \approx \sigma \qquad \xi\sigma^2 \ll 1, \tag{8}$$

and

$$\phi \sim \exp\left(\frac{\sigma}{4\kappa}\right) \qquad \xi\sigma^2 \gg 1, \tag{9}$$

where $\kappa = \sqrt{6 + \chi\xi^{-1}}/4$.

We must also pay attention to masses of fermion fields representing ordinary matter fields in the new CF. We introduce a simple Yukawa coupling of ϕ to a fermion field ψ from which mass term of the fermion is derived;

$$\mathcal{L}_{\text{coupling}} = -\sqrt{-g} f \bar{\psi}\psi\phi. \tag{10}$$

This coupling is as weak as gravity and the mass is constant asymptotically after the conformal transformation $\psi = F_G^{3/4}\psi_*$;

$$m_{\psi_*} = f\phi F_G^{-1/2} \to f\xi^{-1/2}. \tag{11}$$

For these reasons we reasonably anticipate that we are in the starred CF. Since we expect that m_{ψ_*} is $O(1\text{GeV})$, we must choose a very small $f \sim O(10^{-19})$; the coupling is too weak to reheat the universe after inflation.

The constant term Λ is multiplied by a function of ϕ;

$$V = \Lambda F_G^{-2}. \tag{12}$$

This serves as a potential of the scalar field. A reasonable assumption on $F_G(\phi)$ leads to a potential falling off monotonically toward the asymptotic value zero. The scalar field goes down the hill slowly to infinity, hence resulting in the decay of the effective cosmological constant. The absence of the minimum of the potential is essential to the successful decay scenario. Using (8),(9), we find that the potential (12) as a function of σ is given by

$$V(\sigma) = \Lambda(1 - 2\xi\sigma^2), \qquad \xi\sigma^2 \ll 1, \tag{13}$$

and

$$V(\sigma) \sim \exp\left(-\frac{\sigma}{\kappa}\right), \qquad \xi\sigma^2 \gg 1. \tag{14}$$

Since we reasonably assume that the initial value of σ is Planck scale at the Planck time, sufficient inflation is expected to occur in the early epoch if ξ is sufficient

small $\sim O(10^{-2})$ from (13). In the late epochs the potential (14) is an exponential potential of σ and we find that we must choose an appropriate χ ($-6\xi < \chi < -2\xi$) to obtain the radiation-dominant universe. Successful cosmology (primordial nucleosynthesis), hence, excludes a usual and simple kinetic term of $\phi(F_K = 1)$ requiring an extended form with $\chi < 0$.[6]

We point out that the cosmological constant in this CF can be large enough in the past to cause inflation. Historically, the inflaton, a scalar field expected to drive inflation followed by reheating, has been recruited from the list of the fields in the standard model of elementary particles. The inflaton of this type, e.g. the Higgs, differs from the gravitational scalar field we considered above in two respects. One is that the usual inflaton potential has a minimum; there is no guarantee that the value of the potential at this minimum is exactly equal to zero (or extremely small), hence raising the cosmological constant problem. As the second difference, the ordinary inflaton couples to other fields rather strongly, hence producing sufficient reheating, whereas the gravitational scalar field has a much weaker coupling, nearly as weak as gravity.

We point out that there is a natural coupling of this gravitational scalar field to another scalar field Φ, like the Higgs scalar, after the conformal transformation $\Phi = F_G^{1/2}\Phi_*$;

$$\mathcal{L}_{\text{kin}\Phi} = \sqrt{-g}\left(-\frac{1}{2}g^{\mu\nu}\partial_\mu\Phi\partial_\nu\Phi\right) \tag{15}$$

$$= \sqrt{-g_*}\left(-\frac{1}{2}g_*^{\mu\nu}D_\mu\Phi_*D_\nu\Phi_*\right), \tag{16}$$

where $D_\mu = \partial_\mu + (1/2)\partial_\mu(\ln F_G)$. This coupling, derived from conformal noninvariance of the kinetic term of a spinless field, contains derivatives, and hence is sufficiently strong to give reheating in the early epoch but is as weak as the gravitational interaction in late epochs. Spinor and vector fields do not have this kind of coupling. In many models including those discussed previously,[2] a dissipative term

which converts the energy of the inflaton field to the radiation energy has been introduced by hand. To take the derivative coupling nature correctly into account, we derive the dissipative term explicitly based on the quantum theory.[4] Among many methods proposed, we choose the Morikawa-Sasaki-Ringwald recipe[7] which allows us to calculate the backreaction of quantum fluctuations of the gravitational scalar field. We limit our calculation to the one-loop order in an adiabatic approximation.

We solved the cosmological equations numerically by using this dissipative term. We show an example in Fig.1, plotting a, ϕ, ρ_r/ρ, p_v/ρ_v, ρ_r and ρ_v vs. t for $\Lambda = 1$, $\xi = 0.8 \times 10^{-2}$, $\chi = -4.48 \times 10^{-2}$ and the initial value $\phi = \dot{\phi} = 1$ at $t = 1$ where $p_v = \dot{\sigma}^2/2 - V$ is the "pressure" of the vacuum. These values of ξ and χ have been chosen to obtain sufficient inflation and successful primordial nucleosynthesis, respectively.

We find: (i) An exponential growth of $a(t)$ to $\gtrsim e^{60}$ ending at $t_1 \sim 10^3$ (in units of the Planck time) emerges naturally from the potential V with (13) having a "plateau". From t_1 to $t_2 \sim 10^{17}$ the scale factor a evolves according to a power-law $\sim t^{1/3}$ and expands like $\sim t^{1/2}$ after t_2. By the way, primordial nucleosynthesis occurs at about $t \sim 10^{45}$ and non-relativistic matter energy becomes dominant at $t = t_{eq} \sim 10^{54}$. This example, hence, reproduces successful cosmology.

(ii) The scalar field ϕ also grows exponentially until t_1. The asymptotic solution $\phi \sim t^{1/2}$ begins at $t_4 \sim 10^{40}$. Note that ϕ stays nearly constant from t_2 to t_4 owing to non-linear effects.

(iii) The curve of ρ_r/ρ shows that the radiation energy becomes dominant after t_2 and begins to converge to the asymptotic value around t_4. Notice the corresponding behaviors of a and ϕ at t_2 and t_4. The ratio p_v/ρ_v, so to say, representing an equation of state of the vacuum, shows a very interesting behavior due to non-linear effects. This behavior is often called a "relaxation oscillation" and is one of common phenomena in nature. Most interesting is the behavior between $t_3 \sim 10^{32}$

and t_4 showing that ρ_v behaves like a "suspending" cosmological constant. Around t_4, p_v/ρ_v begins to damped-oscillate as a function of $\ln t$ and finally settles to 1/3. It is interesting to notice that the vacuum ρ_v does not claim its own "equation of state." It adjusts itself always to obey the same equation of state which we assume for the matter.

(iv) After the end of inflation, dissipation quickly pushes up ρ_r which had supercooled. The dissipative interaction, however, begins to dwindle, as was expected. Also the growth of $a(t)$ is still quite fast. As a consequence ρ_r shows a rapid decrease, leaving a spike-like behavior. It then starts decreasing slowly like $\sim t^{-4/3}$ at t_1. Combining this with the power-law expansion $a(t) \sim t^{1/3}$ from t_1 to t_2, we find that entropy production is no longer appreciable. We may define the reheating temperature T_{reh} by ρ_r at the onset of this power-law behavior. We find that sufficient reheating $T_{reh} \sim 10^{14}$GeV can be obtained in this mechanism despite the absence of an oscillating phase.

(v) The energy density of the vacuum ρ_v behaves like a "cosmological constant" at the beginning and decays like $\sim t^{-2}$ from t_1 to t_2 and like $\sim t^{-8/3}$ from t_2 to t_3. Again it behaves like a "cosmological constant" from t_3 to t_4 and the asymptotic solution ($\sim t^{-2}$) begins after t_4. This behavior may provide a natural explanation of the present cosmological constant which is 10^{-120} times as small as m_{Pl}^4.

Many features sketched above are quite general, insensitive to the choice of parameters and initial conditions, given the rate of the inflationary expansion and the asymptotic value of ρ_v/ρ.

In Fig.2, we show an example in which the suspending cosmological constant equals about 10^{-120}. Unfortunately this suspending cosmological constant is too small to make up the difference between the recently observed small Ω and the prediction $\Omega = 1$ from inflation. Some "recent evidences" for the nonzero Λ,[8,9,10] however, can be explained by introducing another scalar field.[11]

To summarize, a gravitational scalar field is responsible for causing inflation, providing sufficient reheating and relaxing the cosmological constant.

References

1. Y.Fujii, Phys.Rev.**D26**(1982)2580.
   A.D.Dolgov, in *The Very Early Universe*, Proc. Nuffield Workshop, England, 1982, edited by G.W.Gibbons and S.T.Siklos (Cambridge University Press, Cambridge, England, 1982).
   L.H.Ford, Phys.Rev.**D35**(1987)2339.

2. Y.Fujii and T.Nishioka, Phys.Rev.**D42**(1990)361.

3. Y.Fujii and J.M.Niedra, Prog.Theor.Phys.**70**(1983)412.
   Y.Fujii, Mod.Phys.Lett.**A.4**(1989)513.
   Y.Fujii and Y.Okada, Univ. of Tokyo Rep. No. UT-Komaba 85-1,1985 (unpublished).
   O.Bertolami, Nuovo Cimento.**93B**(1985)36.
   R.D.Peccei,J.Sola, and C.Wetterich, Phys.Lett.**B195**(1987)183.
   C.Wetterich, Nucl.Phys.**B302**(1988)645; **B302**(1988)668.
   M.Endou and T.Fukui, Gen.Relativ.Gravit.**8**(1977)833.

4. T.Nishioka and Y.Fujii, to be appeared in Brief Report of Phys.Rev.

5. R.W.Hellings et al., Phys.Rev.Lett.**51**(1983)1609

6. K.Sato et al., in *The Quest for the Fundamental Constants in Cosmology*, Poc. of the IXth Moriond Astrophysics Meeting, edited by J.Audouze. Publisher City 1989.
   K.Freese et al., Nucl.Phys.**B287**(1987)797.

7. M.Morikawa and M.Sasaki, Prog.Theor.Phys.**72** (1984)782.
A.Ringwald, Ann.Phys.**177**(1987)129.

8. M.Fukugita et.al.,Ap.J.**361**,L1(1990).

9. G.Efstathiou et al., Nature**348**(1990)705.

10. K.Tomita and C.Hayashi, Prog.Theor.Phys.**30**(1963)691.

11. Y.Fujii and T.Nishioka, Phys.Lett.**B254**(1991)347.

Figure Captions

Fig.1: An example of the numerical solutions a, ϕ, ρ's and p_v plotted against $\log_{10} t$, with in units of the Planck time. (The epoch of nucleosynthesis, the end of the radiation-dominated universe and the present age correspond roughly to 45, 54 and 60, respectively, on the abscissa.) Parameters chosen are $\Lambda = 1$, $\xi = 0.8 \times 10^{-2}$ and $\chi = -4.48 \times 10^{-2}$ in the unit system of $8\pi G = 1$. Initial conditions are given by $\phi = 1$, $\dot{\phi} = 1$ and $\rho_r = 1$ at $t = 1$.

Fig.2: An example with $\chi = -4.692 \times 10^{-2}$ with the same values of the other parameters as in Fig.1. The example shows that the "suspending cosmological constant" equals about 10^{-120}.

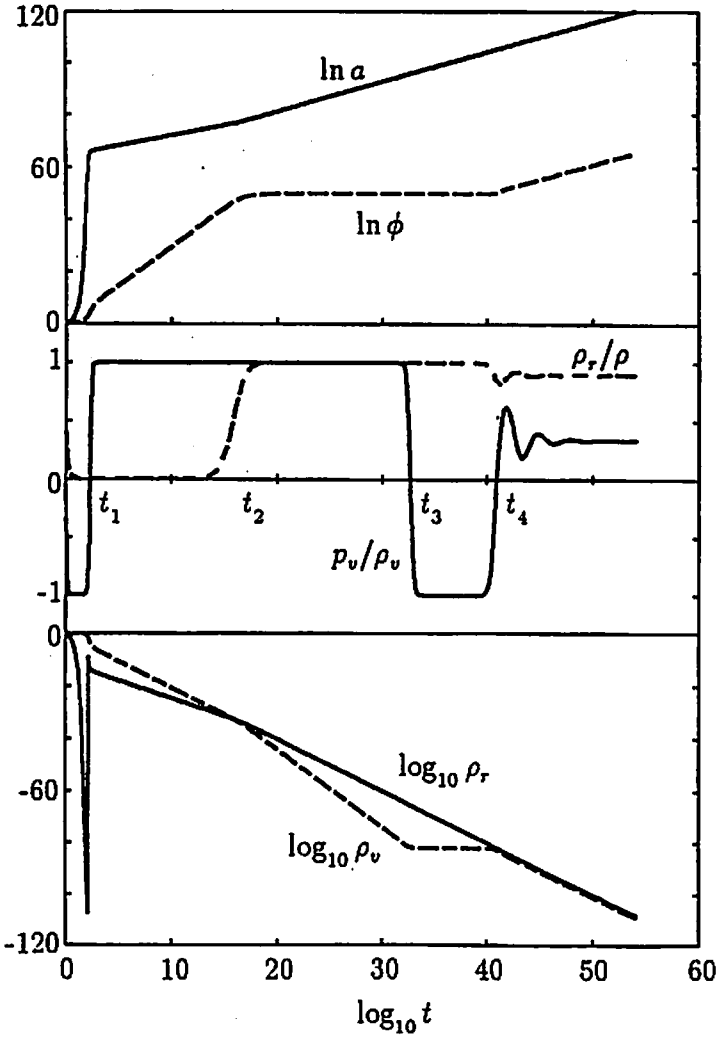
120
60
0
ln a
ln φ
1
0
-1
ρ_r/ρ
t_1
t_2
t_3
t_4
p_υ/ρ_υ
0
-60
-120
log_10 ρ_r
log_10 ρ_υ
0
10
20
30
40
50
60
log_10 t

Fig.1

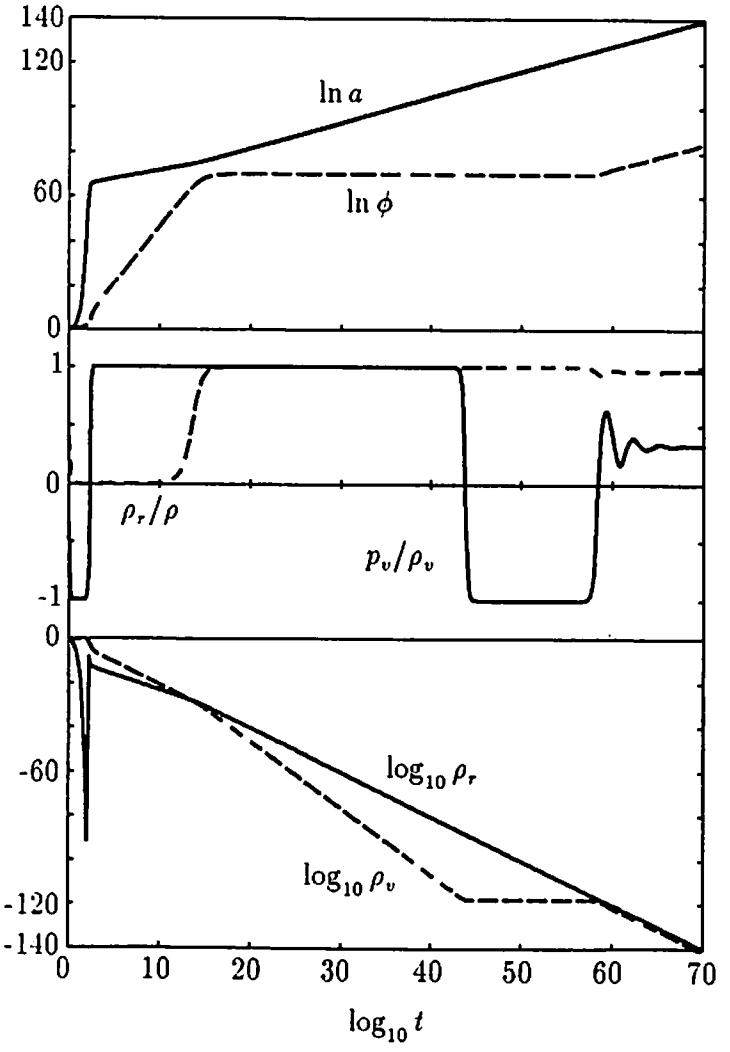
140
120
60
0
ln a
ln φ
1
0
-1
ρr/ρ
pv/ρv
0
-60
-120
-140
log10 ρr
log10 ρv
0
10
20
30
40
50
60
70
log10 t

Fig.2

Gluing Schwarzschild-deSitter Space-Times along the Null Shells

Jiro SODA

Uji Research Center
Yukawa Institute for Theoretical Physics
Kyoto University, Uji 611, Japan

Dray-t'Hooft showed how to join two Schwarzschild space-times, possibly of different masses, along a null cylinder representing a spherical shell of massless matter.[1] They then showed how to join four Schwarzschild regions by colliding two such shells. Dray and Joshi generalized their results by showing how to join Reissner-Nordström space-times along null cylinders corresponding to charged, pressureless dust clouds moving at the speed of light.[2] In this work, we further extend their works to the cosmological context, *i.e.*the Schwarzschild-deSitter space-time.

Let us introduce coordinates $\tilde{U}$ and $\tilde{V}$, which are labels for outgoing and ingoing, radial, null geodesics;

$$ds^2 = 0 = -(1 - \frac{2m}{r} - H^2r^2)dt^2 + (1 - \frac{2m}{r} - H^2r^2)^{-1}dr^2. \qquad (1)$$

More precisely, outgoing geodesics are given by $\tilde{U} = const$, where

$$\tilde{U} = t - r^* \qquad (2)$$

and ingoing geodesics are given by $\tilde{V} = const$, where

$$\tilde{V} = t + r^*. \tag{3}$$

Here

$$r^* = \mu_- \log \mid \frac{r}{r_-} - 1 \mid + \mu_S \log \mid \frac{r}{r_S} - 1 \mid + \mu_D \log \mid \frac{r}{r_D} - 1 \mid \ . \tag{4}$$

The radius r_-, r_S and r_D are determined by

$$\begin{aligned} f(r) &= r^3 - \frac{1}{H^2} r + \frac{2m}{H^2} \\ &= (r - r_-)(r - r_S)(r - r_D), \qquad r_- < 0 < r_S < r_D \ , \end{aligned} \tag{5}$$

and μ_-, μ_S and μ_D are defined as

$$\begin{aligned} \mu_- &= -\frac{1}{H^2} \frac{r_-}{(r_- - r_S)(r_- - r_D)} < 0, \\ \mu_S &= -\frac{1}{H^2} \frac{r_S}{(r_S - r_-)(r_S - r_D)} > 0, \\ \mu_D &= -\frac{1}{H^2} \frac{r_D}{(r_D - r_-)(r_D - r_S)} < 0. \end{aligned} \tag{6}$$

Now we are in a position to introduce the Gibbons-Hawking coordinate system;

$$\begin{aligned} u &= -\exp[-\frac{\tilde{U}}{2\mu_S}] \ , \\ v &= \exp[\frac{\tilde{V}}{2\mu_S}] \ . \end{aligned} \tag{7}$$

At this point, we treated the Schwarzschild horizon specially. The resulting

metric is

$$ds^2 = \frac{4H^2\mu_S^2 f(r)}{rG_S(r)}dudv + r^2 d\Omega^2 \ , \tag{8}$$

where r is implicitly defined by

$$-uv = G_S(r) = (\frac{r}{r_-} - 1)^{\frac{\mu_-}{\mu_S}}(\frac{r}{r_S} - 1)(\frac{r}{r_D} - 1)^{\frac{\mu_D}{\mu_S}}. \tag{9}$$

In this coordinate system, the coordinate singularity at r_S disappears although another coordinate singularity remains. Of course, the converse treatment is also possible.

The Penrose diagram is obtained by the appropriate conformal transformation and is shown in Fig.1.

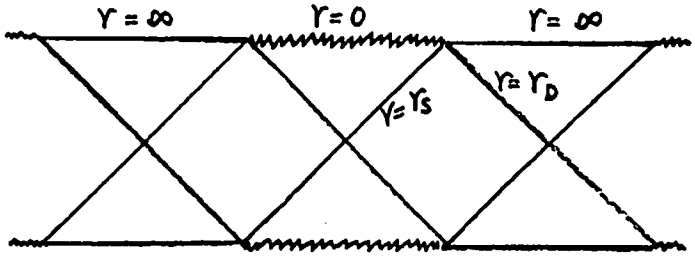

Fig. 1

We now join two Schwarzschild-deSitter space-times of different masses and cosmological constants, with metrics given by

$$\begin{aligned} ds^2 &= \frac{4H^2\mu_S^2 f(r)}{rG_S(r)}dudv + r^2 d\Omega^2, \quad (u \leq \alpha), \\ ds^2 &= \frac{4H^2\mu_S^2 f(r)}{rG_S(r)}dUdV + r^2 d\Omega^2, \quad (u \geq \alpha), \end{aligned} \tag{10}$$

where $U = U(u), U(\alpha) = \beta, V = V(v)$, and

$$\begin{aligned} -uv &= G_S(r), \quad (u \leq \alpha), \\ -UV &= \bar{G}_S(r), \quad (u \geq \alpha). \end{aligned} \tag{11}$$

Here, the bared quantities denote that of replacing the H, m in terms of $\bar{H}, \bar{m}$. As we want to match the metrics at $u = \alpha$, the following conditions are imposed

$$\frac{\alpha}{\mu_S} = \frac{\beta}{\bar{\mu}_S U'(\alpha)} = \gamma_S. \tag{12}$$

From the continuous but not smooth space-time,

$$g_{ab} = (1 - \theta(u - \alpha))g^-_{ab} + \theta(u - \alpha)g^+_{ab}, \tag{13}$$

we can easily compute the Ricci tensor. The only non-zero component is

$$R_{uu} = -\frac{2}{r}[\frac{\partial r}{\partial u}]\delta(u - \alpha), \tag{14}$$

where $[Q] \equiv \lim_{u\to\alpha^+} Q - \lim_{u\to\alpha^-} Q$. In the present case, we obtain

$$\begin{aligned} R_{uu} = \frac{2}{\gamma_S r}\left[\frac{2(\bar{m} - m)}{r} + (\bar{H}^2 - H^2)r^2\right]\delta(u - \alpha) \\ + \text{regular terms}, \end{aligned} \tag{15}$$

where we used the junction condition (12) in the above calculation.

From eq.(15), the interesting results can be extracted. If we assume $\alpha < 0$ then $\gamma_S < 0$. And we assume $m > \bar{m}, \bar{H} > H$, the eq.(15) becomes

$$R_{uu} = \frac{2}{|\gamma_S| r}\left[\frac{2(m-\bar{m})}{r} - (\bar{H}^2 - H^2)r^2\right]\delta(u-\alpha) + \text{regular terms.} \tag{16}$$

The curvature (16) changes its sign at the point

$$r_0^3 = \frac{2(m-\bar{m})}{\bar{H}^2 - H^2}, \tag{17}$$

hence the radius r larger than r_0 is physically excluded. How to interpret this result is similar to that of Reisner-Nortström.[2] As we imposed the light velocities on the shell motion, we get the apparent contradiction. That point must be the turning point of the shell motion. To confirm this observation, we shall examine the collision of the shells. (Fig.2)

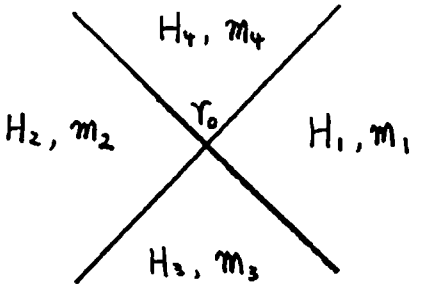

Fig. 2

To remove the conical singularity at r_0, we must impose the consistency

condition

$$(1-\frac{2m_1}{r_0}-H_1^2r_0^2)(1-\frac{2m_2}{r_0}-H_2^2r_0^2)=(1-\frac{2m_3}{r_0}-H_3^2r_0^2)(1-\frac{2m_4}{r_0}-H_4^2r_0^2). \quad (18)$$

If we consider the case, $m_1 = m_3 = m_4 = m, m_2 = \bar{m}, H_1 = H_3 = H_4 = H, H_2 = \bar{H}$, the eq.(18) reduces to the eq.(17). This situation can be understood as in Fig.3.

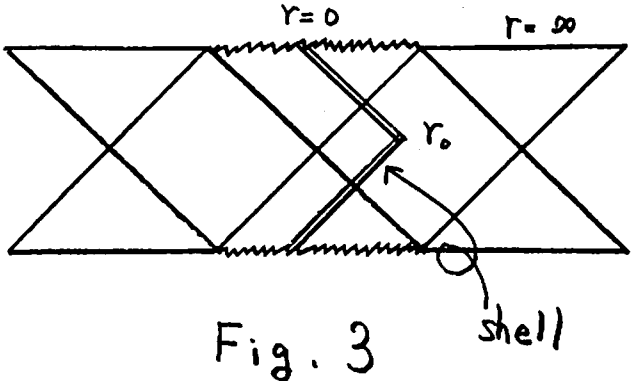

Fig. 3

In this work, we have shown what condition must be imposed for gluing two Schwarzschild-deSitter space-times. To keep the positivity of the energy, it turns out that the collision of two such shells must be considered. As a result, the qualitative aspects of the dynamics of the shells are understood from that of the null shells. Consideration of the extreme situation such as the null shells makes the analysis of the shell dynamics simple. So it naturally leads us to the study of the quantum counterpart of this analysis. Up to now, we know that the homogeneous and isotropic universe can be quantized using a mini-superspace model. If we include the matter fields and inhomogeneity, the problem becomes tremendously difficult. As for this direction, the quantization of the null shell model is of interest. It may be formulated as a topological field theory.

ACKNOWLEDGEMENTS

I am grateful to the Japan Society for the Promotion of Science for the partial support under the Grand-in-Aid for Scientific Research for the Ministry of Education, Science and Culture No.02952045.

REFERENCES

1. T. Dray and t'Hooft, *Comm. Math. Phys.* 99 (1985) 613.
2. T. Dray and P. Joshi, *Class. Quantum Grav.* 7 (1990) 41,
   T. Dray, *Class. Quantum Grav.* 7 (1990) L131.

Bubble Dynamics and Space-Time Structure in Extended Inflation

NOBUYUKI SAKAI and KEI-ICHI MAEDA*
Department of Physics, Waseda University
Shinjuku-ku, Tokyo 169-50, Japan

January, 1992

Abstract

Developing a thin-shell formalism in inhomogeneous spacetime, we study the evolution of bubbles nucleated by a first-order phase transition in extended inflation. We find that : (1) The world-hypersurface of any true vacuum bubble expands rapidly to become asymptotically null; this contradicts the result of Goldwirth-Zaglauer, who maintain that bubbles created initially later collapse. (2) Wormholes can be produced as well as in old inflation, resulting in the multi-production of universes.

1 Introduction

La and Steinhardt proposed extended inflation (EI)[1] to solve the graceful exit problem[2] in old inflation. In EI, gravity is described by the Brans-Dicke (BD) theory[3] instead of the Einstein theory. The BD field decelerates the expansion of the Universe so that true vacuum bubbles can coalesce, thus ending the phase transition driving inflation.

In this paper we investigate within the context of EI the dynamics of bubbles and the space-time structures to which their evolution may lead. We address the following two questions: (a) What is the fate of true vacuum bubbles surrounded by false vacuum? (b) What is the fate of false vacuum remnants surrounded by shell-like true vacuum regions? We base our answers on the assumption that the boundary layers of created bubbles are spherical and thin.

Answering question (a) is necessary to understand the percolation process in the late stages of inflation. Several authors have pointed out that the constraint from the homogeneity of the cosmic microwave background requires a BD parameter $\omega < 25$[4], which

*BITNET address:maeda@jpnwas00

is inconsistent with the experimental bound $\omega > 500$[5]. Those authors assume, however, that bubbles expand with the velocity of light[6]. It is important to determine whether this assumption remains valid in the BD theory. Goldwirth and Zaglauer have recently extended the thin-shell formalism first devised by Israel (Gauss-Codazzi formalism)[8] to obtain the equation of motion for a bubble in EI[7]. They found that the interior of a true vacuum bubble cannot be homogeneous. Hence, following the method of Berezin, Kuzumin and Tkachev[9], they rewrote their bubble equation of motion using only those field variables defined outside the bubble. They showed that bubbles nucleated in the early stages of EI later collapse, and that the absence of large bubbles imposes limits on the inhomogeneity due to bubble collisions, thus loosening the bounds on ω.

Though their equation of motion is correct, Goldwirth and Zaglauer failed to consider a regularity constraint on the bubble initial data: to ensure the flatness of spacetime at the center of a bubble, the BD field must be regular there. We reinvestigate the evolution of true vacuum bubbles in EI, taking this constraint into account.

As for the problem (b), we note that the evolution of false vacuum remnants and the resulting spacetime structure were first studied by Sato *et al*[10] in the context of old inflation, and several authors[9,11] have discussed it using the thin-shell formalism. We investigate the same problem in EI. Particularly we are interested in worm-hole solutions, and in the possibility of production of child universes.

2 Evolution of True Vacuum Bubbles

The field equations in the BD theory are written as ($8\pi G = 1$)

$$R_{\mu\nu} - \frac{1}{2} g_{\mu\nu} R = \hat{T}_{\mu\nu}, \tag{2.1}$$

$$\phi^{;\rho}{}_{;\rho} = \frac{\mathrm{Tr}T}{3 + 2\omega}, \tag{2.2}$$

where

$$\hat{T}_{\mu\nu} \equiv \frac{T_{\mu\nu}}{\phi} + \frac{\omega}{\phi^2}(\phi_{,\mu}\phi_{,\nu} - \frac{1}{2} g_{\mu\nu}\phi_{;\rho}\phi^{;\rho}) + \frac{1}{\phi}(\phi_{;\mu\nu} - g_{\mu\nu}\phi^{;\rho}{}_{;\rho}), \tag{2.3}$$

and $T_{\mu\nu}$ is the energy-momentum tensor of the matter fluid including a Higgs-like inflaton field. The BD field ϕ is normalized to unity at the present epoch. Replacing $T_{\mu\nu}$ in the Einstein theory with $\hat{T}_{\mu\nu}$, we can use the thin-shell formalism developed in the Einstein theory[8,9,11]. To describe the behaviour of the shell, we introduce a Gaussian normal coordinate system (n, τ, θ, ϕ), where τ is chosen to be the proper time on the shell.

Here we consider only vacuum energy as our matter fluid, so that $T_{\mu\nu}$ for the case with true vacuum bubbles is described as

$$T_{\mu\nu}(\text{outside}) = -\rho_0 g_{\mu\nu}, \quad T_{\mu\nu}(\text{inside}) = 0, \tag{2.4}$$

$$T_{\mu\nu}(\text{shell}) = -\sigma\delta(n)h_{\mu\nu}, \tag{2.5}$$

where ρ_0 is the false vacuum energy density, σ is the surface energy density of a shell and $h_{\mu\nu}$ is the three-geometry of the shell's world hypersurface.

If the universe (old phase region) is assumed to be homogeneous, isotropic and flat, the metric is given by

$$ds^2 = -dt^2 + a^2(t)(dr^2 + r^2 d\Omega^2). \tag{2.6}$$

We know the solutions of EI[1],

$$a(t) = a(0)\left(1 + \frac{\chi}{\alpha}t\right)^{\omega+\frac{1}{2}}, \tag{2.7}$$

$$\phi(t) = \phi(0)\left(1 + \frac{\chi}{\alpha}t\right)^2, \tag{2.8}$$

where $\chi^2 \equiv \rho_0/3\phi(0)$, $\alpha^2 \equiv (3+2\omega)(5+6\omega)/12$, and $t = 0$ is the time when EI starts.

Goldwirth and Zaglauer showed that the inner region is not homogeneous from the junction condition of the BD field. Without knowing the inner inhomogeneous solution, one can derive the equation of motion only in terms of the outer field variables[7]. In this paper, we rewrite that equation in a more tractable form,

$$\frac{d\beta}{dt} = -(1-\beta^2)\left(\beta H + \frac{2}{R}\right) + (1-\beta^2)^{\frac{3}{2}}\left(\frac{\rho_0}{\sigma} - \frac{3}{4}\frac{2\omega}{3+2\omega}\frac{\sigma}{\phi}\right). \tag{2.9}$$

where

$$R \equiv ar, \quad \beta \equiv a\frac{dr}{dt}, \quad \text{and} \quad H \equiv \frac{da/dt}{a}. \tag{2.10}$$

represent the circumference radius of the shell, the peculiar velocity relative to the outer background expansion and the Hubble expansion parameter in the outer region, respectively. The relationship between R and β is given by

$$\frac{dR}{dt} = \beta + HR. \tag{2.11}$$

From the (n,τ) component of the field equations (2.1) across the shell, we can also show

$$\frac{d\sigma}{d\tau} = 0, \tag{2.12}$$

which is the same result as in the Einstein theory.

Once initial conditions are given, we can find the evolution of the shell from Eqs.(2.9) and (2.11) because σ is constant.(2.12) Assuming $\beta = 0$ at the nucleation time t_0, the initial parameters are t_0, σ and $R(t_0)$. In the Einstein theory, we cannot give σ and $R(t_0)$ independently, if we assume that the inside of the bubble is Minkowski space-time. A similar situation occurs here although we do not know the inner inhomogeneous solution. An additional condition is obtained from requiring the flatness of space at the bubble's center, i.e., regularity at the origin. We have to set up initial conditions which are consistent with this condition.

For this purpose, we solve for the inner space-time on an initial hypersurface assuming a distribution of the BD field. We calculate σ as an eigenvalue problem, by integrating iteratively the constraint equations of the field equations (2.1) with boundary conditions specified at the shell. As the result of numerical calculation, we find

$$\sigma \approx \sigma_{\rm Min} \equiv \frac{3+2\omega}{\omega}\frac{\phi}{R}\left\{\sqrt{1+\left(\frac{dR}{d\tau}\right)^2}-\sqrt{1+\left(\frac{dR}{d\tau}\right)^2-H^2R^2}\right\} \tag{2.13}$$

independently of the values assigned to the adjustable parameters, where $\sigma_{\rm Min}$ means the value that results when we take the inner region to be Minkowski space-time.

Next we analyze the dynamical equation (2.9) and investigate the σ dependence for given $R(t_0)$. If $\beta(t_0) = 0$, Eq.(2.9) becomes

$$\frac{d\beta}{dt}(t_0) = -\frac{2}{R(t_0)} + \left(\frac{\rho_0}{\sigma} - \frac{3}{4}\frac{2\omega}{3+2\omega}\frac{\sigma}{\phi(t_0)}\right). \tag{2.14}$$

Then the critical surface energy density $\sigma_{\rm cr}$ between expansion and contraction is approximately given by $\sigma_{\rm cr} \approx \rho_0 R(t_0)/2 \approx 1.5\sigma_{\rm Min}$. Numerical calculation shows $\sigma_{\rm cr} \approx (1.5-1.6)\sigma_{\rm Min}$, which confirms the above result. Hence we can conclude that every bubble expands and no bubble collapses, because $\sigma \approx \sigma_{\rm Min} < \sigma_{\rm cr}$. The speed of the shell approaches the velocity of light soon after nucleation, and the asymptotic coordinate radius of the bubble is almost the same as that of null geodesics,

$$r_{\rm null}(t_0) \equiv \int_{t_0}^{\infty}\frac{dt}{a(t)} = \frac{\alpha}{\gamma(\omega-\frac{1}{2})}\frac{1}{(1+\frac{\chi}{\alpha}t_0)}. \tag{2.15}$$

This result is verified for any parameters and for any functional forms of the BD field. We can conclude that the effect of the BD field has little influence upon the bubble motion and the approximation of null geodesics is valid even in the BD theory.

Our result is contrary to that of Goldwirth and Zaglauer, who insist that bubbles collapse if

$$f \equiv \frac{\rho_0}{\gamma\sigma}\sqrt{\frac{\phi(t_0)}{\phi(0)}} \le 1. \tag{2.16}$$

This difference comes from their different method of determining initial conditions. We solved in the inner region to get nonsingular initial data, while they extended the formula with gravitational effects[12] as

$$R(t_0) = \left[\frac{3+2\omega}{2\omega} \frac{\rho_0}{3\sigma} + \frac{2\omega}{3+2\omega} \frac{\sigma}{4\phi(t_0)} \right]^{-1}. \tag{2.17}$$

We give a discussion of Eq.(2.17) here. Rewriting Eq.(2.13), we have

$$\left(\frac{dR}{d\tau} \right)^2 = \left[\left(\frac{\omega + \frac{1}{2}}{\alpha} \right)^2 \frac{3+2\omega}{2\omega} \frac{\rho_0}{3\sigma} + \frac{2\omega}{3+2\omega} \frac{\sigma}{4\phi(t_0)} \right]^2 R^2 - 1. \tag{2.18}$$

If $dR/d\tau(t_0) = 0$, $R(t_0)$ agrees with Eq.(2.13) except for the factor $\{(\omega + \frac{1}{2})/\alpha\}^2$. Since $0.95 < \{(\omega + \frac{1}{2})/\alpha\}^2 < 1$ for $\omega > 25$, their formula (2.18) is not so different from our results. To find the solution for Eq.(2.13), however, parameters are constrained as

$$\left(\frac{\omega + \frac{1}{2}}{\alpha} \right)^2 \frac{3+2\omega}{2\omega} \frac{\rho_0}{3\sigma} > \frac{2\omega}{3+2\omega} \frac{\sigma}{4\phi(t_0)}, \tag{2.19}$$

which results in $f > 1.1$ for $\omega > 25$. Though in their model σ is chosen to be so large that $f \leq 1$ is realized in the early stages of EI, in such a situation either bubbles are not nucleated or the thin-shell approximation does not apply.

In order to know whether bubbles are nucleated when Eq.(2.19) is violated, and if they are, whether the resulting bubbles expand or contract, we will have to investigate the nucleation process without using the thin-shell formalism.

3 Evolution of False Vacuum Remnants

We will now discuss the evolution of false vacuum remnants. As in [10], we make the simplifying assumption that an infinite number of bubbles are nucleated on a sphere simultaneously at time t_0. The universe is divided into three regions as shown in Fig.1. From causality, the inner false vacuum region A and the outer false vacuum region C are the homogeneous EI space-time and are described by the metric (2.6). We are interested in the evolution of the shells Σ_1, Σ_2 and the spacetime structure of the true vacuum region B. Since the BD field is inhomogeneous in true vacuum region, the metric in B is not given analytically in contrast to the Einstein theory. However we can derive and solve the equations of motion for shells using the metric on the homogeneous side of each shell, if and only if we give physically consistent initial values.

Equations of motion for Σ_1 and Σ_2 are given by

$$\frac{d\beta_i}{dt} = -(1-\beta_i{}^2)\left(\beta_i H + \frac{2}{R_i}\right) + \varepsilon_i(1-\beta_i{}^2)^{\frac{3}{2}}\left(\frac{\rho_0}{\sigma_i} - \frac{3}{4}\frac{2\omega}{3+2\omega}\frac{\sigma_i}{\phi}\right), \quad (i=1 \text{ or } 2) \quad (3.1)$$

where $\varepsilon_1 = -1$ and $\varepsilon_2 = 1$. If we assume $\beta_1(t_0) = \beta_2(t_0) = 0$, the remaining initial parameters are t_0, σ_1, σ_2, $R_1(t_0)$ and $R_2(t_0)$. However, as in the previous case, these parameters are not independent of each other because of the constraint equation in the space-time B and the boundary conditions on Σ_1 and Σ_2. In order to set up initial conditions, we must solve for the space-time B assuming some spatial distribution of the BD field, which may be determined by a complicated numerical simulation of bubble nucleation and collision processes. Although the cosmic time in A differs, in general, from that in B, we think that these are the same time t_0 on the initial slice by using constant-mean-curvature slicing.

We regard σ_1, $R_1(t_0)$ and the proper distance between Σ_1 and Σ_2 as free parameters, in addition to ω and t_0, and we integrate the constraint equations iteratively until the boundary conditions are satisfied. We find numerically that the space-time structure of B depends mostly on two parameters, $R(t_0)/H^{-1}(t_0)$ and $\sigma_1/\sqrt{\phi(t_0)\rho_0}$. We thus classify the solutions by these two parameters.

A physical restriction is the energy condition $\sigma_2 > 0$. If σ_1 is chosen too large, then the region B becomes a closed space and Σ_2 cannot be connected to it with positive σ_2. The critical values are plotted as the solid line in Fig.2. We also present the critical values that the bottle-neck structures appear initially as the dotted line.

Now we evolve the equations of motion (3.1) for obtained initial values. As a result, Σ_2 always expands and the comoving radius asymptotically approaches null geodesics. Σ_1 expands or collapses depending on initial parameters. This critical values $R_1(t_0)_{cr}$ are also illustrated as the dashed line in Fig.2. It is found that in the range $\sigma_1/\sqrt{\rho_0\phi} < 1$, $R_1(t_0)_{cr} \approx H^{-1}(t_0)$, which agrees with the analysis in the previous paper[10]. In the range $\sigma_1/\sqrt{\rho_0\phi} > 1$, there is a narrow region where small scale bubbles still expand.

For small value of ω, the BD field is initially small and then the effective gravitational constant becomes initially large. However we can classify the solutions just with parameters $R_1(t_0)/H^{-1}(t_0)$ and $\sigma_1/\sqrt{\phi(t_0)\rho_0}$ as in Fig.2. Hence the results do not depend on ω or t_0. As long as the boundary conditions are satisfied, the results do not depend too much on the configuration of BD field, either.

Finally, we discuss the evolution of the space-time B. If $\sigma_1/\sqrt{\rho_0\phi} \ll 1$, the bottle-neck structures are not formed initially unless $R_1(t_0) \gg H^{-1}(t_0)$. In the Einstein theory the region B is the Schwarzschild space-time and if $R_1(t_0) > H^{-1}(t_0)$, Σ_1 and Σ_2 go out of

a white hole into separate two regions, that is, a worm-hole is created between Σ_1 and Σ_2[10]. We predict that the evolution of the space-time is similar to that in the Einstein theory and the space-time also changes into a worm-hole if $R_1(t_0) > H^{-1}(t_0)$ in the BD theory. It is natural to think that a worm-hole appears when Σ_1 expands, because the regions A and C are in the inflationary phase while the region B is not. To know the evolution of the spacetime B exactly, we must solve the dynamical equations of the field equations (2.1) and (2.2) numerically. This work is in progress.

Acknowledgement

NS would like to thank Dr. Laurens D.Gunnarsen for his careful reading of our report. This work was supported partially by the Grant-in-Aid for Scientific Research Fund of the Ministry of Education, Science and Culture No.02640238 and No.03250213.

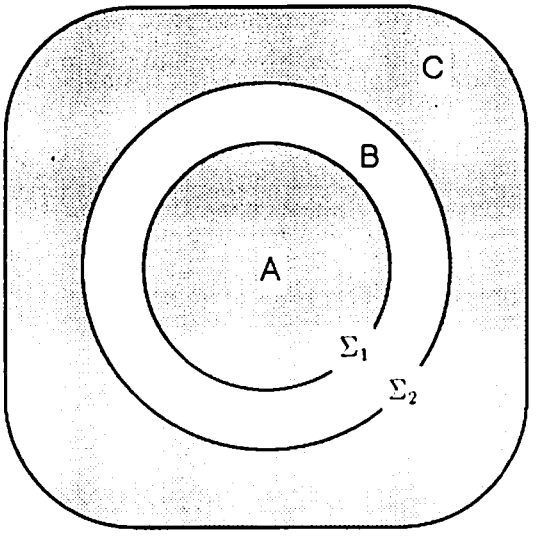

Figure 1: a false vacuum surrounded by true vacuum bubbles

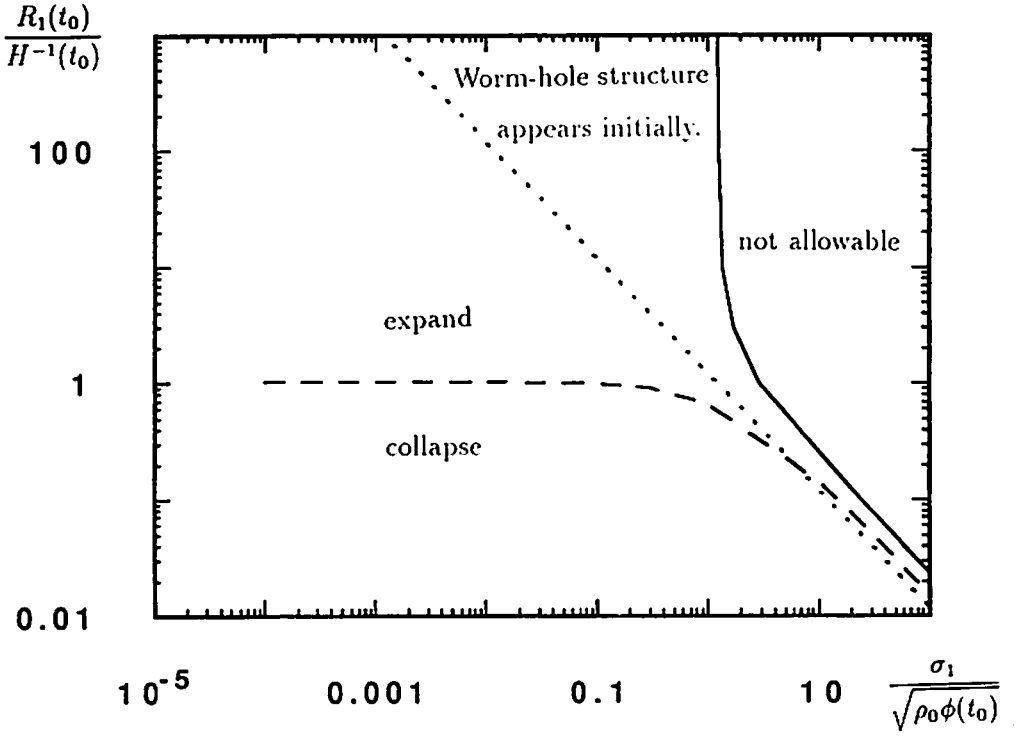

Figure 2: an example of classification of solutions

($\omega = 25$, at the end of inflation)

References

[1] D. La and P.J. Steinhardt, Phys. Rev. Lett. **62**, 376 (1989); Phys. Lett. **220B**, 375 (1989).

[2] A.H. Guth and E.J. Weinberg, Phys. Rev. **D23**, 321 (1981); Nucl. Phys. **B212**, 321 (1983).

[3] C. Brans and R.H. Dicke, Phys. Rev. **24**, 925 (1961).

[4] D. La, P.J. Steinhardt and E.W. Bertschinger, Phys. Lett. **231B**, 231 (1989); E.J. Weinberg, Phys. Rev. **D40**, 3950 (1989).

[5] R.D. Reasenberg *et al.*, Astrophys. J. **234**, L219 (1979).

[6] S. Coleman, Phys. Rev. **D15**, 2929 (1977).

[7] D.S. Goldwirth and H.W. Zaglauer, Phys. Rev. Lett. **26**, 3639 (1991).

[8] W. Israel, Nuovo Cim. **44B**, 1 (1966).

[9] V.A. Berezin, V.A. Kuzumin and I.I. Tkachev, Phys. Rev. **D36**, 2919 (1987).

[10] K. Sato, M. Sasaki, H. Kodama and K. Maeda, Prog. Theor. Phys. **65**, 1443 (1981); M. Sasaki, H. Kodama, K. Sato and K. Maeda, Prog. Theor. Phys. **66**, 2052 (1981); K. Sato, Prog. Theor. Phys. **66**, 2287 (1981); H. Kodama, M. Sasaki and K. Sato, Prog. Theor. Phys. **68**, 1979 (1982); K. Maeda, K. Sato, M. Sasaki and H. Kodama, Phys. Lett. **B108**, 98 (1982); K. Sato, H. Kodama, M. Sasaki and K. Maeda, Phys. Lett. **B108**, 103 (1982).

[11] V.A. Berezin, V.A. Kuzumin and I.I. Tkachev, Phys. Lett. **B120**, 91 (1983); S.K. Blau, E.I. Guendelman and A.H. Guth, Phys. Rev. **D35**, 1747 (1987).

[12] S. Coleman and F.D. Luccia, Phys. Rev. **D21**, 3305 (1980).

Worm Hole Formation in Numerical Cosmology

Yasusada NAMBU[†] **and Masaru SIINO**[‡]

Department of Physics, Tokyo Institute of Technology,
Oh-Okayama Meguroku, Tokyo 152, Japan
15th January 1992

abstract. Using a spherically symmetric inhomogeneous code we study the evolution of the inflationary inhomogeneous universe. The formation of a worm hole is discussed by embedding the spatial hypersurface into a higher dimensional flat space and determining apparent horizons.

I. Introduction

Many cosmologists pay much attention to the inflationary model because it can solve problems in the standard cosmology and explain the origin of the large scale structure. In the inflationary phase, the universe experiences de Sitter (quasi-de Sitter) expansion which implies the existence of cosmic event horizon. Initial small inhomogeneity and anisotropy are erased out by rapid cosmic expansion. Then the resultant universe becomes homogeneous and isotropic.

To utilize these aspects of inflation, it is important to discuss whether the universe can enter into the inflationary phase from the wide range of initial condition. This implies that the inflationary phase is an attracter solution in the considering dynamical system. 'Cosmic no hair conjecture'[1] is a very naive statement which represents the property of the inflation. R.M.Wald[2] proved this conjecture partially for homogeneous Bianchi type models. By his theorem, we can conclude that most of homogeneous universe with positive cosmological constant goes into

† E-mail address: ynambu@jpnrifp.bitnet
‡ E-mail address: msiino@cc.titech.ac.jp

the inflationary phase. However we cannot say so much things for inhomogeneous models. In fact, a remarkable inhomogeneity may cause the formation of cosmological global inhomogeneous structure like a worm hole. The spacetime with worm hole can be regarded as the counter examples of the 'cosmic no hair conjecture' since the global structure of spacetime is completely different from the de Sitter spacetime. Using the thin wall approximation, Maeda, Sato, Kodama and Sasaki[3] showed that the structure of a worm hole (child universe) is formed in the spherically symmetric inhomogeneous universe. From their discussion, the worm hole structure is formed when certain the condition for the inhomogeneity is satisfied. Then the universe is no longer 'no hair'.

Our purpose is to understand the dynamics of worm hole formation for various initial conditions. To do this we numerically analyze the evolution of the spherically symmetric inhomogeneous universes[4]. Our main interests are differences between the result with the thin wall approximation and the result without any approximation. We must set up the scalar field bubble with finite wall thickness and calculate its dynamics numerically. In our system, the inflationary phase is driven by a massive scalar field Φ with potential $V(\Phi) = \lambda(\Phi^2 - \sigma^2)^2$.

To establish numerical calculation we fix the topology of the universe to 3-sphere. This choice of spatial topology enables us to treat outer boundary condition easily. We introduce an extra massless scalar field Ψ, by which constraint equations for initial data are simplified successfully. In our expanding universe the contribution of the Ψ field to the total matter fields rapidly damps in time and this field has no effect on the evolution of geometry soon.

To investigate the worm hole formation, we determine apparent horizons[5] instead of determining event horizons, because apparent horizons can be determined without knowing the global structure of the spacetime. A spatial hypersurface at each timestep is embedded into higher dimensional flat space. From these information we judge whether worm hole or black hole are formed.

II. Thin wall approximation

In the context of the first order phase transition in the early universe, Maeda, Sato, Kodama and Sasaki[3] considered a spherically symmetric inhomogeneous universe with thin wall approximation. In Fig.1, the region A and C have cosmological constant Λ_1 and the region B has a cosmological constant Λ_2 that satisfies $\Lambda_1 > \Lambda_2 > 0$. Supposing that the domain wall runs with the speed of light, the region A, B and C are causally disconnected each other. Then in the region A and C, the spacetime is de Sitter and the metric is given by

$$ds^2 = -dt^2 + R_0^2 e^{2H_1 t}(d\chi^2 + \chi^2 d\Omega^2) \ , \tag{1}$$

$$; \ H_1 = \sqrt{\frac{\Lambda_1}{3}} \ . \tag{2}$$

In the region B, the spacetime is Schwartzschild de Sitter:

$$ds^2 = -(1 - \frac{2m}{r} - \frac{\Lambda_2}{3}r^2)d\tau^2 + (1 - \frac{2m}{r} - \frac{\Lambda_2}{3}r^2)^{-1}dr^2 + r^2 d\Omega^2, \tag{3}$$

where m is the Schwartzschild mass of the region A. In the table, we summarize their results classified by the ratio of Λ_2 to Λ_1 and the scale of initial inhomogeneity. The ratio of the inhomogeneous scale to the initial horizon scale is

$$\gamma = \frac{R_0 \chi_0}{(1/H)} \ . \tag{4}$$

The global structure of spacetime changes at the value of $\gamma = 1, \gamma^*$ where γ^* is related to the ratio $x = \Lambda_2/\Lambda_1$ as

$$\gamma^* = \frac{1}{\sqrt{3}}\left(\frac{1}{x^{1/2}(1-x)}\right)^{1/3} > 1 \ . \tag{5}$$

In the case of $\gamma > \gamma^*$ ('large inhomogeneity'), the metric (3) has no event horizon. In this case, the whole spacetime becomes de Sitter like. If $\gamma < \gamma^*$, the

metric (3) has de Sitter and Schwartzschild event horizons and there are three possibilities. When $\gamma < 1$ ('small inhomogeneity'), a black hole is formed since inner domain wall W^- fall into the singularity within the Schwartzschild horizon. If $\gamma^* > \gamma > 1$ and $\Lambda_2 > \Lambda_1/3$, the spacetime becomes de Sitter like because the world lines of the domain walls cross no event horizon. Worm hole formation requires the condition $\gamma^* > \gamma > 1$ and $\Lambda_2 < \Lambda_1/3$, which imply the world lines of the domain walls cross the both of de Sitter and Schwartzschild horizon.

III. Calculation

A general form of the metric of the spherically symmetric inhomogeneous space is reduced to

$$dl^2 = A(\chi)^2 d\chi^2 + B(\chi)^2(d\theta^2 + \sin^2\theta d\phi^2) \ . \tag{6}$$

Now using the gauge freedom corresponding to shift vector $N^\chi = \beta$, we can rewrite spatial metric in natural style of the closed 3-sphere space. We use the geodesic timeslice that lapse function is equal to one, so that the timeslice actively approaches to a source of gravity. After all, the spacetime metric in our calculation is given by

$$ds^2 = -dt^2 + R(\chi,t)^2\left[(d\chi + \beta dt)^2 + \sin^2\chi d\Omega^2\right] \ . \tag{7}$$

Using this metric form, we solve the Einstein equations by finite differencing on numerical grids[4].

To set up numerical calculation, we must prepare the set of initial data that satisfies the Hamiltonian constraint and momentum constraints. But it is not so easy in a inhomogeneous situation. The Hamiltonian constraint is

$$^{(3)}\mathcal{R} = 2\rho_{total} + \frac{3}{2}\tilde{K}^2 - \frac{2}{3}(\mathrm{Tr}K)^2 \ , \tag{8}$$

where $\tilde{K}$ is the traceless part of the extrinsic curvature K_{ab} and $^{(3)}\mathcal{R}$ is the 3-Ricci

scalar :

$$^{(3)}\mathcal{R} = -\frac{4}{R^3}\left(R_{,\chi\chi} + 2\frac{R_{,\chi}\cos\chi}{\sin\chi} - \frac{R_{,\chi}^2}{2R}\right) + \frac{6}{R^2}\ , \tag{9}$$

and momentum constraints are left only one independent component

$$\frac{\partial}{\partial\chi}(R^3\sin^3\chi\tilde{K}) = R^3\sin^3\chi(J_\chi + \frac{2}{3}\mathrm{Tr}K_{,\chi})\ , \tag{10}$$

where

$$J_\chi \equiv T^0_\chi\ . \tag{11}$$

As the matter fields, we use a massive scalar field Φ with potential $V(\Phi) = \lambda(\Phi^2-\sigma^2)^2$. To circumvent solving constraint equations, we determine the spatial distribution of the massless scalar field to make total energy density $\rho_{total} = \rho_\Phi + \rho_\Psi$ becomes homogeneous. As the universe expands, the contribution of the Ψ field to total energy density becomes small quickly, and we can simulate the evolution of Φ field inhomogeneity. The Hamiltonian constraint becomes homogeneous initially:

$$\frac{6}{R^2} = 2\rho_{total} - \frac{2}{3}(\mathrm{Tr}K)^2\ . \tag{12}$$

In this method, we can solve momentum constraints trivially too.

It is also difficult to establish the well behaving boundary condition in numerical analysis. In our system, since the topology of the universe is S^3, the boundary condition is reflection symmetry at $\chi = \pi/2$. This condition is not so difficult compared to the case of open universe, in that case we must demand suitable asymptotic boundary condition at outer boundary.

In our analysis, it is necessary to know whether a black hole or a worm hole is formed in the numerically generated spacetime. The best way is to determine an event horizon, which becomes possible if the global structure of the spacetime is known. However, knowing the global structure of the spacetime is much difficult because the region of the spacetime in which we can follow the evolution of initial

data is limited. The practical method is to determine the apparent horizon. The apparent horizon can be determined without knowing the global structure of a spacetime. In the general spacetime the existence of an apparent horizon implies the existence of the event horizon[5]. An apparent horizon is a 2-surface on which a null geodesic congruence has zero expansion θ,

$$\theta = \nabla_\mu k^\mu = 0 \ . \tag{13}$$

We calculate the expansion θ_+ and θ_- for outgoing and ingoing null geodesic congruence about origin, respectively. For the metric (7),

$$\theta_\pm \propto R\dot{R} + (\pm 1 - R\beta)(R_{,\chi} + R\cot\chi) \ . \tag{14}$$

By observing the sign of these expansions, we can determine the apparent horizons related to the de Sitter and Schwartzschild horizons. This information suggests us the formation of a black hole and a worm hole.

IV. Results and discussion

In the calculation reported here, the grid size is $\delta\chi = \pi/2 \times 1/100$ and the timestep is $\delta t = 0.02$. This δt satisfies the Courant condition. We continue the calculation until 10000 timestep.

We prepare the initial inhomogeneous scalar field as

$$\Phi = \Phi_0 + \frac{A}{1 - e^{-\frac{1}{D^2}}}\left[\exp(-(\frac{\cos\chi}{D})^2) - \exp(-(\frac{1}{D})^2)\right] \ . \tag{15}$$

Initially ρ_Φ is distributed on a 3-sphere like Fig.2. The main result of the our calculation with parameters $A = 0.35, D = 0.2, \Phi_0 = 0.045, \rho_{total} = 2.0$ and $\mathrm{Tr}K = -2.4$ is shown in Fig.3. In this calculation, we evaluate a numerical error by computing the Hamiltonian constraint at each timestep. The absolute value of the error ΔH was below 2×10^{-3}, as seen in Fig.4.

Fig.3 is obtained by embedding the spatial grid points into a higher dimensional flat space at each time step. The x-axis is Schwartzschild coordinate $r = R\sin\chi$ and the y-axis is appropriate extra dimension, which is determined so that the length along the curve coincides with the proper distance on 3-surface. Each grid point is drawn by four kinds of markers which are distinguished by the sign of the expansions θ_+ and θ_-. The small, middle, large, and white dots are correspond to $\{\theta_+ > 0, \theta_- < 0\}$, $\{\theta_+ < 0, \theta_- < 0\}$, $\{\theta_+ > 0, \theta_- > 0\}$ and $\{\theta_+ < 0, \theta_- > 0\}$ respectively. The initial inhomogeneity of the matter deforms the homogeneous universe into a bottle neck structure, and apparent horizons appear. In Fig.3(d), three apparent horizons appear at the place where different kind of markers adjoin. We can identify each apparent horizon: two correspond to de Sitter and one to Schwartzschild event horizon. Schwartzschild event horizon appears at a throat of bottle neck structure. This indicates that the Einstein-Rosen bridge is formed.

Now we present some comments and physical implications about our calculation. In this article we showed only a little part of our analysis. We demonstrated that the worm hole formation is possible when appropriate parameters are selected. As shown in the section II, Maeda, Sato, Kodama and Sasaki discussed the initial condition for the formation of the worm hole in the thin wall approximation. On the other hand, we studied the worm hole formation numerically without thin wall approximation. Physical situation of our calculation is much different from the case of the thin wall approximation in the following points: The thickness of the bubble wall is finite and may change during its time evolution. Furthermore spacetime inside the bubble is not completely de Sitter because the energy-momentum tensor inside the bubble is not always the form of false vacuum. These facts may affect values of the parameter which is necessary to form the worm hole. According to the result of the thin wall approximation, the collapsing bubble cannot generate a worm hole because it hits a black hole singularity. But if one consider the effect of time varying wall thickness, the situation may change drastically and we expect that worm hole formation is pos-

sible. These differences will be analyzed and discussed in detail in a forthcoming paper[6].

REFERENCES

1. G. W. Gibbons and S. W. Hawking *Phys. Rev.* **D 15** (1977) 2738.
2. R. M. Wald *Phys. Rev.* **D 28** (1983) 2118.
3. K. Maeda,K. Sato,M. Sasaki and H. Kodama *Phys. Lett.* **108B** (1982) 98.
4. D. S. Goldwirth and T. Piran *Phys. Rev.* **D 40** (1989) 3263.
5. See, e.g., R. M. Wald, *General Relativity* (University of Chicago Press, Chicago,1984).
6. Y. Nambu and M. Siino, in preparation.

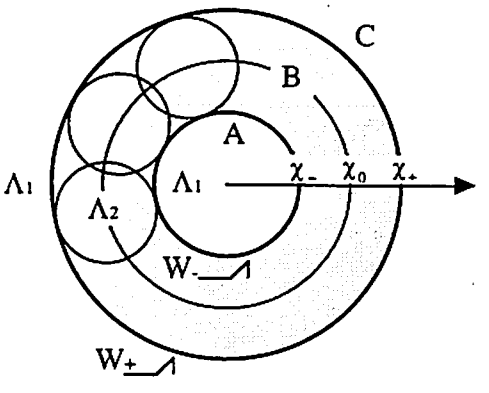

Fig.1

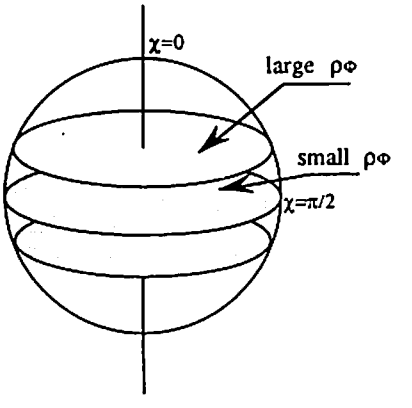

Fig.2

Fig.3

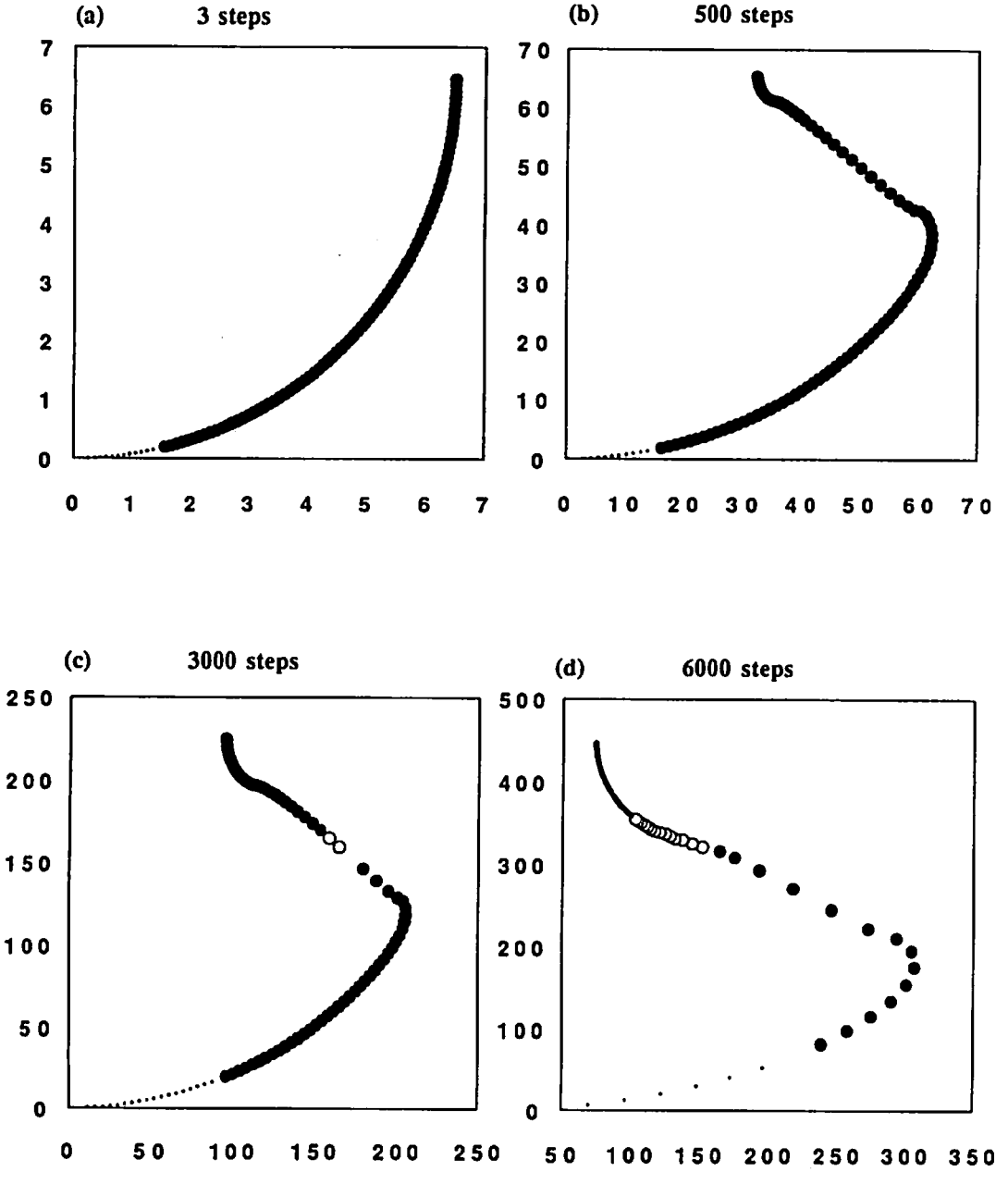

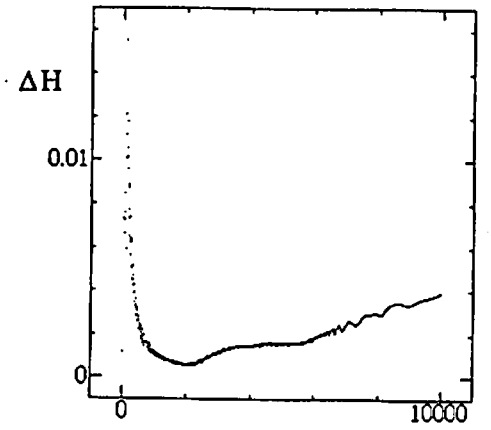

Fig.4

	$\Lambda_2 < \Lambda_1/3$	$\Lambda_1/3 < \Lambda_2 < \Lambda_1$
small	Black Hole	
middle	Worm Hole	De Sitter like
large	De Sitter like	

table

Wesson's 5D Space-Time-Mass theory of gravity

T. Fukui
Faculty of Liberal Arts, Dokkyo University, Soka, Saitama, Japan

Abstract. Wesson's 5D Space-Time-Mass theory of gravity(1983) is reviewed, and the basic equations of a cosmological model are presented for the preparation of studying the effects of the theory on the baryon synthesis in the early Universe. Also the comparison of the theory with the Brans-Dicke theory of gravity is touched upon.

1. Introduction

Wesson(1983, 1984) proposed the 5D Space-Time-Mass theory of gravity by introducing a new variable $x^5=Gm/c^2$ to the standard 4D Space-Time theory of gravity. Originally Wesson introduced the fifth coordinate on the two grounds, firstly to attempt to construct variable-gravity theory where mass m should be variable, and secondly to regard m with the gravitational constant G as a coordinate along the same line as regarding time t with the velocity of light c as the fourth coordinate. By solving the 5D Einstein tensor in vacuum $G_{ij}=0$, Wesson presented a solution which is the 5D analog of the 4D Schwarzschild solution, and studied the rate of change of rest mass by applying the solution to the 5D geodesic equation. In order to compare his theory with the Kaluza-Klein cosmology which is the subject of special interest among particle physicists, Wesson(1985, 1986) also studied a 5D cosmological model that is homogeneous and isotropic, and suggested that the fifth coordinate will contribute to the physical consequence of the present 4D Universe. Fukui(1987, 1988a) obtained another particular cosmological solution and studied the rate of change of rest mass, and showed explicitly the contribution of the fifth coordinate. And again Fukui(1988b) obtained the other solution of the metric coefficient with off-diagonal components to study the possibility for yielding a new natural constant which might be required in unifying the gravitational interaction with the other three interactions(Wesson, 1981). Ponce de Leon(1988) presented other cosmological solutions in the more comprehensive manner. And Chatterjee(1986) and Grøn(1988) obtained other solutions in the cosmic time coordnate, which are useful in studying physical processes in the early Universe. In order to see the effects of the theory on the

cosmological processes, Çoley(1990) studied helium formation with the solution obtained by Grϕn and set limits on the value of the non-negative parameter appearing in the model. Quite recently Wesson (1991) studied particle horizons with the solutions obtained so far to have a kind of theory for the origin of mass which is consistent with the cosmological observation. In Section 2 of the present article, we derive analytical equations showing the effects of the theory(Fukui, 1992) before we proceed to the numerical calculation of baryon synthesis. Section 3 is devoted to comparison of the theory with the Brans-Dicke theory, because both of them are variable-gravity theories and may probably correspond with each other. Some comments are made in Section 4.

2. Effects of 5D-STM theory

The metric to be concerned is

$$ds^2=e^{\nu}dt^2-e^{\omega}(dx^2+dy^2+dz^2)+e^{\mu}dm^2. \tag{1}$$

The last term in RHS of Eq. (1) is the mass coordinate which Wesson introduced on the grounds mentioned in Introduction. Actually t and m should be written as ct and Gm/c^2 if conventional physical dimensions are desired. From the 5D Einstein tensor in vaccum $G_{ij}^{(5)}=0$,

$$G_{00}^{(5)}=-3\dot{\omega}^2/4-3\dot{\omega}\dot{\mu}/4-e^{\nu-\mu}(3\overset{**}{\omega}/2+3\overset{*}{\omega}^2/2-3\overset{*}{\omega}\overset{*}{\mu}/4)=0, \tag{2}$$

$$G_{05}^{(5)}=3\dot{\overset{*}{\omega}}/2+3\dot{\omega}\overset{*}{\omega}/4-3\overset{*}{\nu}\dot{\omega}/4-3\overset{*}{\omega}\dot{\mu}/4=0, \tag{3}$$

$$G_{11}^{(5)}=G_{22}^{(5)}=G_{33}^{(5)}=e^{\omega-\nu}(\ddot{\omega}+3\dot{\omega}^2/4+\ddot{\mu}/2+\dot{\mu}^2/4+\dot{\omega}\dot{\mu}/2-\dot{\nu}\dot{\omega}/2-\dot{\nu}\dot{\mu}/4)+$$
$$+e^{\omega-\mu}(\overset{**}{\omega}+3\overset{*}{\omega}^2/4+\overset{**}{\nu}/2+\overset{*}{\nu}^2/4+\overset{*}{\nu}\overset{*}{\omega}/2-\overset{*}{\omega}\overset{*}{\mu}/2-\overset{*}{\nu}\overset{*}{\mu}/4)=0, \tag{4}$$

$$G_{55}^{(5)}=-3\overset{*}{\omega}^2/4-3\overset{*}{\nu}\overset{*}{\omega}/4-e^{\mu-\nu}(3\ddot{\omega}/2+3\dot{\omega}^2/2-3\dot{\nu}\dot{\omega}/4)=0, \tag{5}$$

where $(\cdot)$ and $(*)$ denote partial derivatives with respect to t and m, respectively. In this Section, we use most general matter-free cosmological solution in the cosmic time coordinate obtained by Chatterjee. The solutions are

$$e^{\nu}=f(m)t^2+g(m)t+h(m), \tag{6}$$

$$e^{\mu}=-\{\overset{*}{f}(m)t^2+\overset{*}{g}(m)t+\overset{*}{h}(m)\}^2/[4f(m)\{f(m)t^2+g(m)t+h(m)\}], \tag{7}$$

where $f(m)$ is interrelated with $g(m)$ and $h(m)$ as

$$f(m)=\{g(m)^2+2C\}/\{4h(m)\}, \tag{8}$$

where C is an arbitrary constant. Here we tentatively assume $h(m)=\text{constant}(=h_0)$ for simplicity. When we divide the Einstein tensor $G_{ij}^{(5)}$ into two functions, $G_{ij}^{(4)}$, the part which is proper to 4D, and the remainder, H_{ij}, (Fukui 1988a)

$$G_{ij}^{(5)}=G_{ij}^{(4)}+H_{ij}, \tag{9}$$

then the non-zero components H_{ij} are obtained as follows,

$$H_{00}=3[\{(g^2+2C)t+2h_0g\}/A]^2, \tag{10}$$

$$H_{11}=-(g^2+2C)/2h_0+\{(g^2+2C)t+2h_0g\}^2/(4h_0A), \tag{11}$$

where $g(m)$ and $A(t,m)=(g^2+2C)t^2+4h_0gt+4h_0^2$ are abbreviated as g and A respectively. If these quantities can be regarded as those giving the physical state of the 4D Universe, the components H_{00} and H_{11} correspond to the energy momentum tensors T_{00} and T_{11} of the 4D Universe, respectively, which give the total density and pressure of the Universe in the case of a perfect fluid. Taking the ratio of $H_{11}e^{-\nu}$ to H_{00} then results in the equation of state,

$$p/\rho c^2=-\{2(g^2+2C)A\}/[3\{(g^2+2C)t+2h_0g\}^2]+1/3. \tag{12}$$

When the fifth coordinate shrinks to zero, $\overset{*}{g}(m)=0$, then g^2+2C in the first term of RHS of Eq. (12) can be assumed to be zero and Eq. (12) leads the Universe to a radiation-dominated state. Therefore, the first term can be regarded as a term produced by variable rest mass. To see the effects of the fifth coordinate more specifically, we study the trajectory of a test particle described by the 5D geodesic equation,

$$d^2x^k/ds^2+\Gamma^k_{ij}(dx^i/ds)(dx^j/ds)=0 \quad (i,j,k=0,1,2,3,5). \tag{13}$$

The evaluations of Eq. (13) for k=1, 2, and 3 give

$$dx/ds=4h_0t_x/A, \tag{14}$$

$$dy/ds=4h_0t_y/A, \tag{15}$$

$$dz/ds=4h_0t_z/A, \tag{16}$$

where t_x, t_y, and t_z are integration constants.
For k=0, the geodesic equation can be transformed to

$$d^2t/ds^2+4h_0t_0^2\{(g^2+2C)t+2h_0g)\}/A^2+$$
$$+\overset{*}{g}^2t(gt+2h_0)\{(g^3+2Cg)t^3+6h_0g^2t^2+12h_0^2gt+8h_0^3\}/$$
$$/\{(g^2+2C)A^2\}\cdot(dm/ds)^2=0, \tag{17}$$

where $t_0^2=t_x^2+t_y^2+t_z^2$.
And for k=5, Eq. (13) can also be transformed to

$$\overset{*}{g}t(gt+2h_0)/\{(g^2+2C)A\}\cdot(d^2m/ds^2)+2\overset{*}{g}\{(g^3+2Cg)t^3+6h_0g^2t^2+12h_0^2gt+$$
$$+8h_0^3\}/\{(g^2+2C)A^2\}\cdot(dt/ds)\cdot(dm/ds)-4h_0t_0^2/A^2+$$
$$+t[\overset{**}{g}(g^2+2C)(gt+2h_0)A+\overset{*}{g}^2\{(4C^2-g^4)t^3-(6h_0g^3+4Ch_0g)t^2-12h_0^2g^2t-$$
$$-8h_0^3g\}]/\{(g^2+2C)^2A^2\}\cdot(dm/ds)^2=0. \tag{18}$$

With Eqs. (17) and (18)

$$(g^2+2C)^{1/2}\cdot(dt/ds)+\overset{*}{g}t(gt+2h_0)\{(g^2+2C)t+2h_0g\}/$$
$$/\{(g^2+2C)^{1/2}A\}\cdot(dm/ds)=\zeta, \tag{19}$$

where ζ is an integration constant. By taking the metric Eq. (1) into account, we get

$$dt/ds=\{(g^2+2C)t+2h_0g\}^2(\zeta\pm B^{1/2})/\{8h_0^2C(g^2+2C)^{1/2}\}+$$
$$+\zeta/(g^2+2C)^{1/2}, \tag{20}$$

$$\overset{*}{g}\cdot(dm/ds)=(g^2+2C)^{1/2}\{(g^2+2C)t+2h_0g\}A(-\zeta\mp B^{1/2})/\{8h_0^2Ct(gt+2h_0)\}, \tag{21}$$

where $B=[1+8h_0^2C/\{(g^2+2C)t+2h_0g\}^2]\zeta^2-$
$$-8h_0^2C(g^2+2C)\{4h_0t_0^2/A+1\}/\{(g^2+2C)t+2h_0g\}^2. \tag{22}$$

Eqs. (20) and (21) teach us the evolutionary path of the rest mass of a test particle with time. That is, rest mass changes till it saturates at the compactification of the fifth dimension. The equations correspond to Eqs. (11) and (13) in Grϕn. The time variation of rest mass is also studied by Wesson(1986), Fukui(1988a, 1988b), Banerjee et al. (1990), and Coley.

In case of $\zeta=0$, the total differential equation Eq. (20) can be solved analytically as

$$(g^2+2C)^{1/2}\{(g^2+2C)t^3/3+4h_0gt^2/2+4h_0^2t\}=0. \tag{23}$$

By using this relation in Eq. (12), the equation of state becomes

$$p/\rho c^2=-(Ct^2+2h_0^2)/(2Ct^2+3h_0^2)+1/3. \tag{24}$$

It deserves notice that Eq. (24) admits the existence of the state of stiff matter in the early Universe(Raine 1981). The first term of RHS should be zero at the time (say, t_c) when the fifth dimension shrinks to zero, and one has

$$Ct_c^2+2h_0^2=0. \tag{25}$$

Eq. (24) then reduces to the equation of state for radiation at $t=t_c$ through a stiff matter state. According to the scenario just described, Eqs. (12) and (24) should be applicable only to the period before t_c in the early Universe, not for t very large.

By fitting e^w, Eq. (6) to $e^w=(-2C)^{1/2}t+h_0$ and g, Eq. (23) to $g=(-2C)^{1/2}$ at $t=t_c$, we get a spatial component before $t_c=(-2h_0^2/C)^{1/2}$ as follows,

$$e^w=[-h_0+\{-(2Ct^2+3h_0^2)\}^{1/2}]/2 \tag{26}$$

and negative values of h_0 and C. Actually the scenario in this Section is applicable to the following period

$$\{-3h_0^2/(2C)\}^{1/2}\leqq t\leqq\{-2h_0^2/C\}^{1/2}. \tag{27}$$

3. Relations for the Brans-Dicke cosmology with the Wesson's theory

According to Bergmann(1968) and Wagoner(1970), we take a Brans-Dicke Lagrangian modified by a variable cosmological term $\Lambda(\phi)$ which is a function of a scalar field ϕ;

$$0=\delta\int\left[\phi\{R^{(4)}-2\Lambda(\phi)\}+16\pi L_m/c^4-\omega_0\phi_{,i}\phi^{,i}/\phi\right](-g)^{1/2}d^4x. \tag{28}$$

Here $R^{(4)}$ is the scalar curvature and L_m the Lagrangian density of matter in the 4D Universe and ω_0 the Brans-Dicke parameter. The field equation for the metric is

$$R_{ij}^{(4)}-g_{ij}R^{(4)}/2+g_{ij}\Lambda=8\pi T_{ij}/(\phi c^4)+\omega_0(\phi_{,i}\phi_{,j}-g_{ij}\phi_{,k}\phi^{,k}/2)/\phi^2+$$
$$+(\phi_{,i;j}-g_{ij}\Box\phi)/\phi, \tag{29}$$

where

$$T^{ij}=2/(-g)^{1/2}\cdot d\{(-g)^{1/2}L_m\}/dg_{ij}. \tag{30}$$

While the field equation for ϕ is obtained by varing ϕ and $\phi_{,i}$ in the Lagrangian

$$R^{(4)}-2\Lambda-2\phi\cdot(d\Lambda/d\phi)=\omega_0\phi_{,i}\phi^{,i}/\phi^2-2\omega_0\Box\phi/\phi. \tag{31}$$

Using Eqs.(2), (4), and (29), we get the following relation,

$$\{\gamma(3\overset{*}{\omega}\overset{*}{\mu}/2+3\overset{*}{\omega}^2/2-3\overset{*}{\omega}\overset{*}{\mu}/4)-(\overset{*}{\omega}\overset{*}{\mu}+3\overset{*}{\omega}^2/4+\overset{*}{\nu}\overset{*}{\mu}/2+\overset{*}{\nu}^2/4+\overset{*}{\nu}\overset{*}{\omega}/2-\overset{*}{\omega}\overset{*}{\mu}/2-\overset{*}{\nu}\overset{*}{\mu}/4)\}e^{-\mu}$$
$$=\{\ddot{\mu}/2+\dot{\mu}^2/4+\dot{\omega}\dot{\mu}/2-\dot{\nu}\dot{\mu}/4+\omega_0/2\cdot(\dot{\phi}/\phi)^2+\ddot{\phi}/\phi+\dot{\omega}\dot{\phi}/\phi-\dot{\nu}\dot{\phi}/(2\phi)-$$
$$-\gamma(3\dot{\omega}\dot{\mu}/4-\omega_0/2\cdot(\dot{\phi}/\phi)^2+3\dot{\omega}\dot{\phi}/(2\phi)\}e^{-\nu}+(1-\gamma)\Lambda, \tag{32}$$

where $\gamma=p/(\rho c^2)$. And Eq.(31) with Eqs.(2)-(5) gives the following relation,

$$-(3\overset{*}{\omega}\overset{*}{\mu}+3\overset{*}{\omega}^2+\overset{*}{\mu}\overset{*}{\nu}+\overset{*}{\nu}^2/2+3\overset{*}{\nu}\overset{*}{\omega}/2-3\overset{*}{\omega}\overset{*}{\mu}/2-\overset{*}{\nu}\overset{*}{\mu}/2)e^{-\mu}$$
$$=[\omega_0\{(\dot{\phi}/\phi)^2-2\ddot{\phi}/\phi+\dot{\nu}\dot{\phi}/\phi-3\dot{\omega}\dot{\phi}/\phi\}+\ddot{\mu}+\dot{\mu}^2/2+3\dot{\omega}\dot{\mu}/2-\dot{\nu}\dot{\mu}/2]e^{-\nu}+2\Lambda+$$
$$+2\phi\cdot(d\Lambda/d\phi). \tag{33}$$

Therefore Eqs. (32) and (33) are the relations for the Brans-Dicke cosmology with the Wesson's theory to be investigated in the future work.

4. Comments

The effect of the fifth coordinate is conspicuous in Eq. (12), and the equation of state of stiff matter in the early Universe can be derived without making any assumptions about the physical contents of the 4D Universe. It is natural therefore to expect that the physical state, especially in the very beginning, of the 4D Universe is inherited from the geometrical property of the 5D Universe. This supports the suggestion made by Wesson(1990). Therefore, the present procedure is quite helpful in inferring the early physical state of a lower-dimensional Universe from the geometrical property of a higher-dimensional Universe. The analytical study in the present procedure prepares us well for further numerical calculations of cosmological phenomena in the early Universe, e.g. baryon synthesis.

And the relations presented in Section 3 will surely be useful in clarifying the significance of the Wesson's theory.

Last of all, we would like to make speculative comment that if the present string theory tries to explain the origin of a physical contents in terms of the frequency of a string, then the present theory implies that there are ripples in the 5D Universe and the 4D Universe with the physical contents is embedded at the crests or troughs of the ripples.

Acknowledgements. The author wishes to express his gratitude to P.S.Wesson and A.A.Coley for their valuable suggestions.

References

Banerjee, A., Bhui, B.K., and Chatterjee, S.: 1990, Astron. Astrophys. 232, 305
Bergmann, P.G.: 1968, Int. J. Theor. Phys., 1, 25
Chatterjee, S.: 1986, Gen. Rel. Grav. 18, 1073
Coley, A.A.: 1990, Astron. Astrophys. 233, 305
Fukui, T.: 1987, Gen. Rel. Grav. 19, 43
Fukui, T.: 1988a, Astrophys. Space Sci. 141, 407
Fukui, T.: 1988b, Astrophys. Space Sci. 146, 13
Fukui, T.: 1992, Astron. Astrophys. in press
Grφn, φ.: 1988, Astron. Astrophys. 193, 1

Ponce de Leon, J.: Gen. Rel. Grav. 20, 539
Raine, D. J.: 1981, The Isotropic Universe, Adam Hilger, Bristol (150p.)
Wagoner, R. V.: 1970, Phys. Rev. 1D, 3209
Wesson, P. S.: 1981, Phys. Rev. D23, 1730
Wesson, P. S.: 1983, Astron. Astrophys. 141, 407
Wesson, P. S.: 1984, Gen. Rel. Grav. 16, 193
Wesson, P. S.: 1985, Astron. Astrophys. 143, 233
Wesson, P. S.: 1986, Astron. Astrophys. 166, 1
Wesson, P. S.: 1990, Gen. Rel. Grav. 22, 707
Wesson, P. S.: 1991, Preprint, University of Waterloo, Canada.

Ashtekar variables and their applications

HITOSHI IKEMORI

Department of Economics, Shiga University,
Baba 1-1-1, Hikone 522, Japan

ABSTRACT

The fundamentals of the formalism for nonperturbative canonical gravity proposed by Ashtekar are reviewed. The procedure of transition to the new variables is recapitulated as the steps of rewriting the covariant action, in which the Ashtekar theory is understood as a kind of gauge theory that contains the self-dual connection as its gauge field.

1. Introduction

The Ashtekar formalism is one of the most interesting subjects in the recent study of general relativity, which seems especially suitable for quantum description of the theory. It is a problem of great importance in fundamental physics to construct a consistent quantum theory of gravity. There is no room for doubt that Einstein's general relativity is the most superior theory of gravity, because of its confirmed consistency and great elegance. Though it has been established in the regime of classical theory, no one have yet been successful with the quantum theory of general relativity. As it stands, the Einstein theory is perturbatively unrenormalizable. Although an attempt based on the superstring theory has been expected to save the situations, it has not been a satisfying theory because of its lack of predictive power in the low energy physics. It seems that the nonperturbative quantum effects and the techniques to reveal them are increasing their importance for the investigations of quantum theory of gravity. Recently Ashtekar sheds a light on the nonperturbative canonical theory of gravity by proposing new variables [4,5,6].

2. Appearance of Ashtekar variables

First let us go back to a canonical formalism of the Einstein theory. The Einstein-Hilbert action

$$S_E[g] = \int d^4x\sqrt{-g}R \tag{1}$$

can be put into a canonical theory by means of the ADM method, in which the space-time metric $g_{\mu\nu}$ is decomposed as

$$ds^2 = g_{\mu\nu}dx^\mu dx^\nu = -N^2dt^2 + q_{ij}(dx^i + N^i dt)(dx^j + N^j dt) \quad ; \tag{2}$$

$$g_{\mu\nu} = \begin{pmatrix} -N^2 + N_kN^k & N_j \\ N_i & q_{ij} \end{pmatrix} \quad , \tag{3}$$

where N and N^i are the lapse function and the shift vectors respectively, and q_{ij} is the spatial or 3-dimensional metric.

Then the canonical action is given by

$$S_E[q,p] = \int d^4x \left[\dot{q}_{ij}p^{ij} - \left(N_i\mathcal{H}^i_M + N\mathcal{H}_H \right) \right] \tag{4}$$

where

$$\begin{cases} \mathcal{H}^i_M := -2^{(3)}\nabla_j p^{ij} \\ \mathcal{H}_H := G_{ijkl}p^{ij}p^{kl} - \sqrt{q}\,{}^{(3)}R \quad ; \end{cases} \tag{5}$$

$$\left(\quad G_{ijkl} := \frac{1}{2\sqrt{q}}(q_{ik}q_{jl} + q_{il}q_{jk} - q_{ij}q_{kl}) \quad \right) \quad .$$

In this case the dynamical variables are the spatial metric q_{ij} and its conjugate momentum p^{ij} which is essentially the extrinsic curvature. As there are constraints $\mathcal{H}^i_{\rm M} \approx 0$ and $\mathcal{H}_{\rm H} \approx 0$ accompanied by the Lagrange multipliers N and N^i, the phase space of the Einstein theory which has the coordinates (q_{ij} , p^{ij}) should be reduced to a physical one on account of these constraints. They are first class and called the momentum constraints and the Hamiltonian constraints respectively. They are non-polynomial in q_{ij} due to the existence of the inverse metric q^{ij} in ${}^{(3)}\Gamma^i_{jk}$ and ${}^{(3)}R$, which causes many troubles in either case of classical or quantum theory. Especially the troubles in the quantum theory with regards to the Hamiltonian constraint seems to be serious and the quantum version of this constraint known as the Weeler-DeWitt equation has never been tractable except for some extremely reduced models.

The new variables proposed by Ashtekar allows a reformulation that makes the theory more promising and may even solve this problem. The translation from the standard canonical variables (q_{ij} , p^{ij}) to the Ashtekar variables $(\tilde{E}^i_I , {}^+\mathcal{A}^I_i)$ is a kind of canonical transformation, however, to the complex variables. Ashtekar employs a densitised inverse triad $\tilde{E}^i_I$ as a canonical coordinate and a new connection ${}^+\mathcal{A}^I_i$ as its conjugate momentum. Roughly speaking, ${}^+\mathcal{A}^I_i$ is related to the standard variables by

$$ {}^+\mathcal{A} = p - i\,{}^{(3)}\Gamma(q) \quad , \tag{6}$$

then we can recast the constraints into new forms

$$\begin{cases} \mathcal{C}_{{\rm M}i} := -\tilde{E}^j \cdot {}^+\mathcal{F}_{ij} & \sim \mathcal{H}^i_{\rm M} \\ \mathcal{C}_{\rm H} := -i\,\dfrac{1}{2}\,(\tilde{E}^i \times \tilde{E}^j) \cdot {}^+\mathcal{F}_{ij} & \sim \mathcal{H}_{\rm H} \end{cases} \tag{7}$$

by means of its curvature ${}^+\mathcal{F}^I_{ij}$. And an additional constraint

$$\mathcal{C}^I_{\rm G} := -{}^+\mathcal{D}_i\tilde{E}^i_I \approx 0 \tag{8}$$

which means a requirement of invariance under a gauge transformation introduced in the new formalism. New constraints $\mathcal{C}_{{\rm M}i}$, $\mathcal{C}_{\rm H}$ and $\mathcal{C}^I_{\rm G}$ are at most quadratic polynomial of new variables, and we may hope them to make things manageable.

3. Lagrangian formalism for Ashtekar theory

It seems easier to understand the transition to Ashtekar theory in the framework of Lagrangian formalism [35-40], though Ashtekar has introduced the new variables through a kind of canonical transformation in the Hamiltonian formalism.

The procedure of transition to the new variables consists of three steps of rewriting the action. The first step is consideration of the first-order formalism and the second is the introduction of internal symmetry which means the use of the tetrad instead of the metric. The last step of the transition is the use of the self-dual connection instead of the spin connection. These steps are summarized in the following table.

Theory	order of ∂_μ	independent variables	
Einstein Einstein-Hilbert action	2nd order	metric $g_{\mu\nu}$	
Palatini action	1st order	metric $g_{\mu\nu}$	affine connection $\Gamma^{\lambda}_{\mu\nu}$
Tetrad Palatini action	1st order	tetrad e^a_μ	spin connection ω^{ab}_μ
Ashtekar Jacobson-Smolin action	1st order	tetrad e^a_μ	self-dual connection $+\omega^{ab}_\mu$

3.1. First order formalism

The first order formalism of general relativity is well known as the Palatini form and the action employed in this formalism consists of the terms with the first order derivatives in contrast with the Einstein-Hilbert action which contains second order derivatives. The Einstein-Hilbert action

$$S_{\rm E}[g] = \int d^4x\sqrt{-g}R(g) \sim g\partial^2 g + (\partial g)^2 \tag{9}$$

consists of the terms with the second order derivative or the square of first order derivative of metric $g_{\mu\nu}$. The Palatini's idea is to consider the affine connection $\Gamma^{\alpha}_{\mu\nu}$ to be independent of the metric $g_{\mu\nu}$. The Palatini action with the independent variables $g_{\mu\nu}$ and $\Gamma^{\alpha}_{\mu\nu}$;$(\Gamma^{\alpha}_{\mu\nu} = \Gamma^{\alpha}_{\nu\mu})$ is

$$S_{\rm P}[g,\Gamma] = \int d^4x\sqrt{-g}g^{\mu\nu}R_{\mu\nu}(\Gamma) \sim g(\partial\Gamma + \Gamma\Gamma) \quad , \tag{10}$$

which is equivalent to the Einstein-Hilbert action $S_{\rm E}[g]$ when a $\Gamma^{\alpha}_{\mu\nu}$ equation is satisfied. The equation of motion that follows from the variation with respect to $\Gamma^{\alpha}_{\mu\nu}$; $\frac{\delta}{\delta\Gamma^{\alpha}_{\mu\nu}}S_{\rm P}[g,\Gamma] = 0$ is satisfied when the affine connection is equal to the usual Christoffel symbol $\Gamma^{\alpha}_{\mu\nu} = \Gamma^{\alpha}_{\mu\nu}(g) \sim$

∂g consisting of the metric. Substitution of this result into the Plaltini action shows that it is equal to the Einstein-Hilbert action.

$$\begin{aligned} \frac{\delta}{\delta\Gamma^{\alpha}_{\mu\nu}} S_{\rm P}[g,\Gamma] = 0 \quad &\rightarrow \quad \Gamma^{\alpha}_{\mu\nu} = \Gamma^{\alpha}_{\mu\nu}(g) \sim \partial g \\ &\Downarrow \\ &S_{\rm P}[g,\Gamma(g)] = S_{\rm E}[g] \end{aligned} \tag{11}$$

3.2. Tetrad formalism

The next step is introduction of the internal symmetry, that is, considering the local Lorentz transformation as a gauge symmetry. We employ the orthonormal tetrad e^{a}_{μ} instead of the metric $g_{\mu\nu}$, which acts as a basis of the local Lorentz frame. And we also employ the spin connection ω^{ab}_{μ} instead of the affine connection $\Gamma^{\lambda}_{\mu\nu}$, which acts as a gauge field of the local Lorentz algebra $so(3,1)$. So far as the internal indices $a, b, \cdots$ are concerned, lowering and raising the indices are performed by the metric $\eta_{ab} = \mathrm{diag}(-1,1,1,1)$. As is well known the tetrad plays a role of a square root of the metric and they are related as

$$g_{\mu\nu} = \eta_{ab} e^{a}_{\mu} e^{b}_{\nu} \quad . \tag{12}$$

The Palatini action in the tetrad form is

$$S_{\rm T}[e,\omega] = \int d^{4}x \; e \; E^{\mu}_{a} E^{\nu}_{b} R^{ab}{}_{\mu\nu}(\omega) \tag{13}$$

where e is the determinant of e^{a}_{μ} ; ($e := \det e^{a}_{\mu} = \sqrt{-g}$) and E^{μ}_{a} is the inverse tetrad. The action is equivalently written as

$$S_{\rm T}[e,\omega] = \int \frac{1}{2} \varepsilon_{abcd} R^{ab}(\omega) \wedge e^{c} \wedge e^{d} \tag{14}$$

making use of differential forms.

Now that the internal symmetry is taken into consideration, the Riemann curvature $R^{\alpha}{}_{\beta\mu\nu}$ will be replaced by the curvature $R^{ab}_{\mu\nu}(\omega)$ of the spin connection ω^{ab}_{μ} defined by

$$R^{ab}_{\mu\nu}(\omega) := \partial_{\mu}\omega^{ab}_{\nu} - \partial_{\nu}\omega^{ab}_{\mu} + \omega^{a}_{\mu c}\omega^{cb}_{\nu} - \omega^{a}_{\nu c}\omega^{cb}_{\mu} \quad , \tag{15}$$

that is to say, the curvature 2-form R^{ab} is defined from the spin connection 1-form ω^{ab} by

$$R^{ab}(\omega) := d\omega^{ab} + \omega^{a}{}_{c} \wedge \omega^{cb} \tag{16}$$

in the language of differential forms.

After Palatini we consider the spin connection ω_μ^{ab} to be independent of the tetrad e_μ^a, we only require the antisymmetry in its indices $\omega_\mu^{ab} = -\omega_\mu^{ba}$. The situation is much the same as the metric Palatini formalism. The equation of motion with respect to ω^{ab}; $\frac{\delta}{\delta\omega^{ab}} S_{\rm T}[e,\omega] = 0$ is nothing but a torsion free condition

$$De^a := de^a + \omega^a{}_b \wedge e^b = 0 \tag{17}$$

and is satisfied when the spin connection is equal to the Levi-Civita connection $\omega^{ab} = \omega^{ab}(e)$ consisting of the tetrad e_μ^a. Substituting this result into the tetrad Palatini action, we obtain the Einstein-Hilbert action written in the tetrad form.

$$\begin{aligned} \frac{\delta}{\delta\omega^{ab}} S_{\rm T}[e,\omega] = 0 \quad \rightarrow \quad & \omega^{ab} = \omega^{ab}(e) \\ & \Downarrow \\ & S_{\rm T}[e,\omega(e)] = \int d^4x e R(\omega(e)) = \int d^4x \sqrt{-g} R(g) \end{aligned} \tag{18}$$

3.3. Self-dual connection

As the last step of the transition, the self-dual connection should take place of the spin connection. Let us explain a self-duality of connection, which is the self-duality with respect to internal indices and should not be confused with the self-duality with respect to space-time indices.

Suppose F_{ab} is an antisymmetric tensor with respect to its internal indices a and b, then the duality transform will be defined as

$${}^*F^{ab} := \frac{1}{2}\varepsilon^{abcd} F_{cd} \quad , \tag{19}$$

making use of the totally antisymmetric symbol ε^{abcd}. We should remark the fact that the dual of dual is equal to the multiplication by -1,

$${}^*({}^*F_{ab}) = -F_{ab} \quad , \tag{20}$$

when we choose the Lorentzian signature and use the metric $\eta_{ab} \equiv \mathrm{diag}(-1,1,1,1)$ to lowering and raising the internal indices.

As a result of this fact, we recognize that the eigen values of the duality transform operation are $\pm i$ and the eigen states are supplied by the complex combinations

$$ {}^{\pm}F_{ab} = \frac{1}{2}(F_{ab} \mp i {}^{*}F_{ab}) \quad , \tag{21} $$

which satisfy the eigen equations

$$ {}^{*}({}^{\pm}F_{ab}) = \pm i {}^{\pm}F_{ab} \quad . \tag{22} $$

The notion of self-duality means an eigen state of the duality transform operation and we call ${}^{+}F_{ab}$ self-dual part (and ${}^{-}F_{ab}$ anti-self-dual part) of F_{ab}.

The spin connection 1-form ω^{ab} which has a pair of antisymmetric internal indices can be uniquely decomposed into the self-dual and anti-self-dual part :

$$ \omega^{ab} = {}^{+}\omega^{ab} + {}^{-}\omega^{ab} \quad . \tag{23} $$

Substitution of this relation into the definition of the the curvature 2-form R^{ab} brings us the result

$$ R^{ab}(\omega) = R^{ab}({}^{+}\omega + {}^{-}\omega) = R^{ab}({}^{+}\omega) + R^{ab}({}^{-}\omega) \quad , \tag{24} $$

which means that the curvature 2-form R^{ab} can be also decomposed additively according to the decomposition with respect to the self-duality. Where $R^{ab}({}^{+}\omega)$ is the curvature of self-dual connection ${}^{+}\omega^{ab}$ and is nothing but the self-dual part of $R^{ab}(\omega)$, and the curvature $R^{ab}({}^{-}\omega)$ of anti-self-dual connection ${}^{-}\omega^{ab}$ is the anti-self-dual part of $R^{ab}(\omega)$ in the same way.

Previously mentioned tetrad Palatini action

$$ S_{T}[e,\omega] = \int \frac{1}{2}\varepsilon_{abcd} R^{ab}(\omega) \wedge e^{c} \wedge e^{d} = \int {}^{*}R_{cd}(\omega) \wedge e^{c} \wedge e^{d} \tag{25} $$

is decomposed as

$$ S_{T}[e,\omega] = {}^{+}S[e,{}^{+}\omega] + {}^{-}S[e,{}^{-}\omega] \quad ; \tag{26} $$

$$ {}^{\pm}S[e,{}^{\pm}\omega] = \int {}^{*}R_{ab}({}^{\pm}\omega) \wedge e^{a} \wedge e^{b} \quad , \tag{27} $$

with regard to the contributions of (anti)-self-dual connections.

The idea of the Ashtekar formalism is to consider just a self-dual part of the action. The equivalence to the Einstein-Hilbert action is still preserved with regard to just a half of duality components. There is little difference between the self-dual connection theory and the tetrad Palatini theory in reasoning an equivalence to the Einstein theory.

The ${}^+\omega^{ab}$ equation $\frac{\delta}{\delta {}^+\omega} {}^+S[e, {}^+\omega] = 0$ is satisfied when the self-dual connection is equal to the self-dual part of the Levi-Civita connection; ${}^+\omega^{ab} = {}^+\omega^{ab}(e)$ and the use of this result makes the self-dual action equal to the Einstein-Hilbert action multiplied by $\frac{1}{2}$.

$$\begin{aligned} \frac{\delta}{\delta {}^+\omega} {}^+S[e, {}^+\omega] = 0 \quad \rightarrow \quad & {}^+\omega^{ab} = {}^+\omega^{ab}(e) \\ & \Downarrow \\ & {}^+S[e, {}^+\omega(e)] = \frac{1}{2} S_T[e, \omega(e)] = \frac{1}{2} S_E[g] \end{aligned} \tag{28}$$

To be convinced of this fact, we should recall that the curvature of self-dual connection is given by the complex combination

$$R^{ab}({}^+\omega) = {}^+R^{ab}(\omega) = \frac{1}{2}\left(R^{ab}(\omega) - i {}^*R^{ab}(\omega) \right) \quad . \tag{29}$$

The action turns out to be

$$\begin{aligned} {}^+S[e, {}^+\omega(e)] &= \int \frac{1}{2} {}^* \left(R_{ab}(\omega(e)) - i {}^*R_{ab}(\omega(e)) \right) \wedge e^a \wedge e^b \\ &= \int \frac{1}{2} \left[{}^*R_{ab}(\omega(e)) + i R_{ab}(\omega(e)) \right] \wedge e^a \wedge e^b \\ &= \frac{1}{2} S_T[e, \omega(e)] \; + \; i \int \frac{1}{2} \left[R_{ab}(\omega(e)) \wedge e^a \wedge e^b \right] \\ &= \frac{1}{2} S_E[g] \end{aligned} \tag{30}$$

when we use the relation ${}^+\omega^{ab} = {}^+\omega^{ab}(e)$ required by the ${}^+\omega^{ab}$ equation, because the imaginary part of the action vanishes by virtue of the 1st Bianchi identity

$$R^a{}_b(\omega(e)) \wedge e^b \equiv 0 \tag{31}$$

which is the cyclic identity $R_{\mu[\nu\alpha\beta]} \equiv 0$ in the tensor form.

This means that the self-dual action would lead to the same equation of motion as the Einstein equation so far as the tetrad or equivalently the metric is concerned. The anti-self-dual action can be employed instead in the same way and the situation is quite the same as the case of the self-dual action.

4. Ashtekar theory from self-dual action

The Ashtekar formalism can be regarded as a canonical theory starting from the self-dual action stated in the previous section [36,43]. Let us consider the 3+1 decomposition of the self-dual theory in the tetrad form after the ADM decomposition in the metric form in order to relate the self-dual action with the Ashtekar theory. The self-dual action can be written in the form

$$ {}^{+}S[E, {}^{+}\omega] = \int d^4 \, e \, E^{\mu}_{a} E^{\nu}_{b} R^{ab}{}_{\mu\nu}({}^{+}\omega) \tag{32} $$

employing the inverse tetrad E^{μ}_{a} rather than the tetrad e^{a}_{μ}, which is just the same action previously described in the notation of differential forms. It is convenient to choose the gauge condition $E^{0}_{I} = 0$ and denote $E^{\mu}_{0} = \left(\frac{1}{N}, -\frac{N^{i}}{N}\right)$ then the inverse tetrad has the form of

$$ E^{\mu}_{a} = \begin{pmatrix} E^{0}_{0} & E^{i}_{0} \\ E^{0}_{I} & E^{i}_{I} \end{pmatrix} = \begin{pmatrix} \frac{1}{N} & -\frac{N^{i}}{N} \\ 0 & E^{i}_{I} \end{pmatrix} \quad , \tag{33} $$

where we use the notation $I, J, \cdots = (1, 2, 3)$ for the spatial indices out of the internal indices $a, b, \cdots = (0, 1, 2, 3)$ and the notation $i, j, \cdots = (1, 2, 3)$ for the spatial indices out of the space-time indices $\mu, \nu, \cdots = (0, 1, 2, 3)$.

This choice allows us to think of E^{μ}_{0} as a normal vector field to the spacelike hypersurface spanned by the condition of $t = x^{0} = const.$ which plays the same role as that of ADM.

It is easy to verify that E^{i}_{I} acts as an inverse triad from which we can define the inverse of space metric q^{ij} by

$$ q^{ij} := E^{i}_{I} E^{j}_{I} \tag{34} $$

and that the inverse of space-time metric obtained by $g^{\mu\nu} = \eta^{ab} E^{\mu}_{a} E^{\nu}_{b}$ is exactly the same as that given in the ADM decomposition. It deserves an attention that this gauge choice is not a restriction on the general coordinate transformation but on the local Lorentz transformation.

Under the above gauge condition the rotational group $SO(3)$ survives as an internal symmetry out of the local Lorentz group $SO(3, 1)$, which will be in accord with the situation that the self-dual connection is in fact a complex $so(3)$ connection.

We may think of the complexified algebras to make things clear, then the decomposition of the spin connection into the self-dual and anti-self-dual parts is understood as the

decomposition of the complexified Lorentz algebra into a couple of the complexified $so(3)$ algebras; $so(3,1;\mathbf{C}) = so(4;\mathbf{C}) = so(3;\mathbf{C}) \oplus so(3;\mathbf{C})$.

Actually we define the $so(3;\mathbf{C})$ connection ${}^{+}\mathcal{A}_{\mu}^{I}$,

$$ {}^{+}\mathcal{A}_{\mu}^{I} := 2\,{}^{+}\omega_{\mu}^{0I} = \omega_{\mu}^{0I} - \frac{i}{2}\,\epsilon^{IJK}\omega_{\mu}^{JK} \quad , \tag{35} $$

from the $so(3,1)$ connection ω_{μ}^{ab} . The new connection ${}^{+}\mathcal{A}_{\mu}^{I}$ is equivalent to the self-dual connection ${}^{+}\omega_{\mu}^{ab}$, because ${}^{+}\omega_{\mu}^{0I}$ carries all the elements of ${}^{+}\omega_{\mu}^{ab}$ due to the relation ${}^{+}\omega_{\mu}^{0I} = -\frac{i}{2}\,\epsilon^{IJK}\,{}^{+}\omega_{\mu}^{JK}$ brought by its self-duality.

Now we are ready to write over the action for the Ashtekar theory, making use of the gauge choice and the variables described above, the self-dual action can be written as

$$ {}^{+}S[E,{}^{+}\mathcal{A}] = \int d^{4}x \left[{}^{+}\dot{A}_{i}\cdot\tilde{E}^{i} - ({}^{+}A_{0}\cdot\mathcal{C}_{\mathrm{G}} + N^{k}\mathcal{C}_{\mathrm{M}k} + \underset{\sim}{N}\mathcal{C}_{\mathrm{H}}) \right] \tag{36} $$

where

$$ \begin{cases} \mathcal{C}_{\mathrm{G}}^{I} := -{}^{+}\mathcal{D}_{i}\tilde{E}_{I}^{i} \\ \mathcal{C}_{\mathrm{M}k} := -\tilde{E}^{j}\cdot{}^{+}\mathcal{F}_{jk} \\ \mathcal{C}_{\mathrm{H}} := -i\,\dfrac{1}{2}\,(\tilde{E}^{j}\times\tilde{E}^{k})\cdot{}^{+}\mathcal{F}_{jk} \quad . \end{cases} \tag{37} $$

The notations employed here are as follows. The inner and outer products concerned with the internal indices $I, J, K, \cdots$ are denoted as $\tilde{E}^{j}\cdot{}^{+}\mathcal{F}_{jk} := \tilde{E}_{I}^{j}\,{}^{+}\mathcal{F}_{jk}^{I}$ and $(\tilde{E}^{j}\times\tilde{E}^{k})^{I} := \epsilon^{IJK}\tilde{E}_{J}^{j}\tilde{E}_{K}^{k}$. The quantities which transform as densities under the space coordinate transformation are denoted as

$$ \begin{cases} \tilde{E}_{I}^{i} := \sigma E_{I}^{i} & \text{density of weight } 1 \\ \underset{\sim}{N} := \sigma^{-1}N & \text{density of weight } -1 \quad , \end{cases} \tag{38} $$

where $\sigma := \left(\det(E_{I}^{i})\right)^{-1} = \sqrt{q}$ and q is the determinant of the space metric q_{ij}. The covariant derivative ${}^{+}\mathcal{D}_{i}$ and the field strength ${}^{+}\mathcal{F}_{ij}^{I}$ of the connection ${}^{+}\mathcal{A}_{i}$ are defined by

$$ \begin{cases} {}^{+}\mathcal{D}_{i} := \partial_{i} - i\,{}^{+}\mathcal{A}_{i}\times \\ {}^{+}\mathcal{F}_{ij}^{I} := \partial_{i}{}^{+}\mathcal{A}_{j}^{I} - \partial_{j}{}^{+}\mathcal{A}_{i}^{I} - i({}^{+}\mathcal{A}_{i}\times{}^{+}\mathcal{A}_{j})^{I} \quad . \end{cases} \tag{39} $$

It is obvious that ${}^{+}\mathcal{A}_{0}^{I}$, N^{i} and $\underset{\sim}{N}$ act as Lagrange multipliers that accompany the constraints $\mathcal{C}_{\mathrm{G}}^{I} \approx 0$, $\mathcal{C}_{\mathrm{M}i} \approx 0$ and $\mathcal{C}_{\mathrm{H}} \approx 0$ respectively. These constraints are first class and

they are often called the gauge constraint (or the Gauss law constraint), the momentum constraint (or the vector constraint) and the Hamiltonian constraint.

It seems natural at a glance to consider the canonical variables (${}^{+}\mathcal{A}_i^I$, $\tilde{E}_I^i$) as the coordinates of the phase space for this theory. They are nothing but the Ashtekar's new variables. Thus we have reached the Ashtekar theory starting from the covariant action for the self-dual theory. To summarize the decomposition employed in our procedure, we will schematize the variables and their degree of freedom as follows.

covariant variables	⇒	canonical variables	gauge conditions	Lagrange multipliers (associated constraints)	
E_a^μ	⇒	$\tilde{E}_I^i$	$E_I^0 = 0$	N^i	$\underset{\sim}{N}$
16		9	3	3	1
				($\mathcal{C}_{\mathrm{M}i}$)	($\mathcal{C}_{\mathrm{H}}$)
${}^{+}\omega_\mu^{ab} = {}^{+}\mathcal{A}_\mu^I$	⇒	${}^{+}\mathcal{A}_i^I$		${}^{+}\mathcal{A}_0^I$	
12		9		3	
				($\mathcal{C}_{\mathrm{G}}^I$)	

5. Discussions

5.1. Comparison of Ashtekar and Einstein theory

Let us itemize the difference between the Einstein theory and the Ashtekar theory.

Einstein theory	Ashtekar theory
purely geometrical theory	gauge theoretical features
2nd order derivative theory	1st order derivative theory
dynamical equations are non-polynomial	dynamical equations are polynomial
does contain the inverse of variables	does not contain the inverse of variables
does not admit degenerate metric	does admit degenerate metric

The polynomiality of dynamical equations in the Ashtekar theory is indebted to the fact that all the constraints which rule dynamics are polynomials of the new variables as it has been seen. It owes largely to this polynomiality that the Ashtekar theory has preferable aspects to the Einstein theory especially in considering a nonperturbative quantum gravity.

As far as the constraints are concerned, they are more manageable than those in the Einstein theory in either case of classical or quantum theory. Furthermore these dynamical equations does not contain the inverse of $\tilde{E}^i_I$ employed as a fundamental variable and they works even if $\tilde{E}^i_I$ is degenerate [14-16]. In the Einstein theory, it is not allowed for the metric q_{ij} to be degenerate because the constraints and the dynamical equations contain the inverse of space metric q_{ij} and they never work if q_{ij} is degenerate. It seems possible for a solution of the equations of motion to go over singularities when they are written with the Ashtekar variables, then one may discuss a possibility of topology change [17] even in the classical theory. There are expected wider classes of classical solutions because of the extended nature of the phase space in the Ashtekar formalism. The extended phase space is that of a complexified Yang-Mills theory, though it should be reduced to a physical one by virtue of constraints. The gauge theoretical features suggest that various techniques in gauge theories may be applicable to study the quantum gravity in this formalism [18-22,24,25].

5.2. Reality condition problem

Not all properties of the Ashtekar formalism are welcome and there is a price to pay, that is, a reality condition problem. It seems curious that one of the new "canonical" variables, ${}^+\mathcal{A}^I_i$ is complex and the other, $\tilde{E}^i_I$ is real. Though one may be inclined to consider $\tilde{E}^i_I$ to be also complex, it is not allowed if one thinks of a strict equivalence to the Einstein theory. On the contrary, one should claim $\tilde{E}^i_I$ to be real throughout its time evolution in this case. The consistency of the reality with the time evolution requires that the imaginary part of ${}^+\mathcal{A}^I_i$ is to be determined as a function of $\tilde{E}^i_I$ (or e^I_i). Recalling the definition of ${}^+\mathcal{A}^I_i$ (35)in which one finds $\Im m({}^\pm\mathcal{A}^I_i) = -\frac{i}{2}\,\varepsilon^{IJK}\omega^{JK}_i$, this requirement means that the imaginary part of ${}^+\mathcal{A}^I_i$ should be equal to the the spatial part of $\omega^{JK}_i(e)$ or 3-dimensional Levi-Civita connection. This substitution seems to breakdown the polynomiality of constraints and to cause undesired difficulties. But there will be a remedy for the reality condition problem, though it seems that there has never been an exhaustive discussion on this problem. For example, it is pointed out [2,3] that the reality condition can be recasted into a polynomial form, however it is cubic. More detailed investigations on the issue will be necessary anyway.

5.3. Applications

The Ashtekar formalism has been applied to various directions and has revealed its relations to some other theories. As Ashtekar's main aim has been the quantum gravity, most of related works are concerned with this subject and a lot of papers [29-34] are written especially on the loop-space representation of the non-perturbative quantum gravity. There are excellent lecture notes [1,2] and review articles [3], to which we will leave detailed explanations and comprehensive references. One can find also a readable survey of applications within the classical theory in one [3] of them.

There is no room to enumerate all the related topics but some selected references will be found in the end of this report and it will serve for a rapid survey.

REFERENCES

Lecture Notes

[1] Ashtekar, A. "New Perspectives in Canonical Gravity." (Bibliopolis, Naples 1988)

[2] Ashtekar, A. "Lectures on Non-perturbative Canonical Gravity." (World Scientific, Singapore 1991)

Review Articles

[3] Rovelli, C. "Ashtekar Formulation of General Relativity and Loop Space Nonperturbative Quantum Gravity: A Report." Class. Quantum Grav. **8** (1991) 1613-1676.

Primary Works by Ashtekar

[4] Ashtekar, A. "New Variables for Classical and Quantum Gravity." Phys. Rev. Lett. **57** (1986) 2244-2247.

[5] Ashtekar, A. "A Note on Helicity and Selfduality." J. Math. Phys. **27** (1986) 824-827.

[6] Ashtekar, A. "New Hamiltonian Formulation of General Relativity." Phys. Rev. **D36** (1987) 1587-1602.

Inclusion of Matter Fields

[7] Ashtekar, A., Romano, J.D. and Tate, R.S. "New Variables for Gravity: Inclusion of Matter." Phys. Rev. **D40**, (1989) 2572.

Extension to Supergravity

[8] Jacobson, T. "New Variables for Canonical Supergravity." Class. Quantum Grav. **5** (1988) 923.

[9] Gorobey, N.N. and Lukyanenko, A.S. "The Ashtekar Complex Canonical Transformation for Supergravity." Class. Quantum Grav. **7** (1990) 67-71.

Extension to Higher Dimensions

[10] Seriu, M. and Kodama, H. "New Canonical Formulation of the Einstein Theory." Prog. Theor. Phys. **83** (1990) 7.

Classical Symmetric Solutions

[11] Bombelli, L. and Torrence, R.J. "Perfect Fluids and Ashtekar Variables, with Applications to Kantowski-Sachs model." Class. Quantum Grav. **7** (1990) 1747-1765.

[12] Fukuyama, T. and Kamimura, K. "Schwarzschild Solution in Ashtekar Formalism." Mod. Phys. Lett. **A6** (1991) 1437-1442.

[13] Kamimura, K., Makita, S. and Fukuyama, T. "Spherically Symmetric Vacuum Solution in Ashtekar's Formulation of Gravity." Preprint TOHOFP-91-40, Jun 1991.

Degenerate Metric

[14] Koshti, S. and Dadhich, N. "Degenerate Spherical Symmetric Cosmological Solutions Using Ashtekar's Variables." Class. Quantum Grav. **6** (1989) L223-L226.

[15] Bengtsson, I. "Some Remarks on Space-time Decompositions and Degenerate Metrics in General Relativity." Int. J. Mod. Phys. **A4** (1989) 5527.

[16] Bengtsson, I. "Degenerate Metrics and an Empty Black Hole." Class. Quantum Grav. **8** (1991) 1847-1858.

Topology Change

[17] Horowitz, G.T. "Topology Change in Classical and Quantum Gravity." Class. Quantum Grav. **8** (1991) 587-602.

Gravitational Instantons

[18] Samuel, J. "Gravitational Instantons from the Ashtekar Variables." Class. Quantum Grav. **5** (1988) L123-l125.

[19] Capovilla, R., Jacobson, T. and Dell, J. "Gravitational Instantons as SU(2) Gauge Fields." Class. Quantum Grav. **7** (1990) L1-l3.

[20] Torre, C.G. "A Topological Field Theory of Gravitational Instantons." Phys. Lett. **B252** (1990) 242-246.

[21] Torre, C.G. "Perturbations of Gravitational Instantons." Phys. Rev. **D41** (1990) 3620.

[22] Uehara, S. "A Note on Gravitational and SU(2) Instantons with the Ashtekar Variables." Class. Quantum Grav. **8** (1991) L229-l234.

Selfdual Einstein Equation

[23] Ashtekar, A., Jacobson, T. and Smolin, L. "A New Characterization of Half Flat Solutions to Einstein's Equation." Commun. Math. Phys. **115** (1988) 631

Relations to Yang-Mills Theory

[24] Mason, L.J. and Newman, E.T. "A Connection Between the Einstein and Yang-mills Equations." Commun. Math. Phys. **121** (1989) 659-668.

[25] Bengtsson, I. "Selfdual Yang-Mills Fields and Ashtekar's Variables." Class. Quantum Grav. **7** (1990) L223-l227.

Relations to Penrose's Twistor Theory

[26] Mason, L.J. and Frauendiener, J. "The Sparling 3-form, Ashtekar Variables and Quasi-local Mass." In *Twistors in Mathematics and Physics,* LONDON MATHEMATICAL SOCIETY LECTURE NOTE SERIES 156.

Initial Data Problem

[27] Saraykar, R.V. "Structure of The Space of Solutions of Einstein's Equations : A New Variables Approach." J. Math. Phys. **29** (1987) 186-196.

[28] Wagh, S.M. and Saraykar, R.V. "Conformally Flat Initial Data for General Relativity in Ashtekar's Variables." Phys. Rev. **D39** (1989) 670-672.

Loop Space Representation (see also [2] and [3] with references therein)

[29] Rovelli, C. "Knot Theory and Quantum Gravity." Phys. Rev. Lett. **61** (1988) 1155.

[30] Jacobson, T. and Smolin, L. "Nonperturbative Quantum Geometries." Nucl. Phys. **B299** (1988) 295.

[31] Rovelli, C. and Smolin, L. "Loop Space Representation of Quantum General Relativity." Nucl. Phys. **B331** (1990) 80.

[32] Rovelli, C. "Loop Representation in Quantum Gravity: The Transform Approach." In *Cavalese 1988, Proceedings, General relativity and gravitational physics* 615-628.

[33] Smolin, L. "Nonperturbative Quantum Gravity via the Loop Representation." In *Proc. of Osgood-hill Conf. on Conceptual Problems of Quantum Gravity* 440-489.

[34] Ashtekar, A., Rovelli, C. and Smolin, L. "Gravitons and Loops." Phys. Rev. **D44** (1991) 1740-1755.

Covariant Action

[35] Samuel, J. "A Lagrangian Basis for Ashtekar's Reformulation of Canonical Gravity." Pramāna-J. Phys. **28** (1987) L429-L432.

[36] Jacobson, T. and Smolin, L. "Covariant Action for Ashtekar's Form of Canonical Gravity." Class. Quantum Grav. **5** (1988) 583.

[37] Nelson, J.E. and Regge, T. "Group Manifold Derivation of Canonical Theories." Int. J. Mod. Phys. **A4** (1989) 2021-2030.

[38] Dolan, B.P. "On the Generating Function for Ashtekar's Canonical Transformation." Phys. Lett. **B233** (1989) 89-92.

[39] Henneaux, M., Schomblond, C. and Nelson, J.E. "Derivation of Ashtekar Variables from Tetrad Gravity." Phys. Rev. **D39** (1989) 434-437.

[40] Kamimura, K. and Fukuyama, T. "Ashtekar's Formalism in First Order Tetrad Form." Phys. Rev. **D41** (1990) 1885.

Reality Conditions

[41] Bengtsson, I. "Reality Conditions for Ashtekar's Variables." Preprint GOTEBORG-89-4a, Oct 1989.

[42] Tate, R.S. "Polynomial Constraints for General Relativity Using Real Geometrodynamical Variables." Preprint (SYRACUSE) Jun 1991. Submitted to Class. Quantum Grav.

Exact Solutions of Quantum Constraints

[43] Kodama, H. "Holomorphic Wave Function of the Universe." Phys. Rev. **D42** (1990) 2548-2565.

Quantum Cosmological Models

[44] Kodama, H. "Specialization of Ashtekar's Formalism to Bianchi Cosmology." Prog. Theor. Phys. **80** (1988) 1024. see also [43]

[45] Ashtekar, A. and Pullin, J. "Bianchi Cosmologies: a New Description." Preprint (SYRACUSE) (Nov 1989)

[46] Husain, V. and Smolin, L. "Exactly Solvable Quantum Cosmologies from Two Killing Field Reductions of General Relativity." Nucl. Phys. **B327** (1989) 205.

[47] Husain, V. and Pullin, J. "Quantum Theory of Space-times with One Killing Field." Mod. Phys. Lett. **A5** (1990) 733.

General Relativity without Metric

[48] Capovilla, R., Jacobson, T. and Dell, J. "General Relativity without the Metric." Phys. Rev. Lett. **63** (1989) 2325.

[49] Bengtsson, I. "Selfduality and the Metric in a Family of Neighbors of Einstein's Equations." Preprint GOTEBORG-91-4, Feb 1991.

[50] Husain, V. and Kuchar, K.V. "General Covariance, New Variables and Dynamics without Dynamics." Phys. Rev. **D42** (1990) 4070-4077.

[51] Capovilla, R., Dell, J., Jacobson, T. and Mason, L. "Self-dual 2-forms and Gravity." Class. Quantum Grav. **8** (1991) 41-57.

[52] Capovilla, R., Dell, J., Jacobson, T. and Mason, L. "A Pure Spin-connection Formulation of Gravity." Class. Quantum Grav. **8** (1991) 59-73.

[53] Ikemori, H. "Introduction to 2-form Gravity and Ashtekar Formalism." Preprints YITP-K-922 (Mar 1991). In *Proc.of Workshop on Quantum Gravity and Topology, INS, Tokyo, Japan.*

[55] Peldan, P. "Legendre Transforms in Ashtekar's Theory of Gravity." Class. Quantum Grav. **8** (1991) 1765-1784.

Issue of Time

[56] Ashtekar, A. "Old Problems in the Light of New Variables." Preprint (SYRACUSE) (Apr 1989). In *Proc. of Osgood-hill Conf. on Conceptual Problems of Quantum Gravity.*

[57] The contributions in the section of *The Issue of Time in Quantum Gravity* in *Proc. of Osgood-hill Conf. on Conceptual Problems of Quantum Gravity.*

CP Problem

[58] Ashtekar, A., Balachandran, A.P. and Jo, S. "The CP Problem in Quantum Gravity." Int. J. Mod. Phys. **A4** (1989) 1493.

[59] Bengtsson, I. "P, T and the Cosmological Constant." Int. J. Mod. Phys.**A5** (1990) 3449-3460.

Lattice Gravity (Regular Lattice)

[60] Renteln, P. and Smolin, L. "A Lattice Approach to Spinorial Quantum Gravity." Class. Quantum Grav. **6** (1989) 275-294.

[61] Renteln, P. "Some Results of SU(2) Spinorial Lattice Gravity." Class. Quantum Grav. **7** (1990) 493-502.

(2+1) Dimensional Analogues

[62] Ashtekar, A. and Romano, J. "Chern-simons and Palatani Actions and (2+1) Gravity." Phys. Lett. **B229** (1989) 56.

[63] Ashtekar, A., Husain, V., Rovelli, C., Samuel, J. and Smolin, L. "(2+1)-quantum Gravity as a Toy Model for the (3+1) Theory." Class. Quantum Grav. **6** (1989) L185.

[64] Ashtekar, A. "Lesson from (2+1)-dimensional Quantum Gravity." Preprint (SYRACUSE) Mar 1990. To appear in Strings '90, Superstring Workshop, College Station, TX, Mar 12-17, 1990.

[65] Witten, E. "(2+1)-dimensional Gravity as an Exactly Soluble System." Nucl. Phys. **B311** (1988) 46.

[66] Witten, E. "Topology Changing Amplitudes in (2+1)-dimensional Gravity." Nucl. Phys. **B323** (1989) 113.

[67] Nelson, J.E. and Regge, T. "Homotopy Groups and (2+1)-dimensional Quantum Gravity." Nucl. Phys. **B328** (1989) 190.

[68] Nelson, J.E. and Regge, T. "Homotopy Groups and (2+1)-dimensional Quantum De-Sitter Gravity." Nucl. Phys. **B339** (1990) 516-532.

[69] Waelbroeck, H. "2+1 Lattice Gravity." Class. Quantum Grav. **7** (1990) 751-769.

Vacuum Polarization around Black Holes and Quantum Hair[1]

Kiyoshi SHIRAISHI

Akita Junior College

Shimokitade-sakura, Akita-shi, Akita 010, Japan

Properties of black holes (BHs) with quantum hair [1] have been discussed recently [2]. The quantum hair is supported by virtual string loops surrounding the BH. In this talk, we examine the renormalized value of $\langle\phi^+\phi\rangle$ and stress tensor for a scalar field in the Hartle-Hawking vacuum around Schwarzschild BHs in the presence of the virtual string loops.

First of all, consider an Abelian Higgs model in D-dimensional spacetime. Suppose that the Higgs scalar has the U(1) charge Ne, where N is an integer larger than one. Another complex, free, scalar field is introduced, which has the charge e. In this system, a vortex,

[1] This talk is based on ref. [0].

which has (D-3)-dimensional extension, is made from the circular configuration of the Higgs field. Although this extended object (string) is invisible for a classical measurement, the additional complex scalar field feels the existence of the for the vortex quantum-mechanically.

A virtual loop of the string can be created around an O(D-1)-symmetric BH in the D-dimensional spacetime. The (D-2) dimensional world-sheet of the string can wrap the membrane of the event horizon of the BH. The virtual motion of the object induces a virtual electric field, though the field strength is confined at the wake of the loop if the string is assumed very thin.

At spatial infinity, a field strength takes a topologically-determined value in the presence of the virtual string world-sheet wrapping the horizon *k*-fold. We can simply express the field strength by the following gauge field:

$$A_\tau \to \frac{2\pi k}{N\hbar e\beta}, \tag{1}$$

where $\beta^{-1}=(D-3)\hbar c/(4\pi r_g)$ and r_g is the Schwarzschild radius.

The higher components in the Fourier expansion with respect to the periodic Euclidean time (τ) are irrelevant for the quantum nature of the

complex scalar field. We can also neglect other components of the gauge field, because their contribution to quantum effect is small at $r>>r_g$.

Now we start with the estimation of the vacuum polarization of the complex scalar field with the charge e in the Schwarzschild spacetime with the back ground gauge field configuration (1).

The asymptotic value of $\langle\phi^+\phi\rangle$ at spatial infinity in D-dimensional Schwarzschild spacetime with the back ground gauge configuration is [0]

$$\langle\phi^+\phi\rangle_k \to \frac{\hbar\Gamma((D-2)/2)}{2\pi^{D/2}c(\beta\hbar c)^{D-2}} \sum_{n=1}^{\infty} \frac{\cos(2\pi kn/N)}{n^{D-2}}. \qquad (2)$$

Next we examine the quantum energy-momentum tensor which comes from the polarization of the scalar field. The asymptotic value at spatial infinity in D-dimensional spacetime turns out to be

$$\langle T^{\mu}_{\nu}\rangle_k \to \frac{2\hbar\Gamma(D/2)}{\pi^{D/2}c(\beta\hbar c)^{D}} \sum_{n=1}^{\infty} \frac{\cos(2\pi kn/N)}{n^{D}} \mathrm{diag.}(-(D-1), 1, ..., 1). \qquad (3)$$

Finally, we consider the sum over the possible configurations. If the system including the BH has a charge Q, then the expectation value for $\langle\phi^+\phi\rangle$ can be presented as

$$\langle\phi^{+}\phi\rangle_{Q} \rightarrow \frac{1}{Z_{Q}} \sum_{k=-\infty}^{\infty} \exp\left(-i\frac{2\pi kQ}{Nhe}\right) \langle\phi^{+}\phi\rangle_{k}\, e^{-S_{st.}/\hbar i} , \tag{4}$$

where $S_{st.}$ is the action for the extended object (string) and can be approximated using the tension κ as

$$S_{st.} \approx \kappa|k|\frac{2\pi^{(D-1)/2}}{\Gamma((D-1)/2)} r_{g}^{D-2} \equiv \kappa|k|A . \tag{5}$$

Z_{Q} is defined as to keep the identity $<1>_{Q}=1$. $<T^{\mu}{}_{\nu}>_{Q}$ can be defined in the same manner.

Then the asymptotic value of $\langle\phi^{+}\phi\rangle$ at spatial infinity for the D-dimensional case is approximated by

$$\langle\phi^{+}\phi\rangle_{Q} \rightarrow \frac{\hbar\Gamma((D-2)/2)\,\zeta(D-2)}{2\pi^{D/2}c(\beta\hbar c)^{D-2}} \times f_{D-2}(Q/\hbar e, N, \kappa A) , \tag{6}$$

and similarly $<T^{\mu}{}_{\nu}>_{Q}$ at infinity is given by

$$\langle T^{\mu}_{\nu}\rangle_{Q} \rightarrow \frac{2\hbar\Gamma(D/2)}{\pi^{D/2}c(\beta\hbar c)^{D}} f_{D}(Q/\hbar e, N, \kappa A)\cdot \mathrm{diag.}(-(D-1), 1, \ldots, 1) , \tag{7}$$

where

$$f_x \equiv \frac{1}{2\zeta(x)}\sum_{n=1}^{\infty}\frac{1}{n^x}\left\{\frac{\cosh\kappa A - \cos(2\pi Q/N\hbar e)}{\cosh\kappa A - \cos(2\pi/N(Q/\hbar e-n))} + \frac{\cosh\kappa A - \cos(2\pi Q/N\hbar e)}{\cosh\kappa A - \cos(2\pi/N(Q/\hbar e+n))}\right\}. \quad (8)$$

For large κA, we obtain

$$f_x \approx 1 - \frac{2}{\zeta(x)}e^{-\kappa A}\cos\frac{2\pi Q}{Nhe}\sum_{n=1}^{\infty}\frac{1}{n^x}\sin^2\frac{n\pi}{N}. \quad (9)$$

We have found that the amount of the Hawking radiation of the bose gas is suppressed if the total charge of the system vanishes (Q=0). (but it never becomes negative value.) Provided that the extrapolation to the region of small κA is permitted, the rise in the Hawking temperature may take place in the presence of quantum hair.

There seems to be much difficulty in the thermodynamical interpretation of the system, because the proper temperature of BH (β^{-1}) and the temperature of the charged boson gas take different values; the equilibrium of the total system is not attained in general, according to our result.

In this talk, we have studied the quantum property of the BHs with

virtual loops of strings. Numerical calculations for the precise value of physical quantities near a BH with virtual string loops will be necessary for the future analyses.

References

[0] K. Shiraishi, preprint AJCHEP-3 (Nov. 1991).

[1] L. M. Krauss and F. Wilczek, Phys. Rev. Lett. **62** (1989) 1221.

L. M. Krauss, Gen. Rel. Grav. **22** (1990) 253.

J. Preskill and L. M. Krauss, Nucl. Phys. **B341** (1990) 50.

L. M. Krauss and S.-J. Rey, Phys. Lett. **B254** (1991) 355.

T. Banks, Nucl. Phys. **B323** (1989) 90.

K. Li, Nucl. Phys. **B361** (1991) 437.

M. G. Alford and J. March-Russell, NSF-ITP-91-48, PUPT-1234, April 16, 1991.

[2] J. Preskill, Physica Scripta **T36** (1991) 258.

S. Coleman, J. Preskill and F. Wilczek, Mod. Phys. Lett. **A6** (1991) 1631; Phys. Rev. Lett. **67** (1991) 1499.

Inner-Horizon Thermodynamics and Stability of Kerr Black Holes

Osamu Kaburaki

Astronomical Institute, Faculty of Science, Tohoku University, Sendai 980, Japan

ABSTRACT

Thermodynamic formulation for the physical states of the event horizons (or outer horizons) of Kerr black holes is extended also to their inner horizons, according to Curir's suggestion. From a mathematical standpoint, this corresponds to extending the range of variation of the rotation parameter, $h = a/r_H$ where a is specific angular momentum of a hole, by letting r_H stand for the 'radius' not only of the outer horizon but also of the inner horizon. For a given set of observable quantities of a kerr hole, its mass M and angular momentum J, all other thermodynamic variables defined on both types of horizons are obtained as double roots of corresponding quadratic equations. However, the physical meanings of these quantities on the inner horizon have not clarified fully yet.

By using the linear series expressing the equilibrium states of both outer and inner horizons, the thermodynamic stability (which is known to be equivalent to local dynamic stability) of these horizons are examined in four different circumstances. The results may be summarized as that the stability is generally different for different circumstances.

Among the four ensembles representing the above four different cicumstances, canonical and microcanonical ensembles are of special interest. The former describes isolated Kerr holes and there is no change of stability on both horizons. Combining with the knowledge for dynamic stability of a Schwarzschild hole, we can conclude that any Kerr hole is stable to axisymmetric perturbations. On the other hand, the latter describes the holes in heat baths and, in this case, there is a change of stability on the event horizon but nothing on the inner

horizon. It can be seen that, in a heat bath of infinite size, a Schwarzschild hole is unstable but angular momentum has a stabilizing effect.

The peculiarity of the extreme Kerr holes is also suggested from these analyses.

The details will be found in the following papers.

"The 'Inner-Horizon Thermodynamics' of Kerr Black Holes"

by I. Okamoto and O. Kaburaki, Mon. Not. Roy. Astron. Soc., in ress.

"Thermodynamic Stability of Kerr Black Holes"

by O. Kaburaki, I. Okamoto and J. Katz, Phys. Rev. D, submitted.

Rindler Noise and Thermalization Theorem in the Flat Spacetime with a Boundary

Kouji OHNISHI

Department of Physics, Tohoku University, Sendai 980, Japan

ABSTRACT

The vacuum noise of a quantum field as viewed by a uniformly accelerated observer is studied in the flat spacetime with a static boundary. The noise consists of the ordinary thermal term and a boundary-effect term, which has some special properties. These properties are understood from the view point of a quantum correlation among Rindler particles. By introducing a Minkowski Bessel mode that is a Fourier transform of a Minkowski plane-wave mode, we investigate the nature of this correlation. We find that a modified thermalization theorem holds with the same structure as the thermalization theorem in the absence of a boundary, provided that the boundary is located at a special position. This result holds regardless of the dimension of the spacetime and for massive as well as massless fields.

§ 1. Introduction

The world line of a Rindler observer (a uniformly accelerated observer) is a hyperbola on the Minkowski spacetime(see Fig 1). Hence, Rindler observers confined to the right wedge R ($x > |t|$) can not obtain information of the spacetime as a whole. How does the existence of the horizon influence quantum theory? One of the consequences is the Unruh effect;[1~6] a Rindler observer in the Minkowski vacuum feels as if he were in a thermal bath of temperature $T = a/2\pi(\equiv \hbar a/2\pi c k_B)$ where a is his proper acceleration .

To be precise, consider a system (a ***detector***) endowed with internal degrees of freedom and coupled linearly to a quantum field $\phi(x)$ which was initially in the Minkowski vacuum state. When this detector is accelerated uniformly, its transition probability per unit time from an internal energy level E to another level $E+\omega$ is proportional to the ***Rindler noise*** $\mathcal{F}(\omega)$ [2,3], which is defined as

$$\mathcal{F}(\omega) \equiv \int_{-\infty}^{\infty} d\tau \int_{-\infty}^{\infty} d\tau' e^{-i\omega(\tau-\tau')} G^+(\tau,\tau') \quad , \qquad (1\cdot 1)$$

where G^+ is the positive frequency Wightman function

$$G^+(\tau,\tau') \equiv \langle O|\, \phi(x(\tau))\phi(x(\tau'))\, |O\rangle \quad ,$$

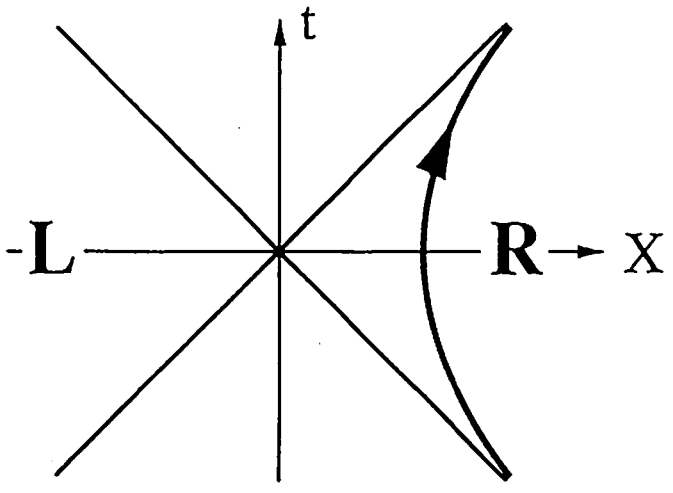

Fig.1 Rindler observer and Minkowski spacetime

The world line of a Rindler observer is a hyperbola on Minkowski spacetime, so Rindler observers confined to R have horizons.

where G^+ is the positive frequency Wightman function

$$G^+(\tau,\tau') \equiv \langle O|\,\phi(x(\tau))\phi(x(\tau'))\,|O\rangle \quad ,$$

where $x(\tau)$ is a world line of a uniformly detector and τ is a proper time of a detector. Hence Rindler noise "the power spectrum" $\mathcal{F}(\omega)$ is just a Fourier transform of two point correlation function along a uniformly accelerated observer. And this noise turns out to be of Planckian form

$$\mathcal{F}(\omega) = \mathcal{F}_M(\omega) \propto \frac{\omega}{\exp(\omega/T)-1} \quad , \qquad (1\cdot 2)$$

which satisfies the KMS condition,

$$\mathcal{F}(\omega) = \exp(-\omega/T)\mathcal{F}(-\omega) \quad . \tag{1·3}$$

Under this thermal property of Rindler noise lies the following thermalization theorem[4,5] ,which states that "*the pure state(i.e. Minkowski vacuum state) which is the vacuum from the point of view of inertial observers is a canonical ensemble from the point of view of Rindler observers* ".

The regions R and L($x < -|t|$) of spacetime are causally disconnected. But the Minkowski vacuum state $|O_M\rangle$ is a coherent state in which R-Rindler particles b^R and L-Rindler particles b^L are pair-wise correlated (product of two-mode squeezed states):

$$|O_M\rangle \propto \prod_{\omega,\vec{k}} \exp\left[e^{-\pi\omega} b^{R+}_{\omega,\vec{k}}\, b^{L+}_{\omega,-\vec{k}}\ \right] |O_R\rangle\,, \tag{1·4}$$

where $|O_R\rangle$ is the Rindler vacuum: $b^R|O_R\rangle = b^L|O_R\rangle = 0$. The mode functions(Rindler mode)associated with b^R and b^L are completely localized to R and L ,respectively(see(2.14)).

As a result, when a physical observation is made entirely in R, the L-Rindler particles, which can not be observed,play the role of a thermal bath. Moreover the expectation value of the Rindler particle number turns out to be given by the Bose distribution function,

$$\begin{aligned} \langle O_M| b^{R}_{\omega\vec{k}}{}^{+} b^{R}_{\omega'\vec{k}'} |O_M\rangle &= N(\omega)\delta(\omega-\omega')\,\delta(\vec{k}-\vec{k}') \\ \langle O_M| b^{R}_{\omega\vec{k}} b^{R}_{\omega'\vec{k}'} |O_M\rangle &= 0 \\ N(\omega) &\equiv [\exp(2\pi\omega)-1]^{-1} \quad . \end{aligned} \tag{1·5}$$

Recall that the theorem is closely related to Thermo-Field Dynamics(TFD)[7,8]; degrees of freedom in R correspond to the physical-field degrees of freedom , those in L to the tilde-field degrees of freedom , and the Minkowski vacuum state to the thermal vacuum state. As a result of the thermalization theorem, $\mathcal{F}(\omega)$ satisfies the KMS condition.

In order to understand the role played by the region L and the nature of quantum correlation among Rindler particles in more detail,we examine the Rindler noise in the case when a part of L is absent,that is, when there is a boundary at $x = -b_0 < 0$. [9,10]

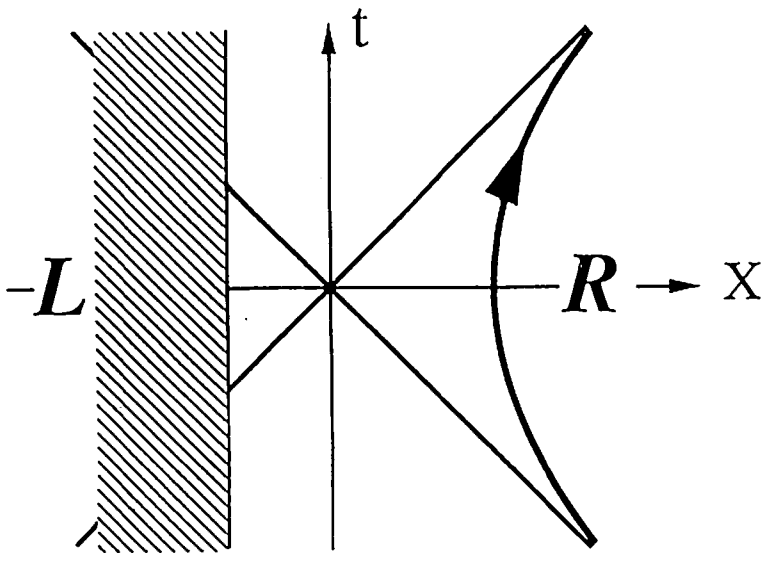

FIG.2 Rindler observer and the boundary

These is a static boundary at $x = -b_0$ in the flat spacetime .

Previously,we found that $\mathcal{F}(\omega) = \mathcal{F}_M(\omega) + \mathcal{F}_B(\omega)$ where the boundary effect is represented by a term $\mathcal{F}_B(\omega)$, which has a remarkable property

$$\lim_{b_0 \to 0} \mathcal{F}_B(\omega) \propto \delta(\omega) \quad . \tag{1 \cdot 6}$$

In one explanation, this special property can be interpreted as the consequence of specific types of interference among various Minkowski modes of the field. Detailed investigation has been given elsewhere[11].

In order to understand the properties of the Rindler noise in terms of quantum correlation among Rindler particles, we shall formulate a modification of the thermalization theorem, and find that a modified thermalization theorem for the case of boundary at $b_0 = 0$ has the same structure as the thermalization theorem in the absence of a boundary.

§ 2. Modification of thermalization theorem

To understand the thermal property of the noise in the presence of the boundary at $x = -b_0$ (see Fig 2), we shall introduce the Minkowski-Bessel(MB) mode[12,13] as an intermediate step, and extend the thermalization theorem by using the properties of the MB mode.

§2.1 Definition of modified Minkowski Bessel mode

Let P_θ be the two-dimensional part of the Minkowski plane wave,

$$\begin{aligned} P_\theta(U,V) &= \frac{1}{\sqrt{4\pi}} \exp\{i(\, k_x x - \omega_k t\,)\} \\ &= \frac{1}{\sqrt{4\pi}} \exp\{-i\frac{\mu}{2}(\, Ue^{\theta} + Ve^{-\theta}\,)\} \quad , \end{aligned} \tag{2·1}$$

where (U,V) is null coordinates ; $U = t - x$, $V = t + x$, and $k \equiv (\omega_k, k_x, \vec{k})$, $\omega_k \equiv \sqrt{k_x^2 + \mu^2}$, $\mu^2 = \vec{k}^2 + m^2$ where m is the mass of the field and θ is rapidity ;

$$\begin{cases} k_x = \mu \sinh\theta \\ \omega_k = \mu \cosh\theta \end{cases} .$$

MB mode is defined

$$\begin{aligned} B_\nu(U,V) &\equiv \frac{1}{\sqrt{2\pi}} \int_{-\infty}^{\infty} d\theta e^{-i\nu\theta} P_\theta(U,V) \\ B_q(U,V) &= B_\nu(U,V) e^{i\vec{k}\cdot\vec{y}}\, (2\pi)^{1-n/2} \quad , \end{aligned} \tag{2·2}$$

where n is dimension of spacetime and $q = (\nu, \vec{k})$. From this definition, MB mode has following properties.

property 1

MB mode is complete and orthogonal in Minkowski spacetime.

property 2

The vacuum state of MB particle is the same as the Minkowski vacuum state.

From the property 1 ,we can write a quantum scalar field as

$$\begin{aligned} \phi(x) &= \int_{-\infty}^{\infty} d\vec{k} \int_{-\infty}^{\infty} dk_x \{a_k \frac{1}{\sqrt{4\pi\omega_k}} e^{i(k_x x - \omega_k t)} e^{i\vec{k}\cdot\vec{y}}\, (2\pi)^{1-n/2} + c.c.\} \\ &= \int_{-\infty}^{\infty} d\vec{k} \int_{-\infty}^{\infty} d\theta \{a_{\theta\vec{k}} P_\theta(U,V) e^{i\vec{k}\cdot\vec{y}}\, (2\pi)^{1-n/2} + c.c.\ \} \quad , \end{aligned} \tag{2·3}$$

where $a_{\theta\vec{k}}$ is a Minkowski particle related to the ordinary Minkowski particle a_k as

$$a_{\theta\vec{k}} \equiv \sqrt{\mu \cosh\theta} a_k \quad . \tag{2 · 4}$$

And also using MB mode ,we can write as

$$\phi(x) = \int_{-\infty}^{\infty} d\vec{k} \int_{-\infty}^{\infty} d\nu \{d_q B_q(U,V) + c.c\} \quad . \tag{2 · 5}$$

Comparison shows that MB particle

$$d_q = \frac{1}{\sqrt{2\pi}} \int_{-\infty}^{\infty} d\theta \; e^{i\nu\theta} a_{\theta\vec{k}} \quad , \tag{2 · 6}$$

is a linear combination of Minkowski particles. Hence,the vacuum state of MB particle is the Minkowski vacuum state,

$$\forall q \qquad d_q |O_M\rangle = 0 \quad . \tag{2 · 7}$$

property 3

MB mode is an eigenfunction of the Lorentz-boost ;

$$(x\frac{\partial}{\partial t} + t\frac{\partial}{\partial x}) B_\nu(U,V) = -i\nu B_\nu(U,V) \quad . \tag{2 · 8}$$

property 4

A parallel displaced MB mode is

$$B_\nu(U - b_0, V + b_0) = \sqrt{2} \int_{-\infty}^{\infty} d\nu' B_{\nu'}(U,V) B_{\nu-\nu'}(-b_0, b_0) \quad . \tag{2 · 9}$$

From above properties,we can extend the MB mode in the presence of a boundary.

§2.2 MB mode in the presence of a boundary

A Minkowski plane wave satisfying the Dirichlet boundary condition at $x = -b_0 < 0$ is

$$\frac{1}{\sqrt{\pi}} \sin k_x(x + b_0) e^{-i\omega_k t} = P^+_\theta(\tilde{U}, \tilde{V}) - P^+_{-\theta}(\tilde{U}, \tilde{V}) \quad : \ (\theta > 0) \ , \qquad (2 \cdot 10)$$

where $\tilde{U} = U - b_0$, $\tilde{V} = V + b_0$. We can write in the terms of MB mode as

$$\begin{aligned} P_\theta(\tilde{U}, \tilde{V}) - P_{-\theta}(\tilde{U}, \tilde{V}) &= \frac{1}{\sqrt{2\pi}} \int_{-\infty}^{\infty} d\nu \{ e^{+i\nu\theta} - e^{-i\nu\theta} \} B_\nu(\tilde{U}, \tilde{V}) \ , \ (\theta > 0) \\ &= \frac{1}{\sqrt{2\pi}} \int_0^{\infty} d\nu 2i \sin \nu\theta \{ B_\nu(\tilde{U}, \tilde{V}) - B_{-\nu}(\tilde{U}, \tilde{V}) \} \ . \end{aligned} \qquad (2 \cdot 11)$$

Here, a modified Minkowski-Bessel(MMB) mode is defined as

$$\bar{B}_q(\tilde{U}, \tilde{V}) \equiv i \{ \ B_q(\tilde{U}, \tilde{V}) - B_{-\tilde{q}}(\tilde{U}, \tilde{V}) \ \} \qquad : \nu > 0 \ , \qquad (2 \cdot 12)$$

where $q \equiv (\nu, \vec{k})$, $\tilde{q} \equiv (\nu, -\vec{k})$ and $\nu > 0$, and this MMB mode is also complete and orthogonal in the region $x > -b_0$ of Minkowski spacetime.

We consider a particle $\bar{d}_q$ associated with MMB mode. From the definition, $\bar{d}$ particles satisfy

$$^\forall \nu > 0, \vec{k} \qquad \bar{d}_q \ |O_B\rangle = 0 \qquad , \qquad (2 \cdot 13)$$

where $|O_B\rangle$ is the Minkowski vacuum state modified by the presence of the boundary at $x = -b_0 < 0$.

§2.3 Modification of thermalization theorem

We introduce the Rindler coordinates$(\eta, \xi, \vec{y})$ by

$$t = |\xi| \sinh \eta \ , \quad x = \xi \cosh \eta \ , \quad \vec{y} = \vec{y}_{Minkowski} \ .$$

In terms of these coordinates ,the Rindler mode is defined as

$$\begin{aligned} u^{(\sigma)}_q(\eta, \xi, \vec{y}) &= \theta(\sigma\xi)(2\nu\pi^2)^{-1/2}(2\nu \sinh \pi\nu)^{1/2} \ K_{i\nu}(\mu|\xi|) e^{i\vec{k}\cdot\vec{y}} (2\pi)^{1-n/2} e^{-i\nu\eta} \\ &\propto e^{-i\nu\eta} \quad (\ 0 < \nu < +\infty) \qquad , \end{aligned} \qquad (2 \cdot 14)$$

where σ stands for + in R(i.e.,$\xi > 0$) and − in L (i.e.,$\xi < 0$), and this mode is complete and orthogonal in the region R and L,respectively.

On the other hand,a MB mode is as

$$
\begin{aligned}
B^{\sigma}_{\nu}(\eta,\xi) &= \frac{1}{\sqrt{8\pi^2}}\int_{-\infty}^{\infty} d\theta\ \mathrm{e}^{-i\nu\theta}\exp\{\sigma i\mu|\xi|\sinh(\theta-\sigma\eta)\} \\
&= \frac{1}{\sqrt{2\pi^2}}K_{i\nu}(\mu|\xi|)\exp(\sigma\pi\nu/2)\exp(-\sigma i\nu\eta) \\
&\propto \mathrm{e}^{-\sigma i\nu\eta} \quad (-\infty<\nu<\infty) \quad ,
\end{aligned}
\tag{2·15}
$$

where σ denotes + in R and − in L as above and ν now takes not only positive but also negative values. Note that these modes are normalized with respect to Klein-Gordon inner product.

To see the relationship between $\bar{d}$ particles and Rindler particles b associated with the Rindler mode, let us calculate the Bogoliubov coefficient in region R.

$$
b_p = \frac{i}{\pi\sqrt{2\sinh\pi\omega}}\int_0^{\infty} d\nu\Big\{P(\omega,\nu)\bar{d}_q - Q(\omega,\nu)\bar{d}^{\dagger}_{\tilde{q}}\Big\} \tag{2·16}
$$

where $p\equiv(\omega,\vec{k})$, $\tilde{p}\equiv(\omega,-\vec{k})$,

$$
\begin{aligned}
P(\omega,\nu) &\equiv \Big\{\mathrm{e}^{\pi\nu/2}\cdot K_{i(\nu-\omega)}(\mu b_0) - \mathrm{e}^{-\pi\nu/2}\cdot K_{i(\nu+\omega)}(\mu b_0)\Big\} \\
Q(\omega,\nu) &\equiv \Big\{\mathrm{e}^{\pi\nu/2}\cdot K_{i(\nu+\omega)}(\mu b_0) - \mathrm{e}^{-\pi\nu/2}\cdot K_{i(\nu-\omega)}(\mu b_0)\Big\}
\end{aligned}
\quad . \tag{2·17}
$$

Using this relation, the expectation value of the Rindler particle number in vacuum state $|O_B\rangle$ can be calculated;

$$
\begin{aligned}
\langle O_B|\, b^{\dagger}_p\, b_{p'}\ |O_B\rangle &= \frac{\delta(\vec{k}-\vec{k}')}{2\pi^2\sinh\pi\omega}\int_0^{\infty} d\nu\ Q^*(\omega,\nu)\ Q(\omega',\nu) \\
&= \delta(\vec{k}-\vec{k}')\Big[\frac{\delta(\omega-\omega')}{\mathrm{e}^{2\pi\omega}-1} - \frac{K_{i(\omega+\omega')}(2\mu b_0)}{\pi\sqrt{2\sinh\pi\omega\cdot 2\sinh\pi\omega'}}\Big] \quad ,
\end{aligned}
\tag{2·18}
$$

and

$$
\begin{aligned}
\langle O_B|\, b_p\, b_{p'}\ |O_B\rangle &= -\frac{\delta(\vec{k}+\vec{k}')}{2\pi^2\sinh\pi\omega}\int_0^{\infty} d\nu\ P(\omega,\nu)\ Q(\omega',\nu) \\
&= \delta(\vec{k}+\vec{k}')\frac{K_{i(\omega-\omega')}(2\mu b_0)}{\pi\sqrt{2\sinh\pi\omega\cdot 2\sinh\pi\omega'}} \quad .
\end{aligned}
\tag{2·19}
$$

The second term of $< b^{+}b >$ as well as $< bb >$ represents the boundary effect; thermalization theorem of(1·5) does not hold.

Two limiting cases are particular interest. One is the case of $b_0 \to \infty$;

$$\begin{aligned} \langle O_B | b_p^+ \, b_{p'} \, | O_B \rangle &= \frac{1}{e^{2\pi\omega} - 1} \delta(p - p') \\ \langle O_B | b_p \, b_{p'} \, | O_B \rangle &= 0 \quad . \end{aligned} \tag{2 · 20}$$

This result coincides with the no-boundary case as expected for the boundary effect of the noise. The second is the case of $b_0 \to 0$;

$$\begin{aligned} \langle O_B | b_p^+ \, b_{p'} \, | O_B \rangle &= \frac{1}{e^{2\pi\omega} - 1} \, \delta(p - p') \\ \langle O_B | b_p \, b_{p'} \, | O_B \rangle &= \frac{e^{\pi\omega}}{e^{2\pi\omega} - 1} \, \delta(p - \tilde{p}') \quad . \end{aligned} \tag{2 · 21}$$

§2.4 Modified thermalization theorem when $b_0 = 0$

In the special case of $b_0 = 0$, $(2 · 16)$ reduces to

$$\begin{pmatrix} b_q \\ b_{\tilde{q}}^+ \end{pmatrix} = \begin{pmatrix} u & v \\ v & u \end{pmatrix} \begin{pmatrix} i\bar{d}_q \\ i\bar{d}_{\tilde{q}}^+ \end{pmatrix} \tag{2 · 22}$$

where

$$u = (N_\nu + 1)^{1/2}, \quad v = N_\nu^{1/2}, \quad N_\nu = (e^{2\pi\nu} - 1)^{-1} \quad .$$

This Bogoliubov transformation can be invoked to find the relationship between the modified Minkowski vacuum state $|O_B\rangle$ and the Rindler vacuum state$|O_R\rangle$. Restricting our attention to the two modes $(\bar{d}_q \, , \, \bar{d}_{\tilde{q}})$ or $(b_q \, , \, b_{\tilde{q}})$ only, we examine the conditions

$$\begin{aligned} 0 = i\bar{d}_q \, |O_B\rangle &= (u b_q - v b_{\tilde{q}}^+) \, |O_B\rangle \\ 0 = i\bar{d}_{\tilde{q}} \, |O_B\rangle &= (-v b_q^+ + u b_{\tilde{q}}) \, |O_B\rangle \quad . \end{aligned} \tag{2 · 23}$$

Then we fine

$$|O_B\rangle \propto \prod_q \exp(e^{\pi\nu} b_q{}^+ b_{\tilde{q}}{}^+) \, |O_R\rangle \quad . \tag{2 · 24}$$

Comparing this with Eq.$(1 · 4)$, we see that quantum correlation between b_q^R and $b_{\tilde{q}}^R$ endows the thermal character to $< b_q^{R+} b_q^R >$ for which boundary effects are absent as shown in Eq.$(2 · 21)$, where $b_{\tilde{q}}^R$ now plays the role of $b_{\tilde{q}}^L$.

A crucial difference,however,is that $< b_q^R b_{\tilde{q}}^R >$ does not vanish;indeed boundary effect to the Rindler noise just comes from this term , which offers an alternative explanation to Eq.$(1 \cdot 6)$.

In the foregoing discussion we have excluded the 2-dimensional massless case, where rapidity θ could not be defined . Therefore we reexamine this case. It can be shown that the same structure is found if boundary is at $x = b_0 = 0$ by using a Minkowski Mellin mode that a Fourier transform of right(left) moving Minkowski plane wave. The result is

$$|O_B\rangle \propto \prod_{\omega} \exp(e^{\pi\omega} b_\omega^{RMW+} b_\omega^{LMW+}) |O_R\rangle \quad , \qquad (2 \cdot 25)$$

where b^{RMW} and b^{LMW} are right(left) moving massless Rindler particles in 2-dimensional spacetime. Hence we conclude that modified thermalization theorem of the form above hold regardless of the dimension of the spacetime and for massive as well as massless fields.

Acknowledgements

The author would like to acknowledge the continuing guidance and encouragement of Professor S.Takagi. The author are grateful to Professor T.Tuzuki , Professor A.Hosoya and Professor S.Tadaki for helpful discussions. The author also would like to special thank Dr. T.Mishima and Dr. A.Nakayama for helpful suggestions and comments.

Reference

1. W.G.Unruh, Phys.Rev.**D14**(1976),870
   ;in *Quantum Mechanics in Curved Space-Time*
   ed.J.Audretsch and V.de Sabbata(Plenum Press,1990),p.89
2. N.D.Birrell and P.C.Davies, *Quantum Fields in Curved Space*
   (Cambridge University Press,1982),chap.3
3. B.S.DeWitt,in *General Relativity* ed.S.W.Hawking and W.Israel
   (Cambridge University Press ,1979),p.680
4. G.L.Sewell,Ann.of Phys.**141**(1982),201.
5. S.Takagi,Prog.Theor.Phys.Suppl.**88**(1986),1
6. V.L.Ginzburg and V.P.Frolov,Sov.Phys.Usp.**30**(1987),1073.
7. Y.Takahashi and H.Umezawa , Collective Phenomena **2**(1975),55
8. W.Israel, Phys.Lett**A57**(1976),107
9. T.D.Lee,Nucl.Phys.**B264**(1986),107
10. T.Mishima,Prog.Theor.Phys.**82**(1989),930
11. K.Ohnishi and S.Takagi ,in *Thermal Field Theories* ed.H.Ezawa,
    T.Arimitsu and Y.Hashimoto (Elsevier Science Publishers B.V.,1991),p.539
12. U.H.Gerlach ,Phys.Rev.**D38**(1988)514
13. L.N.Pringle ,Phys.Rev.**D39**(1989) 2178

Equilibrium States of General Relativistic Rotating Stars

Y. ERIGUCHI

Department of Earth Science and Astronomy,

College of Arts and Sciences, University of Tokyo

ABSTRACT

Techniques and schemes to study equilibrium states of rotating stars which are available up to now are briefly reviewed. General relativistic treatments are mainly explained but Newtonian cases are also referred to. As one application of numerical computations some results of rapidly rotating neutron stars are discussed.

1. Introduction

Equilibrium configurations of rotating bodies have been investigated since Newton discovered the gravity and applied it to the shape of the earth. Classically the shapes of rotating *fluid* were pursued because it was relatively easy to treat constant density configurations.

Maclaurin discovered that spheroidal configurations can be in equilibrium when they rotate uniformly or rigidly (Maclaurin spheroids). This sequence (Maclaurin sequence) is characterized only by one parameter such as the ellipticity of the meridional cross section or the angular momentum. It should be noted that the angular velocity is not a good parameter to specify the Maclaurin spheroid because there are two different equilibrium states for one value of the angular velocity. About 100 years later Jacobi discovered that ellipsoids can be equilibrium states of uniformly rotating fluid (Jacobi ellipsoids). This Jacobi sequence exists only when the angular momentum of the fluid exceeds a certain critical value. It implies that uniformly and slowly rotating fluids must be axisymmetric but that rapidly rotating fluids can become non-axisymmetric as well as axisymmetric. Furthermore since the Jacobi sequence bifurcates from the Maclaurin sequence, this change can occur continuously by increasing the

amount of the rotation.

Riemann introduced uniform vorticity as well as the uniform rotation and found that, as far as the velocity field is expressed by a linear combination of the coordinate, ellipsoidal configurations are allowed to be in equilibrium states (Riemann ellipsoids). In other words constant density fluids can be in equilibrium when there is a special kind of internal motion together with the uniform rotation. As a special case of Riemann ellipsoid there is an ellipsoidal configuration whose shape is maintained only by the internal motion. This configuration is called Dedekind ellipsoid.

As for the compressible stars the effect of rotation has been tried to include by many authors. However for a long time, since the problem is difficult to treat exactly and no powerful numerical computational ability was available, a perturbational technique was the only method to attack the problem. Although, as far as slowly rotating compressible gases are concerned, some understandings had been obtained, effects of rapid rotation on stars had been estimated from those classical equilibrium configurations.

The appearance of high speed computers seemed to give us a useful tool which helped to compute equilibrium models for rapidly rotating stars. However a moderate numerical computational power was not enough to obtain equilibrium structures of compressible gaseous stars. Mathematically speaking we have to solve an boundary value problem for an elliptical partial differential equation with free boundary. In an ordinary situation elliptical type equations are approximately solved by solving a set of linear equations, i.e. inverting a matrix. Even for axisymmetric configurations the matrix becomes very large and requires a huge amount of computational time. Moreover since one boundary is the surface of the star which is also unknown quantity, it is difficult to apply boundary conditions to the partial differential equation.

Under such a situation, equilibrium configurations of rapidly rotating compressible Newtonian stars was first solved by James in 1964. Around 1970 Ostriker and his colleagues developed the self-consistent-field (SCF) method and applied it to rotating Newtonian barotropes. However, their SCF method cannot be applied to highly deformed and/or very rapidly rotating configurations. Around 1980 Eriguchi and Hachisu succeeded in developing powerful but simplified numerical schemes for obtaining equilibrium structures of rotating compressible stars. They computed many kinds of configurations and found many new equilibrium sequences. Thus as far as the Newtonian gravity is concerned, we have reasonable and practical numerical schemes for rotational problems.

Concerning the strong gravity, since no exact solutions has been found, the effect of the rotation has been estimated and/or extrapolated from the results of Newtonian configura-

tions. It was in 1967 that the problem for slowly rotating configurations was formulated perturbationally by Hartle. Using this formulation slowly rotating configurations have been computed many authors. As for rapidly rotating configurations a thin disk was first solved by Bardeen and Wagoner (1971). The thin disk can, however, be included just as the boundary condition to the Einstein equation. Therefore it would be fair to say that Bardeen and Wagoner solved vacuum solutions with special boundary conditions on the equator.

The internal structure of general relativistic rotating matter was, therefore, first solved by Wilson (1972, 1973). He found that an ergo-region appears inside the matter for rapidly rotating models. However, one of his boundary conditions is Newtonian-like and so his solutions cannot be accepted as accurate ones. Almost the same time Bonazzola and Schneider (1974) used a different numerical scheme and computed relativistic incompressible fluids and ideal Fermi gas models. In their treatment there is a very severe restriction that the metric component g_{tt} can never become positive (here $(-,+,+,+)$ convention is used). Thus they cannot solve very strong gravity cases.

Concerning general relativistic incompressible fluids Butterworth and Ipser (1975, 1976) have succeeded in computing equilibrium structures even for very strong gravity. Their numerical scheme is an extension of the Newtonian scheme developed by Stoeckly (1965). The non-linear differential equations, i.e. Einstein equations, are solved by a Newton-Raphson-like iteration scheme. Therefore they treated carefully the boundary conditions. However its scheme did not work for the compressible gas (Butterworth 1976).

Although the reason of the failure of their scheme for compressible gases is not clearly shown, it may be that their scheme could not be applied to significantly deformed configurations. It may sound strange that the scheme can give solutions for very rapidly rotating and very strong gravity fluids but not for rapidly rotating and strong gravity gases. In order to understand this result we need to think about the nature of the rotation and the gravity. Although the rotation deforms configuration, the gravity acts to gather matter to the central region which results in decreasing the deformation. For the incompressible fluid case the gravity is large even in the outer region of the star and so the deformation is not so large even for significantly rapidly rotating models. On the contrary for the compressible gases the density of the outer region is so low that the rotational effect is not decreased. Thus the numerical scheme which would succeed in solving general relativistic *compressible* gas must be able to handle a significantly deformed configurations.

Komatsu, Eriguchi and Hachisu (1989) have succeeded in developing such a computational scheme. They extended the Newtonian scheme developed by Hachisu (1986). They can compute any kinds of configurations even for very soft equation of states. Thus even in the

general relativistic cases we have basic tools in our hands and have come to the stage to solve structures of rapidly rotating bodies in a practically short time.

It seems that almost every problem can be solved by just computing numerically if a problem is properly posed. However we have to remark that the problem of rotational equilibrium can be handled only for barotropes in general relativistic cases. Rapidly rotating baroclinic stars are just begun to investigate even in the framework of Newtonian gravity. The development of Newtonian field from now on will give us many clues to extension to the general relativity.

2. Axisymmetric Equilibrium States of Rotating Stars

2.1. Assumptions

The equilibrium configurations of rotating stars are considered under the following assumptions.

The space-time and the matter are *axially symmetric* and *stationary*. It implies that there are two Killing vectors. In the framework of general relativity rotating non-axisymmetric space-time and configurations will not be in equilibrium state, although there can be non-axisymmetric equilibrium states in Newtonian gravity. We assume that the matter is confined to a compact region in the space so that the space time is *asymptotically flat*. Concerning the matter it is assumed to be a *perfect fluid*. The energy momentum tensor can be expressed as

$$T^{ij} = (\varepsilon + p)u^i u^j + pg^{ij}, \tag{1}$$

where T^{ij}, ε, p, u^i, and g^{ij} are the energy momentum tensor, the energy density, the pressure, the four velocity and the metric, respectively. Moreover as written in the introduction the equation of state is assumed *barotropic*, i.e.

$$p = p(\varepsilon). \tag{2}$$

2.2. Metric

The stationary and axisymmetric space time can be expressed by the following metric (see e.g. Bardeen 1970; Thorne 1971):

$$ds^2 = g_{00}dt^2 + 2g_{03}dtd\varphi + g_{33}d\varphi^2 + g_{11}(dx^1)^2 + g_{22}(dx^2)^2, \tag{3}$$

where t and φ are the time and the azimuthal coordinates corresponding to two Killing vectors, respectively. When if we use spherical coordinates (r, θ, φ), this metric can be written as:

$$ds^2 = -e^{2\nu}dt^2 + e^{2\alpha}(dr^2 + r^2 d\theta^2) + r^2 \sin^2\theta e^{2\beta}(d\varphi - \omega dt)^2, \tag{4}$$

where ν, α, β and ω are four gravitational potentials. In particular ω is the frame dragging potential (see e.g. Bardeen 1970).

When we treat only the vacuum region, the potential $\beta + \nu$ can be set to vanish and the metric can be reduced to simplified form such as (Papapetrou 1966),

$$ds^2 = f^{-1}[e^{2\gamma}(d\rho^2 + dz^2) + \rho^2 d\varphi^2] - f(dt - \omega d\varphi)^2. \tag{5}$$

However we will not refer to this metric in this review any more.

2.3. Boundary conditions

Since the matter is confined to the compact region, there is a surface of the matter distribution which is defined by the place where the pressure vanishes. When a rotating star or a black hole is surrounded by axisymmetric configuration(s) such as toroid(s), we need to consider two or more surfaces corresponding to matter configurations.

Concerning the metric the asymptotically flat conditions are written for the metric (4) as

$$\nu \to -\frac{M}{r} + O(\frac{1}{r^2}), \tag{6a}$$

$$\beta \to \frac{M}{r} + \frac{\beta_0}{r^2} + O(\frac{1}{r^3}), \tag{6b}$$

$$\omega \to \frac{2J}{r^3} - \frac{6MJ}{r^4} + O(\frac{1}{r^5}), \tag{6c}$$

$$\alpha \to \beta + O(\frac{1}{r^4}), \tag{6d}$$

where M, J and β_0 are the gravitational mass, the total angular momentum and a certain constant, respectively.

When we consider a rotating star, the gravitational potential must be regular at its center. However when we consider a (rotating) black hole and a surrounding axisymmetric matter configuration, the metric should behave on the horizon of the black hole as follows if we use coordinates in which the horizon is set to $r = constant$ (see e.g. Bardeen 1973):

$$e^{\nu} = 0, \tag{7a}$$

$$\omega = \omega_H (= \text{constant}), \tag{7b}$$

and

$$\beta = \text{finite}, \tag{7c}$$

where ω_H is the dragging of the horizon.

One more boundary condition is obtained from the local flatness of the space-time on the rotation axis, which reads

$$\alpha = \beta, \qquad \text{z} - \text{axis}. \tag{8}$$

The problem is, therefore, only to solve the Einstein equations derived from the metric (4) with boundary conditions mentioned above which are suitable for the situation considered. However it is not easy to solve them directly. Historically speaking, as discussed in the introduction, weak gravity cases and/or slow rotation cases have been investigated first.

3. Newtonian and Post-Newtonian Rotating Stars

Concerning equilibrium configurations for Newtonian stars details are not reviewed in this paper but references are listed for those who are interested in them.

When the gravity becomes strong but not so strong, the problem can be handled in the post-Newtonian frame. Chandrasekhar (1965) formulated the problem to the order of $1/c^2$ and after that Chandrasekhar and Nutku (1969) extended it to the order of $1/c^4$.

In the post-Newtonian treatment of uniformly rotating stars the metric can be expressed by using three potentials, U, Φ and D as follows:

$$g_{00} = -c^2 \left(1 + 2\frac{U}{c^2} + \frac{2U^2 + 4\Phi}{c^4}\right), \tag{9a}$$

$$g_{11} = g_{22} = g_{33} = 1 + \frac{2U}{c^2}, \tag{9.b}$$

$$g_{01} = -\frac{4\Omega x_2 D}{c^3}, \tag{9c}$$

and

$$g_{02} = \frac{4\Omega x_1 D}{c^3}, \tag{9d}$$

where Ω and (x_1, x_2, x_3) are the angular velocity and the Cartesian coordinates, respectively. These potential must satisfy the following differential equations:

$$\nabla^2 U = 4\pi G\rho, \tag{10a}$$

$$\nabla^2 D + \frac{1}{r}\frac{\partial D}{\partial r} - \frac{\mu}{r^2}\frac{\partial D}{\partial \mu} = 4\pi G\rho, \tag{10b}$$

and

$$\nabla^2 = 4\pi G\rho\left[\Omega^2 r^2(1-\mu^2) - U + \frac{1}{2}\Pi + \frac{3}{2}\frac{p}{\rho}\right], \tag{10c}$$

where $\mu = \cos\theta$, ρ and $\rho\Pi$ are the mass density and the internal energy density which is defined as

$$\varepsilon = \rho(1+\Pi). \tag{11}$$

The hydrostatic equilibrium equation can be written as

$$\left[1 - \frac{\Pi + p/\rho}{c^2}\right]\nabla p = \rho\nabla\left[-U + \frac{1}{2}\Omega^2 r^2 \sin^2\theta\right.$$

$$\left. + \frac{1}{c^2}\left(\frac{1}{2}(\Omega r\sin\theta)^4 - 2U(\Omega r\sin\theta)^2 - 2\Phi + 4(\Omega r\sin\theta)^2 D\right)\right]. \tag{12}$$

These equations are solved for slowly rotating polytropes by Fahlman and Anand (1971) when $1.5 \leq N \leq 3$ where N is the polytropic index. For rapidly rotating cases Miketinac and Barton (1972) applied the Stoeckly's scheme (1965) and obtained equilibrium configurations for $N = 1.5$ and $N = 3$ sequences.

4. Slow Rotation Approximation

The rotation can be parametrized by the following quantity

$$\omega^2 \equiv \frac{\Omega^2}{4\pi G\varepsilon}. \tag{13}$$

This parameter is roughly equal to the ratio of the centrifugal force to the gravitational force or the ratio of the rotational energy to the gravitational energy. Thus when stars rotate slowly, this parameter is so small that we can expand physical quantities in terms of this parameter.

The first attempt of this slow rotation approach was tried by Hartle (1967). The metric for slowly rotating stars can be expressed as

$$ds^2 = -e^{2\nu}dt^2 + e^{2\lambda}dr^2 + r^2e^{2\mu}[d\theta^2 + \sin^2\theta(d\varphi - \omega dt)^2], \tag{13}$$

where

$$e^{2\nu} = e^{2\nu_0}[1 + 2h_0(r) + 2h_2(r)P_2(\cos\theta)], \tag{14a}$$

$$e^{2\lambda} = e^{2\lambda_0}\left(1 + \frac{e^{2\lambda_0}}{r}[1 + 2m_0(r) + 2m_2(r)P_2(\cos\theta)]\right), \tag{14b}$$

$$e^{2\mu} = 1 + 2k_2(r)P_2(\cos\theta), \tag{14c}$$

and the quantities with subscript $_0$ are those for spherical models. From the Einstein equation the dragging term ω must satisfy

$$\frac{1}{r^4}\frac{d}{dr}\left(r^4 j\frac{d\bar{\omega}}{dr}\right) + \frac{4}{r}\frac{dj}{dr}\bar{\omega} = 0. \tag{15}$$

where

$$\bar{\omega} \equiv \Omega - \omega, \tag{16}$$

and

$$j \equiv e^{-(\nu_0+\lambda_0)}. \tag{17}$$

The boundary condition to this equation is

$$\bar{\omega} \to \Omega - \frac{2J}{r^3}. \tag{18}$$

Thus we can solve the dragging term without knowing other perturbed quantities. Other perturbed quantities are solved afterwards. These equations are numerically solved by Hartle and Thorne (1968) for Harrison-Wheeler equation of state, V_γ equation of state and for massive stars with $N = 3$ polytrope. They applied their results to obtain the increase of the mass due to rotation and found that rotation can increase the mass about 20% as far as uniform rotation is concerned. This formulation has been used by many authors for various situations which are considered to be rotate slowly (Chandrasekhar and Miller 1974; Miller 1977) and for slowly rotating neutron stars (Datta and Ray 1983; Ray and Datta 1984).

5. Rapidly Rotating Relativistic Disks

Although thin disks are not interesting objects from the standpoint of the internal structure, the behavior of the space-time deserves investigation because the rotational effect of the matter may be understood. Bardeen and Wagoner (1971) treated uniformly rotating infinitesimally thin disks. As for the metric they used the same type as Eq.(4) in the cylindrical coordinates (ρ, z, φ). Since almost all space are vacuum except on the equatorial plane, the metric component $\beta + \nu$ can be set to vanish, i.e.

$$\beta + \nu = 0. \tag{19}$$

Two components of the Einstein equations for the vacuum can be written as:

$$\nabla^2\nu = \frac{1}{2}\rho^2 e^{-4\nu}\nabla\omega\nabla\omega, \tag{20a}$$

and

$$\rho^{-2}\nabla(\rho^2\nabla\omega) = 4\nabla\nu\nabla\omega. \tag{20b}$$

Here it should be noted that in these equations the metric α does not appear. Thus we can solve two metric components ν and ω first and then solve for α which satisfies a first order differential equation which we will not write here.

The boundary conditions which can be obtained from integration of the Einstein equation with matter terms through the disk are written as

$$\frac{\partial\nu}{\partial\xi} = 2\pi a|\eta|\sigma\frac{1+v^2}{1-v^2}, \tag{21a}$$

$$\frac{\partial\omega}{\partial\xi} = -8\pi a|\eta|\sigma\frac{\Omega-\omega}{1-v^2}, \tag{21b}$$

where ξ and η are oblate spheroidal coordinates defined by

$$\rho = a(1+\xi)^{1/2}(1-\eta^2)^{1/2}, \qquad z = a\xi\eta, \tag{22}$$

$$\sigma \equiv \int \varepsilon e^{2\alpha} dz, \tag{23}$$

and a is the coordinate radius of the disk.

In practice Bardeen and Wagoner made use of the expansion of physical quantities with respect to the quantity γ which is defined as

$$\gamma \equiv 1 - e^{2\nu_c}, \tag{24}$$

where ν_c is the value of the metric at the center of the disk. This quantity measures the strength of the gravity or is related to the red shift factor at the center z_c as

$$\gamma = \frac{z_c}{1+z_c}. \tag{25}$$

For example the metric ν is expanded as

$$\nu = \sum_{n=1}^{\infty} \nu_n(\xi,\eta)\gamma^n. \tag{26}$$

In this way Bardeen and Wagoner obtained the binding energy (E_b), the gravitational mass (M) and so on of the thin disks. They can be written as:

$$\frac{E_b}{M_0} = \frac{\gamma}{5}[1 + \frac{2}{5}\gamma + 0.1879\gamma^2 + 0.1002\gamma^3 + \cdots], \tag{27}$$

$$\frac{M^2}{J} = \frac{10}{3\pi}\gamma^{1/2}[1 + 0.05\gamma - 0.02362\gamma^2 - 0.02399\gamma^3 - \cdots], \tag{28}$$

where M_0 and J are the rest mass and the total angular momentum, respectively. The limiting values for $\gamma \to 1$ of these quantities are

$$\frac{E_b}{M_0} \to 0.373, \tag{29}$$

$$\frac{M^2}{J} \to 1.00014. \tag{30}$$

These vales are those of extreme Kerr metric and so in this limit the space-time will reach that of Kerr space-time. One special nature of the space-time around the thin disk is the appearance of the ergo-toroid region, i.e. the topology of the ergo-region is not spheroidal but toroidal where the rotation axis is not included inside the ergo-region.

Salpeter and Wagoner (1971) treated the effect of the pressure of the disks.

6. Rapidly Rotating Relativistic Stars

Wilson (1972) computed the structure and the space-time around the massive star with the polytropic index $N = 3$ in the framework of the general relativity. He wrote down the Einstein equations and solved the differential equations iteratively and obtained solutions.

However his treatment had two shortcomings. First he fixed the matter distribution. Thus he obtained the gravitational field and the rotation law which are consistent with the prescribed matter distribution. In this kind of approach unless we know the matter distribution rather precisely, we cannot obtain physically realistic models.

Second point is related to the boundary condition of the metric. Since in the numerical computation we can only handle a finite region, we need to be very careful about the *asymptotically flat* condition. Wilson applied Newtonian-like boundary condition to the metric ν. Therefore his computation might be significantly different from the real solutions especially when very strong gravity is treated.

Although his scheme was limited in the sense mentioned above, he found the ergo-toroidal region for the first time for the matter.

Wilson (1973) computed rapidly rotating neutron star models by revising his code whose details, however, were not be clearly described. He computed differentially rotating models and applied the stability criterion of the Newtonian analysis that rotating configurations may become unstable against the $m = 2$ deformation mode when the ratio of the rotational energy to the gravitational energy exceeds 0.14. In doing so he concluded that the rotation might increase the gravitational mass of the neutron star by $50 - 70\%$ compared with that of the spherical cases.

Almost the same time Bonazzola and Schneider (1974) developed a completely different numerical scheme to handle general relativistic rotating stars. Their idea was to use the integral representation of the potentials. Of course the Einstein equations are not linear equations the potentials cannot be represented explicitly as the case for Newtonian potential. However if the non-linear terms with respect to the potentials are treated as the source terms, the remaining linear differential operators have been integrated by using appropriate Green functions corresponding to the operators. The most important point in this kind of treatment is that we can easily include the boundary condition at the infinity. This is essential for the numerical computation because we can only treat a finite region.

Therefore their basic ideas were fine but their metric was not nice. They used $\ln(-g_{tt})$ as one of the variables. It implies that they cannot treat the space-time in which a region where $g_{tt} > 0$ appears, i.e. very strong gravity case. (In Bonazzola and Schneider paper the sign convention is taken as $(+,-,-,-)$ but in this paper the sign convention is taken as $(-,+,+,+)$.)

They computed the incompressible fluids and completely degenerate Fermi gas models. For incompressible fluids their results were compared with results of Newtonian (Maclaurin sequence) and post-Newtonian treatments. The agreement was good and as far as the strength of the gravity is not so large. Their results showed that there appeared prolate iso-density regions in the central region of the degenerate gases. However it is very difficult to deform the central region to prolate shape by rotation, although they interpreted that the effect of the dragging could work to prolate configuration. The dragging potential can never exceed the angular velocity at the same point and so they cannot act as "anti-centrifugal" force which might result in prolate shape. Thus there may be something wrong with their codes, which should not be said officially(?).

First satisfactory configurations for rapidly rotating and highly general relativistic stars were obtained by Butterworth and Ipser (1975,1976). They solved the differential equations

by applying Newton-Raphson-like iteration scheme. In doing so the boundary conditions were carefully analyzed because of the finite region requirement in numerical computations mentioned before. In practice multipole expansions for the metric were done to the orders $1/r^5$, $1/r^7$ and $1/r^6$ for ν, ω and β, respectively.

If a set of non-linear equations, i.e. Einstein equations, were properly treated by Newton-Raphson scheme, a very large size of matrix would be inverted, which would be very time consuming and far from practical. Thus they handled as follows. When the second order differential of a certain metric appears in a certain equation, its equation is treated as the equation for its metric by assuming that other metrics which are necessarily included in the equation are already known. Therefore its equation is linearized with respect to the metric concerned and the "Newton-Raphson" iteration scheme is applied. After the iteration converges, the second metric and the second equation are chosen ad the same procedure is followed. In solving the second metric the newly converged values for the first metric is used. The convergence of this scheme is not assured but as far as the uniformly rotating incompressible fluids they have succeeded in computing many equilibrium configurations.

Their models for the incompressible fluid cover very wide range of rotation and the gravity space. For very strong gravity model sequences they found that an ergo-toroidal region appears for rapidly rotating cases. Therefore their scheme may be said very satisfactory for investigation of general relativistic rotating stars.

However it may sound strange that their scheme did not give solution for *Newtonian* or *post-Newtonian* configurations if the rotation is very rapid or it should be said that the deformation becomes considerable. They can only obtain equilibrium configurations with the axis ratio less than 0.4, $r_p/r_e < 0.4$, where r_p and r_e are the polar radius and the equatorial radius of the star, respectively. For very strong gravity models strong gravity acts as gathering mass towards the central region and thus even very rapid rotation does not deform the star considerably as far as the incompressible fluid is concerned.

Butterworth (1976) applied this scheme to the compressible stars. However his code could not give equilibrium solutions for rapidly rotating and strong gravity models. Butterworth wrote that the reason of the failure was unclear. Although there may be some errors in the numerical codes, one reason may be that their scheme is not suitable for highly deformed configurations.

Anyway Butterworth computed polytropic configurations with $0.5 \leq N \leq 3.0$. The strength of gravity can be parametrized by the following quantity

$$\kappa \equiv \frac{p_c}{\varepsilon_c}, \tag{31}$$

where subscript $_c$ denotes that the quantities are evaluated at the center. Models he could

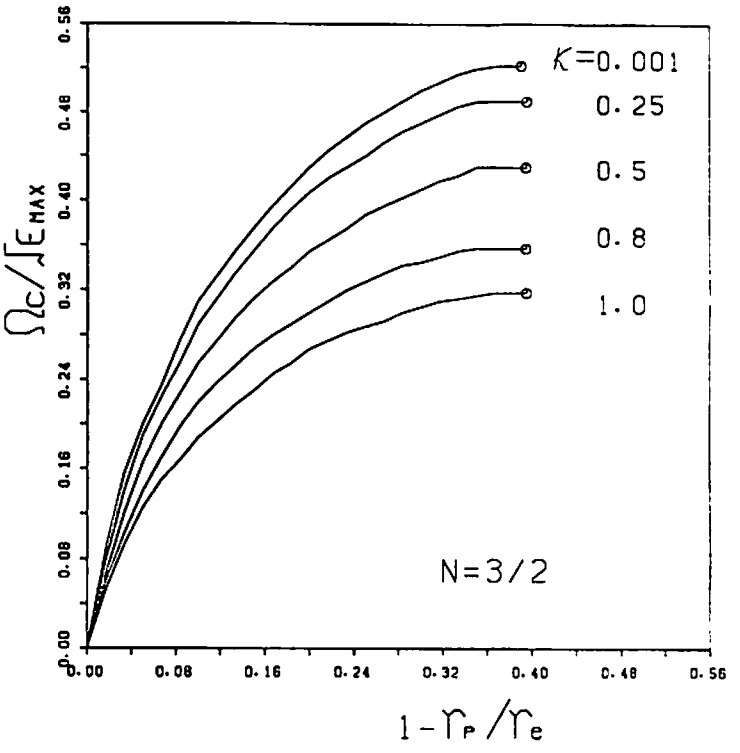

Fig. 6.1 The non-dimensional angular velocity $\Omega/\varepsilon^{1/2}$ is plotted against the coordinate ratio r_p/r_e for $N = 1.5$ polytrope. The numbers attached to curves are the values of the strength of gravity κ. The open circles denote critical states where mass-shedding begins.

computed were those with $\kappa < 0.25$, which are not so highly relativistic. This is contrasted with the fact that for the incompressible cases their code gave solutions even for $\kappa = 2 \sim 3$.

Butterworth and Ipser's scheme are, therefore, nice for rather wide range of parameters but not be satisfactory for any parameters of models. If possible more powerful numerical schemes are desired.

In the Newtonian framework Hachisu (1986) succeeded in formulating a very versatile scheme to treat any kind of rotation law and any kind of deformations so far as barotropes are concerned. The basic idea of Hachisu's scheme is the extension of the SCF method by Ostriker et al. In the SCF method the problem is divided into two parts: the potential part and the density part. In the potential part the assumed density distribution is used to compute the gravitational potential. After obtaining the gravitational potential, the density is solved

form the hydrostatic equilibrium equation by using the obtained gravitational potential. This iteration cycle is pursued until the density and the potential converge. In this iteration scheme the most important point is the choice of model parameters whose values are fixed all through iteration cycles. If improper parameters are chosen, the iteration will diverge.

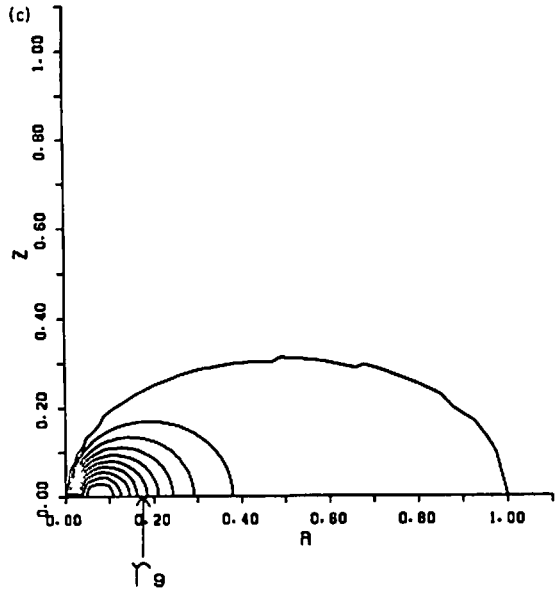

Fig. 6.2 The energy density in the meridional cross section is drawn for $N = 1.5$ polytrope when $\kappa = 0.4$. Contours are linearly spaced by 1/10 of the maximum energy density. The arrow with r_g denotes the radius of the gravitational radius corresponding to the total mass of the "ring".

Komatsu et al.(1989) have extended the Hachisu's scheme to general relativistic stars. In doing so they combined the integral representation of the Einstein equation which Bonazzola and Schneider (1974) formulated and the Hachisu's scheme for iteration to solve non-linear equations. This scheme has worked almost perfectly as far as problems treated thus far and seems to have almost no limitations for its applicability.

Komatsu et al.(1989) computed rapidly rotating relativistic polytropes with uniform rotation without any difficulty. They found that the critical states where the "centrifugal" force balances the gravity at the equatorial surface are characterized by the same axis ratio irrespective of the strength of the gravity for $N = 1.5$ polytropes (Fig.6.1)

They also applied their scheme to differentially rotating polytropes. For highly differentially rotating cases equilibrium configurations become ring-like. One example is shown in

Fig.6.2, in which the iso-density contours are shown for $N = 1.5$ polytrope. The gravitational radius corresponding to the total mass is show by the arrow. As seen from this figure that this configuration is highly relativistic and considerably deformed.

As shown by Komatsu et al.(1989) we are now at the stage that any configurations in general relativity can be solved as far as barotropes are concerned (of course in the weak gravity cases Hachisu's scheme (HSCF-scheme) (1986) or Eriguchi and Müller's scheme (SFNR-scheme) (1985) can give solutions for almost every situation). Therefore we should apply these schemes to realistic states such as rapidly rotating neutron stars or extend their schemes to treat baroclinic states, which may be very difficult.

7. Rapidly Rotating Neutron Stars

Although the equation of state is uncertain for the nuclear matter region and beyond from the analysis of theories and experiments on the earth, the existence of the neutron star may give us information about the equation of state. Since soft equations of state results in relatively small radius of the neutron star, rather rapid rotation can be allowed. On the other hand, for stiff equations of state, rapid rotation will cause to shed mass from the equator by the centrifugal force because of its rather large radius. Thus it is important to determine how rapidly neutron stars can rotate for each equation of state proposed thus far for the neutron star matter.

As mentioned in the previous section several authors (Butterworth and Ipser 1975, 1976; Butterworth 1976; Komatsu, Eriguchi and Hachisu 1989) have succeeded in solving Einstein equations by different schemes. These schemes can be applied to obtain structures of rapidly rotating neutron stars.

Friedman et al. (1984, 1986, 1988, 1989) have used the same formulation as Butterworth and Ipser's (1975) and developed an independent numerical code. They have applied it to realistic neutron stars by using many kinds of equation of states for the high density region and obtained many equilibrium configurations. However they did not explicitly mention that their code gives different results from those by Butterworth who wrote that Butterworth's method (1976) did not give solutions for highly relativistic and rapidly rotating *compressible* models as mentioned before.

Since the existence and the structure of the realistic neutron stars affect the nuclear matter physics, it is desirable to compute the same problem by totally different numerical scheme and compare results with theirs. Komatsu et al.'s code (1989) has been applied to

models with very wide range of the rotation rate and the compressibility, and their scheme seems to have no limitation in the strength of the relativity and the rotation rate. Eriguchi et al. (1992) have used Komatsu et al.'s scheme (1989) to compute realistic neutron star models.

The metric is that of Eq.(4). Uniformly and differentially rotating models are computed. Concerning the equation of state, four different equations of states are used : (1) Pandharipande's equation of state for neutron matter (1971); (2) Friedman - Pandharipande's equation of state (1981); (3) and (4) Bethe -Johnson's equations of state (I) and (V) (1979).

For uniformly rotating neutron stars the results are summarized in Fig.7.1. In Fig.7.1 the maximum angular velocity is drawn against the total mass of the neutron star. As seen from this figure results by Eriguchi et al.(1992) (E-H-N) are in good agreement with those of Friedman et al.'s computation (1989) (F-I-P) except in rather high energy density region. The difference of the maximum angular velocity is several percent at the most highest density region especially for the Friedman-Pandharipande's equation of state.

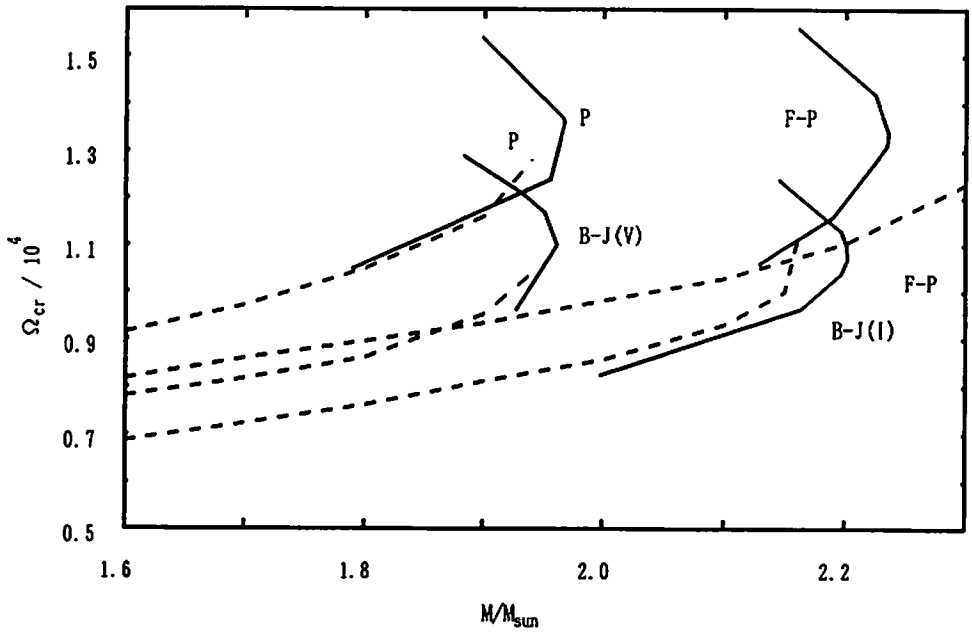

Fig.7.1 The maximum angular velocities for uniformly rotating neutron stars are drawn against the gravitational mass of the neutron star. Different curves correspond to different equations of states whose abbreviations are attached to curves. P : Pandharipande's neutron matter. F-P: Friedman - Pandharipande's equation of state. B-J: Bethe-Johnson's equation of state. Full curves denote present results and dashed curves denote Friedman et al.'s results.

This may come from the difference of formulations and numerical codes. In order to obtain the maximum angular velocity we have to compute the equatorial radius of the neutron star as accurate as possible. If the radius determined by one numerical code may be a little larger than a true value, the angular velocity obtained will becomes smaller than a true value and vice versa. In particular the accuracy of the obtained model for very high energy density region becomes crucial for that problem. In this region the central energy density and the ratio (κ) of the central pressure p_c to the central energy density ε_c are :

$$\kappa \equiv p_c/\varepsilon_c = 0.67, \quad \epsilon_c \sim 3.4 \times 10^{15}\mathrm{g/cm^3}, \quad \mathrm{E-H-N}$$

$$\kappa \sim 0.38, \quad \varepsilon_c \sim 2.5 \times 10^{15}\mathrm{g/cm^3}. \quad \mathrm{F-I-P}$$

Therefore the difference may come from the limitation of applicability of numerical schemes in computing structure of rotating matter with very strong gravity.

REFERENCES

Relativistic Rotating Stars

Review

J.M. Bardeen: 1973, *in Black Holes (Les Houches 1972)*, ed. C. DeWitt and B.S. DeWitt : Gordon and Breach, New York, p.241-289

K.S. Thorne: 1971, *in General Relativity and Cosmology*, ed. R.K. Sacks : Academic Press, New York, p.237-283

Slow Rotation

J.B. Hartle: 1967, *Astrophys.J.*, **150**, 1005

J.B. Hartle and K.S. Thorne: 1968, *Astrophys.J.*, **153**, 807

S. Chandrasekhar and J.C. Miller: 1974, *Mon. Not. Roy. Astr. Soc.* , **167**, 63

B. Datta and A. Ray: 1983, *Mon. Not. Roy. Astr. Soc.* , **204**, 75p

J.C. Miller: 1977, *Mon. Not. Roy. Astr. Soc.*, **179**, 483

A. Ray and B. Datta: 1984, *Astrophys.J.*, **282**, 542

Variational Principle

J.M. Bardeen: 1970, *Astrophys. J.*, **162**, 71
J.B. Hartle and D.H. Sharp: 1965, *Phys. Rev. Lett.*, **15**, 909
J.B. Hartle and D.H. Sharp: 1967, *Astrophys. J.*, **147**, 317
M.A. Abramowicz and R.V. Wagoner: 1978, *Astrophys. J.*, **226**, 1063

Vacuum Solution

R.P. Kerr: 1963, *Phys. Rev. Lett.*, **11**, 237
A. Papapetrou: 1966, *Ann. Inst. H. Poincaré*, **A-4**, 83
A. Tomimatsu and H. Sato: 1972, *Phys. Rev. Lett.*, **29**, 1344

Rapidly Rotating Stars

[Disks]

J.M. Bardeen and R.V. Wagoner: 1971, *Astrophys. J.*, **167**, 359
E.E. Salpeter and R.V. Wagoner: 1971, *Astrophys. J.*, **164**, 557

[Spheroidal and Toroidal Configurations]

E.M. Butterworth: 1976, *Astrophys.J.*, **204**, 561
E.M. Butterworth and J.R. Ipser: 1975, *Astrophys.J.*, **200**, L103
E.M. Butterworth and J.R. Ipser: 1976, *Astrophys.J.*, **204**, 200
J.L. Friedman, J.R. Ipser and L. Parker: 1984, *Nature*, **312**, 255
J.L. Friedman, J.R. Ipser and L. Parker: 1986, *Astrophys.J.*, **304**, 115
J.L. Friedman, J.R. Ipser and L. Parker: 1988, *Nature*, **336**, 560
J.L. Friedman, J.R. Ipser and L. Parker: 1989, *Phys. Rev. Lett.*, **62**, 3015
H. Komatsu, Y. Eriguchi and I. Hachisu: 1989, *Mon. Not. Roy. Astr. Soc.*, **237**, 355
H. Komatsu, Y. Eriguchi and I. Hachisu: 1989, *Mon. Not. Roy. Astr. Soc.*, **239**, 153
S. Bonnazola and J. Schneider: 1974, *Astrophys. J.*, **191**, 273
J.M. Lattimer, M. Prakash, D. Masak and A. Yahil: 1990, *Astrophys.J.*, **355**, 241
J.R. Wilson: 1972, *Astrophys.J.*, **176**, 195
J.R. Wilson: 1973, *Phys. Rev. Lett.*, **30**, 1082
X. Wu, H. Müther, M.Stoffel, H. Herold and H. Ruder: 1991, *Astron. Astrophys.*, **246**, 411

Equation of States for Neutron Stars

W.D. Arnett and R.L. Bowers: 1977, *Astrophys. J. Suppl.*, **33**, 415
G. Baym, C. Pethick and P. Sutherland: 1972, *Astrophys. J.*, **170**, 299
H.A. Bethe and M. Johnson: 1974, *Nucl. Phys.*, **A230**, 1
B. Friedman and V.R. Pandharipande : 1981, *Nucl. Phys.*, **A361**, 502
V.R. Pandharipande : 1971, *Nucl. Phys.*, **A174**, 641
V.R. Pandharipande : 1971, *Nucl. Phys.*, **A178**, 123

Post-Newtonian Treatment

S. Chandrasekhar: 1965, *Astrophys. J.*, **142**, 1488
S. Chandrasekhar and Y. Nutku: 1969, *Astrophys. J.*, **158**, 55
J.M. Bardeen: 1971, *Astrophys. J.*, **167**, 425
M.J. Miketinac and R.J. Barton: 1972, *Ap. Sp. Sci.*, **18**, 437
G.G. Fahlman and S.P.S. Anand: 1971, *Ap. Sp. Sci.*, **12**, 58
S.L. Shapiro and A.P. Lightman: 1976, *Astrophys.J.*, **207**, 263

Self-gravitating-toroid (BH-toroid, Star-toroid)

C. Will: 1974, *Astrophys. J.*, **191**, 521
C. Will: 1975, *Astrophys. J.*, **194**, 41
S. Nishida, Y. Eriguchi and A. Lanza: 1991, *Astrophys. J.*, , submitted
A. Lanza: 1992, *Astrophys. J.*, , in press
S.K. Chakrabarti: 1988, *J. Astrophys. Astron.*, **9**, 49

Newtonian Rotating Stars

Book

S. Chandrasekhar: 1969, *Ellipsoidal Figures of Equilibrium*, Yale University Press, New Haven

Y. Hagihara: 1970, *Theories of Equilibrium Figures of a Rotating Homogeneous Fluid Mass*, NASA SP-186
R.A. Lyttleton: 1953, *The Stability of Rotating Liquid Masses*, Cambridge Univ. Press, Cambridge
L. Lichtenstein: 1933, *Gleichgewichtsfiguren Rotierender Flüssigkeiten*, Springer, Berlin

J.L. Tassoul: 1978, *Theory of Rotating Stars*, Princeton University Press, Princeton

Classical

G.H. Darwin: 1901, *Phil. Trans. Roy. Soc. London*, **A197**, 1
G.H. Darwin: 1902, *Phil. Trans. Roy. Soc. London*, **A198**, 301
G.H. Darwin: 1903, *Phil. Trans. Roy. Soc. London*, **A203**, 111
F.W. Dyson: 1893, *Phil. Trans. Roy. Soc. London*, **A184**, 43
F.W. Dyson: 1893, *Phil. Trans. Roy. Soc. London*, **A184**, 1041
M.P. Humbert: 1915a, *Comptes Rendus de Acad. Sci. Paris*, **160**, 509
M.P. Humbert: 1915b, *Comptes Rendus de Acad. Sci. Paris*, **160**, 594
M.P. Humbert: 1915c, *Comptes Rendus de Acad. Sci. Paris*, **161**, 340
M.P. Humbert: 1918, *Comptes Rendus de Acad. Sci. Paris*, **167**, 776
H. Poincaré: 1885, *Acta Math.*, **7**, 259

Slow Rotation

S. Chandrasekhar: 1933, *Month. Not. Roy. Astron. Soc.*, **93**, 390
S. Takeda: 1934, *Mem. College Sci. Kyoto Imp. Univ.*, **17**, 197
J. Faulkner, I.W. Roxburgh and P.A. Strittmatter: 1968, *Astrophys. J.*, **151**, 203
R. Kippenhahn and H.-C. Thomas: 1970, *in Stellar Rotation*, ed. A. Slettebak : Reidel, Dordrecht, p.20
I.W. Roxburgh: 1974, *Astrophys. Sp. Sci.*, **27**, 425
I.W. Roxburgh, J.S. Griffith and Sweet, P.A.: 1965, *Z. Astrophys.*, **61**, 203
J.J. Monaghan and I.W. Roxburgh: 1965, *Month. Not. Roy. Astron. Soc.*, **131**, 13
J.C.B. Papaloizou and J.A.J. Whelan: 1973, *Month. Not. Roy. Astron. Soc.*, **164**, 1
J.A.J. Whelan, J.C.B. Papaloizou and R.C. Smith: 1971, *Month. Not. Roy. Astron. Soc.*, **152**, 9p

Rapid Rotation

[Pioneering Work]

R.A. James: 1964, *Astrophys. J.*, **140**, 552
R. Stoeckly: 1965, *Astrophys. J.*, **142**, 208

[SCF-Method]

S.I. Blinnikov: 1975, *Sov. Astron.*, **19**, 151
P. Bodenheimer: 1971, *Astrophys.J.*, **167**, 153
P. Bodenheimer and J.P. Ostriker: 1970, *Astrophys.J.*, **161**, 1101
P. Bodenheimer and J.P. Ostriker: 1973, *Astrophys.J.*, **180**, 159
S. Jackson: 1970, *Astrophys.J.*, **161**, 579
J. W-K. Mark: 1968, *Astrophys.J.*, **154**, 627
J.P. Ostriker and P. Bodenheimer: 1968, *Astrophys.J.*, **151**, 1089
J.P. Ostriker and F.D.A. Hartwick: 1968, *Astrophys.J.*, **153**, 797
J.P. Ostriker and J. W-K. Mark: 1968, *Astrophys.J.*, **151**, 1075

[EFGH-Method, SFNR-scheme, HSCF-scheme]

Y. Eriguchi: 1978, *Publ. Astron. Soc. Japan*, **30**, 507
Y. Eriguchi and I. Hachisu: 1982, *Prog. Theor. Phys.*, **67**, 844
Y. Eriguchi and I. Hachisu: 1983, *Prog. Theor. Phys.*, **69**, 1131
Y. Eriguchi and I. Hachisu: 1983, *Prog. Theor. Phys.*, **70**, 1534
Y. Eriguchi and I. Hachisu: 1985, *Astron. Astrophys.*, **142**, 256
Y. Eriguchi and I. Hachisu: 1985, *Astron. Astrophys.*, **148**, 289
Y. Eriguchi, I. Hachisu and D. Sugimoto: 1982, *Prog. Theor. Phys.*, **67**, 1068
Y. Eriguchi and E. Müller: 1985, *Astron. Astrophys.*, **146**, 260
Y. Eriguchi and E. Müller: 1985, *Astron. Astrophys.*, **147**, 161
Y. Eriguchi, E. Müller and I. Hachisu: 1986, *Astron. Astrophys.*, **168**, 130
Y. Eriguchi and D. Sugimoto: 1981, *Prog. Theor. Phys.*, **65**, 1870
I. Hachisu: 1986, *Astrophys. J. Suppl.*, **61**, 479
I. Hachisu: 1986, *Astrophys. J. Suppl.*, **62**, 461
I. Hachisu and Y. Eriguchi: 1982, *Prog. Theor. Phys.*, **68**, 206
I. Hachisu and Y. Eriguchi: 1984, *Publ. Astron. Soc. Japan*, **36**, 239
I. Hachisu and Y. Eriguchi: 1984, *Publ. Astron. Soc. Japan*, **36**, 259
I. Hachisu and Y. Eriguchi: 1984, *Publ. Astron. Soc. Japan*, **36**, 497
I. Hachisu, Y. Eriguchi and D. Sugimoto: 1982, *Prog. Theor. Phys.*, **68**, 191
I. Hachisu, J.L.Tohline and Y. Eriguchi: 1987, *Astrophys. J.*, **323**, 592
E. Müller and Y. Eriguchi: 1985, *Astron. Astrophys.*, **152**, 325

[Other 3-Dimensional Model]

J.R. Ipser and R.A. Managan: 1981, *Astrophys.J.*, **250**, 362

A GENERAL RELATIVISTIC RING AROUND A BLACK HOLE

SHOGO NISHIDA[1], YOSHIHARU ERIGUCHI[1] AND ANTONIO LANZA[2]

[1]Department of Astronomy and Earth Science,
College of Arts and Sciences, University of Tokyo, Meguro,Tokyo, Japan 153

[2] International School for Advanced Studies,
Strada Costiera 11, 34024 Trieste, Italy

ABSTRACT

We have got solutions of general relativistic equilibrium structure of black hole - ring systems. Our computational method are without any approximations about gravity of the ring or the rotation of the black hole. The ring around the black hole is a thick toroid of the polytropic gas. This is the first solutions of the Einstein's equation consisting of a self-gravitating thick toroid around a black hole, and our method has no limitation about the mass of the ring relative to the black hole's. Here we investigate the highly relativistic effect of the ring to the black hole or the external space. Dragging of inertial frame caused] by the ring is studied through the black hole's mass - angular momentum - angular velocity relation.

I. INTRODUCTION

Since Schwarzshild discovered the black hole as a solution of the vacuum Einstein equation, many works have been done for the black hole physics analytically or numerically. There are many solutions representing the black holes in the pure vacuum. But it is very difficult to solve the Einstein equation which has non-vanishing stress-energy tensor.

Will(1974,1975) got stationary axisymmetric solutions of the infinitesimal ring around a slowly rotating black hole by perturbing Schwarzshild solution to the first order of the ratio of the ring's mass to the hole's mass and to the second order of the hole's angular velocity. Chakrabarti(1988) used vacuum static axisymmetric solution for the infinitesimal ring configuration around a hole. But they didn't solve the matter equation $T^{\mu\nu}_{;\nu} = 0$. There is no analytical solution for matter until now. Practically it seems impossible to handle the matter distribution analytically. Then only numerical computation is what we can do in order to solve the non vacuum Einstein equation more generally.

Even numerically it is difficult to solve non-vacuum equation. There is only one calculation solving the relativistic self-gravitating disk around a black hole(Lanza;1991). Lanza's method deals with stationary axisymmetric infinitesimally thin disk around a black hole.

We have succeeded in obtaining the general relativistic solutions of self-gravitating thick polytropic fluid around a rotating hole. Our method basically allows any mass ratio of the ring to the hole. So our method can be applied to not only astrophysically reasonable models but also astrophysically unrealistic but physically interesting ones. As the latter case, we discuss the dragging of inertial frame due to the ring and the hole, tidal force to the hole by the ring. All of these are the ring's highly relativistic effect in the spacetime. These effects are described by the changes of macroscopic quantities of the black hole i.e. gravitaional mass, angular momentum, angular velocity, surface area, effective temparature. These quantities are ralated by only one equation in the general stationary axisymmetric case, although Kerr black hole have only two independent quantity.

From the astrophysical point of view, it is important to investigate the structure of accreting ring around the black hole. Stability of a thick toroidi has been discussed by many people. Abramowicz(1983) suggested runaway instability will occur by the ring's axisymmetric accretion to the hole. This is the result of changing the location of the cusp from which accretion occurs. Abramowicz used Newtonian effective potential of Schwartzshild metric modeling the ring's accretion. Wilson(1984) denied this conclusion by introducuing Kerr metric and angular momentum transport by accretion. But these discussions don't use self-gravitating ring, so fully self-gravitating equilibrium configurations must be needed to end these discussions.

We will describe the outline of this paper. In the section II the problem is described and some assumptions are discussed. Further we make a few simplification to the matter distribution for the ring. This simplification is adequate in application to astrophysical problems. In the section III we show the basic equations to be solved in this paper. The existence of a general stationary axisymmetric black hole is described as a boundary conditions on the event horizon. Equations are transformed to the integral representations which are suitable to treat the boundary condition for the metric on the event horizon and in the asymptotically flat region. In the section IV we present the computational scheme to solve the basic equations.

II. PROBLEM AND ASSUMPTIONS

We will solve both the space-time and the structure of a system which consists of a black hole and the surrounding toroid.

We make several assumptions for the matter and the space-time. The space-time is *stationary (pseudostationary)*. There is a Killing vector field $\bar{\xi}$ that is timelike at least in the asymptotic distant region. The word "pseudostationary" implies that this Killing vector field is not everywhere timelike. The space-time is assumed *axisymmetric*. We can define a Killing vector field $\bar{\eta}$ which vanishes on the axis of symmetry and is spacelike everywhere. This implies that there exist integral curves which are topologically circular. Two Killing vector fields mentioned above are assumed to commute, i.e.

$$[\bar{\xi}, \bar{\eta}] = 0. \tag{2.1}$$

It follows from three assumptions mentioned above that the metric can be written as

$$ds^2 = -e^{2\nu}dt^2 + e^{2\alpha}(dr^2 + r^2 d\theta^2) + e^{2(\gamma-\nu)}r^2 \sin^2\theta(d\phi - \omega dt)^2, \tag{2.2}$$

where t and ϕ are the coordinates associated with time and axial Killing vectors, respectively : $\bar{\xi} = \partial/\partial t$, $\bar{\eta} = \partial/\partial\phi$. Coordinates r and θ are chosen so that the metric can be written as that of the spherical coordinates in flat 3-space except for the factor $e^{2\alpha}$. Metric components α, γ, ν and ω are functions which depend only on r and θ. We choose the units $c = G = 1$ throughout this paper.

Concerning the matter we assume that the matter is *perfect fluid*. Therefore the energy momentum tensor T^{ab} is written as:

$$T^{ab} = (\varepsilon + p)u^a u^b + pg^{ab}, \tag{2.3}$$

where ε, p, u^a and g^{ab} are the energy density, the pressure, the four-velocity and the metric tensor, respectively. We use *polytropic* relation as the equation of state:

$$p = K\varepsilon^{1+1/N}, \tag{2.4}$$

where K is a constant and N is the polytropic index. The matter is assumed to have *only circular motion*. This implies that the four-velocity is a linear combination of two Killing vectors, i.e. r and θ components of the four velocity do vanish. Thus the four-velocity can be written as follows:

$$u^a = \frac{e^{-\nu}}{\sqrt{1-v^2}}(1, 0, 0, \Omega), \tag{2.5}$$

where v is the velocity of a fluid element measured from an inertial frame of the zero angular momentum observer, i.e.:

$$v = (\Omega - \omega)r\sin\theta e^{(\gamma-2\nu)}, \tag{2.6}$$

and Ω is the angular velocity measured from infinity i.e.:

$$\Omega = \frac{d\phi}{dt}. \tag{2.7}$$

Moreover the matter is assumed in equatorial symmetric and consequently all quantities are *equatorial symmetric*, i.e.

$$f(\theta) = f(\pi - \theta), \tag{2.8}$$

where f represents a physical quantity such as the density or the metric. Further since we are considering a system of finite size, the space-time must be *asymptotically flat*. This condition is expressed as

$$\nu \sim O(\frac{1}{r}), \quad \gamma \sim O(\frac{1}{r^2}), \quad \omega \sim O(\frac{1}{r^3}), \tag{2.9}$$

when $r \longrightarrow \infty$.

By the requirement of local flatness, we must set the condition on the axis:

$$\alpha = \gamma - \nu. \tag{2.10}$$

In stationary axisymmetric and circular case we can express the existence of black hole in a simple manner. On the event horizon (smooth null hypersurface spanned by two Killing vectors) metric coefficients must behave as follows:

$$e^{\gamma} = 0, \ e^{\nu} = 0, \ \omega = \omega_H = const. \tag{2.11}$$

We can make the coordinate locus of the horizon a sphere of constant radius $r = h$ without loss of generality.These can be regarded as a complete set of boundary conditions on the horizon.

III. BASIC EQUATIONS

Although basic equations are almost the same as that of our last paper(1992) , we made some changes to treat the present problem. So we will show an outline of whole discussion again for readers' convenience. The Einstein equations for ν, γ and ω can be written as follows:

$$\Delta\lambda = S_\lambda(r,\mu), \tag{3.1}$$

$$(\Delta + \frac{1}{r}\frac{\partial}{\partial r} - \frac{1}{r^2}\mu\frac{\partial}{\partial \mu})B = S_B(r,\mu), \tag{3.2}$$

$$(\Delta + \frac{2}{r}\frac{\partial}{\partial r} - \frac{2}{r^2}\mu\frac{\partial}{\partial \mu})\omega = S_\omega(r,\mu), \tag{3.3}$$

where

$$S_\lambda = 4\pi\lambda e^{2\alpha}[(\varepsilon + p)\frac{1+v^2}{1-v^2} + 2p] + \frac{1}{2}r^2(1-\mu^2)B^2\lambda^{-3}\nabla\omega\cdot\nabla\omega - \nabla(\gamma-\nu)\cdot\nabla\lambda, \tag{3.4}$$

$$S_B = 16\pi pBe^{2\alpha}, \tag{3.5}$$

$$S_\omega = \nabla(4\nu - 3\gamma)\cdot\nabla\omega - 16\pi e^{2\alpha}(\varepsilon + p)\frac{\Omega-\omega}{1-v^2}. \tag{3.6}$$

Here

$$B = e^{\gamma}, \ \lambda = e^{\nu},$$

Δ and ∇ are the Laplacian and the gradient in the flat 3-space, respectively, and $\mu = \cos\theta$, and subscript , denotes differentiation with respect to the variable followed. As for the equation for α, by using the Einstein

equations, we come to the following expression:

$$
\begin{aligned}
\alpha_{,\mu} = & -\nu_{,\mu} - \{(1-\mu^2)(1+rB^{-1}B_{,r})^2 + [\mu-(1-\mu^2)B^{-1}B_{,\mu}]^2\}^{-1} \\
& [\frac{1}{2}B^{-1}\{r^2B_{,rr} - [(1-\mu^2)B_{,\mu}]_{,\mu} - 2\mu B_{,\mu}\}[-\mu+(1-\mu^2)B^{-1}B_{,\mu}] \\
& + rB^{-1}B_{,r}[\frac{1}{2}\mu + \mu rB^{-1}B_{,r} + \frac{1}{2}(1-\mu^2)B^{-1}B_{,\mu}] \\
& + \frac{3}{2}B^{-1}B_{,\mu}[-\mu^2+\mu(1-\mu^2)B^{-1}B_{,\mu}] - (1-\mu^2)rB^{-1}B_{,\mu r}(1+rB^{-1}B_{,r}) \\
& - \mu r^2\nu_{,r}^2 - 2(1-\mu^2)r\nu_{,\mu}\nu_{,r} + \mu(1-\mu^2)\nu_{,\mu}^2 - 2(1-\mu^2)r^2B^{-1}B_{,r} \\
& \times \nu_{,\mu}\nu_{,r} + (1-\mu^2)B^{-1}B_{,\mu}[r^2\nu_{,r}^2 - (1-\mu^2)\nu_{,\mu}^2] + (1-\mu^2)B^2e^{-4\nu} \\
& \times \{\frac{1}{4}\mu r^4\omega_{,r}^2 + \frac{1}{2}(1-\mu^2)r^3\omega_{,\mu}\omega_{,r} - \frac{1}{4}\mu(1-\mu^2)r^2\omega_{,\mu}^2 + \frac{1}{2}(1-\mu^2) \\
& \times r^4B^{-1}B_{,r}\omega_{,\mu}\omega_{,r} - \frac{1}{4}(1-\mu^2)r^2B^{-1}B_{,\mu}[r^2\omega_{,r}^2 - (1-\mu^2)\omega_{,\mu}^2]\}].
\end{aligned}
\tag{3.7}
$$

As for the matter, the equation for the hydrostatic equilibrium can be written as

$$
\nabla p + (\varepsilon + p)[\nabla\nu + \frac{1}{1-v^2}(-v\nabla v + v^2\frac{\nabla\Omega}{\Omega-\omega})] = 0. \tag{3.8}
$$

In addition to these basic equations we must specify the rotation law of the central star and the toroid. According to Komatsu, Eriguchi and Hachisu(1989) from the integrable condition of the equation of motion we choose the following relation as the rotation law:

$$
A^2(\Omega_c - \Omega) = \frac{(\Omega-\omega)r^2\sin^2\theta e^{2(\gamma-2\nu)}}{1-(\Omega-\omega)^2r^2\sin^2\theta e^{2(\gamma-2\nu)}}, \tag{3.9}
$$

where A is a constant which we will call a rotation parameter. If we choose this rotation law, specific angular momentum measured by the proper time of the matter must increase as far as angular velocity of the matter decrease . The smaller the rotation parameter becomes, the stronger the degree of differential rotation. This relation becomes in the Newtonian limit as follows:

$$
\Omega/\Omega_c = A^2/(A^2 + r^2\sin^2\theta). \tag{3.10}
$$

This rotation law with small value of A represents that for the constant specific angular momentum except near the rotation axis region.

IV. METHOD OF SOLUTION

Since the boundary conditions (2.9)-(2.11) for the metric can be easily taken into account by using Green functions, we rewrite Eqs.(3.1)-(3.3) in the integral form as was done by Komatsu et al. (1989). The integral representation of Eqs.(3.1)-(3-3) are

$$
\lambda = 1 - \frac{h}{r} - \sum_{n=0}^{\infty}\int_h^{\infty}dr'\int_0^1 d\mu' r'^2 f_{2n}^2(r,r')P_{2n}(\mu)P_{2n}(\mu')S_\lambda(r',\mu'), \tag{4.1}
$$

$$r\sin\theta B = (1-\frac{h^2}{r^2})r\sin\theta - \frac{2}{\pi}\sum_{n=1}^{\infty}\int_h^{\infty}dr'\int_0^1 d\mu' r'^2 f^1_{2n-1}(r,r')\frac{1}{2n-1}\sin(2n-1)\theta$$
$$\times \sin(2n-1)\theta' S_B(r',\mu'), \tag{4.2}$$
$$r\sin\theta\omega = \frac{\omega_H h^3}{r^2}\sin\theta - \sum_{n=1}^{\infty}\int_h^{\infty}dr'\int_0^1 d\mu' r'^3\sin\theta' f^2_{2n-1}(r,r')\frac{1}{2n(2n-1)}P^1_{2n-1}(\mu)$$
$$\times P^1_{2n-1}(\mu')S_\omega(r',\mu'), \tag{4.3}$$

where

$$f^1_n(r,r') = (r'/r)^n - \frac{h^{2n}}{(rr')^n}, \quad for\ r'/r \le 1,$$
$$(r/r')^n - \frac{h^{2n}}{(rr')^n}, \quad for\ r'/r > 1, \tag{4.4}$$

and

$$f^2_n(r,r') = (1/r)(r'/r)^n - \frac{h^{2n+1}}{(rr')^{n+1}}, \quad for\ r'/r \le 1,$$
$$(1/r')(r/r')^n - \frac{h^{2n+1}}{(rr')^{n+1}}, \quad for\ r'/r > 1. \tag{4.5}$$

The equation of motion for the toroid is integrated to give

$$(1+N)\ln(K\varepsilon^{1/N}+1) + \nu + \frac{1}{2}\ln(1-v^2) - \frac{1}{2}A^2(\Omega-\Omega_c)^2 = C, \tag{4.6}$$

where C is the integral constant. The rotation law for the toroid is

$$A^2(\Omega_c - \Omega) = \frac{(\Omega-\omega)r^2\sin^2\theta e^{2(\gamma-2\nu)}}{1-(\Omega-\omega)^2 r^2\sin^2\theta e^{2(\gamma-2\nu)}}, \tag{4.7}.$$

In order to obtain one equilibrium state, we must specify seven independent parameters. We choose followiong quantities as seven parameters:

1) the ratio of the radius of the event holizon h to the outer boundary of the ring r_{out};
2) the dragging of innertial frame on the horizon ω_H (angular velocity of the black hole;
3) the relative thickness of the toroid r_{in}/r_{out}, where r_{in} and r_{out} are the distances to the inner edge of the ring and the outer edge from the rotation axis, respectively;
4) the ratio of the maximum pressure to the maximum energy density of the ring $\kappa = p_{max}/\varepsilon_{max}$ of the ring ;
5) the maximum density of the ring ε_{max};
6) the polytropic index of the ring N;
7) the rotation parameter of the ring A.

Numerical procedure begins with specifying seven parameters mentioned above. Next we need to prepare initial guesses for the variables ν, γ, ω, α, ε, p and Ω. Substituting them into the right hand side of Eqs.(4.1)-(4.3), we can obtain new values of ν, γ and ω. Using these new values, we can integrate Eq.(3.7), starting from the rotation axis and ending at the equator, to obtain a new value for α. After that we compute ε and Ω in order to keep consistency with new potentials ν, γ, ω and α using Eqs.(4.6)-(4.7)

We regard newly obtained values as an improved set of guesses and return to the next iteration step by keeping the model parameters fixed. We continue this iteration cycle until the differences of each physical quantity between two successive cycles become sufficiently small and then we regard those values as true values which satisfy the basic equations and the boundary conditions.

IV. RESULTS

Since there are seven parameters which we can freely specify, we need seven dimensional parameter space to see the whole structure of the solution space. Here we will discuss mainly the effect of the existence of the toroid on the black hole. This can be done by fixing the model parameters of the black hole and changing the size of the toroid.

The gravitational mass M_r and the total angular momentum J_r of the ring are defined by

$$\begin{aligned} M_r &= \frac{1}{2}\int\int r^2 \sin\theta dr d\theta \nabla\cdot[B\nabla\nu - \frac{1}{2}r^2\sin^2\theta B^3 e^{-4\nu}\omega\nabla\omega] \\ &= 2\pi\int\int r^2\sin\theta dr d\theta B e^{2\alpha}[(\varepsilon+p)\frac{1+v^2}{1-v^2} + 2p + 2r\sin\theta(\varepsilon+p)\frac{v\omega e^{\gamma-2\nu}}{1-v^2}], \end{aligned} \tag{5.1}$$

$$\begin{aligned} J_r &= -\frac{1}{8}\int\int r^2\sin\theta dr d\theta\nabla\cdot[r^2\sin^2\theta B^3 e^{-4\nu}\nabla\omega] \\ &= 2\pi\int\int dr d\theta r^3\sin^2\theta(\varepsilon+p)\frac{v}{1-v^2}B^2 e^{2\alpha-2\nu}, \end{aligned} \tag{5.2}$$

respectively. It is obvious that we can rewrite the above formula for gravitational mass and the total angular momentum using the surface integral on the event horizon and infinity. It is natural to define the mass and angular momentum of the black hole from the surface integral of the black hole. And the total mass and angular momentum are given by surface integral at the infinity:

$$M = \frac{1}{2}\int_0^\pi \sin\theta d\theta[r^2 B\frac{\partial\nu}{\partial r} - \frac{1}{2}\sin^2\theta r^4 B^3 e^{-4\nu}\omega\frac{\partial\omega}{\partial r}], \tag{5.3}$$

$$J = -\frac{1}{8}\int_0^\pi d\theta sin^3\theta r^4 B^3 e^{-4\nu}\frac{\partial\omega}{\partial r}. \tag{5.4}$$

So we separate the total quantities into two part:

$$M = M_h + M_r, \tag{5.5}$$

$$J = J_h + J_r, \tag{5.6}$$

where subscript h denotes the surface integral on the event horizon.

We draw the typical behaviour of the dragging of innertial frame caused by the ring's rotation in Fig.1 . This is the 2-D plotting of the ω on the plane containing the rotation axis. Two peaks nearly correspond to the density maximum and there is the black hole of $\omega_H = 0$ between the peaks. In this model M_h and M_r is nearly constant. To see the ring's dragging effect, we plotted J_h of a sequence changing the thickness of the ring and fixing other parameters($\omega_H = 0$) in Fig.2 . This shows that the larger the ring's gravity become, the larger the black hole's angular momentum become in order to maintain zero angular velocity.

Fig.3 presents the comparison with pure vacuum case i.e. Kerr black hole. In this figure the angular momentum of the black hole is plotted against the angular velocity. A solid line denotes the sequence of solutions of black hole - ring systems, and a dashed line is that of Kerr black holes which have the same mass with hole - ring systems. From this figure we can read the angular momentum and angular velocity of a black hole may have different signature due to the dragging by the ring. Beacause ergosphere covering the black hole disappears only when $\omega_H = 0$, there is the case in which the zero angular momentum black hole have ergosphere. That is to say, the ring helps to make ergosphere around the black hole. When the black hole rotates rapidly, the ring's role changes from the motor to the anchor. The black hole must have large angular momentum to have the same angular velocity and same mass as that of Kerr black hole .

REFERENCES

Abramowicz, M.A., Calvani, M., Nobili, L. 1983, Nature, **302**, 597

Chakrabarti, S. 1988, J. ApJ & A, **9**, 49

Komatsu, H., Eriguchi, Y., Hachisu, I. 1989, MN, **237**, 355

Lanza, A. 1991, SISSA preprint, ,

Nishida, S., Eriguchi, Y., Lanza, A. 1992, preprint, ,

Will, C.F. 1974, ApJ, **191**, 521

Will, C.F. 1975, ApJ, **196**, 41

Wilson, D, B 1984, Nature, **312**, 620

Figure captions

Fig.1 2-D Plottining of the dragging of inertial frame in the meridian plane. Model parameters are as follows: $h/r_{out} = 0.03$, $\omega_H = 0$, $r_{in}/r_{out} = 0.38$, $\kappa = 0.01$, $N = 1$, $A = 0.1$.

Fig.2 Plotting of J_h/M_h^2 versus M_r/M_h. In this sequence only r_{in}/r_{out} are changed and ω_H is fixed to zero.

Fig.3 The solid line is the sequence of the black hole - ring system obtained by changing ω_H. Dashed line is the sequence of Kerr black hole that has the same gravitational mass as the solid line. The values of M_h and M_r are nearly the same.

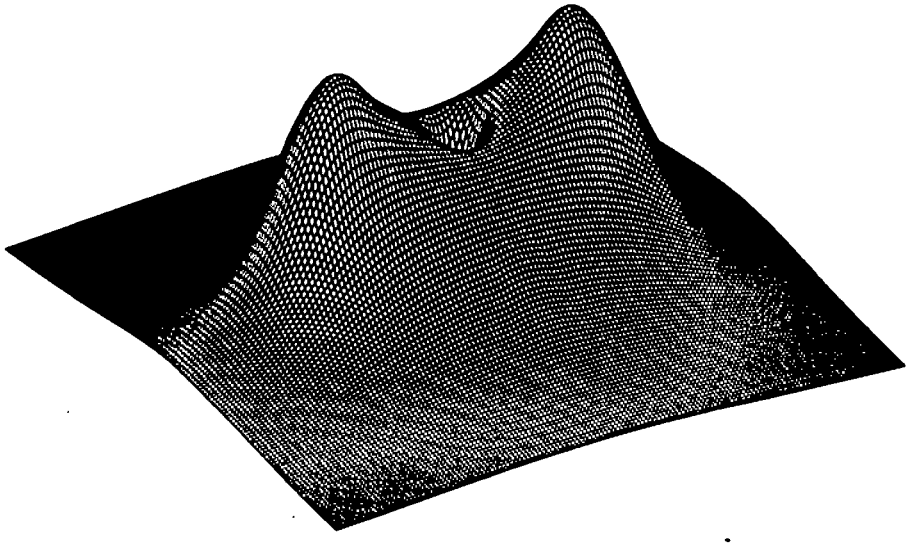

Fig.1

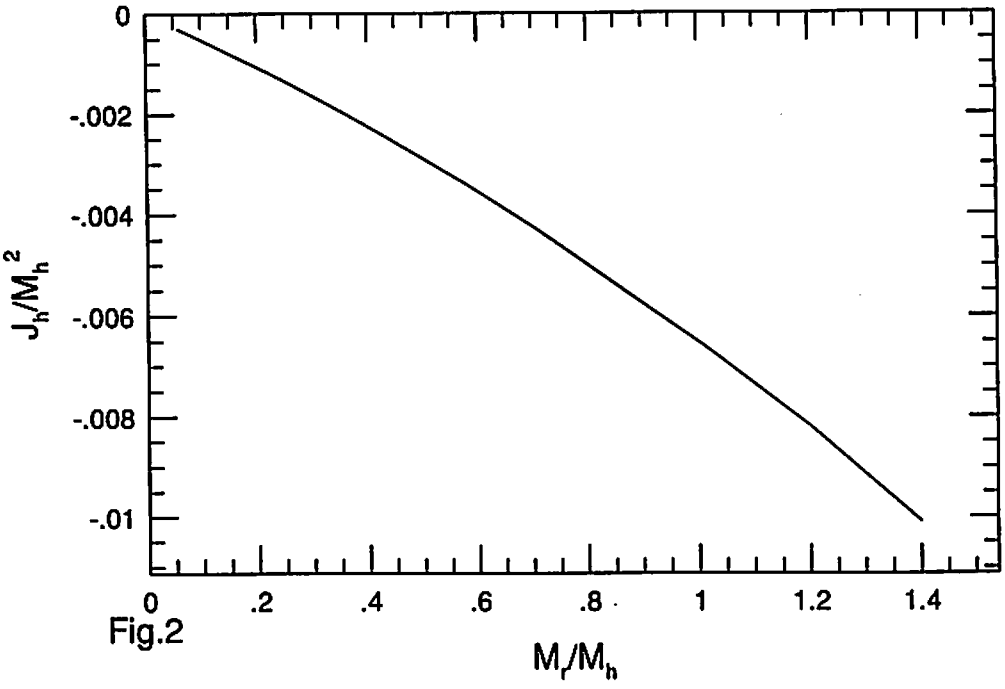
0
-.002
-.004
-.006
-.008
-.01
J_h/M_h^2
0
.2
.4
.6
.8
1
1.2
1.4
M_r/M_h

Fig.2

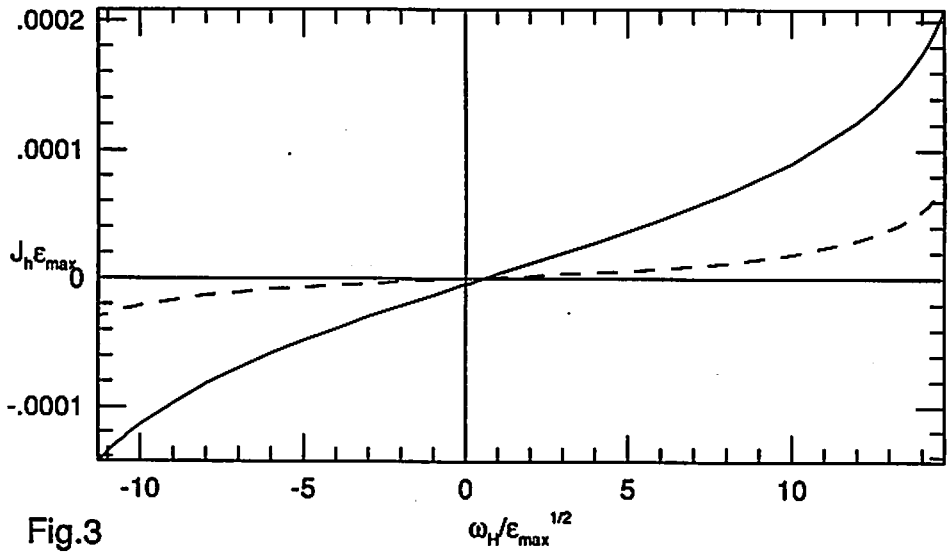
.0002
.0001
0
-.0001
$J_h\varepsilon_{max}$
-10
-5
0
5
10
$\omega_H/\varepsilon_{max}^{1/2}$

Fig.3

Gravitational Soliton Solutions in General Relativity

Akira Tomimatsu

Department of Physics, Nagoya University, Nagoya 464-01, Japan

We give a brief review of solution-generating techniques applied to the vacuum Einstein equations. Some properties of the soliton solutions which describe interacting black holes or colliding waves are discussed.

1 Introduction

A main mathematical difficulty in general relativity is to solve the highly nonlinear Einstein equations. We have no method to treat the general solutions as yet. However, considerable efforts have been devoted to the developments of analytical techniques for obtaining the exact solutions. If we limit our discussions to symmetric spacetimes with two commutable Killing vectors, various solution-generating techniques have been found. These are closely related to the mathematical methods well-known in soliton physics. Now it is straightforward to derive an interesting family of the metrics which may be called the gravitational soliton solution.

The metrics which we consider here have the form

$$ds^2 = f\ (\ \epsilon\ (dq^1)^2 + (dq^2)^2\ ) + g_{\alpha\beta}dp^\alpha dp^\beta, \tag{1}$$

where $\epsilon = \pm 1$, and the metric functions f and $g_{\alpha\beta}$ $(\alpha, \beta = 1, 2)$ depend on the coordinate variables q^1 and q^2 only. When $\epsilon = +1$, the determinant of the matrix $(g_{\alpha\beta})$ must be negative. The spacetime can be interpreted to be stationary and axisymmetric, and the spatial cylindrical coordinates ρ, φ, z and the time coordinate t are introduced as follows,

$$p^1 = t,\ p^2 = \varphi,\ q^1 = \rho,\ q^2 = z. \tag{2}$$

When $\epsilon = -1$ and $\det(g_{\alpha\beta}) > 0$, we obtain gravitaitonal wave solutions, which are cylindrically symmetric ($q^1 = t, q^2 = \rho$) or plane symmetric ($q^1 = t, q^2 = z$).

In Sect.2 we shall give a brief review of the solution-generating techniques applied to the vacuum Einstein equations for the metrics (1). The soliton solutions can describe interacting black holes or colliding waves. Their physical properties are discussed in Sect.3 and Sect.4. Our purpose is to shed a light on such interesting problems in general relativity in terms of the soliton solutions.

2 Solution-Generating Techniques

The essential part of the vacuum Einstein equations for the metrics (1) is reduced to the form

$$\epsilon \frac{\partial}{\partial q^1} [\, W(\frac{\partial}{\partial q^1} g) g^{-1} \,] + \frac{\partial}{\partial q^2} [\, W(\frac{\partial}{\partial q^2} g) g^{-1} \,] = 0, \tag{3}$$

where g is the two-rowed matrix $(g_{\alpha\beta})$, and its determinant is equal to $-\epsilon W^2$. The function W must satisfy the simple equation

$$(\epsilon \frac{\partial^2}{\partial q^1 \partial q^1} + \frac{\partial^2}{\partial q^2 \partial q^2}) W = 0. \tag{4}$$

For example, plane waves give the solution $W = a(t-z) + b(t+z)$, where a and b are arbitrary functions. For stationary and axisymmetric spacetimes, a natural choice is that $W = \rho$. If g is given, the equation for the remaining metric function f is easily integrable.

Instead of the matrix g we can introduce a complex potential E which is called the Ernst potential. For the stationary and axisymmetric metric ($\epsilon = +1$) of the form

$$ds^2 = f(d\rho^2 + dz^2) - h(dt - \omega d\varphi)^2 + h^{-1} W^2 d\varphi^2, \tag{5}$$

the Ernst potential is defined by $E = h + i\psi$, where

$$\partial\psi/\partial\rho = W^{-1} h^2 \partial\omega/\partial z, \;\; \partial\psi/\partial z = -W^{-1} h^2 \partial\omega/\partial\rho. \tag{6}$$

The compatibility condition for these two equations is satisfied by virtue of the original Einstein equations for g, which can be rewritten in the form

$$(E + E^*)[\, \frac{\partial}{\partial\rho}(W\frac{\partial}{\partial\rho}) + \frac{\partial}{\partial z}(W\frac{\partial}{\partial z}) \,]\, E = 2W \,[\, (\frac{\partial E}{\partial\rho})^2 + (\frac{\partial E}{\partial z})^2 \,]. \tag{7}$$

For the plane symmetric waves ($\epsilon = -1$) with the line element

$$ds^2 = f(-dt^2 + dz^2) + W\ [\ \chi dy^2 + \chi^{-1}(dx - \omega dy)^2\ ], \tag{8}$$

the Ernst potential is defined by $E = \chi + i\omega$.

There exists an internal symmetry in the Einstein equations for g and the Ernst equation for E, and a new metric generated through some transformations of a known metric can satisfy these equations. The important point is that such a new metric can contain extra parameters. We obtain a more general solution compared with its seed solution. Let us discuss the solution-generating transformations.

(1) One of the solution-generating transformations is based on the Geroch transformation, which was originally applied to spacetimes with one Killing vector $\xi^a (a = 0 \sim 3)$. The new metric g^N_{ab} generated by the Geroch transformation has the form

$$g^N_{ab} = FG(g^S_{ab} - F^{-1}\xi_a\xi_b) + GN_aN_b, \tag{9}$$

where g^S_{ab} is a seed metric, and F, G and N_a are given by ξ_a and an arbitrary parameter.

If two commutable Killing vectors exist, the successive transformations become possible by using their different combinations. A useful realization of the Lie algebra of the Geroch group was constructed by Kinnersley et al (see Xanthopoulos [1]). The transformations act on an infinite sequence of complex potentials, in which the Ernst potential is included. Through a suitable choice of a set of transformations, the procedure to derive new metrics (with an arbitrary number of mass and angular momentum parameters for stationary and axisymmetric spacetimes) is reduced to only algebraic manipulations.

(2) The method of Bäcklund transformations which generate the soliton solutions was introduced by Neugebauer [2]. This originates from the transformation theory in differential geometry (or in total differential equations) and can be applied to the Ernst equation. For plane-wave metrics, its essential part is the Neugebauer-Kramer involution between the seed Ernst potential $E^S = \chi + i\omega$ and the new one $E^N = \Psi + i\Phi$, where $\Psi = W\chi^{-1}$, and

$$\frac{\partial}{\partial t}\Phi = W\chi^{-2}\frac{\partial}{\partial z}\omega,\ \ \frac{\partial}{\partial z}\Phi = W\chi^{-2}\frac{\partial}{\partial t}\omega. \tag{10}$$

For stationary and axisymmetric metrics, we need two successive procedures of the involution to obtain a mapping of real metrics to real ones.

(3) In general, Bäcklund transformations can be reduced to fundamental linear equations of inverse scattering methods. For example, let us consider stationary and axisymmetric metrics with $W = \rho$. We can construct a system of linear differential equations for scattering problem with a complex spectral parameter λ as follows [3],

$$D_1\psi = \frac{\rho V - \lambda U}{\lambda^2 + \rho^2}\psi, \ D_2\psi = \frac{\rho U + \lambda V}{\lambda^2 + \rho^2}\psi, \tag{11}$$

where $\psi = \psi(\lambda, \rho, z)$ is a two-rowed matrix, and $U = \rho(\partial g/\partial\rho)g^{-1}$, $V = \rho(\partial g/\partial z)g^{-1}$. The differential operators defined by

$$D_1 = \partial_z - \frac{2\lambda^2}{\lambda^2 + \rho^2}\partial_\lambda, \ D_2 = \partial_\rho + \frac{2\lambda\rho}{\lambda^2 + \rho^2}\partial_\lambda \tag{12}$$

are commutable, and the integrability condition $(D_1D_2 - D_2D_1)\psi = 0$ is satisfied by virtue of the vacuum Einstein equations for g.

The matrix function ψ is related to the metric g via the equation $\psi(\lambda = 0, \rho, z) = g$. Hence, from a seed metric and Eq.(11), we obtain a seed complex function ψ^S, which is transformed via the matrix $\chi(\lambda, \rho, z)$ into a new complex function ψ^N ($= \chi\psi^S$). The transformation matrix χ may contain n simple poles at $\lambda = \mu_k (k = 1 \sim n)$ in λ plane as follows,

$$\chi = I + \sum_{k=1}^{n} R_k/(\lambda - \mu_k). \tag{13}$$

where I is a two-rowed unit matrix. Then, the metric g^N corresponding to ψ^N is called the n-soliton solution. (Its topological property was investigated by Belinskii [4].)

For wave metrics, by a slight modification of the above-mentioned inverse scattering technique, we can obtain the soliton wave solutions. The relationship between stationary, axisymmetric solutions and wave solutions is not so clear. Any complex transformations of the coordinates and parameters may not succeed in deriving the physical wave metrics from the stationary, axisymmetric metrics, and vice versa.

There exist some different methods which were not mentioned here (for example, the method of homogeneous Riemann-Hilbert problem [5]). More detailed explanation of the

solution-generating methods can be seen in Tomimatsu and Sato [6] for stationary and axisymmetric metrics and in Griffiths [7] for wave metrics. The relationship between the technique of Bäcklund transformations and other methods has been discussed by Cosgrove [8]. In the following, however, we shall not refer to further mathematical developments of the techniques. Let us focus our attention on physical properties of the soliton solutions generated via the inverse scattering method.

3 Interacting Black Holes

First we consider stationary and axisymmetric spacetimes. The simplest seed metric is the flat Minkowski metric

$$ds^2 = d\rho^2 + dz^2 - dt^2 + \rho^2 d\varphi^2. \tag{14}$$

If the number of simple poles in the soliton-transformation matrix χ given by (13) is odd, the deteminant of g^N becomes positive, and we have no physical stationary, axisymmetric solution. The double-soliton transformation is fundamental, and the transformation matrix χ has two poles $\lambda = \mu_+, \mu_-$ satisfying the equations $\mu_\pm^2 - 2(w_\pm - z)\mu_\pm - \rho^2 = 0$. By acting this transformation on the seed metric (14), we obtain the well-known Kerr-NUT metric. The parameters $w_\pm$ may be written in the form $w_\pm = z_0 \pm (m^2 - a^2)^{1/2}$. The Kerr-NUT object (which is a black hole if the NUT parameter is chosen to be zero) is located at $z = z_0$ on the axis $\rho = 0$, and m and a are mass and angular momentum parameters, respectively.

In the same manner the four-soliton transformation generates the two-Kerr-NUT metric. Two rotating masses are located at a distance on the axis of symmetry. This stationary metric may represent two black holes in equilibrium due to a balance between their attractive force and spin-spin repulsive force. Such an interpretation is valid only when the following requirements are satisfied;

(1) local flatness on the axis,

(2) no curvature singularities outside the horizons,

(3) positive masses which are defined by the Komar surface integrals on each event horizon

$H_k(k = 1, 2)$, i.e.,

$$M_k = -\frac{1}{8\pi}\int_{H_k}\frac{1}{2}(\xi^{a;b} - \xi^{b;a})dS_{ba} > 0. \tag{15}$$

Unfortunately, any choice of parameters involved in the metric cannot satisfy all the requirements for equilibrium [9], [10]. A head-on collision of two black holes will occur to generate pulsed gravitaitonal waves propagating along the axis [11].

Because any stationary state of many interacting black holes is unlikely, we consider only the double-soliton solution. Here, the seed metric is the Weyl metric written in the form

$$ds^2 = f(d\rho^2 + dz^2) - e^{2\nu}dt^2 + \rho^2 e^{-2\nu}d\varphi^2. \tag{16}$$

The gravitational potential is assumed to be regular in an inner region surrounded by matter (for example, accretion disk). Then, the metric function ν in the inner region should be given by

$$\nu = \sum_{n=0}^{\infty} A_n P_n(\eta) P_n(\mu), \tag{17}$$

where A_n and P_n are arbitrary parameters and the Legendre polynomials, respectively. The coordinates η and μ are defined by the equations

$$\rho^2 = m^2(\eta^2 - 1)(1 - \mu^2),\ z = m\eta\mu. \tag{18}$$

The double-soliton transformation of the Weyl metric can generate a Kerr black-hole metric deformed by the gravitational field ν of the surrounding matter [12], [13]. We can calculate the mass M and the angular momentum J through the Komar surface integrals on the event horizon (a spatial 2-sphere). Then we obtain the well-known black-hole mass formula

$$M = \frac{\kappa S}{4\pi} + 2\Omega_H J, \tag{19}$$

where κ, S and Ω_H are the surface gravity, the area and the angular velocity of the horizon, respectively. No effect due to the interaction between the black hole and the surrounding matter appears explicitly in this formula. However, such an interaction can induce interesing effects. For example, the maximum angular momentum of the black hole is given by

$$J_{max} = M^2 \exp(-2\sum_{n=0}^{\infty} A_{2n}). \tag{20}$$

If the gravitational field of the surrounding matter has a negative potential at the poles (i.e., $\sum_{n=0}^{\infty} A_{2n} < 0$), the maximum angular momentum of interacing holes becomes larger than that of isolated holes with the same mass. To determine the parameters A_{2n}, we must give a model of the surrounding matter. This remains in future works.

4 Colliding Waves

Now let us study the soliton solutions representing gravitational cylindrical or plane waves. In general, gravitational waves have two dynamical degrees of freedom (+ and × modes). For waves of pure + mode, it is not so difficult to solve the vacuum Einstein equations. (Note that the metric component g_{12} vanishes just like the Weyl metric given in the previous section. The × mode plays the role of rotation in stationary and axisymmetric metrics.) However, no general solution of two modes is known. The soliton transformation is a useful procedure to generate × mode from + mode, and through the soliton solution we can observe nonlinear interactions between the two modes.

(1) Cylindrical Waves

For cylindrically symmetric metrics, the determinant of the matrix g may be chosen to be equal to ρ^2. Then we can use the flat metric written by the cylindrical coordinates as a seed metric. The cylindrical soliton gravitational field on the flat background spacetime contains pulsed waves of two modes outogoing from and ingoing to the axis $\rho = 0$, where a non-propagating disturbance is always excited. The outgoing and ingoing waves interact at some region near the axis. The ratio of the amplitudes of two modes changes as these waves propagate in the interaction region. This effect is a gravitational analogue of the electromagnetic Faraday rotation, which was first pointed out by Piran, Safier and Stark [14]. For the soliton waves [15], the + mode dominates at the axis, and its complete conversion to the × mode occurs at the interaction region. Through the subsequent interaction between the outgoing and ingoing waves, a part of the × mode changes into the + mode. The mode conversion stops at a region far distant from the axis. The soliton solution presents a good example which shows a very

effective gravitational Faraday rotation.

(2) Plane Waves

For plane symmetric metrics, the determinant of g for the flat metric should be chosen to be equal to unity. Then, the soliton transformation cannot generate any non-trivial metrics from the flat seed metric. Here we consider cosmological metrics as the seed metrics. The soliton field describes a cosmological inhomogeneity.

For the Friedmann background model which does not satisfy the vacuum Einstein equations, a matter field should be introduced into the field equations. Then, the inverse scattering technique may not be applicable. Fortunately, this obstacle can be overcome for the scalar-coupled Einstein equations

$$R_{ab} = \nabla_a \phi \nabla_b \phi. \tag{21}$$

Because the scalar field ϕ depends only on the two coordinates t and z, it does not contribute to the equations for the matrix g. To study the evolution of the cosmological soliton waves, Belinskii [16] obtained the single-soliton solution on the Friedmann background model

$$ds^2 = t\,(-dt^2 + dz^2 + z^2 dx^2 + dy^2). \tag{22}$$

The soliton perturbation defined by $H_{yy} = (g^N_{yy} - g^S_{yy})/g^S_{yy}$ is initially localized at the region $z \simeq 0$, and it begins to die away via the production of a wave. The wave propagates to infinity with the speed of light, and its amplitude decreases as the cosmological expansion of the Friedmann background goes on. This shows a decay of initial inhomogeneity due to the cosmological expansion.

The final topic is concerned with the soliton collision, which obeys the vacuum Einstein equations. The problem of collision of plane waves has been studied by many works. It has been found that when the rightward-traveling waves collide with the leftward-traveling waves at some region, a focusing of the null congruences occurs. This singularity theorem [17] is a result of the Raychaudhuri equation for null geodesics. Some Riemann scalar curvature may become infinite at the singularity (curvature singularity). Then, the metric near the singularity

behaves like an inhomogeneous Kasner metric [18]. Some simple solutions for colliding plane waves were given by Szekers [19], and Khan and Penrose [20].

By using the Kasner seed metric which is an anisotropic cosmological solution of the vacuum Einstein equations, Ibañez and Verdaguer [21] derived the four-soliton solution. It is shown that the collision between the rightward-traveling and leftward-traveling solitons does not induce any convergence of null rays to a singularity. The cosmological expansion of the Kasner background can suppress the focusing effect of null rays.

The role of polarization of plane waves also is interesting. The Szekeres solution is collinear (pure + mode), and the curvature singularity does occur. Through the soliton transformations of the Szekeres solution, we obtain colliding-wave solutions of two modes [22]. By virtue of the noncollinear generalization, the curvature singularity found in the Szekeres solution turns into the Cauchy horizon. The interaction between different polarization modes can affect the formation and structure of singularity.

It is clear that we can obtain many informations of nonlinear interactions of gravitational waves from the soliton solutions. However, this solution-generating technique is applicable only to wave solutions with complete cylindrical or plane symmetry. It will be necessary to show how the soliton solutions become an approximation of realistic waves of finite energy and finite extent. To establish the notion of graviton in general relativity, quantum effects in the nonlinear interactions also should be investigated. Quantum theories of colliding waves will become important in future research.

References

[1] B. C. Xanthopoulos, in *Geometric Aspects of the Einstein Equations and Integrable Systems*, ed. R. Martini (Lecture Note in Physics No.239, Springer-Verlag, Berlin, 1985) pp.77-108.

[2] G. Neugebauer, J. of Phys. **A12** (1979), L67.

[3] V. A. Belinskii and V. E. Zakharov, Soviet Phys. JETP **48** (1978), 985 ; **50** (1979), 1.

[4] V. A. Belinskii, Phys. Rev. **D44** (1991), 3109.

[5] I. Hauser and F. J. Ernst, J. Math. Phys. **21** (1980), 1126.

[6] A. Tomimatsu and H. Sato, Prog. Theor. Phys. Suppl. No.70 (1981), 215.

[7] J. B. Griffiths, *Colliding Plane Waves in General Relativity* (Clarendon Press, Oxford, 1991).

[8] C. M. Cosgrove, J. Math. Phys. **21** (1980), 2417.

[9] A. Tomimatsu and M. Kihara, Prog. Theor. Phys. **67** (1982), 1406.

[10] W. Dietz and C. Hoenselaers, Ann. of Phys. **165** (1985), 319.

[11] A. Tomimatsu, Gen. Rel. Grav. **21** (1989), 1233.

[12] A. Tomimatsu, Phys. Lett. **103A** (1984), 374.

[13] R. Geroch and J. B. Hartle, J. Math. Phys. **23** (1982), 680.

[14] T. Piran, P. N. Safier and R. F. Stark, Phys. Rev. **D32** (1985), 3101.

[15] A. Tomimatsu, Gen. Rel. Grav. **21** (1989), 613.

[16] V. A. Belinskii, Sov. Phys. JETP **50** (1979), 623.

[17] F. J. Tipler, Phys. Rev. **D22** (1980), 2929.

[18] U. Yurtsever, Phys. Rev. **D38** (1988), 1731 ; **D40** (1989), 329.

[19] P. Szekeres, Nature **228** (1970), 1183 ; J. Math. Phys. **13** (1972), 286.

[20] V. A. Khan and R. Penrose, Nature **229** (1971), 185.

[21] J. Ibañez and E. Verdaguer, Phys. Rev. Lett. **51** (1983), 1313.

[22] A. Wang, Int. J. Mod. Phys. **A6** (1991), 2273.

Static Gravitational Solitons and the Ring Solution

Takahiro AZUMA

Faculty of Liberal Arts, Dokkyo University
Soka, Saitama 340, Japan

ABSTRACT

We study the soliton solutions to the static vacuum Einstein equation which are obtained by means of the inverse scattering method. In the 4-soliton case with complex pole trajectories there appears an intriguing ring solution.

1. Introduction

Belinskii and Zakharov[1] showed that the soliton technique known as the inverse scattering method(ISM) gives a systematic way of solving the stationary vacuum Einstein equation with axial symmetry. They obtained an infinite series of solutions which are classified by the even soliton number n and showed that the 2- soliton solution is just the well-known Kerr solution. The "nonlinear superposition" of two Kerr solutions has the soliton number 4 and in the degenerate pole case it is known as the Tomimatsu-Sato solution[2] with $\delta = 2$.

Alekseev and Belinskii[3] investigated the structure of the general n-soliton solution in the static case which corresponds to the superposition of multi-Schwarzschild solutions and found the "weak singularities" between two Schwarzschild solitons. In the stationary case several people[4] also studied the structure of the multi-Kerr solution.

In these soliton solutions the soliton number n corresponds to the number of the single poles in the complex λ plane where λ is the parameter appearing in the linear system of ISM. The infinite series of solutions starting with the Schwarzschild and Kerr solution mentioned above are obtained by adopting only the real poles in the static and stationary case, respectively.

In this report we consider the soliton solutions which are obtained by adopting the complex poles in the static case. In Sec. 2 we give the generalized n-soliton solution which includes an extra arbitrary parameter q. This q comes from our renormalization of metric coefficient which is different from that in Ref. [1]. In Sec. 3 we study the 2- and 4-soliton solutions with complex pole trajectories and show that there appears an intriguing ring solution in the 4-soliton case. In the last section we propose a classification of the series of solutions by means of the combinations of real and complex pole trajectories[5]. We also show that among these combinations there is an interesting solution which describes a black hole accompanied by rings.

2. Generalized n-soliton solution

We consider the metric given by

$$-ds^2 = f^{-1}Q(d\rho^2 + dz^2) + (-fdt^2 + f^{-1}\rho^2 d\phi^2), \tag{2.1}$$

where f and Q are functions of the cylindrical coordinates (ρ, z). For the metric coefficients in the last two terms in Eq. (2.1) we define a diagonal matrix g by

$$g = \mathrm{diag}(-f, f^{-1}\rho^2). \tag{2.2}$$

We apply ISM to the integration of the vacuum Einstein equation for g and obtain a nontrivial solution g' from the vacuum metric $g_0 = \mathrm{diag}(-1, \rho^2)$. But g' does not satisfy the normalization $\det g = -\rho^2$, which forces us to renormalize the matrix g'. Belinskii and Zakharov[1] renormalized their non-diagonal g' by multiplying it by an overall factor $-\rho(-\det g')^{-1/2}$. On the other hand, we can renormalize our diagonal g' to get a physical metric $g^{(ph)}$ as

$$g^{(ph)} = Ng', \tag{2.3}$$

where N is a 2×2 matrix given by

$$N = \mathrm{diag}\{[\rho(-\det g')^{-1/2}]^q, [\rho(-\det g')^{-1/2}]^{2-q}\}. \tag{2.4}$$

Here we introduce an arbitrary parameter q. Using this renormalization we obtain a generalized static n-soliton solution

$$f = \left(i^n \frac{\mu_1 \mu_2 \cdots \mu_n}{\rho^n}\right)^q, \tag{2.5}$$

$$Q = \left[\frac{\rho^{n^2/2} \prod_{k>l} (\mu_k - \mu_l)^2}{\prod_k (\rho^2 + \mu_k^2) \prod_l \mu_l^{n-2} C^{(n)}}\right]^{q^2}, \tag{2.6}$$

with the pole trajectories

$$\mu_k = w_k - z \pm \sqrt{(w_k - z)^2 + \rho^2} \qquad (k = 1, 2, \cdots, n), \tag{2.7}$$

and the constant

$$C^{(n)} = 2^{\frac{n(n-2)}{2}} \prod_{k>l}^{n} (w_{2k-1} - w_{2l-1})^2 (w_{2k} - w_{2l})^2. \tag{2.8}$$

Here w_k's are constants which could be real or complex corresponding to the real or complex pole trajectories. The $\pm$ sign in Eq. (2.7) is to be determined so that the metric may become asymptotically flat.

In order to see the meaning of the parameter q, let us consider the simplest case, i.e., the 2-soliton solution with real pole trajectories. In this case μ_k's are chosen as

$$\mu_1 = w_1 - z + \sqrt{(w_1 - z)^2 + \rho^2}, \tag{2.9a}$$

$$\mu_2 = w_2 - z - \sqrt{(w_2 - z)^2 + \rho^2}, \tag{2.9b}$$

with the real constants

$$w_1 = z_0 + \sigma, \tag{2.10a}$$

$$w_2 = z_0 - \sigma, \tag{2.10b}$$

and the solution is given by

$$f = (-\mu_1\mu_2/\rho^2)^q, \tag{2.11}$$

$$Q = \left[\frac{\rho^2(\mu_1-\mu_2)^2}{(\mu_1^2+\rho^2)(\mu_2^2+\rho^2)}\right]^{q^2}. \tag{2.12}$$

Introducing the prolate spheroidal coordinates (u, v) with the constant σ by

$$\rho = \sigma\sqrt{(u^2-1)(1-v^2)}, \tag{2.13}$$

$$z - z_0 = \sigma uv, \tag{2.14}$$

we can write f and Q as

$$f = \left(\frac{u+1}{u-1}\right)^q, \tag{2.15}$$

$$Q = \left(\frac{u^2-1}{u^2-v^2}\right)^{q^2}, \tag{2.16}$$

which is referred to as the Weyl solution if we put $q = -\delta$. Therefore we find that the parameter q is necessary in order to obtain the Weyl solution with the arbitrary distortion parameter δ by means of ISM.

3. The solutions with complex pole trajectories

We first consider the 2-soliton case where we replace σ by $i\sigma$ in Eq. (2.10). Note that the pair of pole trajectories in Eq. (2.9) are not complex conjugate even by this assignment of w_k. The solution is given by Eqs. (2.11) and (2.12) but the parameter q must be pure imaginary in this case to keep the reality of metric. In the oblate spheroidal coordinates (x, y)

$$\rho = \sigma\sqrt{(x^2+1)(1-y^2)}, \tag{3.1}$$

$$z - z_0 = \sigma xy, \tag{3.2}$$

f and Q are expressed as

$$f = \exp(-2\bar{\delta}\tan^{-1}x), \tag{3.3}$$

$$Q = \left(\frac{x^2+y^2}{x^2+1}\right)^{\bar{\delta}^2}, \tag{3.4}$$

where $\tilde{\delta} = -iq$. This is the well-known solution which is obtained by transforming the Weyl solution to the expression in the oblate spheroidal coordinates. We now refer to this solution as the 2-soliton solution with non-complex conjugate pole trajectories. The solution in Eqs. (3.3) and (3.4) is known to have the naked singularity of ring type at $x = y = 0(\rho = \sigma, z = z_0)$. The curvature of space-time becomes infinite at the ring, which is caused by the fact that Q tends to zero as $x, y \to 0$. We note that the 2-soliton solution with complex conjugate poles does not satisfy the condition of asymptotic flatness.

We next proceed to the 4-soliton case. It is easily expected from the above discussion about the 2-soliton solution that there is a solution constituted of two ring singularities in the 4- soliton case. In addition to this we have another intriguing solution constructed from two pairs of complex conjugate pole trajectories

$$\mu_1 = z_1 + i\Sigma_1 - z + \sqrt{(z_1 + i\Sigma_1 - z)^2 + \rho^2}, \tag{3.5a}$$

$$\mu_2 = z_2 + i\Sigma_2 - z - \sqrt{(z_2 + i\Sigma_2 - z)^2 + \rho^2}, \tag{3.5b}$$

$$\mu_3 = \overline{\mu}_1, \tag{3.5c}$$

$$\mu_4 = \overline{\mu}_2. \tag{3.5d}$$

What is different from the 2-soliton case with complex conjugate poles is that we can choose the signs in front of the square root in Eq. (3.5) so that the metric may satisfy the asymptotic flatness condition. Using these trajectories f and Q are written as

$$f = (|\mu_1|^2|\mu_2|^2/\rho^4)^q, \tag{3.6}$$

$$Q = \left[\frac{\rho^8|\mu_1 - \mu_2|^4|\mu_1 - \overline{\mu}_2|^4(\mu_1 - \overline{\mu}_1)^2(\mu_2 - \overline{\mu}_2)^2}{2^8\Sigma_1^2\Sigma_2^2|\mu_1^2 + \rho^2|^2|\mu_2^2 + \rho^2|^2|\mu_1|^4|\mu_2|^4}\right]^{q^2}, \tag{3.7}$$

with real q.

In order to investigate the behavior of this solution let us assume that $\Sigma_1 < \Sigma_2$ and $z_1 = z_2 = z_0$ for simplicity. We then notice that the numerator of Q does not vanish for any ρ and z, while the denominator of Q becomes zero at $\rho = \Sigma_k (k = 1, 2)$ and $z = z_0$. This causes the divergence of Q and the metric

singularities of ring type at $(\rho, z) = (\Sigma_1, z_0)$ and (Σ_2, z_0). However, in the case where $q = 1$ we find that Q has a finite expression at the inner ring($\rho = \Sigma_1$) in such oblate spheroidal coordinates as

$$\rho = \Sigma_1 \sqrt{(x^2+1)(1-y^2)}, \tag{3.8}$$

$$z - z_0 = \Sigma_1 xy. \tag{3.9}$$

We can also see that all the metric functions and their derivatives approach finite values as $\rho \to \Sigma_1$ and $z \to z_0 (x, y \to 0)$. Similarly, we find that the metric becomes finite as $\rho \to \Sigma_2$ and $z \to z_0$ in the oblate spheroidal coordinates with the constant Σ_2. Therefore the curvature invariant $R^{\alpha\beta\gamma\delta}R_{\alpha\beta\gamma\delta}$, which is independent of the choice of coordinates, naturally has finite limits at these rings:

$$R^{\alpha\beta\gamma\delta}R_{\alpha\beta\gamma\delta} \to \frac{3 \times 2^{12}\Sigma_2^4\left(4\Sigma_2^2 - \Sigma_1^2 - 3\Sigma_2\sqrt{\Sigma_2^2 - \Sigma_1^2}\right)}{(\Sigma_2^2 - \Sigma_1^2)^3\left(\Sigma_2 + \sqrt{\Sigma_2^2 - \Sigma_1^2}\right)}, \text{ as } \rho \to \Sigma_1, \tag{3.10}$$

$$R^{\alpha\beta\gamma\delta}R_{\alpha\beta\gamma\delta} \to \frac{3 \times 2^{12}(4\Sigma_2^2 - \Sigma_1^2)}{(\Sigma_2^2 - \Sigma_1^2)^3}, \text{ as } \rho \to \Sigma_2. \tag{3.11}$$

Furthermore, for null geodesics we have the equation

$$\dot{x}^2 + \dot{y}^2 = \frac{1}{\Sigma_k^2 Q(x^2+y^2)}\left[E^2 - \frac{f^2L^2}{\Sigma_k^2(x^2+1)(1-y^2)}\right] \qquad (k = 1 \text{ or } 2), \tag{3.12}$$

where the dot denotes differentiation with respect to an affine parameter, and E and L are constants. As we approach the inner or outer ring($x, y \to 0$) Eq. (3.12) behaves as

$$\dot{x}^2 + \dot{y}^2 \sim \frac{2^4}{\Sigma_2^2 - \Sigma_1^2}\left(E^2 - \frac{L^2}{\Sigma_k^2}\right) \qquad (k = 1 \text{ or } 2), \tag{3.13}$$

the right hand side of which is finite. This means that the geodesics starting from the ring have a finite length for a finite affine parameter. On the other hand, in the case of the ring singularity mentioned before $\dot{x}^2 + \dot{y}^2 \to \infty$ as $x, y \to 0$, and so the geodesics cannot be extended through the ring.

In the above discussion we have clarified the difference between the rings mentioned in the 4-soliton case with complex conjugate pole trajectories and

the ring singularity appearing in the 2-soliton case with non-complex conjugate pole trajectories. The difference is caused by the fact that Q diverges at the ring in the former case while it becomes zero at the ring singularity in the latter case. These behaviors of Q are determined by whether the parameter q is real or imaginary corresponding to the case of complex conjugate or non-complex conjugate poles. Taking these facts into consideration, we shall call this 4-soliton solution "the ring solution" in order to distinguish it from the solutions with the ring singularity.

4. Classification of static soliton solutions

In the previous sections we have shown the static soliton solutions to the vacuum Einstein equation which are characterized by the even soliton number. In the real pole case there is a series of static solutions starting with the Weyl solution in Eqs. (2.15) and (2.16). These are understood as the nonlinear superposition of multi-Weyl solutions[3,6]. In the complex pole case we have two kinds of solutions, i.e., the ring solution and the solution with ring singularities. We must consider all these solutions in the classification of the series of solutions. For the higher soliton numbers this classification becomes complicated because we can mix the various cases of pole trajectories. In table 1 we list the the possible solutions with the soliton number 2, 4 and 6.

Last of all we comment on the 6-soliton solution with two pairs of complex conjugate pole trajectories and one pair of real trajectories. Although the solution is much complicated, we can distinguish the two parts of solution which come from the real and complex poles. In the case where $q = 1$ the one part constructed from real pole trajectories describes a black hole with the event horizon and the other describes the two rings mentioned in Sec. 3 which are located outside the horizon. There is of course an effect of interaction between the above two parts but the event horizon evade defectiveness. We thus have an interesting solution constituted of a black hole and two rings. We already found the solution which describes a black hole accompanied by two rings in the vacuum six-dimensional space-time[7]. Here we have shown the similar solution also in

four-dimensional space-time.

soliton number	real pole	complex pole	
2	Weyl	[c.c. poles]	—
	SBH($q=1$)	[non-c.c. poles]	Weyl'(ring singularity)
4	superposed	[c.c. poles]	Ring sol.($q=1$)
	Weyl	[non-c.c. poles]	two ring singularities
	2 SBHs($q=1$)	[mixture]	—
	[mix. of real and c.c. poles]		—
	[mix. of real and non-c.c. poles]		Weyl + ring singularity
6	superposed	[c.c. poles]	—
	Weyl	[non-c.c. poles]	three ring singularities
	3 SBHs($q=1$)	[mixture]	Ring sol. + ring singularities($q=1$)
	[mix. of real and c.c. poles]		SBH + Ring sol.($q=1$)
	[mix. of real and non-c.c. poles]		Weyl + ring singularities

Table. 1 The possible solutions with the soliton number 2,4 and 6. In this table SBH and c.c. stand for Schwarzschild black hole solution and complex conjugate, respectively. — means no asymptotically flat solution. Weyl' is the solution given by Eqs. (3.3) and (3.4).

REFERENCES

[1] V.A. Belinskii and V.E. Zakharov, Sov. Phys. JETP **50**(1979)1.

[2] A. Tomimatsu and H. Sato, Phys. Rev. Lett. **29**(1972)1344;
Prog. Theor. Phys. **50**(1973)95.

[3] G.A. Alekseev and V.A. Belinskii, Sov. Phys. JETP **51**(1980)655.

[4] K. Ohara and H. Sato, Prog. Theor. Phys. **65**(1981)1891;
M. Kihara and A. Tomimatsu, Prog. Theor. Phys. **67**(1982)349;
A. Tomimatsu and M. Kihara, Prog. Theor. Phys. **67**(1982)1406.

[5] T. Azuma and T. Koikawa, preprint TMUP-HEL-9108.

[6] T. Koikawa, preprint TMUP-HEL-9112.

[7] T. Azuma and T. Koikawa, Phys. Lett. **A**(to be published).

Superposed Weyl Solitons —String Connecting Black Holes—

TAKAO KOIKAWA

Department of Physics, Tokyo Metropolitan University
Minami-Ohsawa 1-1, Hachioji-Shi 192-03, Japan

ABSTRACT

We study an exact solution of the vacuum Einstein equation which consists of a string and two Weyl's at the ends. Estimation of the string tension shows that its repulsive force is balanced by the attractiove force between two Weyl's.

1. Introduction

Lately we classified the static solutions of the vacuum Einstein equation with axial symmetry [1]. Two infinite series of gravitational solitons starting with the Weyl solution and the ring singularity appear in the classification. The difference of two series lies in the fact whether they take real poles or complex poles in constructing the solutions. We have clarified an interesting features of a ring solution appearing in the complex pole trajectories in ref.[1] . Here we focus on the real pole trajectories. The solutions appearing in this series are classified by their even soliton numbers. The first solution with the soliton number 2 is the well known Weyl solution. The next solution has the soliton numer 4 and can be understood as a nonlinear superposition of the solutions. We will discuss the features of the solution in detail in the next section. In section 3 we give an interpretation of the 4-soliton solution as a system composed of two Weyl solitons and a string connecting them at the ends. This turns out to give a natural interpretation of the balancing of the attractiove force by two massive Weyl's and the string tension by the string. Here the string tension yields a repulsive force and so can be balanced against the gravitational attractive force between the two Weyl solitons. In the last section we discuss the lensing effect due to the string.

2. Features of the superposed Weyl solitons

In order to clarify the meaning of the 4-soliton solutions we consider several limits of the parameters. For that purpose we first study the 2-soliton solution, that is, the Weyl solution:

$$-ds^2 = -fdt^2 + f^{-1}\{Q(d\rho^2 + dz^2) + \rho^2 d\phi^2\}, \tag{2.1}$$

where f and Q are given by

$$f = \left(-\frac{\mu_1\mu_2}{\rho^2}\right)^{-\delta}, \tag{2.2}$$

$$Q = \left(\frac{\rho^2(\mu_2 - \mu_1)^2}{(\rho^2 + \mu_1^2)(\rho^2 + \mu_2^2)C^{(2)}}\right)^{\delta^2}, \tag{2.3}$$

where $C^{(2)}$ is a constant. Here μ_1 and μ_2 are real poles and now given by

$$\mu_1 = w_1 - z + \sqrt{(w_1 - z)^2 + \rho^2}, \tag{2.4a}$$

$$\mu_2 = w_2 - z - \sqrt{(w_2 - z)^2 + \rho^2}. \tag{2.4b}$$

Here w_1 and w_2 are real constants guaranteeing the reality of the pole trajectories with an order $w_1 < w_2$. It is known that this solution reduces to the Schwarzshild solution with mass m when δ equals 1. The behaviour of f and Q near $\rho = 0$ are given by

$$f \sim \left(\frac{w_1 - z}{w_2 - z}\right)^{-\delta}, \; Q \sim 1, \; for \; z < w_1, \tag{2.5a}$$

$$f \sim \left(\frac{z - w_1}{z - w_2}\right)^{\delta}, \; Q \sim 1, \; for \; w_2 < z. \tag{2.5b}$$

In the 4-soliton case, f and Q are given by

$$f = \left(\frac{\mu_1\mu_2\mu_3\mu_4}{\rho^4}\right)^{-\delta}, \tag{2.6a}$$

$$Q = \left(\frac{\rho^8(\mu_2 - \mu_1)^2(\mu_3 - \mu_1)^2(\mu_4 - \mu_1)^2(\mu_3 - \mu_2)^2(\mu_4 - \mu_2)^2(\mu_4 - \mu_3)^2}{(\rho^2 + \mu_1^2)(\rho^2 + \mu_2^2)(\rho^2 + \mu_3^2)(\rho^2 + \mu_4^2)\mu_1^2\mu_2^2\mu_3^2\mu_4^2 C^{(4)}}\right)^{\delta^2}, \tag{2.7}$$

where $C^{(4)}$ is a constant. Their behaviour near $\rho \sim 0$ are given by

$$f \sim \left(\frac{(w_1 - z)(w_3 - z)}{(w_2 - z)(w_4 - z)}\right)^{-\delta}, \; Q \sim 1, \; for \; z < w_1, \tag{2.8a}$$

$$f \sim \left(\frac{(z - w_1)(w_3 - z)}{(z - w_1)(w_4 - z)}\right)^{-\delta},$$

$$Q \sim \left(\frac{(w_4 - w_1)(w_3 - w_2)}{(w_4 - w_2)(w_3 - w_1)}\right)^{\delta^2}, \; for \; w_2 < z < w_3. \tag{2.8b}$$

$$f \sim \left(\frac{(w_2-z)(w_4-z)}{(w_1-z)(w_3-z)}\right)^{-\delta}, \; Q \sim 1, \; for \; w_4 < z. \tag{2.8c}$$

Let us introduce new variables z_1, z_2, σ_1 and σ_2 by

$$\begin{aligned} w_1 &= z_1 - \sigma_1, \\ w_2 &= z_1 + \sigma_1, \\ w_3 &= z_2 - \sigma_2, \\ w_4 &= z_2 + \sigma_2. \end{aligned} \tag{2.9}$$

with an order $w_1 < w_2 < w_3 < w_4$. We can understand that this is a superpositon of two Weyl solitons by taking the Taylor expansion around each solitons. Taking the limit that $|z_2 - z_1| \gg \sigma_1, \sigma_2$, we find that the above solution becomes

$$f \sim \left(\frac{w_1-z}{w_2-z}\right)^{-\delta} \{1 + O\left(\frac{\sigma_2}{z_2-z_1}\right)\}, \; Q \sim 1, \; for \; z \lesssim w_1, \tag{2.10a}$$

$$f \sim \left(\frac{z-w_1}{z-w_2}\right)^{\delta} \{1 + O\left(\frac{\sigma_2}{z_2-z_1}\right)\}, \; Q \sim 1 + O\left(\frac{\sigma_1\sigma_2}{(z_2-z_1)^2}\right), \; for \; w_2 \lesssim z. \tag{2.10b}$$

Next we consider the case that two Weyl's get contact with each other or $w_2 \to w_3$. The result is that the two Weyl's fuse into one Weyl with the additive mass of the original two masses. We also consider the case that two Weyl's get overlapped onto each other, or $w_1 \to w_2$ and $w_3 \to w_4$ simultaneously. In order this to occur the original two masses should agree with each other. The resultant solution is the Weyl with the same mass as those of the old Weyl's. It has been examined how the superposed Kerr solution behaves in the several limiting cases of the parameters [2]. Since we can regard the present superposed Weyl solution is obtained from the superposed Kerr solution by taking the zero angular momentum limit, the present analysis does not give anything particular. However we believe that simpleness is deserving of pedagogical value.

3. String attached by two Weyl solitons

It is natural to ask how they can be gravitationally balanced. As far as we assume that both masses of the Weyl solitons at the ends of the string are positive, there should be some repulsive force against the attractive force between two Weyl solitons. In the case of Kerr solution, the spin-spin interaction can be a candidate of the repulsive force between them. It was investigated if the flat metric is possible around the string in this case and found to be impossible to impose the Euclidean nature around the string[2]. We can not expect such a spin-spin interaction in the Weyl solution case. Instead we expect one-dimensional object lying along the z-axis between two Weyl's rather than nothing as has been discussed before in the superposed Kerr solution case. We, therefore, do not expect any Euclidian nature around the string between two Weyl's. Just as we expect massive entitiy is filled inside of horizon in the black hole, we expect that the entity, which is a long,thin and straight string with the string tension μ, lies between two Weyl solitons,which turns out to break the Euclidean nature around it. In order to measure the deviation of space-time around the string from the Euclidean space-time, we define P_0 by [3]

$$P_0^2 = \lim_{\rho \to 0} \left(\frac{g_{\varphi\varphi}}{\rho^2 g_{\rho\rho}} \right). \tag{3.1}$$

It is easy to see that $P_0 = 1$ in the Euclidean case. The present 4-soliton metric yields

$$P_0 = \left(\frac{(z_2 - z_1)^2 - (\sigma_2 - \sigma_1)^2}{(z_2 - z_1)^2 - (\sigma_2 + \sigma_1)^2} \right)^{\delta^2} \geq 1. \tag{3.2}$$

It is easy to find in the limit that the two Weyl's are separated infinitely

$$P_0 \sim 1 + \frac{4G^2 m_1 m_2}{(z_2 - z_1)^2}. \tag{3.3}$$

where $m_1 = \delta\sigma_1/G$ and $m_2 = \delta\sigma_2/G$ are masses defined in the Newtonian potential in the isolated limit. Note that $(P_0 - 1)$ becomes positive or negative depending on whether both masses are positive or either of them is negatibe. They correspond

to the repulsive force or attractive force, respectively. As an origin of this non-Euclidity, suppose the stress energy tensor assciated with a long, thin and straight string given by

$$T^{\mu}{}_{\nu} = \mu\delta(x)\delta(y)diag(1,0,0,1). \tag{3.4}$$

The metric outside of the string was solved by Vilenkin [4] in the limit $G\mu << 1$:

$$-ds^2 = -dt^2 + dz^2 + d\rho^2 + (1-4G\mu)^2\rho^2 d\varphi^2. \tag{3.5}$$

This yields

$$P_0 \sim 1 - 4G\mu. \tag{3.6}$$

Comparing this with eq.(3.3), we find that the present space-time is induced by a string of which tension is given by

$$\mu = -\frac{Gm_1m_2}{(z_2-z_1)^2}. \tag{3.7}$$

Note that negative μ means the repulsive force rather than the attractive force in the z direction when both masses are positive. On the other hand the gravitational force between two far separated Weyl solitons is given by

$$f = -G\frac{m_1m_2}{(z_2-z_1)^2}. \tag{3.8}$$

This shows that the gravitational force between the two positively massive Weyl's could be balanced by the string tension which works repulsively in z-direction.

4. Discussion

It has been well known that there lies a weak singularity between two Kerr solutions, and so does the present two Weyl soliton case. It is interesting to ask if the light can really reach to the weak singularity. Before discussig it, let us consider the Weyl solution case. Suppose that the light is emitted inward from outside of the singularity and travels only on the plane including the equator of the Weyl solution. The equation reads

$$\frac{dk^\mu}{d\lambda} + \Gamma^\mu{}_{\rho\sigma} k^\rho k^\sigma = 0, \tag{4.1}$$

where $k^\mu = dx^\mu/d\lambda$ are the 4 components of a null vector of light and $\Gamma^\mu{}_{\rho\sigma}$ is the Levi-Civita symbol. Since k^μ is a null vector, we also have

$$g_{\mu\nu} k^\mu k^\nu = 0, \tag{4.2}$$

which leads to

$$(k^1)^2 = -(\frac{E^2}{g_{00}} + \frac{L^2}{g_{33}})/g_{11} = -\frac{E^2}{g_{00}g_{11}}\left(1 + B^2\frac{g_{00}}{g_{33}}\right), \tag{4.3}$$

where E and L are the constants corresponding to energy and angular momentum. Here we note that the non-negative condition of the RHS yields a prohibited region where the light can not enter, and the size of the region depends on one parameter known as the impact parameter $B = E/L$. In the case that $\delta \geq \frac{1}{2}$ there exists a critical impact parameter B_C which separates absorption from scattering of light from far infinity. It is given by

$$B_C = \frac{(2\delta+1)^{(2\delta+1)/2}}{\delta(2\delta-1)^{(2\delta-1)/2}} M, \tag{4.4}$$

which coincides with the well known value for the Schwarzschild black hole when $\delta = 1$. In the case that $0 < \delta < \frac{1}{2}$, we find that

$$B_C = 0, \tag{4.5}$$

which means that the absorption cross section equals zero. In other words, when

the angular momentum is non-zero, no light from outside can reach the equator of the singular surface of the Weyl solution as far as we limit that the light travels only on the plane including the equator of the Weyl solutin. This originates from the fact that the second term on the RHS in eq.(4.3) can be as large as we want in the limit $x \to 1$, which corresponds to approaching to the singular surface of the Weyl solution.

The similar situation can also be found in the string case which we are now discussing. We consider the behavior of light emitted inward toward the string with two massive Weyl's at the ends. We found that $B_C = 0$, which means that the light approaching the string is scattered off from the string and never gets the string if the angular momentum is non-zero. This is because as far as the angular momentum of light is non-zero, the second term in eq.(4.3) gets dominant as the light approaches the string. The only case that the light is absorbed to the string is when the impact marameter is zero, which means the measure of the absorption cross section by the string with unit length is zero. This might be that strings do not cause any serious trouble physically, even if they might be subject to the mathematical weak singularity. The details will be published elsewhere[5].

The author would like to thank all the organizers of the workshop. He acknowledes Prof.Azuma for invaluable discussion on this paper. Without the discussion this work has not been completed. He also acknowledges Iwanami Fūjukai for financilal support.

references

[1] T. Azuma and T. Koikawa, preprint TMUP-HEL-9108;

T. Azuma, paper included in this proceeding.

[2] M. Kihara and A. Tomimatsu, Prog. Theor. Phys. 67(1982) 349;

67(1982)1406; K. Ohara and H. Sato, Prog. Theor. Phys. 65(1981)1891.

[3] G. A. Alekseev and V. A. Belinskii, Zh. Eksp. Teor. Fiz. 78(1980)1297.

[4] A. Vilenkin, Phys. Rev. D23(1981)852.

[5] T. Azuma and T. Koikawa, in preparation.

Black Holes from Cosmic Strings †

Hisakazu Minakata

Department of Physics, Tokyo Metropolitan University
1-1 Minami-Osawa, Hachioji, Tokyo 192-03, Japan

Abstract

An estimation is given for the formation rate of primordial black holes from cosmic strings. The plausibility of the underlying assumptions for the estimation is critically examined. It is found that the formation rate is negligibly small contrary to the claim in the literature.

† Talk given at the Workshop on General Relativity and Gravitation held at Tokyo Metropolitan University, December 4-6, 1991.

Primordial black holes are interesting objects which can be used as a probe into the largest and the smallest structure of the matter. This possibility arises due to the phenomenon of Hawking's radiation [1] through which the very existence of the primordial black holes is detectable. They can probe the density inhomogenity in the early universe at far earlier epoch than that can be investigated by other observational means. They are also of interest from the particle physics point of view. They can probe the fundamental structure of the matter at energy scales far beyond that amenable to accelerators [2].

In order to use them as a useful probe it is of key importance to identify the formation mechanism of primordial black holes. The candidate mechanism, so far proposed, include (1) density inhomogenity in the early universe [3], (2) bubble collisions at the time of cosmological phase transition [4], and the collapse of cosmic strings [5,6]. Probably, many more are on the waiting list. At the moment we cannot identify the right mechanism. (Even two or three of them would be competing!) To prepare possible future observations it is important to thoroughly examine the known mechanisms to estimate the formation rate and the mass distribution of primordial black holes.

In this talk I address the third mechanism of the formation of primordial black holes; callapse of cosmic strings. It is very natural to expect that cosmic strings are the intense source of primordial black holes. If we consider the GUTs cosmic string its energy density per unit length would be $\mu \simeq (10^{16}\ \mathrm{GeV})^2 \sim 10^{43}$ erg/cm. It is imaginable that such high concentration of the energy density can lead to the copious formation of black holes. It turns out, however, that an estimation [7] which I will present here indicates that this naive expectation is wrong. It appears to us that we can extinguish this mechanism form the list of the candidate mechanism for formation of primodial black holes.

How can one estimate the formation rate of black holes form cosmic strings? Our estimation which I present below relys on the following assumptions [8] :

1) Our method estimates the formation rate assuming that cosmic strings are doing quasi-free motion.
2) String's quasi-free motion is disturbed by the emission of gravitational waves. We assume that this effect does not invalidate our key asumption 1).
3) We assume that the network of cosmic strings is in the scaling solution [9].

It is not difficult to justify (though not in a rigorous sense) the assumptions 1)~3). Let us begin with the third assumption. It is now well established in detailed numerical simulations [10-12] that the network of cosmic strings eventually approachs to the scaling solution. In this scaling solution the energy densities of long strings, loops, and the radiations (including gravitational waves off loops) are in peaceful coexistence, all have the identical time dependence, $\propto \mu/t^2$ in the radiation dominated era.

The second assumption is next easier to justify. Cosmic strings radiate gravitational waves at a rate

$$\dot{E} = -\Gamma G\mu^2 \qquad (1)$$

where $\Gamma \simeq$ 50-100. The effect of emitting gravitational waves for quasi-freely moving strings may be quantified by estimating $T_p\dot{E}/E$, the energy loss rate per one period of oscillation T_p. Using (1) $\dot{E}/E = -\Gamma G\mu/L$ and one period of oscillation is, on the order of magnitude, Tp~L where L is the length of the string. Then the energy loss rate during one period of oscillation is estimated to be $\sim\Gamma G\mu$. Since we are interested in the parameter region of $G\mu\sim10^{-6}$ required by structure formation scenario (or by grand unified theories), the energy loss rate is $\sim10^{-4}$. Therefore, the effect of the gravitational wave emission can be safely treated as a pertarbation to the quasi-free motion of cosmic strings.

We now turn to the assumption 1). It is known [13] that the viscosity due to interactions with surrounding particles has negligible effect on cosmic string

motion except for very early epoch. The interaction between strings is described as the crossing and the simultaneous intercommutation of strings. The frequency of intercommtation per unit time can be estimated as follows. Let us take the analytic model of the scaling cosmic string network presented by Albrecht and Turok [10]. As in the discussion of the effect of gravitational wave emission, the frequency of the string intercommutation may be quantified by the rate of loop production per one period of oscillation. $T_p[d\rho_l(L) / dt] / \rho_l(L)$, where $\rho_l(L)dL$ is the energy density of loops with length L~L+dL. In their analytic model the loop energy density obeys the equation

$$\frac{d}{dt}\rho_l(L) = -3H\rho_l(L) + \frac{\mu}{\xi^4} f\left(\frac{L}{\xi}\right) \qquad (2)$$

where H stands for the Hubble parameter, ξ the curvature scale of the strings, and f(x) is the scale-invariant loop production function. Using the formulas given in Ref. [10] it is easy to obtain the loop production rate per one period of oscillation averaged over loop length:

$$\left\langle T_p \frac{\rho_l(L)}{dt} / \rho_l(L) \right\rangle \simeq \frac{\xi}{R_H} \left\langle \left(\frac{L}{\xi}\right)^2 \right\rangle \qquad (3)$$

where R_H denotes the Hubble radius. In (3) $\langle x^2 \rangle$ should be understood as follows:

$$\langle x^2 \rangle = \int dx\, x^2 \cdot \sqrt{x} f(x) \,/\, \int dx \sqrt{x} f(x) \qquad (4)$$

for the radiation dominated era, and

$$\langle x^2 \rangle = \int dx\, x^2 f(x) \,/\, \int dx f(x) \qquad (5)$$

for the matter dominated era. In deriving (3) we have ignored the effect of gravitational wave emission since it is a small perturbation. If we use

$$f(x) = A\frac{1}{\sqrt{x}} e^{-Bx} \qquad (6)$$

as suggested in Ref. [10], then loop production rate can be estimated as $\sim(\xi/R_H)\cdot B^{-2}$. Since $(R_H/\xi)^2 \simeq 210$ and $B \simeq 2.6$ in the radiation era Albrecht-Turok simulation the loop production rate per one period of oscillation is ~ 1/100. We also obtain similar result for the matter dominated era. Thus it appears that the intercommutation of the strings is not so frequent that hardly affects significantly the quasi-free motion of cosmic strings. We have relied upon the functional from of f(x) as well as the values of parameters of Albrecht and Turok since the corresponding informations on the loop production function have not been reported in more recent Bennett-Bouchet simulation [11].

This completes our arguments to justify the assumptions 1)~3). Of course if the string motion would be completely free then the collapse to black holes could not occur since the motion of loops is completely harmonic [5]. But, as we have just learned, there are several sources of perturbation which make the motion of strings deviate from the exactly harmonic ones.

We now proceed to the estimation of formation rate of black holes from cosmic strings based on our assumptions 1)~3). Our presentation will essentially follow our paper, Ref. [7]. Broadly speaking we treat the quasi-free motion of strings basically as a sequence of random walks of the string segments. In the rest of my lecture I try to make this statement more precise..

It is well known since Kibble and Turok [14] that the equation of motion of free relativistic string can be solved by superposing left- and right-moving components;

$$\mathbf{r}(\sigma, \tau) = \frac{1}{2}[\mathbf{a}(\sigma+\tau)+\mathbf{b}(\sigma-\tau)]. \tag{7}$$

The functional forms of **a** and **b** are arbitrary apart from the condition

$$|\mathbf{a}'|^2=|\mathbf{b}'|^2=1. \tag{8}$$

Here we are working with the gauge $\tau=t$ (t is our time coodinate) and the primes in (8) imply the derivative with respect to their dependent variables $\sigma\pm\tau$.

The solution (7) means that by arbitrarily generating **a** and **b** subject to the condition (8) we can have a solution of relativistic equation of motion of strings. Then, it is very natural to regard them as random variables: By randomly generating **a** and **b** we can simulate the quasi-free relativistic motion of strings.

To carry it out we latticise $\sigma\pm\tau$ space for **a** and **b** variables. Then the constraint (8) implies that the sequence of **a** and **b** variables forms two independent random walks whose step length are unity. After n-steps **a** variable can be written as (let us take $\tau=t=0$)

$$\mathbf{a}(\sigma_n)=\Delta\sigma\sum_{i=1}^{n}\mathbf{a}'(\sigma_i), \tag{9}$$

where $\Delta\sigma$ is the quantity which must exist in (9) on dimensional ground. The physical interpretation of $\Delta\sigma$ is the correlation length [5], or the curvature scale

of cosmic strings. Following Ref. [5] we denote $\Delta\sigma$ as s hereafter. Thus we have set up the random walk picture of quasi-free motion of relativistic strings.

Now it is straightforword to evaluate the formation probability of black holes. We define that a black holes has formed if at certain time all the string coodinates $\mathbf{r}(\sigma,\tau)$ of a particular loop are within the Schwarzschild radius $r_S=2GL\mu=2Ly$. ($y\equiv G\mu$) Let us estimate the probability that such event occurs. The probability that a string remains within r_S after one steps of **a**-and **b**-walk is given by

$$\frac{\pi(2Ly)^2}{4\pi\left(\frac{s}{2}\right)^2} = 4x^2y^2 \tag{10}$$

where we have defined x=L/s. This is the ratio of the area of the Schwarzschild circle to that of the whole globe which can be reached after a **b**-step as represented in Fig.1 (next page). Since it is the random walk the probability of confining into the Schwarzschild radius after n-steps is

$$P = (4x^2y^2)^{n-1} \tag{11}$$

where we have taken into account the fact that tha loop is closed (n−1, not n).

The step number n is not the physical quantity by itself. It is an antificial quantity because we latticised σ-space by hand. Nevertheless, when we make up our mind on what is the black hole n is self-consistently determind. Let L be length of the string black hole. On the other hand, since all the string configurationis are within the Schwarzscild radius, the string length must be of the order of $\sim r_S n$. Eliminating L form both side of the equation

$$L \approx r_s n = 2Lyn. \qquad (12)$$

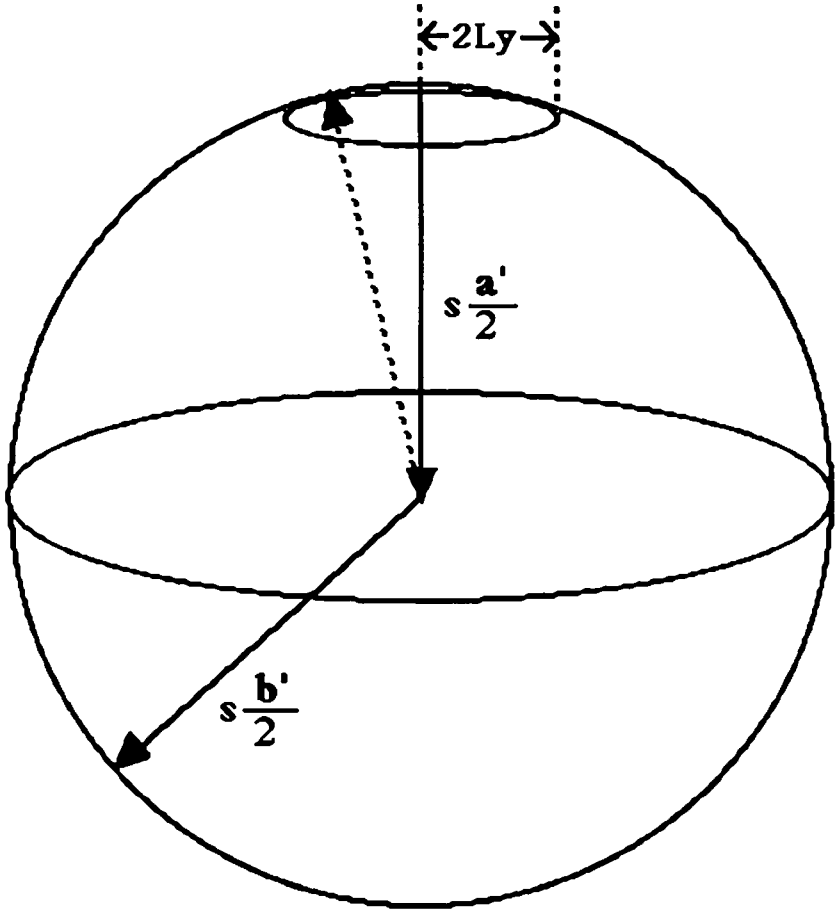

Fig. 1. Set of one steps of random **a**- and **b**-walks is drawn for the case that xy<<1, or equivalently, the correlation length s is much larger than the Schwarzschild radius r_s=2Ly. A globe with radius $\frac{s}{2}$ is depicted such that an **a**-step starts at the north pole and ends at the center of the globe. The following **b**-step ends at somewhere on the globe as shown by the solid line. For a black hole configuration it must end in the arctic region of radius r_s as indicated by the dashed line.

we obtain

$$n \approx \frac{1}{2y} \tag{13}$$

which is a very large number $\sim 10^6$ for $y=G\mu=10^{-6}$. Then the black hole formation probability we finally obtain is [15]

$$P = (4x^2y^2)y^{-1}/2-1. \tag{14}$$

We refer Ref.(7) for the discussion of estimating x. The result is, on the order of magnitude, $x\sim 10$. With $x=10$ and $y=G\mu=10^{-6}$ the black hole formation probability (14) takes the value

$$P \sim 10^{-5\times 10^6} \tag{15}$$

which is entirely negligible.

Why the formation rate of black hole so tiny? The answer is clearly exhibited in (12). The step number n is the ratio between L and r_s (=2Ly). With $y=G\mu \ll 1$ the Schwarzschild radius is so small that n must be a very large number. If the step number is huge there is almost no probability that the string configuration remains within the Schwarzschild radius.

The reason why we reach to a conclusion quite different from that of Hawking [5] is explained in more detail in Ref.(7). Our conclusion is not inconsistent with Ref. [6] since they do not really address the absolute rate of black hole formation.

I have described a way of estimating formation rate of primordial black holes from cosmic strings. In particular, I presented some critical discussions on the underlying assumptions for the estimation. Our result indicates that even if a characteristic signal for the evapolating black hole would be observed in the future it is not the one from cosmic strings.

References

[1] S. W. Hawking, Nature 248, 30(1974); Comm. Math. Phys. 43, 199(1975).

[2] For a recent comprehensive review, see F. Halzen, E. Zas, J. H. MacGibbon, and T. C. Weekes, Nature 353, 807(1991).

[3] B. J. Carr, Astrophys. J. 201, 1(1975).

[4] S. W. Hawking, I. G. Moss, and J. M. Stewart, Phys. Rev. D26, 2681(1982).

[5] S. W. Hawking, Phys. Lett. B231, 237(1989).

[6] A. Polnarev and R. Zembowicz, Phys. Rev. D43, 1106(1991).

[7] H. Honma and H. Minakata, preprint TMUP-HEL-9109, September, 1991.

[8] I have to mention that these assumputions are those taken, explicitly or implicitly, by Hawking in Ref. [5]. In fact, our arguments essentially follow his except for the last crucial point of departure.

[9] T. W. B. Kibble, Nucl. Phys. B252, 227(1985).

[10] A. Albrecht and N. Turok, Phys. Rev. D40, 973(1989).

[11] D. P. Bennett and F. R. Bouchet, Phys. Rev. D41, 2408(1990).

[12] B. Allen and E. P. Schellard, Phys. Rev. Lett. 64, 119(1990).

[13] A. Vilenkin, Phys. Rep. C121, 263 (1985).

[14] T. W. B. Kibble and N. Turok, Phys. Lett. B116, 141(1982).

[15] To my understanding this probability P is the quantity which gives rise to the energy density of black holes at time t when multiplied by $\rho_l(t)$, the energy density of loops, and may be better denoted as the "black hole fraction".